Transactions

of the

ASME

OCTOBER, 1951

VOL. 73, No. 7

Transactions

of The American Society of Mechanical Engineers

Published on the tenth of every month, except March, June, September, and December

---

Published monthly by The American Society of Mechanical Engineers. Publication office at 20th and Northampton Streets, Easton, Pa. The editorial department is located at the headquarters of the Society, 29 West Thirty-ninth Street, New York 18, N. Y. Cable address, "Dynamic," New York. Price $1.50 a copy, $12.00 a year for Transactions and the *Journal of Applied Mechanics* to members and affiliates, $1.00 a copy, $6.00 a year. Changes of address must be received at Society headquarters four weeks before they are to be effective on the mailing list. Please send old as well as new address. . . . By-Laws: The Society shall not be responsible for statements or opinions advanced in papers or . . . printed in its publications (B13, Par. 4). . . . Entered as second-class matter, March 2, 1928, at the Post Office at Easton, Pa., under the Act of August 24, 1912. . . .

Simplified Process for Determining Steam Purity

By S. T. POWELL[1] AND I. G. McCHESNEY[2]

A method and apparatus are described for measuring electrical conductivity of steam from boilers and vapor from evaporators. The stainless-steel capillary sampling line throttles the flow and condenses part of the sample by radiation, normally requiring no cooling water. The condensed part of the sample is kept at the boiling point and continuously swept by uncondensed vapor so that gases cannot go into solution. No reboiling or degassing is required. Design and operating details are given, based upon successful operation for many months, with no attention or adjustment required.

THE problems of measuring accurately the dissolvable solids in steam by conductivity methods have been solved with varying degrees of success by a number of different testing procedures. The objective has been to measure only the dissolved solids which are contained in the condensed steam. The basic principle upon which the conductivity method depends is to collect a representative sample of the steam and to process the sample in such a manner that the conductivity of the steam condensate can be measured without interference from dissolved gases or impurities picked up in the sampling and testing apparatus. Frequently, conductivity recorders are used to show the changes which take place in steam quality under various boiler operating conditions.

Many papers have been published in the technical press and in the proceedings of societies describing the apparatus used and the results obtained under varying operating conditions (1 to 5).[3]

The most troublesome of all the problems involved in the measurement of steam contamination by electrical conductivity is that of preventing gas contamination or degassifying a contaminated sample. Because dissolved gases often combine chemically with the condensate, the best solution for this problem is to prevent the initial contamination of condensate as it is formed in the sampling and measuring system. This result can be accomplished if the steam sample is drawn off at high velocity in such a manner that the exposed surfaces of the condensate particles are scrubbed thoroughly by steam passing through the sampling tube. If this passage is at high velocity, condensate particles clinging to the wall of the tube and those torn from the wall of the tube by the steam, all tend to lag behind steam flowing through any increment of the sampling line. This assures that the exposed surfaces of all condensate particles are at or very close to the boiling point for the pressure established at any particular point in the sampling line. Fig. 1 shows the apparatus required for sampling and collecting and measuring the specific conductivity of condensate without gas contamination.

The sample enters a standard sampling nozzle in the steam main, passes through a high-pressure stainless-steel gate valve and into a sampling line of stainless-steel capillary tubing which Fig. 1 shows in the form of a coil. Actually, this tubing may be 50 to 150 ft long, since it serves as an orifice to limit the total sample flow, and also as an air-cooled radiating condenser which will deliver a mixture of steam and condensate to the apparatus. In practice, any excess of sampling line between the nozzle and conductivity unit is formed into a helix or flat serpentine on a rigid mounting.

The apparatus is designed for use when sampling steam in a pressure range from somewhat above atmospheric to extremely high pressures, and it discharges at atmospheric pressure. Because of constant discharge pressure, automatic temperature compensation is not required. The flow of sample to the cell can be adjusted by using the proper length of sampling tube or preferably by sampling at a rate in excess of the requirements for the condensate cell and passing the excess through a by-pass line to a vent as shown in Fig. 1.

The partially condensed sample of steam and vapor enters the condensate cell where the electrical conductivity is measured and is finally discharged to waste. The operation of the condensate cell is shown schematically in Fig. 2.

Steam, condensate, and gases enter this cell tangentially and while the condensate particles are collected and flow down the walls of the condensate cell, their exposed surfaces are being continuously scrubbed by steam. Level regulation in this condensate cell is automatic, particles being thrown from the condensate surface out through the discharge pipe. As the condensate surface approaches the vertical outlet pipe, an orifice is formed causing an appreciable pressure drop at the surface of the condensate. High turbulence and surface boiling are the results. This not only carries away excess condensate, but prevents absorption of gases in the condensate that is temporarily collected within the cell. The turbulence caused is useful in thoroughly mixing condensate held in the cell. The length of travel through the discharge passage is sufficient to prevent the diffusion of gases from the atmosphere back through the discharge and into the cell. The conductivity electrodes inserted in the condensate cell thus measure the specific conductivity of the condensate without the effect of gas contamination. The condensate cell in operation is shown in Fig. 3.

This cell is sampling saturated steam from a 1350-psi source with the sampling line adjusted to a suitable flow rate. No by-pass valve is used. The contamination by boiler-water carry-over is about 0.4 to 0.5 ppm.

The length and size of sampling lines are estimated to a first approximation from the graph shown in Fig. 4. However, before mounting the sampling line permanently, the total flow and steam:condensate ratio should be measured, and the length adjusted if necessary.

---

[1] Consulting Chemical Engineer, Baltimore, Md. Fellow ASME.

[2] Assistant Superintendent, Rochester Gas & Electric Corporation, Rochester, N. Y. Mem. ASME.

[3] Numbers in parentheses refer to the Bibliography at the end of the paper.

Contributed by the Joint Research Committee on Boiler Feedwater Studies and the Power Division and presented at the Annual Meeting, New York, N. Y., November 26–December 1, 1950, of THE AMERICAN SOCIETY OF MECHANICAL ENGINEERS.

NOTE: Statements and opinions advanced in papers are to be understood as individual expressions of their authors and not those of the Society. Manuscript received at ASME Headquarters, October 9, 1950. Paper No. 50—A-85.

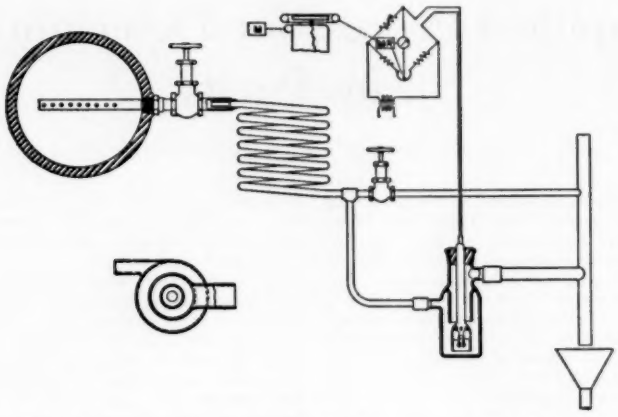

FIG. 1 APPARATUS FOR MEASURING SPECIFIC CONDUCTIVITY OF HIGH-PRESSURE-STEAM SAMPLES

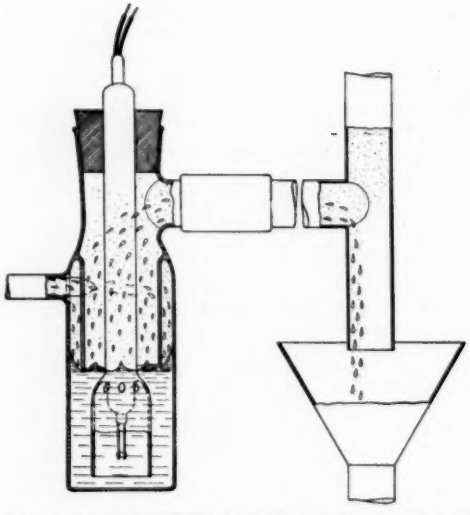

FIG. 2 DIAGRAM SHOWING OPERATION OF CONDENSATE CELL

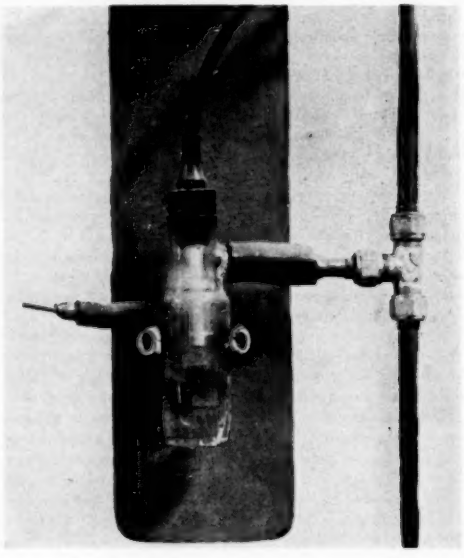

FIG. 3 CONDENSATE CELL IN OPERATION

APPARATUS FOR SAMPLES AT LOW PRESSURE

If the pressure at the sample point is variable, such as in the vapor lines from evaporators, the adjustment of water temperature to the boiling point may not be automatic, especially if the design flow rate is small. Therefore it may be necessary to provide additional controls for rate of flow. In extreme cases a temperature compensator may be added in the electric circuit of the conductivity equipment, such as shown in Fig. 5. In this case the temperature-compensating element is placed in the flow cell along with the conductivity-dip cell.

In a typical installation the apparatus would receive the sample from an evaporator with steam pressure varying from 25 to 10 psia and discharging the steam and condensate to the first heater having a pressure range from 6 to 2.5 psia. Under such conditions, and with properly adjusted flow through the system, the sampling line and coil will always be considerably above the ambient temperature, and the apparatus functions without attention throughout the full range of operation.

At maximum load condition the flow of sample to the condensate cell is adjusted to the maximum amount possible without ex-

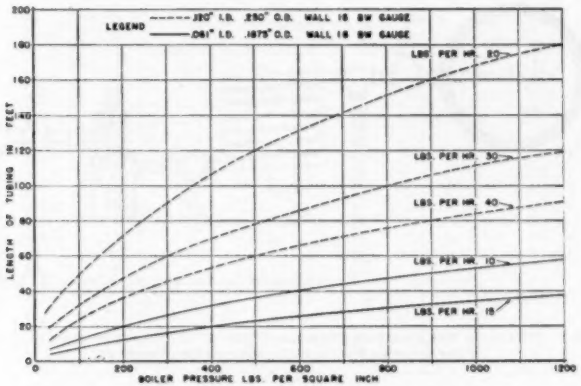

FIG. 4 GRAPH USED IN ESTIMATING SIZE AND LENGTH OF SAMPLING LINES

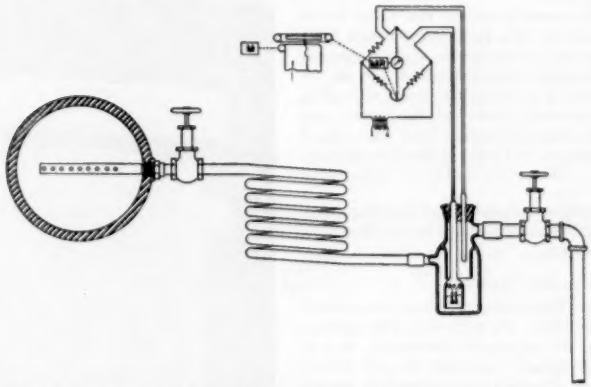

FIG. 5 APPARATUS FOR MEASURING SPECIFIC CONDUCTIVITY OF STEAM SAMPLES TAKEN NEAR ATMOSPHERIC PRESSURE

posing the electrodes as a result of extreme turbulence. Under this condition it is satisfactory if the sample is from 25 to 50 per cent condensed. The maximum flow rate for the experimental condensate cell is between 8 and 10 lb per hr. If this maximum-flow adjustment is made, the device will operate satisfactorily at light loads. For instance, if the flow were to drop to 3 to 4 lb per hr with condensation in the range of 50 to 75 per cent, there would be no change in the recorded conductivity because of this flow change. Experiments have demonstrated that a 4-to-1 change in the rate of sample flow will not affect the conductivity measurement. In adjusting the flow, the only requirement is that at maximum flow the high turbulence in the condensate cell will not expose the electrodes, and that the minimum flow at light load will cause surface boiling and sufficient turbulence for level regulation in the cell.

If the pressure of the sample is below that of the atmosphere, it is most convenient to use cooling water in order to condense the required amount of steam for the conductivity reading. Typical apparatus which is used for this service is illustrated in Fig. 6.

Here, two conditions, as follows, are required for successful operation:

(*a*) A pressure drop across the sampling and measuring system sufficient for turbulent flow at fairly high velocity throughout the system.

(*b*) A cooling agent other than air because the sampling line and coil may be close to or below the ambient temperature.

When operating the device at low absolute pressure, it is satisfactory to connect the condensate-cell discharge in a $1^1/_2$-in. isolated line to the condenser. This permits the condensate cell to operate close to the absolute pressure of the main condenser. A suitable source of cooling water is the condensate or booster-pump discharge. This discharge should be reasonably close to the vacuum temperature in the main condenser. Connecting the conductivity sampling and measuring system in this way, there is no possibility of undercooling the sample as the condensate used in cooling automatically follows the pressure and temperature changes in the main condenser and condensate cell. For this reason, the quantity of cooling water flowing is not at all critical. If any other source of cooling water is used, it is important that its temperature and flow be regulated carefully so that a very small temperature difference occurs between the cooling water entering the coil and the steam-and-condensate mixture being admitted to

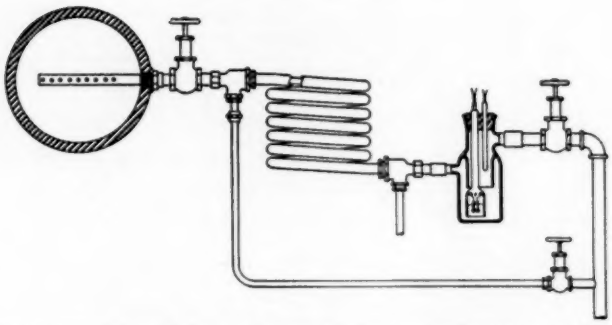

FIG. 6 APPARATUS FOR MEASURING SPECIFIC CONDUCTIVITY OF STEAM SAMPLES TAKEN FROM SOURCES BELOW HALF-ATMOSPHERIC PRESSURE

the cell. If this is not done, undercooling of the condensate will cause gas absorption in the sample.

A steam sampling and measuring system was set up on an evaporator at Russell Station of The Rochester Gas and Electric Corporation to measure the contamination of the discharged steam. The evaporator pressure varied between 25 psia and 10 psia. This installation required the use of condensate for cooling the sampled steam. As previously described, the coolant was taken from the condenser pump discharge. There have been 9 months of satisfactory operation, and many calibrations made by total evaporation methods. A typical record of the performance is shown in Fig. 7.

The usual carry-over of this evaporator is between 0.2 and 0.35 ppm. One reason for this low contamination is an operating head on the evaporator of only 46 Btu.

OPERATING TESTS

Early experiments on two installations at 650 psi were carried out in February and March, 1948. The range of flow for satisfactory operation was one of the important experiments. It was found that the per cent condensation and also the total flow of sample to the cell was not at all critical and that the cell operated satisfactorily at high rates of flow up to the point where extreme turbulence was still not sufficient to expose the electrodes in the conductivity cell. The minimum flow limit was such that surface boiling occurred in the cell, and there was sufficient turbulence to throw condensate particles upward through the outlet of the cell.

One of the unexpected difficulties occurring during the early stages of experimental work on the apparatus was the diffusion of gases through the discharge line into the cell. Cells operating with a short discharge, 2 to 4 in. long, recorded conductivities of 2 to 3 times as great as cells having longer discharge lines. Connecting an 18-in. piece of rubber tubing to the discharge of the conductivity cell was sufficient to prevent gas diffusion into the cell. Under such conditions, the conductivity record would show about $1^1/_2$ micromhos. On removal of the rubber tubing, the conductivity would immediately increase to 4 to $4^1/_2$ micromhos and again reduce to $1^1/_2$ micromhos when the tube was reconnected. This indicated the requirement for a discharge sufficiently long to provide a vapor seal against diffusion of gases.

Another series of tests that was conducted over a period of several weeks was for the purpose of demonstrating whether or not a true sample could be withdrawn from a tee connection on the sampling line so that a by-pass line would be permissible in

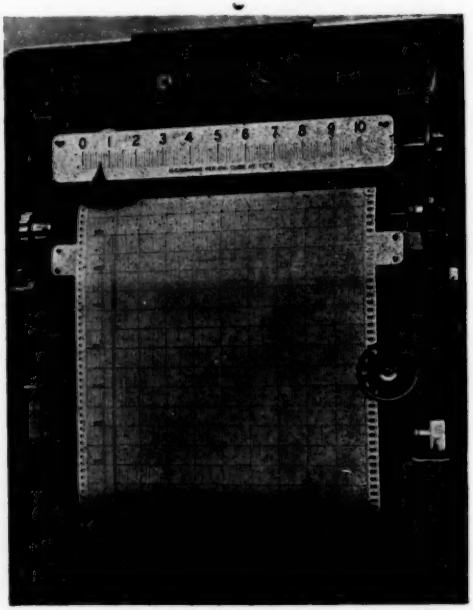

FIG. 7 RECORD OF CONDUCTIVITY OF EVAPORATOR STEAM AT RUSSELL STATION

adjusting the flow to the condensate cell. In order to do this, two cells were connected successively on the same sampling line. The total flow of sample was 30 lb per hr. The flow to the first condensate cell installed on the sampling line was 5 lb per hr, and that to the second cell 3 lb per hr with 22 lb per hr by-passed. The second cell was installed approximately 6 in. from the first cell. The cells were calibrated carefully and the electric circuit checked and compared to standards. Over a period of several weeks the record of the two cells was in close agreement. A record taken during one of the sampling periods is shown in Fig. 8.

Several measurements correlating specific conductivity with

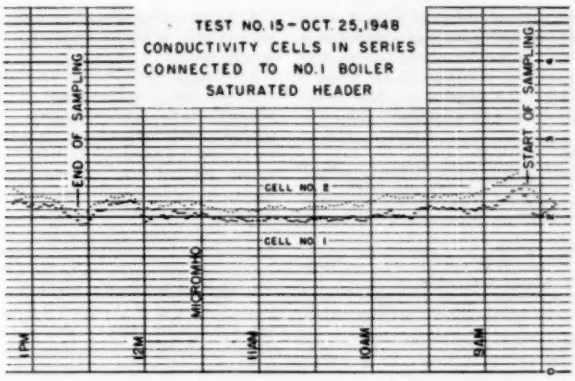

FIG. 8 RECORD OF CONDUCTIVITY CELLS CONNECTED IN SERIES DURING A SAMPLING INTERVAL

total dissolved solids by evaporation are shown in Table 1.[4] These figures are applicable to steam samples. Table 2 shows comparable data for evaporator vapor samples.

In addition to the test and developmental work described, one of the authors has supervised experimental work with this apparatus in other stations. It was installed to measure the quality of saturated steam at 600 psig delivered from boilers of a generating unit, and once the proper sample flow and steam:condensate ra-

[4] Conductivity measurements were corrected to 25 C by a fixed resistance added to the bridge circuit. The values for K are lower than the customary range of 0.50 to 0.65, because at very low dissolved-solids concentrations, K does not fall on the curve $c = f(\bar{L})$ as determined at high concentrations, where c is equal to the concentration in parts per million and $\bar{L}$ is the specific conductance.

TABLE 1 RATIO BETWEEN TOTAL SOLIDS IN STEAM AND SPECIFIC CONDUCTIVITY DETERMINED BY EVAPORATION OF CONDENSED-STEAM SAMPLE TAKEN AT STATION NO. 3

Date 1948	Specific conductivity, mho × 10^{-6}	Total solids by evaporation, ppm	Ratio: $\frac{\text{Total solids}}{\text{Conductivity}} = K$	Specific conductivity × avg K	Difference + or − ppm
10–1 10–5	1.65	0.50	0.30	0.57	+0.07
10–6 10–11	1.80	0.60	0.33	0.63	+0.03
10–12 10–16	1.65	0.70	0.42	0.57	−0.13
10–25 10–28	1.43	0.50	0.35	0.50	0.00
10–29 11–3	1.70	0.50	0.29	0.59	+0.09
11–4 11–8	1.52	0.60	0.39	0.53	−0.07
11–8 11–12	1.43	0.50	0.35	0.50	0.00

Average ratio = 0.35 = K

TABLE 2 RATIO BETWEEN TOTAL SOLIDS IN EVAPORATOR VAPOR AND SPECIFIC CONDUCTIVITY DETERMINED BY EVAPORATION OF CONDENSED-STEAM SAMPLES FROM EVAPORATOR DISCHARGE AT RUSSELL STATION

Date 1949	Specific conductivity, mho × 10^{-6}	Total solids by evaporation, ppm	Ratio: $\frac{\text{Total solids}}{\text{Conductivity}}$	Specific conductivity × avg K	Difference + or − ppm
7/27 8/5	0.70	0.38	0.54	0.29	−0.08
8/8 8/15	0.60	0.20	0.33	0.25	+0.05
8/15 8/22	0.63	0.19	0.30	0.26	+0.07
8/26 9/2	0.60	0.31	0.52	0.25	−0.06
9/7 9/15	0.58	0.27	0.46	0.24	−0.03
9/16 9/23	0.72	0.24	0.33	0.31	+0.07
9/23 9/30	0.67	0.32	0.48	0.28	−0.04
10/3 10/13	0.78	0.30	0.38	0.33	+0.03

Average ratio = 0.42 = K

tio were established, the apparatus has functioned without attention. Another of these sampling assemblies was installed at a 900-psig central station subject to considerable ammonia contamination and has been operating satisfactorily for about 3 months, giving readings of 1.0 to 2.5 micromhos. After initial adjustment the apparatus has required no attention.

BIBLIOGRAPHY

1 "Steam Contamination-III, Determination of Steam Quality," by S. T. Powell, *Combustion*, vol. 9, November, 1937, pp. 25–31.
2 "Symposium on Problems and Practice in Determining Steam Purity by Conductivity Methods," Proceedings of the ASTM, vol. 41, 1941, pp. 1261–1340.
3 "Degasification of Steam Samples for Conductivity Tests," by P. B. Place, Proceedings of the ASTM, vol. 41, 1941, pp. 1302–1312; also, *Combustion*, vol. 13, August, 1941, pp. 31–35.
4 "An Automatic Degasser for Steam Sampling in Power Plants," by H. M. Rivers, W. H. Trautman, and G. W. Gibble, Trans. ASME, vol. 72, 1950, pp. 511–518.
5 "A New Degasifying Steam Condenser for Use in Conductivity Determinations," by F. G. Straub and E. E. Belson, Trans. ASME, vol. 63, 1941, pp. 645–648.

Discussion

W. N. Greer.[5] This proposed method of steam-purity measurements is a move in the proper direction in that better results should be obtained under conditions which prevent the solution of gases in the condensed sample to be measured. Its mere simplicity may lead some to question its practicability. The answer to this is that it appears to have been proved in practice.

The lag in this system is materially less than in any of the previously devised arrangements for steam-purity measurements. The lag in the sample line, under normal conditions, should be negligible. With a volume of condensed sample of approximately 60 cc in the cell, the theoretical lag, with an instantaneous change in dissolved solids of steam being sampled, is approximately 2.5 min to record 90 per cent of the change in solids content, and 4.5 min to record 99 per cent of the change. In other words, with instantaneous change in dissolved-solids content, the recorder would almost immediately begin to indicate a change, would require about 2.5 min to have recorded 90 per cent of the change, and 4.5 min to have practically reached the full value.

Referring to Tables 1 and 2, the value of K, the factor by which the micromho reading is multiplied to obtain ppm, is probably affected by errors in determining the dissolved-solids content by evaporation. The average value of K often used has been 0.6. This value actually is a function of the concentration of dissolved solids, being high for high-solids content, and decreasing as the dissolved-solids content decreases. At the lower concentrations the relatively high conductance of the hydrogen and hydroxyl ions, due to the dissociation of water, become effective, and must necessarily result in a lower value for K.

R. A. Lorenzini.[6] The writer believes that an "ideal" degasser can be defined as one which has the following requisites:

1 It must remove completely the gases which contribute to the conductivity of the condensed-steam sample.
2 It must be simple, foolproof, and should require little or no attention for its operation.
3 It should be reliable and should require little or no maintenance.
4 It should be flexible enough to fulfill the requirements of representative sampling.
5 It should be low in cost.

A degasser which has all of these qualifications would be enthusiastically acclaimed by all those interested in steam-purity determinations.

The degasser described by the authors is certainly simple, and simplicity and reliability quite often go hand in hand. It is claimed that the degasser requires little or no attention once the necessary initial adjustments are made and it is certainly a blessing to have a degasser which does not require continuous compensations for variations in condensate temperature. While the writer has no information on the cost of this degasser, it is believed that it will be low.

The authors have presented no data on the initial and residual contents of carbon dioxide and ammonia. The inclusion of these data would add materially to the value of the paper.

It appears obvious that any factor which changes the ratio of steam and water in the cell will influence the results obtained as this will have the effect of diluting or concentrating the sample whose conductivity is measured. If the heat transferred from the coil or sampling line remains constant, the quality of steam condensed also will remain constant. However, if the sampling rate is changed the ratio of condensate and steam will also change.

If the sampling rate is increased, the ratio of condensate to steam will decrease and the concentration of salts in the condensate must necessarily increase. On the other hand, if the sampling rate is decreased, the ratio of condensate to steam will increase, and the concentration will decrease.

The same results will be obtained if the sampling rate remains constant and the heat transfer to the surroundings changes. To illustrate this, assume that the sampling line consists of $^1/_4$-in-OD capillary tubing 100 ft long and that the sampling rate is constant at 40 lb per hr. If there is no air motion relative to the sampling line then the heat is transferred from the tubing to the surroundings by free convection and radiation and the over-all heat-transfer coefficient will be about 5.4 Btu/(sq ft)(hr)(deg F), and the steam condensed will be 12 lb per hr or 30 per cent of the total flow. However, if the air velocity relative to the line is 2 mph or only 2.9 fps, the over-all heat-transfer coefficient to the surroundings becomes about 12.5 Btu/(sq ft)(hr)(deg F), and 27.8 lb will be condensed or 70 per cent of the steam sampled. Thus the concentration of solids will be in the ratio of 2.3 to 1 for these two conditions. In order to eliminate this effect, it would be necessary to shelter the tubing carefully.

To control the sampling rate the authors recommend that a portion of the partially condensed sample be diverted from the cell. From our experience it is extremely difficult to split a two-phase stream into two streams, each having the same proportion of steam and condensate. The degree of success depends largely upon the ratio of liquid to vapor and also the ratio of the flows in the two branches and the orientation of the tee which is used for splitting the stream.

The writer cannot follow the arrangement of cells described by the authors where it is said that "two cells were connected successively on the same sampling line" with a flow of 5 lb per hr to the first cell and 3 lb per hr in the second cell and with 22 lb per hr by-passed. The writer would appreciate having the authors' clarification on this point.

F. G. Straub.[7] The authors of this paper show a simple method for measuring the electrical conductivity of steam which eliminates the necessity for frequent temperature corrections. They show that for the plants tested they have been able to obtain a fairly straight curve. However, it is difficult to interpret their data.

---

[6] Technical Sales, Leeds & Northrup Company, Philadelphia, Pa.
[6] Mechanical Engineer, Research Department, Foster Wheeler Corporation, New York, N.Y. Jun. ASME.

[7] Research Professor of Chemical Engineering, University of Illinois, Urbana, Ill.

In Tables 1 and 2 reports are given on the total solids by evaporation and the specific conductance as determined with their cell. How was the sample obtained for evaporation? The construction of the cell is one that apparently does not allow a sample of the solution in the cell to be removed without some modification. These data merely show that the steam being sampled was free from variation in solids. No data are given as to the specific conductance of parallel samples determined by means of a standard condensing coil or to the possible gas contamination. It would be advisable to run tests of this nature. Where conductance of steam and condensate are compared for determination of condenser leakage, this cell establishes a curve for the steam but no similar curve will be available for the condensate.

It would be desirable to run tests using this type of cell on steam which has some contamination with both soluble solids and gas, and see how effective it would be.

H. M. Rivers.[8] Designed to measure the conductivity of steam condensate at its boiling temperature, with minimum opportunity for subcooling, the present apparatus embodies two very important features: Contaminating gases are sparingly soluble under these conditions and are less likely to affect the conductivity value; and the conductivity can be measured at relatively constant temperature, a decided advantage where continuous records are required. The first of these principles has been recognized for a long time[9] and, as a matter of fact, both were successfully incorporated in the steam-sampling apparatus used by Mumford about a decade ago.[10] A conductivity-flow cell of improved design has been included, as well as certain refinements which minimize subcooling of the condensate whose conductivity is being measured; but in all practical regards, the present apparatus is about the same as that described by Powell[11] and by Powell, Bacon, McChesney, and Henry,[12] 13 years ago.

The problem of excluding or removing gases from steam condensate is difficult, but not insuperable. An essential requirement, however, is that much of the original sample must be vented away to carry off the contaminating gases. All mineral impurities remain in that portion of the sample which is not vented off. But data representing the concentration of mineral impurities in the gas-free condensate are meaningless unless the weight ratio of such condensate to the original sample is accurately known. It makes a great deal of difference whether the solids are measured in a portion of condensate which corresponds to 25, 50, or 75 per cent of the total sample; for measured values must be multiplied by a suitable factor (0.25, 0.50, or 0.75, respectively, for the figures just given) to put the data on an original sample basis. Therefore, if steam-purity data are to be capable of meaningful interpretation—beyond some rough qualitative indication that carry-over is or is not taking place—the weight-ratio of gas-free condensate to total sample must be known, and it must remain substantially constant for continuous recording of the data.

The foregoing requirement has not been met in the design of this apparatus, which makes no provision for measuring continuously the ratio of gas-free condensate to total steam sample, nor does it attempt to control this ratio in any way whatever. The authors state that moderate changes in sample flow rate (changes comparable to those encountered in actual practice) can alter the percentage of condensation by as much as 100 per cent. But this necessarily introduces an error of like magnitude in the steam-purity data. A 4 to 1 change in rate of sample flow, which the authors seem to regard as inconsequential, could put the data 400 per cent in error, due to the effect this change could have on the percentage of condensation. As has been pointed out, reasonable changes in the temperature and velocity of air surrounding the atmospheric condenser may affect greatly the percentage of condensation and, consequently, the accuracy of the data. Other errors of gross and unknown magnitude may be introduced when a large amount of partially condensed sample is by-passed around the conductivity cell, for here again the condensate being tested represents a totally unknown fraction of the original sample.

Why, then, do the authors find no significant change in conductivity even though the percentage of condensation—and, consequently, the concentration of solids in the condensate being tested—varies at random over a wide range? Only one logical explanation seems possible; the samples must contain some slight but nevertheless significant residual of dissolved gas. The amount of mineral impurities present, even when concentrated 1.5 to 4 times, must be too low to permit accurate measurement by conductometric means. The point being emphasized in this discussion is that the steam-purity data, when expressed on an original sample basis—as they must be for intelligible interpretation—may be 50 to 300 or 400 per cent in error, due to uncontrollable and unknown variations in the percentage of condensation. It may be interesting, however, to examine the experimental results to see whether they are consistent with this conclusion.

Consider, for example, the data in Table 1 of the paper. Presumably, on the basis of tests which found the concentrations of dissolved gases to be zero or very low, the authors assumed that the conductivity values were not influenced by gas contamination. This required their assuming, further, that 1 micromho of specific conductivity corresponds to about 0.35 ppm of boiler-water solids—a "*K*-factor" considerably lower than expected, as the authors recognize. Now, regarding the authors' explanation for this inconsistency, it is true that the ratio of concentration to conductivity does decrease as the concentration becomes less. But, in the case of boiler-water solids, this decrease is comparatively slight—on the order of only a few per cent at most—and could not reasonably account for such a wide discrepancy in *K*-factor values.

If it is assumed, not without considerable experimental justification, that 1 micromho of specific conductivity corresponds to about 0.65 ppm of boiler-water solids in steam condensate, the solids values in Table 1 can be divided by 0.65 to give the corresponding conductivities due to solids alone. The difference between these and the measured conductivity values ranges from 0.57 to 0.93 micromho (0.74 average) and might conceivably be due to the presence of dissolved gases, for such is the "gas error" attributable to traces of carbon dioxide and/or ammonia barely detectable by conventional analytical methods.[13] Similar treatment of the data in Table 2 suggests a possible gas error ranging from 0.09 to 0.36 micromho (0.23 average), which is well within the limit of experimental accuracy. It may be pointed

[8] Assistant Director of Engineering Service, Hall Laboratories, Inc., Pittsburgh, Pa.

[9] "Some Fundamental Considerations of Corrosion in Steam and Condensate Lines," by R. E. Hall and A. R. Mumford, Trans. American Society of Heating and Ventilating Engineers, vol. 38, 1932, pp. 121–190.

[10] "A New Type of Conductivity Apparatus for Use With Boiler Waters and Steam Samples," by A. R. Mumford, "Symposium on Problems and Practice in Determining Steam Purity by Conductivity Methods," Proceedings of the American Society for Testing Materials, vol. 41, 1941, pp. 1314–1325.

[11] "Steam Contamination," by S. T. Powell, *Combustion*, vol. 9, no. 3, 1937, pp. 36–40; no. 4, pp. 27–31; no. 5, pp. 25–31.

[12] "Design and Development of Apparatus for Measurement of Steam Quality by Electrical Conductivity Methods," by S. T. Powell, H. E. Bacon, Jr., I. G. McChesney, and F. Henry, Trans. AIChE, vol. 33, 1937, pp. 116–138.

[13] "Determination of Purity of Steam by the Electrolytic-Conductivity Method," by W. B. Gurney, M. C. Schwartz, and T. E. Crosan; discussion by A. Watson, Trans. ASME, vol. 62, 1940, pp. 728–733.

out, in this connection, that ammonia is extremely difficult to remove from steam condensate, it defies accurate analysis in very low concentration, and has a comparatively high conductivity.

Unfortunately, the authors neglected to include any actual data on the amounts of gaseous contamination in either the original steam or the samples used for conductivity measurement. A sprinter's running time is meaningful only in relation to the distance covered; some reference to influent- and effluent-gas concentrations would have enhanced this paper considerably. However, data which are available do admit the possibility that contamination by dissolved gas may be responsible for a substantial percentage of the conductivity. For any given installation of the apparatus, it would be reasonable to expect this "low minimum gas residual" to stay fairly constant without regard to the percentage of condensation; thus, if the amount of mineral contamination is slight, wide changes in the percentage of condensation might occur without greatly affecting the conductivity. A conductivity record which remains unchanged, despite variations of 100 per cent and more in the percentage of condensation, could hardly be explained in any other way.

Reference is made to various total-solids values determined by evaporation—0.50 to 0.70 ppm in Table 1, and 0.19 to 0.38 ppm in Table 2. If these determinations were made on samples drawn from the apparatus, as presumably they were, what were the corresponding concentrations of solids in the original steam? Do these different values represent true variations in steam purity, or do they merely reflect changes in the percentage of condensation?

Equipment designers, plant operators, and water-conditioning consultants can use steam-purity data profitably only if those data are known to be truly indicative of boiler or evaporator operating conditions. The data mentioned in this paper are of some relative value, of course, in showing that steam samples of very high purity were flowing through the apparatus. Some such qualitative indication of steam purity may be entirely adequate in those plants where steam contamination is negligible and, in which, therefore, no carry-over problem exists nor is likely to occur. But where there is a problem—as evidenced by superheater failures, turbine deposits, excessive trap maintenance, and the like—precise, quantitative steam-purity data are prerequisite to wise diagnosis and effective application of corrective measures.

Authors' Closure

Most of the questions about the operation of the apparatus have been thoroughly analyzed during the experimental and development stages, covering a period of $1^1/_2$ years. This work was carried out at several plants. It is not possible to cover all these experiments in a paper of reasonable length.

One of the important causes for the variation in value of K is described by Dr. Greer. The values given in Tables 1 and 2 are all for solid concentrations below 1 ppm, some of them considerably below, and for this reason, the dissociation of water has a very important effect on the value of K. The observed conductivity includes both the conductivity caused by dissolved solids in the solution and by the hydrogen and hydroxyl ions.

Mr. Lorenzini asked for information on tests for the initial and residual carbon-dioxide and ammonia contents of condensate passing through the apparatus. Many measurements of the efficiency of gas removal were made at Station No. 3 on two boilers. Due to a fairly high percentage of make-up, the initial CO_2 in the steam leaving the boilers ranges from 10 to 14 ppm. Condensate was carefully sampled from the cell chamber and analyzed for residual CO_2 by the standard method of the American Public Health Association but using long comparator tubes as described in an earlier paper (12). Results of tests in all cases were negative. Samples for determining the residual ammonia content were drawn from the cell chamber at a flow rate sufficiently low to permit high turbulence and surface boiling within the cell. The samples were collected under Nujol and tested for residual ammonia also by the American Public Health Association method. No measurable amounts of ammonia occurred. The initial content of ammonia in the steam from the boilers is usually about 0.2 ppm. This is the equivalent of 3.1 micromhos. Throughout the year, the ammonia content of the steam covers a wide range. In the summer months it ranges between 0.2 to a record low of 0.02 ppm. In the spring months the ammonia content increases to 0.8 to 1.0 ppm maximum. Measurements of the residual content of ammonia were taken for samples collected in January and February at a time when the ammonia content would be in the order of 0.2 to 0.3 ppm. Efficient removal of ammonia is also cited for a 900 psig central station in the last paragraph of the paper.

The change in sampling rate and steam condensate ratio will be discussed later in the closure.

The tests questioned by Mr. Lorenzini, "Two cells connected successively on the same sampling line" were particularly designed to demonstrate that representative samples can be drawn from a tee connection in high-velocity sampling lines. A simple sketch of the test arrangement is shown in Fig. 9.

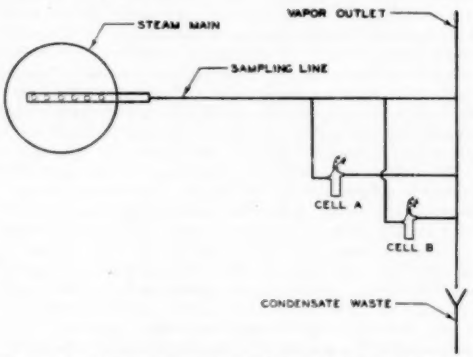

Fig. 9 Test Arrangement for Successive Sampling From Tee Connections in Sampling Line

Dr. Straub was concerned with our method of determining total solids by evaporation and sampling for such tests. These procedures have been developed since early tests in 1936. This work was done by Dr. H. E. Bacon, P. B. Place, and Frank Henry. In the early stages, two 10-liter block-tin sampling cans were made. They have seen considerable use in the past 15 years and all traces of iron on the inner surface of the cans has long since been removed. A description of the evaporating apparatus is beyond the scope of this paper but its development has been over the same period of time and in its present state will give very accurate and consistent results. Due to numerous requests, an adequate description of the apparatus and experience in its development will be prepared for presentation before a suitable group. The sample is fed to an electrically heated platinum dish by a "chicken-feeder" type of flow regulation that holds a fairly constant amount of sample in the dish. Heat regulation prevents boiling and the sample is protected against overflowing the dish by an electronic relay having a fine-wire contact with the condensate surface. Air used to displace the sample and remove vapor from the dish is thoroughly cleaned

by first passing through a large commercial air filter made of flannel and then through two successive cotton filters. Air for removing vapor is jetted against the fine drawn tip that discharges the sample into the dish in order to prevent vapor lock in the feeding line. The electric heater, platinum dish, feeding line, and air lines are glass-enclosed with a water seal at the base. A slight negative pressure is drawn on this glass enclosure to cause air and vapor removal. At the completion of the sample run and before the sample has dried, the platinum dish is removed and the final drying occurs in an oven. A careful weighing of the platinum dish before and after the test run determines the solids content of the original sample. The determination of total solids by evaporation usually takes about one week.

He also asked about samples withdrawn from the cell for gas analysis. No drains or other similar connections are shown on the cell described in the paper. This cell is the result of experimental and development work and in its present form is for practical use and not for further study of the device itself. However, in the course of development of the cell, two methods for withdrawing samples were used. A short length of small-bore glass tubing with a small rubber tube attached was inserted into the cell through the cell discharge opening. The small tubing was concentric with an 18 in. length of $^3/_8$-in. rubber tubing that formed a vapor seal. In another case, a special cell was made wherein a glass by-pass tube was connected below the condensate level in the cell chamber and sealed concentrically in the glass discharge tube. Again, a small rubber tube was connected to this glass by-pass inside of a $^3/_8$-in. tube for vapor seal. In both cases, the small-bore rubber tubing, after thorough purging, was inserted in the sampling bottle and the sample collected under Nujol. The results of tests for gas contamination were all negative. Particular care was taken during the sampling period to see that the sampling rate did not interfere with high turbulence and surface boiling within the cell. Gas contamination of the condensate would result if such interference were to occur.

The authors were not aware of the existence of a standard condensing coil for the determination of specific conductivity. However, tests of this nature have been run. Over a period of more than one year, several carefully calibrated runs were made with the sample divided in the manner shown in Fig. 9 where one of the conductivity measurements was made with apparatus described in an earlier paper (12) and the other sample was measured by the apparatus described in this paper. No undercooling of the sample occurred during the test runs with the old apparatus and under such conditions, it has efficient degassing characteristics. During these tests the new apparatus recorded about $^1/_2$ micromho below the old apparatus, indicating a more effective gas removal. The conductivity of steam for these tests was in the order of 2 micromhos as measured by the new apparatus.

There would be no difficulty in simultaneously recording conductivity of a steam sample and that of a condensate sample. A simple flow cell would suffice for making the latter measurement.

Mr. Rivers refers to earlier work on the recording of steam conductivity. The important advantages of the sampling method now used were well appreciated in apparatus described 13 years ago (12). Both the ASME and ASTM have written standards for the collection of representative steam samples. These standards can only be used as a guide in test work and do not guarantee representative sampling. High turbulence in a mixture of steam, gas, and dry solids does not lend itself to analysis required to establish accurate sampling procedures because of segregation that is bound to occur near vortexes, bends, and obstructions.

The authors cannot concur with Mr. Rivers' statements concerning sampling. They are:

(*a*) "*All* mineral impurities remain in that portion of the sample which is not vented off."

(*b*) "It makes a great deal of difference whether solids are measured in a portion of the condensate which corresponds to 25, 50, or 75 per cent of the sample. . . ."

(*c*) That for meaningful interpretation of steam-purity data ". . . the weight ratio of gas-free condensate to total sample must be known, and remain substantially constant. . . ."

He is evidently thinking in terms of a totally condensed sample, a somewhat different condition from that existing in the method described in this paper. Superheated steam consists of dry, wet, and vaporized solids, steam, and gases. Even though a saturated-steam sample is drawn off, the high pressure gradient in the small tube causes it to immediately superheat and this condition exists before sample condensation starts. If particles are small enough, it is not possible to drive them against any surface. This particle size is in the order of a fraction of a micron. This effect has been well established by work on gas-turbine blading done by Yellott. So it is reasoned that small particles of salts or moisture can pass through the sampling tube and conductivity cell without striking any surface or going into solution along these surfaces. Moisture particles tend to seed out on foreign particles such as dry salts but the moisture and dry-salt particles will have to acquire sufficient mass before striking any surface in the system. As radiation occurs, some of the moisture particles will pass this critical size while others, often in concentrated salt solution, never gain sufficient size to contact surfaces. The phenomena that occur in a condensing sample of steam are certainly very complex and not all subject to experimental analysis. It is quite obvious to the author that all the salts in the sampling procedure are not caught in the condensed sample as stated by Mr. Rivers. It is conceivable that these salts are collected in the measuring cell in a manner somewhat proportional to the percentage of condensate collected. This conforms with many observations that have been made on one of the boilers at Station No. 3 where many pieces of apparatus have been tested at varying sampling rates, radiation constants, and lengths of sampling tubing.

In the past, because of fairly high steam contamination, the relationship between specific conductivity and dissolved solids was determined by multiplying by a "*K*-factor" of about 0.6. The steam produced by boilers of recent design often has a very low contamination. Recent evaporator designs have reduced solids carry-over to a range between a $^1/_4$ and $^1/_2$ ppm. Besides the effect of the dissociation of water, mentioned in the last of Dr. Greer's discussion, other experimental errors add to the difficulty of determining the factor *K*. These include solution of various metals and glass used in the storing of samples taken for total evaporation, the possible dust contamination of the sample in spite of extreme precautions to prevent such contamination. There are further errors in final drying and weighing of the sample. With all these handicaps the conductivity apparatus described gives a very sensitive and reasonably accurate guide to the percentage of dissolvable solids in steam and is an excellent monitor for the indication of unsafe operating conditions due to carry-over.

In July, 1950, this apparatus was loaned to the Lummus Company to make evaporator tests. During the fall of 1950 the American Locomotive Company also used this apparatus for extensive tests on one of their evaporators. Both these companies were well satisfied with the performance of the apparatus during the tests.

It was designed as a practical operating device for the control

of turbine-blading deposits and other allied operating difficulties that result from steam contamination. A record of the amount of influent—and effluent—gas concentration does not bear on this operating problem.

In all cases, the samples reported on in Tables 1 and 2 were samples collected from the original steam source through the same sampling tube used for the conductivity apparatus. The sample was drawn off close to the steam source so that the radiation constant of the sampling line was not affected. In all cases, conductivity was recorded throughout the entire sampling period.

In view of a considerable amount of successful experience with the proper application of this apparatus, the author feels that it will prove a satisfactory guide for plant operators.

The Prevention of Embrittlement Cracking

By A. A. BERK,[1] COLLEGE PARK, MD.

Data are presented to show that nitrate, quebracho tannin, and zero-caustic treatment have been applied successfully in stationary plants to prevent cracking in embrittlement-detector specimens. On one large railroad prevention of cracking in detector specimens has paralleled a spectacular decrease in boiler-seam cracking in locomotive engines. The principal conclusion from a survey of cracking in stationary boilers in the last 10 years is that embrittlement is not a frequent occurrence.

BOILER-seam cracking results from intercrystalline corrosion by caustic solutions which are concentrated from the boiler water in contact with the stressed steel of the seams. The embrittlement detector[2] is a device attached to a boiler so that partial evaporation and concentration of the boiler water takes place on the stressed surface of the test specimen which forms part of an especially designed seam. Thus the detector reproduces closely the conditions in an actual boiler seam in which cracking could occur. Development of cracks in the small test surface indicates that the boiler water can cause embrittlement failure of such seams in the boiler.

The embrittlement-detector test (1)[3] not only will show if an unsafe condition exists, but the effect of treatments to prevent cracking can be evaluated in terms of test-specimen resistance to failure. Many such tests, reported at the Annual Meeting of the Society in 1941, confirmed previously obtained laboratory indications that the method of chemical control previously available for preventing cracking in riveted seams was at best uncertain (2, 3, 4, 5, 6); this was the maintenance of the sulphate-alkalinity ratios, first recommended in the ASME Boiler Code in 1926, and still appearing in the most recent edition of 1949 (7).

Between 1935 and 1940, three practical treatments were found to prevent embrittlement cracking in detector units under laboratory conditions. That two of these treatments should be effective had previously been indicated by the results of earlier tests published in 1930, by F. G. Straub (8); using a different type of apparatus, he found that tannic acid and sodium nitrate, among other materials, prevented cracking of his test specimens. The effectiveness of organic substances such as tannin and lignin, of sodium nitrate, and of eliminating free sodium hydroxide from the boiler water by maintaining only the alkalinity corresponding to trisodium phosphate has been proved on operating boilers by embrittlement-detector tests during the past decade. Results reported to the Bureau of Mines through 1949, from approximately 2000 such tests obtained with 600 detectors in 500 boiler plants have been summarized for this paper. Some 500 additional tests on railroad locomotive boilers are discussed for their special significance with respect to nitrate treatment. Also, 26 cases of boiler-seam cracking studied during the past 10 years provide related information of interest.

Tests in Stationary Boiler Plants

In summarizing the embrittlement-detector test data, the results have been tabulated to show the effectiveness of nitrate (9), tannin (9), and zero-caustic (9, 10, 11) treatments on the prevention of cracking of embrittlement-detector test specimens. Nitrate and quebracho tannin are inhibitors of intercrystalline corrosion in hot concentrated caustic solutions. The zero-caustic treatment, also called the "co-ordinated phosphate" method (11) or the "captive alkalinity" method (12), prevents formation of concentrated solutions of caustic.

Table 1 shows the number of plants in which preventive treatment stopped cracking of the test specimens. Of the 500 plants from which data were obtained, 113 applied nitrate treatment, all successfully; in some instances the minimum nitrate-alkalinity ratio[4] required was as high as 0.3. Similarly, 23 plants successfully applied quebracho-tannin treatment; in other plants the quebracho-alkalinity ratio[4] of 0.3 was not sufficient to prevent cracking of the test specimens, and in a few instances even 0.4 was inadequate, but cracking was stopped completely when such plants changed over to nitrate treatment. Fourteen plants have reported that cracking of detector specimens stopped when the boiler water was treated to contain no caustic alkalinity. The pressure ranges given in this table are those reported and are not necessarily exclusive; however, it is possible that special conditions would cause nitrate or quebracho tannin to be unstable at the higher pressures in the respective ranges.

TABLE 1 EFFECTIVENESS OF PREVENTIVE TREATMENT[a]

Type of treatment	Plants in which treatment stopped cracking of test specimens	Pressure range, psi
Nitrate	113	100–900
Tannin	23	100–700
Zero caustic	14	300–1400

[a] In several instances tannin treatment did not prevent cracking completely and the plant changed to nitrate, which was always successful; zero-caustic treatment was also always successful.

Table 2 contains the over-all summary of individual tests in stationary plants; that is, a series of six tests on one boiler are reported as six tests. The results of tests in which sodium nitrate was the principal treating chemical show clearly its effectiveness as an inhibitor. In four tests the specimens were reported to be cracked when a 0.3 minimum ratio was maintained; but in every instance it appeared that the nitrate concentration had been very low for a significant period of the test, generally during the early days. As already mentioned, quebracho extract has not been as effective as nitrate; however, the ratio of cracked to total specimens is good compared to results with no treatment. As would be expected, when the boiler water contained no free caustic cracking did not result. Most of the tests proving the effectiveness of nitrate and zero-caustic treatments were run for 90 days or more, some as long as a whole year.

Because of the interest for a quarter of a century in the sulphate-alkalinity ratios, the data for pressures to 250 psi were re-

[1] Supervising Chemist, Boiler Water Research Section, Bureau of Mines.

[2] U. S. Patents 2,283,954 and 2,283,955.

[3] Numbers in parentheses refer to the Bibliography at the end of the paper.

Contributed by the Joint Research Committee on Boiler Feedwater Studies and the Power Division and presented at the Annual Meeting, New York, N. Y., November 26–December 1, 1950, of The American Society of Mechanical Engineers.

Note: Statements and opinions advanced in papers are to be understood as individual expressions of their authors and not those of the Society. Manuscript received at ASME Headquarters, October 2, 1950. Paper No. 50—A–84.

[4] Sodium nitrate or quebracho tannin to alkalinity (sodium carbonate plus sodium hydroxide) as sodium hydroxide; all ratios on a weight basis.

TABLE 2 OVER-ALL SUMMARY OF STATIONARY PLANT TESTS WITH EMBRITTLEMENT DETECTOR

Principal testing chemical	Specimens not cracked — 30 days	60 days	90 days or more	Total	Specimens cracked, inhibitor ratio high[a] — 30 days	60 days	90 days or more	Total
Sodium nitrate[b]	190	140	404	734	1	1	2	4[c]
Quebracho extract	78	46	49	173	4	4	6	14
Zero caustic	7	21	38	66	...	...	...	0
None of foregoing[d]	194	100	104	398	305	152	129	586[e]
				1371				604

[a] A ratio of sodium nitrate or quebracho tannin to alkalinity (carbonate plus hydroxide) as NaOH of 0.3.
[b] Includes tests in which the boiler water had a high natural nitrate concentration.
[c] There were good reasons for believing that the nitrate concentrations had not been maintained at the indicated level, especially during the early days of the test; no cracks resulted when the tests were repeated under more careful supervision, sometimes with somewhat higher nitrate-alkalinity ratios.
[d] Includes approximately 50 test specimens not cracked when the boiler water was known to contain a high concentration of tannin-type organic matter from natural sources, silica equivalent to or greater than otherwise "free sodium hydroxide," or high concentrations of sodium chromate; also includes many tests for which the analytical data were incomplete.
[e] 586 cracked in a total of 984 (60 per cent).

examined; 57 tests were found for which the sulphate-carbonate ratios recommended in Section 7 of the ASME Boiler Code were satisfied, caustic soda was present, and nitrate or tannin was not present in significant amounts. Cracking resulted in 39 of these tests, which is approximately the frequency of failure in the group of tests representing no treatment. In contrast, there were no failures when the concentration of free caustic was zero, fewer than 1 per cent when the water was treated with nitrate, and fewer than 8 per cent when quebracho-tannin treatment was used.

The table contains 984 tests for which the boiler water was not treated by one of the three methods listed. Approximately 50 test specimens not cracked in this group were tested with water known to contain a high concentration of tannin-type organic matter from natural sources, or silica at least equivalent to otherwise "free sodium hydroxide," or high concentrations of sodium chromate. About 60 tests were not included in the table because the tests were known to be too poorly run or because no information was available for the conditions under which the tests were run. Nearly 200 of the 398 specimens recorded as "not cracked" were included in the summary because some data were available or because it was not known definitely that the test was improperly conducted.

In addition to presenting the totals of cracked and uncracked specimens for each type of treatment, Table 2 also classifies the tests as having been run 30, 60, or 90 days. The longer tests are regarded as more significant, especially as it has been demonstrated that false conclusions might be drawn when failure did not occur in the shorter test periods (11). The standard method of test (1) provides for 30, 60, and 90-day runs to reduce this uncertainty.

In a summary made in 1942 (9), an analysis of the significance of a negative test showed that for runs of 30, 60, and 90 days, the chances that an embrittling water would cause failure in the specimens were, respectively, 68, 84, and 95 in 100. A similar analysis has now been made of approximately 800 tests for which the boiler water presumably was not treated and had caused at least one of a series of specimens to crack. Probably because the earlier analysis was made on tests run under relatively close supervision by the Bureau of Mines laboratory and over-all control of the tests run since 1942 has been less uniform, a considerable decrease in test accuracy has been found for 60 and 90-day tests. Several of the plants started test programs with 60 or 90-day runs and found no cracking; then, having learned how to operate the unit properly, they discovered a second test specimen to be broken in two in 15 or 20 days. The latest analysis shows the probability of cracking by an embrittling water in 30, 60, or 90 days to be 79, 74, and 88 in 100, respectively; if the approximately 200 tests for which the data are incomplete were excluded from the compilation, it is estimated that these figures would become 86, 90, and 96, respectively. On the other hand, the percentage values would be somewhat lower if an allowance were made for uncracked specimens excluded from the analysis incorrectly; for example, in some boilers the water may possibly have been potentially embrittling although no cracking resulted in any of the tests that were made.

Tests on Chesapeake & Ohio Railway System Locomotive Boilers

Boiler-seam cracking was a very serious problem on the Chesapeake & Ohio Railroad during the period 1930 to 1940. Nitrate treatment was introduced in 1941 (13, 14) and has been extended to cover the entire system. Table 3 shows that failures have been essentially eliminated, and cracks were found in only one engine of the hundreds examined in 1949. Boilers are inspected every 4 years during outages for classified repairs, and almost all of the cracks found since 1944 have been described as "insignificant and possibly missed during previous 4-year inspections."

The embrittlement detector has been used at 18 principal terminals to test the effectiveness of the preventive treatment. The last column in Table 3 shows that the decrease in the number of cracked specimens preceded or paralleled the decrease in boiler cracking. The improvement effected by nitrate treatment is brought out even more clearly in Table 4, which compares the number of cracked specimens in relation to the total tested during the prenitrate, concentration-adjustment, and nitrate-treatment periods. The latter group of tests averaged considerably more than 120 days each and produced no severe cracking.

Experience has shown that embrittlement cracks in locomotive boilers occur most frequently along the major axis of the elliptical deformation produced in the boiler shell by the service road stresses. Probably the metal in such deformed areas is subjected to considerably higher stress than is usual in stationary-boiler seams. In any case, it has been found advisable to set the minimum sodium nitrate-alkalinity ratio at 0.4 to prevent embrittlement failure in locomotive boilers.

Despite the higher ratio, the cost of nitrate treatment on the C & O in 1949 was less than $20 per locomotive per year, or 40 cents per million gross-ton-miles in terms of service.

Boiler-Seam Cracking in Stationary Plants

Twenty-six cases of cracking of stationary boilers were investigated by the author during the period 1942 through 1949; of these, 24 could be definitely called "embrittlement" because the cracks were intercrystalline. The boilers ranged in size from a riveted, downdraft, horizontal-firebox steam generator producing 1400 lb per hr at 50 psi to several welded-drum water-tube boilers producing more than 100,000 lb of steam per hr at 630 psi. Two

TABLE 3 LOCOMOTIVE BOILER CRACKING ON THE C&O

Year	Total engine-[a] miles, millions	Boilers found cracked	Detector test specimens cracked[b]
1930–1937...	21.9 (avg)	161	..
1938.....	19.2	31	..
1939[c].....	20.6	33	..
1940.....	22.6	19	34
1941[d].....	24.6	13	8
1942.....	27.8	10	8
1943.....	30.0	6	5
1944.....	31.2	8	2
1945.....	30.7	5	0
1946.....	28.6	5	2
1947.....	33.2	6	1
1948.....	31.9	4	0
1949.....	23.4	1	2

[a] Steam locomotives only.
[b] Includes slightly cracked test specimens.
[c] Organic treatment begun.
[d] Nitrate treatment substituted for organic treatment.

TABLE 4 EMBRITTLEMENT DETECTOR TESTING ON THE C&O

Period	Specimens tested	Specimens cracked
Before nitrate treatment[a].....	104	38
Early nitrate treatment[b].....	163	17
1944–1949, inclusive.....	243	7[c]

[a] Includes tests of tannin-type organics.
[b] Period of adjustment to optimum concentrations.
[c] Almost every crack was small and shallow.

boilers at one plant developed intercrystalline cracking in tube seats about 30 days after they were placed in service; 10 boilers were 20 to 25 years old. At six of the plants the boiler drums were welded; the others were riveted with internal, external, or combined calking. Cracks were found in butt straps, drum metal, tube seats, and tube ligaments. Methods of water conditioning ranged from no treatment at all to substantially complete removal of all dissolved and suspended material.

In no instance was nitrate or a tannin-type inhibitor present in concentrations shown by embrittlement-detector tests to prevent cracking of test specimens. In 10 of the plants embrittlement-detector test results were available, and all confirmed the dangerous quality of the boiler water. In four instances test specimens failed before the cracks in the boiler seams were found.

The effectiveness of the sulphate-alkalinity ratios cannot be scientifically proved or disproved by the relatively crude data obtainable. Five of the plants, of which four were operated at pressures below 400 psi, maintained ratios at the time of the failures; however, none of the plants had complete data to show that the ratios had always been maintained. In one plant a large number of tubes were lost in a cross-drum straight-tube boiler operated at 180 psi. Eighteen months after the boiler was retubed, cracking was found in the seats of the new tubes between the drum and the rear header; during this period the plant used sulphate treatment, but some of the ratios of sulphate to alkalinity were as low as 1.5. Most of the other plants adopted nitrate treatment and their embrittlement troubles did not recur.

Two boilers operated at 615 to 630 psi lost about 15 tubes owing to embrittlement cracking. To date, this is the highest pressure at which boiler-seam cracking has been reported. However, the first failure occurred only 28 days after the boilers were placed in service, and the trouble may have started when the new boilers were boiled out for 48 hr or longer with relatively strong caustic soda. Nitrate treatment has stopped embrittlement cracking at this plant.

Acknowledgments

The investigation on embrittlement cracking was conducted under a co-operative agreement between the Joint Research Committee on Boiler Feedwater Studies and the Bureau of Mines. It was supervised by a subcommittee under the direction of the late J. H. Walker and was carried out at the Bureau under the leadership of W. C. Schroeder. Many have co-operated in the extensive test program or made other contributions to the studies, and their support and assistance is gratefully acknowledged. Companies licensed under the embrittlement patents include Allis-Chalmers Manufacturing Company, W. H. and L. D. Betz, Dearborn Chemical Company, Gilbert Associates, Hagan Corporation, National Aluminate Company, the Permutit Company, and Cyrus Wm. Rice & Company. They have all generously made available such tests as were obtained; it is only fair, however, to state that more than half the material for Tables 1 and 2 was supplied by the Hagan Corporation through its subsidiary, Hall Laboratories, Inc.

It would be impractical to list all of the plants that supplied the test data. Those that contributed the results of ten or more tests include: American Viscose Corporation, Atlantic Refining Company, Boston Edison Company, Buckeye Cotton Oil Company, Canadian Kodak Company, Carbide and Carbon Chemicals Corporation, Celanese Corporation of America, Chesapeake Corporation, Chile Exploration Company, Consolidated Edison Company of New York, Continental Oil Company, Crossett Lumber Company, The Detroit Edison Company, Duquesne Light Company, Erie Lighting Company, Firestone Tire and Rubber Company, Ford Motor Company, Fort Howard Paper Company, General Motors Corporation, Goodyear Tire and Rubber Company, Gulf Refining Company, Humble Oil and Refining Company, Hunt Oil Company, International Paper Company, Johns-Manville Corporation, Koppers Company, Lago Oil and Transport Company, Magnolia Petroleum Company, Mathieson Chemical Corporation, Metropolitan Transit Authority, Minnesota and Ontario Paper Company, Monsanto Chemical Company, New Jersey Zinc Company, New York State Electric and Gas Corporation, Oscar Mayer & Company, Pennsylvania Salt Manufacturing Company, Phillips Petroleum Company, Pittsburgh Plate Glass Company, Procter and Gamble Company, Public Service Electric and Gas Company, Shell Oil Company, Sinclair Refining Company, Tennessee Eastman Corporation, Tennessee Valley Authority, The Texas Company, United Illuminating Company, U. S. Industrial Chemicals, U. S. Naval Installations, Virginia Electric and Power Company, West Penn Power Company, West Texas Utilities Company, West Virginia Pulp and Paper Company.

The results of the tests on the Chesapeake & Ohio Railway System were made available by R. C. Bardwell and his chief chemist, J. J. Dwyer. The data on boiler-seam cracking in stationary boilers was developed with the assistance of W. H. and L. D. Betz, The Bird-Archer Company, The Employers' Liability Assurance Corporation, Fidelity and Casualty Company of New York, Hartford Steam Boiler Inspection and Insurance Company, Mutual Boiler Insurance Company, The Ocean Accident and Guarantee Corporation, The Travelers Insurance Company, and Union Iron Works.

BIBLIOGRAPHY

1 "Standard Method of Corrosivity Test of Industrial Water (United States Bureau of Mines Embrittlement Detector Method)," American Society for Testing Materials Designation: D807-49. ASTM Standards, Part 5, pp. 1462–1468.

2 "Intercrystalline Cracking of Boiler Steel and Its Prevention," by W. C. Schroeder and A. A. Berk. U. S. Government Printing Office, Washington, D. C., Bureau of Mines Bulletin No. 2,443, 1941.

3 "Embrittlement of Boiler Steel—Experiences With the Embrittlement Detector," by T. E. Purcell and S. F. Whirl, Trans. ASME, vol. 64, 1942, pp. 397–402.

4 "Field Data From the Embrittlement Detector," by E. P. Partridge, C. E. Kaufman, and R. E. Hall, Trans. ASME, vol. 64, 1942, pp. 417–425.

5 "Studies on the Cracking of Boiler Plate," by P. G. Bird and E. G. Johnson, Trans. ASME, vol. 64, 1942, pp. 409–416.

6 "Summary of Papers Composing the Symposium on Embrittlement," by W. C. Schroeder and A. A. Berk, Trans. ASME, vol. 64, 1942, pp. 427–430.

7 "Suggested Rules for Care of Power Boilers," ASME Boiler Construction Code, 1949, Sect. 7, pp. 58–59.

8 "Embrittlement in Boilers," by F. G. Straub, University of Illinois Experiment Station Bulletin no. 216, 1930, pp. 79–81.

9 "A Practical Way to Prevent Embrittlement Cracking," by A. A. Berk and W. C. Schroeder, Trans. ASME, vol. 65, 1943, pp. 701–711.

10 "Water Treatment to Prevent Embrittlement Cracking," by W. C. Schroeder and A. A. Berk, U. S. Patent 2,454,258 granted November 16, 1948.

11 "Protection Against Caustic Embrittlement by Coordinated Phosphate pH Control," by T. E. Purcell and S. F. Whirl, Proceedings of the Third Annual Water Conference, Engineers Society of Western Pennsylvania, 1942, pp. 45–60.

12 "A New Approach to the Problem of Conditioning Water for Steam Generation," by R. E. Hall, Trans. ASME, vol. 66, 1944, pp. 457–488.

13 "Railroad Boiler Seam Cracking Controlled by Nitrate Treatment," by A. A. Berk, *Industrial and Engineering Chemistry*, vol. 40, 1948, pp. 1371–1375.

14 "Experience With Intercrystalline Cracking on Railroads," by R. C. Bardwell and H. M. Laudemann, Trans. ASME, vol. 64, 1942, pp. 403–407.

Discussion

R. C. Bardwell.[5] The summary of the studies and work on prevention of embrittlement cracking as presented in this paper is of considerable interest and indicates careful study and check of the conditions influencing this trouble, and results secured.

This study is of special interest to the railroads. Trouble from embrittlement cracking was first reported by the Chicago and North Western Railway in 1912, and caused considerable concern and expense during the following 15 years, until experience had demonstrated the efficiency of certain organic inhibitors which are still in use by that company. This trouble was followed by similar cracking on other railroads and by an epidemic, of cracked boiler courses on The Chesapeake & Ohio Railway, beginning about 1930. Studies reported by Straub at the University of Illinois which resulted in adoption of recommendations for a sulphate-alkalinity ratio for protection as shown in the Section entitled "Suggested Rules, Care of Power Boilers" of the ASME Boiler Code did not appear to be in line with steam-boiler experience on railroads.

Railroad water conditions are followed up closely by the Water Service Committee of the American Railway Engineering Association, which is composed of membership in charge of water supplies on most of the large railway systems in the country, so that information is available from a wide territory and is not confined to local conditions. Railroad experience indicated that most of the embrittlement cracking occurred in territories carrying comparatively high sulphate ratios; maybe not as high as the ASME recommendations. However, practically no cracking was being experienced in territories with low or practically no sulphates and high alkalinities. Another factor of importance was that it had been found necessary to carry high alkalinities even up to 30 per cent of dissolved solids in locomotive-boiler operation in order to protect against corrosion which formerly caused considerable trouble and much greater expense than the embrittlement cracking. An increase in sulphates resulting in increasing the salt concentration, in many cases above the critical foaming point, caused carry-over and interfered with operation.

In view of these conditions, the Railroad Water Committee could not support the sulphate-alkalinity ratio recommendations.

The co-operative research at the Bureau of Mines, which was supervised by the Joint Committee on Boiler Feedwater Studies on which the railroads were consistently represented, was followed with interest, and their failure to substantiate the sulphate protection against embrittlement was in line with the railroad experience. In fact, the possibility of water quality causing this trouble was viewed with considerable skepticism until the development of the embrittlement detector which demonstrated conclusively that cracking in stressed steel exposed to concentrated caustic solutions could result unless an inhibitor was present. Sulphates appeared to be of little or no importance while sodium nitrate seemed to give the best results, with certain lignins and tannins also effective.

Confirming the efficiency of the embrittlement detector, one of these instruments was first installed on a locomotive in one of the worst embrittling territories on the Chesapeake and Ohio Railway. Much to the surprise of all concerned, the test specimen was practically shattered in 12 to 15 days. With the addition of lignins or sodium nitrate in accordance with the findings of the Bureau of Mines research, these specimens now run regularly in this territory over 120 days with no cracking. To confirm the operation of the detector, the inhibitor was held out for a period, and again the specimen was found to be badly cracked in less than 20 days. As a matter of further interest, no cracking has taken place in any boiler in this territory since the addition of an inhibitor, either lignin or sodium nitrate in accordance with findings at the Bureau of Mines, and the comparatively small amount required has not affected the foaming point or carry-over troubles.

The railroads have been interested in this matter, not only from a locomotive standpoint, but also power-plant-boiler operation. Locomotive boilers undoubtedly are more susceptible to such cracking as no embrittlement cracks have been found in any of the 78 power-plant boilers in service on the Chesapeake and Ohio, although considerable trouble was experienced with the locomotive boilers as brought out by the author. In addition to Table 3 of the paper, the writer can advise that so far, in 1950, no embrittlement-cracked boiler has been reported on the Chesapeake and Ohio as we have been consistently treating the water with sodium nitrate to carry the amount of this material equal to 40 per cent of the alkalinity as sodium hydroxide.

Although the co-operative research work by the Bureau of Mines under the supervision of the Joint Research Committee on Boiler Feedwater Studies has shown definitely that the inhibiting effect of sodium nitrate as well as some lignins and tannins, is much superior to sulphates, a sodium sulphate-alkalinity ratio is still carried as the only preventive for embrittlement cracking in the 1949 issue of "Suggested Rules, Care of Power Boilers," although this has been contrary to the recommendation of the ASME Boiler Code Chemists Committee for the past 7 years. Although this recommendation comes under the heading of "Suggested Rules," it is still part of the Boiler Code which has a semilegal status in many states, and this is a matter of some concern to the railroads.

In view of the apparent hesitancy and long delay of the ASME Boiler Code Committee in bringing the information in the Boiler Code up to date, the Railroad Water Service Committee at a meeting in October, 1950, unanimously approved a recommendation to the railroads which report has been published.[6] This report states in part: "Due to the fact that the sodium sulphate-hydroxide ratio maintained in steam boilers was found worthless as an inhibitor in railroad service, it is the opinion of your Committee that the results secured at the Bureau of Mines, as well as in various railroad laboratories, supplemented by experience in actual railroad operation, have furnished sufficient

[5] Chesapeake & Ohio Railway, Richmond, Va.

[6] American Railway Engineering Association Bulletin no. 490, November, 1950.

information to prevent embrittlement of steam boilers in railroad service, to formulate the following recommendations:

"1 It is the opinion of your Committee that the railroads should disregard the sodium sulphate - alkalinity ratio recommendation as outlined in The American Society of Mechanical Engineers Boiler Code of 1949 which ratio is of questionable value and increases operation difficulties in railroad steam boilers.

"2 Complete investigation of boiler feed waters with special reference to alkaline content and the presence of natural inhibitors.

"3 Installation of embrittlement detectors on boilers operating in suspected water districts on the various railroads.

"4 Properly supervised and controlled use of sodium nitrate or lignin in water known to have embrittling tendencies, as outlined in previous reports of your Committee.

"5 Proper workmanship resulting in tight boiler seams in all boiler construction."

This recommendation will be considered at the Annual Meeting of the American Railway Engineering Association in March, 1951, and with the approval by this authoritative scientific body, will have some effect in counteracting the importance of the present unsatisfactory ASME Boiler Code suggestions.

In closing, it is desired to call particular attention to the last sentence in the summary at the beginning of the paper which is to the effect that with present recommended treatments, prevention of embrittlement cracking is no longer considered a serious problem.

C. E. KAUFMAN.[7] The organization with which the writer is associated has supervised a considerable number of the detector tests described by the author. From some 1200 tests in over 400 plants we have necessarily come to the same general conclusions as has the author.

A few years ago we relied to an appreciable extent on the use of organic materials in combating waters which were potentially embrittling. Currently, however, we prefer the addition of sodium nitrate or the maintenance of boiler water at essentially zero free-caustic alkalinity. Nitrate appears to be more positive in its action than organic materials, is easier to test for, does not introduce discoloration which may interfere with certain testing procedures, and is relatively inexpensive.

In addition to the evidence of the detector tests, we have found in several instances that actual tube-end cracking caused by embrittlement has been eliminated through the addition of nitrate.

Analysis of our results and of the additional data supplied in the paper causes us to have no faith in the sulphate-alkalinity ratio for the prevention of embrittlement.

We consider it quite fortunate that factors of stress and concentration are required in addition to certain boiler-water conditions for the production of embrittlement. Since these physical factors have happily been absent in many cases, actual embrittlement of the boiler has been avoided although the waters involved have been potentially dangerous.

F. G. STRAUB.[8] This paper is a very good summary of the results obtained in the operation of the embrittlement detector in various power plants and on locomotive boilers. It shows that the results obtained in the laboratory are in agreement with those obtained in the power plants. This is to be expected since the conditions of operation of the embrittlement detector are the same in both places.

In the laboratory the detector indicated that nitrate would stop cracking whereas sulphate would not. We would expect to find the same results to be obtained in the plants and they were. The author states: "Many such tests (referring to embrittlement-detector tests) reported at the Annual Meeting of the Society in 1941, confirmed previously obtained laboratory indications (again referring to the embrittlement-detector tests) that the method of chemical control previously available for preventing cracking in riveted seams was at best uncertain; this was the maintenance of the sulphate-alkalinity ratios, first recommended in the ASME Boiler Code in 1926, and still appearing in the most recent edition of 1949."

Why does the author say that the method recommended by the ASME Boiler Code Committee since 1926, is "at best uncertain?" Is it because the sulphate has not been effective in preventing failure in actual operating stationary boilers or is it because it does not stop cracking in the embrittlement detector? He cites 2000 tests with embrittlement detectors operating on boilers, which tests should indicate the sulphate to be ineffective, but he talks about only 26 cases of boiler metal cracking actually studied in ten years. Of these cases he says only 24 could be called embrittlement. He does not give the actual water analyses from any of these plants but says that in ten of the plants embrittlement detector showed the dangerous quality of the boiler water. He states that only 5 of the 24 plants maintained sulphate ratios at the time of the failure; however, none of the plants had complete data to show the ratios had always been maintained. This certainly cannot be given as proof that the sulphate ratios were ineffective in preventing embrittlement. In fact, it certainly appears to be evidence that the sulphate ratios were not maintained in the 24 plants which had encountered embrittlement.

The author appears to want to eliminate the use of sulphate to prevent embrittlement in favor of the phosphate, nitrate, and organic substances. The work carried on at the University of Illinois in the period from 1904 to 1930, reported the following as part of its conclusions:

1 The presence of sodium sulphate in boiler water tends to retard the embrittling effect of the sodium hydroxide, and if in proper proportions will stop it entirely.

2 The presence of phosphates, tannates, chromates, nitrates, acetates, etc., will inhibit the embrittling action of caustic soda if these salts are present in the boiler water in proper amounts.

3 Methods for the introduction of some of the newer inhibiting agents to feedwaters have been worked out and are in operation in large power plants.

The author states: "Between 1935 and 1940 three practical treatments were found to prevent embrittlement cracking in detector units under laboratory conditions." The three practical treatments he refers to are the phosphate treatment, nitrate, and organic. He ignores the practical method which was found to be effective in actual power plants—but unfortunately not effective on the Bureau of Mines detector—mainly the sulphate ratio.

We at the University of Illinois have no objection to the use of inhibitors other than sulphate—as the writer has stated already—since as far back as 1930 we recommended these other methods of treatment. However, we do object to the practice being used by certain groups of not giving credit to the effectiveness of sulphate. There are at least four methods of treatment which may prevent embrittlement. Each plant has its own operating conditions which will dictate which of these will be best for its particular conditions of operation.

[7] Hall Laboratories, Pittsburgh, Pa.

[8] Research Professor in Chemical Engineering, University of Illinois, Urbana, Ill.

Author's Closure

The reception of the summary has been most gratifying, and the author is indebted to Messrs. Bardwell, Kaufman, and Straub for their written discussion.

Mr. Bardwell's announcement that there was no boiler-seam cracking in the C & O's nitrate-treated locomotive boilers during 1950 is a most welcome addition to the data. Mr. Kaufman's confirmation of the general conclusions of the summary is based on many years of practical application of engineering skill to water problems in stationary boilers and is especially appreciated. Professor Straub's statement is considerably less negative than usual.

Mr. Bardwell's detailed explanation of why the railroads' water-service engineers are irritated by the Code-recommended sulphate-alkalinity ratios, Mr. Kaufman's flat statement that his company has no faith in sulphate-alkalinity ratios, and Professor Straub's conclusion that three practical methods of treatment may be superior to sulphate-alkalinity ratios under "particular conditions of operation," all argue for revision of the Code. The principal obstacle is disagreement on what should be added and what should be deleted.

To eliminate the confusion shared by many boiler operators and to enable them to take advantage of the best information available, so that the frequency of boiler-seam cracking will continue to decrease, the author suggests the following wording:[9]

> Research and experience have indicated that this type of crack failure can be prevented.
>
> *a* Nitrate treatment has been successful in the range through 700 psi. In some plants a weight ratio of sodium nitrate to alkalinity (sodium hydroxide plus sodium carbonate as NaOH) of 0.4 was required, but many found much smaller ratios to be adequate for protection.
>
> *b* Zero-caustic treatment, in which the boiler-water alkalinity is substantially equivalent to the trisodium phosphate content of the water, has also been successful. Because of practical considerations, use of this method is limited to boilers operated with distilled-water make-up or its equivalent in quality.
>
> *c* Treatment with tannin-type organic matter is not regarded as highly as nitrate treatment but has been used successfully in many plants.
>
> *d* Sulphate treatment, recommended and used for many years, has been shown to be less reliable than the foregoing methods.

[9] To replace paragraph 49, Proposed Revisions and Addenda to Suggested Rules for the Care of Power Boilers, *Mechanical Engineering*, June, 1948, pp. 557–560.

The Solubility of Quartz and Some Other Substances in Superheated Steam at High Pressures

By G. W. MOREY[1] and J. M. HESSELGESSER,[1] WASHINGTON, D. C.

An apparatus and method for determining the solubility of silica in superheated steam at high pressures are described. At 752 F (400 C), the solubility of quartz in steam increases from 1.0 ppm at 500 psi to 1548 ppm at 15,000 psi; at 932 F (500 C), the solubility increases from 4.3 ppm at 500 psi to 2596 ppm at 15,000 psi. The curves representing the solubility results at 752 F and 932 F cross at two pressures. Between these two pressures the solubility is greater at 752 F than at 932 F; below and above these pressures the solubility is greater at 932 F than at 752 F. This crossing is ascribed to the pressure-density relationships of water at the two pressures, which are affected by the proximity at 752 F of the critical point of water. When the solubility is plotted against the density of steam at each measured point, the curves do not cross, and the solubility at 932 F is greater than at 752 F. The solubilities of some other substances in superheated steam at high pressures are given also.

Introduction

THE dynamic method to be described of determining the solubility of quartz and other substances in superheated steam at high pressures was devised and tried in 1945, and some results were obtained with quartz at 932 F (500 C) and 15,000 psi. Our interest in the problem at this time was geological, and press of other work caused further experiments to be postponed indefinitely. Hall Laboratories, Inc., of Pittsburgh, Pa., became interested in the work, and the present study, extended downward to pressures within the range of modern steam-boiler practice, is the result of their interest and financial support.

The solubility of quartz and other substances in gases, especially superheated steam at high pressures, is of interest to the geologist because of its bearing on the formation of veins and pneumatolytic deposits, and to the engineer because of its bearing on the deposition of silica and other substances on the blades of high-pressure turbines. That gases can dissolve solids has long been known, but the pertinent literature is scanty. One of the earliest to show the solubility was Hannay (1),[2] and Villard (2), and Talmadge (3) added confirmatory evidence. Smits (4) has discussed the theoretical aspects in connection with critical endpoints, and Niggli (5) has considered the geological implications. Several studies have been made of organic systems (6) in which the gaseous solubility of a solid has been measured. Morey and Ingerson (7) published an annotated and theoretical discussion of the relationships in systems of this type, and Morey (8) discussed the solubility of solids in water vapor, with numerous examples from his own experimental work and that of others.

The geologist has been concerned chiefly with equilibrium between gas and solid, the engineer with the equilibrium between a gas, steam, and the boiler water. At first thought, it would appear that it would be the distribution coefficient of SiO_2 between the steam and the dilute solution of silica in the boiler water which is in question, but consideration shows the problem to be not so simple. As the water rises in the boiler tubes, the rapid transfer of heat through the tubes results in violent and turbulent boiling. This boiling occurs primarily at the interface, and at this interface the dissolved material becomes concentrated, and in some areas solid material separates. It is not the distribution coefficient of SiO_2 between steam and a dilute boiler water which is in question, but between steam and a solution of unknown concentration, which at some places becomes saturated solution from which silica (and other substances) may be deposited. The equilibrium values of solubility reported in this paper thus become limiting values which will be approached more or less closely in the steam arising in parts of the boiler tubes.

The engineer's problem is complicated even more by the boiler water containing not silica alone but several dissolved salts. It is a multicomponent system. In a two-component system such as water and quartz, at a given temperature and pressure, only one composition of gas can be in equilibrium with a solid compound or a given liquid composition. A multicomponent system has more degrees of freedom. The solubility of quartz will not be the same in a gas containing dissolved NaCl as in a gas consisting of water alone, and every other substance which is dissolved in the steam affects the solubility of quartz. In general, however, this will be a secondary effect, and the equilibrium values with water are the best guide to the conditions under which silica will separate. This is true even though there is supersaturation, for deposition of silica may take place from a gas supersaturated with respect to silica but not from one that is unsaturated. The saturation values depend on both the temperature and the pressure of the steam, and a steam which is unsaturated under a given set of conditions may be saturated or supersaturated under a different set of conditions.

In the following sections are described the apparatus used and the method of operation. It has been found that the solubility of quarts in steam ranges from 1.0 grams per million grams of water at 752 F (400 C) and 500 psi, to 2596 grams per million at 932 F (500 C) and 15,000 psi, and that the solubility is largely determined by the density of steam at the temperature and pressure of the experiment. Solubilities in superheated steam at high pressures are given also for silica glass and some inorganic salts.

Apparatus and Method

The method used was a dynamic one. Water under pressure was passed over the heated quartz or other substance, which was contained in a high-pressure vessel or bomb. During its passage over the quartz, the water was superheated steam at high pres-

[1] Geophysical Laboratory, Carnegie Institution of Washington.

[2] Numbers in parentheses refer to the Bibliography at the end of the paper.

Contributed by the Joint Research Committee on Boiler Feedwater Studies and the Power Division and presented at the Annual Meeting, New York, N. Y., November 26–December 1, 1950, of The American Society of Mechanical Engineers.

Note: Statements and opinions advanced in papers are to be understood as individual expressions of their authors and not those of the Society. Manuscript received at ASME Headquarters, September 22, 1950. Paper No. 50—A-73.

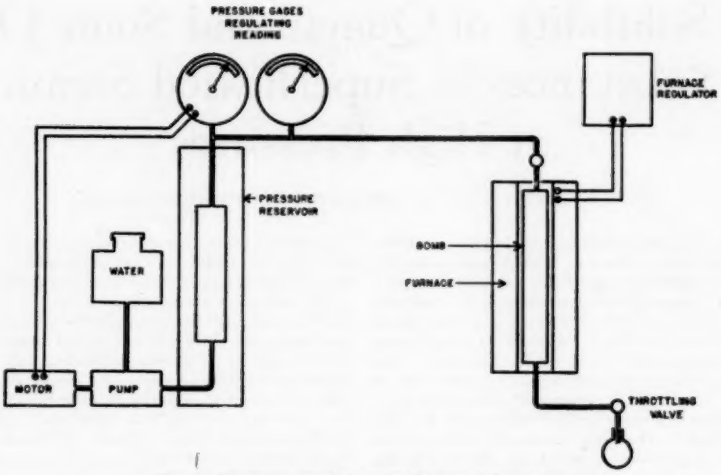

FIG. 1 DIAGRAMMATIC OUTLINE OF PRESSURE APPARATUS

(Distilled water is pumped into pressure line which includes a reservoir, a reading gage, and a regulating gage to maintain the pressure constant. Quartz is contained in bomb and heated in regulated electric furnace. Water is changed to steam, passes over quartz, out of bomb, constant pressure being maintained on cooled water until throttle valve is reached. Condensed water is collected, weighed, and analysed.)

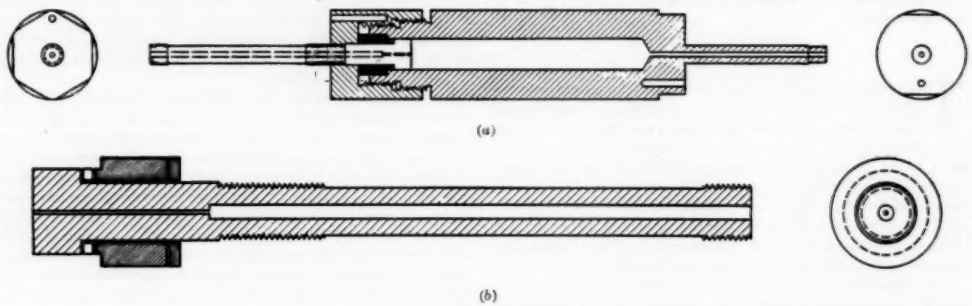

FIG. 2 THE PRESSURE VESSEL

(The pressure vessel consists of a bomb, a cap, and a plunger. Bomb is 2.5 in. OD with a chamber, 0.875 in. bore and 9 in. deep. Cap screws on and holds plunger in place. Closure is made by plunger; initial compression of plunger is by a nut, not shown, but on threaded part of stem. Holes for thermocouples are shown in cap and in bottom of bomb; two additional holes, symmetrically placed, but not shown, are for controlling thermocouple.)

sure and after cooling to liquid water it remained at the high pressure up to a throttling valve. Here the pressure was slowly released, at a rate of from 10 to 40 drops per min, and the condensed water was collected, weighed, and the amount of silica determined by analysis.

The apparatus is shown diagrammatically in Fig. 1. Distilled water is forced by the pump into a pressure line in which there is a cylindrical reservoir, volume 2240 cc, and two pressure gages, a reading gage and a regulating gage. The reading gage was calibrated against a dead-weight gage. The regulating gage has had the glass removed from the screwed-on rim. A square bracket is fastened onto the rim of the regulating gage, and on the part of the bracket parallel to the face of the gage the lamp and phototube holder of a GE CR7505 photoelectric relay is mounted. A small mirror is mounted on the rim behind the plane of travel of the needle of the gage, and a small flag is fastened to the end of the needle. When the light is reflected from the mirror into the photocell, the relay starts the pump, which runs until the light is interrupted by the flag and stops the pump. When pressure falls, the photocell is activated and the pump starts. This controls the pressure to ± 50 psi. The regulating position can be changed by rotating the rim of the gage.

The pressure vessel or bomb is shown in Fig. 2(*a*). It is made of Inconel X, which has given better results than stainless steel in other high-pressure work. The closure is effected by the internal pressure itself, bearing on a silver washer [details are in the enlarged Fig. 2(*b*)]. The head of the plunger fits inside the chamber of the bomb. A collar, or washer, fits over the stem of the plunger and projects $^1/_8$ in. inside the chamber and is held in place by the screwed-on cap of chrome-molybdenum steel. A silver washer, $^1/_8$ in. thick, is imprisoned between the head of the plunger and the bottom of the collar. Initially, this washer is compressed by tightening a nut on the threaded part of the stem, which is above the cap. When pressure is applied within the bomb, it bears on

the end of the plunger and further compresses the silver washer. The area of the head of the plunger is 0.60 sq in., of the silver washer, 0.3 sq in., so, if P is the internal pressure, the pressure on the washer is $2P$. This closure has held perfectly for a long time even though it has been subjected to wide changes in pressure and temperature, and to pressures much greater than any reported in this paper.

The bomb is contained in a furnace electrically heated and controlled by a Brown electronic controller. The main heater is of nichrome wire wound on an alundum tube and current adjustment is by a Variac. An auxiliary pad heater, controlled by another Variac, on the bottom of the heater, not shown in the figure, serves to make up for heat loss at the exit end. In all of the earlier runs the controlling thermocouple was placed adjacent to the main furnace winding, and attempts were made to maintain uniform temperature along the bomb by adjusting the two Variacs, both of which were on the controller. This was difficult because different rates of flow required different power inputs, and a difference in the input distribution. Runs made with this arrangement are indicated in Table 1 as "older runs" when there is a significant difference. Later an auxiliary furnace, not shown in the figure, was placed on top of the main furnace. It was controlled by another Brown electronic controller, activated by a thermocouple placed in a thermocouple well in the cap, similarly placed to that shown in the figure. Temperature was measured by a Pt-Pt-10 Rh thermocouple inserted in another well in the cap; the emf was read on a White potentiometer. The main furnace and the auxiliary pad heater were held at constant temperature by a thermocouple inserted in a well in the bottom of the bomb, and temperature was measured by a thermocouple in another well, not shown in the figure. Thus both top and bottom of the bomb were controlled independently, the bottom to better than ±1 deg, the top to ±2 deg.

The bomb is fastened to the high-pressure line by a standard coupling, and the water under pressure is admitted by a valve. It passes into the hot bomb as steam, over the quartz, out the bottom of the bomb, and through a cooling tube to the throttling valve. Here the rate of flow is adjusted to the desired rate, usually between 10 and 25 drops per min, and the water collected in a weighed flask. At the end of the run the condensed water is weighed, evaporated to dryness in a large platinum vessel, and the silica transferred to a platinum crucible, ignited, and weighed. The silica is then volatilized by evaporation with HF and H_2SO_4, the crucible again weighed, and SiO_2 determined by the difference.

The results at 500 psi were obtained by a colorimetric method by the Hall Laboratories, Inc. The samples were mailed in polyethylene containers. Portions of each of the three runs at 932 F (500 C) were retained by us, combined, and SiO_2 determined gravimetrically as usual. We obtained 4.3 parts per million, as compared with the mean of 3.8 of the colorimetric determinations.

Another comparison between the gravimetric method and the colorimetric method was obtained with the co-operation of the Philadelphia Quartz Company, to whom five samples were sent. The agreement between the two methods was excellent. The first figures in the following were obtained by them, the second by us: 18 and 16; 38 and 38; 85 and 95; 1358 and 1352; 2480 and 2572.

The success of the method depends primarily on the silica dissolved in the condensed steam remaining in solution until it has passed through the throttle. This it does. The exit tube, $^1/_{16}$ in. bore, has never stopped up, although more than 250 grams of SiO_2 have passed through. The greatest difficulty is in adjusting the rate of flow, and at high pressure it requires frequent attention. None of the commercial needle valves was satisfactory, and the modifications tried were not wholly successful. It is comparatively easy to throttle at pressures of 5000 psi or less, but at 15,000 psi there appeared a deformation which slowed or almost stopped the flow. The actual orifice must be very small, but no evidence of stoppage of the valve by deposits could be found.

Tabulated Results

The results summarized in the tables show a satisfactory agreement, considering the difficulty of the problem. It was at first planned to make a series of runs at each temperature and pressure with varying rates of flow, but this was soon found to be unnecessary. That too fast flows give low results is shown by a few results given in the tables, and in numerous unpublished results. But when the rate is of the order of 2 grams H_2O per min a steady state appears to be reached in which the unavoidable, unexplained differences between results show no correlation with rates of flow.

The volume of the bomb is 4.81 cu in. (78.8 cc) and it holds about 75 grams of crushed quartz. This leaves a free volume of about 3 cu in. (50 cc); hence, at a rate of flow of 1 gram per min the water is in contact with quartz for about 50 min. The quartz is crushed to pass a screen of 4, and retained on one of 8 meshes per in. If it is assumed that the average piece is a cube of 2 mm side, the total area will be 1127 sq cm (68.8 sq in.).

Table 1 gives the detailed results for each temperature and pressure. For each run is given the weight of condensed water, the duration of the run, the rate of flow in grams of H_2O per minute, the total weight of SiO_2, and the grams SiO_2 per million grams of H_2O. For each set is given the mean and the mean deviations from the mean. All the results at 500, 1000, and 2000 psi are with the apparatus with temperatures controlled at both top and bottom; at other pressures the two sets of measurements are indicated when there is a difference between them.

Table 2 gives a summary of the results with quartz, expressed in two different ways. Column 2 gives solubility in grams SiO_2 per million grams H_2O; column 4 gives solubility in grams SiO_2 per million ml of H_2O. The values for density of water given in column 3 are by Kennedy (9).

The results at 572 F (300 C) represent solubility in liquid water. They show a wide variation at each pressure, and there is no significant difference at 3000, 10,000 and 15,000 psi. Consequently these are all averaged together. One series of four runs was made at 680 F (360 C) and 5000 psi.

The results in column 2 of Table 2, solubility in grams SiO_2 per million grams H_2O, are shown in Fig. 3. Instead of passing a smoothed curve through the mean value at each temperature and pressure, the observed values are joined by straight lines.[3] The circles represent the mean deviation from the mean at each point. The curves cross in two places. At two different pressures the solubility is the same at 752 F (400 C) as at 932 F (500 C); between these pressures the solubility is greater at 752 F (400 C) than at 932 F (500 C), and above and below these pressures it is greater at 932 F (500 C) than at 752 F (400 C). The surface representing the solubility at different pressures and temperatures evidently has a double curvature, and it does not necessarily follow that the solubility would be the same at an intermediate temperature.

These peculiar relationships are caused in large part by the peculiar pressure-volume relationship of steam at high pressure and temperature, and, in particular, by the proximity of 752 F (400 C) to the critical point of water, 705.4 F (374.1 C) and 3061 psi. It was thought that recalculating the results to grams SiO_2 dissolved per million milliliters of water would remove this crossing. The results so recalculated are in column 4, Table 2. The curves again cross, but at pressures different from before. Fig. 4 shows the solubility expressed in grams SiO_2 per million grams

[3] This method of representation is a personal preference of the authors and contains no implication as to the intervening parts of the solubility curve.

TABLE 1 SOLUBILITY OF QUARTZ IN SUPERHEATED STEAM

Weight condensate, grams	Duration, min	Rate, grams per min	Total SiO_2 grams	Grams SiO_2 per million grams H_2O
		752 F (400 C)		
		500 psi (colorimetric)		
772	855	0.90	...	1.00
497	570	0.87	...	1.08
1125	870	1.29	...	1.04
1125	870	1.29	...	1.04
			Mean.....	1.04
		1000 psi		
771	1080	0.71	0.0024	3.1
980	540	1.81	0.0036	3.7
3879	2330	1.67	0.0118	3.1
2017	1870	1.08	0.0069	3.5
858	1120	0.77	0.0024	2.8
			Mean.....	3.1
			Mean deviation..	0.2
		2000 psi		
708	375	1.94	0.0038	5.4
1116	900	1.24	0.0060	5.4
906	495	1.83	0.0046	5.1
1246	945	1.32	0.0060	4.8
			Mean.....	5.2
			Mean deviation..	0.2
		5000 psi		
274	475	0.58	0.1786	651
356	769	0.46	0.2378	668
295	940	0.31	0.1959	664
310	500	0.62	0.1768	571
754	1080	0.70	0.5107	678
701	1026	0.69	0.4843	691
742	315	2.36	0.4592	612
347	480	0.72	0.2319	668
353	300	1.18	0.2387	677
968	900	1.08	0.5717	591
764	540	1.41	0.4505	590
410	900	0.46	0.2414	859
			Mean.....	637
			Mean deviation..	38
		10,000 psi		
383	476	0.80	0.5310	1386
484	555	0.88	0.6068	1249
331	495	0.67	0.4532	1370
960	322	2.98	0.5865	1027
294	407	0.72	0.3375	1285
213	405	0.67	0.3376	1383
455	540	0.84	0.5909	1299
146	...	...	0.1869	1280
452	520	0.87	0.6325	1392
771	455	1.69	0.9123	1183
435	870	0.50	0.5393	1240
628	265	2.37	0.6892	1098
306	326	0.94	0.3993	1305
1910	884	2.16	2.1380	1119
			Mean.....	1259
			Mean deviation..	91
		15,000 psi		
934	560	1.67	1.1399	1220*
349	865	0.40	0.5394	1547
267	840	0.33	0.4995	1680*
391	750	0.52	0.5960	1525
28	501	0.06	0.0490	1750*
540	500	1.19	0.9345	1574
704	471	1.49	0.5865	1245*
302	567	0.53	0.4659	1545
331	474	0.70	0.4630	1400
274	525	0.52	0.4127	1508
119	445	0.27	0.1783	1495
453	765	0.59	0.6602	1457
753	570	1.32	1.1452	1521
151	120	1.26	0.2175	1440
			Mean.....	1501
			Mean deviation..	42
		932 F (500 C)		
		500 psi (colorimetric)		
995	930	1.07	...	3.04
931	930	1.0	...	4.64
600	510	1.10	...	3.64
			Mean.....	3.77
			Gravimetric.....	4.3
		1000 psi		
1434	1740	0.82	0.0238	16.6
504	1868	1.48	0.0244	13.1
1027	1035	0.99	0.0149	14.5
1937	1361	1.42	0.0315	16.3
2834	1360	1.42	0.0354	12.5
2020	1440	1.40	0.0250	12.4
			Mean.....	14.2
			Mean deviation..	1.5
		2000 psi		
1085	595	1.99	0.0342	31.5
981	560	1.75	0.0338	34.5
2800	1620	1.73	0.1088	38.9
729	420	1.73	0.0285	39.1
1184	880	1.41	0.0429	36.2
1109	880	1.26	0.0436	39.3
1677	1400	1.20	0.0603	36.0
1162	975	1.19	0.0365	31.4
564	480	1.18	0.0216	38.4
2072	1938	1.07	0.0733	35.4
1953	2480	0.79	0.0614	31.4
713	900	0.69	0.0262	36.8
			Mean.....	35.7
			Mean deviation..	2.4
		5000 psi		
697	160	4.36	0.1821	261*
646	210	3.08	0.1379	214
398	...	...	0.0873	219
374	315	0.87	0.0579	211
554	453	1.20	0.1191	215
314	390	0.81	0.0692	220
426	420	1.02	0.0974	229
217	...	...	0.0474	218
195	...	...	0.0433	222
1030	510	2.02	0.2164	210
1364	840	1.62	0.2830	208
1170	1390	0.89	0.2411	206
1015	900	1.13	0.2206	217
			Mean.....	216
			Mean deviation..	6
		10,000 psi, older results		
284	430	0.66	0.3239	1384
401	415	0.98	0.5715	1426
342	...	...	0.5076	1485
249	240	1.04	0.3486	1402
562	490	1.15	0.7601	1354
112	455	0.25	0.1654	1480
352	460	0.77	0.5194	1476
			Mean.....	1430
			Mean deviation..	44
		10,000 psi newer results		
1791	455	3.93	2.3793	1329
784	540	1.45	1.0669	1361
599	990	0.61	0.8123	1356
539	600	0.90	0.7415	1376
756	450	1.68	1.0085	1345
1079	910	1.19	1.4317	1327
921	540	1.71	1.2488	1356
1175	960	1.22	1.5656	1335
			Mean.....	1348
			Mean deviation..	14
		15,000 psi, older results		
1238	232	5.57	2.3697	1839*
662	130	5.09	1.2370	1870*
499	471	1.06	1.1514	2307
444	460	0.97	1.0662	2399
320	475	0.67	0.7380	2309
320	516	0.63	0.7678	2309
473	840	0.56	1.1482	2430
205	458	0.45	0.4547	2222
199	495	0.40	0.4627	2327
165	445	0.37	0.3986	2412
104	330	0.32	0.2414	2317
240	2000	0.12	0.5748	2341
			Mean.....	2347
			Mean deviation..	50
		15,000 psi, newer results		
482	326	1.48	1.2384	2573
738	950	0.78	1.9373	2625
763	496	1.54	1.9680	2581
767	900	0.85	2.0054	2615
490	600	0.82	1.2068	2585
			Mean.....	2596
			Mean deviation..	19

* Omitted from mean.

TABLE 2 SUMMARY OF SOLUBILITY RUNS WITH QUARTZ

Pressure, psi	Solubility, grams SiO_2 per million grams H_2O	Density of water	Solubility, grams SiO_2 per million ml of H_2O	Partial pressure SiO_2 atm
		572 F (300 C)		
5, 10, and 15,000	616	0.736	478	
		680 F (360 C)		
5,000	852	0.633	570	
		752 F (400 C)		
1,000	3.1	0.0221	0.069	0.21×10^{-3}
2,000	5.2	0.0572	0.30	0.71×10^{-3}
5,000	637.0	0.4676	298.0	0.217
10,000	1259.0	0.6332	797.0	0.856
15,000	1801.0	0.6971	1079.0	1.580
		932 F (500 C)		
1,000	14.2	0.0202	0.29	0.96×10^{-3}
2,000	35.7	0.0440	1.57	3.3×10^{-3}
5,000	216.0	0.1405	30.35	0.073
10,000	1348.0	0.3993	583.3	0.92
15,000	2596.0	0.5415	1406.0	2.65

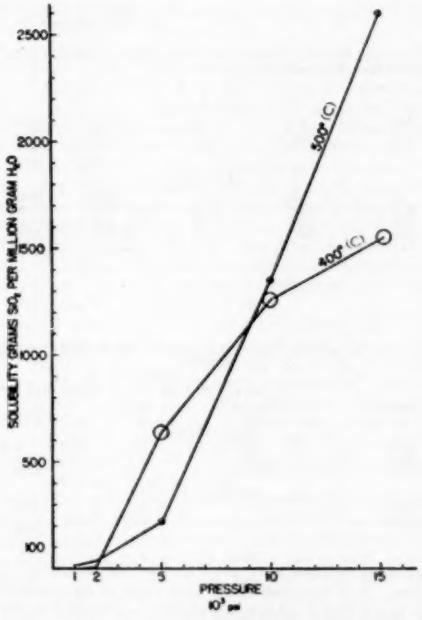

FIG. 3 SOLUBILITY RESULTS WITH QUARTZ, EXPRESSED AS GRAMS SiO_2 PER MILLION GRAMS WATER
(Experimentally determined points are joined by straight lines.)

H_2O, plotted against the density of water at the temperature and pressure of the experiment. When so expressed, the curves no longer cross, and the solubility is higher at 932 F (500 C) than at 752 F (400 C). Fig. 5 shows the results at 500, 1000, and 2000 psi; at 932 F they lie on a straight line, and almost on a straight line at 752 F.

Table 3 gives the detailed results with silica glass. The first glass used was cloudy or translucent silica tubing. This differed in its behavior from any of the other materials. It shattered in

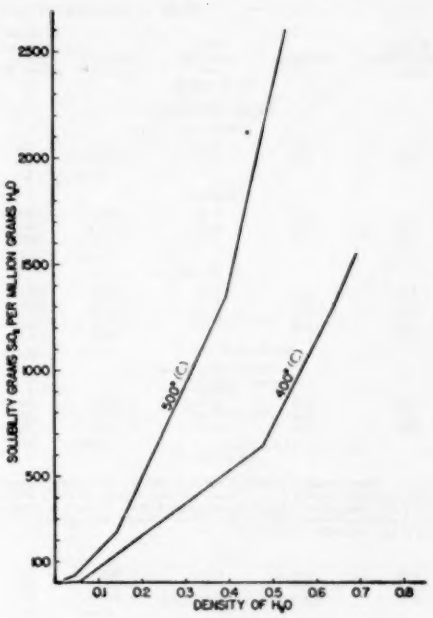

FIG. 4 SOLUBILITY RESULTS WITH QUARTZ, EXPRESSED AS GRAMS SiO_2 PER MILLION GRAMS H_2O, PLOTTED AGAINST DENSITY OF WATER AT SAME PRESSURE AND TEMPERATURE
(Experimentally determined points are joined by straight lines.)

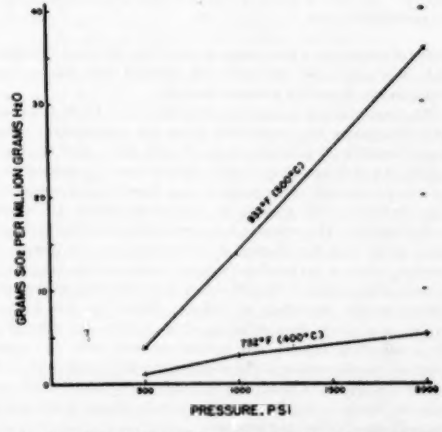

FIG. 5 SOLUBILITY RESULTS WITH QUARTZ, EXPRESSED AS GRAMS SiO_2 PER MILLION GRAMS WATER AT 500, 1000, AND 2000 PSI
(Experimentally determined points are joined by straight lines.)

the bomb and coated the interior of the bomb with a dense adherent coating of silica glass containing much quartz. This coating extended over the bottom of the bomb and finally sealed over the exit. No runs were made with this at 932 F (500 C). Frag-

TABLE 3 SOLUBILITY OF SiO_2 GLASS IN SUPERHEATED STEAM

Weight condensate, grams	Duration, min	Rate, grams per min	Total SiO_2 grams	Grams SiO_2 per million grams H_2O
		752 F (400 C)		
		Opaque Silica Glass		
		2000 psi		
456	600	0.76	0.0132	29
393	545	0.72	0.0169	43
			Mean..	36
		5000 psi		
204	385	0.53	0.2850	1397
502	870	0.58	0.7373	1463
554	500	1.11	0.7115	2283
			Mean..	1381
		10,000 psi		
434	411	1.06	1.0292	2371
755	960	0.79	1.9139	2535
671	435	1.54	1.4578	2173
639	390	1.64	1.7268	2702
1134	...	...	2.6783	2362
			Mean..	2429
		Clear Silica Glass		
		2000 psi		
729	920	0.79	0.0205	28
381	500	0.76	0.0106	28
287	960	0.30	0.0110	38
			Mean..	31
		932 F (500 C)		

NOTE: After preceding runs at 400 F and 2000 psi, this sample of glass was left under pressure at 500 F for a week. At end of series at 2000, 5000, and 10,000 psi, it was found to be completely crystalline. In view of agreement between results obtained with it and those obtained with quartz, it is believed it had crystallized during that time.

		2000 psi		
302	480	0.63	0.0087	29
1094	990	1.11	0.0361	33
902	1360	0.66	0.0234	38
			Mean..	31
		5000 psi		
247	1420	0.17	0.0582	235
166	490	0.34	0.0300	217
473	1680	0.28	0.1015	215
1101	985	1.12	0.2487	226
			Mean..	223
		10,000 psi		
403	480	0.84	0.6018	1492
503	637	0.79	0.7437	1460
822	915	0.90	1.1661	1418
296	555	0.53	0.4243	1431
657	1042	0.63	0.9382	1428
895	1350	0.66	1.2649	1414
496	1320	0.38	0.7064	1425
			Mean..	1438

NOTE: The following series of runs were made with fresh silica glass. At end of series there was a small amount of crystallization to quartz.

		5000 psi		
191	180	1.06	0.0645	338
296	960	0.31	0.1071	362
514	480	1.07	0.1837	357
354	840	0.42	0.1196	338
723	532	1.36	0.2547	352
378	900	0.42	0.1279	338
503	600	0.84	0.1707	339
288	855	0.34	0.0980	340
684	131	5.22	0.1619	237[a]
1228	1320	0.93	0.4273	348
			Mean.....	346
			Mean deviation..	8

NOTE: The following series of runs were made with fresh silica glass. At end of run there was some crystallization.

		10,000 psi		
227	540	0.42	0.5741	2529
511	915	0.56	1.2939	2534
491	473	1.04	1.2529	2553
			Mean..	2539
		15,000 psi		
98	180	0.54	0.4141	4275
533	960	0.56	2.0882	3918
172	1020	0.17	0.7450	4344
645	1005	0.64	2.3577	3656[a]
			Mean.....	4179

[a] Omitted from mean.

ments of clear silica glass, obtained from The Thermal Syndicate, Ltd., were used next, and with this material there was no shattering and no deposit of glass on the walls.

The runs with silica glass are summarized in Table 4, and the solubility values for quartz are given for comparison. Much larger "solubility" values were found with silica glass than with quartz, as was to be expected from the free-energy relationships of the two substances. It is realized that these cannot represent a true solubility. The glass is an amorphous phase, an "undercooled liquid." The criterion for a reversible solubility is usually taken to be that if a change in conditions, e.g., an increase in pressure, causes a material to dissolve; the opposite change, e.g., a decrease in pressure, should cause it to separate in the same thermodynamic condition as before. This does not happen; and when a phase does separate, it is quartz—not silica glass. These solubility values, and values obtained with any amorphous silica, represent rates of solution of silica under fairly well-defined conditions. Constant values may be obtained under constant conditions, but different values may be obtained with amorphous silicas of different histories.

In Table 2, column 5, are given partial pressures of SiO_2 in the steam. These were obtained by multiplying the total pressure in atmospheres by the weight fraction SiO_2, and are not intended to convey any implication as to the molecular condition of SiO_2 in the steam, which will remain a matter of speculation until some method of molecular-weight determination under these somewhat extreme conditions is devised. Nothing is known even about the

TABLE 4 SUMMARY OF SOLUBILITY RUNS WITH SILICA GLASS

Pressure, psi	Solubility, grams SiO_2 per million grams H_2O: Opaque glass	Clear glass	Quartz
	752 F (400 C)		
2000	36	31	5.2
5000	1381	..	637
10000	2429	..	1259
	932 F (500 C)		
5000	..	346	216
10000	..	2539	1348
15000	..	4179	2596

extent of association of water vapor itself at high temperature and pressure. It is improbable that silica exists as SiO_2 molecules. In all probability it exists in tetrahedral co-ordination as orthosilicic acid, or a hydrated orthosilicic acid, but speculations are incapable at present of experimental test. There is no experimental evidence of the existence of any silicic acid as such. Certainly the precipitates obtained by acidifying alkaline silicate solutions are not silicic acids but gels containing amorphous silica. Consequently, the calculation of partial pressures on a weight per cent basis, as given in Table 2, is the only possible method, and contains no implication concerning molecular association of either the water or the silica. The vapor pressure of quartz is primarily determined by the temperature, and the effect of pressure is a secondary effect which can be calculated from well-known thermodynamic considerations, and the same would be true of any "silicic acid." The amount of silica in the steam is

so enormously greater than would be expected from the vapor pressure of quartz that a true solubility in steam is the only possible explanation.

Discussion

The results obtained with quartz show satisfactory agreement, and it is believed that they represent the real, reversible, solubility values. To prove that they do, it would be necessary to show that a solution saturated at a given temperature and pressure would take up more quartz if these parameters were changed in appropriate directions, and, if the parameters were changed in the opposite directions, crystalline quartz would be deposited. Apart from experimental difficulties, this could not be done because of the tendency of silica solutions, gaseous or liquid, to become, and remain, supersaturated. It is true, as shown by Morey and Ingerson (10), and later by many who have tried to commercialize the process, that quartz crystals can be caused to grow by transport in a gas from amorphous silica, but this is too slow a process to use for testing reversibility. The results obtained with silica glass make it probable that the final values represent a real solubility. The results obtained with fresh glass are higher than with quartz, but as the glass crystallizes the values drop to essentially the same as with quartz.

There are few results which are directly comparable to those of this paper. Those of Gruner (11), Hitchen (12), Lenher and Merrill (13), and Kennedy (14), shown in Fig. 6, deal with solubility in liquid water. Gruner found with quartz 958 ppm at 572 F (300 C), as compared to our 616 parts. Kennedy found 1100 parts at 572 F (300 C) and 2000 parts at 680 F (360 C), as compared to our 616 and 852 parts, but he used silica glass.

Van Nieuwenburg and Miss P. M. Van Zon (15) made "Semi-quantitative Measurements of the Solubility of Quartz in Supercritical Steam," at a series of pressures, and at 716 F (380 C), 752 F (400 C), and 797 F (425 C). Their pressure range was from 4166 to 7110 psi, and the order of magnitude of their results is the same as ours. Linear interpolation to 5000 psi at 752 F (400 C) gives 889 ppm, as compared to our 637.

Kennedy measured the solubility of silica glass at 784 F (418 C) and, presumably, 4500 psi. No data are given; the results are given only in a curve which combines his results and those of Gruner. At 752 F (400 C) the curve gives a value of 1200 ppm, as compared to our value of 1381 at 5000 psi. (Kennedy presented a paper at the Section of Volcanology, American Geophysical Union, April 21, 1948, entitled "Effect of Pressure on the Solubility of Quartz in Water at Supercritical Temperatures." This has not been published.)

Straub (16) passed superheated steam over "pure silicic acid" which was prepared by adding hydrochloric acid to a solution of $Na_2O.SiO_2.5H_2O$ in distilled water. The precipitated silicic acid was filtered and washed with distilled water until free from chloride. "With this apparatus, the superheated steam leaving the tube should contain an amount of silicic acid corresponding to the vapor pressure at the temperature and pressure used..... "The silica content of the steam was the same for rates of flow from 2 to 10 lb per hr, indicating that the silica present in the steam represented the equilibrium condition between the silica in the steam and the vapor pressure of the silicic acid." He found that the logarithm of the concentration of silica in the superheated steam plotted against the reciprocal of the absolute temperature resulted "in a series of straight lines for the various pressures. This relationship indicates that the silica present is the result of vapor pressure of silicic acid." Since his experimental data consists of weights of SiO_2 in parts per million, they are directly comparable to ours. The equation of the best straight line representing the logarithm of the silica content of the steam as a function of the reciprocal of the absolute temperature was calculated from the data of his Table 10 for 420 psi, and extrapolated from his highest temperature, 650 F (343 C) to 752 F (400 C). This extrapolation gave 3.1 ppm. We obtained 1.0 ppm at 752 F and 500 psi with quartz, which is an excellent agreement.

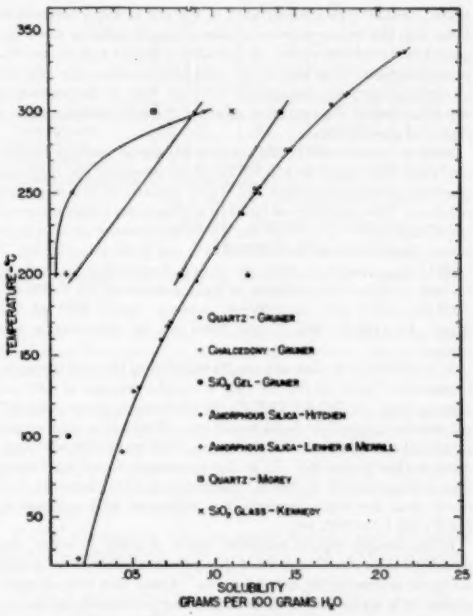

Fig. 6 Results of Several Investigations in Solubility of Quartz, Chalcedony, and Amorphous Silica in Liquid Water

Other work in this laboratory in which the solubilities in superheated steam at high pressure of several substances have been determined will be mentioned. The liquid-solubility curves at 752 F (400 C) of the various solid phases in the system H_2O–Na_2O–SiO_2, and the compositions of the gaseous phases in equilibrium with liquid and solid, have been determined at pressures up to 30,000 psi. At 15,000 psi, the gas in equilibrium with sodium-silicate solution and quartz contains 1.6 per cent of Na_2O and 3.4 per cent SiO_2; at the same temperature and pressure the gaseous solubility of quartz in binary system H_2O–SiO_2 is 0.155 per cent, as shown in Table 2. Mixtures that are more alkaline have not quartz but a sodium silicate as solid phase, but the gases may contain more SiO_2 as well as more Na_2O. An example is a gas found to be in equilibrium with crystalline sodium metasilicate at 30,000 psi, which contained 24.2 per cent Na_2O and 8.4 per cent SiO_2.

Other results in this system show the contrast between the silicates of sodium and potassium, a contrast of importance in boiler-water chemistry. Potassium metasilicate is extremely soluble in water from 500 to 1000 F, and at 752 F (400 C) it will be completely liquefied by a steam pressure of about 140 psi. The work now under way has shown that sodium metasilicate is extremely insoluble in water at high temperature, and at 752 F (400 C) a steam pressure of 30,000 psi is not sufficient to produce metasilicate liquid.

The solubilities of some other salts in supercritical steam at high pressure have been measured. They may be grouped into two

types. In one type the solubility of the salt in water becomes so large that the vapor pressure of this saturated solution never approaches the critical curve. If the solid is heated with steam at a pressure greater than that of the saturated solution, the salt will all melt to form an unsaturated solution; but, if the pressure is less than that of the saturated solution, the solid will remain in a region of gas and solid.

Sodium chloride and potassium chloride are of this type, and in studying their gaseous solubilities it is necessary to keep the pressure of steam less than the vapor pressure of the saturated solution. The solubility of NaCl in H_2O increases with temperatures, and Keevil (17) found the maximum pressure on the three-phase curve to be at 1112 F (600 C) and 5700 psi. At 932 F (500 C) the pressure is 4680 psi. Using the dynamic method described, we found the solubility of NaCl in steam at 932 F (500 C), 1000 psi to be 7 ppm; at 2000 psi, 14 ppm; and at 4000 psi, 304 ppm. At 1121 F (605 C) and 5000 psi, the solubility is 539 ppm.

It is difficult to explain the results of Spillner (18), who found no formation of liquid at 782.6 F (407 C) until a pressure of 3905 psi was reached. At 782.6 F (407 C) the three-phase pressure is 2567 psi, and the crystalline NaCl should have dissolved to form an unsaturated solution above that pressure. Still more difficult to explain are his results with KCl. He apparently found no formation of liquid at 780 F (406 C) and 4544 psi, while Benedict (19) found that the vapor pressure of a saturated KCl solution at 780 F (406 C) is 1922 psi.

In the second type of solubility curve of a salt in water, the solubility is so small that the vapor-pressure curve of saturated solutions intersects the critical curve. Above this critical intersection is a region in which no liquid can be formed, no matter what the pressure. Water-silica forms a system of this type; and so, indeed, do most minerals and many inorganic salts.

Most sulphates have a very small solubility in water at the critical point. Wuite (20) and Schroeder, Berk, Partridge, and Gabriel (21) found the solubility of sodium sulphate in water decreased to practically zero at the critical temperature of water. At 932 F (500 C) the system is in the region of gas and solid at 15,000 psi. By the dynamic method we found the solubility of Na_2SO_4 in steam at 932 F (500 C) to be 4300 ppm. At the same temperature and pressure, the solubility in steam of $CaSO_4$ is only 16 ppm, very much less than quartz.

BIBLIOGRAPHY

1 "On the Solubility of Solids in Gases," by J. B. Hannay and James Hogarth, Proceedings of the Royal Society, London, vol. 29, 1879, p. 324; vol. 30, 1879, pp. 178–188.

2 "Dissolution des liquides et des solides dans Les Gaz," by P. Villard, *Journal de Physique*, vol. 5, 1896, pp. 453–461.

3 "Solubility of Solids in Vapors," by J. M. Talmadge, *Journal of Physical Chemistry*, vol. 1, 1896–1897, pp. 547–554.

4 "Über die Erscheinungen, welche auftreten wenn die Faltenpunktakurve der Löstichkeitskurve begegnet," by A. Smits, *Zeitschrift für Physikalische Chemie*, vol. 51, 1905, p. 193; and numerous other papers.

5 "Die Gasmineralisatoren in Magma," by Paul Niggli, *Zeitschrift für Anorganische Chemie*, vol. 75, 1912, p. 161; and numerous other papers.

6 "On Critical End-Points and the System Ethane–Naphthalene," by Ada Prins, Proceedings of the Royal Academy of Science, Amsterdam, Holland, vol. 17, 1915, pp. 1095–1106.

7 "The Pneumatolytic and Hydrothermal Alteration and Synthesis of Silicates," by G. W. Morey and Earl Ingerson, *Economic Geology*, vol. 32, 1937, pp. 607–701.

8 "Solubility of Solids in Water Vapor," by G. W. Morey, Proceedings of the American Society for Testing Materials, vol. 42, 1942, pp. 980–988.

9 "Pressure—Volume—Temperature Relations in Water at Elevated Temperatures and Pressures," by George C. Kennedy, *American Journal of Science*, vol. 248, 1950, pp. 540–564.

10 "Annual Report of the Director of the Geophysical Laboratory," by L. H. Adams, reprinted from Year Book No. 40, Carnegie Institution of Washington, Washington, D. C., 1941, pp. 35–56.

11 "Hydrothermal Oxidation and Leaching Experiments, Their Bearing on the Origin of Lake Superior Hematite-Limonite Ores," by J. W. Gruner, *Economic Geology*, vol. 25, 1930, pp. 697–719, 837–867.

12 "A Method for the Experimental Investigation of Hydrothermal Solutions, With Notes on Its Application to the Solubility of Silica," by C. S. Hitchen, Institute of Mining and Metallurgy, London, England, Bulletin 364, 1934.

13 "The Solubility of Silica," by V. Lenher and H. B. Merrill, *Journal of the American Chemical Society*, vol. 39, 1917, pp. 2630–2638.

14 "The Hydrothermal Solubility of Silica," by G. C. Kennedy, *Economic Geology*, vol. 39, 1944, pp. 25–36.

15 "Semi-Quantitative Measurements of the Solubility of Quartz in Super-Critical Steam," by C. J. Van Nieuwenburg and Miss P. M. Van Zon, *Recueil des Travaux Chimiques des Pays-Bas*, vol. 53, 1934, pp. 129–132.

16 "Steam Turbine Blade Deposits," by F. G. Straub, University of Illinois, Engineering Experimental Station, Bulletin Series 364, 1946.

17 "Vapor Pressures of Aqueous Solutions at High Temperatures," by N. B. Keevil, *Journal of the American Chemical Society*, vol. 64, 1942, p. 841.

18 "Hochgespannter Wasserdampf als Lösungsmittel," by F. Spillner, *Die Chemische Fabrik*, vol. 13, 1940, pp. 405–416.

19 "Properties of Saturated Aqueous Solutions of Potassium Chloride at Temperatures Above 250 C," by Manson Bendict, *Journal of Geology*, vol. 47, 1939, pp. 252–276.

20 "Das System Natriumsulfat-Wasser," by J. P. Wuite, *Zeitschrift für Physikalishe Chemie*, vol. 86, 1919, pp. 349–382.

21 "Solubility Equilibria of Sodium Sulfate at Temperatures of 150 to 350° C," by W. C. Schroeder, A. A. Berk, Everett P. Partridge, and Alton Gabriel, *Journal of the American Chemical Society*, vol. 57, 1935, pp. 1539–1546.

Discussion

A. A. Berk.[4] The practical importance to the power industry of the transport of silica by steam led to some exploratory testing at the Bureau of Mines some years ago.

Our rough tests were made by suspending either a quartz crystal or a fused-silica tube over water held at 635 F (335 C) in a steel bomb. The bomb capacity was 275 ml. When the total water charged was 50 ml, less than 40 per cent of it vaporized at the operating temperature to form saturated steam at 2000 psi. When the charge of total water was less than 20 ml, all of it vaporized to form dry steam, superheated to 635 F. The pressure of the superheated steam was fixed by the quantity of water in the bomb.

Quartz crystals were pitted or etched by the steam in 10-day tests. Each crystal had a total surface area of approximately 2 sq in., and the maximum weight loss was about 33 mg. As shown in Table 5, herewith, the loss in weight was greatest in the

TABLE 5 QUARTZ IN STEAM AT 635 F

Steam pressure, psi	Average weight loss, mg in 10 days
2000 (sat)	29
1800	22
1200	7

steam saturated at 2000 psi, and became smaller as the pressure decreased. This is in agreement with the authors' finding that, at a given temperature, the solubility of quartz increases with increasing density of the steam.

The tests with fused-silica tubing are also in agreement in so far that the tubes exposed to the saturated steam lost considerably more weight as compared to quartz crystals of the same surface area. Also, saturated steam converted fused silica completely to crystalline quartz during the 10-day tests, and tiny quartz crystals were found on the platinum-wire suspension. However, in superheated steam, the tubes not only did not lose

[4] Supervising Chemist, Boiler Water Research Section, Bureau of Mines, College Park, Md.

weight, but they actually gained a few milligrams each, apparently by hydration (Table 6); there was no conversion to quartz but instead a very thin opaque skin containing crystobalite, a less dense form of crystalline silica, was formed on the exposed surfaces.

TABLE 6 FUSED SILICA IN STEAM AT 635 F

Steam pressure, psi	Average weight loss, mg in 10 days
2000 (sat)	39
1800	gained
1200	gained

In the absence of steam, that is, in air alone, there was no change at 635 F in either the quartz or the fused silica. Steam at this temperature removed silica from quartz crystals. Saturated steam at this temperature converted fused silica to quartz. Superheated steam at this temperature had little effect on the samples of fused silica that were used in the survey.

C. E. IMHOFF.[5] The prevention of deposits in any system can be accomplished by maintaining the concentration of the potential scale former at a value below its normal solubility under the conditions of temperature and pressure which exist in the system. By using data such as that collected by the authors one should be able to set a maximum value for silica in steam below which no deposits could be formed. Unfortunately, the temperatures and pressures of their tests are considerably higher than that present in the usual scaling areas in a steam turbine.

A study of the characteristics of turbine-blade deposits, reported by the writer's company in 1947, indicated that blade deposits might be expected in those stages where the temperature fell below 700 F, but in practically no instance were deposits found in stages whose temperatures were greater than 700 F. This study included deposits from turbines operating at 1300 psi and below. Pressures in the stages operating at 800 F were normally less than 575 psi. This is sufficiently below 1000 psi that it is doubtful if an extrapolation of the authors' data in this range could be warranted.

A somewhat surprising result is the great difference in solubility between quartz and silica glass. The small difference in solubility between two crystal forms such as Calcite (β $CaCO_3$) and Aragonite ($\gamma CaCO_3$) are quite familiar, but the sevenfold difference between quartz and glass, as shown in Table 4 at 2000 psi, is entirely unexpected and suggests that the form of the solid phase greatly affects the quantity which may go into solution. This also brings up the question regarding what solid phase would be expected when silica is precipitated from superheated steam. The authors determined the silica gravimetrically, but those making silica determinations on powerhouse steam must use colorimetric methods because of the very small quantities present. It would be of extreme interest to know if colorimetric procedures would check the gravimetric results and if the original source of the silica in any way influenced its colorimetric reactions.

If quartz has a lower solubility than amorphous silica, then quartz would be first of these to deposit when passing through a turbine. Fig. 7 of this discussion shows the relationship between the five forms of silica commonly found in turbine deposits and the temperature zones for each species. Of the three forms of pure silica, quartz is the first to precipitate as the steam loses temperature and pressure. Usually, not more than three of the five forms are found in accordance with the order listed in Fig. 7.

The presence of two sodium silicates in the list of blade-deposit materials should certainly draw sufficient attention to their importance to promote a study of their solubilities in steam-turbine temperature-pressure ranges.

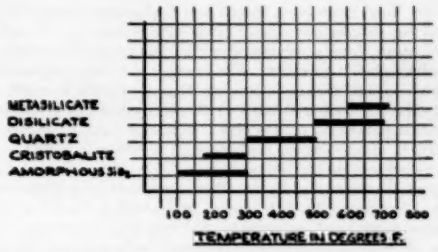

FIG. 7 TEMPERATURE ZONES OF OCCURRENCE OF SILICEOUS TURBINE-BLADE DEPOSITS

E. P. PARTRIDGE.[6] The value of investigations such as the present one does not lie in the immediate reading of data from tables or curves to modify the control limits of an operating boiler. What is truly important is the continuing challenge to think beyond what we now accept as truth. The authors' data present several challenges:

1 The solubility of silica in water increases over the entire range of boiler operation up to the critical point and is surprisingly high.

2 Amorphous silica is much more soluble than crystalline quartz, in steam as well as in water.

3 Steam will dissolve not only silica as such, but also sodium silicate.

4 The ratio of Na_2O to SiO_2 dissolved in the steam may differ from the ratio in the solid sodium silicate over which the steam passes.

5 Many, if not all, substances may be soluble to a measurable extent in steam.

At this point it is worth looking backward briefly.

Transport of silica dissolved in highly compressed water vapor at high temperatures was considered probable by the geophysicists even before it was demonstrated experimentally more than two decades ago by van Nieuwenburg and Blumendal.[7] Nine years ago, information accumulated up to that time from both the laboratory and the power plant was brought out in a round-table discussion sponsored by ASTM Committee D-19 on Industrial Water.[8] In his paper summarizing experimental observations on silicate-water systems, which preceded the general discussion on that occasion, Dr. Morey said, "In all this work there is constantly being obtained evidence of transport of ordinarily nonvolatile materials by high-pressure steam.....The conditions of these experiments are more drastic than those encountered in steam boilers and superheaters, but nevertheless, the very considerable power of steam under these more drastic conditions to transport ordinarily nonvolatile components will be paralleled by a smaller transport power per unit of steam at the lower pressures."

[5] Research Supervisor, Chemical Laboratories, Allis-Chalmers Manufacturing Company, Milwaukee, Wis.

[6] Director, Hall Laboratories, Inc., Pittsburgh, Pa. Mem. ASME.

[7] "Vaporization of Silica With Steam," by C. J. van Nieuwenburg and H. B. Blumendal, *Recueil des travaux chimiques des Pays-Bas*, vol. 49, 1930, pp. 857–860; vol. 50, 1931, p. 338.

[8] "Round-Table Discussion on the Solvent Action of Water Vapor at High Temperature and Pressure," Proceedings of the American Society for Testing Materials, vol. 42, 1942, pp. 977–1022.

Only three years later, Straub and Grabowski[9] reported that small but definite amounts of silica were transported by saturated steam from a solution of sodium silicate under conditions simulating boiler operation. For example, a solution containing enough sodium silicate to provide 20 ppm of SiO_2 at a pH of 10.1–10.5 and boiling at 600 F (1525 psig) would produce steam containing about 0.2 ppm of SiO_2. In related bomb experiments at 600 F, using solutions containing up to 465 ppm of SiO_2 and pH values adjusted in the range from 6.8 to 12.1, steam passing through the solution picked up silica in amounts up to 6.9 ppm of SiO_2. Increasing the SiO_2 content or decreasing the pH of the solution in the bomb increased the SiO_2 content of the steam.

In the same investigation, Straub and Grabowski also showed how much silica could be picked up by passing superheated steam at various pressures over silica in a bomb. Since they used "silicic acid" (amorphous silica) prepared by reacting acid with sodium silicate, their steam presumably dissolved more than would correspond to equilibrium with quartz, just as shown by the comparative data given by the authors in the present paper.

The conclusion of Straub and Grabowski that only silica, rather than sodium silicate, was transported by the steam in their experiments was questioned in discussion by Imhoff, who noted that the pH of most of the samples of steam lay above 7. Actually, there is every reason to believe that Na_2O as well as SiO_2 will enter the steam, but that the ratio of these components in the steam will differ from the ratio in the boiler water. The present paper shows values at pressures far above the boiler range which illustrate this point. Circumstantial evidence suggests that, under the conditions of temperature, pressure, and boiler-water composition in contemporary high-pressure power plants, the amount of Na_2O dissolved in the steam is relatively small compared to the SiO_2, but that it certainly is there.

In many cases, sodium disilicate and in a few cases, sodium metasilicate as well as disilicate have been identified as major constituents of deposits in turbines, occurring consistently in the stages preceding those in which quartz is found. Are we to assume that the same steam, of what would be considered admirable purity, transported the SiO_2 of the sodium silicate in dissolved form, but could only carry the corresponding Na_2O mechanically as a mist of boiler water? Instead, it seems much more likely that the steam from a high-pressure boiler carries dissolved in it minute quantities of many substances and drops out in the turbine those with respect to which it becomes sufficiently supersaturated as the pressure and temperature progressively decrease.

That the complex vapor coming to the turbine comprises more than 999,999 parts of H_2O and much less than 1 part of all the dissolved substances together need not make this case difficult to understand. At the inlet to the turbine, the steam contains less than it could hold of each dissolved substance. However, as it cools during expansion, there will come a moment at which it can no longer hold dissolved together all the Na_2O and SiO_2. If there is enough Na_2O in relation to the SiO_2, sodium metasilicate (Na_2SiO_3) will crystallize on the blades in that stage. If there is less Na_2O in relation to SiO_2, sodium disilicate ($Na_2Si_2O_5$) will be deposited. Only when much of the Na_2O has been used up will the remaining SiO_2 begin to crystallize as quartz. Finally, when the pressure and temperature have dropped still lower, and the amount of SiO_2 which the steam can hold dissolved has further decreased, the excess comes out as amorphous silica. In this same range, the steam can no longer retain all of its dissolved iron oxide.

This interpretation of what actually is found in the turbine agrees with the observation by Straub and Grabowski that steam will not dissolve sodium silicate to as great an extent as it does silica. They found only 0.02 ppm of SiO_2 in steam at 681 psig heated to 600 F in contact with solid sodium silicate, as contrasted to at least 1 ppm of SiO_2 which might be expected in equilibrium with quartz from inspection of the data reported by the authors.

The obvious way to reduce the amount of silica deposited in the turbine is to reduce the amount of silica picked up by the steam from the boiler water. Theoretically, this could be accomplished by maintaining a very high ratio of Na_2O (or of K_2O) as hydroxide with respect to SiO_2 in the boiler water. The smaller amount of total SiO_2 which could be dissolved in the steam would, in the extreme case, also be accompanied by enough dissolved Na_2O so that all of the reduced amount of silica deposited in the turbine would come down as water-soluble sodium silicates, removable by a simple washing operation. There are, however, many practical objections to maintaining a very high caustic content in the water of a high-pressure boiler.

A more satisfactory way of keeping the SiO_2 content of the steam at a minimum is the system of precision control[10] involving the maintenance of a low and carefully controlled concentration of phosphate in the boiler water, at the same time insuring that enough magnesium enters the boiler to combine with the silica as serpentine ($3MgO.2SiO_2.2H_2O$). This substance is so nearly insoluble that the residual silica in the water of a high-pressure boiler may be held as low as 2–3 ppm.[5, 10, 11]

Experience over a period of several years in a number of plants has shown that it is not necessary to eliminate phosphate, nor does it seem desirable in view of the tendency to accumulate calcium in the boiler water until calcium sulphate or calcium silicate begins to deposit as hard scale. The objective is to proportion the phosphate to the calcium and the silica to the magnesium so that the residual soluble silica is a minimum, magnesium phosphate is not formed as an adherent sludge, yet calcium is removed completely as calcium phosphate.

It will be surprising if further progress in the production of power does not raise to importance additional aspects of the action of steam as a solvent. In anticipation of that progress, we should be grateful to the authors for bringing down to what are to them the "low" pressures of 1000 to 2000 psi, the broad scientific viewpoint, as well as the specific data they have been accumulating for many years.

F. G. Straub.[12] When a paper is prepared for presentation before a society such as this the writer believes it should be written and presented in a manner so that it will be of some value to the audience. Primarily, the author should recognize the problem or question which he is trying to answer; then the data that are pertinent to the answer of that problem should be assembled in a manner which the audience or reader can understand.

The writer has attempted to read the paper the authors have prepared in order to see what value it can possibly be to the steam-power-plant industry, but can find practically nothing at

[9] "Silica Deposition in Steam Turbines," by F. G. Straub and H. A. Grabowski, Trans. ASME, vol. 67, 1945, pp. 309–316; also included in "Steam Turbine Blade Deposits," by F. G. Straub, University of Illinois Engineering Experiment Station, Bulletin no. 364, 1946, 92 pp.

[10] "Precision Control of Boiler-Water Conditions," by R. E., Hall, Proceedings of the Ninth Annual Water Conference, Engineers Society of Western Pennsylvania, 1948, pp. 81–95.

[11] "Prevention of Silica Deposits on High-Pressure Turbine Blades," Progress Report by Wisconsin Electric Power Company to Power Station Chemistry Subcommittee, Edison Electric Institute, May, 1945. Discussed in reference 10.

[12] Research Professor in Chemical Engineering, University of Illinois, Urbana, Ill. Mem. ASME.

this stage of their reported work which is of any help either from a research or operating viewpoint.

In their introduction they state: "As the water rises in the boiler tubes the rapid transfer of heat through the tubes results in violent and turbulent boiling. This boiling occurs primarily at the interface and at this interface the dissolved material becomes concentrated, and in some areas solid material separates." If, as they state, there is violent and turbulent boiling, how can the dissolved material become concentrated to the solid at what they call the interface? They go on and say, "It is not the distribution coefficient of silica between steam and dilute boiler water which is in question—but between a solution of unknown concentration, which at some places becomes saturated solution from which silica may be deposited." If we assume that such concentrations may exist, there is, as the authors state, a violent and turbulent boiling which must bring the steam in contact with boiler water and ultimately leave the boiler drum in contact with the boiler water. This will establish the distribution coefficient between the steam and boiler water and not between the steam and the solid. The authors certainly are not familiar with data collected from operating boilers. In these boilers a definite ratio of silica in the steam to soluble silica in the boiler water is established and even when there is known hideout of silica it does not increase this ratio.

The data presented by the authors from their laboratory tests cover very little of the range applicable to boiler operation. In Table 1 of the paper, data are given for superheated steam at 1000, 2000, 5000, 10,000, and 15,000 psi. Assuming the data at 1000, 2000, and possibly 5000 psi are of value—why is the paper burdened with data at 10,000 and 15,000 psi? In Table 1 the data are not presented in a form that the engineer can compare readily with existing data, that is, ppm.

Table 2 makes an attempt at using a terminology similar to parts per million and then confuses the reader further by referring to solubility of SiO_2 in one column and saying partial pressure of SiO_2 in another column. If it's solubility of SiO_2 in steam, then the SiO_2 does not have a partial pressure. Again, in this table, data for extreme pressures are given.

Table 3 gives the so-called solubility of SiO_2 glass in superheated steam with no further definition of glass than opaque or clear silica glass.

Table 4 sums up all the data and it too gives 10,000 and 15,000 psi which do not apply. The data as plotted contribute nothing new to the paper, and do not distinguish between degrees F and C.

They give no data regarding the solubility of other substances.

In their discussion they state, "Straub determined the solubility of precipitated silica in steam." We did not determine solubility. We definitely distinguished between solubility of salts in steam and vaporization of silica acid.

Closure by G. W. Morey

It is interesting that the values in steam found by different authors do not greatly differ. This is shown by Fig. 6 by the results given in the discussion by A. A. Berk, and by the results published by Kennedy[13] since the presentation of this paper which show excellent agreement with those in this paper.

The difference in the "solubility" results obtained with quartz and with silica glass would be expected to be larger than between calcite and araginite. The free energy difference between two crystalline forms would be expected to be relatively greater than between a crystal and a glass, which is thermodynamically an undercooled liquid. Nevertheless, this large difference in solubility at 2000 psi, 752 F, is surprising and larger than found at other temperatures and pressures. It should also be mentioned that not only did the colorimetric determinations made both by the Hall Laboratories and by the Philadelphia Quartz Company agree well with our gravimetric results, but also no difference was found between the samples as received and when treated to convert any "colloidal" silica to "crystalloidal" silica.

[13] "A Portion of the System Silica-Water," by George C. Kennedy, Economic Geology, vol. 45, 1950, pp. 629–653.

Stress and Deflection Tests of Steam-Turbine Diaphragm

By V. C. TAYLOR,[1] NEWPORT NEWS, VA.

This paper gives the results of tests made on a high-pressure and a low-pressure steam-turbine diaphragm. These diaphragms were subjected to loads which were applied uniformly along a semicircular arc. Data were taken on the deflection, reaction distribution, and nozzle-vane stresses. The information derived from these tests is incorporated in a method for calculating diaphragm stresses and deflections.

Introduction

THE solution for the stresses and deflections in a turbine diaphragm is complicated by the fact that it is a split ring rather than a continuous ring. It is, however, necessary to split the diaphragm into halves in order to facilitate assembly of the turbine. The combination of the split diaphragm and the nozzle vanes makes a very complex structure.

Four important factors that must be considered in the mechanical design of a steam-turbine diaphragm are as follows:

1 The deflection of the diaphragm due to steam loading.
2 The distribution of the reaction.
3 The stress in the nozzle vanes.
4 Inner and outer ring stresses.

Because of the complexity of the structure, any mathematical solution must be based on a simplification of the problem. Published literature on this subject involves such simplification that the final result is subject to considerable doubt. Therefore it was considered desirable to run tests to obtain this information.

The first Newport News tests were made in 1940 on a high-pressure diaphragm. In 1948 a design problem necessitated the running of tests on a low (or medium) pressure diaphragm. Since resistance-wire strain gages were in general use in 1948, it was possible to make more complete tests than those made earlier on the high-pressure diaphragm.

The objectives of these tests were to secure information that could be used as follows:

1 To determine whether the particular design of diaphragm was satisfactory for its service.

2 To select a mathematical solution to fit the information obtained from tests.

In 1932 Mr. A. M. Wahl presented a paper in which he analyzed an annular half ring (without nozzles).[2] His method with some modifications has been applied to the applicable data from these tests and has checked reasonably well. In determining the nozzle-vane stress, it is necessary to know the reactions acting on the diaphragm and the behavior of the vanes in transmitting these forces. The reaction calculated by Wahl's method must be adjusted in order to obtain values that are sufficiently close to the actual to be used in finding the blade stresses.

A mathematical solution which is based on a simplification of the problem should be used in the light of test results. The test data available at present are limited. Additional information is needed on diaphragms of other proportions. This would give a better idea of the accuracy of some of the calculations, and could be used to refine others to give increased accuracy.

Apparatus for Low-Pressure-Diaphragm Test

Details of the low-pressure diaphragm are shown in Fig. 1. This is the second-stage low-pressure diaphragm of a 12,500-hp marine turbine. The pressure drop across the diaphragm is 13.6 psi at maximum power. This gives a total load of 5850 lb on each half.

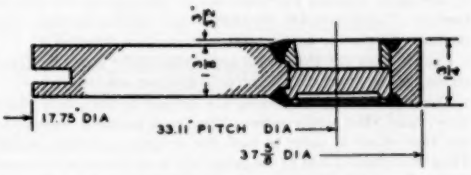

FIG. 1 DETAILS OF LOW-PRESSURE TURBINE DIAPHRAGM

It was not considered necessary to duplicate operating conditions by applying a uniform pressure over the steam-loaded area. A calculation of the stiffness of the diaphragm in resisting bending moments in a radial plane, indicates that the substitution of a load distributed along an arc instead of a uniformly distributed load, would have a negligible effect on the diaphragm deflection. In the test, the diaphragm was subjected to a load uniformly distributed around a semicircle whose center of gravity coincided with the center of gravity of the steam-loaded area.

Figs. 3 and 4 show the arrangement for testing the diaphragm. The force A was applied with a hydraulic testing machine through a ball connection to the rigid loading frame B. The frame transmitted the load to the diaphragm D, through a rubber strip C. This was used to insure even distribution of the load. The diaphragm rested on the aluminum-bronze supporting ring E. Resistance-wire strain gages mounted on this ring were used to determine the reactions. Dial indicators mounted on the base plate gave the deflection of the diaphragm. Location of the indicators is shown in Fig. 3.

---

[1] Engineering Technical Department, Newport News Shipbuilding and Dry Dock Company. Mem. ASME.

[2] "Strength of Semicircular Plates and Rings Under Uniform Pressure," by A. M. Wahl, Trans. ASME, vol. 54, 1932, pp. 311–320.

Contributed by the Power Division and presented at the Annual Meeting, New York, N. Y., November 26–December 1, 1950, of THE AMERICAN SOCIETY OF MECHANICAL ENGINEERS.

NOTE: Statements and opinions advanced in papers are to be understood as individual expressions of their authors and not those of the Society. Manuscript received at ASME Headquarters, August 1, 1950. Paper No. 50—A-49.

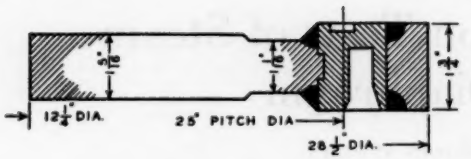

NUMBER OF NOZZLES	40
HEIGHT OF NOZZLES	1/2"
NOZZLE ANGLE	15°
MATERIAL OF INNER AND OUTER RINGS	MILD STEEL
MATERIAL OF NOZZLE RING	A.S.T.M A 276-44T CLASS 410 (13% CR)
MATERIAL OF WELD	25% CR 20% NI

FIG. 2 DETAILS OF HIGH-PRESSURE TURBINE DIAPHRAGM

A view of the supporting ring is shown in Fig. 5. Fig. 6 shows a portion at one end. The ring was cut in segments with gages mounted in the center of each segment. The gages were spaced closer toward the end of the diaphragm because, as will be shown later, the curve of reaction is changing rapidly in this region. At each location where measurements were made on the ring, two gages were mounted, one on the inside and one on the outside. These were connected in series. Any bending in the support ring would decrease the electrical resistance of the strain gages mounted on the side in compression and increase, by the same amount, the resistance of the gage on the side in tension. This eliminated the effect of any bending strains; thus readings of only the compressive reaction were obtained.

Fig. 7 shows the gage wires and some of the gages mounted on the bottom of the diaphragm (steam-outlet side).

The gages used in measuring the stresses in the nozzle vanes were $^1/_8$-in. SR-4 strain gages. They were mounted parallel to the vane edges in order to read the maximum bending stress. These were located first at the points where the maximum stresses were believed most likely to occur. It was found, however, that the stress pattern was considerably more complex than had been expected and additional gages were mounted later.

APPARATUS FOR HIGH-PRESSURE-DIAPHRAGM TEST

Details of the high-pressure diaphragm tested are shown in Fig. 2.

The test arrangement used for applying the load to the high-pressure diaphragm was similar to that used for the low-pressure diaphragm. However, the reaction ring was not used since this test was conducted in 1940, and as mentioned, strain gages were not in general use. For the deflection test, the diaphragm rested on $^3/_{16}$-in. × $^5/_{16}$-in. steel blocks which supported it along the outer edge.

For the reaction measurements, the diaphragm rested on $^1/_8$-in-diam × $^1/_4$-in. brass crushing pins which were located close to the outer edge with their axes radial. A number of pins were calibrated to give a curve of the permanent set versus applied load. From this curve the reactive force of each supporting pin was obtained by measuring the amount of crushing it underwent during the test. It was necessary to run several tests in order to obtain a spacing for the pins which would give equal crushing at all points. Difficulty was encountered in obtaining the readings at the ends because of the extreme concentration of the reaction.

METHOD OF CALCULATION

Wahl's method of calculating stresses and deflections in a diaphragm is shown in the Appendix. This is an approximate solution for a semicircular annular ring. To the author's knowledge there is no exact solution. It is necessary to consider the diaphragm as a semicircular annular ring of uniform thickness, thus neglecting the differences in rigidity between the nozzles and the rings. During loading, a radial section is assumed to remain undistorted (no curvature in a radial plane). Deflection measurements taken during the tests showed that this assumption was justified. The solution gives deflection of the diaphragm, stresses in the ring, and reaction distribution. The resulting reaction consists of a distributed load and a concentrated force at the ends of the diaphragm. This concentration of the reaction at the ends checks reasonably well with the test results.

Though there remains much to be desired in so far as the

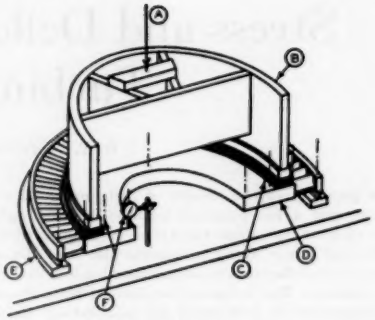

A APPLIED LOAD
B LOADING FRAME
C RUBBER
D DIAPHRAGM
E SUPPORTING RING
F DIAL INDICATORS FOR MEASURING DEFLECTION

FIG. 3 ARRANGEMENT FOR TESTING LOW-PRESSURE DIAPHRAGM

FIG. 4 LOW-PRESSURE DIAPHRAGM IN TESTING MACHINE

FIG. 5 DIAPHRAGM SUPPORTING RING

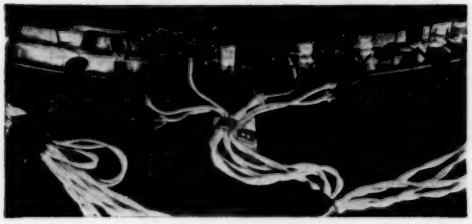

FIG. 6 STRAIN GAGES MOUNTED NEAR END OF SUPPORTING RING

FIG. 7 VIEW OF BOTTOM SIDE OF LOW-PRESSURE DIAPHRAGM SHOWING STRAIN-GAGE CONNECTIONS

method of calculation is concerned, Wahl's method plus the modifications to be suggested later should be satisfactory for design purposes.

DEFLECTION

The deflection measurements from the test on the high-pressure diaphragm are shown in Fig. 8. Because of the short rigid vanes, this diaphragm approaches quite closely the solid ring which was assumed in the calculation. The 60,000-lb load gave a maximum deflection of 0.190 in. This occurred at the end of the diaphragm on the inside corner. Unfortunately, because of testing difficulties, it was necessary to apply the load midway between the outer and inner diameters of the diaphragm. The same load applied uniformly over the area or along a semicircle, whose center of gravity coincided with the center of gravity of the area, would have produced a smaller moment and thus less deflection. Correcting the test reading for this difference gives a deflection of 0.169 in. The calculated figure for this point was 0.181 in.

Measured deflection on the low-pressure diaphragm is slightly lower than the calculated values. The deflection of this dia-

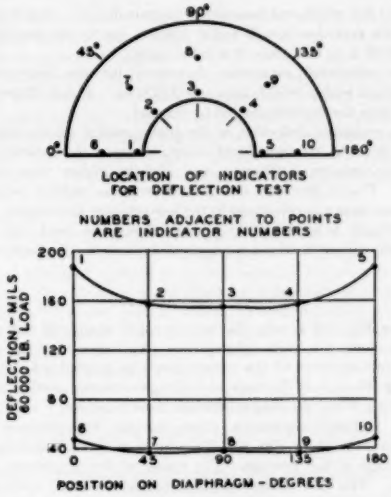

FIG. 8 DEFLECTIONS OF HIGH-PRESSURE DIAPHRAGM

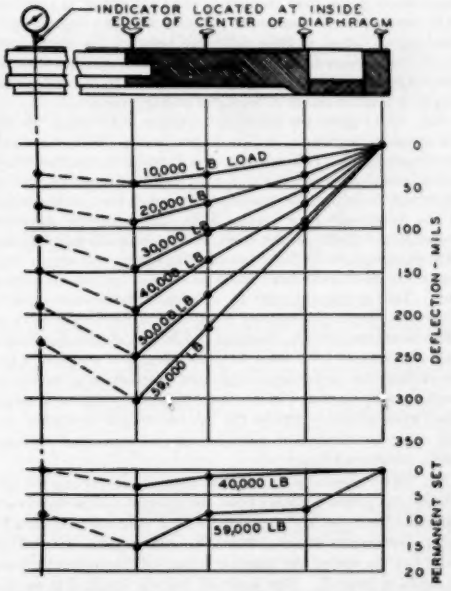

FIG. 9 LOW-PRESSURE DIAPHRAGM—DEFLECTION IN RADIAL PLANE

phragm for a series of loads is shown in Fig. 9. A set of indicators was mounted at each end of the diaphragm, and a single indicator was located at the center of the inner arc. Each of the points connected by solid lines represents the average of two end deflections. These curves show only slight deviation from the

straight line which was assumed in the calculation. It is believed that this variation is sufficiently small to justify the assumption that there is no curvature in a radial plane.

The calculated maximum deflection for the low-pressure diaphragm with a 5850-lb load was 0.0237 in. This is 12 per cent lower than the figure indicated by the test.

The measured deflection of the high-pressure diaphragm was quite close to the calculated value, whereas the deflection of the low-pressure diaphragm was slightly higher than calculated. This is probably due to a decrease in rigidity resulting from the longer nozzle vanes in the low-pressure diaphragm. For this reason a considerable margin should be used for diaphragms whose nozzles are longer than those in the diaphragms tested.

Reaction Distribution

From Fig. 8 it is seen that a very rapid change in deflection occurs along the inside edge of the diaphragm near the ends. This bending down of the corners tends to concentrate the supporting reaction at the ends and along the center portion of the outer ring, while reducing it between these locations.

The reaction-distribution curve for the high-pressure diaphragm is shown in Fig. 10. This curve gives the reaction as a percentage of the average. The center of the diaphragm is at 90 deg. The curve shows the high concentration of reaction at the ends of a diaphragm and gives a general idea of the distribution. The reaction distribution for the low-pressure diaphragm is given for low loads in Fig. 11 and for high loads in Fig. 12. Since strain gages were employed, the data obtained probably were more accurate than those obtained with the high-pressure diaphragm. There is little difference between the distribution for the low loads and the high loads. These curves show that, for this diaphragm, the intensity of the reaction in the supporting ring at the ends is about 16 times the average reaction.

Fig. 13(A) gives the calculated reaction distribution for the low-pressure diaphragm in pounds per degree (Wahl's method, see Appendix 1). This consists of a distributed reaction which varies from a maximum in the upward direction (positive, acts on diaphragm in a direction opposite to the steam load) at the center of the diaphragm to a maximum in the downward direction (crosshatched area) at the ends, and a concentrated upward force F_1 at each end. Since the test diaphragm was simply supported, no downward force could be exerted by the supporting ring. This is not the case in an actual turbine installation, where the diaphragm support is capable of exerting a force in either direction. Since, however, no lifting of the diaphragm from the support ring could be detected at any point, it is believed that the downward diaphragm reaction in a turbine is small, or nonexistent. In order to obtain a reaction diagram which more closely resembles the test results, the downward section must be eliminated and the concentrated load replaced with a distributed load.

Fig. 13(B) illustrates the method used in subtracting the calculated downward reaction from the upward. The downward distributed reaction W_2 is replaced with a concentrated force F_3 and a distributed reaction W_4. The concentrated force F_3 is located at the end of the diaphragm and subtracts directly from the upward force F_1. The resultant force is assumed to be distributed over the first 5 deg varying uniformly from a maximum at zero degrees to zero at 5 deg. This loading can be represented by the concentrated force W_5. The distributed downward reaction (W_4) (crosshatched area) is subtracted from the calculated upward reaction (upper curve in Fig. 13(B), as shown.

In adjusting the calculated reaction, the total moments and the total reaction must be unchanged. Thus

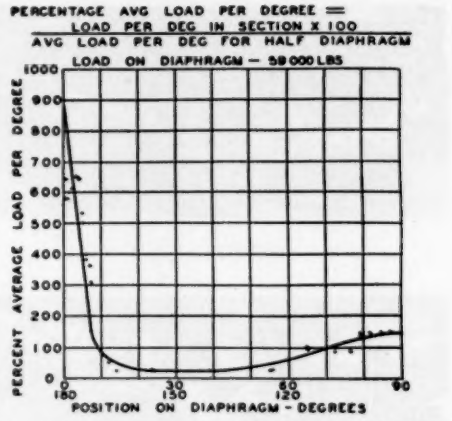

Fig. 10 Reaction Distribution for High-Pressure Diaphragm

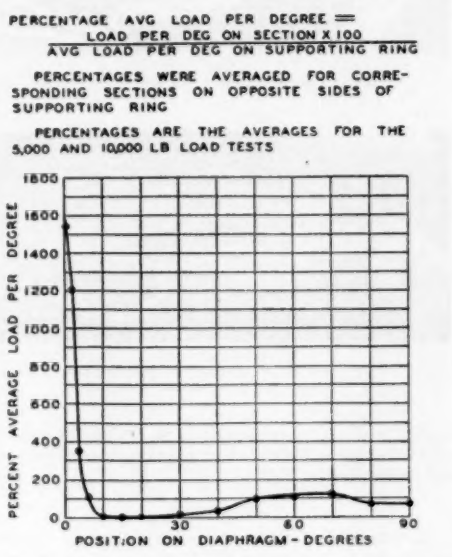

Fig. 11 Reaction Distribution for Low-Pressure Diaphragm, Low Loads

$$W_2 = F_3 + W_4$$
$$W_2 \times L_2 = W_4 \times L_4 - W_5 L_5$$
$$W_5 = F_1 - F_3$$

Moments are taken about the diaphragm joint and the moment arms L are perpendicular to it.

The assumption that reaction W_5 is distributed over an arc of 5 deg was based on the test curves and will vary somewhat, depending upon the stiffness of the particular diaphragm. For the high-pressure diaphragm, this reaction may be considered to extend over about 8 deg. This diaphragm is quite different from

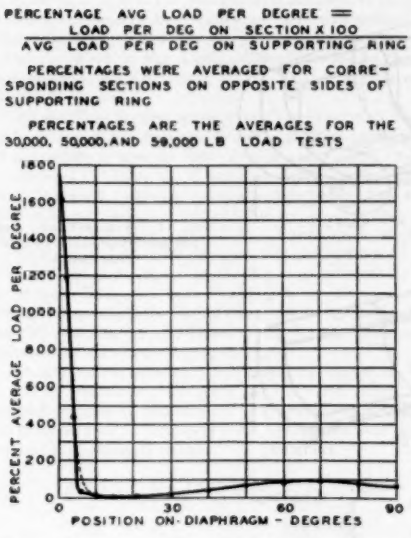

FIG. 12 REACTION DISTRIBUTION FOR LOW-PRESSURE DIAPHRAGM, HIGH LOADS

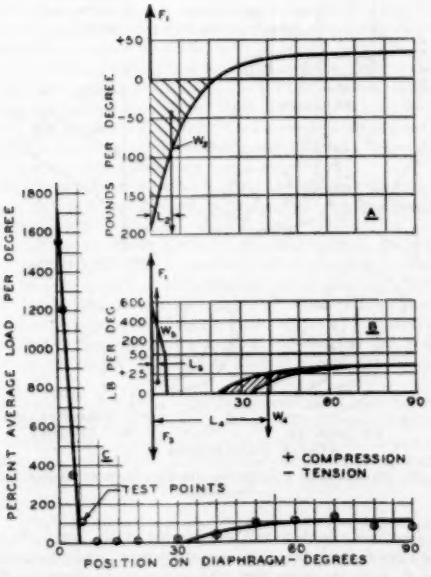

FIG. 13 ADJUSTMENT OF CALCULATED REACTION TO CORRESPOND WITH TEST RESULTS

the low-pressure and the data probably are not as accurate. It is believed that the end reaction could be assumed over the first 5 deg for most diaphragms.

The distribution of W_4 was selected to produce the best agreement between the calculated and the test curves. The curve for the new distributed upward force, formed by the bottom of the W_4 curve, was selected so that most of W_4 would be as close to its original position on the diagram (as part of W_3) as practical and yet form a smooth curve fairing into the original calculated curve.

Fig. 13(*C*) shows the adjusted calculated curve in per cent average load per degree. This agrees very closely with the test points from Fig. 11 which also are shown. Though this reaction distribution appears to be considerably different from the original, Fig. 13(*A*), the net effect on deflection and ring stress, produced by either loading should be approximately the same since this difference is mainly local action. In the calculation of vane stresses, however, it is felt desirable to use the curve which is close to the actual distribution.

VANE STRESS

The concentration of reaction found in the test on the high-

TABLE 1 NOZZLE-VANE STRESSES FOR 9000-LB LOAD—LOW-PRESSURE DIAPHRAGM

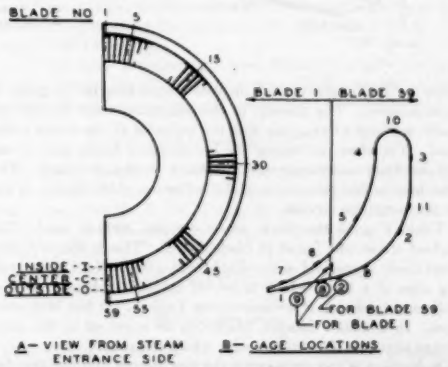

BLADE NO	1	2	3	4	5	15	30	45	55	56	57	58	59
GAGE LOCATION	STRESS IN 1000 PSI - COMPRESSION								+ TENSION				
1 - O	.054	.045	.102	.093						.370	.330	.384	
1 - C	*.171	*.150		*.120						.080	.147	*.195	
1 - I	.354	*.618	*.581	.579	.441				.444	.465	.351	.237	
2 - O													.330
2 - C													*.204
2 - I		.448										*.075	.732
3 - O		.285											
3 - C		.237										*.180	
3 - I		.135										.596	.792
4 - O		*.465	*.446	.342		.255		*.088		.309	.288	.262	.057
4 - C		.210	.174	.111		.045	.036	.054		.135	.204	.219	.282
4 - I		.820	.704	.564	.459	.210	.135	.006	.075	.048	.018	.177	.414
5 - I		.188										.045	.042
6 - O	.252	.081										.375	
6 - C	.078											*.128	
6 - I	.240	.132										.098	
7 - I	*.021												
8 - O		.249										.333	
8 - C		*.120										*.153	
8 - I	*.330	.429										*.616	
9 - I	.080												
10 - O												.006	
10 - C												.225	
10 - I												.376	
11 - I													.093

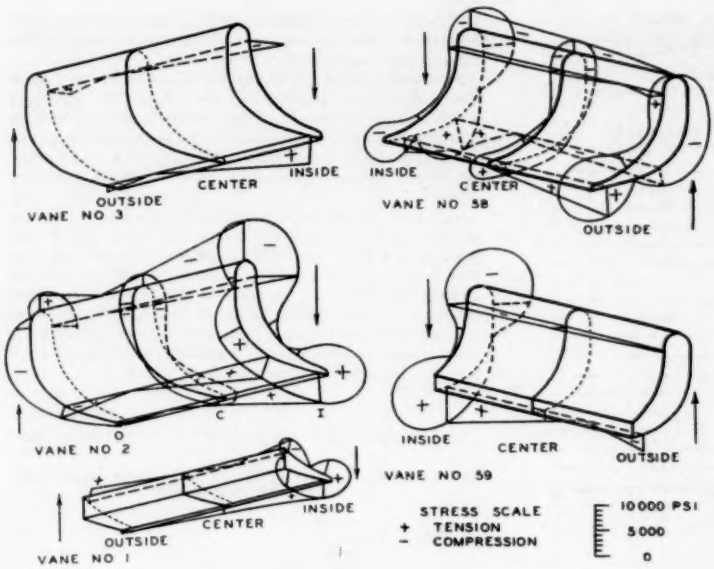

FIG. 14 NOZZLE-VANE STRESS DISTRIBUTION—LOW-PRESSURE DIAPHRAGM

pressure diaphragm caused increased attention to be given to vane stresses. The amount of this reaction carried by the end vanes was not known, nor was the behavior of the vanes under load. Therefore, in testing the low-pressure diaphragm, it was felt necessary to measure vane stress at a number of points. This was done to find the nature of the deflection of the blades as well as the maximum stresses.

Table 1 gives the blade stress for the 9000-lb load. The highest stress was found in blade No. 2. This is the first complete blade at one end of the diaphragm. Blade No. 1 is the trailing edge of a blade which is cut off at the diaphragm joint as indicated in sketch B accompanying Table 1. It has little stiffness. In a similar manner, blade No. 59 is cut off by the joint, except that it is the entering edge which remains.

A diagram of the stresses for the first partial and the first full nozzle vane from each end is shown in Fig. 14. The stresses are plotted perpendicular to the vane profile at the points where they were measured. It can be seen that the stresses are extremely complex. The distribution of the stresses in the vanes at one end of the diaphragm is considerably different from the distribution at the other end, but the maximum stresses are approximately the same. The differences are probably due to the nozzle vanes facing in opposite directions relative to the ends of the diaphragm.

In what follows a rational though approximate approach is made to the solution of vane stresses, and an example is calculated. While this calculation contains drastic simplifications, it will serve to show the nature of blade behavior under the reaction loading.

In the calculation which follows, the first full blade (No. 2) has been chosen because it is the most highly stressed. This blade has been assumed to carry the reaction for the first 3.1 deg of the arc (3.1 deg = vane spacing) Fig. 15(*A*) curve No. 1. The effect of the partial vanes has been neglected. The blades have been assumed to act as guided cantilevers fixed at the inner ends and loaded at the outer ends with the reaction. Under

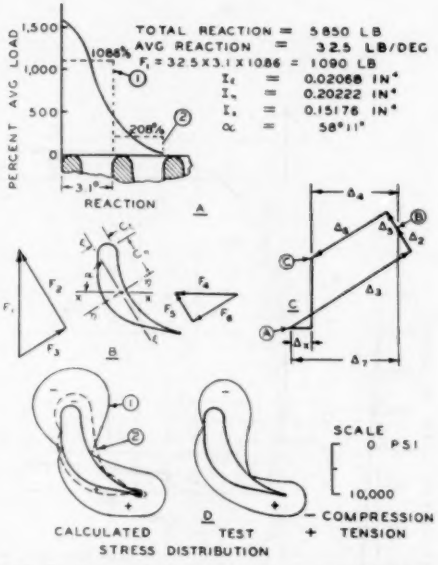

FIG. 15 DIAGRAMS OF PROCEDURE FOR CALCULATING NOZZLE-VANE STRESSES

this condition, the blade will be subjected to two forces, the upward force F_1, from the reaction of the support, and a tangential force F_4, from the outer ring. These forces are shown in Fig. 15(*B*). The force F_1 may be resolved into the components F_2

and F_3 acting normal to the principal axes of inertia of the blade. The angle α is the angle between the minimum axis and the plane of the diaphragm. The forces F_2 and F_3 produce the deflections Δ_2 and Δ_3, shown in Fig. 15(*C*). These combine to form the resultant deflection $\overline{AB}$ caused by F_1. The component of $\overline{AB}$ along the X-axis is Δ_7.

The force F_4 is likewise resolved into components F_5 and F_6, which produce the deflections Δ_5 and Δ_6. The deflections Δ_5 and Δ_6 combine to give the deflection $\overline{CB}$ produced by F_4. The component of $\overline{CB}$ along the X-axis is Δ_8. The algebraic sum of Δ_7 and Δ_8 gives Δ_x, which is the resultant deflection along the X-axis. Since the blades are tied together by the outer ring, they must all have the same value of Δ_x. Furthermore, since the tangential stress in the outer ring must be zero at each of its ends, the summation of F_4 from 0 to 180 deg must be equal to zero, that is, some blades will have F_4 acting in one direction, while others have it acting in the opposite direction. By making use of these two relationships, the forces acting on any blade can be calculated as shown in the Appendix 2(*A*).

Table 2 gives the calculated and measured stresses for blade No. 2 (first complete blade from the end) and No. 3. The measured stresses are taken from the 9000-lb-load test, but have been reduced to correspond with the 5850-lb load used in obtaining the calculated stresses.

TABLE 2 CALCULATED AND MEASURED STRESSES FOR BLADES NOS. 2 AND 3

	Upward force (P_0) lb	(A) Max calc stress, psi	(B) Max meas stress, psi	(A) ÷ (B)
(1) Vane No. 2	1090	7195	5330	1.35
(2) Vane No. 3	210	1941	4570	0.43
(3) Per cent diff $\frac{(1)-(2)}{(1)} \times 100$	80	73	14	

It is seen in Table 2 that the calculated stress for blade No. 2 is 35 per cent above the measured, whereas the calculated value for blade No. 3 is 57 per cent below the measured. This indicates that a portion of the force from the supporting ring that was assumed to be taken by blade No. 2 is actually carried by blade No. 3. This is probably due to a twisting moment being transmitted through the nozzle vanes. As yet the author is unable to give a satisfactory method by which the actual loading on the vanes can be determined from the reaction of the support on the outer ring. It is believed that a more detailed solution of the forces acting would prove very complex.

Line (3) of Table 2 shows that the percentage difference between the calculated stresses on blades 2 and 3 is less than the percentage difference of the applied force. This is due to the fact that the higher the portion of the total reaction that is carried by a blade, the closer its neutral axis will approach the X-axis, and thus the greater will be its resistance to bending. The effect that the load has on the location of the neutral axis is illustrated with a plot of the stress shown in Fig. 15(*D*). Blade No. 2 with the higher load, has a neutral axis close to the X-axis, whereas the neutral axis of blade No. 3 is close to the minimum axis.

If blade No. 2 is assumed to bend about the X-axis the stress obtained is 5890 lb, as compared with a measured stress of 5330 lb, Appendix 2(*B*). It should be noted that using the X-axis and considering the blade as a fully guided cantilever are optimistic assumptions. The use of too high a load acting on vane No. 2 compensated for this.

A simplified method that may be used in calculating the blade stress is to assume that the full concentrated force P, obtained by Wahl's method, is acting on the end of the blade. This eliminates the necessity for determining other points on the reaction curve. The stress obtained by using the full end reaction and the X-axis is 14,950 psi, or about 2½ times the measured value, Appendix 2(*C*). In cases where vane stresses are not high, this method could be used in place of a more detailed calculation.

Some have advocated the use of the full concentrated end force and the minimum axis. The stress obtained with these assumptions is 40,000 psi or about 8 times the measured, Appendix 2(*D*). Such conditions are far too severe.

The stress in the vanes can be allowed to be quite high since, if one vane should yield, the load would be thrown on the adjacent vanes which have lower stresses.

Conclusions

1 It is indicated by these tests that, in most cases, the deflection will be the limiting factor in diaphragm design. Wahl's method gives deflections which are reasonably close for diaphragms with short vanes, but are too low for diaphragms with longer vanes.

2 The reaction-distribution curve should be known or estimated before vane stresses can be calculated. This can be done by using Wahl's method and distributing the negative reaction over the adjacent diagram.

3 Approximate vane stresses may be calculated using the methods described in Appendix 2(*A*) or 2(*B*).

4 It is suggested that stresses in the diaphragm rings be calculated by taking a section through the center and calculating the difference (algebraic sum) between the moments produced by the steam-loading and the reactions (see Appendix 1 for an example of this procedure).

5 Since stress measurements were obtained on only one diaphragm, caution should be used in applying the results to diaphragms whose proportions vary greatly from the one tested.

Acknowledgment

The author wishes to thank the Newport News Shipbuilding and Dry Dock Company for permission to publish the data from these tests; and Mr. R. W. Nolan, Mr. J. R. Kane, and Mr. J. Halliday for their assistance in preparing this paper.

Appendix 1

Wahl's Solution

This method of solution for the stresses and deflections in a semiannular ring is taken from Wahl's paper.[3] A brief outline of his derivation is given, however, in order to clarify the source of the factors used in the calculation form.

The sign of one of the terms in the expression given by Wahl for γ (Equations [18] and [19][3]) is not in agreement with that derived herewith. It is believed that this is a typographical error. One of the calculated deflection curves given by Wahl has been checked using the signs obtained in this derivation. The deflection obtained was the same as that on the curve in Wahl's paper.

It should be noted that in the curves shown throughout this paper, the end of the diaphragm was designated as 0 deg, the center 90 deg, and the opposite end 180 deg. In the case of the following calculations (Wahl's method), the center is taken as 0 deg and the end as 90 deg.

Nomenclature

The following nomenclature is used in this Appendix (shown also in Fig. 16):

[3] Reference 2, p. 314.

M = bending moment
H = twisting moment
Q = shear force
C = torsional rigidity of rectangular cross section
E = modulus of elasticity
r = mean radius of plate
p = uniform pressure
q = reaction of support per unit length of circumference
G = modulus of rigidity
I = moment of inertia of section perpendicular to mean circumference
h = thickness of plate
a = half width of plate
R = outer radius of plate
α = polar angle in plane of plate
w = deflection

NOTE: $\frac{C}{EI} = \frac{4G}{E}\left(1 - \frac{0.625h}{2r}\right)$ (Wahl[2] equation 15

It is assumed that the diaphragm deflects without curvature in radial planes. Considering the segment contained by the angles α and $\alpha + d\alpha$, the equations for equilibrium are

$$\Sigma F_v = 0$$

$$2aprd\alpha + \frac{d\alpha}{d\alpha} = qRd\alpha$$

$$2apr + \frac{dQ}{d\alpha} = qR \quad \ldots\ldots [1]$$

$\Sigma M_T = 0$ (moments about an axis tangent to outside circumference)

$$-\frac{dH}{d\alpha} + M + \frac{2}{3}a^2p = qRa \quad \ldots\ldots [2]$$

$\Sigma M_R = 0$ (moments about a radial axis)

$$-\frac{dM}{d\alpha} - H + Qr = 0 \quad \ldots\ldots [3]$$

Boundary conditions:

(a) $M = 0$ at $\alpha = \frac{\pi}{2}$

(b) $H = Pa$ at $\alpha = \frac{\pi}{2}$ P = concentrated reaction at $\alpha = \frac{\pi}{2}$ (joint)

(c) $Q = -P$ at $\alpha = \frac{\pi}{2}$

(d) $H = 0$ at $\alpha = 0$

The law of deformation is expressed as follows (from theory of curved bars bent out of plane of initial curvature)

$$\frac{M}{EI} = \frac{w}{ar} - \frac{1}{r^2}\frac{d^2w}{d\alpha^2} \text{ Wahl[2] equation 63} \quad \ldots\ldots [4]$$

$$\left.\begin{aligned} \frac{H}{C} &= \frac{1}{r^2}\left(1 + \frac{r}{a}\right)\frac{dw}{d\alpha} = \frac{R}{ar^2}\frac{dw}{d\alpha} \\ \frac{dw}{d\alpha} &= \frac{ar^2}{CR}H \end{aligned}\right\} \quad \ldots\ldots [5]$$

In these five equations there are five unknowns: w, H, M, Q, and q. Eliminating all unknowns except w, the fundamental equation for the deflection is obtained

$$\frac{a^2}{r^3}\frac{d^4w}{d\alpha^4} - \left(\frac{2a}{r} + \frac{C}{EI}\frac{R^2}{r^2}\right)\frac{d^2w}{d\alpha^2} + W = \frac{2a^4pr}{EI}\left(\frac{r}{a} - \frac{1}{3}\right)$$

A general solution for this equation is

$$W = C_1 \cosh \gamma_1\alpha + C_2 \cosh \gamma_2\alpha + \frac{2a^4pr}{EI}\left(\frac{r}{a} - \frac{1}{3}\right)$$

in which

$$\gamma_1 = \sqrt{A + 2B\sqrt{K}} \qquad \gamma_2 = \sqrt{A - 2B\sqrt{K}}$$

where

$$A = \frac{r}{a} + \frac{R^2}{2a^2}\frac{C}{EI} \qquad B = \frac{R^2}{2a^2}\frac{C}{EI} \qquad K = \frac{ra}{R^2}\frac{EI}{C} + \frac{1}{4}$$

Substituting the boundary conditions (a) $M = 0$ at $\alpha = \frac{\pi}{2}$ and (b) $H = Pa = Qa$ at $\alpha = \frac{\pi}{2}$ the following equations are obtained

$$C_1[\gamma_1^2 - A'\gamma_1]\sinh \gamma_1\frac{\pi}{2} + C_2[\gamma_2^2 - A'\gamma_2]\sinh \gamma_2\frac{\pi}{2} = 0 \ldots [6]$$

$$A' = \frac{r}{a} + \frac{R^2}{a^2}\frac{c}{EI}$$

$$C_1\left(\frac{1}{a} - \frac{1}{r}\gamma_1^2\right)\cosh \gamma_1\frac{\pi}{2} + C_2\left(\frac{1}{a} - \frac{1}{r}\gamma_2^2\right)\cosh \gamma_2\frac{\pi}{2} + \frac{2a^2pr}{EI}\left(\frac{r}{a} - \frac{1}{3}\right) = 0 \ldots\ldots [7]$$

These two equations are solved simultaneously for C_1 and C_2. With the value of C_1 and C_2, the following can be found

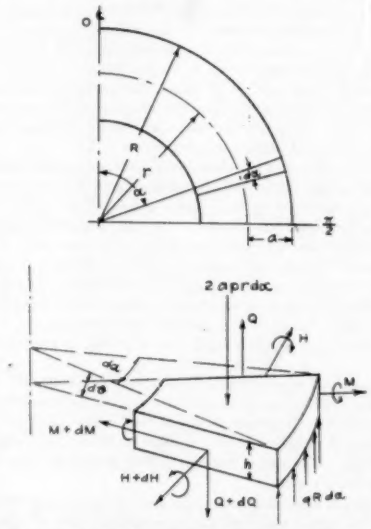

FIG. 16 SYMBOLS FOR CALCULATING STRESS AND DEFLECTION IN A SEMICIRCULAR RING

$$M = \frac{EI}{r^2}\left(\frac{r}{a}\,w - \frac{d^2w}{d\alpha^2}\right) \qquad w = C_1 \cosh \gamma_1\alpha + C_2 \cosh \gamma_2\,\alpha + C_4$$

$$\frac{d^2w}{d\alpha^2} = C_1\,\gamma_1^2 \cosh \gamma_1\alpha + C_2\,\gamma_2^2 \cosh \gamma_2\alpha$$

$$H = \frac{CR}{dr^2}\frac{dw}{d\alpha} \qquad \frac{dw}{d\alpha} = C_1\,\gamma_1 \sinh \gamma_1\alpha + C_2\,\gamma_2 \sinh \gamma_2\alpha$$

The diaphragm used in the calculation which follows is the low-pressure second-stage diaphragm which previously has been described.

Maximum pressure differential	P	psi	13.51
Outside radius	R	in.	18.5625
Mean radius	r	in.	13.40625
Half width	a	in.	5.15625
Mean equivalent plate thickness	h	in.	1.375
	E		30×10^6
	G		11.5×10^6
$C/EI = (1 - 0.625h/2a)\,4G/E$	M		1.4055
EI	EI		67.020×10^6
I	I		2.334
C	C		94.1966×10^6
$1/2\,(R/a)^3\,(C/EI)$	B		9.1076
$(ra/R^2)\,EI/C + 1/4$	K		0.3927
$(r/a + B)$	A		11.7076
$\sqrt{A + 2B\sqrt{K}}$	γ_1		4.8084
$\sqrt{A - 2B\sqrt{K}}$	γ_2		0.5422
$D = A + B$	D		20.8152
$\gamma_1\,(\gamma_1^2 - D)\sinh \gamma_1 \frac{\pi}{2}$	a_{11}		10569
$\gamma_2\,(\gamma_2^2 - D)\sinh \gamma_2 \frac{\pi}{2}$	a_{12}		−10664
$1/r\,(r/a - \gamma_1^2)\cosh \gamma_1 \frac{\pi}{2}$	a_{21}		−1459
$1/r\,(r/a - \gamma_2^2)\cosh \gamma_2 \frac{\pi}{2}$	a_{22}		0.2382
$2\,pa^2r/EI\,(r/a - 1/3)$	b_1		0.001682

Simultaneous Equations:

$$a_{11}\,C_1 + a_{12}\,C_2 = 0 \qquad [8]$$

$$a_{21}\,C_1 + a_{22}\,C_2 + b_1 = 0 \qquad [9]$$

$$C_1 = 1.375 \times 10^6$$
$$C_2 = 1363.1 \times 10^6$$
$$b_1 xa = C_2 = 8672.8 \times 10^6$$

	Center	Horizontal joint
α	0	$\pi/2$
$\gamma_1\,\alpha$	0	7.5530
$\gamma_2\,\alpha$	0	0.8517
$\cosh \gamma_1\,\alpha$	1.0	953.2
$\cosh \gamma_1\,\alpha$	1.0	1.385'5
C_3	8672.8×10^6	8672.8×10^{-6}
$C_1 \cosh \gamma_1\,\alpha$	1.3×10^6	1310.6
$C_2 \cosh \gamma_2\,\alpha$	1363.1×10^6	1888.8
Sum w	10037.2×10^6	11872.2×10^{-6}
$2w$	0.02007	0.02374 defl. on inner edge (in.)
$C_1\,\gamma_1^2 \cosh \gamma_1\,\alpha$	31.79×10^6	30303.8×10^6
$C_2\,\gamma_2^2 \cosh \gamma_2\,\alpha$	400.75×10^6	555.1×10^6
Sum $= d^2w/d\alpha^2$	432.54×10^6	30858.9×10^6
$\sinh \gamma_1\,\alpha$	0	953.2
$\sinh \gamma_2\,\alpha$	0	.95845
$C_1\,\gamma_1 \sinh \gamma_1\,\alpha$	0	6302.1×10^6
$C_2\,\gamma_2 \sinh \gamma_2\,\alpha$	0	708.4
Sum $= dw/d\alpha$	0	7010.5×10^6
$H = CR/ar^2\,dw/d\alpha$	0	13227 = torsional moment (in-lb.)
$(EI/ar)w$	9731.1	11510.1
$(EI/r^2)\,d^2w/d\alpha^2$	161.3	11507.3
Difference $= M$	9569.8	0 = bending moment (in-lb)
$(2/3\,P)(a^2/R)$	12.919	12.919
M/aR	100	0
Sum	112.92	12.919
$[C/(ar)^2]\,[d^2w/d\alpha^2]$	−8.52	−608.321
Difference $= q$	104.40	−595.402 = distributed reaction (lb/deg)

$$P = \frac{H}{a} \qquad \text{2565 = concentrated reaction (lb)}$$

$$\text{Maximum bending stress} = \frac{M_0 h}{2I} = \frac{9569.8 \times 1.375}{2 \times 2.234}$$

$$\text{Maximum bending stress} = 2945 \text{ psi}$$

$$\text{Maximum shearing stress}^4 = H_{\pi/2} \times \frac{3a + 0.9\,h}{2a^3\,h^3} = 13.227 \times \frac{3 \times 5.15625 + 0.9 \times 1.375}{2 \times 5.15625^3 \times 1.375^3}$$

$$\text{Maximum shearing stress} = 2198 \text{ psi}$$

Appendix 2

Maximum Blade Stress

Four methods of calculating the maximum blade stress are given. The last method is one that has been used, but whose assumptions are considered too severe.

In all cases the diaphragm is subjected to a steam load of 5850 lb, and the blades are assumed to bend as guided cantilever beams. The location of the point of maximum stress and its distance C from the neutral axis will vary, depending upon the neutral axis used in the particular method. The axes are shown in Fig. 15(*B*).

(*A*) Total reaction $F = 5850$ lb (load on diaphragm at maximum power)

Number of blades, $N = 58$

Blade length, $l = 2.11$ in.

$I_x = 0.02068$ in.^{4}

$I_y = 0.2022$ in.^{4}

$C_y = -0.79$ in. (these values of C are for the point where the maximum stress was found to occur)

$C_\xi = -0.35$ in.

$\alpha = 58°11'$

$\sin \alpha = 0.850$

$\cos \alpha = 0.527$

$$\Delta_2 = \frac{F_1 l^3 \sin \alpha}{12\,EI_\xi} = 0.109 \times 10^{-6}\,F_1$$

[4] "Formulas for Stress and Strain," by R. J. Roark, McGraw-Hill Book Company, Inc., New York, N. Y., 1938.

$$\Delta_3 = \frac{F_3 l^3 \cos \alpha}{12\, EI_\xi} = 0.665 \times 10^{-6} F_3$$

$$\Delta_5 = \frac{F_5 l^3 \cos \alpha}{12\, EI_\eta} = 0.068 \times 10^{-6} F_5$$

$$\Delta_4 = \frac{F_4 l^3 \sin \alpha}{12\, EI_\xi} = 1.074\, \Delta\, 10^{-6} F_4$$

$\Delta_7 = \Delta_3 \sin \alpha - \Delta_5 \cos \alpha = 0.507 \times 10^{-6} F_3$

$\Delta_6 = \Delta_5 \cos \alpha + \Delta_4 \sin \alpha = 0.948 \times 10^{-6} F_4$

$\Delta_x = \Delta_7 - \Delta_6$

$\Sigma\Delta_x = \Sigma\Delta_7 - \Sigma\Delta_6$

$\Sigma\Delta_6 = 0.948 \times 10^{-6} F_4 = 0$

$\Sigma\Delta_x = N\Delta_x$

$$\Delta_x = \frac{\Sigma\Delta_7}{N} = 0.507 \times 10^{-6} \times \frac{\Sigma F_3}{N}$$

$\Delta_x = 0.507 \times 10^{-6} \times$ avg load per blade

$$\Delta_x = 0.507 \times 10^{-6} \times \frac{5850}{58} = 51 \times 10^{-6}$$

F_3 for second blade = 1090 lb (from reaction curve)

$\Delta_4 = \Delta_7 - \Delta_x = 502 \times 10^{-6}$

$$F_4 = \frac{\Delta_4}{0.948 \times 10^{-6}} = +530$$ (the direction—and sign—of F_4 reverses when $\Delta_x > \Delta_7$)

$F_5 = 530 \cos \alpha = +280$

$F_6 = -(530 \sin \alpha) = -450$

$F_2 = 1090 \sin \alpha = +925$

$F_3 = 1090 \cos \alpha = +575$

$F_3' = F_2 + F_3 = 1205$

$F_3' = F_3 + F_6 = 125$

$$S_6 = \frac{MC_6}{I} = \frac{125 \times 2.11 \times (-0.35)}{2 \times 0.02068} = -2230$$ (compression)

$$S_7 = \frac{MC_7}{I} = \frac{1205 \times 2.11 \times (-0.79)}{2 \times 0.2022} = -4965$$ (compression)

Total stress = $-2230 - 4965 = 7195$ psi (compression)

(*B*) The conditions are the same as used in calculation (*A*), except that the blade is assumed to bend around the *X*-axis.

Force acting on blade..... $F_1 = 1090$ lb

Length..... $l = 2.11$ in.

$I_x = 0.1645$ in.[4]

$C = 0.91$ in.

Maximum stress..... $$S = \frac{F_1 l C_x}{2I_x} = 5890$$ psi

(*C*) The concentrated reaction *P* acting at the end of the outer ring (obtained from Wahl's calculation shown in Appendix 1) is carried by one blade. The blade is assumed to bend about the *X*-axis.

Forcing acting on blade..... $P = 2560$ lb

Maximum stress..... $$S = \frac{PlC_x}{2I_x} = 14950$$ psi

(*D*) The concentrated reaction *P* is carried by one blade. The blade is assumed to bend about the minimum axis.

Angle of minimum axis with surface of diaphragm $\phi = 58°11'$

Component of force acting perpendicular to minimum axis

$P \times \cos 58°11' = 1350$ lb

$I\xi = 0.02068$ in.[4]

$C\xi = 0.58$ in.

Maximum stress $$S = \frac{P \times \cos 58°11' \times l \times C\xi}{2 \times I\xi} = 40{,}000$$ psi

Discussion

R. W. NOLAN.[5] This excellent and much needed paper fits into one of the gaps in the existing literature on steam turbines.

The author's conclusion (1), that "in most cases the deflection will be the limiting factor in diaphragm design," appears to be correct. It is, however, of interest to consider the exception to this rule, that is, the diaphragm in which the vane stress rather than the deflection may govern. This might occur in a turbine where there is ample space for the diaphragm to deflect without fouling its sealing fins or some rotating part.

In the diaphragm which was tested, the calculated vane stress was 7195 psi with a load of 9000 lb. At the designed load of 5850 lb, the calculated stress would be 4680 psi. This is a rather low operating stress. If, the elastic limit of the material were 70,000 psi, the nominal factor of safety would be 14.9, a rather high value. If, however, the diaphragm had lighter vanes, and larger pressures, it might be possible to run the stress up above the elastic limit. In such a case the reaction diagram would change radically. Fig. 17, herewith, shows the reaction diagram from the author's Fig. 12. The reaction curve which would be

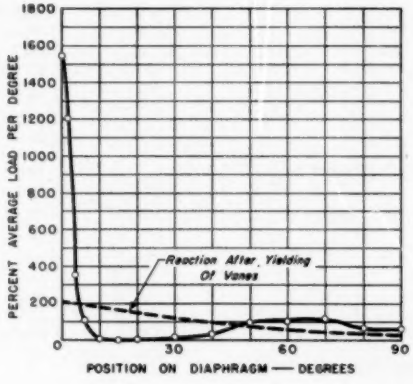

FIG. 17

obtained if the nozzle vanes were extremely flexible has been superposed on this diagram. This is also the reaction diagram which is approached if the nozzle vanes yield. As long as the vane material is sufficiently ductile, this reaction curve will be reached before failure can occur. The values of the reaction were obtained by assuming the reaction to be a linear function of the distance from the joint and then calculating the distribution which would make the resultant of the reaction forces coincide with the resultant of the uniformly distributed load. It will be seen that the maximum reaction is approximately 200 per cent at the diaphragm ends, dropping to 40 per cent at the center. The maximum reaction is thus 1/5 of the value obtained when the diaphragm acts elastically. Using this distribution, the stress in No. 2 vane has been calculated by the method illustrated in Appendix 2(*A*) of the paper. This gave a value of 1900 psi. Appendix 2(*A*), however, assumes the vane to act as a guided cantilever. This assumption could not be expected to hold for very high loading. It therefore appears necessary to treat the vanes as simple cantilevers, thus obtaining a stress of 3800

[5] Newport News Shipbuilding and Dry Dock Company, Newport News, Va.

psi. This is a little over one half of the stress (7195 psi) obtained when the diaphragm behaves elastically, Appendix 2(*A*). There is thus even more margin of safety in the methods of calculation outlined in Appendix 2(*A*) and (*B*) than is indicated by the nominal factor of safety. This additional margin can be kept in mind if a case of high vane stress is encountered.

F. L. Jackson.[6] The Wahl[7] theory for stress and deflection of semicircular plates has not found the broad application it deserves, principally because the final results are not given in a simplified form for numerical calculation. Reference to Wahl's paper or to Appendix 1 of the author's paper reveals the extensive

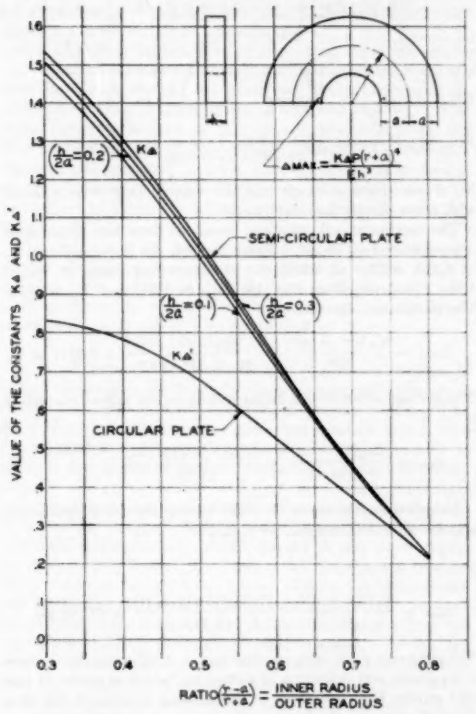

Fig. 18 Curves for Finding K_Δ and K_Δ' in Deflection Formula for Flat Plates;

$$\left[\Delta_{max} = \frac{K_\Delta P(r+a)^4}{Eh^3};\ \Delta'_{max} = \frac{K'_\Delta P(r+a)^4}{Eh^3}\right]$$

analysis required for one particular case. A simple method is presented to enable a designer to apply the results of this theory directly and also to determine the effects of a change in the physical dimensions on maximum deflection and stress. This method was derived by equating the Wahl equations for stress and deflection to corresponding simple plate-theory equations, and obtaining equivalent constants K in terms of the Wahl parameters. These constants for maximum deflection and stress are plotted in Figs. 18 and 19 of this discussion, over a range of the most frequently occurring cases of inner radius to outer radius and thickness to plate width. It is planned to extend these curves and to provide similar curves or data to predict the distribution of stresses and deflections throughout the plate. For this reason, the curves will be discussed only to the extent required for application.

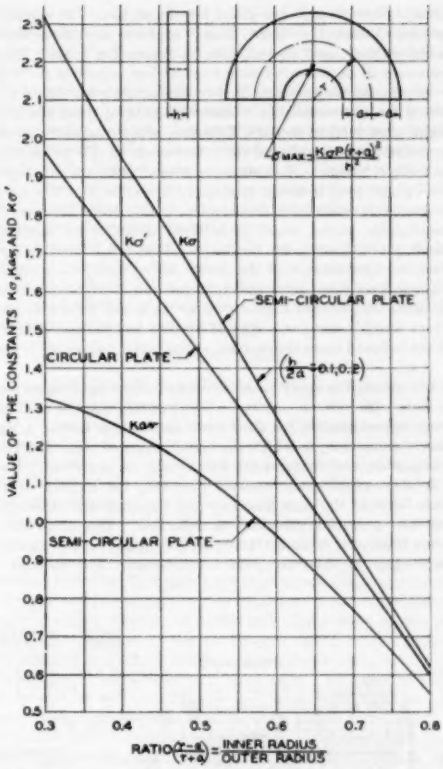

Fig. 19 Curves for Finding K_{avg}, K_σ, and K'_σ in Stress Formula for Flat Plates

$$\left[\sigma_{avg} = \frac{K_{avg}P(r+a)^2}{h^2};\ \sigma_{max} = K_1\sigma_{avg} = \frac{K_\sigma P(r+a)^2}{h^2};\ \sigma'_{max} = \frac{K'_\sigma P(r+a)^2}{h^2}\right]$$

The notation used is identical with that in Wahl's paper except that Δ_{max} is used for maximum deflections, and σ_{avg} for σ'_{max}, the average stress over a radial section on the axis of symmetry. The difference between K_σ and K_{avg} in Fig. 19 is due to the stress multiplication factor[8] K_1, i.e., $\sigma_{max} = K_1\sigma_{avg}$, or $K_\sigma = K_1K_{avg}$. Values of maximum deflection and stress taken from

[6] Research Engineer, De Laval Steam Turbine Company, Trenton, N. J.

[7] "Strength of Semicircular Plates and Rings Under Uniform Pressure," by A. M. Wahl, Trans. ASME, vol. 54, Paper No. APM-54-28, 1932, pp. 311–320.

[8] Reference 7, Equation [34].

circular-plate theory[9] are given for comparison. It should be mentioned that the Wahl theory neglects any distortion in radial sections, and irregularities in supporting edges. Radial sections will be distorted somewhat at low values of $(r - a)/(r + a)$, and irregularities in the supporting edge may be expected for any installation. Although both of these effects are slight, they tend to increase deflection and stress, and any conservative predictions based on these curves should be increased by a slight margin. Test data are needed over a wide range of $(r - a)/(r + a)$ to assess accurately these effects. The curves for maximum deflection are compared with Smith's[10] curve for semicircular plates, which is believed obtained by modifying simple plate theory with factors based on test. Smith's curve gives fair agreement with the curves at $(r - a)/(r + a)$ of 0.3, is about 8 per cent higher at 0.4, 15 per cent at 0.5, and increases to about 35 per cent higher at 0.8. It is not known to what extent Smith's curve was verified by test, but the curves in Fig. 18 are believed more appropriate at the higher values of $(r - a)/(r + a)$.

Any attempt to apply these curves to turbine diaphragms must be done with extreme caution. These curves may be used as a rough approximation for short-vane diaphragms having a rigid joint construction, in which the contribution of vane distortion is negligible, and temperature effects may be neglected. Even with short-vaned constructions, however, the rigidity of the joints between the vane assembly and the inner and outer rings may have a considerable effect on deflection. This effect will be shown from tests made by the writer's company on two identical diaphragms of different joint construction. The method of

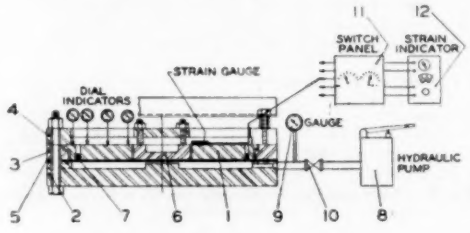

PART NO.	PART NAME
1	TEST DIAPHRAGM
2	COVER
3	SPACER
4	COVER
5	RUBBER DIAPHRAGM
6	CENTER PLUG
7	WOOD FILLER PCS.
8	HYDRAULIC PUMP
9	GAUGE
10	VALVE
11	SWITCH PANEL
12	STRAIN INDICATOR

FIG. 20 DIAPHRAGM TEST APPARATUS

test is shown in Fig. 20, herewith, the diaphragm being loaded with a uniform pressure over the whole diaphragm area. This method is believed to represent more closely actual conditions in steam turbines than that used by the author. The over-all dimensions of the two test diaphragms are given in Fig. 21 of this discussion. Diaphragm No. 1 contained large, double-J welding kerfs in the inner and outer rings so there was considerable depth and area of weld metal next to the vanes. Diaphragm

[9] "Stress and Deflections in Flat Circular Plates With Central Holes," by A. M. Wahl, Trans. ASME, vol. 52, 1930, pp. 29–43.

[10] "Deflections and Stress in Built-Up Half Diaphragms," by D. M. Smith, Proceedings of the Fifth International Congress for Applied Mechanics, 1938, pp. 62–65.

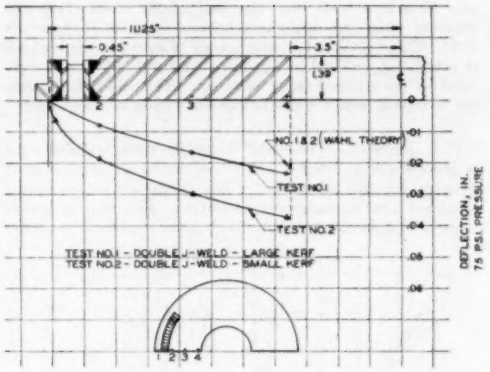

FIG. 21 MAXIMUM DEFLECTION CURVES SHOWING EFFECT OF ROTATION AT JOINTS

No. 2 was identical except that the welding kerfs were reduced with consequently less weld metal.

The maximum deflection and stress for these two diaphragms are calculated at 75 psi. From Fig. 18, for $(r - a)/(r + a)$ of 0.315, $h/(2a)$ of 0.182, the corresponding value of K_Δ is 1.48. Similarly, from Fig. 19, $K_{\sigma_{avg}}$ is 1.31, and K_{σ_r} is 2.25. The maximum deflection is

$$\Delta_{max} = \frac{K_\Delta P(r + a)^4}{Eh^3} = \frac{(1.48)(75)(11.125)^4}{30 \times 10^6(1.39)^3} = 0.0211 \text{ in.}$$

The average stress over a radial section on the axis of symmetry is

$$\sigma_{avg} = \frac{K_{\sigma_{avg}} P(r + a)^2}{h^2} = \frac{(1.31)(75)(11.125)^2}{(1.39)^2} = 6300 \text{ psi}$$

The maximum stress at the inner edge on the axis of symmetry may be obtained from $\sigma_{max} = K_1\sigma_{avg}$

or

$$\sigma_{max} = \frac{K_{\sigma_r} P(r + a)^2}{h^2} = \frac{(2.25)(75)(11.125)^2}{(1.39)^2} = 10{,}800 \text{ psi}$$

The relatively rigid joint construction in diaphragm No. 1 gives a maximum test deflection of 0.0240 in., which is about 11 per cent greater than calculated. This increase is believed due to a slight decrease in thickness in the outer ring, slight distortion of radial cross sections, and irregularities in the supporting edge. Test results for maximum stress give 10,000 psi compared to the calculated value of 10,800 psi, which is acceptable for design purposes. For the weaker joint construction in diaphragm No. 2, the test deflection is 0.0375 in., which is 79 per cent greater than calculated, and 64 per cent greater than in diaphragm No. 1. This 64 per cent increase in deflection is due only to the decreased rigidity of the joint construction. This effect of rotation at the joints in increasing deflections is clearly shown in Fig. 21, herewith, and emphasizes the importance of establishing a rigid joint construction in controlling deflections.

For the low-pressure diaphragm of the author's paper, discrepancies are noted for the dimensions given on the drawing and those in Appendix 1. Assuming that the latter dimensions are correct, calculations from Figs. 18 and 19 give Δ_{max} of 0.0237 in., σ_{avg} of 2947 psi, and σ_{max} of 4470 psi. The fact that

the maximum test deflections are within 12 per cent of the calculated value may be partly due to the increased thickness of the outer ring which tends to stiffen the diaphragm. Test values for maximum stress are not given for comparison. The author's suggestion that the average stress as calculated be used for the maximum stress demonstrates the need of modification of the Wahl theory. This suggestion is rather arbitrary, however, and would apply only to diaphragms of identical configuration.

For the range of diaphragms generally encountered in practice, some modification of the basic theory is necessary. In many cases the structure is of such complicated and geometrically irregular form as to render accurate calculations impossible. More complex stress problems arising from excessive temperature gradients are not included in this discussion.

A more rational approach would be to treat the diaphragm as a combination of three basic elements. These elements are the outer ring, vane section, and inner ring, which are joined together by welding or other means of a "given rigidity." This would involve a solution of the differential equations[7] for the inner and outer rings with appropriate modifications at the edges. The methods suggested by the author for obtaining stresses in the nozzle vanes and determining the actual distribution of reaction are an excellent approach toward a more rational treatment.

The author is to be congratulated on his contribution to the meager information available in the literature on this subject. It is only when more test data becomes available over a wide range of the many variables involved that any correlation between theory and test may be established.

A. W. Rankin.[11] The calculation of stresses and deflections in split diaphragms is one of the most complex problems which a turbine designer must solve, and, as the author points out, all the published analyses employ such simplification that a considerable amount of testing must be done in order properly to calibrate the calculated results. Accordingly, it has been necessary for almost all turbine designers to conduct diaphragm deflection tests at some time in order to check particular features of individual designs. The writer's company, for instance, conducted similar tests to those reported in this paper during the early 1920's, and at that time noted the extreme reaction which occurs in the horizontal joints. This is the major reason why reinforcing bridges are spaced more closely near the horizontal joint than elsewhere on the circumference. The fact that there is still no complete practicable solution for the calculation of diaphragm stresses and deflections, however, lends even more importance to the author's excellent publication, as the more test data available the more nearly correct will be the calibration on the calculated quantities. The industry is indebted to the author and his company for making these results available for general study.

The writer is not in complete agreement with the statement that the bending down of the corners tends to concentrate the supporting reaction at the ends and along the center portion of the outer ring. In the writer's opinion, the high reaction at the ends is caused simply by the necessity for the gravity center of the total reaction to line up with the gravity center of the applied load, and the bending down of the corners of the inner ring is caused to a considerable extent simply by their being unsupported. It also appears that the reaction can be approximated to a satisfactory and practical degree by assuming a double sine wave plus two concentrated shear reactions at the horizontal joint. It is difficult to believe that there will be sufficient bending of an outer ring of practical dimensions to close up the clearance in a diaphragm fit and result in negative reactions.

Some question can be raised concerning the author's conclusion that deflection in most cases will be the limiting factor in diaphragm design. While this conclusion is approached in the low-temperature ends, a close watch must be maintained of stresses at the high-temperature regions, or excessive creep may occur. This, in turn, will result in excessive deflections, but the initial calculations would not predict this unless they are in terms of the allowable creep stresses.

The foregoing comments, which do not invalidate the major portion of the paper, are secondary to the writer's desire to express his appreciation to the author for a timely presentation on a subject which is of great importance in the design of reliable turbines for both land and marine use.

Author's Closure

The author wishes to thank Messrs. Nolan, Jackson, and Rankin for their helpful discussions.

Mr. Nolan has given an interesting analysis of the change in the reaction which would occur if the vanes were stressed beyond the yield point. This lowering of the maximum stress due to the redistribution of the load should be considered if the maximum stress appears high.

The curves presented by Mr. Jackson should be of considerable aid in calculating the stresses and deflections of diaphragms. The extension of these curves to cover the distribution of the stress and deflection throughout the plate should also prove useful.

Mr. Jackson has brought up an important point in his discussion of the effect that the circumferential joints have on the deflection. In the case of the diaphragms tested by the author, little rotation could have occurred in the joints since, as can be seen in Figs. 1 and 2, they were quite rigid. The type of joint that is used, as well as the diaphragm proportions, must be considered in applying the data from the body of this paper.

It is true, as Mr. Jackson states, that the deflection of the low-pressure diaphragm, Fig. 1, would have been greater had it not been for the increased thickness of the outer ring. Probably more important than the effect of the outer ring is the effect of the increased rigidity of the nozzle vanes due to the thickness at this section. Had the entire diaphragm been of the same thickness as the inner ring, the test deflection would have been expected to be greater than the 12 per cent over the calculated. The diaphragm shown in Fig. 21 has a decreased thickness in the outer ring and vane section which also results in a test deflection greater than calculated. It should be noted that the increased deflection of the low-pressure diaphragm was due to the length of the vanes while that of the diaphragm tested by Mr. Jackson was due to decreased thickness of the outer ring and blade section. As stated in the conclusions, it is important to consider carefully the comparative diaphragm proportions in applying the test results from one to the design of another.

The apparent discrepancy between the dimensions shown in Fig. 1 and those used in Appendix I is due to the use of the steam-loaded area for the calculation, rather than the actual dimensions of the diaphragm. The outer radius was considered as being the distance to the point at which the diaphragm was supported by the turbine casing. An inner radius was used which included the sealing ring segment, since this load must be carried by the diaphragm.

The author is unable to give a measured stress for the inner ring of the diaphragm, as requested by Mr. Jackson. In these tests strain gages were not mounted on the inner ring since calculations indicated that stress in the ring was quite low. It was

[11] Assistant Division Engineer, General Electric Company, Schenectady, N. Y. Mem. ASME.

considered more important to concentrate on the determination of the blade stresses and deflection, whose values appeared to be high, and the reaction distribution.

In calculating the bending stress for the inner ring the author did not apply the correction factor given by Wahl. The factor used is for a circular plate where it is necessary for the fibers on the inner radius to elongate during bending in a radial plane. In the case of the circular plate, this stress due to the elongation of the fibers in a circumferential direction, will be constant along any circumferential section. Whereas for the semicircular plate such a stress must be zero at the two ends. It does not appear that the factor used for the circular plate would be applicable to the semicircular plate.

The diaphragm tested by Mr. Jackson gave a deflection which was 11 per cent greater than calculated whereas the maximum stress was 7 per cent less than calculated. This indicates that the stress at the inner radius is considerably less than indicated by the maximum stress. Test data will be needed to tell to what extent the stress at the inner radius may be greater than the average.

The author does not consider, as does Mr. Rankin, that the necessity for the center of gravity of the reaction to line up with that of the applied force is sufficient in itself to explain the reaction distribution of the diaphragm. A relatively smooth curve, as shown in Fig. 17, would fulfill this requirement without the high reactions at the end. With such an explanation the minimum reaction would be expected at the center of the diaphragm, whereas it actually occurs between the center and the ends.

The author concurs with Mr. Rankin's statement that the creep stress may be the limiting factor for the designs of a diaphragm at the high-pressure end. During the process of creep the more highly stressed blades should tend to distribute their load to those less stressed. This would proceed much in the same manner as blades in yielding as discussed by Mr. Nolan. However, as Mr. Rankin states, the creep may result in excessive deflection.

High-Temperature Properties and Characteristics of a Ferritic Steam-Piping Steel

By A. W. RANKIN[1] and W. A. REICH,[2] SCHENECTADY, N. Y.

With the considerable amount of turbine capacity now in operation and being built at the 1000 F and 1050 F levels, there is considerable incentive to develop a stronger ferritic steel for these temperatures. This paper presents a review of the high-temperature properties and manufacturing and heat-treating characteristics of a chromium-molybdenum-vanadium alloy. The authors' company is utilizing this composition for turbine shells, valve casings, and steam leads at both 1000 F and 1050 F. This paper presents the characteristics of the piping form of this alloy. Corresponding properties and operating experiences are also presented on the chromium-free molybdenum-vanadium steel which preceded the chromium-molybdenum-vanadium composition.

Introduction

ONE of the major engineering accomplishments of the last half century is the increase in the generation efficiency of our public-utility power stations, as is shown in Fig. 1. The major reason for this increase in generation efficiency has been the increase in operating temperatures, as is illustrated in Fig. 2, which increases the thermal-cycle efficiency. The use of the higher temperatures has required the continuous introduction of more highly alloyed steels possessing both suitable long-time high-temperature properties and adequate processing characteristics. This has already required lengthy metallurgical developments, but such work must be continued because the factors which demand an increase in generation efficiency are more potent today than at any time in the past.

The maximum steam temperature at present in use for major power generation is 1050 F and the first unit at this temperature level went into operation late in 1948, while the first unit at the 1000 F level went into operation at that temperature only in early 1946. That there will soon be a significant amount of capacity at the 1000 F and 1050 F levels, however, is indicated by the fact that of all the orders received between May 1, 1947, and April 30, 1950, by the authors' company, for units of 10,000 kw and larger, almost 50 per cent of the capacity was for either 1000 F or 1050 F operation.

Design, manufacture, and installation at the 1000 F and 1050 F levels are rendered somewhat difficult, however, by the characteristics of the steels which are deemed satisfactory for such service. These temperatures push the more common ferritic steels, with their customary heat-treatments, to a point where heavy walls are required to maintain satisfactory margins on the creep and rupture strengths; in turbine shells, this may result in difficulty in obtaining a casting of satisfactory soundness, while in piping it may require the use of forged and bored tubing. If

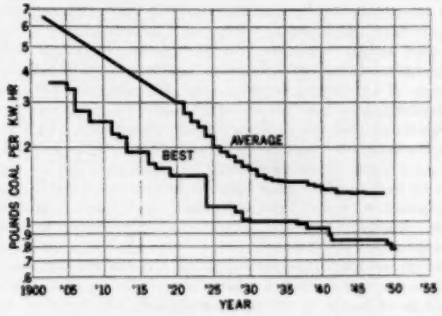

Fig. 1 Increase in Generation Efficiency of Power Stations During Past 45 Years

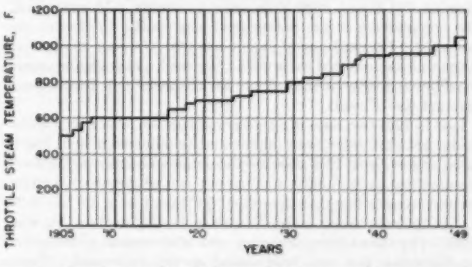

Fig. 2 Increase in Steam-Turbine Operating Temperatures During Past 45 Years

the austenitic steels are used, as has been done for the shells and steam leads of a number of turbines at the 1050 F level, there results an increase in material cost, and, in addition, fabricating and operating difficulties, peculiar to the metallurgy of the austenitic steels, may arise.

In view of these characteristics of the more common steels generally available for high-temperature service, and of the large amount of capacity now being built for 1000 F and 1050 F operation, it is evident that there is much to be gained by the use of a stronger ferritic steel for turbine shells, steam leads, and station piping. It is the purpose of this paper to describe a chromium-molybdenum-vanadium steel which the authors' company has been using for turbine construction at the 1000 F and 1050 F levels.

Chromium-Molybdenum-Vanadium Ferritic Steel

The addition of vanadium to the chromium-molybdenum steel to make an age-hardening alloy which is stronger at high temperatures than the vanadium-free chromium-molybdenum steel is relatively well known as such steels have been used for high-temperature bolting for more than ten years. In 1945 the company with which the authors are associated introduced a va-

[1] Assistant Division Engineer, Steam Turbine Engineering Division, General Electric Company, Mem. ASME.

[2] Section Engineer, Schenectady Works Laboratory, General Electric Company.

Contributed by the Power Division and presented at the Annual Meeting, New York, N. Y., November 26–December 1, 1950, of The American Society of Mechanical Engineers.

Note: Statements and opinions advanced in papers are to be understood as individual expressions of their authors and not those of the Society. Manuscript received at ASME Headquarters, Oct. 12, 1950. Paper No. 50—A-76.

nadium-containing steel for its turbine shells and valve castings at the 1000 F level. This was a molybdenum-vanadium steel with a per cent chemical composition of 0.20 C max, 1.0 Mo, 0.20 V, and a number of units have been installed at 1000 F with this composition. High-temperature tests indicate that this alloy is superior in high-temperature properties to the more common ferritic steels, with their customary heat-treatments, particularly at the 1000 F temperature level and higher. Since this molybdenum-vanadium alloy had adequate high-temperature strength and satisfactory response to heat-treatment for the intended service, chromium was deliberately omitted in order to minimize welding difficulties with these large castings. In the absence of chromium, graphitization resistance was obtained by prohibiting entirely the use of aluminum deoxidization, and a high-temperature normalizing treatment was used. In addition, it was expected that the vanadium as a carbide former would also contribute to the graphitization resistance. There has been no case in which graphitization has ever occurred in this aluminum-free molybdenum-vanadium cast steel although welded specimens have been exposed in the laboratory to 1100 F for more than 20,000 hr.

Shortly after the introduction of the molybdenum-vanadium cast steel, it was pointed out that a similar alloy in piping form would be of benefit to the power-generation industry since the superior high-temperature properties would contribute to thinner pipe walls. The authors' company accordingly assumed the obligation of developing this steel, and using it for turbine steam leads at 950 F and 1000 F in order to obtain field experience. The composition of the piping steel was similar to that of the cast steel. On the basis of experience with the cast steel, chromium was also omitted from the piping steel, although aluminum deoxidization was permitted to the extent of 0.5 lb of aluminum per ton of steel.

Late in 1948 two cases of minor graphitization, which will be discussed in detail later, were discovered in laboratory weld specimens, and early in 1949 the molybdenum-vanadium piping steel was modified by the addition of one per cent of chromium, and its per cent composition then became 0.15 C max 1.0 Cr, 1.0 Mo, 0.20 V. In 1950 the molybdenum-vanadium casting steel was likewise modified by the addition of one per cent of chromium, although no graphitization has ever been found in this cast steel. High-temperature tests of the chromium-molybdenum-vanadium alloy showed it to be similar to its molybdenum-vanadium predecessor in possessing excellent high-temperature strength, and, the authors' company has been actively applying the cast alloy in turbine shells and valves, and has adopted it as its standard alloy for such applications at the 1000 F temperature level. Steam leads of the chromium-molybdenum-vanadium piping alloy are being installed on a number of units for 1000 F operation in order to obtain field experience with this alloy. In addition to the use of this chromium-molybdenum-vanadium alloy for castings and steam leads at the 1000 F level, the authors' company is also using it for the construction of several 1050 F totally ferritic machines in which the design has been held to the stress levels commensurate with the high-temperature long-time strength of this material. In this respect, the chromium-molybdenum-vanadium alloy is displacing, for at least some of the 1050 F units now in design, the austenitic steels customarily used for turbine shells, valves, and steam leads at this temperature level.

With some manufacturing and fabricating experience now available on this steel, and with high-temperature data available to establish its high-temperature strength, it was felt that publication should be made at this time describing the characteristics of this alloy. Although the development of the cast and piping forms of this chromium-molybdenum-vanadium alloy are closely interwoven, this paper is restricted to piping steel. In addition to the characteristics of the chromium-molybdenum-vanadium steel, test data and operating experience with the chromium-free molybdenum-vanadium steel will also be presented. Sufficient high-temperature test data are available to establish the high-temperature properties of the chromium-containing alloy, but they can be reinforced considerably by a study of the corresponding data on the molybdenum-vanadium steel. In a similar manner, operating experience with the molybdenum-vanadium steel is pertinent to a discussion of the chromium-molybdenum-vanadium steel, and will be included.

Operating Experience With Molybdenum-Vanadium Steel

Molybdenum-vanadium steam leads have been in service at 950 F and 1000 F since 1948, and, in general, have performed satisfactorily with respect to fabrication, welding, and service operation. It is relatively well known to the power industry, however, that two cases of minor graphitization of laboratory specimens have been reported with this composition, and a steam lead of this alloy split in June, 1949, while in service at 950 F in the Industrial Canal Station of the New Orleans Public Service, Inc. It is accordingly incumbent on the authors to review these difficulties before further discussing the chromium-molybdenum-vanadium composition.

With respect to the split steam lead, it has been established that a crack almost completely through the wall was in this lead prior to fabrication, and inspection failed to detect it because of the relative insensitivity of the usual commercial methods of testing pipe. The final report on the investigation of this split is being submitted in a companion paper,[3] and the bases upon which the foregoing conclusion was established are discussed in detail in that paper. It should be noted at this point, however, that similar faults have occurred in several other compositions, thereby indicating that the trouble could not be laid on the molybdenum-vanadium chemistry. For example, the ultrasonic inspection method developed during the investigation of the New Orleans split has already located more severe wall cracking in some Type 347 pipe which had successfuly passed the normal commercial inspection methods, and made possible the removal of this pipe from processing prior to any fabrication whatsoever.

The two cases of graphitization of the molybdenum-vanadium alloy occurred in laboratory specimens of pipe welds, and neither of these specimens had been given the complete heat-treatment required by the specifications of the authors' company for this steel. The degree of graphitization in these two cases is shown in Figs. 3*a*, 3*b*, and 4. The graphitization in Figs. (3*a* and *b*) occurred in a laboratory weld specimen which had received no high-temperature treatment and no preheat or postweld treatment, but was tested for graphitization after welding in the condition as received from the pipe mill; this graphitization occurred after 9551 hr exposure at 1100 F, and has progressed no further after approximately 8500 additional hours at 1100 F. The graphitization of Fig. 4 occurred in a laboratory weld specimen which had been given the specified high-temperature treatment except that the preheat and postweld treatment were omitted; this graphitization occurred after 5548 hr exposure at 1000 F and 9000 psi. Since it is generally recognized that the heat-treatment and postweld treatment both contribute to graphitization resistance, it is evident that these specimens were in an unusually susceptible condition. Nevertheless, with these two cases at hand in which the alloy had shown graphitization, even though these were cases in which the complete specified

[3] "Report on Split Steam Lead at New Orleans," by A. W. Rankin and W. A. Reich, presented at the Annual Meeting, New York, N. Y., Nov. 26–Dec. 1, 1950, of The American Society of Mechanical Engineers. Paper No. 50—A-75.

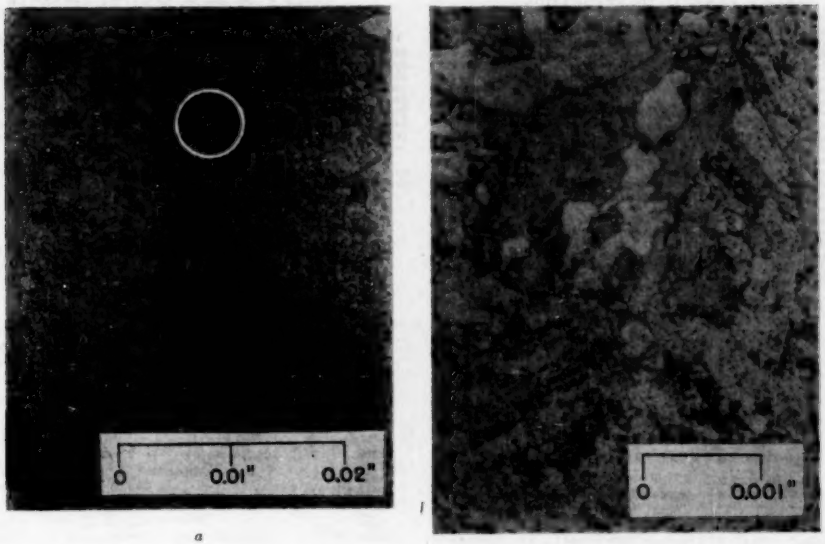

a *b*

FIG. 3 GRAPHITIZATION IN A WELDED LABORATORY SPECIMEN OF WROUGHT MOLYBDENUM-VANADIUM STEEL EXPOSED (UNSTRESSED) TO 1100 F FOR 9551 HR

(*a*, Outer edge of heat-affected area; *b*, circled area of Fig. 3(*a*) at greater magnification. Specimen received no heat-treatment prior to or after welding. Two per cent nital etch.)

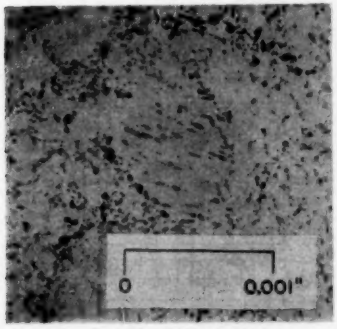

FIG. 4 GRAPHITIZATION IN A WELDED LABORATORY SPECIMEN OF WROUGHT MOLYBDENUM-VANADIUM STEEL EXPOSED TO 1000 F FOR 5548 HR UNDER A STRESS OF 9000 PSI

(Specimen received no postweld heat-treatment. Two per cent nital etch.)

heat-treatment had not been followed, it was decided that chromium would be added to the molybdenum-vanadium composition in order to obtain adequate protection against any inadvertent mishandling in manufacture, fabrication, or assembly. One per cent of chromium was added and, with this addition, the one per cent chromium, one per cent molybdenum, and one-quarter per cent vanadium composition was obtained.

The foregoing review of all the operating vicissitudes which have arisen with the molybdenum-vanadium steel indicates that the general foundation of the chromium-molybdenum-vanadium alloy is sound. The split in the New Orleans steam lead cannot be laid to the molybdenum-vanadium chemistry, and the addition of the chromium should furnish adequate protection against graphitization.

HIGH-TEMPERATURE STRENGTH

High-temperature test data are available from eight test series through which the strength of the chromium-molybdenum-vanadium alloy can be established. Three of these test series are on chromium-molybdenum-vanadium, while the remaining five are on the chromium-free molybdenum-vanadium steel. These tests include rupture tests, flow-rate creep tests, and constant-load creep tests. Some of these tests have been in progress for almost 16,000 hr (approximately two years), and are still running.

These eight test series are identified by "item" numbers (the symbol "CR" after the item number distinguishes the chromium-containing alloys). A general description of these items is given in Table 1; the chemical composition, heat-treatment, and room-temperature physical properties are given in Tables 2, 3, and 4, respectively; the rupture and flow-rate creep strength are given in Tables 5, 6, and 7.

In Fig. 5 are plotted the rupture-test results itemized in Table 5. The full line drawn on this figure is an approximate average of all the data on the chromium-molybdenum-vanadium steel. As an estimate of the strength of this alloy relative to other high-temperature piping steels, the 100,000-hr rupture strength of Type 347 austenitic steel (18 per cent chromium, 11 per cent nickel, columbium-stabilized) has been plotted at the 1100 F temperature.

The chromium-molybdenum-vanadium steel appears from these data to be somewhat stronger than the chromium-free molybdenum-vanadium steel, particularly at the higher tempera-

TABLE 1 GENERAL IDENTIFICATION

Item	
2370	Molybdenum-vanadium; specimen from a commercial heat of piping, silicon-killed; National Tube Company, heat ×22208.
2375	Molybdenum-vanadium; specimen from a commercial heat of piping, silicon-killed; National Tube Company, heat ×22208.
2394 CR	Chromium-molybdenum-vanadium; specimen from an induction heat, aluminum-killed with one pound per ton; General Electric Company, heat 2009.
2395 CR	Chromium-molybdenum-vanadium; specimen from an induction heat, aluminum-killed with one pound per ton; General Electric Company, heat 2010.
2398	Molybdenum-vanadium; specimen from an induction heat, aluminum-killed with one pound per ton; General Electric Company, heat 2013.
2399	Molybdenum-vanadium; specimen from an induction heat, aluminum-killed with one pound per ton; General Electric Company, heat 2014.
2491	Molybdenum-vanadium; specimen from a commercial heat of piping, silicon-killed; Babcock & Wilcox Tube Company, heat 26485.
2645 CR	Chromium-molybdenum-vanadium; specimen from a commercial heat of piping, silicon-killed; National Tube Company, heat ×32782.

TABLE 2 PERCENTAGE CHEMICAL COMPOSITION

Item	c	mn	si	cr	mo	v
2370	0.20	0.58	0.26		1.04	0.21
2375	0.20	0.58	0.26		1.04	0.21
2394 CR	0.11	0.49	0.14	1.03	1.10	0.27
2395 CR	0.19	0.37	0.12	0.85	1.10	0.25
2398	0.08	0.44	0.11		1.05	0.28
2399	0.22	0.34	0.18		1.07	0.13
2491	0.11	0.49	0.30		0.99	0.17
2645 CR	0.08	0.48	0.24	0.99	0.86	0.21

TABLE 3 HEAT-TREATMENT

Item	Heat-treatment
2370	1922 F (1050 C), 4 hr, air cool; 1202 F (650 C), 4 hr, furnace cool
2375	1922 F (1050 C), 4 hr, furnace cool to 1742 F (950 C), air cool 1202 F (650 C), 4 hr, furnace cool
2394 CR	1922 F (1050 C), 4 hr, air cool; 1202 F (650 C), 4 hr, furnace cool
2395 CR	1922 F (1050 C), 4 hr, air cool; 1202 F (650 C), 4 hr, furnace cool
2398	1922 F (1050 C), 4 hr, air cool; 1202 F (650 C), 4 hr, furnace cool
2399	1922 F (1050 C), 4 hr, air cool; 1202 F (650 C), 4 hr, furnace cool
2491	1922 F (1050 C), 4 hr, air cool; 1202 F (650 C), 4 hr, furnace cool
2645 CR	1922 F (1050 C), 2 hr, air cool; 1300 F (704 C), 12 hr, furnace cool

TABLE 4 ROOM-TEMPERATURE PHYSICAL PROPERTIES

Item	Ultimate strength, psi	Proportional limit, psi	Elongation in 2 in., per cent	Reduction of area, per cent
2370	143,900	114,900	23.5	60.1
2375	139,900	109,900	21.0	62.3
2394 CR	86,400	39,900	24.5	60.6
2395 CR	133,900	82,400	15.5	42.5
2398	74,900	46,900	30.0	66.5
2399	116,900	69,900	17.0	40.4
2491	115,400	71,000	21.0	58.6
2645 CR	83,900	54,400	27.0	73.9

tures, and this is a result which had not been counted on originally as it is believed in many quarters that chromium does not add appreciably to high-temperature strength. In the present case, however, it is believed that the chromium has combined with the molybdenum and vanadium to form a complex carbide which maintains its strength at higher temperatures than its chromium-free counterpart. In particular, the 1100 F rupture strength of the chromium-containing material is unusually high and even compares favorably with the austenitic steel at this temperature. In view of the fact that only one test point is available at this temperature, however, it does not appear justifiable to take full advantage of the strength shown at this temperature by the chromium-molybdenum-vanadium alloy. For this reason, the suggested average curve is drawn considerably below the 1100 F strength shown at this temperature by the 2645 CR test.

In Fig. 6 are plotted the flow-rate creep-test results itemized in Table 6 for a creep rate of 10^{-7} per hr (one per cent per 100,000 hr). Again, an approximate average curve is drawn for the test data of the chromium-molybdenum-vanadium steel.

Fig. 7 is similar to Fig. 6, but with the flow rate creep strength evaluated for 10^{-8} per hr (0.1 per cent per 100,000 hr) rather than the 10^{-7} per hr as in Fig. 6.

Figs. 8 and 9 show the results of constant-load creep tests conducted at 1000 F and 1100 F, respectively. Plotted on these

TABLE 5 100,000-HR RUPTURE STRENGTH

(Figures in parentheses give duration of test)

Item	900 F	1000 F	1100 F
2370		18,300 psi (16,746 hr)	
2375		20,000 psi (13,737 hr)	
2394CR	52,500 psi (7728 hr)	29,000 psi (9456 hr)	
2395CR	86,000 psi (11,013 hr)	33,000 psi (4756 hr)	
2398	54,000 psi (10,238 hr)	22,500 psi (7315 hr)	
2399	61,000 psi (12,627 hr)	28,000 psi (7078 hr)	
2491	67,000 psi (1158 hr)	33,000 psi (5942 hr)	11,500 psi (5963 hr)
2645CR	40,000 psi (2956 hr)	23,000 psi (2767 hr)	21,200 psi (2242 hr)

NOTE: The stresses given in this table are the values of the 100,000-hr rupture strength as extrapolated from tests whose duration was as shown by the figures in parentheses.

TABLE 6 FLOW-RATE CREEP STRENGTH

10^{-7}/hr (1.0% per 100,000 hr)

(Tests at approximately constant total strain of 0.2%)

Item	900 F	1000 F	1100 F
2370	39,000 psi	20,800 psi	
2375		21,800 psi	
2394 CR		21,000 psi	
2395 CR		25,800 psi	
2398		17,300 psi	
2399		18,300 psi	
2491		24,500 psi	10,300 psi
2645 CR	34,800 psi	23,000 psi	10,500 psi

TABLE 7 FLOW-RATE CREEP STRENGTH

10^{-8}/hr (0.1% per 100,000 hr)

(Tests at approximately constant total strain of 0.2%)

Item	900 F	1000 F	1100 F
2370	24,500 psi	12,400 psi	
2375		12,000 psi	
2394 CR		14,400 psi	
2395 CR		18,800 psi	
2398		12,300 psi	
2399		12,800 psi	
2491		12,400 psi	5,300 psi
2645 CR	31,500 psi	18,000 psi	5,900 psi

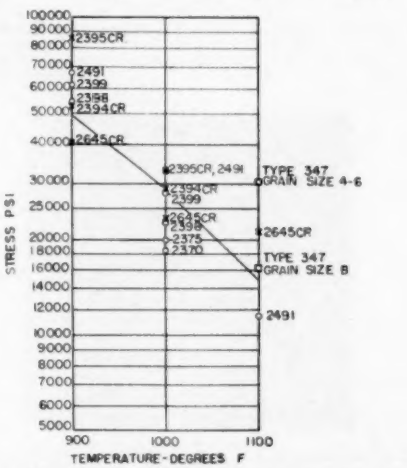

FIG. 5 100,000-HR RUPTURE STRENGTH OF MOLYBDENUM-VANADIUM STEEL (CIRCLES), CHROMIUM-MOLYBDENUM-VANADIUM STEEL (CROSSES), AND TYPE 347 AUSTENITIC STEEL (SQUARES, 1100 F ONLY)

(Data on Type 347 steel taken from Timken "Digest of Steels," 1946.)

figures are per cent plastic strain versus time in hours. As can be seen, the tests on the molybdenum-vanadium steel have been running for approximately 16,000 hr (2 years); it is planned to continue these tests to about 25,000 hr (3 years). The tests on the chromium-molybdenum-vanadium steel have been in progress, as of October 2, 1950, for only about 3500 hr, but it is planned to continue these tests also to approximately 25,000 hr.

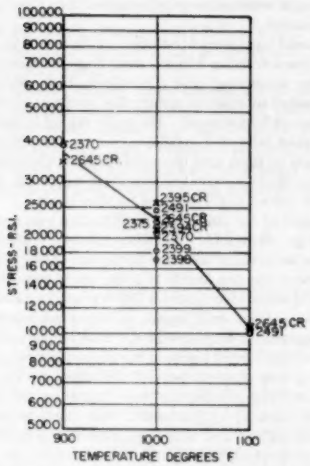

FIG. 6 FLOW-RATE CREEP STRENGTH FOR RATE OF 10^{-7} PER HR (ONE PER CENT PER 100,000 HR) FOR MOLYBDENUM-VANADIUM STEEL (CIRCLES) AND CHROMIUM-MOLYBDENUM-VANADIUM STEEL (CROSSES)

(Tests made at an approximately constant total strain of 0.2 per cent.)

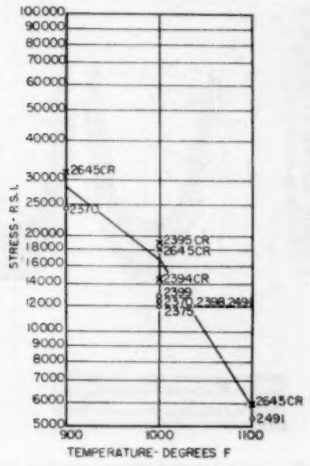

FIG. 7 FLOW-RATE CREEP STRENGTH FOR RATE OF 10^{-8} PER HR (0.1 PER CENT PER 100,000 HR) FOR MOLYBDENUM-VANADIUM STEEL (CIRCLES) AND CHROMIUM-MOLYBDENUM-VANADIUM STEEL (CROSSES)

(Tests made at an approximately constant total strain of 0.2 per cent.)

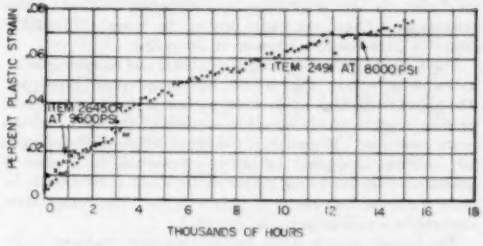

FIG. 8 1000 F CONSTANT-LOAD CREEP TESTS, FOR MOLYBDENUM-VANADIUM STEEL (DOTS), AND CHROMIUM-MOLYBDENUM-VANADIUM STEEL (CROSSES)

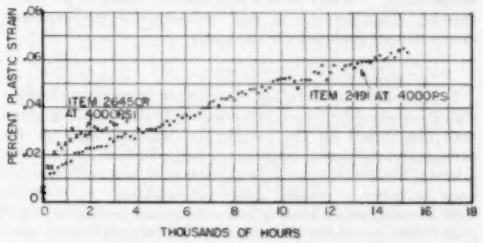

FIG. 9 1100 F CONSTANT-LOAD CREEP TESTS FOR MOLYBDENUM-VANADIUM STEEL (DOTS), AND CHROMIUM-MOLYBDENUM-VANADIUM STEEL (CROSSES)

SPECIFICATION PROPERTIES

The chromium-molybdenum-vanadium pipe specification in current use by the authors' company requires the following percentage chemical composition: carbon, 0.15 max; manganese, 0.30–0.60; phosphorus, 0.035 max; sulphur, 0.035 max; silicon, 0.10–0.35; chromium, 0.80–1.20; molybdenum, 0.80–1.10; vanadium, 0.15–0.25.

Aluminum deoxidization is restricted to one-half pound of aluminum per ton of steel.

The basic electric process of melting which was used for the production of the original molybdenum-vanadium piping has also proved satisfactory for the chromium-molybdenum-vanadium alloy. Silicon was used for deoxidization because of the aluminum restriction.

The normal manufacturing process used for medium alloys is satisfactory for billet manufacture, hot piercing and rolling. Like the molybdenum-vanadium alloys, the chromium-molybdenum-vanadium exhibits pronounced age-hardening during tempering. Accordingly, after hot-rolling and before cold-straightening, the pipe is held at 1650 F (899 C) for one hour, and furnace-cooled or cooled in still air. This treatment, which results in a hardness in the neighborhood of 150 Brinell, produces sufficient notch toughness to minimize the possibility of cracking during the cold-straightening operation. After this 1650 F (899 C) treatment, the minimum physical properties are specified as follows: tensile strength, 60,000 psi; yield strength (0.02 per cent offset), 25,000 psi; elongation (0.5-in-diam test specimen), 15 per cent (long) 10 per cent (trans.).

A flattening test is required by this specification in which the constant e (deformation per unit length) is maintained at 0.08 which corresponds to the value used for piping steels listed in the ASTM specifications A106, A158, A280.

FABRICATION AND HEAT-TREATMENT

For fabrication operations such as hot-bending, only the normal practice for medium-alloy steels is required. After the hot-bending operation, the pipe is held for two hours minimum in the range 1877–1967 F (1025–1075 C), and air-cooled. When desired, this treatment may be modified to permit furnace-cooling to 1742 F (950 C), followed by air-cooling. After the normalizing

treatment, the pipe is subjected to a tempering treatment which consists of a 12-hr (min) hold within the range 1275–1325 F (690–719 C), followed by furnace or air-cooling.

The purpose of the foregoing normalizing and tempering treatment is to obtain the desired high-temperature properties. The object of the high-temperature portion of this treatment is to produce a substantially complete solution of the alloy carbides in the austenite. This solution treatment, followed by cooling in air, enables subsequent tempering treatments to produce a pronounced age-hardening characteristic which is believed to be of fundamental importance in obtaining good high-temperature strength in a vanadium-containing steel.

The tempering part of the high-temperature treatment is designed to produce overaging to well below the peak hardness in order to obtain the best compromise between notch toughness at low temperature and good creep and rupture strength at high temperature. Further details regarding the study of the heat-treating characteristics of this chromium-molybdenum-vanadium alloy are given later in this paper.

Welding

No unusual difficulties are encountered in welding provided that the electrode, preheat, and postweld treatments are selected with due regard for the metallurgical characteristics of this chromium-molybdenum-vanadium alloy. Because of the considerable hardenability exhibited by this steel, proper precautions must be taken to prevent underbead cracking. An electrode with a low-hydrogen coating and a minimum preheat of 482 F (250 C) are specified in the fabrication instructions for this steel, and sound welds have been obtained consistently with these precautions. In order to obtain as uniform a structure and composition in the welded joint as is practicable, the per cent composition of the deposited weld metal is specified as 0.5 chromium, 1.0 molybdenum, 0.25 vanadium. The lower chromium content of the weld deposit results in somewhat easier welding, and is justified by the findings of many investigators that welds in piping are more resistant to graphitization than base metal of the same composition.

The postweld treatment must take cognizance of the secondary hardening characteristics which a vanadium-containing alloy exhibits during tempering, and a relatively high postweld treatment is required in order to reduce the hardness of the weld deposit and heat-affected zone. Since the piping is welded in the normalized and tempered condition, only a subcritical postweld treatment can be used, and the welding instructions for this steel specify a postweld treatment of four hours minimum in the range 1275–1325 F (690–719 C) followed by slow cooling.

Photographs of the procedure qualification test specimens are shown in Figs. 10 and 11. Ductility values are obtained which are comparable to those obtained in the less-strong alloy steels in all tests except the free bend. In the latter test, although the specimen withstood successfully a 180-deg bend without cracking, the elongation of the weld deposit is somewhat less than the 30 per cent required by various codes. This is not indicative of a deficiency in ductility of the weld metal, but is simply a result of the age-hardening characteristic of this alloy during tempering. During the welding process, the weld deposit experiences a high-temperature normalizing treatment, while the base metal, which is already normalized and tempered, experiences further tempering during the postweld treatment. Accordingly, the base metal is not as hard as the weld deposit, and during the free-bend test the major portion of the deformation will occur in the base metal. The welding instructions of the authors' company recognize this characteristic, and require an elongation of only 20 per cent in the free-bend test. That the weld is sound and satisfactory for the intended service is shown by its ability to take a 180-deg bend without cracking.

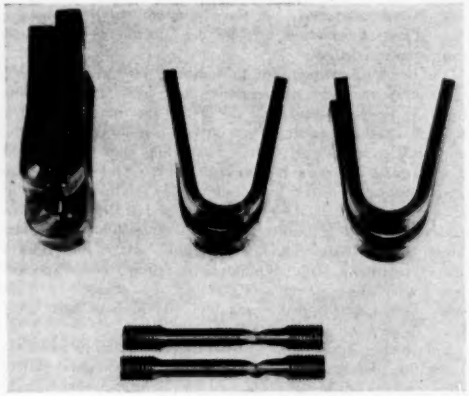

Fig. 10 Weld Qualification Tests on Chromium-Molybdenum-Vanadium Steel

(Metal-arc-welded in fixed horizontal position using electrode of 1/2 per cent chromium, 1 per cent molybdenum, 1/4 per cent vanadium. *Upper left:* free bends; *upper right:* side bends; *lower:* transverse tensile tests.) Free-bend elongation: 27.3% and 32.0%

Results of Transverse Tensile Tests

Ultimate strength	Yield strength	Elongation in 2 in.	Reduction of area
74,900 psi	43,900 psi	21.5%	78.0%
70,400 psi	42,400 psi	20.0%	78.3%

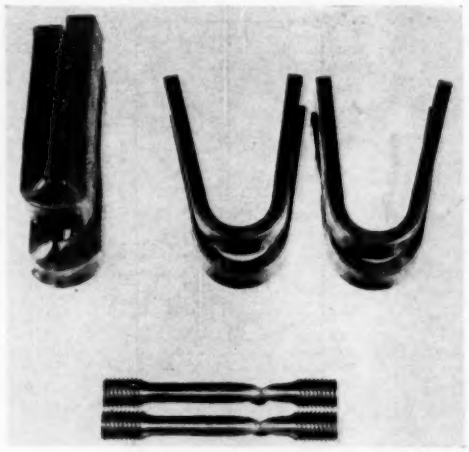

Fig. 11 Weld Qualification Test on Chromium-Molybdenum-Vanadium Steel

(Metal-arc-welded in fixed vertical position using electrode of 1/2 per cent chromium, 1 per cent molybdenum, 1/4 per cent vanadium. *Upper left:* free bends; *upper right:* side bends; *lower:* transverse tensile tests.) Free-bend elongation: 21.5% and 23.0%

Results of Transverse Tensile Tests

Ultimate strength	Yield strength	Elongation in 2 in.	Reduction of area
73,900 psi	45,900 psi	16.0%	78.2%
72,900 psi	42,900 psi	20.5%	78.3%

Heat-Treating Characteristics

Studies of the heat-treating characteristics of this alloy were obtained on specimens taken from the production heat of piping of item 2645 CR, Table 2.

In Fig. 12 Brinell hardness curves are plotted for this alloy as functions of time at a tempering temperature of 1300 F (704 C) when air-cooled from normalizing temperatures of 1742 F (950 C), 1832 F (1000 C), 1922 F (1050 C), and 2012 F (1100 C). These curves illustrate the increased hardening which occurs with increasing normalizing temperatures. In addition, a hardness

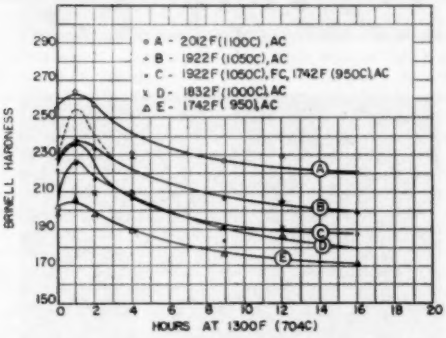

Fig. 12 Hardness Versus Tempering Time at 1300 F (704 C) for Normalized Chromium-Molybdenum-Vanadium Steel

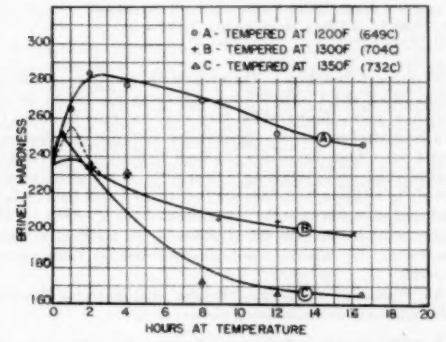

Fig. 13 Hardness Versus Tempering Time at Various Tempering Temperatures for Chromium-Molybdenum-Vanadium Steel Normalized From 1922 F (1050 C)

curve is shown for the condition of furnace-cooling from 1922 F (1050 C) to 1742 F (950 C) followed by air-cooling. This latter curve justifies the permissible production practice of heat-treating in this manner to minimize deterioration of the furnaces.

In Fig. 13 Brinell hardness curves are plotted for specimens tempered for various lengths of time at 1200 F (649 C), 1300 F (704 C), and 1350 F (732 C) after air-cooling from a normalizing temperature of 1922 F (1050 C).

The Charpy impact test, performed in a 220 ft-lb pendulum-type testing machine using the standard keyhole specimen, was used as a qualitative measure of notch ductility. Table 8 lists impact energy, temperature of test, Brinell hardness, and heat-treatment for several longitudinal specimens taken from the aforementioned production heat. Fig. 14 is a plot of the impact energy versus temperature for various conditions of heat-treatment. Investigators have described this characteristic of metals by the term "transition temperature." In the plot of impact energy versus temperature, the transition temperature has been variously described as the temperature at which the impact energy begins to decrease, decreases to a minimum or to half the maximum value, or when the fracture changes from the ductile type to a brittle cleavage, etc. In the opinion of the authors and their associates, a rough correlation can be established between the transition temperature of a material and the tendency for cracks to propagate through it during welding and forming operations. In general, the lower the transition temperature, the less is the crack propagating tendency. Materials with high transition temperatures require more careful handling and higher preheats in welding. The welding preheat temperature is placed well above the transition temperature as determined in the Charpy-impact test. This is necessary, in the authors' opinion, because forming and welding operations often impose more severe multiaxial stress conditions than does the Charpy-impact test, and it is well known that the transition temperature is markedly affected by acuity of notch as well as by speed of application of the stress system. It should be emphasized that the keyhole charpy test is used by the authors in a qualitative manner to describe and compare notch toughness because of the relative ease of making the test specimens and performing the test. It is not felt that this or any of the many other tests of this sort in current use is capable of more than a qualitative measure of the ability of a material to withstand all of the complex conditions imposed during pipe manufacture and assembly.

TABLE 8 AVERAGE KEYHOLE CHARPY IMPACT ENERGY (FT LB)

Temperature	Condition of heat-treatment D	B	C	A
−13 F (−25 C)			6	6
32 F (0 C)			10	
77 F (25 C)	3	20	27	65
122 F (50 C)	9	38	43	87
212 F (100 C)	40	50	45	75
302 F (150 C)	48	58	45	75
392 F (200 C)	48	50	45	90

A, 1652 F (900 C), annealed; 125 Brinell
B, 1922 F (1050 C), air cool; 1300 F (704 C), 20 hr; 180 Brinell
C, 1832 F (1000 C), air cool; 1300 F (704 C), 12 hr; 175 Brinell
D, 1922 F (1050 C), air cool; 1300 F (704 C), 4 hr; 220 Brinell

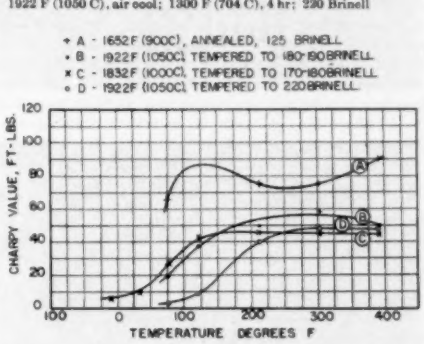

Fig. 14 Keyhole Charpy Impact Energy Versus Temperature for Heat-Treated Chromium-Molybdenum-Vanadium Steel

Again referring to Fig. 14, the annealing treatment is shown to be effective in giving good notch ductility to the material to enable it to withstand the operations of cold-straightening, shipping, and handling. When the 1922 F (1050 C) treatment is used to produce the high-temperature strength, notch toughness can be obtained by tempering to 175–200 Brinell. The regular temper-

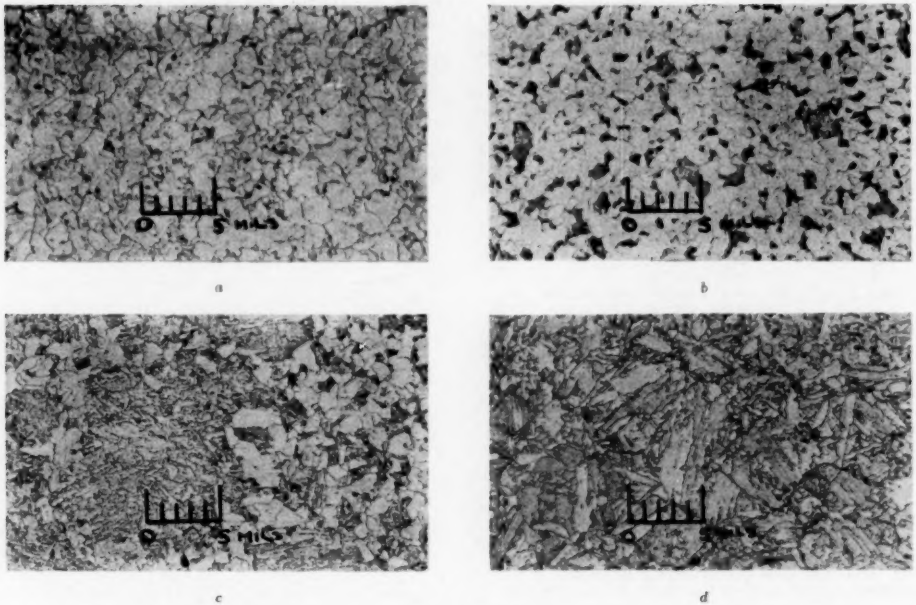

FIG. 15 MICROSTRUCTURES OF CHROMIUM-MOLYBDENUM-VANADIUM STEEL AFTER VARIOUS HEAT-TREATMENTS
[*a*, Furnace-cooled from 1652 F (900 C), ×100; *b*, air-cooled from 1832 F (1000 C), ×100; *c*, air-cooled from 1922 F (1050 C), ×100; *d*, air-cooled from 2012 F (1100 C), ×100.]

ing treatment of 12 hr minimum at 1300 F (704 C) serves to bring the hardness into this range for service conditions.

The microstructures obtained after various heat-treatments are shown in Fig. 15.

ACKNOWLEDGMENT

The authors take great pleasure in acknowledging the contributions of the many persons who contributed to this development, including the engineers of the Public Service Electric and Gas Company, New Jersey. In particular, advice on manufacture and assembly was obtained from the engineers of several pipe mills and fabricators. Specific acknowledgment is made of the contributions of Messrs. R. M. Curran, W. L. Fleischmann, G. C. Naylon, D. L. Newhouse, B. R. Seguin, and J. L. VanUllen of the General Electric Company.

Discussion

H. S. BLUMBERG.[4] The authors of this paper and the General Electric Company are to be complimented for their progressive approach in the development of a new piping material for the increasingly high temperatures at which steam power is being more efficiently generated.

This paper gives a logical presentation of the background for the selection of this Cr-Mo-V steel, the outstanding characteristic of which is its superior high-temperature strength at temperatures at which units are being currently constructed and operated. The authors have described in some detail the specification limits for fabrication operations, and there is no need therefore to repeat these here. The writer's company has been fabricating Mo-V and Cr-Mo-V compositions in production for the past four years, during which time steel has been furnished by two large steel producers. Several thousand feet of pipes from over a dozen heats have been processed by hot-bending, welding, heat-treating, and machining. Bent sections are ultrasonically tested; in addition, test rings are heat-treated with each furnace load and photomicrographs are submitted for approval by the customer as a check on the response of the material to heat-treatment. No difficulty has been experienced in handling this material.

An evaluation of the potentialities of any piping material takes into account the following phases:

1 Mill behavior and characteristics: (*a*) in melting and casting, (*b*) in hot-working to pipe, (*c*) heat-treatment, and (*d*) room-temperature properties as an index of quality.

2 Fabrication behavior and characteristics: (*a*) in hot-bending, (*b*) in cold-bending, (*c*) in forging, (*d*) in welding, (*e*) in heat-treatment, and (*f*) in machining.

3 Service behavior and characteristics: (*a*) load-carrying ability, (*b*) surface stability, and (*c*) structural stability.

A review of our observations of these two compositions in the light of the foregoing is here briefly given. A sufficient number of melts and pipes have now been processed by the steel mills to indicate that the mill behavior of the Cr-Mo-V steel is controllable to give piping of desirable characteristics. By application of a normalizing or annealing heat-treatment, the steel reaches the fabricator in a ductile condition with desirable impact values at ordinary temperatures. The inclusion of ultrasonic testing at the mill insures a more thorough inspection than has been

[4] Head, Materials and Metallurgical Engineering Division M. W. Kellogg Company, Jersey City, N. J.

the case heretofore. Fabrication behavior and resulting characteristics of the steel are understood; current inspection methods, with the addition of ultrasonic testing, appear to be adequate. Knowledge regarding characteristics for service is available from the results of laboratory high-temperature test data reported by the authors and others in the U. S. A. and abroad. In addition, this steel has service background already mentioned. There is agreement regarding the high load-carrying ability of the steel at current steam-generating temperatures, and there appears to be no unusual behavior of the material in relation to surface and structural stability at operating temperatures.

The behavior of this steel which requires the most careful consideration is one which has been dealt with in detail by the authors in their paper. It has been shown that a close relationship exists between time and temperature in the tempering operation and (*a*) high-temperature strength, (*b*) notch sensitivity at ordinary temperatures, and (*c*) ability to satisfactorily pass weld bend tests required by conventional specifications.

Paradoxically, these relations act in opposite directions, in that the treatment which gives the best high-temperature properties acts to yield the poorest notch sensitivity and weld ductility. The authors have logically chosen a compromise heat-treatment which sacrifices some high-temperature strength in favor of improved notched-bar impact properties. Careful control of this phase of heat-treatment is necessary, but this is not an unusual requirement. Shops which are equipped properly are able to control their procedures to insure that specified heat-treatments are carried out, with records thereof. In conclusion, one may say that the outstanding high-temperature strength of the ferritic steel fostered by the General Electric Company is extremely attractive.

Ernest L. Robinson.[5] The writer desires to point out the continuity between this paper and one prepared by himself three years earlier.[6] This earlier paper gave the preliminary results of certain long-time rupture tests on plain moly-vanadium material which have since been completed so that they are now reported in final form by Rankin and Reich.

The sequence of estimated long-time strengths as the tests progressed and successively attained greater validity is of interest.

PREDICTED 100,000-HR RUPTURE STRENGTH PSI. AT 1000 F
(1% Mo, 0.2% V)

Item no.	Date of prediction July, 1947	Sept., 1948	Final
2370	18,500	13,000	18,300
2375	23,000	15,000	20,000

In recording the low values in September, 1948, the writer, in his closure at that time, noted that "any further breaks in the still unbroken bars can only improve these results which still show a marked superiority of moly-vanadium over the low-chromium-molybdenum compositions." When the final breaks came, they showed the writer had been unduly conservative in his estimate based on unbroken bars.

Now, with the addition of 1 per cent of chromium, the results are even better.

E. H. Krieg[7] and F. F. Dedrick.[8] Messrs. Rankin and Reich are to be congratulated on the fine paper they have presented.

It is to be hoped that the chrome-molybdenum-vanadium steel soon will be listed in the various allowable stress tables of the ASME Boiler Code and the Code for Pressure Piping. Such listings give a widespread use of the material and make it possible for the designer to use it readily without requiring a great deal of effort to obtain the necessary basic data.

With two cases of graphitization of molybdenum-vanadium weld specimens in mind and recognizing that these specimens were in a susceptible condition because of lack of heat-treatment or postweld treatment, the authors state it has been decided to add chromium to the molybdenum-vanadium composition to obtain adequate protection against any inadvertent mishandling in manufacture, fabrication, or assembly. It would be of interest to know what mishandling the authors contemplate would be corrected by adding chromium.

H. D. Newell.[9] The writer has read with interest the description of the high-temperature properties and characteristics of a ferritic steam-piping steel which is a chromium-containing modification of the earlier molybdenum-vanadium alloy steel which had been used by General Electric Company for that purpose. One would agree that the more common ferritic steels such as the 1¼ per cent chromium, 2 per cent chromium, and 2¼ per cent chromium steels with molybdenum, with their customary heat-treatments, require heavy walls for 1000 and 1050 F steam service to maintain the required margins on creep and rupture strength to the extent that a new stronger steel of ferritic type would be welcomed by industry. The chromium addition should provide insurance against the possibility of graphitization which appears to be a possibility in the straight molybdenum-vanadium composition. Perhaps more will be known on this when the present molybdenum-vanadium piping installations have had a more extended sojourn at service temperature.

The split steam lead at New Orleans of molybdenum-vanadium steel, mentioned in this paper, was due to a brittle crack partly through the pipe wall which was formed prior to installation. The susceptibility to such brittle cleavage fracture is undoubtedly related to the chemical composition of the molybdenum-vanadium steel and was influenced to a considerable extent by the heat-treatment given which resulted in a high transition temperature and low notch strength at ordinary temperature. Annealed steel of the same composition has adequate impact strength at or about room temperature. That this characteristic is also present in the chromium modification appears evident from the data given in the paper (see Table 8) but can be improved by modification of heat-treatment to either annealing or to a more extended tempering time following the air cool from high temperature. As pointed out by the authors, greater care in handling and higher preheats in welding would be required and such practices would be warranted in order to gain the advantages of high creep and rupture strength in this steel.

In considering the possible use of the chromium-molybdenum-vanadium steel for superheater application, one is led to ask what the properties of this new steel would be in the fully annealed condition at temperatures of 1000 F and 1100 F. Manufacture of superheater sections involves considerable welding, forming, hot-bending, and it would be necessary thereafter to submit the completed section to the high-temperature treatment followed by tempering at 1300 F. Such a heat-treatment would likely result in considerable scaling and distortion where built-up sections comprising several loops would be involved. Since we are presently using ferritic superheater materials to 1100 F, one is led

[5] Structural Engineer, Turbine Engineering Divisions, General Electric Company, Schenectady, N. Y. Fellow ASME.

[6] "Some 1000 F Steam-Pipe Materials," by Ernest L. Robinson, Trans. ASME, vol. 70, 1948, pp. 855–865.

[7] Stone & Webster Engineering Corporation, Boston, Mass. Fellow ASME.

[8] Stone & Webster Engineering Corporation, Boston, Mass. Mem. ASME.

[9] Chief Metallurgist, The Babcock & Wilcox Tube Company, Beaver Falls, Pa.

also to ask how permanent the high-strength properties might be at that temperature level when tests have been extended through 10,000 hr or more. Results of longer-time tests will be awaited with interest as well as comment by the authors as to whether the high-strength characteristics of this steel are principally due to composition or are in large measure due to the special heat-treating practices employed for their particular applications. The elongation values obtained in rupture testing on the heat-treated steel and the annealed steel would be of considerable interest to those contemplating the use of this new composition.

C. L. CLARK.[10] As the authors have indicated chrome-molybdenum-vanadium steels are not new in so far as high-temperature service applications are concerned. The writer's company has produced a steel of this type for many years, designated as 17-22A, for bolting and similar applications and, during the past few years, the lower-carbon variety of this steel (0.28/0.33 C) has been widely used for the braking disk in heavy bombers and high-speed planes. This steel differs from the authors' in that it contains 0.50, rather than 1.0 molybdenum, and has a silicon content of 0.55/0.75 per cent.

In all of the work that we have done, including that on Mo-V and Cr-Mo-V type steels it has been found that for a given type of heat-treatment and a given type of analysis both the creep and rupture strength at 900 and 1000 F are directly proportional to the room-temperature hardness. This does not appear to be true with the authors' results. For example, Heats 2370 and 2399 having respective hardness values of about 280 and 230 Brinell, as indicated by their room-temperature strength values, Table 4, have respective rupture-strength values at 1000 F of 18,300 and 28,000 psi. Since those two heats were given the same heat-treatment, Table 3, and possessed essentially the same composition, Table 2, it would be interesting to know the authors' explanation for their differences in hardness.

With the Cr-Mo-V steels the rupture strengths at both 900 and 1000 F do appear to be proportional to the hardness so the question again arises as to what hardness level can be permitted in piping systems. In so far as pipe is concerned, most ASTM specifications limit the hardness, by specifying tensile and ductility values, to 179 Brinell max even in the more highly alloyed steels of the 7.0 and 9 Cr grades. In the authors' work the maximum rupture strength was obtained with 270 Brinell although the values at a Brinell level of 170 (Heat 2394 Cr) were also very acceptable.

J. J. HELLER.[11] The Cr-Mo-Va steels, such as those described by the authors, hold forth promise for high-temperature service in the steam-power industry.

The writer would like to comment on the rupture strengths observed for the Cr-free Mo-Va steels. The scattering of data in the authors' results, the difference in rupture strength when compared to other work on Mo-Va steels, and work at the University of Michigan all tend to indicate that the test results on these steels are rather sensitive to the heat-treated condition in which they are tested. The authors' results appear to indicate, in general, higher strengths than were observed for comparable steels both at the University of Michigan and also in England, by Glen. However, the results of these various investigations are not exactly comparable. The heat-treating temperature, both for normalizing and tempering, differed, and Glen's work was carried out on $^1/_2$Mo-$^1/_4$Va steel rather than 1Mo-$^1/_4$Va. Comparison is also difficult as the majority of the authors' data are at 1000 F and below, with only one Mo-Va steel, No. 2491, being at 1100 F, while the work at the University of Michigan was at 1050 F, and Glen's work was at 1022 F and 1112 F. However, if steel No. 2491 may be taken as an indication of the results to be expected, the strengths observed are somewhat higher than observed in the work at Michigan and also by Glen.

It is reasonably apparent that the high-temperature strength of the Mo-Va steels is dependent upon the heat-treated condition prior to testing. Work at Michigan indicates comparable strengths between the "as-rolled and tempered" condition and the "normalized and tempered condition"; however, the higher elongation observed in the normalized condition is believed to be desirable. The annealed condition shows markedly lower strengths, especially for short-time period tests, than the normalized condition. It is interesting to note also that the hardness values of the as-rolled and the normalized conditions are comparable, while the hardness of the annealed material is substantially lower. Comparison of the test results and the heat-treating temperatures employed tend to indicate that a more severe tempering produces somewhat lower rupture strengths for short-time periods, but equal or slightly higher strengths for long-time periods; perhaps indicating a more stable structure is developed by more severe tempering.

It is somewhat surprising to note that the authors make no mention of the ductility of either the Mo-Va or the Cr-Mo-Va steels, except as in room-temperature physical tests. The work at Michigan showed very low elongation values in the as-rolled and tempered condition as observed from rupture tests at 1050 F. Elongation values were in the range of 1.5 to 2.0 per cent in 2 in. even for short-time test periods. Normalizing at 1750 F and tempering at 1200 F raised the elongation values to 10 to 15 per cent for test periods less than 1000 hr and 7.5 to 8.0 per cent for test periods beyond 1000 hr. These values are in the range of those observed by Glen at 1022 F. It would be interesting to note if the authors observed elongation values in the ranges just indicated.

A. B. WILDER.[12] The development of chromium-molybdenum-vanadium (Cr-Mo-V) steel for piping by the General Electric Company is an important contribution to our knowledge of steels for power-plant service. Utilization of the principle of "age-hardening" in an effort to improve the creep properties of ferritic steels is a logical approach to the problem. Other methods, such as the addition of molybdenum, have been exploited. The useful purpose of chromium additions in controlling oxidation and graphitization of high-temperature alloys is well established. With higher steam-operating temperatures the basic problem is to improve the creep strength of ferritic steel and eliminate the necessity of employing extremely heavy-wall pipe or austenitic alloys.

The stability of age-hardening alloys at high temperatures is a fundamental consideration which requires thorough evaluation. Although the authors have exposed creep specimens for periods exceeding 16,000 hr, additional information of this type is desirable. The writer's company is conducting long-time exposure tests of Cr-Mo-V steel in an effort to further evaluate the stability of this type of material. The importance of evaluating stability with respect to creep is illustrated in Table 9.[13] The creep-rupture strength of coarse-grained $^1/_2$ Cr - $^1/_2$ Mo steel was reduced about 50 per cent after 10,000 hr exposure at 1050 F.

[10] Metallurgical Engineer, Steel and Tube Division, Timken Roller Bearing Company, Canton, Ohio. Mem. ASME.

[11] Engineering Research Institute, University of Michigan, Ann Arbor, Mich.

[12] Chief Metallurgist, National Tube Company, U. S. Steel Corporation Subsidiary, Pittsburgh, Pa.

[13] "Long-Time Elevated Temperature Test of Chromium Molybdenum Steel," by A. B. Wilder and J. O. Light, a paper presented at the Annual Meeting of American Society for Metals, Chicago, Ill., October 24, 1950. (See authors' closure of discussion for creep data.)

TABLE 9 CREEP RUPTURE PROPERTIES OF CR-MO STEELS

Steel[a]	Stress (1000 psi) for rupture in 10,000 hr — 900 F A[a]	900 F B[a]	1050 F A	1050 F B	1200 F A	1200 F B
1/2 Cr–1/2 Mo (12B)	53.5	59.0	11.2	20.0	2.6	3.4
1/2 Cr–1/2 Mo (12D)	51.5	....	8.7	10.2	2.4	2.4
3 Cr–1 Mo (32D)	27.5	29.0	10.5	11.3	5.4	5.1

[a] Steel 12B melted to coarse-grained deoxidation practice. Steels 12D and 52D fine-grained practice. A, exposed 10,000 hr at temperature before creep testing; B, unexposed before creep testing.

TABLE 10 GRAPHITIZATION CHARACTERISTICS OF MO-V AND CR-MO-V STEEL WELDS

Steel	Al[a]	Hr exposure	Graphitization 900 F	Graphitization 1050 F
1 1/2 Mo–1/4 V (55)	0.0	10,000	None	Moderate
		34,000	Slight	Moderate
1 1/2 Mo–1/4 V (56)	0.4	10,000	None	Moderate
		34,000	Moderate	Moderate
1 1/2 Mo–1/4 V (57)	1.3	10,000	None	Moderate
		34,000	Moderate	Slight
1 Mo–1/4 V (70)	0.5	10,000	Trace	Slight
1/2 Cr–1 Mo–1/4 V (81)	0.0	10,000	None	None

[a] Lb/N.T. aluminum used for deoxidation.

However, the creep-rupture properties of the 1/2 Cr - 1/2 Mo steel, made to a fine-grained deoxidation practice, was less affected and the 3 Cr - 1 Mo steel was not much changed by the 10,000-hr exposure treatment.

In the development of a new type of steel for high-temperature service the prevention of graphitization must be considered. In Table 10[13,14] are shown results obtained in the heat-affected zone of weld bead tests after long periods of exposure at elevated temperatures. The molybdenum-vanadium (Mo-V) steels showed evidence of graphitization after exposure at 900 F and 1050 F, although in two of the steels very little aluminum was used for deoxidation and in one of the steels no aluminum was used. In the Mo-V steel (70) furnace-cooled from 1925 F to 1750 F and air-cooled to ambient temperature followed by a 1300 F draw, no graphitization was observed. The 1/2 Cr-1 Mo -1/4 V steel did not graphitize after 10,000 hr of exposure at 900 F and 1050 F. Additional exposure tests including 1 Cr-1 Mo-1/4 V steels are in progress. The possibilities of graphitization occurring in the Cr-Mo-V steel described by the authors is remote, as sufficient chromium has been added and very little aluminum used in the deoxidation practice.

With reference to the Charpy impact data shown in Fig. 14 and Table 8 of the paper, it would be desirable, after hot-rolling, to have a minimum Charpy impact value of about 15 ft-lb at ambient temperature. This would reduce the possibilities of cracking the material during processing. After fabrication, the material would be given final heat-treatment and then placed in service.

R. W. Emerson.[15] This paper should be considered as the first milestone along the path toward the achievement of one or more vanadium-bearing material specifications for high-temperature central-station piping. The General Electric Company, who have pioneered in the use of this material for high-temperature steam-turbine-inlet piping, have recognized that precipitation hardening occurs upon tempering of the vanadium-bearing material, and due to this inherent advantage, such materials should receive greater general recognition. In this respect, it is hoped that this paper will stimulate further publications on the metallurgical and physical characteristics of low-carbon vanadium-bearing steels for use in high-temperature service.

This discussion is presented to supplement and confirm the authors' data. The authors, in discussing the welding of the Cr-Mo-V material made reference to its hardenability. The Jominy end-quench hardenability of both the Mo-V and Cr-Mo-V materials is shown in Fig. 16. It is to be noted that end-quenching of the Cr-Mo-V specimen from 1675 F resulted in a relatively low hardenability, whereas quenching from 1950 F produced a relatively high hardenability comparable to that obtained on the Mo-V material quenched from 1675 F. Whereas the carbon content of the Mo-V specimen was somewhat higher than that of the Cr-Mo-V, the difference in the two hardenability curves of the specimens having a comparable quenching temperature is due

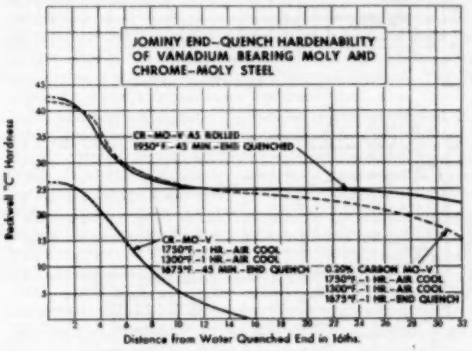

FIG. 16

principally to the extent to which the vanadium carbide went in solution. From Fig. 16 it appears that the vanadium carbide or complex chrome-vanadium carbide in the Cr-Mo-V specimen is more difficultly soluble and requires a higher solution (quenching) temperature than does the Mo-V material.

This was further substantiated in initial tests to determine the precipitation-hardening effects obtained using the Cr-Mo-V analysis. Precipitation-hardening obtained on specimens originally air-cooled from 1800 F was found to be very slight as compared with the marked effect obtained on Mo-V specimens originally air-cooled from the same temperature.

Fig. 17 is presented in substantiation of the marked precipitation hardening of the Mo-V specimens at 1100 and 1200 F following the 1800 F air cool (For chemistry of this material see item 2370, Table 2). The extent to which advantage can be taken of the precipitation-hardening effects of the vanadium-bearing steels, is believed to be primarily a function of the solution temperature used prior to tempering. It is to be noted from Fig. 18 that exceptionally high hardness can be obtained in a 0.10 per cent carbon-moly-vanadium material upon tempering at 1200 F following a 1950 F air cool whereas the same tempering treatment following a 1750 F air cool results in only a moderate increase in hardness (For chemistry of this material see item 2491, Table 2). This variation is believed to be due solely to the extent to which the vanadium (presumably vanadium carbide) has dissolved in the austenite.

To take advantage therefore of the precipitation hardening afforded by the use of vanadium, high normalizing (solution) temperatures are required. If a high solution temperature is not used the primary benefit derived from the use of vanadium is believed to be lost.

A comparison of the 1200 and 1300 F aging curves for the Cr-Mo-V material shown in Fig. 13 reveals a reasonably close check with similar data given in Fig. 19.

Additional data on the mechanical properties of Cr-Mo-V

[14] "Stability of Steel at Elevated Temperatures," by A. B. Wilder and J. D. Tyson, Transactions American Society for Metals, vol. 40, 1948, p. 233.

[15] Metallurgist, Pittsburgh Piping & Equipment Company, Pittsburgh, Pa.

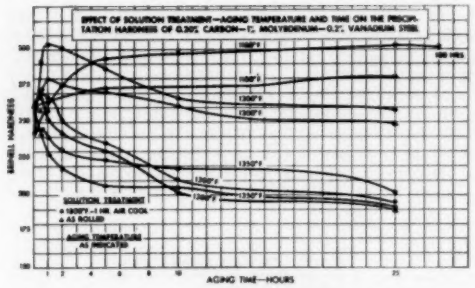

FIG. 17

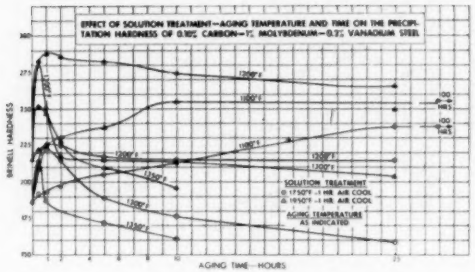

FIG. 18

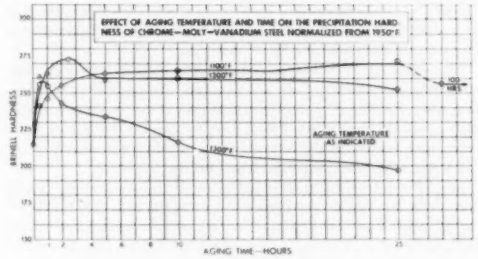

FIG. 19

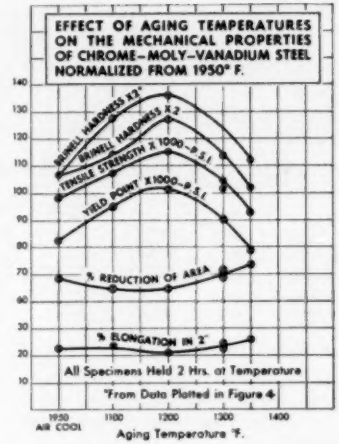

FIG. 20

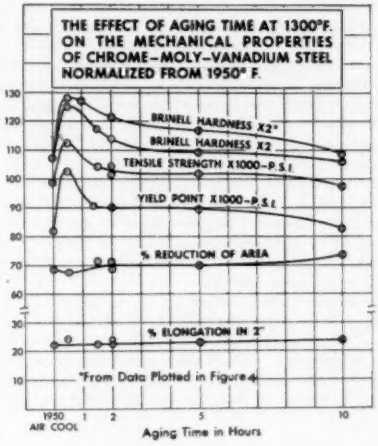

FIG. 21

steel are presented in Figs. 20 and 21. From Fig. 20 it is to be noted that a maximum of 115,000 psi tensile strength can be developed by aging at 1200 F for 2 hr. With this tensile and correspondingly high yield point, it is surprising that this is achieved with only a slight loss in elongation and reduction of area. The data plotted in Figs. 20 and 21 were obtained from 0.505-in-diam tensile bars machined from $1^1/_8$ in. × $1^1/_8$ in. × 6-in-long heat-treated bars cut longitudinally from $8^5/_8$-in-OD × $1^1/_8$-in. wall pipe of the analysis covered by item 2645 CR, of Table 2.

Since the cooling rate of these bars from the 1950 F treatment was more rapid than that to be obtained in commercial car-type furnaces, the yield and tensile values may be slightly higher than that obtained in actual fabrication. These curves do indicate the trend of values to be expected, however, and based upon the heat-treating specifications given by the authors it may be seen from Fig. 21 that assemblies fabricated from this grade of material will go into service with a yield point in the range of 68,000–75,000 psi and a tensile strength of 85,000–95,000 psi. These values seem, and are, high in terms of certain of the more conventional materials but it must be recognized that as the demand increases for high-temperature strength some sacrifices must be made in a "30 per cent elongation standard" at 70 F.

AUTHORS' CLOSURE

In acknowledging the excellent discussions of Messrs. Blumberg, Clark, Emerson, Newell, and Wilder, the authors wish to express their appreciation of the fine co-operation and the many contributions made to this and other development projects of the authors' company by the steel manufacturers and fabricators. Their observations of pilot operations on new materials as well as

their experimental work must be weighted heavily in development of new materials and the processing thereof for high-temperature structural service. Mr. Blumberg's three-point summary of the evaluation of piping materials is especially pertinent in this regard.

With reference to Mr. Clark's discussion, the authors have not been successful in correlating room-temperature hardness and long-time, high-temperature strength even when compositions and heat-treatments were similar. Certain trace elements, such as aluminum, have a marked effect upon high-temperature strength when the heat-treatment is kept constant, and even when heat-treatment is adjusted to give similar microstructures as well as room-temperature physical properties. In this regard Item 2370 was from a commercial heat of pipe. The heat-treatment involved cooling a half section 6⅜ in. OD × 0.718 in. thick from the normalizing temperature in still air. The heat was also silicon-killed and made in an electric furnace. Item 2399 was from an aluminum-killed induction furnace heat (lower nitrogen content) and was air-cooled from the normalizing temperature as a ¾-in. octagon in a 3-in. pipe, packed with cast-iron chips. This treatment is customarily applied to smaller samples to represent cooling rates measured on relatively large heat-treating batches in the shop.

The data referred to by Mr. Clark, Tables 1 through 7, were given as a background to justify the selection of the average high-temperature strengths noted in Figs. 5, 6, and 7 of the paper. For the type of analysis mentioned by Mr. Clark, much more detailed data are desirable. As a case in point, Item 2645 CR is listed in Table 5 as having 100,000 hr rupture strength of 23,000 psi. Only 2767 hr of testing had been completed at the time of this listing, and as these tests have progressed it becomes evident that this extrapolated figure may finally be as high as 28,000 or 30,000 psi.

Short-time high-temperature tests have been found to correlate better with room-temperature hardness than do the long-time values. It is the authors' belief that this comes about because of the greater similarity in the behavior of material under stress in these short-time tests. The mechanisms of flow and fracture in the long-time rupture test differ markedly from those in the short-time test, as evidenced by the "break" or change in slope of the log-stress versus log-time to failure plot at elevated temperature. Perhaps at lower testing temperatures or where the composition and heat-treatment of the material are such that straight log-stress versus log-time to failure plots are obtained, the correlation referred to by Mr. Clark is better. A concerted effort is being applied to correlation studies because development programs are lengthened unduly by the necessity for obtaining long-time creep and rupture strengths for evaluation purposes.

Mr. Clark's comments concerning permissible hardness levels in piping systems are very pertinent. The authors attempted to express their awareness of the desirability of keeping hardness levels low. However, as noted by Messrs. Blumberg, Newell, and Emerson in their discussions of the subject paper, it is apparently true that the attainment of better high-temperature strength in ferritic piping steels will necessitate some increase in hardness over that normally encountered and some sacrifice in room-temperature ductility, which will require better control of handling procedures.

Mr. Emerson's discussion constitutes a notable addition to the information at hand on vanadium-containing piping steels, and the authors are grateful for its presentation. The authors agree with Mr. Emerson's conclusions in all respects. The curves presented in Fig. 18 of Emerson's discussion, illustrate very well not only the higher levels of hardness obtained as a result of higher solution treatments but also a greater resistance to tempering incorporated in the material as a result of higher solution treatment. It is felt that this bears directly on the problem of stability relative to mechanical strength after prolonged exposures to service temperatures.

In response to Messrs. Krieg and Dedrick's discussion, the authors would like to point out that at this time the specimens from silicon-deoxidized electric-furnace heats of molybdenum-vanadium piping steel with the high-temperature normalizing treatment and draw, preheated before welding and stress-relieved after welding, have not graphitized in test; while, as noted by Krieg and Dedrick, specimens taken from heats made differently or lacking the afore-mentioned heat-treating and welding procedure have been shown to graphitize. The authors by "inadvertent mishandling" referred to the possibility that a user of such Mo-V steel, perhaps not needing the ultimate in high-temperature strength, might inadvertently leave out some important steps in this process and put the steel into high-temperature service in a condition susceptible to graphitization. The addition of 1 per cent Cr minimizes this possibility.

The authors concur with Mr. Wilder in his feeling that the possibility of graphitization is remote in the 1 Cr-1 Mo-¼ V steel. It may very well be that additional chromium may be found desirable as service temperatures are raised to combat excessive scaling in service. This matter is being investigated intensively in the authors' laboratory. A principal role of age-hardening in the vanadium-containing steels is in increasing the resistance to tempering reaction in service and thereby lending stability in the sense of mechanical strength.

Mr. Robinson's comments relative to predicted rupture strengths on the basis of short-time tests are interesting, and it is probable that in the case of Item 2645 CR, mentioned previously, the authors have been similarly conservative in their estimations; however, in view of the variations in composition and heat-treatment which are experienced as a matter of course in production, and the relatively slight amount of knowledge available on the effects of these variations on long-time, high-temperature properties, the authors feel such initial conservatism to be justified.

With respect to Mr. Newell's question relative to the strength of annealed Cr-Mo-V piping steel, the authors would expect the properties to be influenced markedly by the austenitizing temperature. Using 950 C or lower, the annealed steel is probably no better than the ½ Cr-½ Mo pipe in the annealed condition. The data given in Table 11, herewith, seem pertinent in this regard.

With respect to the stability of these age-hardening materials, the latest values for the tests plotted in Fig. 8 or Fig. 9 of the paper are given in Table 12.

As noted in the paper, the Cr-Mo-V piping material is tempered to produce rather severe overaging. As stated before, this is in the interests of obtaining the best compromise between high-temperature strength and notch ductility at low temperatures. However, it also should result in a rather high degree of stability relative to the age-hardening mechanism.

In response to the request by Messrs. Newell and Heller for elongation values obtained in the rupture tests presented in the paper, the data in Table 13, herewith, were obtained from the time to failure versus per cent elongation plots made in conjunction with these tests.

It should be noted in passing that long-time rupture tests sometimes exhibit a somewhat fictitious high per cent elongation value when the break is of the intercrystalline variety and is accompanied by many secondary breaks and fissuring along the gage length.

Relative to Mr. Newell's request for comment as to whether the high strength characteristics of the Cr-Mo-V piping steel is due to composition or, in a large measure, due to the heat-treating practices employed, the authors feel that the high-temperature strength of this alloy is largely due to the pronounced age-harden-

TABLE 11 DATA ON THE STRENGTH OF Cr-Mo-V PIPING STEELS AND CASTINGS

Item no.	Composition	Heat-treatment
2490 A	Pipe 0.11 C 0.99 Mo-0.17 V	950 C 8 hr AC; 700 C 4 hr FC
2501 A	Pipe 0.11 C 0.99 Mo-0.17 V	950 C 8 hr FC; 650 C 4 hr FC
2218 A	Casting 0.16 C 0.91 Mo-0.10 V	1050 C FC 600 C/hr; 650 C 2 hr AC
2224 A	Casting 0.16 C 0.91 Mo-0.10 V	1050 C FC 135 C/hr to 835 C, FC at 25 C/hr; 650 C 2 hr AC
2246 A	Casting 0.14 C 1.1 Mo-0.14 V	1050 C FC 400 C/hr; 650 C 3 hr
2247 A	Casting 0.14 C 1.1 Mo-0.14 V	1050 C FC 100 C/hr; 650 C 3 hr

Item no.	Rupture strength
2490 A	100000 hr rupture, 1000 F, 9900 psi
2501 A	100000 hr rupture, 1000 F, 23000 psi
2218 A	100000 hr rupture, 1000 F, 16000 psi
2224 A	100000 hr rupture, 1000 F, 14000 psi
2246 A	0.1%/100000 hr creep strength, 1000 F, 3500 psi
2247 A	0.1%/100000 hr creep strength, 1000 F, 2500 psi

TABLE 12 STABILITY OF AGE-HARDENING—VALUES FOR TESTS OF FIGS. 8 OR 9

Temperature deg F	Item no.	Strain, per cent	Stress psi	Hours
1000	2491 Mo-V	0.08	8000	20000
1000	2645 CR Cr-Mo-V	0.041	9600	8000
1100	2491 Mo-V	0.075	4000	20000
1100	2645 CR Cr-Mo-V	0.045	4000	8000

TABLE 13 ELONGATION VALUES OBTAINED IN RUPTURE TESTS

Item no.	Temperature, deg F	Rupture ductility, 10 hr	100 hr	1000 hr
2370	1000 F	(1)	0.8	0.5
2375	1000 F	(2.5)	[1.7)	0.5
2394 CR	900 F	11.8	12.5	13
	1000 F	15.8	10.7	9.5
2395 CR	900 F	6.2	4.2	2.8
	1000 F	(7)	(4.6)	2.6
2398	900 F	(24)	(17)	16
	1000 F	(15)	13.8	9
2399	900 F	(10.5)	8	6.2
	1000 F	(10)	8.4	6.8
2491	900 F	(4.5)	3.5	2.8
	1000 F	11.2	5.4	1.5
	1100 F	(1.7)	1.2	1.7
2645 CR	900 F	(12)	10.6	10
	1000 F	(19)	16.5	(7.8)
	1100 F	(18)	12.8	5.8

( ) = extrapolation

ing reaction, which is evident in the vanadium-containing steel after a suitable high-temperature normalizing treatment (1000 C or higher). Reference to Fig. 12 of the paper shows the dependency of this reaction upon solution temperature; and straight Mo or Cr-Mo steels are not characterized by such a pronounced hardening reaction on tempering. Thus composition and heat-treatment must be ascribed equal importance in obtaining good high-temperature strength. This was noted in Mr. Emerson's discussion of this paper also.

With further reference to Mr. Heller's discussion, the authors also have noted a high degree of response to age-hardening during tempering of "as-hot-rolled" vanadium-containing steel, but the use of the material in the as-rolled and tempered condition is not thought advisable because of the difficulty of controlling sufficiently the finish temperatures to obtain adequate uniformity of properties in steels so sensitive to heat-treatment. With reference to Mr. Heller's comments on the effects of heat-treatment on rupture ductility, it is also our experience that lower normalizing temperatures result in better ductility in long-time rupture tests; however, this increase in ductility is obtained only at the expense of high-temperature strength.

In the fabrication of Cr-Mo-V piping, particular attention must be paid to the high-temperature strength of the welds. As pointed out previously, the high-temperature strength of a vanadium-containing steel is dependent upon the heat-treatment as well as the chemical composition, and since, in general, the fabrication welds cannot be fully heat-treated, their high-temperature strength is less than that of the normalized and tempered vanadium-containing base material. Accordingly, when full advantage is taken of the high-temperature strength of the base material, it may be advisable to crown the welds more than the usual practice with the more common weaker alloys.

The authors are extremely gratified by the thoughtful and valuable discussion attending this paper and await with great interest the complete publication of the various experimental programs on vanadium-containing steels referred to by those participating in the discussion.

Effect of Molecular Weight of Entrained Fluid on the Performance of Steam-Jet Ejectors

By W. C. HOLTON,[1] COLUMBUS, OHIO

A program of research sponsored by the Heat Exchange Institute[2] involved pumping 13 pure gases and 12 mixtures of gases with small commercial single and two-stage steam-jet ejectors supplied by two manufacturers. Results were calculated in terms of "air equivalent" or "entrainment ratio," which is the ratio of the flow rate of gas to that of air under similar conditions. Entrainment ratios were found to be a function of the molecular weight of the gases handled and were plotted as a smooth curve, which is independent of pressure, design characteristics of ejectors, and is applicable to mixture of gases. It is concluded that the curve may be used to predict results obtainable with any ejector system.

MANUFACTURERS and users of steam-jet ejectors have long been faced with the problem of specifying the correct size of ejector to be used to pump a gas whose physical properties differ widely from those of air. One method of evaluation would involve the running of full-scale tests with expensive gases at high flow rates. Various member companies of the Heat Exchange Institute had run limited tests on molecular-weight entrainment, but the results of various manufacturers' tests did not agree closely. Furthermore, only a limited amount of test information has appeared in the literature,[3] and often this has been considered impractical in view of the limitations of the tests which have been run.

For the purpose of developing a suitable standard, the Heat Exchange Institute authorized an investigation at Battelle Memorial Institute in August, 1946. For this work, both single and two-stage ejectors were to be used with 13 pure gases and a total of 12 mixtures of gases. As a secondary objective of this investigation was to determine the effect of ejector design characteristics on performance, two HEI member companies each supplied a two-stage ejector for the tests. These ejectors are designated A and B. The units were standard stock models of practical size for process work. The two stages of ejector A were taken apart and the second stage used alone for single-stage work. Ejector B was welded together, and motive steam was supplied only to the second stage for single-stage tests.

Tests on single-stage ejectors were run from shutoff to 20 in. Hg abs and on two-stage ejectors from shutoff to 10 in. Hg abs. All tests were conducted at room temperature, nominally 80 F.

Apparatus

The main problem involved in performing the tests was that of measuring accurately both flow rate and pressure of the gas being tested. For the measurement of flow rate, nozzles developed by the HEI[4] were used. Diameters of these nozzles were 0.06299, 0.09402, 0.12501, 0.18799, 0.25002, and 0.31303 in. Mercury U-tube manometers were used to measure pressures on each side of the nozzle. The pressure of the gas at the inlet of the first operating ejector was measured by a floating-scale mercury manometer which made it possible to read differential pressures directly. A standard barometer was located on the instrument panel. The temperature of the gas was measured by mercurial thermometers inserted through rubber stoppers into the gas stream.

Fig. 1 shows the general arrangement of the equipment used for the tests with air. Three of the six gas chambers are visible at the left of the picture. The metering nozzles were installed in

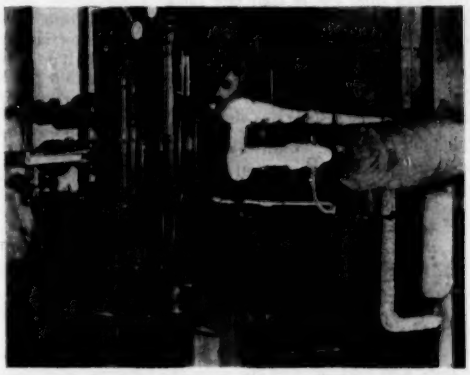

FIG. 1 GAS CHAMBERS CONTAINING METERING NOZZLES, MIXING CHAMBER, MANOMETER PANEL, AND TWO-STAGE EJECTOR WITH THERMAL AND SOUND INSULATION ON INLET AND DISCHARGE

mounting plates between the flanges shown in the center of the gas chambers. The chambers connect through Nordstrom valves to the mixing chamber, which is a steel cylinder, baffled internally to assure mixing of gases. The ejectors were bolted to a Nordstrom valve on the right-hand end of the mixing chamber. Motive steam for the ejectors, supplied from a small steam generator, was dried thoroughly by being passed through two steam separators and was discharged to the atmosphere through a crude muffler. Steam pressure was measured by a conventional Bourdon gage, and steam temperature was measured by thermocouples.

For testing pure gases and gas mixtures, cylinder gases were piped, at full cylinder pressure, to a steam-jacketed high-pressure

---

[1] Research Engineer, Fuels Division, Battelle Memorial Institute.

[2] Members of the HEI are the Elliott Company, Foster Wheeler Corporation, Ingersoll-Rand Company, Schutte and Koerting Company, Westinghouse Electric Corporation, C. H. Wheeler Manufacturing Co., and Worthington Pump and Machinery Corporation.

[3] "Performance of Ejectors as a Function of the Molecular Weights of Vapors," by L. T. Work and V. W. Haedrich, *Industrial and Engineering Chemistry*, vol. 31, 1939, p. 464.

Contributed by the Power Test Code Committee on Steam Jet Compressors, Research Committee on Fluid Meters, and the Hydraulic Division and presented at the Annual Meeting, New York, N. Y., November 26–December 1, 1950, of THE AMERICAN SOCIETY OF MECHANICAL ENGINEERS.

NOTE: Statements and opinions advanced in papers are to be understood as individual expressions of their authors and not those of the Society. Manuscript received at ASME Headquarters, Oct. 25, 1950. Paper No. 50—A-114.

[4] "Standard Nozzles Mean Better Fluid-Flow Measurements," by H. S. Bean, W. H. Reynolds, and R. M. Johnson, *Power*, vol. 89 1945, pp. 578 and 670.

throttling valve. Two needle valves, giving both coarse and fine control of flow rate, followed the main throttling valve and regulated the flow of gas into a heat exchanger. This contained steam coils and was operated to maintain the temperature of the gas at the metering nozzles close to 80 F. Gas was piped from the heat exchanger, through a manifold, to the six gas chambers.

Test Procedure

Before each test the system was checked for air tightness by closing the six Nordstrom valves at the gas chambers, evacuating the mixing chamber with the ejector, and closing the Nordstrom valve at the ejector suction. The rate of pressure rise inside the mixing chamber was then noted, and testing was begun only when this rate was less than 0.1 in. Hg in 10 min. This corresponds to an in-leakage of 0.015 lb per hr. In many cases this rate was much lower.

The upstream pressure was held at a constant value, near atmospheric pressure, for any given test to simplify calculations. Readings of gas temperature and pressure upstream of the metering nozzle, of differential pressure across the nozzle (for noncritical flow only), of pressure at the ejector suction, and of the barometer were recorded for each test point. In addition, data on the condition of the motive steam were also recorded regularly. Readings were taken as soon as pressure equilibrium had been reached; this was determined by observing fluctuations in the level of the floating-scale manometer.

Experience showed that tests could be run more rapidly by proceeding from low to high flow rates. Consequently, each test was started with a no-load (or shutoff) reading before the metered fluid was admitted through the smallest flow nozzle. Use of the flow nozzles both singly and in parallel made it possible to obtain pressure readings for flow increments of 2 to 6 lb per hr. At the conclusion of each test, a no-load check was again made. A second reading was also taken of pressure at an average flow rate.

$$W = \frac{A_2 C P_1}{\sqrt{R}\sqrt{T_1}} \times 14182.9 \sqrt{\frac{k}{k-1}\left[\left(\frac{P_2}{P_1}\right)^{\frac{2}{k}} - \left(\frac{P_2}{P_1}\right)^{\frac{k+1}{k}}\right]}$$

where

W = gas-flow rate, lb per hr
A_2 = area of nozzle throat, sq in.
C = nozzle coefficient of discharge
P_1 = absolute pressure at nozzle entrance, in. Hg at 32 F
R = gas constant for fluid being handled, ft-lb per (lb)(R)
T_1 = absolute temperature at nozzle entrance, F,
k = specific-heat ratio
P_2 = static pressure at nozzle outlet, in. Hg abs

Entrainment ratio, in ejector terminology, is defined as *the ratio of flow of gas to that of air under the same conditions.* To determine this ratio, graphs of absolute pressure as a function of gas-flow rate were made for each gas tested. From smooth curves drawn through the test points, values of flow rates at small pressure intervals (usually 0.5 in. Hg abs) were tabulated for each gas. The entrainment ratios were then calculated at these same pressures and were averaged for each gas tested. Since the compositions of gas mixtures could not be maintained constant over a load range, entrainment ratios were calculated for each mixture separately and were not averaged.

Results of 35 tests, comprising a total of 279 individual test points, are included in this report.

Gases Tested

Table 1 summarizes the combinations of pure gases and ejectors which were tested. Each gas was tested in the pressure range of shutoff to 20 in. Hg abs for single-stage ejectors, and shutoff to 10 in. Hg abs for two-stage ejectors.

Table 2 shows the compositions of the mixtures of gases (other than air) used for the tests. Performance tests with air were made with both ejectors, single and two stage. Since the gases to be mixed were metered in separate gas chambers and were combined in the mixing chamber, it was convenient to use a given mixture at only one rate of flow; consequently, only one pressure reading was obtained for each mixture.

TABLE 1 SUMMARY OF PURE GASES TESTED WITH GIVEN EJECTORS

Ejector A

Single stage		Two stage	
Gas	Molecular weight	Gas	Molecular weight
Ammonia	17.03	Helium	4.00
Natural gas	18.32	Ammonia	17.03
Carbon dioxide	44.01	Nitrogen	28.02
		Isobutane	58.12
		Isopentane	72.15
		Freon-12	118.13
		Freon-11	137.37

Ejector B

Single stage		Two stage	
Gas	Molecular weight	Gas	Molecular weight
Ammonia	17.03	Hydrogen	2.02
Natural gas	18.32	Oxygen	32.00
Carbon dioxide	44.01	Argon	39.94
		Isobutane	58.12
		Freon-21	109.22
		Freon-12	118.13

TABLE 2 COMPOSITIONS OF GAS MIXTURES TESTED WITH GIVEN EJECTORS

Components of mixture				Molecular weight of mixture
Gas	Mol per cent	Gas	Mol per cent	
Ejector A				
Carbon dioxide	13.67	Ammonia	86.33	20.72
Carbon dioxide	21.66	Ammonia	78.34	22.87
Carbon dioxide	58.27	Ammonia	41.73	32.75
Carbon dioxide	84.86	Freon-11	15.14	58.15
Carbon dioxide	80.66	Freon-11	19.34	62.07
Carbon dioxide	52.59	Freon-11	47.41	88.27
Carbon dioxide	45.16	Freon-11	54.84	95.20
Ejector B				
Helium	78.57	Ammonia	21.43	6.80
Helium	50.00	Ammonia	50.00	10.52
Helium	49.30	Ammonia	50.70	10.60
Helium	35.71	Ammonia	64.29	12.38
Helium	29.91	Ammonia	70.09	13.14

Tests with room air were run using the foregoing procedure. Pressure upstream of the nozzle was maintained by throttling at the inlet to the gas chamber. Tests with cylinder gases were slightly more complicated because of the difficulty in maintaining a constant pressure upstream of the flow nozzle. It was also necessary to regulate rather closely the temperature of the gas at this point. Tests with mixtures of gases were made by disconnecting some of the six gas chambers from the heat-exchanger manifold and then connecting these to a separate manifold. To this manifold was connected the cylinder or container of the second gas being tested.

Through all tests the temperature and pressure of the motive steam to the ejectors were closely watched. Manufacturers' recommendations of steam pressure and superheat were rigidly followed.

Flow rates of gases were calculated using the following formula, recommended by the HEI[4]

[4] "Tables for Computation of Air Flow Through HEI Standard Flow Nozzles," by P. Freneau and R. Crippen, Heat Exchange Institute, 1945.

Results of Tests

Fig. 2 shows calculated entrainment ratios plotted as a function of the molecular weight of the gases tested. The smooth curve drawn through these points has been accepted by the HEI for its forthcoming revision of the "Standards of the Heat Exchange Institute, Steam-Jet Ejector and Vacuum-Cooling Section."[6]

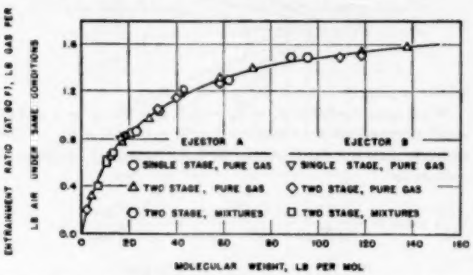

Fig. 2 Entrainment Ratio as a Function of Molecular Weight for Pure Gases and for Mixtures of Gases Tested With Two Steam-Jet Ejectors

Examination of the plotted data shows, first, that design characteristics of the ejectors tested have no effect on performance as tested. The single smooth curve passes equally well through entrainment-ratio values obtained with both ejectors. Thus the conclusion is reached that the curve may reasonably be used to predict results obtainable with any ejector system.

A second conclusion is that results obtained from testing both single and two-stage ejectors are comparable, regardless of the different absolute pressures maintained by the two machines. Independence of these data from the limitation of pressure permits extrapolation of the results to cover ejectors handling gases at absolute pressures lower than were maintained with the single and two-stage units.

Finally, the fact that the test points for mixtures of gases lie on the curve shows that this plot is not restricted for use with only pure gases. Since most ejector applications require use of mixtures of gases where molecular weight can be calculated, the applicability of the test results is thus greatly extended.

Acknowledgments

The co-operation and valuable suggestions of the Technical Committee, Steam-Jet Ejector and Vacuum-Cooling Section, Heat Exchange Institute, and, particularly, those of L. S. Stinson, chairman, and L. A. Droescher, are gratefully acknowledged. The author also wishes to express appreciation for the assistance of R. B. Engdahl, under whose supervision this work was done.

Discussion

F. Lustwerk.[7] The data presented offer, for the first time, a good experimental evaluation of the effects of molecular weight and temperature on the performance of ejectors. In the few previous papers the data, as a whole, were not satisfactory, because the test ejectors were not properly operated and because of the small size and poor design of the ejector (for the requisite tests).

There are, however, a few minor criticisms. The effect of k (the isentropic coefficient c_p/c_v) was not considered. However, the effects from this cause are quite small since only steam was used for the primary fluid. Most of the low-molecular-weight gases which were used had a $k = 1.4$ and the higher-molecular-weight gases probably had values of $k = 1.1$ so that the transition was fairly smooth along the curve. The use of steam as the driving fluid for these tests is not a serious omission since this driving fluid represents the most common usage.

Part of the scatter in the temperature curves was undoubtedly due to heat-transfer effects. In ejectors with more than a single stage, and of differing design, it should be expected that wider discrepancies occur than for single-stage designs. Probably some account could be taken of the amount of heat transfer to the surroundings and to the primary nozzle and steam chest.

All in all, the data show excellent correlation despite the effects mentioned herein. The difficulties involved in the test procedure with such a wide variety and latitude of results appear to have been met with unusual success.

However, important items such as the pressure and temperature of the primary fluid seem to have been overlooked. The effects of changes in temperature of the primary fluid certainly influence secondary flow. These data should be included to complete the report.

A. V. Saharoff.[8] The relative performance of a steam-jet ejector of any given design when compressing various kinds of gas is, of course, susceptible to analysis based on nothing more than a consideration of conditions under which the apparatus is operated, together with the thermodynamic and other properties of the gases in question. Assuming that the performance of the ejector when compressing one mixture (for example, steam and air) is known, then the equivalent performance when handling another mixture can be analyzed and accurately evaluated. Such analysis should be of interest to the author as a further means of appraising the results reported. In the hope that the author will study further his unpublished data, which he undoubtedly has, and comment again in the light of this discussion the writer presents herewith such analysis. In developing it, it is necessary to make several assumptions, three of which may be stated as follows; others will be evident in the development of the formula:

1 The total net amount of energy available from motive gas or steam is the same for each mixture to be compressed.

2 Having the same amount of energy available for compression of each mixture *equal total weights* will be compressed regardless of the composition of the mixture, provided, of course, that all other conditions remain the same.

3 The effects of change in exponent N and compression ratio alter the ratio of gas-air mixture by inverse ratio of corresponding energies required for the compression of the mixtures under consideration.

Assign subscripts 1 and 2 to steam and air, respectively, in a steam and air mixture (1 + 2) to be compressed in ejector and subscripts 3 and 4 to steam and gas, respectively, in a steam and gas mixture (3 + 4) to be substituted for the former.

Let

s = entropy
r = ratio of compression
W = weight
MW = molecular weight
T = initial temperature (same for all gases and mixtures)

[6] Copies of this curve are available upon request to the Heat Exchange Institute, 90 West Street, New York 6, N. Y.

[7] Gas Turbine Laboratory, Massachusetts Institute of Technology, Cambridge, Mass. Jun. ASME.

[8] Worthington Pump and Machinery Corporation, Buffalo, N. Y. Mem. ASME.

p = pressure (total for mixtures, partial for each ingredient)
V = volume
Z = compressibility factor

$$N = \frac{c_p}{c_v} \text{ or } \frac{N-1}{N} = \left[\frac{\delta(\ln T)}{\delta(\ln P)}\right]_s \text{ as required}$$

$$R = \text{Gas constant} = \frac{1546}{(MW)}$$

A, B, C, D = Mole fraction of steam, air, steam, gas, respectively, in above mixtures

By definition

$$A + B = C + D = 1.0 \quad [1]$$

$$P_2 = BP_{(1+2)} \quad [2]$$

$$P_4 = DP_{(3+4)} \quad [3]$$

By assumption

$$W_1 + W_2 = W_3 + W_4 \quad [4]$$

Equations of state

$$P_{(1+2)}V_{(1+2)} = (W_1 + W_2)\, R_{(1+2)}T_{(1+2)}Z_{(1+2)} \quad [5]$$

$$P_2V_2 = W_2R_2T_2Z_2 \quad [6]$$

$$P_{(3+4)}V_{(3+4)} = (W_3 + W_4)\, R_{(3+4)}\, T_{(3+4)}Z_{(3+4)} \quad [7]$$

$$P_4V_4 = W_4R_4T_4Z_4 \quad [8]$$

From which

$$\frac{\text{Gas}}{\text{Air}} \text{ ratio} = \frac{W_4}{W_2} = \frac{P_4V_4R_2T_2Z_2}{P_2V_2R_4T_4Z_4} \quad [9]$$

$$\text{Substituting in place of } \frac{V_4}{V_2} \text{ ratio } \frac{V_{(3+4)}}{V_{(1+2)}} \quad [10]$$

and because of definitions and assumptions

$$\frac{\text{Gas}}{\text{Air}} \text{ ratio} = \frac{D\, R_{(3+4)}T_{(3+4)}Z_{(3+4)}R_2T_2Z_2}{B\, R_{(1+2)}T_{(1+2)}Z_{(1+2)}\, R_4\, T_4Z_4} \quad [11]$$

$$\text{Since } R_{(1+2)} = \frac{1546}{(MW)_{(1+2)}} \quad [12]$$

$$R_2 = \frac{1546}{(MW)_2} \quad [13]$$

$$R_{(3+4)} = \frac{1546}{(MW)_{(3+4)}} \quad [14]$$

$$R_4 = \frac{1546}{(MW)_4} \quad [15]$$

$$T_2 = T_4 = T_{(1+2)} = T_{(3+4)} \quad [16]$$

and substituting in place of molecular weights of mixtures their equivalents in terms of individual molecular weights and mole fractions

$$(MW)_{(1+2)} = A\,(MW)_1 + B\,(MW)_2 \quad [17]$$

$$(MW)_{(3+4)} = C\,(MW)_3 + D\,(MW)_4 \quad [18]$$

and expressing ratio of energies per unit volume for the two mixtures in usual terms, and remembering that subscripts 1 and 3 refer to steam, 2 to air, and 4 to gas

$$\frac{\text{Gas}}{\text{Air}} \text{ ratio} = \frac{D\,(MW)\text{gas}}{B\,(MW)\text{air}} \cdot \frac{A(MW)\text{ steam} + B(MW)\text{air}}{C(MW)\text{ steam} + D(MW)\text{gas}} \cdot \frac{N_{(1+2)}\,[N_{(3+4)}-1]}{N_{(3+4)}\,[N_{(1+2)}-1]} \cdot \frac{\left(r^{\frac{N_{(1+2)}-1}{N_{(1+2)}}}-1\right)}{\left(r^{\frac{N_{(3+4)}-1}{N_{(3+4)}}}-1\right)} \cdot \frac{Z_2Z_{(3+4)}}{Z_4Z_{(1+2)}} \quad [19]$$

which is general formula for gas-air ratio.

When compressibility $Z_2 = Z_4 = Z_{(1+2)} = Z_{(3+4)} = 1$ and assuming normalization of the type $A = B = C = D = 1/2$, . . . [20] which is none too contradictory for some conditions, the formula reduces to

$$\frac{\text{Gas}}{\text{Air}} \text{ ratio} = \frac{(MW)\text{gas}}{(MW)\text{air}} \cdot \frac{(ME)\text{steam} + (MW)\text{air}}{(MW)\text{steam} + (MW)\text{gas}} \cdot X \cdot$$

$$= 1.6214\, \frac{(MW)\text{gas}}{18 + (MW)\text{gas}} \cdot X \quad [21]$$

where X is ratio of energies of compression per unit volume as represented by third and fourth terms of Equation [19].

A plot of Equation [21] with X value taken as unity is shown in Fig. 3.

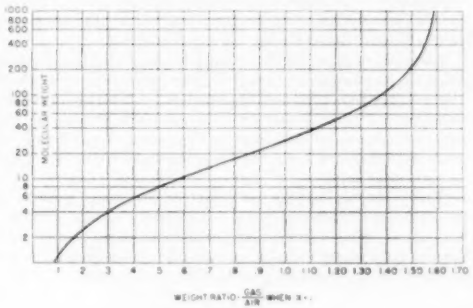

FIG. 3

Value of X may be calculated from $\frac{N-1}{N}$ curves shown in Fig. 4 for various mole percentages of steam-gas mixtures. It is, of course, necessary to exercise care in selecting percentages and gases for which the values are needed.

Fig. 5, which compares the curve of Fig. 3 with Battelle experimental results, shows how close the two come together and when the proper value of X for any particular mixtures under consideration is introduced, the coincidence, in spite of stated and tacit assumptions, is remarkable. It must be realized, however, that in the light of this analysis other gases not used in these experiments, as, for example, monatomic gases of group zero of periodic table, would not show such close coincidence with the Battelle curve. Does the author believe that this "average" curve is valid for such gases?

When motive gas is other than steam, and especially if it is used near pressure and temperature where compressibility of gases must be taken into consideration, the reader is referred to

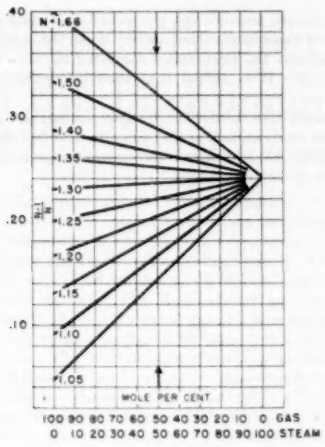

FIG. 4

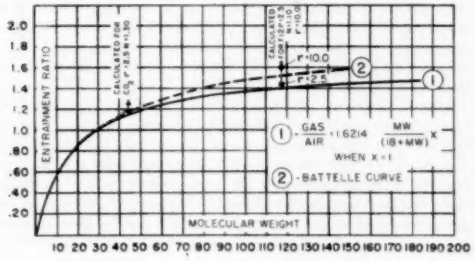

FIG. 5

compressibility charts and their application to problems involving pressure-volume-energy relation for real gases.[9]

PAUL DISERENS.[10] Engineers concerned with the selection and operation of steam-jet ejectors used in chemical process work should be grateful for the data which the author has made available. The curve showing an average or approximate relation between air-gas ratio and molecular weight, should be quite satisfactory for the range of gases selected for the reported tests. It must be appreciated, however, that change in air-gas ratio cannot be defined in terms of molecular weight as a single parameter since the N value of the gas, the number of compressions through which it is compressed, and possibly other factors, also have a direct influence upon the ratio. It seems, therefore, that when and if the reported test results are correlated with some acceptable theory defining the relationship in terms of all three of the factors, molecular weight, N value, and ratio of compression, we may hope to have something which will be useful to the designer of steam-jet apparatus as well as to the engineer who uses or plans to use jet ejectors. (See discussion by A. V. Saharoff.)

Unfortunately, individual tests are not reported in the paper, and without them only an approximate analysis is possible. Assuming, however, that for the tests of the two-stage units, the compression ratio in the first stage was always approximately 3, and the mol per cent in the mixture to be compressed is 50–50, then the gas-air ratio computed from the Saharoff formula will compare with the average values reported in the paper, as shown in the following table:

	Gas-Air Ratio	
Gas	Battelle curve	Calculated
Air	1.0	1.00
Helium	.3	.29
Ammonia	.8	.8
Nitrogen	1.0	.99
Isobutane	1.3	1.315
Isopentane	1.4	1.38
Freon 12	1.5	1.5

It will be seen, therefore, that the calculated values for the gases used during tests are in agreement with the proposed Battelle curve. In using the curve, however, it would be prudent to confine its application to the particular type of gases used for the tests. This will be evident if we consider the gas Xenon having N value of 1.66, and a molecular weight of 130. The Battelle curve shows a gas-air ratio of about 1.57 for a gas having a molecular weight of 130, whereas the ratio calculated from the Saharoff formula for Xenon shows a ratio of 1.38.

AUTHOR'S CLOSURE

Mr. Lustwerk's suggestion that heat-transfer effects may account for part of the scatter in the temperature curves (presented in the companion paper[11]) is appreciated. More data are certainly required to determine the magnitude of these effects on performance data. No attempt was made to correlate such effects with the test results in this investigation.

The ejectors were operated with motive steam at constant pressure and with motive steam temperature as close as possible to design conditions, which specified operation at 125 psig with a superheat of 5 to 10 deg.

Mr. Saharoff's derivation of a formula for the calculation of the entrainment ratio is a real contribution to the literature. The author wishes to suggest, however, that this treatment be expanded in the form of a technical paper and that the derivation be written more completely for the convenience of the reader. The test data used by the author could then be presented in a discussion to Mr. Saharoff's paper.

The author wishes to take exception to Mr. Saharoff's second assumption which seems to be incorrect. It is true that the same amount of energy is available for compression. By the same token, the same weight of steam is used for compression. In the notation of the discusser (and following Equation [4])

$$W_1 = W_2$$

The test data, as shown in Fig. 2, show that

$$W_2 \neq W_4$$

unless subscript 4 refers to air in the special case. Thus Equation [4] does not hold. By the same reasoning, Equation [10] is incorrect.

The "normalization" which Mr. Saharoff uses in Equation [20] applies only over a narrow range of operation. The author wishes to caution against the use of Equation [21] for the solution of general problems for this reason.

The curve of Fig. 2 is presented as an "average" and, as Mr. Saharoff notes, might not be true for gases whose physical properties vary widely from those of the gases tested. Most problems

[9] Worthington Research Bulletin P-7637, July, 1949.

[10] Consulting Engineer, Director of Research, Worthington Pump & Machinery Corporation, Harrison, N. J. Fellow ASME.

[11] "Effect of Temperature of Entrained Fluid on the Performance of Steam-Jet Ejectors," by W. C. Holton and E. J. Schuls. See pages 911–913 in this issue of Transactions.

encountered by ejector manufacturers, however, deal with gases more similar to those tested than those of group zero of the periodic table.

Mr. Saharoff's suggestion that the compressibility of gases must be considered in special cases should be expanded for the information of the reader. The limitations of the use of Fig. 4 should be clearly stated. Both of these points could be well covered in the expansion of this discussion which the author suggests.

The interstage pressure was not recorded on most of the tests reported. Consequently the author does not have sufficient data to perform the calculations suggested by Messrs. Saharoff and Diserens. It is agreed that such information would be valuable.

The constructive discussions are appreciated, and it is hoped that further analysis such as that submitted by Mr. Saharoff will produce additional information for a more comprehensive understanding of ejector action.

Effect of Temperature of Entrained Fluid on the Performance of Steam-Jet Ejectors

W. C. HOLTON[1] AND E. J. SCHULZ[2]

An investigation of the performance of small commercial single and two-stage steam-jet ejectors handling air and steam at temperatures to 1000 F was conducted under the sponsorship of the Heat Exchange Institute.[3] The results of tests are expressed in terms of "entrainment ratio," which is the ratio of the flow rate of gas at a given temperature to that of the same gas at a base temperature. Entrainment ratio was found to be a linear function of temperature. The test results given appear to be independent of pressure and of design characteristics of the ejectors tested. Therefore the plot of the variation of entrainment ratio with temperature is, within the limits of the test accuracy, thought to be applicable to any ejector system.

THE equation for critical flow indicates that the weight rate of flow of gas pumped by an ejector is inversely proportional to the square root of the absolute temperature. However, practical testing has not verified this indication. This behavior has evidently never been explained, as no reports of investigations into the problem have been found in the technical literature. Various member companies of the Heat Exchange Institute had run limited tests on temperature entrainment, but the results of various manufacturers' tests did not agree closely. To supplement an earlier investigation[4] on the performance of ejectors when handling various gases, the Heat Exchange Institute sponsored a series of tests with air and steam at elevated temperatures to develop an accurate method of predicting ejector performance at high temperature.

Laboratory tests were conducted at Battelle Memorial Institute beginning in May, 1949. Two-stage ejectors, of practical size for chemical process plants, were supplied by two HEI member companies. These ejectors are designated "A" and "B" in this report. The two stages of ejector A were taken apart and only the second stage was used for single-stage tests. Single-stage tests were run from shutoff to 10 in. Hg abs, and two-stage tests from shutoff to 6 in. Hg abs. The maximum temperature reached in these tests was 1000 F.

Apparatus

A 65,000-Btu per hr Selas heater, equipped with a compressor and a premixing valve, was used to heat the test gas (air or steam) before it entered the ejector suction. The outlet of the heater was bolted to a stainless-steel pipe tee, to which the ejector was fastened. The tee was operated as an adiabatic thermocouple shield, that is, the tee metal was maintained at the same temperature as that of the gas inside the tee by the use of electrical strip heaters. The entire tee was heavily lagged to reduce loss of heat to the surrounding air. A plain thermocouple bead of 36-gage chromel-alumel wire was placed in the center of the gas stream in the tee. This bead was protected from radiation effects by sheet-silver baffles placed in the pipes both upstream and downstream of the thermocouple. The temperature of the tee proper was observed by a thermocouple peened deep into the metal. The discharge of the ejectors was vented to the atmosphere through a crude muffler.

For tests with air at high temperature, the same metering and pressure-measurement system was used as that described in the investigation previously mentioned.[4] The flow rate of air was measured by determining the pressure drop across the orifices in the gas chambers. The Selas heater was connected to the outlet of the mixing chamber. A floating-scale mercury manometer was used to measure pressure at the ejector suction. A manual potentiometer was used to read all thermocouples.

To test with steam as the secondary, that is, the entrained fluid, required some modification of the apparatus. The gas chambers and mixing chamber were not used because of the difficulty in eliminating condensation of the steam after passing through the flow nozzle. A new gas chamber was constructed by placing one of the two smallest HEI nozzles between two "spool" pieces of pipe, connected at one end to the steam line through a Nordstrom valve and a separator and bolted to the Selas heater at the downstream end. Nozzles used were 0.06299 and 0.09402 in. in diam. Both of the spool pieces were heated to above steam-saturation temperature to prevent condensation, and the entire section was heavily lagged with insulation. A bleed was provided in the upstream spool piece to assure drainage of any condensate. Temperatures of the spool pieces were taken with thermocouples. For the steam tests, thermocouples were wired to a 12-point high-speed recording potentiometer. This was more satisfactory than the manual potentiometer used for the air tests, as it gave a printed record of temperatures by which the test operator could keep the entire system under close temperature control.

Test Procedure

As a measure of the tightness of the test apparatus, readings of the absolute pressure at the ejector suction were recorded for no-load operation; this was found to be a satisfactory leak check. The entire system, including the ejectors, was leak-checked, both before and after the series of tests with air, by evacuating with a mechanical vacuum pump, sealing off the system, and observing the rate of pressure rise. The maximum rate tolerated was 0.1 in. Hg in 10 minutes, which corresponds to 0.015 lb per hr. However, the in-leakage was much less for most tests.

For tests with air, flow rates were varied by using several combinations of flow nozzles while operating at a constant pressure upstream of the nozzle. Tests were run at constant temperature by gradually increasing the flow of air while maintaining the tem-

[1] Research Engineer, Fuels Division, Battelle Memorial Institute, Columbus, Ohio.

[2] Laboratory Asst. Fuels Division, Battelle Memorial Institute.

[3] Members of the HEI are: Elliott Company, Foster Wheeler Corporation, Ingersoll-Rand Company, Schutte and Koerting Company, Westinghouse Electric Corporation, C. H. Wheeler Manufacturing Co., and Worthington Pump and Machinery Corporation.

[4] "Effect of Molecular Weight of Entrained Fluid on the Performance of Steam-Jet Ejectors," by W. C. Holton. See pp. 905–910 of this issue.

Contributed by the Power Test Code Committee on Steam Jet Compressors, Research Committee on Fluid Meters, and the Hydraulic Division and presented at the Annual Meeting, New York, N. Y., November 26–December 1, 1950, of The American Society of Mechanical Engineers.

Note: Statements and opinions advanced in papers are to be understood as individual expressions of their authors and not those of the Society. Manuscript received at ASME Headquarters, Oct. 25, 1950. Paper No. 50—A-115.

perature at the ejector suction constant. This was faster than operating at constant flow by varying temperature, because of the lag of the Selas heater.

For tests with steam as the secondary fluid, the flow rate was varied by changing the upstream pressure, because only one flow nozzle was used for each ejector combination. As in the test with air, tests were similarly run at constant temperature and changing load.

Readings of absolute pressure were recorded when the entire system reached temperature equilibrium. Because the absolute pressure at the ejector suction would change rather rapidly with variations in load, it was necessary to wait for the temperature of the tee metal to be brought to the same temperature as that of the gas in the tee. In air tests, these temperatures were observed by rapidly switching the manual potentiometer from one couple to another. The recording potentiometer was used for the steam tests and the temperature trend was recorded on the chart. The length of the tests was determined largely by the temperature lag of the Selas heater and the electric strip heaters on the tee, and by the operator's skill in maintaining these temperatures equal.

Through all tests, the temperature and pressure of the motive steam to the ejectors were carefully observed. Manufacturer's recommendations of steam pressure and superheat were closely followed.

The results of 72 tests, comprising some 374 test points, are included in this report.

Calculations and Plots

The flow rate of air was calculated using the following formula recommended by the HEI.[5]

$$W = \frac{A_2 C P_1}{\sqrt{R}\sqrt{T_1}} \times 14182.9 \sqrt{\frac{k}{k-1}\left[\left(\frac{P_2}{P_1}\right)^{\frac{2}{k}} - \left(\frac{P_2}{P_1}\right)^{\frac{k+1}{k}}\right]}$$

in which

W = gas flow rate, lb per hr
A_2 = area of nozzle throat, sq in.
C = nozzle coefficient of discharge
P_1 = absolute pressure at nozzle entrance, in. Hg at 32 F
P_2 = static pressure at nozzle outlet, in. Hg abs
R = gas constant for fluid being handled, ft-lb per (lb) (R)
T_1 = absolute temperature at nozzle entrance, R
k = specific heat ratio

The rate of flow of steam was calculated by means of the following formula

$$W = 1472.5 \frac{A_2 C P_1}{\sqrt{T_1}}$$

in which

W = steam flow rate, lb per hr
A_2 = area of nozzle throat, sq in.
C = nozzle coefficient of discharge
P_1 = absolute pressure at nozzle entrance, psia
T_1 = absolute temperature at nozzle entrance, R

Test results were plotted first as lines of constant flow as a function of pressure and temperature. These data were then cross-plotted to give lines of constant temperature with flow rate and pressure as the other variables. From smooth curves drawn through these points, values of flow rates at small pressure intervals (usually 1.0 in. Hg abs) were tabulated for each temperature curve. The entrainment ratio, which is the ratio of the rate of flow of gas at the test temperature to that at the base temperature (90 F), was calculated at each pressure. The entrainment ratios obtained for each temperature were then averaged.

As 200 F was the lowest temperature at which steam tests were run, entrainment ratios for steam were calculated on this basis. For the final plot of these results, the average line drawn through the steam points was shifted to a base point of 90 F using the same slope as that found from the original line.

Fig. 1 shows the effect of temperature on entrainment ratio for the tests with air. It will be noted that the maximum deviation

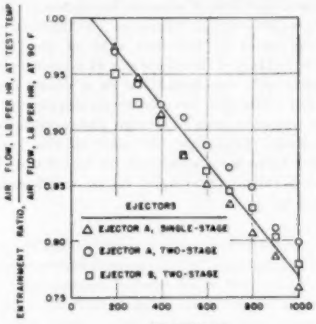

Fig. 1 Entrainment Ratio as a Linear Function of Temperature for Air Tests With Three Ejectors

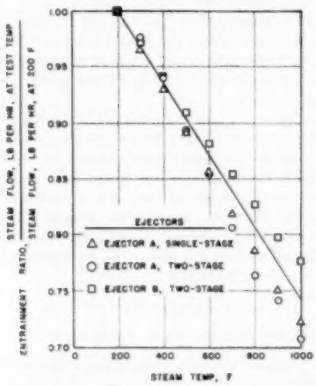

Fig. 2 Entrainment Ratio as a Linear Function of Temperature for Steam Test With Three Ejectors

of any point is less than four per cent. The individual points for any one ejector would lie on an "S" curve; no adequate explanation has been found for this. The straight line shown is thought to be a fair approximation of the average test results.

Fig. 2 presents the variation in entrainment ratio caused by temperature change for steam tests. Again, four per cent is the maximum deviation of any point from the straight line. It will be noted, however, that the results for tests with any one ejector seem to lie in a straight line.

Fig. 3 combines the average lines shown on Figs. 1 and 2. As pointed out before, the line for the steam tests has been shifted

[5] "Tables for Computation of Air Flow Through H.E.I. Standard Flow Nozzles," by P. Freneau and R. Crippen, Heat Exchange Institute, 1945.

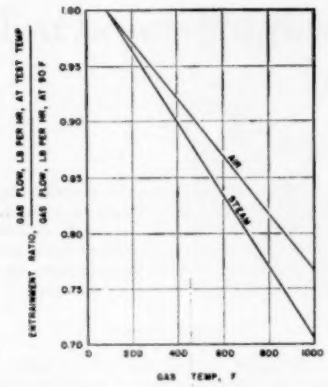

FIG. 3 ENTRAINMENT RATIO AS A LINEAR FUNCTION OF TEMPERATURE FOR AIR AND STEAM TESTS WITH THREE EJECTORS

to the left in order to base the entire curve on performance of the ejector handling gas at 90 F.

CONCLUSIONS

The test results plotted in Figs. 1 and 2 show, first, that entrainment ratio is independent of pressure in the range of 0.2 to 10.0 in. Hg abs. This is evident from the fact that the spread between points plotted for single and two-stage tests is not great. Secondly, the entrainment ratio is independent of design characteristics of the ejector. This conclusion is verified by the relative positions of the points shown. Closer correlation of data and more accurate results would have required a more extensive test program and more elaborate methods of temperature control and measurement than were feasible or necessary for this work. It is felt that the accuracy of these results, plus or minus four per cent, is sufficient for commercial purposes. The correlation of entrainment ratio and temperature shown in Fig. 3 can be used to predict ejector performance at high temperatures. This plot has been accepted by the HEI for its forthcoming revision of the "Standards of the Heat Exchange Institute, Steam-Jet Ejector and Vacuum-Cooling Section."[5]

ACKNOWLEDGMENTS

The co-operation and valuable suggestions of the Technical Committee, Steam Jet Ejector and Vacuum Cooling Section, Heat Exchange Institute, and, particularly of L. S. Stinson, chairman, and L. A. Droescher are gratefully acknowledged. The advice and assistance extended by R. B. Engdahl, under whose supervision this work was conducted, and others of the Battelle staff were major factors in the successful outcome of this investigation.

[5] Copies of this curve are available upon request to the Heat Exchange Institute, 90 West Street, New York 6, N. Y.

Turbojet-Engine Design for High-Speed Flight

By W. V. HURLEY,[1] LYNN, MASS.

The flight mission which a proposed engine is required to fulfill exerts a marked influence on the basic engine design. Missions involving high flight altitudes and high flight speeds tend to throw this problem into sharp relief. Accordingly, this paper discusses the general engine-design problem to meet the requirements of such missions.

Introduction

THE design of an engine may be regarded as a series of choices providing increasing amounts of information regarding the final design as the series proceeds. This is illustrated in Fig. 1.

It is from the set of all possible engine designs, A, that the final choice is to be made. The first step toward this choice is the specification of a mission, i.e., what is required of the engine. This specification will limit the choice to those engines within the subset B. The size of the subset B will depend upon the nature of the "mission" specification. It may be so broad as to eliminate none of the possible designs or so unrealistic as to eliminate all of them.

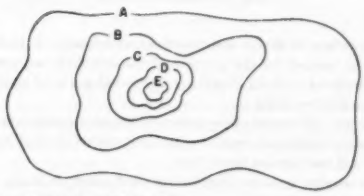

A = The set of all possible designs.
B = A subset of A determined by specifications of mission.
C = A subset of B determined by specification of cycle state conditions.
D = A subset of C determined by specification of aerodynamic design.
E = A subset of D determined by specification of mechanical design.

Fig. 1 Gas-Turbine Design

The next choice to be made is that of the cycle state conditions (pressure ratio, turbine temperature, and so forth). This choice has been limited by the statement of the mission, and in turn limits the number of possible aerodynamic designs. After the cycle has been established (thus placing the final design within the bounds of subset C), it is possible to state the physical dimensions of the engine very roughly.

The aerodynamic design is then made, restricting the possible mechanical designs to those contained in subset D. At this stage physical form and dimensions can be asserted more precisely.

The mechanical design sets forth the physical dimensions in great wealth and detail and narrows the choice of final designs to those lying within the subset E. Of course, subsequent testing and modification continue indefinitely and the "final" design is not obtained until the engine is obsolete.

Our discussion will center, for the most part, around the second and third of the choices outlined—the cycle state conditions and the aerodynamic design. The discussion will in addition be limited to turbojets. Turboprops, ducted fans, and other engine variants will not be considered.

The primary purpose in having the engine aboard the aircraft is to produce thrust for propulsion. To pay for this thrust the aircraft must accommodate the mass and the volume of the engine and its fuel. Thus for an engine of given thrust, the significant criteria, from the aircraft-design standpoint, are its size, weight, and fuel consumption. Though these have extensive mutual relationships we shall take them up in rotation.

Size of Engine

The aircraft drag at the design flight condition very roughly determines the size of the engine once a decision has been made as to the number of engines to be used per airplane. This decision involves many variables outside the compass of this discussion, although a few comments are in order from the engine manufacturer's viewpoint.

1 Two small engines will, in general, weigh less for a given thrust than one large engine.

2 At extreme altitudes the smaller engines will suffer more from Reynolds-number effects.

3 The larger engines will be cheaper to manufacture per pound of thrust. This may not be true of "extremely" large engines involving large amounts of special tooling.

4 The larger engines probably will have a higher strategic-materials content per pound of thrust than the smaller.

After the thrust required per engine has been determined for the design flight condition, a number of other variables come into play.

The air flow needed per pound of thrust depends upon the turbine-inlet temperature, the compressor pressure ratio, the component efficiency level, the flight altitude and Mach number, the anticipated installation losses (including the amount of compressor air bled for aircraft use), and the compressor air required for engine purposes such as cooling.

Fig. 2 is a typical plot of specific air consumption (air flow, pounds per second per pound of net thrust) for flight at a Mach number of 2.0, and altitudes above the tropopause. It is evident that the higher turbine-inlet temperatures and lower cycle pressure ratios will yield smaller lower-air-flow engines under these conditions.

Utilization of the higher turbine-inlet temperatures will depend upon the development of improved materials and improved cooling techniques for both the rotating and stationary parts in the aft portion of the engine. The use of air as a coolant becomes increasingly costly as the flight Mach number is advanced.

[1] Development Engineer, Aircraft Gas Turbine Engineering Division, General Electric Company. Jun. ASME.

Contributed by the Gas Turbine Power and Aviation Divisions and presented at the Annual Meeting, New York, N. Y., November 26–December 1, 1950, of The American Society of Mechanical Engineers.

Note: Statements and opinions advanced in papers are to be understood as individual expressions of their authors and not those of the Society. Manuscript received at ASME Headquarters, October 6, 1950. Paper No. 50—A-130.

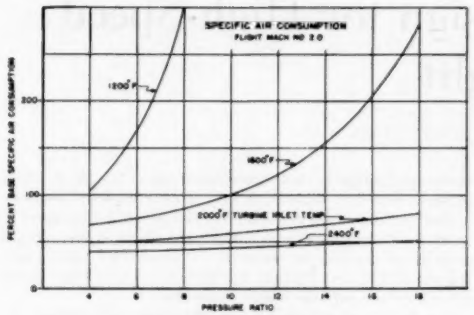

FIG. 2 SPECIFIC AIR CONSUMPTION; FLIGHT MACH NO. 2.0

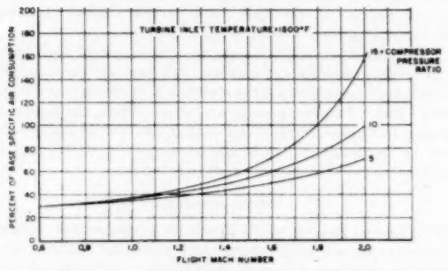

FIG. 3 SPECIFIC AIR CONSUMPTION AS A FUNCTION OF MACH NUMBER

This springs from two sources: Any available air is already fairly hot, thus necessitating the use of a greater quantity; and the drag incurred by taking the air aboard is high. These factors may be so large in some cases as to offset the hoped-for gain from the higher temperature.

The influence of the flight Mach number on the specific air consumption is given in Fig. 3. The effect is shown for three design pressure ratios (5, 10, and 15) and for a single turbine-inlet temperature (1600 F).

Fig. 3, as well as Fig. 2, has incorporated assumed values of the other important variables mentioned. In general, these are dependent upon the major parameters of pressure ratio, turbine temperature, flight altitude, and Mach number. Variations in their level as well as in their functional relationship with the major parameters will produce changes in level and in slope of curves of the type of Figs. 2 and 3. As an example, a lowering of component efficiency level by 1 per cent throughout the machine will result in an increase in specific air consumption in the neighborhood of 5 per cent, but actually dependent in amount upon the values assigned to the other variables.

The net thrust may be approximately doubled by use of exhaust reheat. This is indicated in Fig. 4. The same values of final effective reheat temperature have been assumed for each design, which is roughly equivalent to burning a constant percentage of the available oxygen. At constant values of turbine-inlet and exhaust-reheat temperatures, the higher-pressure-ratio engines have larger rises in temperature in the reheat burner because the turbine-discharge temperature drops with increasing pressure ratio and, therefore, larger increases in thrust. The greatly increased thrust from exhaust reheat is secured at the expense of specific fuel consumption as will be shown later.

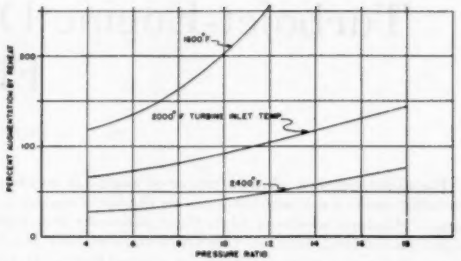

FIG. 4 PER CENT AUGMENTATION BY REHEAT; FLIGHT MACH NO. 2.0

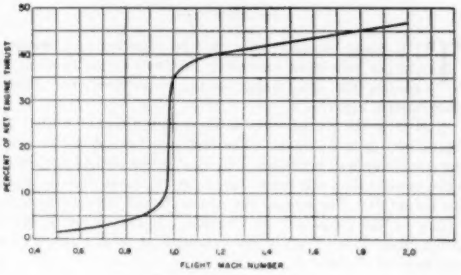

FIG. 5 NACELLE DRAG

The amount of thrust improvement which may be had in this fashion is limited by the portion of the available oxygen which can be utilized without depriving the metal parts of their necessary blanket of cooling air.

There are, of course, other means of thrust augmentation, such as rockets, bleed and burn cycles, and water-alcohol injection, but we will not discuss them here.

If the engine is to be nacelle-installed (and in many cases if submerged), the frontal area is of particular importance at high flight speeds, where the nacelle drag may amount to one half of the engine thrust. Fig. 5 indicates approximate values of nacelle drag as a function of flight Mach number. The drag is expressed as a percentage of the net engine thrust.

The frontal area of the engine hinges upon two primary factors: The cycle state conditions; and the mass flow per unit area inside the diameter of the components which can be attained at a given level of the design art. The influence of the cycle state conditions on specific air consumption has been discussed already; but there is another, less obvious, influence which is demonstrated in Fig. 6. Here the compressor, combustion system, and turbine diameters are plotted against compressor pressure ratio for engines designed to deliver the same thrust at given flight conditions and turbine-inlet temperature. For this plot, the same component design assumptions are maintained for all engines. In a balanced design for a particular cycle pressure ratio, the component limiting in diameter is likely to be less conservatively designed than the others. The necessity of fulfilling other requirements probably would also lead to a variation of design assumptions with pressure ratio, in practice.

The relationships shown in Fig. 6 may be altered by advances in the design art of any or all of the components.

All of the air entering the compressor must do so through the annular space immediately preceding the guide vanes, and we can gain some insight into the compressor problem by inspecting

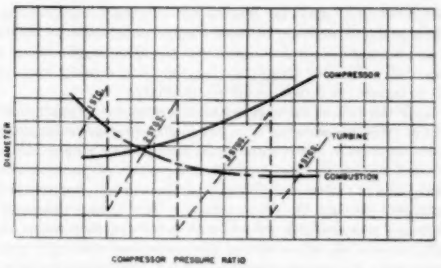

FIG. 6 EFFECT OF CYCLE PRESSURE RATIO ON COMPONENT DIAMETER

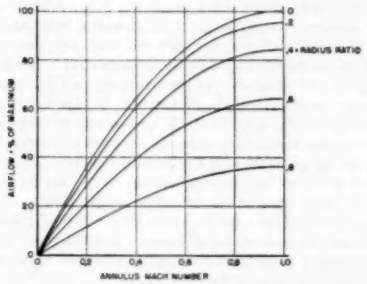

FIG. 7 COMPRESSOR AIR FLOW FOR GIVEN TIP DIAMETER

the flow in this region. Fig. 7 allows us to see in what manner the diameter required to handle a given flow may be reduced. Air flow is plotted against the Mach number of the flow immediately preceding the guide vanes. The parameter is the radius ratio (hub diameter/tip diameter). It is evident that the two means at our disposal are to increase the compressor entering Mach number or to decrease the radius ratio.

The first of these tends to increase the relative Mach number on the compressor blading of at least the first few stages, and thus to make it more difficult to attain a high compressor efficiency. The second goes in the direction of increasing the blading and disk stresses and is conducive of low pressure rise per stage for a given stress.

Moreover, as the radius ratio is reduced, accessories which had been mounted within the outline of the compressor hub must be relocated—usually to a position in which they contribute to engine frontal area.

Increasing the flow per unit area of outside diameter of the combustion system involves a similar situation; either its area must be increased or the average velocity through the chamber must be raised.

The former may incur difficulty in obtaining efficient flow passages from the compressor to the combustion chamber and thence to the turbine, as well as diminish the space available for internal engine structure. The latter makes the achievement of high efficiency more difficult and tends to make the combustion section longer in order to accommodate a longer flame length.

The turbine must produce the power to drive the compressor with a maximum of energy left over for the jet. Furthermore, this energy must be in a form which may be utilized with high efficiency by the exhaust system. This means that the fluid must leave the turbine at a reasonably low Mach number and with little angular rotation. As the flow per unit diameter is raised, the annulus area must be increased in order to maintain these conditions, resulting in a higher stress level. The situation is analogous to that obtaining at the compressor, but generally brings on more alarming consequences since the materials in the turbine are operating under severe conditions of temperature and stress in any successful aircraft gas turbine.

The exhaust reheat system diameter depends upon the Mach number to which the fluid must be diffused to insure efficient combustion and low pressure loss for the degree of augmentation desired. The required diffusion usually can be obtained within the diameter of the other components.

When the net nacelle thrust is considered, it becomes apparent that the engine of minimum frontal area for a given net engine thrust may not yield maximum nacelle thrust. At supersonic flight speeds, by far the major portion of the nacelle drag is wave, or pressure drag. Hence the air flow swallowed per unit engine frontal area can, in itself, have a major influence on the drag. Fig. 8 discloses this effect, which must be taken into account if it is desired to optimize the design for a nacelle installation.

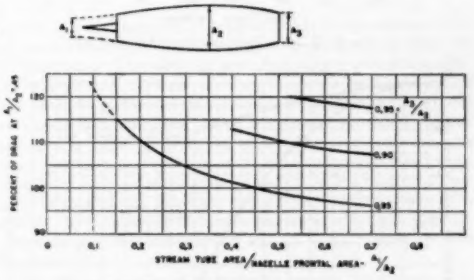

FIG. 8 NACELLE DRAG AT M = 1.6

The length of the engine is affected predominantly by the level of the component design art and by the design cycle pressure ratio just as in the case of the engine frontal area. Improvements in the pressure ratio obtainable per stage of compression are reflected directly in reduced length. So also are decreases in combustion flame length. Similarly, if the energy which may be handled by a turbine stage is increased, in many cases the turbine may be shortened. Length, however, generally plays a secondary role in determination of the number of turbine stages to be used.

Ingenuity in the mechanical design can do much toward holding down the length as well as the diameter of the engine.

WEIGHT OF THE ENGINE

The size of the engine has, of course, a prominent influence on the weight, although there are a large number of other significant factors.

Although the engine may be designed aerodynamically for a particular flight-altitude condition, the stress-limited condition will, in general, occur at sea level. Hence this condition is extremely important from a weight standpoint.

Fig. 9 shows how various of the engine-design parameters vary with flight Mach number at sea-level conditions for a typical engine run at military rpm. At the same Mach number, but a higher altitude, the values will be lower. It is apparent from this plot that the higher the Mach-number limit is set, the heavier will be the resulting engine design. As the limiting Mach number is advanced, it becomes necessary to incorporate thicker

sections in the compressor, combustion, and turbine casings, in order to withstand the higher differential pressures. Parts which may be made of light alloy for the lower flight speeds must be converted to steel on account of the higher temperatures. Greater gas bending loads on the compressor and turbine blading may demand increased blade chords, resulting in considerably heavier wheel blanks and additional compressor and turbine length with the attendant weight.

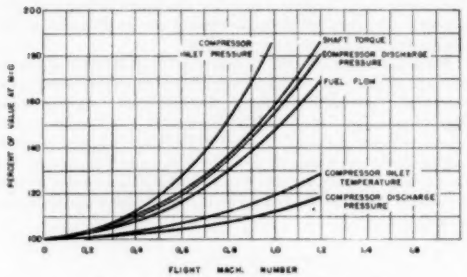

FIG. 9 DESIGN PARAMETERS; SEA LEVEL

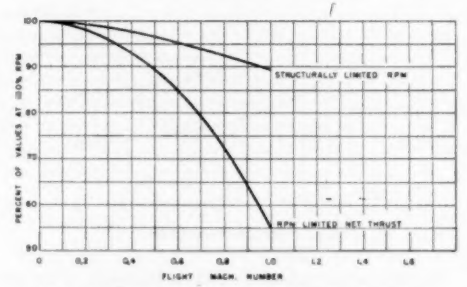

FIG. 10 DERATED ENGINE; SEA-LEVEL OPERATION

An engine designed structurally for a flight Mach number of 2.0 at 50,000 ft is capable of only 0.95 on a standard day at sea level. An engine designed structurally for 1.0 Mach number at 50,000 ft cannot run at military rpm at sea level on a standard day.

To the extent that take-off and climb thrust may be compromised, such an engine as the latter may be "derated" at the lower altitudes to save weight, that is, the allowable engine rpm may be reduced at the lower altitudes to avoid exceeding structural limits specified by the high-altitude condition. As a rough indication of the thrust sacrifice, Fig. 10 has been prepared for an engine which will just run at military rpm at sea level on a standard day. Plotted against flight Mach number are the allowable rpm and the net thrust, expressed as a percentage of that which would be available at 100 per cent rpm. This engine would be mechanically strong enough for 100 per cent rpm operation at a Mach number slightly above 1.2 at 50,000 ft.

The amount of weight which can be saved by such derating depends entirely on the specific engine design and application. If the engine is a small one, many of the metal parts already may be at the minimum thickness tenable for manufacturing or dimensional stability reasons. It may be undesirable because of Reynolds-number effects to decrease blade chords if high-altitude specific fuel consumption is important. Shaft sizes and blade chords already may be limited by vibration considerations. There probably also will be some weight contribution in the form of an automatic control to insure that the operating limits are not exceeded. The net weight saving thus conceivably may turn out to be zero, or it may be quite appreciable.

As in the case of the engine size, the weight is strongly related to the cycle pressure ratio. The higher-pressure-ratio designs not only require more compressor and turbine stages but also demand thicker sections in the latter portion of the compressor casing and in the combustion and turbine casings, because of the increased pressure in these regions. The higher compressor-discharge temperatures will indicate the use of steel rather than light alloys in the aft section of the compressor and in the transition section to the combustion chamber. For engines designed on a consistent basis, the weight, therefore, continues to rise indefinitely with the design pressure ratio.

For a particular pressure ratio, the component design can affect the weight greatly.

The pressure rise per stage of compression is a function primarily of the wheel speed, the fluid velocities, and the amount of turning of the fluid which can be accomplished. By increasing the last two, the number of stages necessary may be reduced and the weight correspondingly decreased. If this takes place at the expense of efficiency, however, an increase in turbine weight will occur since the turbine must now have more output, and less energy in the gases leaving the turbine results. The fuel consumption will also rise, and the additional fuel weight consumed during the flight may offset the engine weight saving. Increases of wheel speed, if they do not result in exorbitant stresses, also may be used to provide fewer stages. But this may not result in lower weight because of the marked effect of wheel speed on the weight of the compressor wheel disks.

The combustion-system weight may be reduced by improving the space rate of heat release so that the chamber may be diminished in size. Again, if this is done at the expense of fuel consumption, it may not result in an over-all weight saving for the aircraft. If it incurs a poor turbine-inlet temperature distribution, severe mechanical difficulties can result.

The turbine weight is dependent to a large extent upon the compressor design, since the compressor fixes the output and rpm of the turbine. Within these limits the weight is controlled to a high degree by factors peculiar to the particular design, such as the vibratory stresses. Some weight saving is generally effected by designing the turbine with a small amount of angular rotation in the discharge gases. If carried too far, this would result in lower exhaust-system efficiency, and therefore fuel consumption.

Perhaps the salient influence is the ingenuity of the mechanical design. Highly efficient structure can make severe inroads on weight. Similarly, significant gains can be made by ingenious use of flow distributions, and so forth, by the aerodynamic designer, and by proper integration and balance of the over-all aerodynamic design.

In the foregoing discussion of weight, engines designed for the same thrust have been assumed. Hence weight and specific weight (weight per pound of thrust) have been synonymous. Specific weight, however, tends to vary with size. If an engine is scaled down geometrically, the thrust decreases as the square of the dimension while weight decreases as the cube. Therefore the specific weight would decrease as the $^3/_2$ power of the dimension. In practice, this will not occur. Engines cannot realistically be scaled geometrically because of such items as minimum manufacturing dimensions, Reynolds-number effects, and blade-tip clearance effects. Actually, the specific-weight exponent for scaling will itself vary with engine size. At the extreme large sizes it should approach the geometric value of 1.5. As the size

is reduced, the exponent will decrease, reaching 1.0 at some relatively small size and dropping below this value as the dimensions are further diminished.

Fuel Consumption

As in the case of the specific air consumption, the specific fuel consumption (pounds of fuel per hour per pound of thrust) depends upon the turbine-inlet temperature, the compressor pressure ratio, the component efficiencies, the flight altitude and Mach number, the anticipated installation losses, and the compressor air required for engine use. Fig. 11 embodies assumed values of those variables and illustrates the variation of specific fuel consumption with the cycle pressure ratio and temperature at a Mach number of 2.0 and altitudes above the tropopause. Again, analogously to specific air consumption, the level of the values assumed for the variables as well as their assumed functional relationships will have a strong bearing on this curve and the succeeding one, Fig. 12, which indicates the change of specific fuel consumption with flight Mach number.

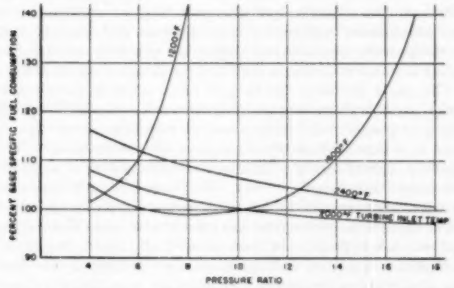

Fig. 11 Specific Fuel Consumption; Flight Mach Number 2.0

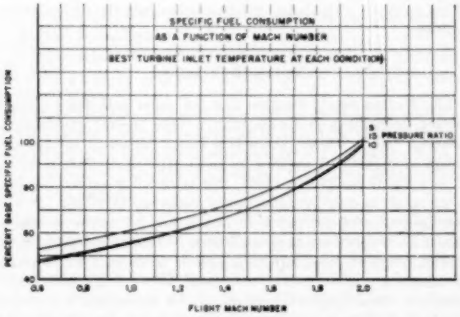

Fig. 12 Specific Fuel Consumption as a Function of Mach Number

(Best turbine-inlet temperature at each condition.)

If the duration of flight at high speed is to be short, exhaust reheat may prove profitable. The specific fuel consumption for this mode of operation is shown in Fig. 13. While the specific air consumption has been nearly halved, the specific fuel consumption has been increased by approximately 50 per cent. An exhaust-reheat engine under these conditions will produce the thrust of two nonreheat engines of equivalent air flow but will burn fuel at a rate equal to that of three such engines. At such high fuel rates a relatively short period of time may suffice to consume a quantity of fuel equal in weight to an additional engine, though the required time rises appreciably as the flight altitude is increased.

The engine with exhaust reheat can be profitable for flights of short duration. For flights of long duration, it is generally de-

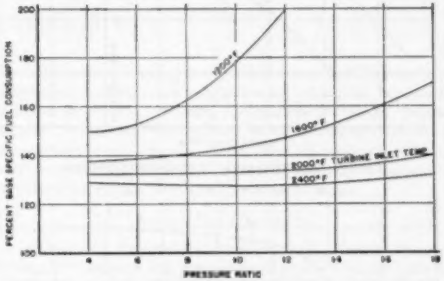

Fig. 13 Reheat Specific Fuel Consumption; Flight Mach Number 2.0

sirable to meet the required cruising thrust in a nonreheat cycle at a condition other than that yielding minimum specific fuel consumption. The reasoning in the foregoing two cases is similar. As shown in Fig. 11, small sacrifices in specific fuel consumption can result in significant decreases in design pressure ratio and turbine-inlet temperature, which may result in notable weight and cost savings. Some of our studies have indicated that the design pressure ratio yielding minimum combined specific weight (weight of fuel plus engine per pound of thrust) may be 50 per cent of that giving minimum specific fuel consumption. The shorter the duration of flight and the higher the flight altitude, the more the fuel consumption can be compromised to save engine weight.

The ratio of the thrust at minimum specific fuel consumption to that at military power may be adjusted somewhat for a specific engine design through manipulation of the compressor design. The matching of the compressor stages may be adjusted to produce peak compressor efficiency at various rpm. This is illustrated in Fig. 14. The compressor represented by curve A will cause the engine to have minimum specific fuel consumption at a lower thrust than for the same engine incorporating compressor B. This change in stage matching alters completely the characteristics of the compressor and hence the whole engine performance is affected markedly. In general, the higher the rpm at which peak compressor efficiency occurs, the poorer will be the part-speed performance. Of course somewhat equivalent variations may be had by adjusting the speeds where the other components attain maximum efficiency. But changes in the compressor produce the largest effects because they influence air flow as well as efficiency.

The aerodynamic design has perhaps the most important bearing on specific fuel consumption. Ingenuity, knowledge, and research must be combined to increase the level of component performance above the already high levels attainable today. The mechanical designer also can make an important contribution by providing low running tip clearances for the compressor and turbine blading, avoiding obstructions in the flow path, keeping air-seal leakages to a minimum, and by maintaining good finish, angle, and contour control on the aerodynamic surfaces.

If the engine is designed for high-altitude operation, two other items attain high significance: Reynolds-number effects and combustion efficiency.

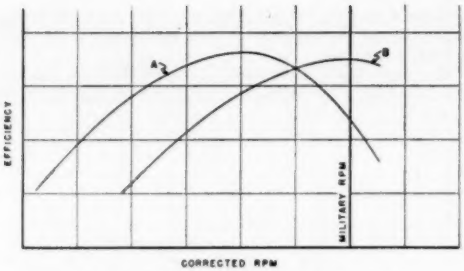

FIG. 14 ALTERNATIVE COMPRESSOR DESIGNS

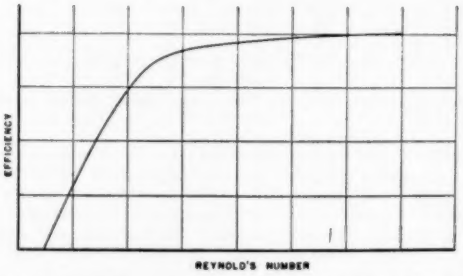

FIG. 15 ROTOR EFFICIENCY AS A FUNCTION OF REYNOLDS NUMBER

Fig. 15 is typical of the variation of rotor efficiency with Reynolds number. At medium altitudes most engines operate on the relatively flat portion of this curve. As the flight altitude rises, Reynolds number decreases, and severe losses in efficiency can result for the smaller engines. This may be avoided to some extent by increases in blade chord with suitable design modifications.

Combustion efficiency tends to become poor at the low-pressure levels encountered during high-altitude flight. This tendency may be countered somewhat by the use of higher compression and by combustion-chamber and fuel-nozzle modifications.

Both the combustion efficiency and Reynolds-number effects are improved by increasing the flight speed, thus resulting in higher compressor entrance pressures for a given altitude.

CONCLUSION

As we have seen, the problem of optimizing an engine design is an extremely complex one. In addition to the many interrelated variables discussed in the foregoing, manufacturing economy, use of strategic materials, engine maintenance, and overhaul time, and many similar subjects must be considered. In practice, an effective balance of the design must depend primarily upon the co-operation, experience, and abilities of the many persons involved. Many factors must be evaluated intuitively or through judgment based on experience, and no one person can be expected to have at his command the necessary background. Much insight can be gained, however, by continued generalizing studies which encompass many of the variables on a consistent basis.

ACKNOWLEDGMENT

The author wishes to thank Mr. W. H. Krase, Mr. M. F. Dowell, and other of his associates for assistance in the preparation of this paper.

Discussion

D. F. WARNER.[2] This paper should prove to be of great interest to the aircraft-engine industry, users of the engines, and to those whose duty it may be to define the missions of future applications of the aircraft gas turbine.

It is apparent that the versatility of application of any engine is becoming increasingly restricted as new aims in altitude and aircraft performance are specified. The bomber, fighter, missile, and civil requirements are even now so divergent that specially tailored engines are proper for each such purpose and, in many cases, variations of engine are properly called for to satisfy separate instances in each of these classes of application.

The paper describes the factors which affect aircraft-engine design and performance, and attempts to establish values wherever possible. In many cases, at this stage of our knowledge, it is impossible to place numbers against the trend. The problem of establishing values is a complex one since many of the factors are interdependent. The paper is provocative of thought, however, and to the writer one of its principal virtues lies in the fact that the author has portrayed in a fine manner the field which is in great need of an accurate and continuing study. The paper summarizes well the knowledge available at this date. The aim in the continued study is, of course, to enable the future aircraft-engine designer quickly to translate into form and design the features which best meet the increasingly exacting demands of the services. The paper admirably presents the extent of the problem.

AUTHOR'S CLOSURE

Mr. Warner clearly discerns that the paper goes much further toward delineating problems than it does toward providing a solution. As he states, there is a strong tendency toward the design of specialized engines for each type of aircraft mission. If, in a highly competitive field, this tendency is carried too far, it can result in overdiversification of the industrial effort. It was not the intent of the paper to imply that an optimum engine should be designed for each application. In fact, comprehensive studies frequently indicate that only a small sacrifice is made by adapting a given engine to several different missions. The extent to which engine design should be specialized is a major problem which is in urgent need of comprehensive and detailed study. The author wishes to thank Mr. Warner for his incisive and kind comments.

---

[2] Aircraft Gas Turbine Division, General Electric Company, Lynn, Mass. Mem. ASME.

Review of Combustion Phenomena for the Gas Turbine

By D. G. SHEPHERD,[1] ITHACA, N. Y.

Combustion-chamber design information is comparatively meager except for over-all performance data from existing gas turbines, such as combustion intensity and fractional pressure loss. Some information is available from established practices in other fields but many new or intensified problems remain. However, there is a rapidly increasing interest in the basic mechanism of combustion from the viewpoint of the physical chemistry of ignition, flame propagation, and burning, which together with reconsideration of the older empirical data of a fundamental nature shows promise of being fruitful. The purpose of this paper is to present a survey of some of this basic material as a step in helping the combustion engineer to correlate it with his knowledge of existing over-all performance.

DESIGN data for combustion in gas turbines is negligible when compared with that available for the other major components, which, if conservatively designed, can be relied upon to give a performance close to that expected, whereas even a conventional combustion chamber requires extensive development and testing under both simulated and operating conditions. Although combustion is a separate self-contained process with no other functions to consider, the stringent requirements with respect to space, weight, and power loss, together with the complex chemical, physical, and aerodynamic phenomena involved, combine to render it a formidable problem. Such data as exist at the present time may be divided into the following groups:

1 Meager statistical data from existing gas turbines, such as combustion intensity and fractional pressure loss.

2 Information on combustion behavior in analogous circumstances, e.g., in oil and gas furnaces, spark and compression-ignition engines.

3 Empirical data on general combustion phenomena, which of recent years are being reconsidered in the light of reaching an understanding of the basic mechanism of combustion by fundamental studies of the physical chemistry of ignition, flame propagation, and burning.

It is this last group which holds the most promise for the gas-turbine engineer. At the present time it presents a rather unwieldy mass of material which is only beginning to shed light on the complex problem of burning a mixture of hydrocarbons in a turbulent high-velocity stream of air. The combustion engineer is confronted with a large body of scattered information which often appears to be remote from the practical design of a combustor, and it is the purpose of this paper to attempt a brief survey of some of this fundamental investigation and to correlate it with existing combustion-chamber performance. To the physicists and chemists working in the fundamental field, it may seem premature to attempt such a correlation at this time, but the information is already becoming indigestible to the combustion engineer. It is hoped that an interim review may serve to clarify his empirical results, to give some clues on probable behavior under varying conditions, and to provide him with a measure of control and prediction which he now so sadly lacks.

Design Requirements

A satisfactory combustion chamber must provide complete burning, low pressure loss, smooth combustion, freedom from deposits, uniform exit temperature, ease of ignition, reliability, and endurance. All these qualities must be provided over a relatively large range of air flow, pressure, temperature, and mixture strength for a possible range of fuels from gas to heavy fuel oil and be accomplished within a structure of minimum weight and volume, the latter requirement at times being a major consideration. Thus gas-turbine combustion design is compounded of many technical skills, and the present state of development has been accomplished largely by empirical means, so that the results of any change of operating conditions have to be met by test with little margin for satisfactory prediction. The combustion engineer knows that because flame speeds are low and combustion temperatures must be high, a primary zone must be isolated by means of a stabilizing baffle, and that mixing to produce the correct final temperature must be accomplished separately. From then on it is a trial-and-error procedure. It is the purpose of fundamental research to help him in establishing design parameters and at least to show him the way to provide the most favorable conditions to satisfy the requirements.

The fundamental work on the combustion mechanism is necessarily done with as few variables as possible, in order to isolate the effect of these variables. Thus it may appear that the mechanism of combustion of homogeneous nonturbulent mixtures or of pure diffusion flames is far removed from gas-turbine conditions. Nevertheless, at some stage in the combustor process, such conditions are established in a greater or lesser degree, and it is important that the control of these stages be understood. Eventually they will be assimilated to build up to a significant body of design information. Some of what appear to be the basic phenomena of importance will now be discussed.

Flame Propagation

The flame speed[2] of all combustible mixtures is low compared to the air-flow velocities encountered; for instance, a gasoline-air mixture has a flame speed of only 2 to 3 fps under normal conditions. Note that flame speed as defined in this manner is a constant of a particular combustible mixture at given pressure and temperature conditions and is independent of the particular method of burning. With turbulence, an apparent or effective flame speed is obtained, greater by a factor of 10 or more than the basic flame speed which is usually measured in quiescent mixtures or in laminar flow. Because of the very low values of flame speed, it is necessary to introduce a stabilizing baffle to provide a region of very

---

[1] Associate Professor, Department of Heat Power, Sibley School of Mechanical Engineering, Cornell University. Jun. ASME.

Contributed by the Gas Turbine Power and Fuels Divisions and presented at the Annual Meeting, New York, N. Y., November 26–December 1, 1950, of The American Society of Mechanical Engineers.

Note: Statements and opinions advanced in papers are to be understood as individual expressions of their authors and not those of the Society. Manuscript received at ASME Headquarters, October 3, 1950. Paper No. 50—A-96.

[2] Flame speed = velocity of flame front in a direction perpendicular to its surface relative to unburned mixture = "transformation," "burning," "normal," or "ignition" velocity, etc.

low velocity or even reverse flow in order to maintain ignition. The laminar flame speed is a property which is basic for an understanding of the mechanism of flame propagation, and a considerable amount of attention has been paid to it.

For gas-turbine combustion, exact values of flame speed are not so important as an understanding of the factors controlling them so that optimum conditions can be provided if possible. Markstein and Polanyi (1)[2] have presented a critical review of existing theories of flame propagation, including the older purely thermal theories and the newer theories, involving the kinetics of chain reactions, together with the effects of turbulence and hydrodynamic factors. At the present time there is no certainty as to whether the controlling effect is a purely thermal one, that is, rate of heat conduction to the unburned mixture or a kinetic one, or diffusion of active atoms and radicals from the flame into the unburned mixture. Thus Tanford and Pease (2) have shown that flame speed can be represented by a product of terms, the most important of which is the square root of the sum of equilibrium free radical concentrations each multiplied by its coefficient of diffusion into unburned gas, hydrogen having a controlling effect because of its high value of diffusion coefficient. This approximate square-root law of flame speed has predicted values successfully for mixtures containing H_2,CO and hydrocarbons.

The role of the diffusion of hydrogen atoms is supported by work of Gaydon and Wolfhard (4), although they sound a note of caution with respect to accepting it completely, a view which is supported by Townend (5) and particularly by Linnett and Hoare (6), who have shown that some of the same experimental results correlated with the square-root law also can be predicted successfully by a purely thermal theory.

An important corollary of any theory is to be able to predict the effect of pressure and temperature. Tanford and Pease are able to show that flame speed should vary inversely with the fourth root of the absolute pressure (approximately), but experimental results are somewhat contradictory. There is still some uncertainty about the accuracy of experiments, but recent work of Garner, Long, and Ashforth (3) by a method believed to be correct to within 5 per cent, shows flame speed of certain mixtures to obey an inverse cube-root relationship with pressure (down to 0.35 atm). Previously, others, Linnett (8), Ubbelohde (9), Badin, Stuart, and Pease (10), and Johnston (11) have demonstrated increase of flame speed with decrease of pressure, some results showing a critical subatmospheric pressure below which flame speed rapidly decreases. This critical pressure may be connected with the important phenomenon demonstrated by Hubner and Wolfhard (7) that the minimum pressure at which combustion can be sustained at all is dependent upon the burner port size, resulting in the simple relation that pressure is inversely proportional to burner diameter. Measurements of flame speed by Wolfhard, et al. (4, 7), varying burner diameter according to this relationship, showed no change with pressure. Thus there may be an effect of burner diameter in some experiments, although this was tested in the work of Garner, et al. (3) with negative result.

In general, it would appear that pressure has a relatively small effect until some critical subatmospheric pressure is reached when the flame speed decreases sharply (but the effect of burner diameter should be noted). Such critical pressures as have been demonstrated are approximately 0.4 atm and thus are significant for gas turbines in aircraft.

Increase of temperature is always beneficial. Johnston (11) has shown that the flame velocity of natural gas-air mixtures increases from peak values of 1.5 to 8.25 fps for an increase of initial temperature from 137 to 902 F. These results show that, roughly, flame speed is proportional to absolute temperature, and Broeze (12) reports similar results for propane-air and butane-air mixtures over a range of temperature from 70 to 400 F although the rate of increase with temperature is considerably less than that found by Johnston. With respect to mixture strength, the peak flame speed (other conditions fixed) occurs at the stoichiometric or slightly rich air/fuel ratio, with a further shift to the rich side at reduced pressure, Johnston (11).

Because different fuels have different flame speeds, there may be some advantage in selecting fuel to give a high value, although in practice the choice of fuel is likely to be quite restricted. Within a given range of fuel, however, it may be possible to select the type of base or structure, and experiments of Reynolds and Ebersole (13), using the uniform flame-propagation velocity[4] in a 2.5-cm tube as being proportional to the true flame speed, present preliminary conclusions as to the effect of degree of unsaturation, chain length, and size of molecule.

It is recognized that OH and H radicals have a marked effect on combustion in some cases and, therefore, the addition of water vapor or pure hydrogen might be expected to affect flame speed. Data are scanty but Kapp (14) reports that in butane-air mixtures, increase of water-vapor content from 0.08 to 2.6 per cent reduced the peak flame speed by 9 per cent.

It was stated earlier that turbulent flame speeds were higher than laminar flame speeds, and Williams and Bollinger (15) in experiments on Bunsen flames of hydrocarbon-air mixtures have developed the following relationship

$$V_T = 0.18\, V_N d^{0.26}\, \mathbf{R}^{0.14}\ (\text{cm/sec})$$

where V_T and V_N are the turbulent and normal (laminar) flame speeds, respectively, d is the port diameter in cm, and $\mathbf{R}$ is the Reynolds number. Attempts have been made to predict the effect of turbulence on flame speed, notably Damkohler (16) and Shelkin (17). These two papers are discussed by Markstein and Polanyi (1), and the experimental work of Williams and Bollinger shows that the conclusions are generally not valid except for the qualitative dependence of turbulent flame speed on laminar flame speed, quantitative predictions not being substantiated.

Caldwell, et al. (18), report Bureau of Standards experiments showing an apparent flame speed of 30 fps and greater for propane-air mixtures in steady flow past a simple baffle, the laminar flame speed being about 1.5 fps for the given mixture. Combustion of this sort is quite different from ignition of quiescent mixtures and Bunsen-type flames, and is closer to actual gas-turbine conditions. A detailed study of this sort has been made by Scurlock (19) with homogeneous mixtures of propane-air and city gas-air in steady flow in a rectangular duct 3 in. × 1 in., using various stabilizers in the form of rods, 30 deg open and closed "gutters" (wedge shapes with apex upstream) and flat plates, the size varying from $^1/_{16}$ to $^1/_2$ in. Tests were made at atmospheric pressure, at inlet temperatures from 30 to 70 C, and flow velocities from 20 to 350 fps. This investigation demonstrated that the increase in apparent flame speed may be ascribed to reverse eddies and turbulence[5] and some approach to a quantitative analysis was made. It was also shown that approach stream turbulence is usually masked by that occurring downstream of the baffle.

Ignition of quiescent mixtures in tubes produces a flame-front

[2] Numbers in parentheses refer to the Bibliography at the end of the paper.

[4] Uniform flame speed (UFS)

$$= \frac{\text{Fundamental flame speed} \times \text{area of flame surface}}{\text{Cross-sectional area of flame}}.$$

[5] Small scale or microscopic turbulence, three-dimensional velocity fluctuations from the bulk velocity, not turbulence as sometimes used in the sense of a large-scale mixing effect.

velocity considerably in excess of true flame speeds (cf. uniform flame speed referred to earlier) and may be considerably increased by special means. The most spectacular results are reported by Evans, et al. (20, 21), the latter quoting maximum flame-front velocities up to 1000 fps by interposing grids in the path of the burning gases. The effect is due to the greatly increased reaction surface and the accelerated mixing by jet effect.

This summary of some of the existing work on flame speed leads to the following tentative conclusions:

1 Increase of initial temperature is beneficial.

2 The pressure effect is uncertain but appears to be relatively small until a certain limiting low pressure is reached when flame speed may drop sharply (but note effect of port size).

3 Type of fuel and basic structure affect flame speed, thus giving notice that fuels of nominally the same physical characteristics may exhibit different behavior.

4 Atmospheric humidity and addition of water vapor affect flame speed but do not exert a major control.

5 Apparent flame speeds in turbulent flow may be very much higher than laminar flame speeds and are related to it by port diameter and Reynolds number. They may reach very high values by special mixing effects.

6 Initial small-scale turbulence has a minor effect.

Stability Limits

In steady-flow combustion, the usual limits of inflammability of an air-fuel mixture are dependent on the flow velocity and the baffle system, the main interest lying in the extent of the range obtained by plotting mixture strength against velocity. Quantitative results are rather meager and are somewhat dependent on the type of baffle system used. Most attention has been paid to homogeneous mixtures, and here it appears that some degree of correlation is being obtained.

Extensive tests of the stability limits of homogeneous mixtures with a variety of baffle shapes have been made by Scurlock (19, 19*a*, 19*b*), Longwell (22, 24), and DeZubay (23). Scurlock's tests were two-dimensional as the baffle extended across the full width of the duct with only one dimension being varied, the baffles used being rods, wedges, and flat plates from $^1/_{16}$ to $^1/_2$ in. width. Propane-air and city gas-air mixtures were used at approximately atmospheric pressure and temperature, flow velocities ranging from 30 to 350 fps. The results showed the following:

1 The mechanism of stabilization differs from a Bunsen flame in that it depends on an eddy region which supplies continuous ignition to fresh mixture.

2 Correlation for the stabilizers of various shapes and sizes was obtained by plotting air/fuel ratio against $V_{BO}/d^{0.45}$, where V_{BO} is the blowont limit velocity and d is the characteristic dimension of the stabilizer transverse to flow.

3 Heating the stabilizer extends the limits considerably and cooling narrows them.

4 The stability limits of a given baffle are unaffected by the width of the duct within a range of duct width/stabilizer dimension of about 10 to 80.

5 The expression $V_{BO}/d^{0.45}$ is a direct function of laminar flame speed and the difference of combustion temperature and initial temperature. It is also dependent on the type of fuel, but the magnitude of the effect is unknown.

6 Increased intensity of initial turbulence decreases the stability limits, with the effects becoming less as ratio of baffle diameter to the scale of the turbulence increases.

The tests made by Longwell were with cylindrical baffles having the longitudinal axis parallel to the air stream. The duct diameter was 6 in., the baffles ranged from 0.75 to 2.87 in. diam, the fuel used was volatile petroleum naphtha, and flow velocities were as high as 900 fps. The baffles were both solid and open at the downstream end and included a simple cone, but it was found that shape did not affect the results except when the downstream end was rounded off. Fully streamlining the trailing edge resulted in very poor operation. Longwell's results correlated well using V_{BO}/d as parameter against air/fuel ratio. As given by him, air/fuel ratio is plotted against R/V_{BO} where R is the baffle radius, showing that above a value of R/V_{BO} of about 20×10^{-6} the lean limit approached a constant value of 24/1 and the rich limit 9/1.

Tests with varying pressure showed that a range from 1 to 3 atms had little effect, but a reduction to 0.2 atm reduced the limits, although this single result was at a velocity of 470 fps, compared with 400 fps for the higher pressures. This was for the 2.87-in. baffle, and a larger effect at lower pressures was observed with the smaller baffles. At atmospheric pressure and 275 fps velocity, using the 0.75-in. baffle, increasing the air temperature from 205 to 500 F increased the lean limit progressively from 19.5 to 22, with small effect on the rich limit. The effect of changing the fuel from naphtha to propylene oxide was to widen the limits relative to the stoichiometric mixture. In both cases the static-inflammability limit could be approached closely on the lean side at a velocity of 300 fps but blowout was at a much leaner mixture than the static limits on the rich side.

DeZubay performed stability tests with flat circular plates $^1/_4$ to 1 in. diam. in a $2^3/_4$-in. duct, the maximum flow velocity being 550 fps and the fuel being commercial propane. Humidity and temperature (90 F ± 30 F) were kept constant but the pressure was varied from 0.2 to 1 atm. Correlation of results showed that the fuel/air ratio is a function of $V_{BO}/P^{0.33}d^{0.336}$ which is fair agreement with Longwell ($F/A \propto V_{BO}/d$). DeZubay also shows that Scurlock's two-dimensional results give excellent agreement, since the dimension d in this case was proportional to area, and his own results can be written as fuel/air ratio being a function of

$$\frac{V_{BO}}{P^{0.33}A^{0.336}} \propto \frac{V_{BO}}{P^{0.33}(d^2)^{0.168}}$$

showing a comparison of coefficients of 0.45 to 0.428. Thus there appears to be favorable correlation of results for stability limits in homogeneous mixtures.

With heterogeneous conditions, i.e., injection of liquid-fuel drops or of gaseous fuel immediately at the combustion zone, similar stability limits are imposed, usually both rich and lean limits being higher than the stoichiometric. There are almost no systematic data available for heterogeneous conditions as the particular injection system obviously must have a controlling effect, and there is a great need for investigation here to see whether any correlation can be obtained for simple stabilizer systems akin to that for homogeneous mixtures.

Lloyd (25) shows a typical stability diagram for the liquid-injection case, and interprets the lean limit line as one where the flame blows out due to sufficient heat not being brought back by flow reversal to ignite the entering fuel and the rich-limit line as one of upper inflammability limit or of pulsating combustion exciting resonance effects. The lean limit is affected adversely by anything which tends to lower the temperature of the flow reversal (e.g., falling air entry temperature), or to raise the ignition temperature (e.g., falling static pressure). The former effect is demonstrated by the extension of the lean limit with increased inlet-air temperature, with little change in the rich limit. This is the usual experience, though Caldwell, et al. (18) report results from the injection of petroleum ether through numerous concentric ports, showing in this instance that the lean limit is

considerably narrowed by increase of air temperature from 50 F to 350 F. A possible explanation for this is given as increasing homogeneity at the higher temperature since the fuel was highly volatile. Other work too shows that often increasing heterogeneity leads to increased stability, which is reasonable if it is considered that such a mixture will be likely to have at least one local zone where combustion is possible even though the over-all mixture strength is out of the range.

The position with respect to stability limits may then be summarized as follows:

1 For homogeneous mixtures, shape of baffle is unimportant, providing that it is not streamlined downstream.

2 There appears to be a correlation between blowout velocity, pressure, air/fuel ratio, and baffle size, represented by the expression $V_{BO}/P^x d^y$ = const for homogeneous mixtures of a given air/fuel ratio. This relationship is unaffected by the ratio of duct width to baffle diameter down to a value of 10. Experimental data to date place the value of x as 0.95, and the value of y between 0.86 and 1.0.

3 For homogeneous mixtures, increase of temperature, either of the mixture or of the baffle itself, is helpful in extending the lean limit. For heterogeneous mixtures, the effect is uncertain but would appear to extend the lean limit considerably for the less volatile fuels.

4 Pressures above atmospheric have little effect on the limits, but subatmospheric pressures may have a narrowing effect approximately in direct relationship.

5 Small-scale turbulence is unlikely to have much effect in gas-turbine chambers where relatively large baffles are used.

6 There appears to be a need for data on stability limits of heterogeneous mixtures for simple injection systems, e.g., upstream, downstream, and radial injection from single and multiple ports with and without plane or coned circular baffles.

In actual gas-turbine combustors, stabilizers have taken a variety of forms but they may be divided into two classes, those operating on the basis of swirl and those operating with "controlled turbulence." Swirling the primary air around the fuel spray is very common on many types of combustion apparatus as it provides excellent mixing conditions and good stability. The essence of its action appears to be the formation of a low-pressure core along the axis, burning gases and fresh air from downstream being drawn into this core and flowing in reverse direction upstream to the fuel nozzle, thus providing constant ignition and mixing. Such a system is difficult to analyze as the effect is distributed over the whole duct cross section and development has been purely empirical.

Systems of controlled turbulence are used in which air is admitted through a number of plane orifices, permitting a more controllable mixing process. Again, the air jets must form a pattern which causes eddies or flow reversal to obtain continuous ignition at or near the point of fuel injection. A large number of existing combustors use such a pattern of jet mixing, combined with downstream fuel injection. Upstream injection of the fuel may provide better stabilization than downstream injection, and an example of this combined with controlled turbulence is given by Lloyd (25) and Ashwood (26). Fuel is injected upstream from a low-dispersion nozzle against the apex of a perforated inner cone which supplies air to the center of the spray, and through the spray annulus to provide good mixing. The inner cone is surrounded by an outer hemispherical shell or cone to provide a stabilizing and mixing zone of greater diameter, this shell being attached to a liner in one form of the combustor suited for a normal gas turbine.

Ignition Temperature

Ignition temperature and the associated delay time or lag are of considerable importance, both in the primary region where stabilization is dependent on the continuous ignition of fresh mixture by recirculating burning or burned gases and in the succeeding combustion and mixing zones, where injudicious admixture of diluting air may quench or chill the reaction below the ignition point. There is some difficulty in establishing values of spontaneous ignition temperature and delay time because so much depends on the method. The total delay time with a liquid fuel consists of a physical delay due to the evaporation of the droplet and diffusion of the vapor into air and a chemical delay time. The physical delay time is dependent on the rate of heat transfer to the fuel and the size of the fuel droplets. Chemical delay time is mainly dependent on the temperature and the particular fuel in question. It would appear possible to obtain similar total delay times with two very dissimilar fuels each having different physical and chemical delay times.

The combustion of liquid drops is discussed later, but Lloyd (25, 27) has studied the delay time in direct fashion by spraying liquid fuel into a stream of air at controlled high temperatures (1400 F — 1800 F) and observing the distance (and hence time if flow rate is known) before a flame front is formed. Under these conditions it is shown that the logarithm of delay time is inversely proportional to the absolute temperature of the air, and that there is very little difference between fuels over a range including kerosene, gas oil, and rubber solvent. The delay times at the temperatures given in the foregoing varied from approximately 30 to 2 millisec.

Results of Muller, quoted by Elliott (28) for α methylnaphthalene and cetene do not show a linear relationship for log t versus $1/T$, and Elliott interprets this as the effect of a physical delay and a chemical delay, each obeying the foregoing law, the sum of the two giving the total delay. The Muller tests were by injection of fuel into a bomb at temperatures ranging from about 500 F to 1150 F, that is, much lower than those of Lloyd in the steady-flow experiments. A comparison of the two sets of data shows that those of Lloyd give very long apparent delay times (30 millisec at 1500 F), compared to those of Muller (30 millisec at 450 F for cetene, and at 800 F for α methylnaphthalene). Degree of atomization would have some effect, but Lloyd has shown that it does not have a controlling influence. Also the Muller results show a marked difference in the two fuels, where Lloyd's show no great effect for a considerable range of fuels, including the addition of "dopes" for ignition promotion. One interpretation of the last result is that at the high temperatures used by Lloyd, chemical delay is insignificant, which is supported by work on combustion of liquid drops discussed later, which shows that the physical delay times of most hydrocarbon fuels are very similar.

These experiments were performed at atmospheric pressure, and it is well known that variation of pressure has a marked effect on ignition. It is not the place here to discuss the very complex subject of reaction kinetics, and perhaps the most significant result is the relation given by Schmidt (29) which correlates tests in a bomb and in an adiabatic compression apparatus, namely

$$t = \frac{Ae^{B/T}}{p^n}$$

where t = delay time, T = absolute temperature, p = pressure, A and B are constants, and the exponent n is slightly greater than unity. This relation strictly holds only for a homogeneous gas reaction where delay times are short but is apparently valid for at least a limited range in a heterogeneous reaction. Further discussion and references to German work are given elsewhere (30).

Temperature then has a controlling influence on delay time, and the effect on the lean stability limit is readily explained. Reduced pressure lengthens delay time in roughly direct proportion (for the higher pressure range), although this effect on the lean limit is not clearly apparent. At some critical low pressure (possibly subatmospheric), a considerable increase in delay time is expected from a consideration of the literature of reaction kinetics, but the subject is too detailed for generalization.

Mullen, et al., measured ignition temperature in high-velocity streams of combustible gas by means of electrically heated rods. Their results showed that the minimum ignition temperature (t_{ig}) was obtained with stoichiometric mixtures, and that t_{ig} was reduced by increased initial mixture temperature, higher pressure, and larger rod diameter. t_{ig} was increased by greater initial turbulence and addition of water vapor (up to 5 per cent), although ordinary atmospheric humidity caused no measurable variation. Different fuels showed different rates of change of t_{ig} with velocity, hydrogen showing the lowest t_{ig} except at the very lowest velocities, contrary to static ignition tests. Location of the heated area was an important factor, the downstream face of the rod being most effective.

The relationship of ignition temperature, delay time, and the effect of pressure then is still somewhat uncertain and is different for various phases of the combustion process, for instance, in the primary zone where liquid fuel is injected and in the later zones where a gas mixture has to complete combustion. The overriding importance of high temperature is established, but other factors seem to depend on the ratio of physical and chemical delay times. Thus, although dopes have generally been found unhelpful (in the controlled tests of Lloyd and other tests on complete combustion chambers), it is possible that they are not effective where physical delay is predominant but could be beneficial where chemical delay is a controlling factor.

Diffusion Flames

A diffusion flame is one in which there is no premixing of fuel and air and in which combustion occurs in a thin flame front created by the interdiffusion of oxygen and fuel molecules. Examples commonly quoted as diffusion flames are those of a candle or a Bunsen burner with no primary air. There appear to be three cases of diffusion flames, (*a*) where the fuel flows into still air, (*b*) where the fuel and air both flow but with different velocities and (*c*) the special case of (*b*) when air and fuel velocities are the same. The last case (historically the earliest analysis) has been studied by Burke and Schumann (**32**) while, more recently, extensive analytical and experimental studies have been made of flames in still air, for laminar flow by Hottel and Hawthorne (**33**), for turbulent flow by Hawthorne, Weddell, and Hottel (**34**), and for both laminar and turbulent flow by Wohl, Gazley, and Kapp (**35**, **35***a*). Barr and Mullins (**36**) have developed the case for both variable air and fuel velocities, particularly studying the effect of reduced oxygen content of the air. While such idealized cases of diffusion flames occur in the gas turbine only with linear injection of a gas or vapor into the air stream, they are approached at some phase of the combustion process, and it is useful to have some knowledge of the controlling factors.

Wohl, et al., have made an extensive study of the flames of city gas and butane in still air over a range of initial fuel-mixture composition from the pure fuel to the stoichiometric mixture. A theoretical expression for flame height h based upon a diffusion process is deduced

$$h = \frac{Qc_f\left(1 - \frac{c_{st}}{2c_f}\right)}{4\pi K c_{st}}$$

where

Q = volume flow rate
c_f = initial mole fraction of fuel gas in primary mixture
c_{st} = mole fraction of fuel in stoichiometric mixture
K = coefficient of diffusion

The experimental results for laminar and turbulent flow are given for various gas mixtures and by consideration of the nature of the different flames, the basic analytical expression is found to represent the empirical results. Thus, for 100 per cent city gas flames, the introduction of a variable diffusivity in terms of height above the burner port, and for 50 per cent city gas-air flames, consideration of the additional phenomenon of flame propagation in a homogeneous mixture allows the empirical expressions for laminar flow to be correlated with the analytical equation. For turbulent city-gas flames, the substitution of eddy diffusivity for molecular diffusivity has similar effect. For butane flames, consideration of the effects of viscosity allows agreement to be reached, with the conclusion, supported by experiment, that butane flames are of a laminar character even if the flow in the burner tube is wholly turbulent.

For laminar flames, Hottel and Hawthorne have a somewhat different approach, which, however, is again based on a diffusional concept, and Hottel shows that there is fair agreement between their results and those of Wohl (see discussion following reference **35***a*). Both show that flame height depends on volume flow rate and ratio of primary to stoichiometric air and is independent of burner-port diameter. For turbulent flames, however, Hawthorne, et al., discard the diffusional approach for a method based on the mixing action of a fuel jet in ambient air, obtaining a relation applicable to a wide range of fuels in contrast to that of Wohl which requires a knowledge of a factor peculiar to a given mixture. Hottel again shows that both sets of results are in substantial agreement. Thus it may be concluded that expressions are available for calculating flame length under certain conditions or, perhaps more important for the combustion engineer, the main factors controlling the flame length are established, and a basis is available for providing optimum conditions and predicting behavior under other conditions. Results have not been given for pressures other than atmospheric but it may be deduced from the basic expression of Wohl that for a given weight rate of flow, pressure will not affect the height of a diffusion flame.

Other experiments on diffusion flames have been performed by Barr and Mullins (**36**) in connection with the general problem of the effect of vitiated air on combustion behavior. By vitiated air is meant air with less oxygen than pure air, as, for instance, when using exhaust gases for one purpose or another. A vitiation index a is defined as the fractional partial pressure or volume of the oxygen in the air (e.g., pure air has $a = 0.21$). In the course of the work, they investigated diffusion flames of a commercial propane-butane mixture with air, introducing the factor of variable air velocity. A theoretical expression is developed in terms of Bessel functions, with variables of air and fuel velocities V_a and V_f, radii of the inner (fuel) and outer (air) tubes, the flame height h, and diffusion coefficient D. By forming parameters Dh/V_a and V_f/V_a, a single curve is obtained for several values of V_f and V_a. As plotted, for a given value of $D = 0.013$ in^2/cm sec and fixed air and fuel densities and tube dimensions, the parameters Dh/V_a and V_f/V_a are transformed into h/V_a and the fuel/air ratio,[6] respectively. Thus flame height can be obtained for a given mixture strength at a known air velocity. The effect of pressure can be gaged from the two parameters and, since $D \propto$

[6] Note that mixture strength as used here is equivalent only to overall ratio of fuel to air of the system and is not that of a homogeneous mixture.

$1/p$ and at constant air and fuel mass flows, V_a and $V_f \propto 1/p$, neither Dh/V_a nor V_f/V_a are affected by pressure. This was confirmed experimentally, when h was found to be constant down to a pressure of about 1.3 psia, subsequently blowing off at lower pressures.

The foregoing results are for pure air, and the effect of vitiation was to increase the flame height, the change being small at weak mixtures but increasing greatly as the stoichiometric mixture was approached. Unfortunately, it is not possible to compare the results of Barr and Mullins with those of Wohl as the former work was done with such small values of fuel-flow rate that a quantitative comparison is difficult.

The behavior of diffusion flames is important for the case of gas or vapor injection and qualitatively is significant for some phase of the liquid-injection case. It appears as though there are available some data to help initial design and prediction of performance.

Combustion of Liquid Drops

Very little work has been reported on the combustion process of an individual liquid drop although the general process for an atomized fuel spray has been considered for Diesel engines (see, for instance, the review by Elliott) (28). This is understandable in view of the experimental complexities, although lately it has received some attention.

Probert (37) gives the results of a theoretical investigation of the burning of a cloud of droplets whose size distribution conforms to the Rosin-Rammler relation

$$R = 100\, e^{-(x/\bar{x})^n}$$

where

R = per cent by weight or volume over a certain diameter x
$\bar{x}$ = size factor, a measure of the degree of atomization, e.g., droplet size when $R = 50$ per cent
n = diversity factor, a measure of closeness of grading of droplets

Examination of the droplet sizes produced by atomizing nozzles reveals that this expression is a convenient representation, as shown by the work of Joyce (40) in which sizes were measured by the technique of spraying melted wax and sieving the solidified particles. It is generally accepted that the rate of evaporation of a liquid drop is proportional to the diameter, and with this assumption, Probert shows that in the initial stages of an idealized combustion process, then a high diversity factor (low n) accelerates burning, but in the final stages the more uniform spray (high n) is more advantageous.

Combustion of a drop is different from evaporation but the assumption of rate being proportional to the first power of the diameter appears to be validated according to initial tests reported by Godsave (38). Lloyd (27) discusses the available evidence and concludes that the burning rate of a drop is largely dependent on the enthalpy of the fuel to the dew point and the rate of heat transfer to the drop.

Spalding (39) has developed a theory for predicting the combustion rate from the physical properties of the fuel by analogy with heat-transfer processes and correlated it with results of experiments in which kerosene is burned (in air of various oxygen contents) from the surface of a sphere, and from a vertical plate. Using the concept of fuel vapor and oxygen diffusing across a gas film to form a combustion surface between the liquid fuel and the air stream, an effective temperature difference is established as a function of the physical properties of the fuel. It is concluded that those properties chiefly determining the combustion rate are the calorific value, the latent heat of evaporation, and the specific heat of the vapor, values of which do not differ greatly among hydrocarbon fuels. Thus, assuming that chemical ignition delay is negligibly small, combustion rates for gasoline and fuel oil are relatively similar (for similar spray patterns), and Lloyd's results on ignition delay discussed earlier are shown to have an analytical foundation.

Dreyhaupt (41) has analyzed the conditions leading up to the ignition of a fuel droplet, giving ways of calculating the heat required and allowing for the variation of mixture strength at different distances from the surface and for the decrease of droplet size as evaporation occurs. One conclusion is that if the droplets are too small they evaporate completely and do not reach ignition temperature, while for large drops there is insufficient air for combustion, and the drops are cooled below the ignition temperature. If this reasoning is correct a certain size of droplet is required for ignition. This situation is akin to a remark of Boerlage and Broeze (42) anent the Diesel engine that, although turbulence (in the large-scale sense) may shorten the evaporation time, it may cool a local-mixture temperature below the ignition point or decrease the local-mixture strength below the optimum for rapid ignition. In the gas turbine of course there is a continual source of ignition by eddying of hot gases but, nevertheless, such observations as the foregoing are worthy of consideration.

In the high-temperature conditions of the primary zone of a combustor, it is probable that cracking of the fuel in the liquid or vapor phase will occur before evaporation or oxidation. This leads to the formation of free carbon and is particularly severe with the heavier fuels with a high boiling point. It is also accentuated at high air pressures as the equilibrium temperature is higher, the equilibrium temperature being that temperature when heat transfer to the liquid is zero. Lloyd (27) traces the experimental course of a droplet of heavy fuel during combustion, showing that partial evaporation is followed by internal boiling or decomposition with the formation of a solid honeycombed bubble substantially larger than the initial droplet, further heating causing the bubble to pass through a skeleton stage of carbon. Even if swelling does not take place, the final stage of combustion occurs at a solid surface. Thus with a heavy liquid fuel the cenospheres familiar in solid-fuel combustion may appear.

It is apparent that a study of the mechanism of combustion of a liquid drop or a cloud of drops is only now commencing, but it is likely to be fruitful.

The Mixing Process

Mixing here is considered to be the mixing of burning fuel or hot gases with fresh air after passing through the primary combustion zone, which, although requiring mixing action, is essentially a stabilizing zone. Up to now mixing processes have been developed empirically and, because the diluting air amounts to 50–90 per cent of the total air, the problem is a major one. The consequent pressure loss is vitally important because often it is the controlling loss whereas ideally the primary-zone baffle should be the limiting factor.

The most favored method is mixing by jet action, exemplified by holes or slots in the wall of the inner combustion tube, the injected stream of air being more or less perpendicular to the gas stream. Swirl has been tried and found useful but does not appear on existing types of combustor. Some mixing effect can be obtained by introducing the air in annular streams parallel to the gas flow, obtaining more efficient wall cooling at the expense of mixing effectiveness. Other methods which have been tried endeavor to provide more positive mixing by leading the air through ducts which project into the gas stream with the idea of better distribution and lower pressure loss. They have not proved very desirable owing to the possibility of material failure by scaling or "burning" which is inevitable if any part of

the duct is insufficiently cooled, e.g., if there is "breakaway" on the air side. A unique method was employed on the initial combustion chamber for the Elliott 2000-hp experimental marine plant (43) in which the main mixing effect was produced by admitting the air from a single duct at right angles to the chamber, by which means two rotationally opposed vortexes were formed in accordance with the hydrodynamic laws governing such a flow pattern.

In nearly all combustion chambers the combustion zone is surrounded by an annulus conducting the diluting air, the latter being injected into the hot gas. An exception to this was the German Jumo 004 combustor which, although having the usual inner liner, directed the hot gases through chutes into the diluting air which suffered a minimum change of direction. While this particular arrangement is not necessarily commended, the basic idea is worthy of consideration as it avoids having to turn the major part of the fluid through a large angle, and this, undoubtedly, contributed to the low pressure loss of this chamber.

The basic problem is to provide the maximum interface between gas and air and therefore a large number of air entry holes or slots would seem desirable. However, a major characteristic of the mixing air jet must be its ability to penetrate as far as possible into the gas stream and, for the size of combustion chamber usually used and for the pressure loss allowable, sufficient penetration can be obtained only by the use of relatively large holes which are then limited in number.

Quantitative data on the mixing process as applied to gas-turbine combustors is scanty. Callaghan and Ruggeri (44) give the results of an experimental investigation to determine the penetration of a circular air jet directed perpendicularly to an air stream and give a quantitative expression for depth of penetration at a given distance in terms of orifice diameter, and densities and velocities of the jet and free-stream air. An investigation of Fraser (45) shows that the side pressure distribution around the jet appears capable of turning the jet nearly to a downstream direction in a few diameters penetration while further penetration appears attributable to a slow spreading of the jet due to turbulent mixing. Lloyd in some qualitative generalizations (25) states that molecular diffusion is negligible, mixing by random turbulence too slow, and ordered turbulence (e.g., a vortex trail from a cylinder) too limited in application by requiring special stream conditions. It is further stated that penetration and pressure losses of mixers are functions of the moments of the two streams and that pressure losses in typical mixing devices have been found amenable to a complete theoretical treatment, but no quantitative results are given.

In general, results on operating combustion chambers show that penetration is improved by placing numbers of holes in line rather than in a staggered arrangement or by the use of slots with a longitudinal axis. Maximum penetration with the lowest pressure loss is effected by having openings with a rounded entrance and with the least general turbulence in the fluid streams.

The problem of mixing for dilution purposes only is complicated by the requirements that part of the air is utilized as secondary air to complete combustion. The requirement of maximum penetration achieved best by large orifices is then opposite to that of combustion in which too much cool air at one point may quench the burning mixture below its ignition point, thus leading to unburned products. This flame-quenching or chilling effect is thus bound up with the ignition-temperature requirements previously discussed.

Carbon Formation and Ash Deposits

Carbon formation, including deposits on the combustor walls and soot in the exhaust gases, has been from the first a severe problem and one which is accentuated by the growing requirement to burn heavy fuels. The easiest approach to the problem is through the properties of the fuel itself, and this has an unfortunate effect because the natural tendency is to restrict the fuel to one which gives relative freedom from carbon troubles. Thus the gas turbine, which is potentially capable of using all gaseous and liquid fuels because it is not uniquely dependent on carburation or adiabatic compression for its combustion performance, may find itself limited in fuel usage. It would be unfortunate if carbon formation became analogous to knocking tendency as one of the primary qualities by which a fuel is rated. Thus the proportion of aromatics in the fuel is one of the primary criteria for aeroturbines. The accent on fuel properties is understandable as although something is known of the physical factors, they are not easy to control, and often the desiderata for minimum carbon conflict with other desirable conditions for good combustion performance.

Basically, the appearance of free carbon is due to the thermal decomposition or cracking of the fuel before oxidation, and it is recognized by the characteristic, luminous, opaque yellow flame as opposed to the nonluminous blue flame. This free carbon can be oxidized if conditions are suitable, but otherwise is carried out in the exhaust as soot or, in bad cases, deposited on the surfaces of the combustor. Its deleterious effect is not on combustion efficiency, which is very small, but on accumulation leading to blockage, overheating or turbine damage, or as undesirable exhaust smoke.

Thermal decomposition in preference to oxidation is favored by rich mixtures and poor mixing and is therefore almost inevitable to some degree with liquid injection, since, even with a weak over-all mixture, there will be locally overrich zones, particularly with poor atomization, causing large droplets. Nevertheless, it is known that with very good atomization of a reasonably volatile fuel (kerosene) and strong turbulence, it is still possible to obtain a predominantly blue flame at low flow rates. Recent experiments of van de Putte and van den Bussche (46), as reported by Broeze (47), show that in a special atomizing burner of the rotary-cup type in which atomization and mixing had been developed to a maximum of homogeneity, all sufficiently volatile chemical types of hydrocarbons may be burned with a blue flame up to or even over the stoichiometric fuel/air ratio. With heavier fuels, carbon is bound to appear, because the decomposition temperature is reached before evaporation and mixing are complete. The studies on the combustion of fuel droplets should be helpful in this aspect of carbon formation, and Spalding (39) has drawn attention to the concept of fuel/air ratio which he considers misleading for burning in the open air where combustion takes place at stoichiometric proportions at the reaction front only.

Good mixing so that the fuel can find sufficient oxygen in its immediate environment requires either premixing of vapor and air before combustion or, with liquid injection, high turbulence in the primary zone, together with a high degree of atomization. High turbulence implies a higher pressure loss, and good atomization requires either very high fuel pressures or special forms of fuel-injector design. Flame-speed and ignition qualities require high primary temperatures with the mixture strength near the stoichiometric, and these factors tend to promote carbon formation, one of the cases of conflicting requirements. One of the obvious first steps in elimination of excessive carbon formation is the weakening of the primary zone, but this can be taken only to the stage where the reaction has been reduced to the point of unacceptably low combustion efficiencies. The second step might be to increase the turbulence, again to the point where pressure loss becomes too high. Failing these, then a redesign of the primary zone is necessary to provide more intimate mixing by means of better distribution. Basically, two types of informa-

tion are required for control of carbon formation; (*a*) a knowledge of the factors governing the formation of free carbon, and (*b*) knowledge of conditions favorable for burning the carbon if formed.

Turning to the fuel qualities which influence carbon formation, the important physical property is the distillation curve. This term is used because probably it is the proportion of high-boiling-point hydrocarbons which are influential, although normally it is practicable to classify fuels only according to one fixed point, e.g., final boiling point, 50 per cent evaporated temperature, etc., and this is the basis of most reported tests. Ebersole and Barnett (48) in a series of tests, using both an open cup and a small laboratory burner, showed that, in open-cup tests, the smoking tendency is more dependent on the type of hydrocarbon than on the boiling point or burning rate. Gibbons and Jonash (49) in tests on an annular combustor, reported more carbon deposited with ethylbenzene (50 per cent evaporation temperature 271 F) than with benzene (172 F), this being a typical result obtained from the examination of a large number of fuels. It is to be expected that the more volatile fuels would give less carbon, as evaporation and mixing is more likely to be complete before the decomposition temperature is reached but, as other fuel properties may tend to mask the sole effect of boiling point, it is important to single out the various characteristics. It is concluded from the foregoing tests that the higher the boiling point, the greater the tendency to carbon formation but that the effect is not overriding. In connection with volatility, the pressure level is important because increasing pressure raises the boiling point, and Mullins (50) has presented some comprehensive data on the vaporization characteristics of some gas-turbine fuels, showing the effect of pressure for both pure fuel and fuel mixed with various proportions of air. Such data are likely to be of particular use for vaporizing-type combustors where the dew point and heat required for vaporization are important quantities.

Another physical property which enters indirectly is the viscosity, because, other factors being equal, a fuel of higher viscosity will give poorer atomization and more carbon. Comparative tests must, therefore, always take this into account, and heavier fuels must be preheated in order to achieve similar viscosities.

Among the chemical properties which are known to affect carbon formation are the carbon/hydrogen ratio and the type or structure of hydrocarbon. It is a matter of no little difficulty to make decisive tests for chemical factors because so many of the properties are not independent. Howes and Rampton (51) have summarized the information on hydrocarbon gas-turbine fuels and correlated a number of important properties. From their results it is apparent that while the paraffins and naphthenes show very little variation of C/H ratio, aromatics vary quite widely and, more important, that aromatics have consistently higher C/H ratios than either of the first two types. Thus it is not clear whether it is the C/H ratio or aromatic content that is the fundamental basis for carbon formation, and results are reported on both bases.

Gibbons and Jonash explicitly recognize the relationship of aromaticity and C/H ratio and present a correlation of carbon-forming tendency in terms of volumetric average boiling temperature with C/H ratio as a parameter. To show the effect of these variables, the following approximate figures are taken from their chart. At 200 F average boiling point, the carbon formed was increased by a factor of 10 in doubling the C/H ratio from about $6^1/_4$ to $12^1/_2$, while at 500 F the carbon was increased a hundredfold in going from a C/H ratio of $5^3/_4$ to $12^1/_2$.

Lloyd (27) gives some results of combustor bench tests on various fuels preheated to give approximately the same viscosity as kerosene, which was used as a standard. Again, it is apparent that carbon/hydrogen ratio has a controlling effect, the approximate ratio of carbon deposit to that of kerosene being $2^1/_4$ for gas oil, $4^1/_2$ for Diesel oil, 100 for fuel oil, and very great for heavy fuel oil. A high-flash naptha gave 100 times as much carbon as kerosene in spite of its low boiling range.

Ebersole and Barnett (48) give confirmatory evidence, reporting that the smoking tendency of a commercial kerosene was about 4 times that of the same kerosene from which the aromatics had been removed. In tests on a small laboratory burner it was found that the smoking tendency of aromatic fuels was dependent both on the class of hydrocarbon and the fuel/air ratio, and that within experimental error it was a linear function of fuel/air ratio. One interesting feature is that olefins gave considerably more smoke than cycloparaffins although both classes of fuels have the same C/H ratio. The results of Clarke, Hunter, and Garner (52) have been replotted by Lloyd (27) on the basis of smoking tendency versus C/H ratio, again confirming the general trend but, in addition, showing that the many branched molecules are more prone to smoke than the straight-chain type.

A side line on the carbon-formation problem which does not appear to have been explored thoroughly is the effect of the addition of water vapor to the combustion zone. It is known that water vapor decreases carbon, presumably owing to the "water-gas" reaction, but no quantitative data are available. Possibly such large quantities of water are required that any benefit is nullified, although in certain applications it might be fruitful.

The use of heavy residual fuels has raised a somewhat unexpected problem in addition to the actual combustion and carbon-formation aspect. This is the fouling of turbine blades and heat-exchanger surfaces due to ash deposits. The over-all problem is one of erosion, corrosion, and fouling, and most gas-turbine users have experienced it in some degree or other, with very little operating data reported. Erosion does not appear to be a major difficulty, and Meyer (53) states that Brown-Boveri experience is that exhaust carbon is more troublesome than ash. Likewise, no corrosion has been reported, although here only long-term experience with a variety of fuels and blade materials can furnish an answer. Fouling, however, is more common, and a serious case has been reported by Hughes and Voysey (54) to the extent that a comparatively short number of hours' running caused a very severe deterioration in performance. A powdery ash had been deposited on the rotor blades, chiefly on the convex or back side, and had built up to a sufficient depth to alter the aerodynamic qualities of the blades. The deposit was largely water-soluble and was not fused on, so that it could be removed by water-injection or thermal shock. Subsequent tests indicated that sodium sulphate was predominant and that it was deposited from a vapor phase. The effect appeared not one of impingement or attachment due to centrifugal force but due to deposit in regions of eddy motion, as, for instance, appear on the downstream side of a cylinder where flow reversal takes place. The tests and conclusions were tentative, and further experience is required before the full nature and extent of the problem can be assessed.

To summarize the carbon-formation picture, it would appear that the investigation of fuels has progressed to the point where certain over-all fuel properties having a controlling effect have been isolated, and fuel specifications can be formulated to minimize trouble from carbon. This can be regarded only as an interim stage, and information on the chemical behavior activating these effects is required in order to obtain a possible means of control. The investigation of the burning of liquid droplets eventually should throw some light on the combustion conditions which control the cracking process, leading to the often expressed hope that the gas turbine will accept any liquid fuel with minor modification to the apparatus.

Linear Scale

The effect of linear scale is a most important one for the following reasons: The practicing combustion engineer is often called upon to design a combustor to suit an engine of the same general type but smaller or larger than the one for which he has experience, and it is of great help to him if he can give an immediate answer for a change of dimensions. Another reason is not so apparent but is of basic importance, because so much experimental work is being done on small-scale apparatus to facilitate the use of moderate air supply, and it is a question as to how linear scale bears on a particular result. For example, the work of Hubner and Wolfhard (7) and Gaydon and Wolfhard (4) discussed previously indicates that the absolute limit of pressure in sustaining combustion is dependent on the size of the apparatus. Other experience generally corroborates a deterioration or performance when the linear scale is reduced below a given level, and it is possible that some effects which are observed during the investigation of a particular variable may disappear when an operational size of unit is used. Some results may be misleading, therefore, although such dependence on scale has the possibility of being a very useful tool if the controlling factors are fully understood. There is a possibility that linear scale might be used to simulate a variation of pressure level, a state of affairs which would greatly facilitate experimental investigation.

The effect of scale has long been recognized in combustion, in uniform flame speed in a tube, for example, and in reaction kinetics where the ratio of volume to surface area changes with linear scale. Scale is implicit in some of the preceding discussion, as, for instance, the effect of pressure on flame propagation as quoted, the flame height/port diameter in diffusion flames and in the mixing of gas streams where the effects have been found to scale, i.e., are proportional to linear dimension.

To discuss the problem generally, suppose a combustor is doubled in linear scale, with pressure and temperature levels and entry velocity to remain constant. Then the weight rate of air and fuel flow will be quadrupled, and the combustion intensity or heat-release rate in Btu/(hr) (cu ft) atmosphere will be halved. Another useful parameter, the heat-release rate per unit cross-sectional area, will remain as before, as will the length/diameter ratio of the combustor. The pressure drop through a gas-turbine combustor is largely due to the aerodynamic losses from turbulence and friction and only dependent on momentum loss to a minor degree. The latter is constant for the conditions quoted, and it is not to be expected that Reynolds number would cause much change of orifice coefficient, so it would be anticipated that the over-all pressure drop would remain constant with scale. Tests made some time ago by the author on three sizes of an operating type of combustion chamber of outside diameter 5.66 in., 8 in., and 11.31 in. (ratio $1:\sqrt{2}:2$) confirm this conclusion, with the possible exception of the smallest size. This had a slightly higher loss, which could be attributed to Reynolds-number effect although more probably it was due to dimensional tolerances which were necessarily rather wide on the sheet-metal construction of the particular combustor type tested.

On the actual combustion side, it is rather difficult to make an assessment. Flame length scales for a diffusion flame but with liquid injection the picture is more complex. Even if the combustion mechanism of a cloud of droplets injected into an air stream were understood and it has been seen that such work is only in a preliminary stage, there still remains the fact that the atomization does not scale, at least in any simple fashion. It still remains to find a suitable parameter which expresses degree of atomization. There are the size and diversity factors in the Rosin-Rammler relation, the specific surface, Sauter mean diameter, etc., and Lloyd (25) suggests that since evaporation is proportional to diameter, then the mean diameter given by the droplet with the same diameter/volume ratio of the spray is significant.

Although in the case cited for a doubling in scale with velocity constant, the air/fuel ratio and combustion intensity per unit cross-sectional area remain the same, the combustion intensity per unit volume is halved, i.e., is inversely proportional to the linear dimension. This is equivalent to increasing the available reaction time directly to the linear dimension, and it would be expected that with more time for combustion available, loss due to incomplete burning would be less. Thus, other factors being equal, it would appear that the smaller the combustion chamber, the more tendency there is to a lowered combustion efficiency. Final mixing becomes more difficult as size increases when using the conventional perpendicular jet-mixing effect, because of the difficulty of penetration into the core of the flame.

Some existing combustion chambers of a given type have appeared in a variety of sizes, and thus appear to scale successfully, but in nearly all cases there is some variable factor which does not allow any true scale relation to be established. In particular, the variation of atomization of the liquid fuel requires empirical testing to obtain successful operation with the different size.

Effect of Fuel Properties

One of the important comprehensive questions which faces the combustion engineer is to estimate the effect of using a different fuel in the combustor. The effect of fuel properties has been implicit in the discussion of some of the foregoing basic phenomena, but no general pattern emerges. Flame speed is a specific property of a particular fuel, but no correlation is apparent between the latter and the static inflammability limits which are another property of a fuel. The manner of fuel injection was seen to exert a considerable effect, and it appears that it is possible for a more "readily combustible" fuel by being too volatile to allow too homogeneous a mixture to be formed which has narrower limits than a poor mixture. According to the work of Lloyd (27) and Spalding (40), physical delay time is approximately the same for most hydrocarbons and if this is the overriding factor, as it may well be for liquid injection, then fuels may differ little in burning rate in a gas-turbine combustor. The biggest effect of fuel properties is on carbon formation, where it appears that boiling point and C/H ratio are the important properties.

Examining the information on the effect of fuels in operating gas-turbine combustors, the evidence is that at atmospheric pressure and above, a wide range of fuel properties affects combustion efficiency very slightly, although heavy fuels may give a longer flame. Thus Lloyd, in the tests on carbon formation referred to previously, shows that even where carbon deposit was excessive, the efficiency was lowered by only 1 or 2 per cent. Gibbons and Jonash (49) in tests on a complete jet engine for a very wide range of fuels of various boiling points and C/H ratio show that no difference in engine thrust was detectable within the experimental errors.

Under adverse conditions, however, particularly at subatmospheric pressure, a noticeable difference in fuels becomes apparent. Another phenomenon may appear under these conditions, that of a limiting combustion-temperature rise, separate from that of combustion efficiency. At given inlet-air conditions, increase of fuel flow from a low value causes an increasing temperature rise up to a maximum value, further addition of fuel causing at first no further temperature rise, and eventually a decrease until the flame is extinguished. This points to a rich-mixture stability limit, and the more volatile fuels, which give higher combustion efficiency under such adverse conditions, tend to have a lower temperature-rise limit. Gibbons and Jonash in an extensive investigation showed that under subatmospheric

conditions, a more volatile fuel, such as gasoline, had a higher combustion efficiency than kerosene or Diesel oil at a given temperature rise (i.e., air/fuel ratio) up to a limiting value which was lowest for gasoline. At this point Diesel oil showed no rich limit and continued to allow operation to a higher temperature with increasing combustion efficiency. Since the effect is due to forming too rich a mixture, the state of the fuel at injection has a similar effect to volatility, and it was found that poorer atomization was beneficial in extending the range of operation under altitude conditions, although it was detrimental under less extreme conditions. Such results as these are tied to a particular combustor and fuel-injection system and may not necessarily occur in other flow patterns.

Combustor Performance

At the present time, little if any of the preliminary data summarized in the foregoing is capable of direct application to an operating gas-turbine combustor except in a qualitative manner. As design information there exists only the knowledge that the air flow must be split to provide (*a*) a stabilizing zone where the flame can be anchored and a high temperature maintained, and (*b*) a secondary combustion and diluting zone where burning is completed and mixing to a suitably uniform temperature takes place. There are certain performance parameters which help in determining size in relation to the rate of fuel flow and to the allowable pressure loss, the limits having been set by past experience.

The combustion parameters are the heat-release rate per unit cross-sectional area, and the release rate per unit volume, both expressed per unit atmosphere of pressure. The former expresses the loading in terms of frontal area which is important for aero gas turbines, while the latter has a more general significance and allows comparison of various types of combustion apparatus. Together they imply a length/diameter ratio of combustion chamber, and two of these three parameters are required to assess the design. Pressure loss may be expressed as a fraction of the initial pressure, a form which gives information on the cycle performance from a thermodynamic aspect, and as a "pressure-loss factor" obtained by dividing the loss by the dynamic head, based on inlet density and velocity over the total cross-sectional area of the combustor. The latter expression brings in the size of the combustor and is, therefore, an aid in design. Because pressure loss varies with the air/fuel ratio, the pressure-loss factor F is often expressed as

$$F = \frac{\Delta p}{q} = A + B\left(\frac{\rho_i}{\rho_o} - 1\right)$$

where Δp = total pressure loss, q = dynamic head as defined previously, A and B are constants, and ρ_i and ρ_o are the inlet and outlet densities, respectively. Since Δp is usually small compared with the datum pressure, temperatures can be substituted for densities with little error. The constant A expresses the "cold" pressure loss of the combustor and is the minimum loss due to friction and turbulence.

A knowledge of the existing limits of these parameters allows the designer to estimate approximately the dimensions of a required combustor, but he still has to relate it to combustion efficiency, limits of stable operation, the type of fuel used, etc., over the operating range of air flow, pressure, initial temperature, and air/fuel ratio required. Apart from establishing more precise data for initial design than the foregoing performance factors, it is the requirement of research that it provide answers to the combustion behavior over the range of operating conditions, or at least to guide the designer to provide the optimum conditions.

The effect of pressure and temperature is particularly important design information because of the difficulty of simulating operating conditions on the test bench, and because the wide variations encountered in the operating range of a gas turbine lead to some of the main difficulties. Owing to the extensive use of the gas turbine in aircraft, the effect of low pressure and temperature is the major interest of the present time. It was seen that some investigators have found that reducing pressure increases flame speed down to some critical value when it decreases sharply, whereas others have found no effect. The effect of linear scale and pressure has been discussed, and it is puzzling that those investigators who did not vary size of apparatus with pressure found an increase of flame speed with reduced pressure whereas if linear scale was important, an opposite effect would have been expected. Reduced pressure narrows stability limits, but quantitative data are meager. The effect of pressure on ignition temperature is small at higher pressures, ($t_{ig} \propto 1/p^n$, where n is slightly greater than unity), but at subatmospheric pressure the effect is specific and introduces the complex field of reaction kinetics. For diffusion flames, the height of the flame was found to be independent of pressure for a given mass-flow rate. Rate of heat transfer (as to a liquid droplet) is decreased by reduction of pressure but the equilibrium temperature is reduced which tends to lessen the tendency to carbon formation.

Thus most of the fundamental properties or mechanisms tend to make the combustion process more difficult as the pressure is reduced, as those effects which are favorable are relatively small. The problem is now to seek out which effects are predominant in order to provide some control measures, as the difficulties of high-altitude operation are limiting. Operating combustors are hampered by poor efficiency, instability, and blowout under high-altitude conditions, and the effects on one particular combustor have been investigated by Gibbons and Jonash (49). One factor which affects all liquid-spray-injection types is the deterioration of atomization under such conditions, as the reduced density leads to very low fuel pressures. Under extreme conditions the fuel may issue from the nozzle in barely atomized form, and combustion efficiency is bound to be low, and all results, therefore, are related to the characteristics of the particular fuel nozzle used. In the reference cited, the pressure level was reduced to 8 to 10 psia and efficiency dropped to 50 per cent under the worst conditions of very weak or very rich mixtures, the ground-level efficiency being close to 100 per cent. The behavior of different fuels was discussed previously, and the effect of volatility and/or atomization was shown to have opposite effects according to whether the mixture was rich or weak. Increasing velocity at otherwise constant conditions also reduces both combustion efficiency and maximum temperature rise, which is consistent with the known form of stability limits for simple baffles, and with the effect of reduced reaction time available.

Increased initial temperature would be expected to have a beneficial effect on combustion efficiency in accordance with the general behavior of chemical reactions which conform to the Arrhenius equation, and increased temperature was shown to increase flame speed and weak stability limit, as well as to reduce delay. This is found to be true of combustors, especially for weak mixtures, but with low pressure, an increased air temperature, acting similarly to high volatility or increased atomization, may lead to a reduced temperature-rise limit. Gas turbines with heat exchangers, therefore, may be expected to show good efficiency over a wide operating range of mixture strengths. Where there is a requirement to burn at very high air/fuel ratios, it may be of advantage to arrange the combustor design so that the air is warmed as much as possible by convection from the liner before entering the combustion zone.

Discussion

It is apparent that few conclusions can be drawn and little direct data from fundamental research applied to the combustor-design problem in quantitative fashion. It is hoped, however, that the review of the basic mechanisms being investigated will allow the engineer to study his particular problem in combustion behavior with a little more insight and give him reason to hope that gradually more control means will be available to him.

With the very mechanism of flame propagation so imperfectly understood, it is perhaps folly to speculate on future developments but, taking the risk, it would seem that three of the most fruitful fields of investigation at the present time are (*a*) a correlation and understanding of stability limits, (*b*) the mechanism of combustion of a liquid drop, and (*c*) the formation and burning of carbon particles. In the last decade, since gas turbines came into prominence, the combustion engineer has really only gained some knowledge on the importance of fuel atomization and, to some extent, its achievement and some general information on the effect of fuel properties. It is hoped that the next decade will equip him with some more positive tools and methods of design and control.

BIBLIOGRAPHY

1 "Flame Propagation—A Critical Review of Existing Theories," by G. H. Markstein and M. Polanyi, Cornell Aeronautical Laboratory, Bumblebee Service Report No. 61, April, 1947.

2 "Theory of Burning Velocity," by C. Tanford and R. N. Pease, *Journal of Chemical Physics*, vol. 15, 1947, part 1, pp. 433–439; part 2, pp. 561–565.

3 "Effect of Pressure on Burning Velocities of Benzene-Air, n-Heptane-Air and 2,2,4-Trimethylpentane-Air Mixtures," by F. H. Garner, R. Long, and G. K. Ashforth, *Fuel*, vol. 30, 1951, pp. 17–19.

4 "Low Pressure Flames and Flame Propagation," by A. G. Gaydon and H. G. Wolfhard, *Fuel*, vol. 29, 1950, pp. 15–19.

5 "Mechanism of Flame Propagation," by D. T. A. Townend, *Fuel*, vol. 29, 1950, pp. 64–67.

6 "The Mechanism of Flame Propagation," by M. F. Hoare and J. W. Linnett, *Journal of Chemical Physics*, vol. 16, 1948, pp. 747–749.

7 "Combustion at High Altitudes," by H. J. Hubner and H. G. Wolfhard, RAE Translation No. 125, November, 1946.

8 "Propagation of Flame," by J. W. Linnett, *Fuel*, vol. 29, 1950, pp. 13–15.

9 "Explosion and Combustion Processes in Gases," by W. Jöst, McGraw-Hill Book Company, Inc., New York, N. Y., 1946.

10 "Burning Velocities of Butadiene-1,3 with N_2-O_2 and H_2-O_2 Mixtures," by E. J. Badin, J. G. Stuart, and R. N. Pease, *Journal of Physics*, vol. 17, 1948, pp. 314–316.

11 "Flame Propagation Rates at Reduced Pressures," by W. C. Johnston, *Journal of the Society of Automotive Engineers*, vol. 55, 1947, pp. 62–65.

12 "Theories and Phenomena of Flame Propagation," by J. J. Broeze, Third Symposium on Combustion, Flame and Explosion Phenomena, Williams and Wilkins Company, Baltimore, Md., 1948, pp. 146–155.

13 "Effect of Molecular Structure on Uniform Flame Movement in Quiescent Fuel-Air Mixtures," by T. W. Reynolds and E. R. Ebersole, NACA Technical Note No. 1609, June, 1948.

14 Discussion by N. M. Kapp following reference 20, pp. 175–176.

15 "Effect of Reynolds Number in the Turbulent-Flow Range on Flame Speeds of Bunsen-Burner Flames," by L. M. Bollinger and D. T. Williams, NACA Technical Note No. 1707, September, 1948.

16 "The Effect of Turbulence on the Flame Velocity in Gas Mixtures," by G. Damkohler, *Zeitschrift für Elektrochemie und angewandte physikalische Chemie*, vol. 46, 1940, NACA Translation Technical Memo TM1112, 1947.

17 "On Combustion in a Turbulent Flow," by K. I. Shelkin, *Journal of Technical Physics*, USSR, vol. 13, 1943, NACA Translation Technical Memo 1110, February, 1947.

18 "Combustion in Moving Air," by F. R. Caldwell, F. W. Ruegg, and L. O. Olsen, SAE Quarterly Transactions, vol. 3, 1949, pp. 327–340.

19 "Flame Stabilization and Propagation in High-Velocity Gas Streams," by A. C. Scurlock, Meteor Report No. 19, M.I.T., May, 1948.

a "Flame Stabilization and Propagation in High Velocity Gas Streams," by G. C. Williams, H. C. Hottel, and A. C. Scurlock, Third Symposium on Combustion Flame and Explosion Phenomena, Williams and Wilkins Company, Baltimore, Md., 1949, pp. 21–40.

b "Basic Studies on Flame Stabilization," by G. C. Williams, Institute of Aeronautical Sciences, Preprint No. 222, 1949.

20 "A Study of High-Velocity Flames Developed by Grids in Tubes," by M. W. Evans, M. D. Scheer, and L. J. Schoen, Third Symposium on Combustion, Flame and Explosion Phenomena, Williams and Wilkins Company, Baltimore, Md., 1949, pp. 168–175.

21 "Augmented Flames in Half-Open Tubes," by M. W. Evans, M. D. Scheer, L. J. Schoen, and E. L. Miller, *Journal of Applied Physics*, vol. 21, 1940, pp. 44–48.

22 "Combustion Problems in Ram-Jet Design," by J. P. Longwell, Institute of Aeronautical Sciences, Preprint No. 221, 1949.

23 "Characteristics of Disc-Controlled Flame," by E. A. DeZubay, *Aero Digest*, vol. 61, 1950, pp. 54–56, 102–104.

24 "Flame Stabilization by Baffles in a High Velocity Gas Stream," by J. P. Longwell, J. E. Cheveney, W. W. Clark, and E. E. Frost, Third Symposium on Combustion, Flame and Explosion Phenomena, Williams and Wilkins Company, Baltimore, Md., 1949, pp. 40–44.

25 "Combustion in the Gas Turbine," by P. Lloyd, Proceedings of The Institution of Mechanical Engineers, vol. 153, 1945, pp. 462–472; reprinted by the ASME, 1947, "Lectures on the Development of the British Gas-Turbine Jet Unit."

26 "The T-Scheme: A Low-Pressure-Loss Combustion Chamber for Gas Turbine Engines," by P. F. Ashwood, *Flight*, vol. 52, 1947, pp. 630–631.

27 "The Fuel Problem in Gas Turbines," by P. Lloyd, Proceedings of The Institution of Mechanical Engineers, vol. 159, 1948, pp. 220–229; reprinted by the ASME, 1949, "Internal Combustion Turbines."

28 "Combustion of Diesel Fuel," by M. A. Elliott, SAE Quarterly Transactions, vol. 3, 1949, pp. 490–512.

29 "Verbrennungsmotoren," by F. A. F. Schmidt, J. Springer, Berlin, Germany, 1945; reproduced as FIAT Final Report No. 709, 1946, p. 314.

30 "Fundamental Work on Combustion in Germany," BIOS Final Report No. 1612.

31 "The Ignition of High Velocity Streams of Combustible Gases by Heated Rods," by J. W. Mullen, J. B. Feen, and M. R. Irby, Third Symposium on Combustion, Flames and Explosion Phenomena, Williams and Wilkins Company, Baltimore, Md., 1949, pp. 317–329.

32 "Diffusion Flames," by S. P. Burke and T. E. W. Schumann, *Industrial and Engineering Chemistry*, vol. 20, 1928, pp. 998–1004.

33 "Diffusion in Laminar Flame Jets," by H. C. Hottel and W. R. Hawthorne, Third Symposium on Combustion, Flame and Explosion Phenomena, Williams and Wilkins Company, Baltimore, Md., 1949, pp. 254–266.

34 "Mixing and Combustion in Turbulent Gas Jets," by W. R. Hawthorne, D. S. Weddell, and H. C. Hottel, Third Symposium on Combustion, Flame and Explosion Phenomena, Williams and Wilkins Company, Baltimore, Md., 1949, pp. 266–288.

35 "Diffusion Flames," by K. Wohl, C. Gazley, and N. M. Kapp, University of Delaware Engineering Experiment Station, Bulletin No. 1, 1948.

35*a* "Diffusion Flames," by K. Wohl, C. Gazley, and N. M. Kapp, Third Symposium on Combustion, Flame and Explosion Phenomena, Williams and Wilkins Company, Baltimore, Md., 1949, pp. 288–299.

36 "Combustion in Vitiated Atmospheres," by J. Barr and B. P. Mullins, *Fuel*, vol. 28, 1949, pp. 181, 200, 225, 228 and 241.

37 "The Influence of Spray Particle Size and Distribution in the Combustion of Oil Droplets," by R. P. Probert, *Philosophical Magazine*, vol. 37, 1946, pp. 94–105.

38 "Combustion of Droplets in a Fuel Spray," by G. A. E. Godsave, *Nature*, vol. 164, 1949, p. 708.

39 "Combustion of Liquid Fuel in a Gas Stream," by D. B. Spalding, *Fuel*, vol. 29, 1950, pp. 2–7 and 25–32.

40 "The Atomisation of Liquid Fuels for Combustion," by J. R. Joyce, *Journal of the Institute of Fuel*, vol. 22, 1949, pp. 150–156.

41 "On the Theory of the Process of Combustion in Engines," by Dreyhaupt Deutschekraftforschung Technische Forschungsbericht Zwischenbericht, No. 111, 1942, pp. 75–88; summarized in BIOS Final Report No. 1612.

42 "The Combustion Process in the Diesel Engine," by G. D. Boerlage and J. J. Broeze, *Chemical Reviews*, vol. 22, 1938, pp. 61–85.

43 "The Elbow Combustion Chamber," by M. A. Mayers and W. W. Carter, Trans. ASME, vol. 68, 1946, pp. 391–398.

44 "Investigation of the Penetration of an Air Jet Directed Perpendicularly to an Air Stream," by E. E. Callaghan and R. S. Ruggeri, NACA Technical Note No. 1615, June, 1948.

45 "Study of a Jet Penetrating a Stream at Right Angles," by

J. P. Fraser, thesis submitted in 1949 to Cornell University in partial fulfillment of the degree of M. Aero. E.

46 "New Ways of Burning Liquid Fuel," by W. L. van de Putte and H. K. J. van den Bussche, Trans. of the Fuel Economy Conference, The Hague, Holland, vol. 3, 1947, pp. 1183–1205; published by Lund Humphreys and Company, Ltd., London, England, 1948.

47 "Combustion in Internal-Combustion Engines," by J. J. Broese, *Engineering*, vol. 169, 1950, p. 648.

48 "Smoking Characteristics of Various Fuels as Determined by Open-Cup and Laboratory-Burner Tests," by E. R. Ebersole and H. C. Barnett, NACA Wartime Report No. E-190, 1945.

49 "Effect of Fuel Properties on the Performance of the Turbine Engine Combustor," by L. C. Gibbons and E. R. Jonash, ASME paper No. 48—A-104, 1948.

50 "Vaporization of Fuels for Gas Turbines," by B. P. Mullins, *Journal of the Institute of Petroleum*, vol. 32, 1946, pp. 703–737, and vol. 33, 1947, pp. 44–70.

51 "The Properties of Hydrocarbon Gas-Turbine Fuels," by D. A. Howes and H. C. Rampton, *Journal of the Institute of Petroleum*, vol. 35, 1949, pp. 419–435.

52 "The Tendency to Smoke of Organic Substances on Burning," by A. E. Clarke, T. G. Hunter, and F. H. Garner, *Journal of the Institute of Petroleum*, vol. 32, 1946, pp. 627 and 643.

53 "Can Combustion Turbines Run on Cheap Fuel Oil?" by A. Meyer, *Brown-Boveri Review*, vol. 32, 1945, p. 246.

54 "Some Considerations Dealing With the Formation of Deposits in Gas Turbine Plants," by D. F. Hughes and R. G. Voysey, *Journal of the Institute of Fuel*, vol. 22, 1949, pp. 197–203.

Discussion

E. A. Allcut.[7] This paper gives a complete résumé of the initiation and propagation of flame and, therefore, it is all the more remarkable that the author has made no mention of the nuclear theory that was formulated by Prof. H. L. Callendar over 25 years ago and which recently has received remarkable confirmation in the work of his former assistant, Mr. R. O. King, in the Mechanical Engineering Laboratories at the University of Toronto. These researches have been published as a series of papers in the *Canadian Journal of Research* and, if the omission is intentional, it would be very interesting to have a plausible explanation of the results therein described. These include the successful operation of a variable-compression engine on hydrogen at a compression ratio of 10 to 1 and on coal gas at 12 to 1 over wide ranges of mixture strength, without either detonation or preignition.

The importance of nuclei in other physical and chemical operations is well known, and King's original experiments (made in open tubes and therefore analogous to turbine combustion chambers) revealed the fact that not only did the presence of nuclei reduce ignition temperatures remarkably, but these nuclei need not be combustible. Stone dust, metallic oxides, cement particles, and even water drops were all effective igniting agents. This theory, and the supporting evidence, convinced the writer many years ago of the intrinsic importance of nuclei in combustion, and when the opportunity offered, he was very glad to put the matter to the test in the Heat Engines Laboratory. The Defence Research Board of Canada also was sufficiently impressed to provide the necessary equipment and funds, so that the matter could be investigated thoroughly. The results have more than fulfilled the original expectations. In practice, the nuclei may consist of liquid drops, carbon particles from the fuel, or foreign matter; in each case they lower ignition temperatures and speed up the combustion process. With their aid, an engine receiving fuel in the ordinary way from a carburetor has been run for days without the use of a spark plug.

These effects are important in all combustion processes, wherever they may take place, and it would seem that many preconceived notions on the propagation of flames will require considerable revision in the light of the new evidence that has been, and is still being collected.

[7] Professor and Head of the Department of Mechanical Engineering, University of Toronto, Toronto, Can. Mem. ASME.

B. A. Landry.[8] Everyone concerned with the fundamental approach to high-intensity combustion will be grateful to the author for the extensive critical review of the literature presented in this paper. The following remarks, suggested by a number of men of the Battelle staff engaged in combustion research, are presented not in criticism, but to round out some of the material presented in this paper.

Flame Propagation. P. F. Kurz: Whereas Tanford and Pease (2) obtained a straight-line correlation for the flame speed of hydrogen when plotted against the concentration of atomic hydrogen, closer examination of the data shows that a double-value relation should have been plotted depending on whether the fuel/air ratio was on the rich or on the lean side; in other words, for the same concentration of hydrogen atoms, there are two possible values of flame speed depending on the value of the fuel/air ratio. The same observation applies to the relations of flame speed to hydroxyl concentration, whereas Tanford and Pease came to the conclusion that no correlation existed, for the now obvious reason that the spread in flame speed is higher, in this instance, for equal values of concentration.

A. A. Putnam and R. A. Jensen: Regarding the minimum pressure at which combustion can be sustained and the inverse relation of pressure to burner diameter, this can be predicted by dimensional analysis if it is assumed that pressure and thermal diffusivity are two of the important factors in the combustion process. Here, as elsewhere in the study of combustion phenomena, it is of great value to study the dimensionless groups associated with a phenomenon and to make a correlation in terms of these dimensionless groups. This method was used to advantage in the paper by Putnam and Jensen.[9] For the data given by Wolfhard and the Westinghouse Laboratory, the critical pressure for any given tube diameter can be predicted from a dimensionless correlation of flash back, quenching, and blowoff points. It should be noted that quenching refers to extinction of the flame when convective heat losses are greater than the heat supply, whereas in Bunsen blowoff, there is also a diffusion effect which alters the air/fuel ratio.

Stability Limits. A. A. Putnam: Scurlock's correlation factor for blowoff from various stabilizers does not appear to be dimensionally correct and should be re-examined to make it possible to use the results obtained to correlate data for other experimental apparatus. The effect of heating a stabilizer in a gas stream is open to question; we have found that intense heating of a disk flame holder failed to change the blowoff limits obtained without heating.

Lloyd's observation of pulsating combustion at rich blowoff is a result probably associated primarily with apparatus design. Our observations show that pulsation can occur anywhere in the combustible range of air/fuel ratios.

R. A. Jensen: We cannot agree with the conclusion reached in the paper that, for homogeneous mixtures, the shape of flame holder is unimportant, provided that it is not streamlined downstream. Blowoff limits are markedly different for hollow and solid hemispheres, and for disks and solid cones with the apex upstream.

Combustion of Liquid Drops. C. C. Miesse: With reference

[8] Supervisor, Fuels Research Division, Battelle Memorial Institute, Columbus, Ohio. Mem. ASME.

[9] "Applications of Dimensionless Numbers to Flash-Back and Other Combustion Phenomena," by A. A. Putnam and R. A. Jensen, Third Symposium on Combustion, Flame and Explosion Phenomena, Williams and Wilkins Company, Baltimore, Md., 1949, pp. 89–98.

to the Rosin-Rammler equation, the characteristic size factor $\bar{x}$ corresponds to an R-value of 37 per cent rather than to $R = 50$ per cent as stated in the paper. It can be shown by logarithm derivation that the Rosin-Rammler equation is not sufficiently flexible to represent all possible sets of droplet-size distributions. Instances have been found where the relation holds over a small range of sizes only and cannot be extrapolated beyond this range.

Linear Scale. C. C. Miesse: The effect of linear scale preferably should be studied from the standpoint of dynamic similitude, since changes in linear scale bring about corresponding changes in ambient pressure, temperature, etc. A noteworthy reference on the subject is Neihouse and Pepoon.[10]

Carbon Formation. B. A. Landry: Carbon formation is related to fuel properties in the sense that as boiling point increases, ignition temperature decreases and also the temperature decreases at which thermal cracking becomes appreciable. Hence, with increase in boiling temperatures, the temperature interval to ignition becomes narrower and the time available shorter for the process of mixing air with the vapors. Thus ignition temperature may be reached in the relative absence of air and thermal cracking follows. Therefore avoidance of carbon formation would seem to depend primarily on improved mixing.

W. T. Olson.[11] This is indeed an excellent review of fundamental information on combustion phenomena pertinent to the design of a high-heat-release system, such as a gas-turbine combustor. It is always helpful to have a summary of key references to a research field, together with a discerning résumé of the principal conclusions from each reference.

It is clear that scientists and engineers attempting the practical and effective utilization of combustion have a difficult problem in arriving at quantitative design rules. The interrelations of the chemical, physical, and aerodynamic phenomena are sufficiently complicated to preclude an early or easy solution to this problem, as the author points out. Quantitative correlation of fundamental data with combustor performance is barely beginning to appear. However, results of fundamental and empirical studies such as those reviewed by the author do provide a basis and background, and an understanding, of the more applied work of the combustion engineer. New ideas and improvements may have to be based on this understanding rather than on quantitative correlation.

The author has described more combustor-performance characteristics in his paper than he implies exist in his introduction. Actually, instead of "very meager statistical data from existing gas turbines, such as combustion intensity and fractional pressure loss," there are quite extensive data on gas-turbine combustor performance, especially for aircraft turbojet combustors. Admittedly, most of these data are unavailable, yet a number of references[12] quite clearly depict the nature of the combustion problems encountered in present systems for turbojets.

With regard to flame propagation, G. L. Dugger,[13] has shown the effect of initial temperature T_b, on the flame speed of a mixture to be of the form

$$u\alpha \sqrt{T_b^2\, T_f^{4.5}\, \frac{\exp\,(-E/RT_f)}{(T_f - T_b)^3}}$$

where T_f is flame temperature, and E is activation energy.

With regard to "stability limits," the well-known narrowing of the inflammability limits of static, homogeneous combustible mixtures by reduced pressure should be pointed out.

With regard to "ignition temperature," it may be significant to note that according to D. T. A. Townend, L. L. Cohen, and M. R. Mandlekar,[14] the temperature required to ignite homogeneous hydrocarbon-air mixtures increases quite suddenly at about 1/4 to 1/3 atm. This is roughly the pressure range where combustion efficiency deteriorates in aircraft gas turbines.

With regard to "combustor performance," a chart has been prepared by I. I. Pinkel and Harold Shames,[15] from which the total-pressure-loss ratio together with the pressure-loss ratio due to drag and the momentum pressure-loss ratio comprising it can be estimated for known values of the combustor-inlet weight flow, temperature, and pressure, and the combustor-outlet temperature. Also with regard to combustor performance, in addition to the effect of reduced pressure on ignition temperature, on rate of heat transfer to droplets, and on fuel flow cited, it should be pointed out that reduced pressure also provides coarser atomization by virtue of less dense air to break up the injected fuel sheet, decreases aerodynamic mixing processes (lower Reynolds number), and increases "quenching distance."[16]

Under the heading "Discussion", the author has certainly listed three major fields in which more knowledge is desired. If it is not already implicit in the suggested research on stability limits, the general problem of understanding and control of the major gas-flow patterns, or gross swirls, or turbulence, in a combustor is cited. This problem, in contrast with research on fundamental flame speed, is not receiving attention commensurate with its importance.

Author's Closure

The author need only make a very general reply to the discussion, as it was the object of the paper to stimulate such comments and to draw forth observations on additional material. The paper represented the views of only one individual and the comments of the discussers add appreciably to its value.

With respect to the remarks of Professor Allcut, the work of King on the nuclear theory of ignition was by no means overlooked, but was felt to lie in the region of chemical kinetics which was too involved for the scope of the paper. However, it introduces a notable new field of investigation and Professor Allcut's remarks are welcomed as bringing up the matter for attention.

Thanks are due to Mr. Landry and co-workers at Battelle for their detailed analysis of several topics, which amend or extend the author's statements. The comments with respect to dimen-

[10] "Dynamic Similitude Between a Model and Full-Scale Body for Model Investigation at Full-Scale Mach Number," by Anshal I. Neihouse and Phillip W. Pepoon, NACA Technical Note No. 2062.

[11] Chief, Fuels and Combustion Research Division, NACA Lewis Flight Propulsion Laboratory, Cleveland, Ohio.

[12] "Combustion and Combustion Equipment for Aero Gas Turbines," by E. A. Watson and J. S. Clarke, *Journal of the Institute of Fuel*, vol. 21, October, 1947, pp. 2–34.

"Effect of Combustor-Inlet Conditions on Performance of an Annular Turbojet Combustor," by J. H. Childs, R. J. McCafferty, and O. W. Surine, NACA Technical Report No. 881, 1947 (formerly NACA Technical Report 1357).

"Some Aspects of Turbojet Combustion," by A. J. Nerad, *Aero Engineering Review*, vol. 8, December, 1949, pp. 24–26 and 88.

[13] "Effect of Initial Mixture Temperature on Flame Speeds and Blow-Off Limits of Propane—Air Flames," by G. L. Dugger, NACA TN 2170, August, 1950.

[14] "The Influence of Pressure on the Spontaneous Ignition of Inflammable Gas-Air Mixtures," by D. T. A. Townend, L. L. Cohen, and M. R. Mandlekar, Proceedings of the Royal Society of London, vol. 146, series A, August 1, 1934, pp. 113–129.

[15] "Analysis of Jet-Propulsion Engine Combustion-Chamber Pressure Losses," by I. I. Pinkel and Harold Shames, NACA Technical Report 880, 1947 (formerly NACA TN 1180).

[16] "Ignition of Explosive Gas Mixtures by Electric Sparks. III. Minimum Ignition Energies and Quenching Distances of Mixtures of Hydrocarbons and Ether With Oxygen and Inert Gases," by M. V. Blanc, P. G. Guest, Guenther von Elbe, and Bernard Lewis, Third Symposium on Combustion and Flame and Explosion Phenomena, Williams & Wilkins Company, Baltimore, Md., 1949, pp. 363–367.

sional analysis and dynamic similitude are very apposite as this is a phase of the subject which appears overdue for investigation in view of the success of such studies in other fields. The comments on stability limits show very clearly the need for more data, and a detailed review on this single topic would be welcome.

Mr. Olson has performed a service in pointing out additional material and giving further references. Again it should be said that the material on actual combustor performance has not been overlooked as it is the point of departure for anyone interested in the field, but that this paper is an attempt to give the background for some of the results and remaining problems cited in those papers. Mr. Olson's suggestion of a more intensive study of the gas-flow pattern as opposed to the present emphasis on flame speed deserves particular attention, as with so many problems to be solved, the first step is to limit the field by asking the right questions. Agreement among interested parties in selection of the most important problems could have a very desirable focusing effect.

High-Speed Braking

By C. L. EKSERGIAN,[1] PHILADELPHIA, PA.

In contrast with the era when the railroad-car tread brake was adequate for all demands, the car brake of today must meet increases in speed of 33 per cent, axle load 25 per cent, inertia load 100 per cent, including 50 per cent overload, and deceleration 100 per cent. The advent of the "disk brake" has made it possible to meet these drastic requirements. This paper deals with the theoretical considerations as well as the practical application of the disk brake to modern railroad practice.

Introduction

TODAY'S demands of high speed, heavy loads, and high deceleration rates, require railroad brakes of tremendous capacity. Not only must the brake meet these demands, but it must do so without incurring thermal damage—provocative of high maintenance or responsible for hazardous operation—particularly likely under the higher decelerations at the higher speeds, as well as under the prolonged applications on descending grade. Beyond this, today's standards for behavior are far more exacting. The brake at all times must be controllable, quiet, and smooth in operation.

Whereas the tread brake satisfied yesterday's demands, today's requirements have so grown that a new type of brake has been found necessary. Crest speeds have climbed from 75 to 100 mph.

Curiously enough, whereas the trend has been toward lightweight construction, heavy axle loads of 40,000 lb are found in today's operations. The reasons for this paradox are numerous.

The replacement of the six-wheel truck by the four-wheel truck usually has resulted in increasing the axle load, despite a reduction in over-all car weight. Modern demands on air conditioning, with its heavier equipment, batteries, double sash, and ducts, have added markedly to weight. Advanced styling, calling for luxurious accommodations and appointments, usually results in additional weight. However, the largest load augment imposed upon the brake is not so traceable to change in axle load per se, as to the overload, resulting from the now underbraking of the locomotive and other cars of lower performance. Such increase can readily amount to 60,000 lb per axle, or 50 per cent over the axle load.

The overload diminishes to zero as all brakes in the train, including the locomotive, approach the same retarding force per unit wheel load. Thus, formerly when the car performance lay closer to the low level of the locomotive brake, the differential and therefore the overload, were not so consequential.

Beyond increase in speed and load, deceleration rates which may now be employed are 100 per cent greater than what was previously tenable. This advance has been made possible by the advent of the wheel controller—as afforded by the Budd "Rolokron," the Westinghouse" Decelostat," and the American Brake Shoe wheel controller. By so preventing wheel slide, deceleration rates can be raised with impunity. In addition, improvements in sanding, as developed by the New York Air Brake Company, and others, have resulted in providing higher adhesions when required. Thus, summing up the task presented to today's car brake, the speed has increased 33 per cent, the axle load 25 per cent, the inertia load (including 50 per cent overload) 100 per cent, and the deceleration 100 per cent.

Since power is the product of torque and speed, and torque in turn varies directly with deceleration and axle load, it follows that the peak power output of the modern brake must be 3 times that of its predecessor. Of equal if not greater import, the energy which the new brake is called upon to dissipate amounts also to 3 times that previously encountered, since work varies directly with the inertia load and square of the speed.

The advent of the disk brake[2] has made it possible to meet these drastic requirements and accordingly to make capital of the higher performance permitted by the greater effective adhesion now obtainable. It was timely that both developments were concurrent. Fully to enjoy the greater capacity residual in the brake, restrictions from adhesion had to be raised; and, conversely, to utilize these higher limits, greater performance was necessary. Thus each was dependent upon the other to effect the end result.

Although to date little progress has been made with the locomotive brake in developing maximum retardation, as permitted by adhesion, tremendous strides have been made in its holding capacity on grades—thanks to the advent of the dynamic brake in combination with Diesel-electric power. By reversing the locomotive torque which hauls the train on ascending grade, a brake of equal capacity obtains for holding the train on descending grade. Accordingly, the mechanical brake is virtually relieved of all holding duty. It is to be noted, however, that this type of brake contributes little to the peak-power output required at high speed—where deceleration counts most—due to its limited torque capacity. For example, ignoring train resistance, a locomotive with 5000 hp at rail can haul a 1500-ton train (including locomotive) on an ascending 2 per cent grade at 31 mph, or with the same horsepower for braking, it can hold the same train at the same speed when descending the grade.

However, assuming sufficient locomotive adhesion to retard the same train at 3 mphps, the locomotive would have to dissipate 110,000 peak horsepower at 100 mph, or over 20 times the continuous power required on grade. In terms of torque, such a deceleration would require 7 times the torque needed in the grade illustration.

Effectiveness

When introducing the disk brake into train operation, no yardstick appeared to exist for measuring the proportionality between output and wheel load in a manner that the counterpart, braking ratio, defined input proportionality. As long as one type of brake with similar behavior was employed, braking ratio, combined with experience, furnished a general index of performance. However, the mixing of different characteristics occasioned by the advent of the disk brake necessitated the establishment of a proportionate measurement of output.

From the standpoint of the brake, torque or retarding force describes its task. However, the performance or deceleration a re-

---

[1] Executive Engineer, and Assistant to Vice-President, The Budd Company. Mem. ASME.

Paper presented before the Railroad Division of The American Society of Mechanical Engineers, St. Louis, Mo., June 20, 1950.

Note: Statements and opinions advanced in papers are to be understood as individual expressions of their authors and not those of the Society. Manuscript received at ASME Headquarters, July 3, 1950.

[2] This brake, manufactured by the author's company, will be referred to as "disk brake" throughout the paper.

sulting therefrom depends upon the mass M acted upon by the retarding force F

$$a = F/M$$

(Since the inertia of the revolving wheel-and-axle assembly is relatively small, it may be disregarded.)

Under independent deceleration, mass equals wheel load W divided by gravity g, so that

$$a = (F/W)g$$

Thus the ratio of retarding force divided by wheel load designates the independent performance of the brake, and, accordingly, may be regarded as the factor of "effectiveness" e.

Since effectiveness is a numerical ratio, it may be expressed in per cent.

It so happens that the adhesion necessary for a retarding force F and a wheel load W is

$$m = F/W = e$$

Thus a given per cent effectiveness requires or utilizes a like per cent adhesion, so that effectiveness and "working" adhesion are numerically the same. Accordingly, the maximum effectiveness possible equals the maximum adhesion available.

Similarly, if we ignore train resistance, the force F required to hold a given wheel load W at constant velocity on a grade G is

$$F = WG$$
$$e = F/W = G$$

Thus the per cent effectiveness required is also equal numerically to the per cent grade. Effectiveness may be expressed in terms of the independent deceleration which it becomes when multiplying by gravity. Thus the "free car deceleration" is that which would result if a car with brakes of common effectiveness were dissociated from the train.

$$a = eg$$

Train Effectiveness

For smooth operation of a train, it is desirable that the effectiveness, or independent deceleration produced by each brake, be common throughout the consist. This relation is likewise necessary if the maximum adhesion available is to be utilized completely at each and all wheels—a prerequisite for maximum retardation. Accordingly

$$F = eW = kW$$

where $e = k$. Consequently, for common effectiveness, the retarding force must be directly proportional to wheel load. In a train, the effectiveness may be different for the various classes of brakes present. Thus, with a mixed consist of car disk brake, car clasp brake, and locomotive clasp brake, the net train effectiveness becomes

$$e_t = \frac{F_t}{W_t} = \frac{F_c + F_d + F_L}{W_t} = \frac{e_c W_c + e_d W_d + e_L W_L}{W_t}$$

or

$$e_t = e_c \frac{W_c}{W_t} + e_d \frac{W_d}{W_t} + e_L \frac{W_L}{W_t}$$

where the subscripts c, d, L, and t refer, respectively, to car clasp brake, car disk brake, locomotive clasp brake, and train.

In terms of train and independent decelerations

$$a_t = a_c \frac{W_c}{W_t} + a_d \frac{W_d}{W_t} + a_L \frac{W_L}{W_t}$$

Thus the resulting train deceleration equals the sum of the products of the independent decelerations and the corresponding weight ratios.

Braking Ratio and Effectiveness

Since retarding force F varies directly with shoe pressure P and coefficient of brake friction f, with n shoes, brake radius r, and wheel radius R

$$F = \frac{nPfr}{R}$$

Effectiveness expressed in like terms becomes

$$e = \frac{F}{W} = \left(\frac{nr}{R}\right)\left(\frac{P}{W}f\right)$$

For a given class of brakes, such as the car clasp, car disk, or locomotive clasp, n, r, and R are usually constant. Consequently, the ratio P/W, which is established arbitrarily, determines the effectiveness within the range of friction which obtains.

Braking ratio is commonly expressed in per cent for a given brake-cylinder pressure (bcp). Thus a common emergency braking ratio is 150 per cent at 100 psi bcp. This means that the ratio of the total shoe pressure nP—when n designates the number of shoes, and P the pressure per shoe—over the wheel load W is 1.50 when the bcp is 100 psi, or 0.015 psi per lb bcp. Actually the true braking ratio b is a constant, independent of the brake-cylinder pressure, so that the common use of the term "per cent braking" refers to the product bp. By definition

$$bp = \frac{nP}{W}$$

or

$$b = \frac{nP}{pW}$$

The relation between the effectiveness e and the braking ratio b becomes

$$e = \frac{r}{R} fpb$$

With the clasp brake $r = R$, so that

$$e = fpb$$

It will be observed that the braking ratio b determines the performance e only for a given f. Although f may vary greatly with different types of brakes and within any given class, if the proportionate change remains the same, then the effectiveness remains common. Thus, whereas the resulting deceleration rate may vary, uniformity in behavior between cars may still prevail.

Disk-Brake and Clasp-Brake Characteristics

The disk brake is individual in that its coefficient of friction remains extraordinarily constant throughout the entire speed range, being independent of shoe load, inertia load, and speed, within the limits encountered. The reason for this is first attributal to the frictional properties of the composition lining employed, in combination with the cast-iron disk, which remain constant within a given temperature range. Also, by virtue of the disk-brake design, critical temperatures are not exceeded in performing the duty assigned. This constancy is shown in Fig. 1 for deceleration.

Because of such constant friction, the effectiveness can be controlled accurately by brake-cylinder pressure p for the range cor-

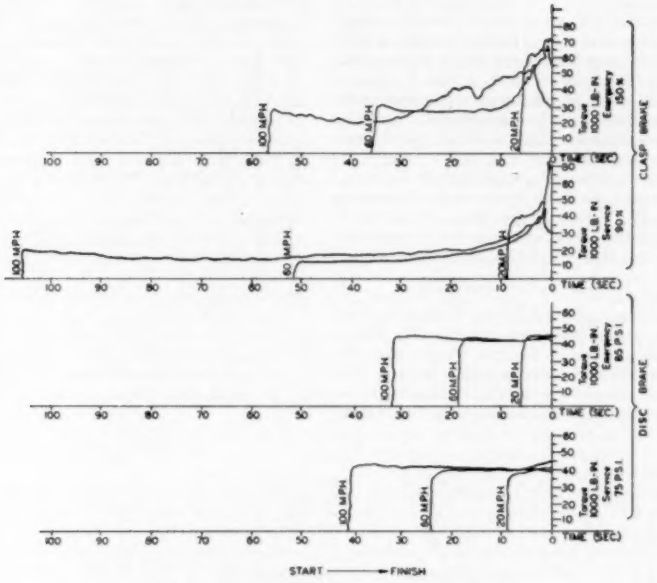

FIG. 1 DYNAMOMETER TESTS—AUTOGRAPHIC CURVES
(Comparison of clasp and disk railroad brakes 19,000-lb inertia load, 36-in-diam wheel.)

responding to the true braking ratio b employed. With b, f, r, and R constant

$$e = kp$$

Thus, not only is the effectiveness from car to car the same, but the resulting car-train deceleration remains directly proportional to control pressure at all times. Accordingly, smooth performance results because of uniformity of behavior and accuracy in control.

The ability to so regulate and therefore limit effectiveness accurately, makes possible setting the effectiveness of each brake close to adhesion limits, thereby obtaining the maximum quota from all brakes—a condition necessary for maximum over-all retardation.

In contradistinction, clasp-brake friction varies inversely with rubbing velocity and surface temperature. In a given train operation, rubbing velocity remains common to all clasp brakes so that whatever the variation in friction attributal to velocity, it likewise remains common. It is largely this situation which makes possible multiple operation in the face of widely varying friction.

On the other hand, surface temperatures do not necessarily vary alike, being a function of shoe pressure and inertia load which may each differ widely in a given train consist.

With a constant braking ratio, the shoe pressure varies as the wheel load, so that proportionately greater power is developed by the brakes with heavy wheel loads, resulting in a more rapid generation of heat and temperature.

Owing to the lower friction incident to the higher temperatures at the heavier-loaded wheels, the effectivness is reduced and, accordingly, the over-all train deceleration. Thus uniformity of behavior is effected by train consist so that common braking ratio does not insure common effectiveness.

Moreover, considering the train deceleration as a whole, the difference in aggregate wheel load from one train to another brings about differences in operating temperatures and, therefore, frictions at like speeds. Accordingly, a fixed schedule of speed-governor control which corrects for speed alone is not universally applicable, due to differences in thermal conditions.

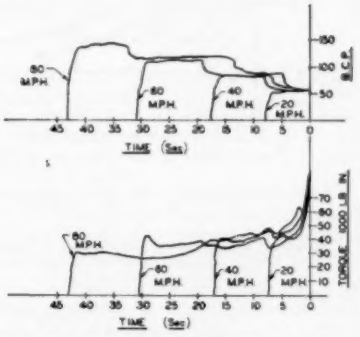

FIG. 1(a) DYNAMOMETER TESTS—AUTOGRAPHIC TORQUE CURVES
(Clasp brakes 250 per cent; speed-governor emergency stops.)

Moreover, the status of heat accumulated preceding the entrance to a given speed bracket may alter the conditions of temperature markedly in the given bracket and, therefore, the extent of correction required. Examples are shown in Figs. 2, 3, and 4. For this reason the adequacy of speed-governor control varies with train consist, which is likely to be unpredictable. Notwithstanding, speed-governor control is highly beneficial and necessary for braking ratios of the order of 250 per cent.

The saving grace lies in the fact that in the high-speed bracket, where temperature is most significant, the range in effectiveness lies below adhesion and, conversely, at low speed, wherein the effectiveness may easily exceed adhesion, temperature becomes subordinate to the effect of speed, to which the controller is tuned.

Emergency and Service Effectiveness

Brake capacity, adhesion, and passenger reaction may limit the selection of maximum braking ratio independently. The passenger can withstand a deceleration of 3 mphps without undue discomfort, and 4 mphps for the occasional emergency demand. The disk-braked *General Pershing*, of the Burlington Railroad, operated entirely satisfactorily with maximum service deceleration

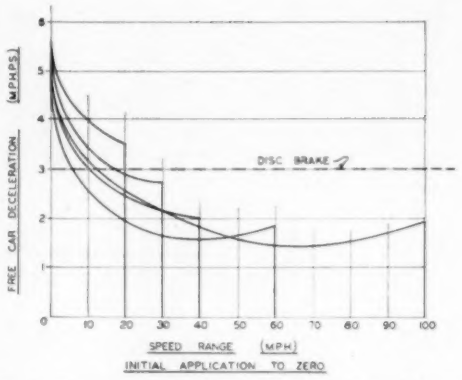

Fig. 3 Deceleration Versus Speed for Clasp Brake Without Speed Governor

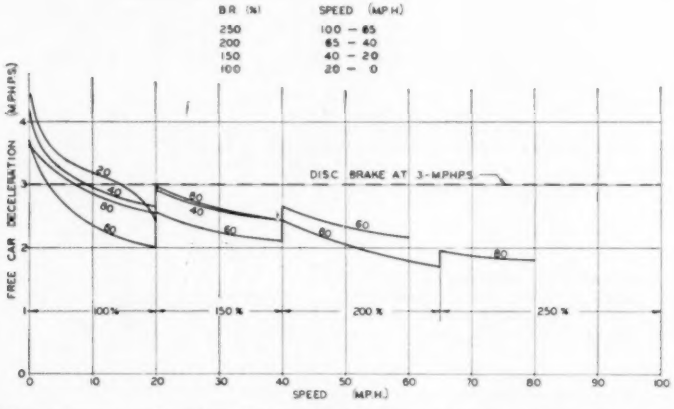

Fig. 2 Torque Characteristics of Clasp and Disk Brakes as Affected by Speed and Point of Initiation of Application (Clasp-brake ratio = 250–100 per cent; as regulated by speed governor; disk-brake effectiveness = 3 mphps.)

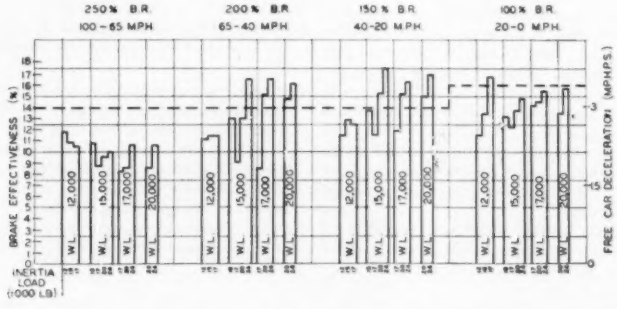

Fig. 4 Effect of Wheel Load and Inertia Load, and Braking Ratio on Clasp-Brake Effectiveness

of 2.8 mphps. This is particularly true if the retardation is smooth, as experienced with the disk brake, and if the rate change of deceleration upon application does not exceed 1 mphpsps. Since adhesion cannot support higher deceleration rates, passenger reaction may be dismissed as a critical factor.

With the disk brake it is possible to develop sufficient torque to utilize at all times the adhesion available, so that adhesion becomes the final limitation for effectiveness. The clasp brake, on the other hand, falls short in utilizing available adhesion at high speed (where deceleration is most effective on stopping distance) due to its thermal limitations. Consequently, at high speed, brake capacity is the limitation. At low speed the clasp-brake effectiveness can easily surpass adhesion due to its peak friction characteristics at low speed, so in this speed bracket adhesion becomes critical.

Due to the determinable and relatively constant coefficient of friction f of the disk brake, and the fact that the sole limitation for maximum effectiveness e' is adhesion m, the braking ratio b for highest emergency performance may be determined directly by equating e' to m and employing maximum brake-cylinder pressure p'

$$b = \left(\frac{e'}{p'f}\right)\left(\frac{R}{r}\right) = \left(\frac{m}{p'f}\right)\left(\frac{R}{r}\right)$$

Such a procedure would be difficult with the clasp brake owing to its extreme variations in friction. Here, experience over years of wide ranges of operation has made it possible to arrive at an optimum braking ratio. When 250 per cent is employed, in order to boost high-speed deficiency in torque, the brake-cylinder pressure is reduced through speed-governor control to compensate for the increase in friction attending reduction in speed. The higher shoe pressures resulting thereby, together with the high speed at which they occur, has resulted in accentuating the inherent thermal limitations of the brake. Beyond this, the loss in shoe friction because of the higher temperatures tends to offset the gain from higher pressure, so that the end improvement in stopping distance is limited. Accordingly, the earlier adopted 150 per cent braking ratio—without need of speed-governor control—is still favored in many quarters.

The true braking ratio b is a fixed quantity, established solely on the basis of maximum conditions of emergency application. The ceiling of the service range is purely an arbitrary matter. It may be assigned to any percentage of emergency desired, by so limiting the brake-cylinder pressure p.

The basis for establishing maximum service effectiveness differs fundamentally from that for emergency; here it is not a matter of what is physically possible but rather what is economically prudent. The gains in schedule from higher decelerations must be pitted against penalties in cost. However, with adequate brake capacity, maintenance is little affected within the limits of nonsanded rail, so that full utilization of this level of adhesion can be made. To employ higher effectiveness would entail intolerable use of sand and/or excessive operation of the wheel protector, which, though justifiable in emergency would not be warrantable for service.

Representative Adhesion

Since adhesion is finally the critical factor in determining maximum effectiveness, it is necessary that the value selected for braking ratio should be representative of conditions encountered. If the selection is unduly low, maximum retardation suffers and, if unsupportable, excessive slip occurs, resulting in longer stopping distances, owing to interruption, or requiring an inordinate use of sand.

Because prevailing adhesions vary over a wide range, reducing representation to a single absolute value becomes a matter of compromise.

To adopt a braking ratio based upon minimum adhesions experienced would curtail retardation intolerably. Consequently, selection must be based upon deliberately countenancing a certain per cent of nonsupport from adhesions encountered. Fortunately, the preponderance of prevailing adhesions lies well above minimum values so that penalties from slip can well be condoned for the higher decelerations more commonly possible. Moreover, with wheel protection, wheel slide is prohibited, slip resulting in causing interruption only. Since such interruption in application can be virtually eliminated by recourse to sand—within limits of sanded-rail adhesion—penalties from such slip become insignificant. However, unduly frequent use of sand is to be avoided because of demands upon limited supply and possible adverse effect upon signals.

It so happens that sand restores the adhesion of wet or poor rail to approximately that of good dry nonsanded rail. Consequently, if a braking ratio is employed which seldom requires sand with dry rail, sanding for the most part will be confined to the more infrequently encountered poor rail.

In an effort quantitatively to determine the range of adhesions that may be encountered, tests were conducted by the author's company, with the assistance of the Pennsylvania Railroad, in August, 1949. The true adhesion is approximately 10 per cent greater than the effective adhesion when the free-car deceleration is 3 mphps, due to weight transfer.

In the present discussion treatment of adhesion refers to the effective adhesion unless otherwise stated.

Values obtained in the adhesion tests referred to are plotted in Figs. 5, 6, 7, 8, in the form of histograms and probability curves.

The results obtained are as follows:

(*a*) 70 per cent of dry-rail adhesions lie between 12 and 20 per cent, averaging 16 per cent.

(*b*) 70 per cent of the wet-rail adhesions lie between 4 and 10 per cent, averaging 7 per cent.

(*c*) Sanding wet rail restores adhesion to nearly dry-rail values, or approximately 13 per cent.

(*d*) Sanding dry rail can raise adhesion to 20 per cent.

(*e*) No perceptible difference was found between range of adhesion values obtained with disk brakes, and clasp brakes, indicating thereby that the wiping effect of the tread shoe is inconsequential.

Experience over the past 10 years with mainliners on the Burlington, Santa Fe, and Milwaukee railroads confirm the foregoing findings.

With wheel protection only (without sand), successful operation has obtained with braking ratios providing a maximum effectiveness of 14 per cent, or a free-car deceleration of 3 mphps. Virtually all disk brakes now operating produce this effectiveness in emergency.

In breakaway tests on the Milwaukee Railroad conducted in May, 1947, the disk-braked free car was stopped from 96 mph in 2220 ft without sand; and from 97 mph in 1961 ft with sand. In the test with nonsanded rail, an effectiveness of 15 per cent was reached without slip occurring, proving that an adhesion of equal or greater value was present. With sand, a deceleration of 4.2 mphps was reached without slip, indicating the presence of 19 per cent adhesion.

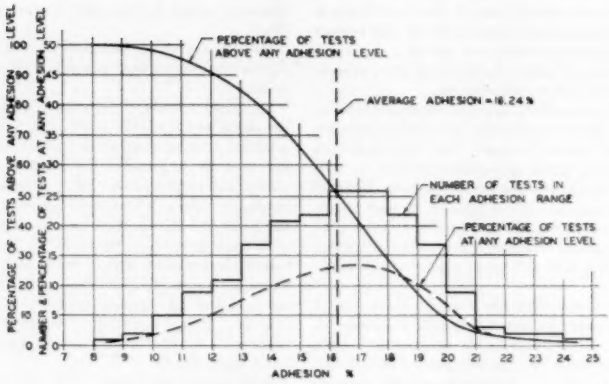

FIG. 5 RESULTS OF DISK-BRAKE DRY-RAIL TESTS
(Speed range, 10 to 90 mph; 196 total tests.)

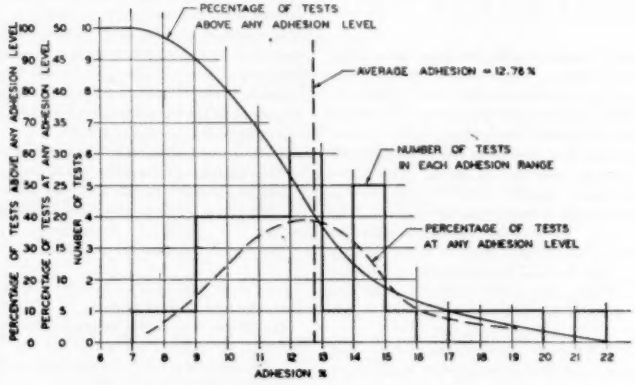

FIG. 6 RESULTS OF CLASP-BRAKE DRY-RAIL TESTS
(Speed range, 10–90 mph; 31 total tests.)

INERTIA LOAD

The inertia load L is the mass M which the brake retards, multiplied by gravity g

$$L = Mg$$

It may be regarded as the mass equivalent necessary for a given torque T, and wheel radius R to produce the net deceleration a resulting—ignoring inertia of the rotating elements. Thus

$$L = \frac{T}{Ra}\,g = \frac{F}{a}\,g$$

where F = retarding force.

In single-car operation in which the effectiveness F/W is the same for each brake, the deceleration is that resulting from the retarding force F, acting on the mass W/g

$$a = \frac{F}{W}\,g$$

so that

$$W = \frac{F}{a}\,g = L$$

Consequently, with such single-car operation, the wheel load is the inertia load.

In train operation, however, with cars and locomotive of different ratios of effectiveness, the resulting train deceleration or effectiveness is not necessarily the same as that of a given individual brake. If the individual effectiveness is higher than that of the train, then the brake suffers from the lower deceleration of the train to the extent of the greater inertia load which results from the given torque producing the lower deceleration. Thus, with a given torque or retarding force, the deceleration may be greater or less than that which occurs when the inertia load equals the wheel load. The difference denotes the amount of overload or underload, or the difference between the inertia load and wheel load.

An extreme example is found in a car with sticking brakes. The aggregate torque of the individual car could be of an order to produce high independent deceleration—were the car free of the train—despite the imperceptible deceleration of the train result-

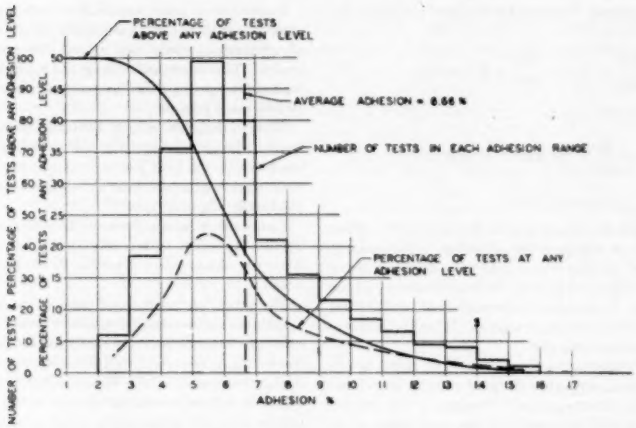

FIG. 7 RESULTS OF DISK-BRAKE WET-RAIL TESTS, INCLUDING RAIN, DEW, AND ARTIFICIAL WETTING
(Speed range, 10 to 90 mph; 448 total tests.)

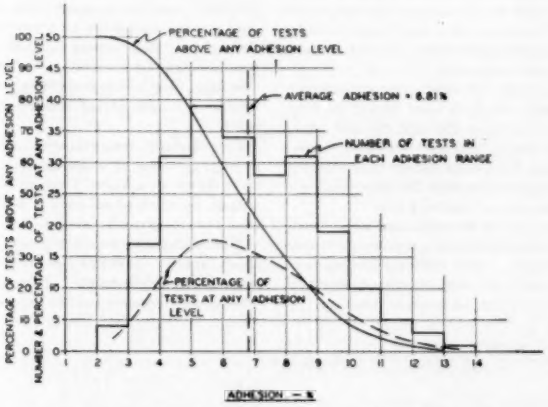

FIG. 8 RESULTS OF CLASP-BRAKE WET-RAIL TESTS, INCLUDING RAIN, DEW, AND ARTIFICIAL WETTING
(Speed range, 10 to 90 mph; 222 total tests.)

ing therefrom. Here the inertia load becomes the weight of the entire train, divided by the number of brakes sticking, assuming equal effectiveness.

The relation between the inertia load L, and the wheel load W, for a given brake producing a retarding force F, or an independent deceleration a, under a train deceleration a_t, becomes, on dividing L by W

$$\left(L = \frac{F}{a_t}\,g\right) \div \left(W = \frac{F}{a}\,g\right)$$

or

$$L = \frac{a}{a_t}\,W = \frac{e}{e_t}\,W$$

where e and e_t represent the corresponding effectiveness ratios.

Thus the inertia load equals the wheel load multiplied by the ratio of the effectiveness or independent deceleration of the individual brake over that for the train.

It will be observed that the provision of relatively higher effectiveness imposes an additive work duty upon the brake, thereby penalizing it for its superior performance. Thus the disk brake, in developing and maintaining maximum torque at high speed, is subjected to an overload when associated with the clasp brake of lower effectiveness in this speed bracket. Note that this overload occurs when power is maximum, thereby imposing the most drastic effect from load.

The ratio of the individual effectiveness to that of the train is likely to vary throughout a given deceleration, either because of individual change in torque of the particular brake, or change in train deceleration as affected by other brakes in the consist. Therefore the inertia load is a variable, depending upon the relative instantaneous behavior of all brakes in the train.

In the Twin Cities Zephyr, car weight approximates 500 tons and locomotive 325 tons. The maximum high-speed decelera-

tion approximates 2.4 mphps; 3 mphps for cars and 1.6 mphps for locomotive

$$a_i = 3 \times \frac{500}{825} + 1.6 \times \frac{325}{825} = 2.4 \text{ mphps}$$

With $W = 20{,}000$

$$L = \frac{a}{a_i} = \frac{3}{2.4} \times 20{,}000 = 25{,}000 \text{ lb}$$

Thermal Duty

The crux of high-speed braking is one of thermal duty. Fundamentally, a brake is an engine in reverse cycle with complete irreversibility. Instead of converting heat into mechanical energy, the duty of the brake is to absorb the kinetic energy of the train and, subsequently, to dissipate it through heat, without incurring at any time deleterious temperatures. It is this temperature proviso that determines capacity.

Under high rates of conversion, or power, heat must be removed from the operating surfaces extremely rapidly lest disastrous temperature climb should ensue. Because of the limited operating areas, coupled with the relatively low coefficients of radiation and convection, these two avenues offer little escape.

Virtually all of the heat developed must be transmitted into the walls of the brake by conduction and at a rate sufficiently paralleling that of its generation through friction so as to prevent undue surface temperature rise. Thereafter, when more time is available, final dissipation into the atmosphere may proceed through the slower paths of radiation and convection.

Hence an added duty of the brake is to serve as an accumulator in storing the heat temporarily which at once cannot be dissipated. For example, in one stop from 100 mph the disk brake can convert 7,000,000 ft-lb of energy into heat within an elapsed time of 20 sec without incurring deleterious surface temperatures. Yet the time required to dissipate the 9000 Btu generated and subsequently stored in the disk amounts to 6 to 8 min.

This tremendous difference between transient and steady-state capacity of a brake is well demonstrated in a comparison between deceleration and drag performance. The 1000 peak horsepower, which can be developed with the disk brake under rapid deceleration, reduces to 75 hp when continuous, as occasioned in drag.

Under steady state, accumulator assistance must be discounted, since the work or heat generated throughout the prolonged period of application easily can exceed the reservoir capacity of the brake. Therefore, under drag, the brake becomes a nonstop path for heat, traveling from operating surface to discharge areas in a steady-state process.

Thus in drag the rate of heat generation, or power, is limited by the dissipation capacity of the brake, for here equilibrium is reached wherein heat leaves as fast as it enters. The peak of the temperature gradient incident thereto should not exceed 600 F lest lining "dusting" result.

Under deceleration, peak surface temperature results from conduction capacity rather than radiation and convection, which latter are of secondary concern. The chief problem is one of conduction.

For given entrance conditions from surface to interior, the maximum surface temperatures reached depend upon two factors—the rate of climb and its duration or length. Because under deceleration, the speed, and therefore power, decrease, the rate of surface temperature rise likewise diminishes. It is readily seen from Fig. 9 that this change in slope of the temperature curve, together with the initial slope, determines the height of the crest. The angle of the slope may be regarded as an index of power, the temperature rising more abruptly the higher the power output. Under high deceleration the power drops quickly so that the temperature curve bends rapidly from the initial slope. Hence the crest is attained quickly at a low level. Thus with high power derived from high torque but low inertia load, maximum temperatures may be moderate. However, if the inertia load is likewise high, then for the same torque the high bracket of power persists for a longer period because of the slower reduction in velocity.

Consequently, temperature climb proceeds for a longer period at high rate and at a less diminishing slope. Accordingly, the crest occurs at a higher temperature. Thus, for a given power output, inertia load determines peak temperatures to the extent that it prolongs maximum power.

Note that the brake relieves itself by its own capacity to reduce speed rapidly. It is this relief in power which the brake depends upon in meeting demands. Take from it this inherent characteristic, and its tremendous peak capacity vanishes.

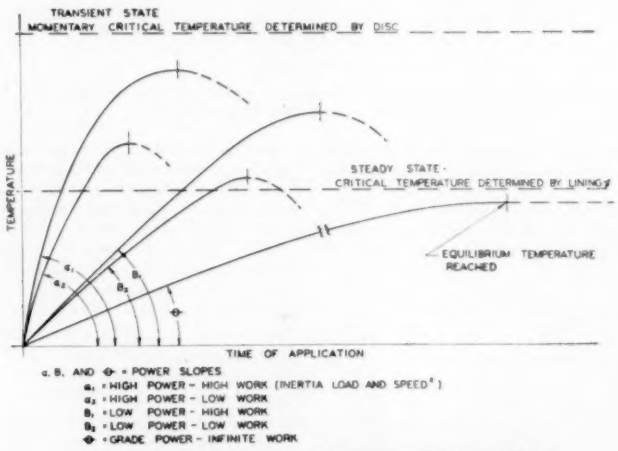

Fig. 9 Surface Temperature as Affected by Power and Work

With the modern railroad brake huge power demands are required because of high speed, and with high braking torques due to heavy wheel loads. An appreciably higher inertia load—brought about by overload—causes an already abrupt temperature ascent to so continue longer, thereby reaching higher ceilings. Thus the inertia load significantly affects power capacity, which accounts for the important role that train consist plays by virtue of its effect on overload.

Note that, whereas the wheel load determines maximum power (for a given effectiveness and speed), the inertia load determines its duration. Hence it is the amount of energy converted in the maximum power range, which is the significant factor, rather than the total energy of the entire stop.

Referring to Figs. 9, 10, and 11, because of the low power demands upon drag, the temperature rise is slow. However, because of the infinitely long application, critical limits can be reached finally if equilibrium does not develop prior thereto. In this case the inertia load becomes infinite under infinite duration of power, so that the bend in the temperature curve from initial slope is the result of dissipation rather than reduction in speed.

Heat Per Engaging Surface

Consider the single-shoe drum brake, Fig. 12, of radius R, and width w, with a shoe arcuate length of $R\theta$, and assume a torque output of T. The total heat W generated between the engaging surfaces of shoe and drum in one revolution is

$$W = 2\pi T$$

and the horsepower developed at n revolutions per second (rps) is $2\pi nT/550$

If the energy absorbed per square inch of shoe surface is W_s, with shoe area A_s, the energy absorbed by the shoe surface per revolution is W_sA_s). Similarly, if the energy absorbed per square inch of drum surface is W_d, with drum area A_d, the energy absorbed by the drum surface per revolution is W_dA_d. The sum must equal the total energy developed

$$W_sA_s + W_dA_d = 2\pi T$$

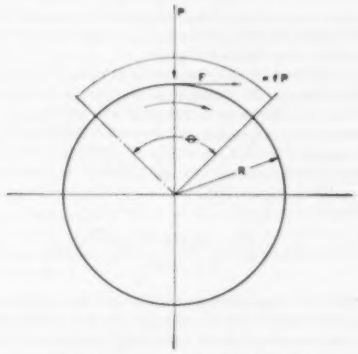

Fig. 12 Single-Shoe Drum Brake

Since all square inches of the shoe surface are continually engaged with the drum, if $K_s(2\pi T)$ represents the portion of total heat which is absorbed by the shoe in one revolution, then the heat absorbed per square inch of shoe surface W_s becomes

$$W_s = \frac{K_s(2\pi T)}{R\theta w}$$

and the horsepower per square inch of shoe surface is

$$\frac{K_s(2\pi nT)}{550\,R\theta w}$$

As the drum makes one revolution, each square inch of drum surface passes under the shoe and in so doing absorbs its proportionate share of the total heat absorbed by the entire drum surface. Consequently, if $K_d(2\pi T)$ represents the portion of heat absorbed by the drum, the heat per square inch becomes

$$W_d = \frac{K_d(2\pi T)}{2\pi Rw} = \frac{K_dT}{Rw}$$

and the horsepower per square inch of drum surface is

$$\frac{K_d(2\pi nT)}{550\,R\theta w}$$

Note that the division of heat which goes to the drum surface film $K_d(2\pi T)$ and the remainder which goes to the shoe surface film $K_s(2\pi T)$ is dependent upon a number of parameters such as the respective instantaneous temperature gradients of shoe and drum, their relative conductivities and masses. Accordingly, K_s and K_d may vary continually throughout the application.

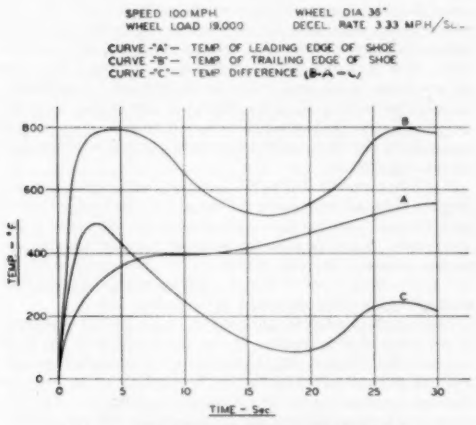

Fig. 10 Disk-Brake Dynamometer Test 52-X
(Speed 100 mph; wheel diameter 36 in.; wheel load 19,000 lb; deceleration rate 3.33 mphps.)

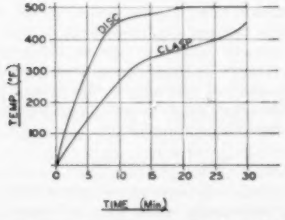

Fig. 11 Comparative Temperature Rise on Grade Between Clasp Brake and Disk Brake
(35 mph; 2.5 per cent grade; 20,000-lb inertia load.)

With the disk brake, $K_d = 1$ virtually, owing to the insulating properties of the shoe.

It is important to point out that due to action and reaction, the friction force per unit area on the shoe is equal and opposite to the friction force per unit area on the drum, and the work developed is the natural friction force times the relative displacement between the two surfaces. Therefore the work and power developed by the brake through friction is localized along the shoe surface for both drum and shoe. Hence the absorption of heat is continuous along the surface of the shoe, but intermittent per revolution for the surface of the drum, heat being transmitted to the drum surface only when passing under the shoe.

It will be observed that the power per square inch for both shoe and drum varies inversely as shoe length, so that maximum unit power occurs for each, when the shoe length is minimum. Whereas the shoe stands only to lose by a reduction in its length, the longer rest period afforded each square inch of drum surface more than compensates for the higher unit power.

With the disk brake, the shoe area is 40 sq in. per face, or 80 sq in. per double face. Assuming uniform pressure distribution, and discounting the differences in unit radii and unit arcuate lengths, the average power per square inch generated between the rubbing surfaces amounts to 12.5 hp, or $^1/_{80} \times 1000$ hp. Such power is developed when an inertia load of 25,000 lb is retarded at 3.3 mphps at 100 mph—a condition commonly encountered with the disk brake.

$$\text{Hp} = \frac{3.3 \times 25{,}000 \times 100}{21.9 \times 375} = 1000$$

Therefore heat is generated on each square inch of the engaging surfaces at the rate of 9 Btu per sq in. per sec, which gives some idea of the tremendous rate at which heat must be removed.

Heat Removal From Operating Surface

With a short shoe of high conductivity, the continuous generation of heat on its surface of limited area, causes an uninterrupted rise in filament temperature. The gradient thereby resulting produces an inrush of heat, which because of the relatively small mass for storage and limited area for dissipation, overtaxes the restricted accumulator capacity of the shoe. Accordingly, surface temperatures pyramid. Thus the shoe represents a poor thermal conveyer, accumulator, and dissipator.

Conversely, the rotating member of the brake—be it wheel, drum, or disk—is inherently far better suited to receive heat.

Primarily a much larger gateway for heat entrance is afforded through its relatively large operating area. Then too, its mass is likely to be more than 10 times that of the shoe, thereby providing correspondingly better storage capacity. Finally, because of the ability to provide large areas exposed to high-velocity air streams—made possibly by rotation—the ability to discharge heat into the atmosphere through radiation and convection is greatly enhanced. Because of these conditions, it follows that operating surface temperatures are held to a minimum by diverting maximum thermal flow into the better-qualified rotating member. This is accomplished effectively by employing in the shoe a highly insulating material—such as the asbestos-composition lining of the disk brake. Here, virtually none of the heat generated in a 100-mph stop enters the shoe, as evidenced by the fact that the shoe can be readily handled directly thereafter. Instead, it is directed into the disk.

Assuming that full recourse has been taken to employ maximum permissible operating area, the temperature head incident to penetration still may result in excessive operating surface temperatures.

Although some assistance may be gained from increasing mass and thereby lowering the level of the gradient, including the peak at operating surface, cost and weight become limiting factors in this direction. Moreover, whereas mass improves accumulator capacity, the very lowering of exit temperatures reduces the temperature head between discharge surface and atmosphere, thereby restricting final dissipation. This limitation is felt in drag applications, and those wherein repetition is frequent.

The most effective manner in preventing excessive climb in surface temperature is to employ a short length of shoe, in combination with one of insulating material.

Since the rate of unit work is maximum, the temperature rise during the work cycle is likewise maximum. This temperature head, magnified by the increased work rate, accelerates thermal flow into the disk or drum during the rest period directly following, resulting in a huge drop in filament temperature. As shown in Fig. 10, this drop amounts to 400–500 F in the early stages of a high-speed application where maximum difference obtains between entrance and exit temperatures. Also note that this drop occurs in less than 50 millisec with a 90-deg shoe at a speed of 100 mph. (The work period is only a matter of 16 millisec.) Accordingly, as an increment area again passes under the shoe, the "recommencement" temperature being so reduced, does not climb to excessive heights during the following work cycles (see Fig. 13).

Although the recommencement temperatures, and, accordingly, the shoe exit temperatures, successively rise during the period of high power output, the fact that such quantities of heat are injected into the interior during the rest cycle, prevents the exit temperatures—maximum in the cycle—from reaching critical limits. Where the work cycle is continuous throughout the revolution, as in the clutch type of circular shoe, the temperature rise per revolution is low and so likewise is the head. Accordingly, thermal flow is relatively slow, causing the heat to dam up at the operating surface and pyramid the uninterrupted rise in surface temperature, thereby reaching higher ceilings, which readily may exceed critical limits.

It will be observed that as the higher surface temperatures are reached, the gradient is more shallow so that the head benefit of peak filament temperatures is not present as in the case of the short shoe. It may be regarded that with the short shoe the operating surface of the disk is "inoculated" with temperature to prevent reaching excessive degrees. This premature temperature head serves as a "thermal pump" to hasten heat flow.

In the early development of the disk brake, a study was made of the effect of shoe length. It was found that with the fully wrapped shoe, 60 mph was the highest speed at application that could be endured before producing "fire bands," or incandescent filament temperatures on the disk operating surfaces. With the short shoe, it was possible to begin application at 100 mph without incurring such deleterious temperatures. Thus, by virtue of the short shoe, the energy capacity was increased threefold.

Although the short shoe increases the lining work and power (inversely with length), the fact that the disk-filament temperatures are so greatly reduced, more than offsets the greater lining duty. The shoe does not wear by abrasion as much as it "dusts off" or melts away by temperature, so that temperature may easily be a more determining factor on wear than pressure.

It has been observed with a given disk brake, that the lining wear with a 120-deg shoe is no greater than with the circular shoe employing 3 times the amount of lining.

Why the Disk Brake?

From the outset of the brake development beginning in 1937, the following fundamental creeds were laid down by the author and have so remained:

1 First it was regarded that the brake should be removed

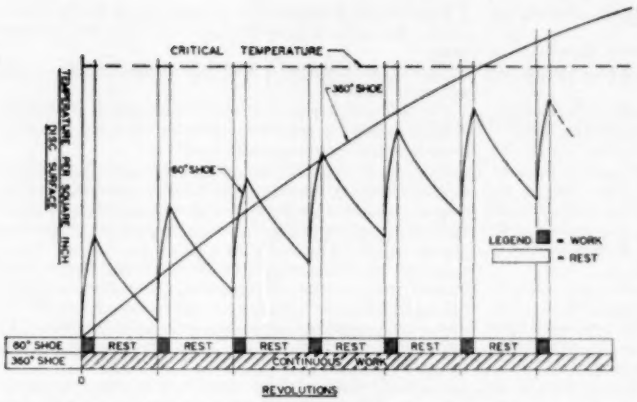

FIG. 13 SCHEMATIC CURVE FOR TEMPERATURE VERSUS REVOLUTIONS, SHOWING EFFECT OF SHOE LENGTH ON TEMPERATURE PER SQUARE INCH OF DISK SURFACE

from the wheel, leaving the wheel free to serve its chief and vital function of load carrying, without hazard from thermal damage and wear from brake shoe. Moreover, by unshackling the brake from restrictions inherent to the wheel, the resulting freedom in design and selection of material made possible optimum choice individual solely to braking considerations.

2 The combination of a shoe with composition lining, largely of asbestos, mating with a cast-iron operating surface on the rotating member. This stipulation was borrowed from automotive experience. After years of trial and error, the industry has settled universally on this combination. The reasons are basic and may be enumerated as follows:

(*a*) The wearing properties of cast iron are excellent. Unlike steel, it is not likely to gall or score—maintaining a smooth satin-like surface—particularly if suitable lining is employed. This is substantiated by the fact that disks are still operating after 10 years of service or 3,000,000 miles.

The chief shortcoming of cast iron as a braking surface is its vulnerability to thermal checking, traceable no doubt to its inherent lack of ductility. Under temperature gradients expansion is restricted by the colder surrounding areas and, therefore, the heated areas plastically upset. Upon cooling they endeavor to return to the now reduced dimensions of the cold state but are restricted in so doing by the same surrounding media that originally produced the hot contraction.

Since the reverse cycle takes place at lower temperatures, and the resulting extension is likely to exceed elastic limits, the material is called upon to shear cold plastically. Accordingly, ductility becomes a requisite in averting thermal checking. However, the lack of ductility of cast iron may be offset by mechanical design—in providing adequate conditions for thermal flow and thereby avert excessively steep temperature gradients.

Note that heat checks do not result from temperature alone, but rather from a differential in temperature. For this reason heat checks seldom occur in drag applications. Though appreciable temperatures may be reached, because of the low power involved, the disk is heated relatively uniformly throughout. Accordingly, peak gradients, conducive to checking, are absent.

(*b*) The composition lining, in combination with cast iron, possesses excellent wearing properties as evidenced by the 90,000-mile lining life obtained with the California Zephyr, which represents one of the most, if not the most, grueling brake operations in the world. Here again, however, it is necessary through mechanical design to prevent the development of excessive temperatures. Characteristically, the resins in virtually all composition-asbestos linings begin to volatilize over 600 F, resulting in rapid wear due to "dusting." Accordingly, when the application is sufficiently long to allow heat to penetrate into the lining, maximum temperatures must be controlled correspondingly.

Fortunately, where the application is sustained, the power is low. Conversely, where the duration is short, higher temperatures can be condoned due to their momentary presence.

(*c*) The application is completely silent and smooth at all times, thereby conspicuously enhancing the much sought for passenger favor.

(*d*) Within proper temperature limits (possible to maintain), the coefficient of friction remains virtually constant at all times. This characteristic is of vital importance to multiple-car control, particularly where each brake must skirt closely to, but not exceed, imposed boundaries, such as those of adhesion. It also provides for smooth and accurate train-handling with minimum effort.

Having established at the outset that the brake should be removed from the wheel, the form or type of brake remained to be determined. After investigating the drum, the clutch-type disk, and the shoe disk, it was decided to adopt the last with the following considerations applying:

1 Because of the high efficiency necessary to handle such enormous power within the space, cost, and weight limits imposed, uniform bearing pressure was paramount. It was essential to distribute the work uniformly over the operating surface, and thereby avoid peak overloads. The disk, unlike the drum, being sensibly impervious to mechanical and thermal distortion, is admirably suited to meet this requirement. It is interesting to note, however, that because of the severity of the imposed demands, it was necessary to resort to measures beyond that enjoyed from the disk form solely.

2 Owing to the fact that the disk may expand diametrically as much as $^1/_8$ in. when hot, it was necessary to provide a partially flexible mount to avoid undue restraint upon the cast-iron ring, which might otherwise fracture under thermal stress. This was accomplished by casting the iron ring integrally with a deep-dished low-carbon-steel tapered stamping, in turn attached to the wheel hub. By virtue of its shape, section, and analysis, this stamping provides the necessary flexibility and toughness required. Absence of this important provision constitutes the chief cause of failure in European attempts with the disk form of brake.

3 Actually, the disk face does not remain planar when heated, but assumes a slightly conical form of both convex and concave contour. Although microscopic, this departure was sufficient to alter uniformity of bearing pressure to the extent of producing fire bands—the forerunner of heat checks. To accommodate this change, the lining was divided into independent segments backed by rubber pads. Each segment was thus free to float and thereby to follow the instantaneous contour of the disk. This one step made it possible to increase the inertia load in a given test from

16,000 lb to 24,000 lb—or 50 per cent—without incurring fire bands, which designate critical limits.

4 By virtue of the double operating faces of the disk, it is possible to provide 700 sq in. for heat conduction as against 400 sq in. of wheel-tread area.

5 Inherently, the disk form lends itself to the inclusion of integrally cast radial vanes, located between the operating surfaces, which may serve as impellers to produce air flow. Thus the enormous exposed area embracing some 7000 sq in., as against 2200 sq in. with the wheel, enjoys direct contact with the air stream, thereby enhancing convection, which is the chief path of final heat dissipation into the atmosphere. It is interesting to note that at 100 mph the radial air velocity through the disk is likewise 100 mph.

This feature of the disk, in so benefiting dissipation, makes it possible to hold a 20,000-lb wheel load at a constant velocity of 35 mph when descending a 3 per cent grade. The application may be sustained indefinitely. At the end of approximately 20 min equilibrium is reached at a noninjurious temperature of 600 F, which remains at this level thereafter as long as the application continues.

6 Perhaps least obvious, but of greatest consequence certainly to deceleration, is the singular ability of the disk to accommodate the single short shoe so vital to conduction. With a pair of free-floating shoes, acting against each other through the disk, no external reactions are introduced, yet each shoe acts singly with respect to the operating face upon which it bears.

Only the disk provides this opportunity. With the drum or wheel brake the bearing is called upon to take the shoe reaction. Moreover, whereas single short-shoe operation is preserved per face, the disk brake in its entirety enjoys the area advantages of a pair of shoes.

Status

With the disk brake in combination with the wheel protector and sanding, as controlled by the protector, a sustained deceleration of 4 mphps from 100 mph with wheel loads of 20,000 lb has been accomplished. Moreover, such emergency performance produces no damage to shoe or disk.

The corresponding theoretical stopping distance of 1840 ft, based upon instantaneous attainment of bcp, has been closely approached with free car operation, utilizing 6 seconds for attainment of full brake-cylinder pressure (2080 ft from 100 mph as interpolated from 97 mph).

It now remains to obtain such performance with the train as a whole.

To do so, requires the following:

1 Adequate car-brake capacity of constant friction.
2 Adequate locomotive-brake capacity of constant friction.
3 Wheel control on both cars and locomotive.
4 Sand regulated by wheel control on both cars and locomotive.
5 Electropneumatic straight air control with full brake-cylinder pressure attained in 2 sec.

Except for the locomotive brake, equipment to satisfy the foregoing requirements is available and in use in varying combinations.

Since no one locomotive-hauled train includes all, full capital is not as yet realized.

The California Zephyr represents a high degree of advanced steps to be found in one train, embracing car disk brake, wheel protection, and electropneumatic straight air.

Although the car disk brake has sufficient capacity to develop an effectiveness of 4 mphps upon emergency demand, a braking ratio was selected to furnish an effectiveness of 3 mphps due to the question of sanding and the restriction in added net performance as curtailed by the locomotive.

In tests, the train stopped from 98 mph in 3365 ft with 90 psi bcp and a total attainment time of nearly 10 sec (the greater portion of brake-cylinder pressure was attained in one half of this time.) At the employed 90 psi bcp the car effectiveness was 2.8 mphps and the locomotive 1.6 mphps, resulting in a train deceleration of 2.4 mphps.

At 100 psi bcp the car effectiveness becomes 3.12 mphps and the locomotive 1.76, resulting in a train deceleration of 2.68 mphps. With 2.5 sec for build up of brake-cylinder pressure, the distance becomes 2940 ft—from 100 mph.

With the combination of sand and a locomotive brake of higher effectiveness, the stopping distance from 100 mph is reduced to 2040 ft.

The combination of all elements is available in the R.D.C. single or multiple-car train built by the author's company. This is made possible by the absence of the locomotive. Emergency and service decelerations are, respectively, 3.4 and 2.7 mphps. The brake has ample capacity to produce a deceleration of 4 mphps.

It is to be pointed out that more experience with sanding is necessary before establishing a practicable emergency effectiveness, so that the rate of 4 mphps should be regarded as a possible goal yet to be substantiated.

The subject of braking is receiving intensified recognition brought about by the many advances which have and are being culminated in this period of outstanding progress.

Acknowledgment

Grateful acknowledgment is expressed for the outstanding support rendered by Mr. H. H. Urbach and Mr. H. I. Tramblie, of the Chicago, Burlington & Quincy Railroad—first to adopt the disk brake; Mr. J. P. Morris and Mr. E. E. Chapman, of the Atchison, Topeka & Santa Fe Railroad, which followed closely thereafter; and Mr. K. F. Nystrom, Mr. V. L. Green and Mr. R. G. Webb, of the Chicago, Milwaukee, St. Paul & Pacific Railroad, and all others who contributed to the development.

Particular acknowledgment is expressed to Mr. William Mann, and Mr. P. W. Gaenssle, of The Budd Company, for their valued assistance in fundamental developments and design of the brake, respectively.

Pressures Developed by Viscous Materials in the Screw Extrusion Machine

By W. T. PIGOTT,[1] AKRON, OHIO

Previously developed equations describing the pressure and discharge rates of Newtonian liquids in the screw-type pump are discussed briefly and are experimentally verified. These equations are then applied to rubberlike materials for the two extreme conditions of extruder operation: Open discharge (with die removed from discharge end of extruder); and zero discharge (with solid plate sealing the discharge end of the extruder). For the condition of closed discharge, calculated pressures agreed with observed pressures. The apparent viscosities of a number of stocks were determined by forcing them through circular orifices at different flow rates and calculating the viscosity from Poiseuille's equation. The effective shear rate was calculated by using an expression for the average volume weighted rate of shear in circular orifices. The effective shear rate occurring in the extruder was calculated for screws with wide thread troughs from the velocity distribution in the troughs and an expression for the average volume weighted rate of shear in rectangular orifices. An experiment was devised to determine the effective shear rate in the extruder at zero discharge. The result agreed with the calculated value. It is concluded that at zero discharge the mechanism for rubberlike materials is one of viscous shearing and that rubberlike materials behave as viscous but highly thixotropic liquids.

Nomenclature

The following nomenclature is used in the paper:

- D = inside diameter of sleeve or circular orifice, cm
- F = constant of integration
- E = constant of integration
- D_m = diameter to centroid portion of screw thread $D_m = D - h$, cm
- w = width of thread land, cm
- s = width of thread trough, cm
- h = height of thread, cm
- λ = lead of thread, cm
- L = effective length of screw; distance from feed port to last effective thread on tip of screw, cm
- l_t = uncoiled length of screw thread, cm

$$l_t = L\sqrt{1 + \left(\frac{\pi D_m}{\lambda}\right)^2}$$

- l = length of orifice, cm
- q = discharge rate of substance flowing through an orifice, cu cm per sec
- θ = helix angle of thread, deg
- C = clearance between thread and sleeve, cm.
- V = linear speed of sleeve relative to screw, cm per sec
- v = velocity of particle of liquid at any point (x, y) in thread trough or orifice cross section, cm per sec
- v_A = average velocity of material flowing through orifice, cm per sec
- d = semi-cross-sectional dimension of screw thread or orifice, cm
- Q = open discharge rate of screw, cm per sec
- Q_l = discharge rate of viscous material in rectangular orifice due to difference of pressure at ends of orifice, cm per sec
- Q_C = backward flow of viscous material through clearance C due to difference of pressure at feed port and discharge port, cu cm per sec
- $f\left(\frac{h}{s}\right)$ = special function calculated by infinite series used in calculation of open discharge rate, dimensionless; see Fig. 2
- $g(s, h)$ = special function calculated by infinite series used in calculation of Q_l, dimensionless; see Fig. 3
- μ = viscosity of Newtonian liquid, poises
- μ_A = apparent viscosity of rubberlike materials, poises
- P = pressure (dynes/cm^2) to convert to psi multiply by 145×10^{-7}
- $\left(\frac{dv}{dx}\right)_A$ = average volume weighted rate of shear, sec^{-1}
- K = the parameter $\frac{P}{\mu l_t}$

Introduction

With the more frequent use of the screw-type extruder, a working knowledge of the mechanism of its basic elements is desirable. The basic extruder elements treated in this investigation are a closely fitting screw with uniform threads and a sleeve equipped with suitable inlet and discharge ports located at the ends of the sleeve. These elements are shown schematically in Fig. 1.

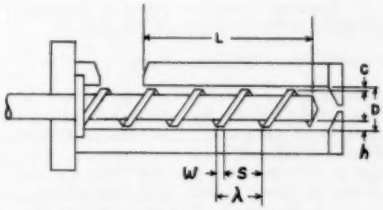

Fig. 1 Schematic of Screw Extruder

The objective of this investigation is to determine the mechanism of this simple combination of elements when various materials are pumped, and to determine the effect of the design and operation of these elements on the pressure and discharge rates. The materials are limited to Newtonian liquids and rubberlike materials. More specifically, the purpose of this investigation is

---

[1] Research Engineer, Goodyear Tire and Rubber Company.

Contributed by the Rubber and Plastics Division and presented at the Annual Meeting, New York, N. Y., November 26–December 1, 1950, of The American Society of Mechanical Engineers.

Note: Statements and opinions advanced in papers are to be understood as individual expressions of their authors, and not those of the Society. Manuscript received at ASME Headquarters, November 20, 1950.

to determine the effect of the screw length L, the thread height h, the thread trough width s, the thread width w, the sleeve diameter D, the clearance C, the speed of rotation of the screw, and the viscosity of the material being pumped on the resulting pressure and discharge rate.

Several mathematical analyses were located which gave the subject a theoretical treatment for the case of Newtonian liquids. Rowell and Finlayson (1, 2)[1] gave very little experimental verification and Rogowsky (3) none. The equations developed by these authors for pressure and discharge rate were experimentally verified using several liquids having different viscosities, screws with different thread dimensions, and screws with different clearances between threads and sleeve.

All the experimental determinations were made using the National Rubber Bench Model extrusion unit and modifications of it. Ordinary hydraulic gages equipped with special fittings were used for pressure determinations. Special equipment was built for viscosity determinations of rubberlike materials, although the same determinations could have been made using various types of apparatus described in the literature.

Open Discharge Rate

The "open discharge rate" is defined as the rate of discharge of a screw with no pressure gradient from the input port to the discharge port. This condition is achieved by operating the machine with the die removed from the discharge end. Under this condition a differential equation describes the velocity distribution of a Newtonian liquid at any point in the thread trough. By successive integration an expression for the volumetric discharge rate can be derived

$$Q = \frac{8s^2 V \cos\theta}{\pi^2} f\left(\frac{h}{s}\right) \quad \ldots\ldots [1]$$

where

$$f\left(\frac{h}{s}\right) = \sum_{m=1}^{m=\infty} \frac{\cosh\left(m\pi\frac{h}{s}\right) - 1}{m^3 \sinh\left(m\pi\frac{h}{s}\right)}$$

and m = odd integers.

Since $f(h/s)$ is merely a function of the ratio (h/s), it can be calculated for a number of different values of (h/s) and used for many computations. The quantity $f(h/s)$ is plotted versus (h/s) in Fig. 2. Equation [1] has been stated by Rogowsky (3) and implicitly stated earlier by Rowell and Finlayson (2).

Zero Discharge

"Zero discharge" is defined as the other extreme, i.e., operation of the extruder with the discharge port completely sealed so that the discharge rate is zero. Under this condition the maximum pressure is achieved in the discharge port. The pressure developed at the sealed discharge port forces the liquid backward through the thread trough and through the annular clearance between the threads and the sleeve. At zero discharge the forward flow rate Q equals the sum of the backward flow rate through the thread trough Q_t, and the backward flow rate through the clearance Q_c

$$Q = Q_c + Q_t \quad \ldots\ldots [2]$$

[1] Numbers in parentheses refer to the Bibliography at the end of the paper.

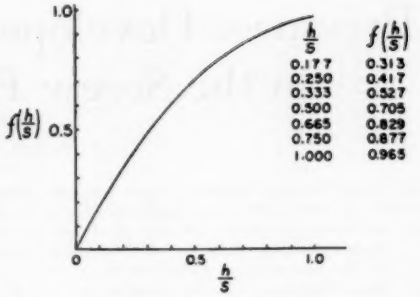

Fig. 2 $f(h/s)$ Versus (h/s) for Open Discharge

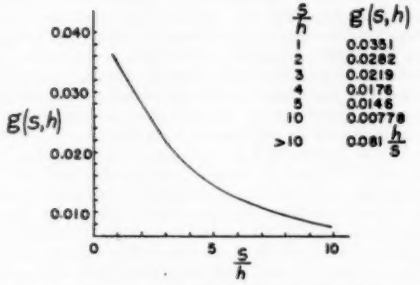

Fig. 3 $g(s, h)$ Versus (s/h) for Flow Through Rectangular Orifice

By using an equation for the flow rate of liquid through a rectangular orifice, Q_l can be evaluated in terms of the dimensions of the thread trough, the viscosity of the liquid, and the difference in pressure at the ends of the orifice

$$Q_l = \frac{P s^3 h^3}{\mu l_t} g(s, h) \quad \ldots\ldots [3]$$

where

$$g(s, h) = \frac{1}{8\left(\frac{s}{h} + \frac{h}{s}\right)} \left\{ \frac{1}{3} + 2 \sum_{m=0}^{m=\infty} \frac{1}{\left(\frac{m\pi}{2}\right)^5} \left(1 - \frac{2}{\left(\frac{m\pi}{2}\right)^3}\right) \left[\frac{s}{h} \tanh\left(\frac{m\pi h}{2s}\right) + \frac{h}{s} \tanh\frac{m\pi s}{2h}\right] \right\}$$

m = odd integers.

Values of $g(s, h)$ for various values of s and h are given in Fig. 3. The complete details of the derivation of Equation [3] have been published elsewhere (4). Similar expressions have been experimentally verified (5).

By using the relation for the flow of liquids through annular spaces, an expression for Q_c in terms of the dimensions of the screw, viscosity of the liquid, pressure, and clearance can be derived

$$Q_c = \frac{P\lambda C^3}{12 L w \mu} \sqrt{\pi^2 D^2 + \lambda^2} \quad \ldots\ldots [4]$$

A series of experiments were carried out by increasing successively the clearance and measuring the zero discharge-head pressure. A Newtonian liquid was used which had a viscosity of approximately 1400 poises at the temperature of the experiment. The zero discharge pressure was calculated by solving Equation [2] for the pressure P. The calculated and observed zero discharge pressures are plotted versus clearance in Fig. 4.

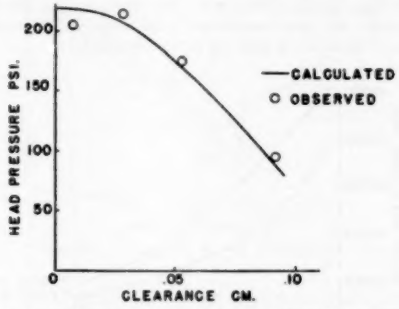

FIG. 4 ZERO DISCHARGE HEAD PRESSURE VERSUS CLEARANCE FOR VISCOUS LIQUID

For closely fitting screws, Q_c is negligible, and Equation [2] becomes

$$Q = Q_t \quad \ldots\ldots\ldots\ldots\ldots\ldots\ldots\ldots\ldots\ldots [5]$$

CONCLUSIONS FOR VISCOUS LIQUIDS

The following is concluded for viscous liquids:

The mechanism is one of viscous shearing for all conditions of operation, i.e., open discharge, zero discharge, and intermediate discharge rates.

From Equation [1] it may be concluded that the open discharge rate of Newtonian liquids is dependent only upon the cross-sectional dimensions of the thread trough and the speed of rotation of the screw. For high thread helix angles, a correction factor $\cos \theta$ must be included. The open discharge rate is independent of both the viscosity of the liquid and the length of the screw. Since there is no pressure gradient from inlet port to the discharge port, the flowback of liquid through the clearance between the threads and the sleeve is negligible. Equation [1] was verified experimentally using a number of screws with different thread dimensions and oils with different viscosities.

The zero discharge pressure is directly proportional to the viscosity of the liquid, the speed of rotation of the screw, and the length of the screw. From Equation [3] it can be seen that greater zero discharge pressures will result when the cross-sectional area of the screw-thread trough is small. The zero discharge pressure decreases as the clearance increases, but the relation is not a linear one. Considerable loss in pressure results from the decrease in viscosity caused by heat generation, hence temperature control is important. Zero discharge head pressures were measured for a number of different viscosity liquids in a number of screws having different thread dimensions. The measured pressures agreed with the pressures calculated from Equation [2].

The relation between discharge rate and pressure is an inverse linear one. The pressure-discharge relation can be determined by calculating the open discharge rate and zero discharge pressure, plotting the two points on rectangular axes of discharge rate and pressure and drawing a straight line between the two points. The linear relation between pressure and discharge rate was verified experimentally by making pressure and discharge-rate determinations on a screw equipped with an adjustable opening on the discharge port.

The pressure and discharge rates were measured with the discharge port completely open, restricted by successive amounts and completely closed. The data from these experiments are shown graphically in Figs. 5 and 6.

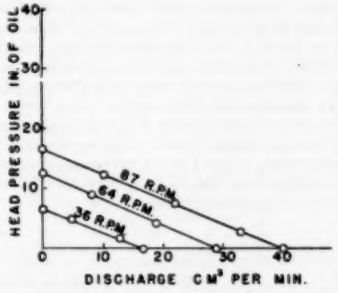

FIG. 5 HEAD PRESSURE VERSUS DISCHARGE RATE FOR 0.5 POISE OIL

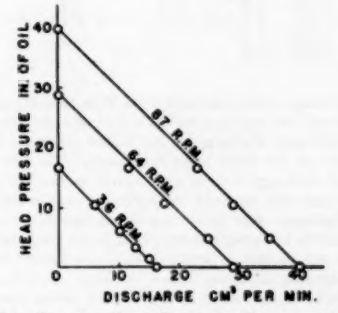

FIG. 6 HEAD PRESSURE VERSU DISCHARGE RATE FOR 1.1 POISE OIL

OPEN DISCHARGE OF RUBBERLIKE MATERIALS

A number of determinations were made using rubberlike materials. These materials are listed in Table 1. A few of their physical properties are given along with the chief component of each stock.

TABLE 1 IDENTIFICATION OF STOCKS

Stock	Composition	Specific gravity at 75 F	Mooney plasticity $ML-212$
A.....	Butyl rubber (compounded)	0.90	49
B.....	Natural rubber (compounded)	0.95	20
C.....	Chemigum (compounded)	1.20	37
D.....	Synthetic rubber (pure gum)	1.20	48
E.....	Polyisobutylene (pure gum)	0.85	56

These stocks were strip-fed into the National Rubber Bench Model screw extruder and the open discharge rates were measured. Screws with uniform threads were used. The sleeve was heated to 212 F in all cases. The area surrounding the feed port was cooled. Even with undercut threads at the feed port, the open discharge rates were far less than the calculated discharge

rates using Equation [1]. Upon dismantling the extruder it was found that the threads were only partly filled with stock.

A different method was then used to measure the open discharge rate. The extruder was operated at zero discharge until no more stock would go into the feed port. The extruder was then stopped and the pressure allowed to subside. The cover plate on the discharge port was then removed. The extruder was turned on again and the stock in the threads discharged and the discharge rate measured. The open discharge rates determined in such a batchwise manner were higher than continuous discharge with strip feeding. The results of these experiments are given in Table 2. The experimental open discharge rates listed in Table 2 were determined over a wide range of screw speeds, the discharge per unit time being directly proportional to the screw speed, and the discharge per screw revolution being constant for any particular stock in any particular screw. The fact that the open discharge rates were much lower with continuous strip feeding than when the full extruder was discharged batchwise indicates that the charging port severely reduced the volumetric efficiency of the extruder.

TABLE 2 OPEN DISCHARGE RATES OF RUBBERLIKE MATERIALS

Stock	Screw dimensions, cm A	Screw dimensions, cm s	Open discharge rate, cu cm/revolution — Calculated	Observed continuous strip feed	Observed batch discharge
C	0.317	2.06	2.48	...	2.14
E	0.317	2.06	2.48	0.67	2.26
B	0.317	2.06	2.48	0.86	1.32
A	0.317	2.06	2.48	0.73	1.97
C	0.317	3.34	3.55	...	2.38
A	0.317	3.34	3.55	0.70	...
C	0.317	4.60	4.43	...	2.58

The discharge rate calculated from Equation [1] was at no time achieved, but was approached as a limit in the case of stock C with batchwise discharge as the thread spacing s decreased (and hence as the helix angle decreased). The fact that the theoretical discharge rate is approached as the helix angle θ decreases and that the open discharge rate varies for different stocks is indicative that the stock is sliding against the wall of the sleeve. At the low pressures prevailing in the stock during open discharge, deformation is largely of an elastic nature, little or no viscous shearing occurring, hence elasticity controls, and the mechanism is largely one of sliding friction rather than viscous shearing.

Zero Discharge of Rubberlike Materials

At high pressures, such as occur throughout most of the stock at zero discharge, the mechanism is more likely to be one of viscous shearing, and Equations [1], [3], [5] should be applicable. It will be shown that this is true and that the zero discharge pressure can be calculated. Close enough agreement between calculated zero discharge pressure and observed values was achieved to make possible fairly close estimations of zero discharge pressure. In order to apply Equations [1], [3], [5] the relation between an apparent viscosity μ_A and the rate of shearing must be known for the stock, because rubberlike materials are known to be thixotropic. In order to make use of this information the effective rate of shear prevailing in the extruder must also be known. The effect of the clearance between the screw threads and the sleeve on the zero discharge pressure was found to be much greater than for Newtonian liquids. No satisfactory method of calculating the decrease in zero discharge pressure due to clearance was found. Therefore the calculation of zero discharge pressure is limited to tightly fitting screws.

A screw was made identical to the one used in determining the data shown in Fig. 4. The zero discharge pressure was measured using stocks A and D and successively increasing the clearance C. The temperature was maintained at 212 F, and the screw was rotated at 25 rpm. The resulting zero discharge pressures are plotted versus the clearance C in Fig. 7. Inspection of Fig. 7 indicates that the per cent decrease in pressure, resulting from the clearance, is much greater than for Newtonian liquids. The greatest slope of the curves in Fig. 7 occurs at the low values of clearance, while the greatest slope of the curve in Fig. 4 occurs at the high values of clearance. The reason for this difference is probably the thixotropic nature of the stocks and the complex nature of the shearing occurring in the clearance C.

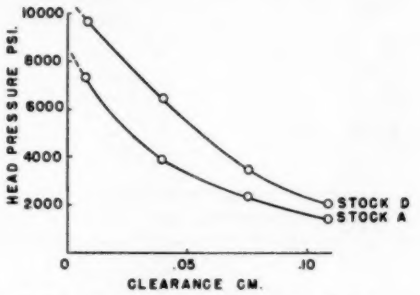

FIG. 7 ZERO DISCHARGE HEAD PRESSURE VERSUS CLEARANCE

Several of the stocks listed in Table 1 were forced through circular orifices, and the discharge rates measured under successively increasing pressures. From these data the apparent viscosity and the average rate of shearing in the orifice were calculated. The apparent viscosity μ_A was calculated from the Poiseuille equation where

$$\mu_A = \frac{P\pi D^4}{128\, l_e} \qquad [6]$$

The average rate of shear was calculated using an expression (6) for the volume weighted average rate of shear. For circular orifices, the expression for the average volume weighted shear

$$\left(\frac{dv}{dx}\right)_A$$

becomes

$$\left(\frac{dv}{dx}\right)_A = \frac{32 v_A}{15\, D} \qquad [7]$$

The values of μ_A were plotted versus

$$\left(\frac{dv}{dx}\right)_A$$

on logarithmic axes and approximately straight lines resulted in the case of each of the stocks. These results are shown in Fig. 8. An inspection of Fig. 8 indicates that μ_A decreases rapidly as

$$\left(\frac{dv}{dx}\right)_A$$

increases. Values of viscosity calculated from the Mooney plasticity (7) for these stocks, agreed favorably with values in Fig. 8 at the corresponding rate of shear. This serves as a check on the

accuracy of this method of viscosity determination at one value of shear rate.

In order to calculate zero discharge pressures for rubberlike materials, the effective shear rate occurring in the screw must be known so that the correct value of viscosity μ_A may be found using the data in Fig. 8. In order to do this, it is necessary to

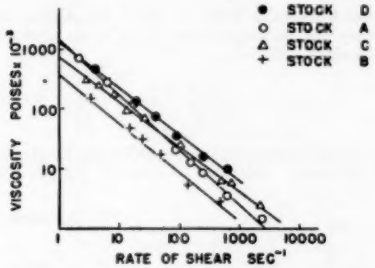

FIG. 8 VISCOSITY VERSUS SHEAR FOR RUBBERLIKE MATERIALS

determine the velocity distribution of a viscous material in the threads under the various conditions of operation and to derive expressions for lines of constant velocity. For widely separated threads, where the ratio s/h is high, the "end effects" due to the presence of the threads is small, and the mechanism becomes one of shearing between two infinitely wide parallel planes separated by the distance h. Equations analogous to Equations [1] and [3] for open discharge and zero discharge, respectively, can be derived with this simplified mechanism if a section s-units wide is considered. From this simplified analysis, expressions can be derived for the velocity distribution across the thread which can be used to calculate an effective shearing rate for various conditions of operation. Since most extrusion screws do have rather high values for the ratio s/h the effective shear rate calculated in this manner should be applicable.

Let the infinitely wide parallel planes A-A and B-B be symmetrically located about the axes x and v as shown in Fig. 9.

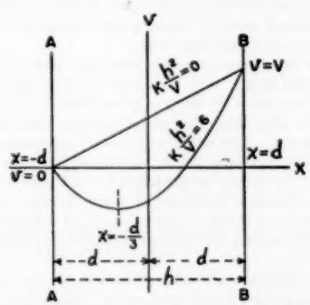

FIG. 9 VELOCITY DISTRIBUTION IN WIDE THREADS

The plane B-B moves with a constant velocity V relative to A-A. Each plane is located at a distance d from the origin so that $2d = h$. If the sleeve of an extruder moves with the velocity V relative to the bottom of the threads on the screw, the plane B-B corresponds to the sleeve and the plane A-A corresponds to the bottom of the screw thread. If the space between the planes is filled with a viscous material, the Laplacian Equation [2] reduces to

$$\frac{\partial v}{\partial x^2} = \frac{P}{\mu l_t}$$

Integrating and letting $P/(\mu l_t) = K$

$$\frac{\partial v}{\partial x} = Kx + C$$

Integrating again

$$v = \frac{K x^2}{2} + Ex + F$$

Since $v = 0$ when $X = -d$, and $v = V$ when $x = d$

$$F = \frac{V - Kd^2}{2}, \quad \text{and} \quad E = \frac{V}{2d}$$

Therefore the general equation for velocity v becomes

$$v = \frac{Kx^2}{2} + \frac{V}{2d} + \frac{V}{2} - \frac{Kd^2}{2} \qquad [8]$$

The expression for volumetric discharge rate is derived by performing the integration

$$\int_{-d}^{d} v dx = Vd - \frac{2Kd^3}{3}$$

At zero discharge this becomes zero, therefore

$$Vd = \frac{2Kd^3}{3}, \quad \text{or} \quad K = \frac{3V}{2d^2}$$

Substituting this value of K in Equation [8]

$$v = \frac{3V}{4d^2} x^2 + \frac{V}{2d} x - \frac{V}{4} \qquad [9]$$

and

$$\frac{dv}{dx} = \frac{3V}{2d^2} x + \frac{V}{2d} \qquad [10]$$

when

$$\frac{dv}{dx} = 0, \frac{3V}{2d^2} x + \frac{V}{2d} = 0$$

and

$$x = -\frac{d}{3}$$

The expression for volume weighted average shear rate in rectangular orifices given by Dillon and Johnston (6) becomes

$$\left(\frac{dv}{dx}\right)_A = \frac{\left|\int_{-d}^{d} \frac{dv}{dx} v dx\right|}{\left|\int_{-d}^{-d/3} v dx\right| + \left|\int_{-d/3}^{d} dv x\right|} \qquad [11]$$

The denominator is separated into two parts and the absolute values indicated, because the integral

$$\int_{-d}^{d} v dx$$

is zero at zero discharge, thus making Equation [11] indeterminate if this is not done.

Substituting Equations [9] and [10] in Equation [11] and calculating

$$\left(\frac{dv}{dx}\right)_A \text{ at zero discharge, } \left(\frac{dv}{dx}\right)_A = 1.69\,\frac{V}{d}$$

Since $h = 2d$

$$\left(\frac{dv}{dx}\right)_A = 3.38\,\frac{V}{h}$$

At open discharge $P = 0$ and K becomes 0. Substituting $K = 0$ in Equation [8]

$$v = \frac{V}{2d}x + \frac{V}{2} \quad \ldots\ldots\ldots\ldots\ldots\ldots [12]$$

and

$$\frac{dv}{dx} = \frac{V}{2d} \quad \ldots\ldots\ldots\ldots\ldots\ldots [13]$$

Substituting Equations [12] and [13] in Equation [11] and calculating

$$\left(\frac{dv}{dx}\right)_A$$

at open discharge

$$\left(\frac{dv}{dx}\right)_A = \frac{V}{2d}$$

Since $h = 2d$

$$\left(\frac{dv}{dx}\right)_A = \frac{V}{h}$$

This value is the expected one for open discharge, because a open discharge the velocity is directly proportional to the distance from the reference plane A-A.

If $K(h^2/V)$ is considered a parameter, which is zero at open discharge and has a maximum value of 6 at zero discharge, the average shear rate

$$\left(\frac{dv}{dx}\right)_A$$

can be calculated for all intermediate values of $K(h^2/V)$.

$$\left(\frac{dv}{dx}\right)_A$$

was calculated for a series of values of the parameter $K(h^2/V)$. These figures are given in Table 3.

TABLE 3 EFFECTIVE SHEAR RATES IN WIDE THREADS

$K\frac{h^2}{V}$	0	1.2	2.4	3.6	4.8	6.0
$\left(\frac{dv}{dx}\right)_A$	$1.00\,\frac{V}{h}$	$1.25\,\frac{V}{h}$	$1.66\,\frac{V}{h}$	$2.16\,\frac{V}{h}$	$2.79\,\frac{V}{h}$	$3.38\,\frac{V}{h}$

The effective shear rate

$$\left(\frac{dv}{dx}\right)_A$$

in the screw at zero discharge was determined experimentally from the zero discharge pressure in the following manner: Since the clearance has a marked effect on the measurement of pressures developed by rubberlike substances, a technique was used which often succeeds in experimental determinations of this kind. Using the zero discharge-pressure data given in Fig. 7, the viscosity μ_A was calculated from Equations [1], [3], [5] and ignoring the clearance C in the calculations. From these calculated viscosities the corresponding shear rates

$$\left(\frac{dv}{dx}\right)_A$$

were found by referring to Fig. 8. From the speed of rotation of the screw and the height of the thread h, the ratio V/h was easily calculated. The ratio

$$\left(\frac{dv}{dx}\right)_A \Big/ \frac{V}{h}$$

was then plotted versus the clearance and the curves extrapolated to zero clearance. This plot is shown in Fig. 10. At zero

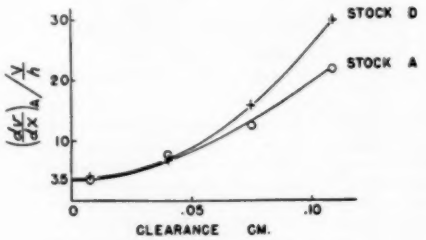

FIG. 10 $\left(\frac{dv}{dx}\right)_A \Big/ \frac{V}{h}$ VERSUS CLEARANCE

clearance the extrapolated curves for both stocks indicate

$$\left(\frac{dv}{dx}\right)_A \Big/ \frac{V}{h}$$

is approximately 3.5, which is close to the theoretical figure of 3.38 for wide threads at zero discharge. One would expect the observed figure to be slightly greater than the theoretical one due to the additional shearing caused by the presence of the threads. Thus the value of effective shearing rate agrees fairly well with the theoretical one for zero discharge.

A series of experiments were carried out to determine the effect of changing the length of the screw on the zero discharge pressure. This was done by shortening the length of a screw successively and measuring the zero discharge pressure for several of the stocks. The results are shown graphically in Fig. 11. As predicted by Equations [1], [3], [5] the zero discharge pressures were found to be directly proportional to the length of the screw. The fact that the zero discharge pressure is directly proportional to the length of the screw is a further indication that at zero discharge the mechanism for rubberlike materials is one of viscous shearing.

Now that a measure of the effective shear rate occurring in the threads of the screw has been worked out, Equations [1], [3], [5] will be applied to closely fitting screws to calculate the zero discharge pressure.

Sample Calculation. Calculate pressure developed at zero discharge by stock C in a closely fitting screw rotating at 10 rpm when the screw has the following dimensions and the temperature is 212 F:

$s = 2.06$ cm	$h = 0.317$ cm	$\lambda = 2.54$ cm
$D = 2.54$ cm	$D_m = 2.22$ cm	$L = 19.0$ cm

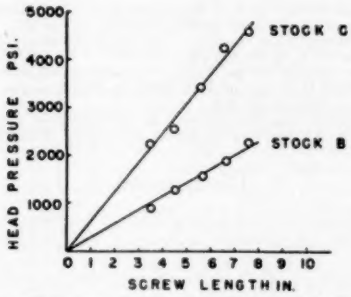

FIG. 11 ZERO DISCHARGE HEAD PRESSURE VERSUS SCREW LENGTH

Open discharge rate:

$$Q = \frac{8s^3\, V \cos\theta}{\pi^3} f\left(\frac{h}{s}\right)$$

At 10 rpm

$$V = \frac{2.54 \times 3.14 \times 10}{60}$$

$$= 1.34 \text{ cm per sec}$$

$h/s = 0.154$, and from Fig. 2, $f(h/s) = 0.28$. Therefore

$$Q = \frac{8(2.06)^3\,(1.34)}{31.0}\,(0.28) = 0.413 \text{ cu cm per sec}$$

The correction $\cos\theta$ is ignored because the helix angle θ is so small that $\cos\theta = 1.00$.

Backward flow through thread:

$$Q_t = \frac{Ps^3h^3}{\mu l_t}\, g(s, h)$$

$$l_t = L\sqrt{1 + \left(\frac{\pi Dm}{\lambda}\right)^2}$$

$$l_t = 19.0\sqrt{1 + \left(\frac{3.14 \times 2.22}{2.54}\right)^2}$$

$$l_t = 55.5 \text{ cm}$$

$s/h = 6.5$, and from Fig. 3

$$g(s, h) = 0.0115$$

Since

$$\left(\frac{dv}{dx}\right)_A$$

was found experimentally to be $3.5\ V/h$, and calculated to be $3.38\ V/h$ for screws with wide threads, let

$$\left(\frac{dv}{dx}\right)_A = 3.5\,\frac{V}{h}$$

$$\left(\frac{dv}{dx}\right)_A = 3.5\left(\frac{1.34}{0.317}\right) = 14.7 \text{ sec}^{-1}$$

Referring to Fig. 8, $\mu_A = 97{,}000$ poises for stock C when

$$\left(\frac{dv}{dx}\right)_A = 14.7 \text{ sec}^{-1}$$

therefore

$$Q_t = \frac{P(2.08)^3\,(0.317)^3}{(55.5)\,(97{,}000)} \times 0.0115 = 9.2 \times 10^{-10}\, P$$

Since $Q = Q_t$ at zero discharge

$$0.412 = \text{P} \times 0.092 \times 10^{-8}$$

$$P = 4.49 \times 10^8 \text{ dynes/cm}^2$$

$$= 4.49 \times 10^8 \times 145 \times 10^{-7} = 6510 \text{ psi}$$

The observed value of zero discharge pressure with this stock under these conditions was found to be 6700 psi which is very close to the calculated figure.

The zero discharge pressure was measured for four of the stocks listed in Table 1 with three different screws with successively increasing values of the thread spacing s. The temperature was maintained at 212 F, and the screws were as close-fitting as possible. The 1-in. National Rubber Bench Model extrusion unit was used in these determinations. The results are plotted versus screw speed in Figs. 12 and 13. The solid lines represent the calculated pressure and the points the observed pressures. Fig. 12 shows the effect of using different stocks with the same screw, and Fig. 13 shows the effect of using different screws with the same stock. Agreement between the calculated curves and the determined curves is close enough to verify the method of calculation and to make possible the estimation of the zero discharge pressure for rubberlike materials. The calculated curves in Figs. 12 and 13 necessarily include the cumulative error of the various measurements upon which the calculations are based, particularly the viscosity determinations. The observed pres-

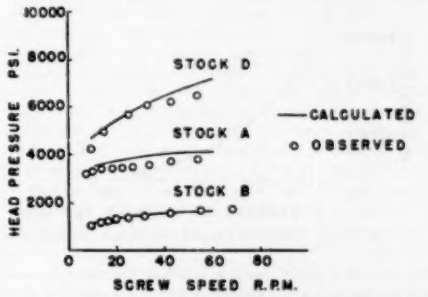

FIG. 12 ZERO DISCHARGE HEAD PRESSURE VERSUS SCREW SPEED

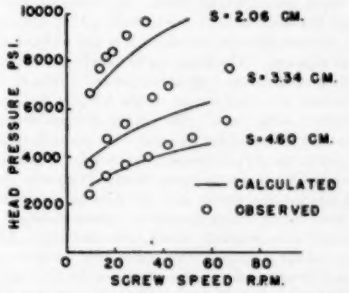

FIG. 13 ZERO DISCHARGE HEAD PRESSURE VERSUS SCREW SPEED

sures decreased varying amounts as a function of time due to heat generation within the stocks. This effect was more pronounced with the tougher stocks than with the softer stocks.

The most striking result of this investigation is that the zero discharge pressure for rubberlike materials is not directly proportional to the rotational speed of the screw.

Pressure-Discharge Relation for Rubberlike Materials

The pressure-discharge rate relation for rubberlike materials is not a simple inverse linear one as in the case of Newtonian liquids, but is markedly curved. This makes the estimation of pressure for intermediate values of discharge rate difficult. The pressure-discharge rate relation for stock E was determined by successively closing the discharge port. The pressures were thus measured for discharge rates ranging from open discharge to zero discharge. This plot is shown in Fig. 14.

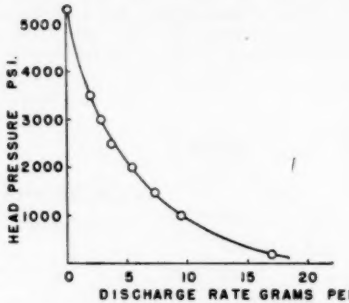

Fig. 14 Head Pressure Versus Discharge for Stock E

The reasons for this characteristic and the changes occurring in the mechanism as the discharge port is successively closed as visualized by the author will now be given.

At open discharge, the inefficiency of strip feeding results in the threads being incompletely filled. In addition, the pressure throughout the stock in the screw threads is low, and there is not sufficient traction between the stock and the walls of the sleeve to prevent slippage. The stock tends merely to rotate with the screw and forward motion is greatly retarded. At open discharge the mechanism is largely one of sliding friction, little or no viscous shearing taking place. The results of open discharge-rate determinations discussed earlier agree with this conception.

As the discharge port is successively closed, the pressure in the forward end of the screw increases enough to prevent slippage of the stock against the sleeve, and the mechanism in this region changes from one of sliding friction to viscous shearing. As the discharge port is successively closed, more and more of the stock undergoes viscous shearing. One could even imagine a point of demarcation between the region of sliding friction and viscous shearing which moves back toward the feed port as the discharge port is closed until at zero discharge all of the stock in the screw threads, with the possible exception of the stock in the immediate region of the feed port, is undergoing viscous shearing.

BIBLIOGRAPHY

1 "Screw Viscosity Pumps," by H. S. Rowell and D. Finlayson, *Engineering*, vol. 114, November 17, 1922, pp. 606–607.

2 "Screw Viscosity Pumps," by H. S. Rowell and D. Finlayson, *Engineering*, vol. 126, August 31, 1928, pp. 249–250 and 385–387.

3 "Mechanical Principles of the Screw Extrusion Machine," by Z. Rogowsky, The Institution of Mechanical Engineers, London, England, advance copy, March 19, 1945.

4 "Memoire sur l'influence des frottenments dans les mouvements reguliers des fluides," by M. J. Boussinesq, *Journal des Mathematiques Pures et Appliquees*, vol. 13, series 2, juillet 27, 1868, p. 377.

5 "A Monograph of Viscometry," by Guy Barr, Oxford University Press, New York, N. Y., 1931, pp. 145–146.

6 "Properties of Several Types of Unvulcanised Rubber Stocks at High Rates of Shear," by J. H. Dillon and N. Johnston, *Physics*, vol. 4, June, 1933, pp. 225–235.

7 "Shearing Disc Plastometer," by Melvin Mooney, *Industrial and Engineering Chemistry*, Analytical Edition, vol. 6, March, 1934, p. 147.

Discussion

G. J. Dienes.[8] It is gratifying to see the increasing interest in such fabrication processes as extrusion from a fundamental viewpoint. From the material standpoint, the rheological properties of thixotropic[4] and viscoelastic[5] materials have been investigated recently under conditions of simple extrusion, i.e., flow through a tube under a constant applied driving pressure. The author analyzes successfully another important part of the extrusion process, namely, the mechanism of developing the driving pressure behind the extrusion die. The techniques given in this paper are of general interest, and the writer would like to see a more detailed description of the pressure-measuring devices used, their exact location in the extruder, and specific methods of attachment. The pressure measurement is the heart of the technique and the author's comments on difficulties encountered by others[6] with plugged connecting tubes would be welcome.

It is only natural, at the present state of knowledge, that considerable idealization is apparent in all these studies. In mapping out the characteristics of the extrusion process, at least one important additional factor will have to be studied carefully. This is the slippage of the material along various surfaces in the extruder. It is well known in practice that lubricants have an important influence on the operation of the extruder and on the properties of the extruded material. However, very little fundamental information is available as to the rheological action of lubricants, particularly at high temperatures. It is also likely that, as a result of lubrication, appreciable temperature differentials may develop within the plastic material leading to considerable rheological complexity.

Silvio Eccher.[7] Many of the author's results and conclusions agree well with those obtained by the writer, working on a 5-cm-diam extruder with pure rubber and rubber compounds.

Referring to Fig. 14 of the author's paper, the writer has also obtained a curve convex to the axes for G.R.I.

For other materials (pure or compounded natural rubber and GR-S), the curve pressure-discharge rate has instead an opposite convexity. Has the author also obtained a similar course? The writer has not been able to vary the clearance, and the author's results therefore appear highly interesting.

Our investigation was carried out with three different leads and three heights of the thread on a 5-cm laboratory extruder. A similar investigation was also made with other extruders in our plant.

As a satisfactory relation has been obtained between dimensions of the screws and discharge rates, in connection with rheometrical parameters of the materials, it will be interesting to know the geometrical dimensions of the screw used by the author in the tests illustrated in Figs. 5 and 6.

[8] North American Aviation, Inc., Downey, Calif.

[4] "Calculating Pressure-Flow Relations for Lubricating Greases," by H. W. Wilson and G. H. Smith, *Industrial and Engineering Chemistry*, vol. 41, 1949, pp. 770–776.

[5] "Extrusion Behavior of Viscoelastic Materials," by F. D. Dexter and G. J. Dienes, *Journal of Colloid Science*, vol. 5, 1950, pp. 228–238.

[6] "The Viscous Flow of Molten Polystyrene," by R. S. Spencer and R. E. Dillon, *Journal of Colloid Science*, vol. 4, 1949, pp. 241–255.

[7] Pirelli Company Laboratories, Milano, Italy.

Author's Closure

In answer to Dr. Dienes's inquiry as to the exact techniques used to measure pressures, the following description is given.

Ordinary hydraulic gages were connected to the head of the extruder through forged steel tubing having an internal diameter of at least one-half inch. The relative positions of the various parts were such that the axis of the tube coincided with the extension of the axis of the screw in the barrel. The gage and the tube were filled with oil and a plug made of very soft rubber (ML, 212 F of 20) was inserted into the tube to form a barrier between the oil and the stock in the head of the extruder. It is best to allow the plug to extend out of the tube a little into the head cavity in order to reduce the flow of stock into the tube as much as possible. Care must be taken not to allow the oil to work its way past the plug into the threads of the rotating screw in the extruder barrel because if this happens a false pressure reading will result due to slippage of the stock against the extruder barrel. For this reason a soft-rubber plug at least two inches long should be used. When the extruder is completely filled and there is no air in the system, a maximum pressure reading should result within 10 seconds after the extruder is turned on.

In the cases where the pressures developed by low-viscosity oils were measured at various points along the extruder barrel, 0.030-in-diam holes were drilled through the barrel, and vertical tubes were attached to them which formed manometers. In this way the pressure heads were measured directly in inches of oil. Such a system may take considerable time to come to equilibrium, however; thus any increase in temperature due to mechanical friction of the rotating screw will result in a somewhat diminished pressure reading.

Dr. Eccher has asked for a more detailed description of the screw used to determine the data shown in Figs. 5 and 6.

Using the same nomenclature, the pertinent dimensions are as follows:

s = 0.317 cm (width of thread trough)
h = 0.317 cm (height of thread)
l_1 = 100 cm (uncoiled length of thread)
D = 2.54 cm (major diam of screw)

Specific gravity of oil, 0.87 to 0.88

This screw was double-flighted. This does not change anything, however, if all computations are based on a single flight of thread. Fairly good agreement was observed between the calculated discharge rates per thread and the head pressure. The screw was closely fitted to the sleeve and hence the clearance was ignored in the computations. The observed pressures were all slightly lower than the computed values, presumably due to a decrease in viscosity due to heat generation.

The author finds Dr. Eccher's observations on the shape of the discharge rate - head pressure curve extremely pertinent. From the calculated values of the effective shear rates in the thread trough under different conditions of operation as given in Table 3, it is postulated that all rubberlike materials should give a discharge rate - head pressure curve having a convexity in the opposite direction to that shown in Fig. 14. Table 3 states mathematically that the effective shear rate is not only directly proportional to the screw speed but also increases from its lowest value at open discharge to its highest value at zero discharge for a constant screw speed. The author was unable to observe such a relation with his particular extruder, however. The immediate reaction to Dr. Eccher's comments is that his extruders may have a more effective feed than ours; thus the threads on his extruder would be more nearly full in the region of the feed port. Perhaps the difference in size between our extruders may have something to do with this. Perhaps the direction of the convexity of the discharge rate - head pressure relation would be a good way of measuring the effectiveness of the feed port.

Pressure-Temperature Relations in Gas-Filled (Class III) Thermometers

By E. E. MODES,[1] SKOKIE, ILL.

Fundamental relations are presented for the pressure within the system of a thermometer or thermal system charged with a perfect gas. An expression is developed which gives the approximate pressure in terms of bulb temperature, ambient temperature, and ratio of bulb volume to ambient volume, this being sufficiently accurate if the volume change of the pressure-responsive element is small. An exact equation for the pressure in the system is developed in terms of the temperatures and volumes of bulb, capillary, and pressure-responsive element, and the volume change of the pressure-responsive element, assuming the volume change to be linear with pressure change. From this relation, means are developed for determining the necessary charging pressure to give a specified pressure change when the bulb is varied through a specified temperature span. An example is included in the Appendix in which charging pressure, pressure-temperature curve, and the effect of ambient-temperature changes are computed by means of the exact expressions developed.

GAS-filled pressure-type thermometers and thermal systems operating on the principle of Charles's law are widely used, and are designated by the industry in general as Class III thermometers. It is the purpose of this paper to set forth fundamental relations between the pressure in and temperatures of such a system, considering the volumes of the various sections and the change in volume of the pressure-responsive element with change in pressure.

Basic Relations

Fig. 1 shows such a system schematically: A being the temperature-sensitive bulb which is immersed in the medium whose temperature is being measured, B the connecting capillary tubing, and C the pressure-responsive element in the form of diaphragm, bellows, Bourdon tube, spiral, or helix, the complete system being charged with an inert gas and hermetically sealed. The pressure-responsive element gives a deflection on the scale through the linkage with variations in internal pressure, caused by variations in temperature of the various sections of the system. The capillary tubing and pressure-responsive element are usually at some ambient temperature which differs from the temperature being measured by the bulb, and in the case of a thermometer with a long length of tubing the tube temperature may differ considerably from the element temperature. The bulb and capillary are constructed in such a manner that their volumes remain substantially constant within the pressure range of the system;

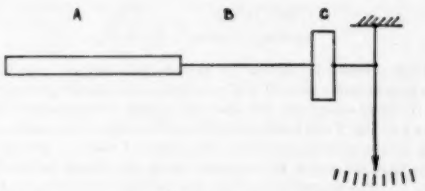

Fig. 1

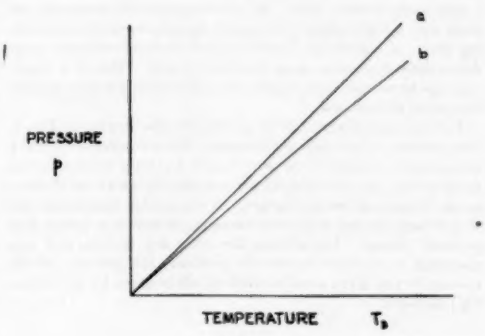

Fig. 2

however, the capillary volume will vary as its length is varied. Since the pressure-responsive element deflects with a pressure change, its volume will be a function of the existing pressure in the system.

For purposes of analysis let us consider a given mass of a perfect gas confined within a chamber of constant volume at absolute pressure P and absolute temperature T. If the temperature of such a system be varied, the internal pressure will vary in accordance with Charles's law as follows

$$p = P \frac{T_B}{T} \quad \ldots\ldots [1]$$

where P is the charging pressure at temperature T, and p is the final pressure at temperature T_B. If pressure be plotted against temperature, the straight line shown at a in Fig. 2 will result, and such a system would have a uniformly graduated scale.

In order to obtain a simplified expression for the pressure within the system shown in Fig. 1, let us assume that the temperature of the capillary B is identical to that of the element C (which is generally true for thermometers with short-length capillaries), and also assume the volume change of the pressure-responsive element with pressure change to be small in comparison to the other volumes in the system. Let the complete system be charged with a perfect gas at absolute pressure P with bulb, capillary, and

---

[1] Development Engineer, Jas. P. Marsh Corporation. Mem. ASME.

Contributed by the Industrial Instruments and Regulators Division and Research Committee on Fluid Meters and presented at the Annual Meeting, New York, N. Y., November 26–December 1, 1950, of The American Society of Mechanical Engineers.

Note: Statements and opinions advanced in papers are to be understood as individual expressions of their authors and not those of the Society. Manuscript received at ASME Headquarters, August 3, 1950. Paper No. 50—A-48.

element at uniform absolute temperature T, and the system sealed. If the temperature of the bulb then be changed to T_B, and the temperature of capillary and element be changed to ambient temperature t, the pressure in the system will be given by

$$p = \frac{P(x+1)}{T\left(\frac{1}{t} + \frac{x}{T_B}\right)} \quad \text{[2]}$$

where

$$x = \frac{\text{bulb volume}}{\text{ambient volume}} = \frac{V_B}{V_C + V_E}$$

If this pressure be plotted for various bulb temperatures with the ambient temperature t held constant at the charging temperature T (as is sometimes the case with actual thermometers) the curve b in Fig. 2 will result considering the origin of co-ordinates to be the charging temperature and pressure T and P. It is to be noted that the curve is no longer linear and drops below the curve a. The magnitude of this nonlinearity depends upon the volume ratio x. By making x sufficiently large the curve can be made linear enough to obtain a reasonable degree of accuracy on a uniformly divided scale. All well-designed thermometers are built with a high volume ratio, some manufacturers recommending 40:1. A high ratio of course means a bulb of relatively large dimensions depending upon capillary length. This is a disadvantage since with some applications there exists a very definite limitation on bulb size.

For an exact analysis of the pressure in the system in Fig. 1, it is necessary to consider the individual temperatures of capillary and pressure-responsive element T_C and T_E, since these may not be identical; also to consider the volume change of the element as its internal pressure changes. A reasonable assumption for this volume change with most elements is that it is linear with pressure change. Considering the foregoing factors, and also assuming a constant barometric pressure, the pressure in the system for any given set of conditions will be given by the following expression

$$p = \sqrt{\left(\frac{V_B T_E}{2KT_B} + \frac{V_C T_E}{2KT_C} + \frac{V_E}{2K}\right)^2 + \frac{T_E P}{K}\left(\frac{V_B + V_C + V_E + KP}{T}\right)} - \left(\frac{V_B T_E}{2KT_B} + \frac{V_C T_E}{2KT_C} + \frac{V_E}{2K}\right) \quad \text{[3]}$$

where P and T are the absolute charging pressure and temperature, V terms are volumes, T terms are absolute temperatures, and the subscripts B, C, E, denote temperatures or volumes of the bulb, capillary, and element respectively; and K is the volume-change constant for the pressure-responsive element, volume change = Kp.

Equation [3] makes it possible to compute the actual pressure in a system in terms of the volumes and temperatures of bulb, capillary, and element, and in terms of the volume change of the element.

Use of Equation [3] will enable the designer to proportion the bulb volume for a given length of capillary to obtain any degree of accuracy on a linearly divided scale, which appears to be superior to past methods of rule of thumb where volume ratios of bulb to ambient were made 40:1 or 20:1, and so forth. The equation is also useful in designing compensators which counteract the effect of ambient-temperature changes about the capillary and element.

Application to Gas-Filled Thermometers

Usual practice with gas-filled thermometers is to employ a system as in Fig. 1, which requires a given pressure change (adjustable by several per cent by means of an adjustable-length link) to cause the pointer to move over full scale. This system may then be used for a variety of temperature ranges by varying the charging pressure P so that the required pressure change is obtained when the bulb is taken from minimum to maximum scale temperature. In order to determine this necessary charging pressure it is convenient to determine the system pressure when the bulb is at the minimum scale temperature by

$$p_1 = \frac{T_1 f[(Kf + V_C + V_E)T_2 + V_B t]}{[(T_2 - T_1)V_B t - 2KfT_1T_2]} \quad \text{[4]}$$

wherein p_1 is the system pressure with bulb at minimum scale temperature T_1 which will result in the required pressure change f when the bulb is taken to the maximum scale temperature T_2, assuming element and capillary to be held at constant ambient temperature t.

With the initial pressure p_1 thus determined, it is now possible to compute the necessary charging pressure P when the complete system is held at uniform charging temperature T. It is generally most convenient to charge at ambient temperature t, and charging pressure under these conditions is given by

$$P = \sqrt{\left(\frac{V_B + V_C + V_E}{2K}\right)^2 + \frac{tp_1}{K}\left(\frac{V_B}{T_1} + \frac{V_C}{t} + \frac{V_E}{t} + \frac{Kp_1}{t}\right)} - \left(\frac{V_B + V_C + V_E}{2K}\right) \quad \text{[5]}$$

With P and T determined, it becomes possible to calculate by means of Equation [3] the pressure in the system under any conditions of bulb, capillary, and element temperatures, if it is desired to charge the system at nonuniform temperature.

Appendix

Nomenclature

The following nomenclature is used in the Appendix:

- B = characteristic gas equation constant[1]
- f = pressure change for full-scale pointer deflection
- K = element volume change per unit pressure change
- M = total mass of gas in complete system
- M_B = mass of gas in bulb
- M_C = mass of gas in capillary
- M_E = mass of gas in element
- P = absolute charging pressure
- p = absolute pressure in system
- p_1 = absolute pressure when $T_B = T_1$ and $T_C = T_E = t$
- t = absolute ambient temperature (capillary and element)
- T = absolute charging temperature (complete system)

[1] "Principles of Thermodynamics," by G. A. Goodenough, third edition, Henry Holt and Company, New York, N. Y., 1932, p. 33.

T_1 = absolute minimum scale temperature
T_2 = absolute maximum scale temperature
T_B = absolute bulb temperature
T_C = absolute capillary temperature
T_E = absolute element temperature
V_B = bulb volume
V_C = capillary volume
V_E = element volume at zero pressure absolute
x = ratio, bulb to ambient volume = $\dfrac{V_B}{V_C + V_E}$

Referring to Fig. 1, when the system is charged the characteristic gas equation gives

$$M = \frac{P(V_B + V_C + V_E + KP)}{BT} \quad \ldots\ldots [6]$$

When bulb is at T_B and capillary and element are at ambient t

$$M_B = \frac{pV_B}{BT_B} \quad \ldots\ldots [7]$$

$$M - M_B = \frac{p(V_C + V_E + Kp)}{Bt} \quad \ldots\ldots [8]$$

By definition

$$V_B = x(V_C + V_E) \quad \ldots\ldots [9]$$

Equations [6], [7], and [9] in Equation [8] and by assumption $K = 0$ gives

$$p = \frac{P(x+1)}{T\left(\dfrac{1}{t} + \dfrac{x}{T_B}\right)} \quad \ldots\ldots [2]$$

To derive Equation [3], applying the characteristic gas equation to the element

$$M_E = \frac{p(V_E + Kp)}{BT_E} \quad \ldots\ldots [10]$$

To the capillary

$$M_C = \frac{pV_C}{BT_C} \quad \ldots\ldots [11]$$

$$M = M_B + M_C + M_E \quad \ldots\ldots [12]$$

Equations [6], [7], [10], and [11] in Equation [12] gives

$$\frac{Kp^2}{T_E} + \left(\frac{V_B}{T_B} + \frac{V_C}{T_C} + \frac{V_E}{T_E}\right)p - \frac{(V_B + V_C + V_E + KP)P}{T} = 0 \quad \ldots\ldots [13]$$

Applying the quadratic form

$$p = \frac{-\left(\dfrac{V_B}{T_B} + \dfrac{V_C}{T_C} + \dfrac{V_E}{T_E}\right) \pm \sqrt{\left(\dfrac{V_B}{T_B} + \dfrac{V_C}{T_C} + \dfrac{V_E}{T_E}\right)^2 + \dfrac{4KP}{T_E}\left(\dfrac{V_B + V_C + V_E + KP}{T}\right)}}{2K/T_E} \quad \ldots [14]$$

Considering the numerator of the right-hand member only, the term under the radical will always be greater than the first term in parentheses, and, since the concept of a negative absolute pressure is absurd, the — sign in the ± notation may be neglected giving

$$p = \sqrt{\left(\frac{V_B T_E}{2KT_B} + \frac{V_C T_E}{2KT_C} + \frac{V_E}{2K}\right)^2 + \frac{T_E P}{K}\left(\frac{V_B + V_C + V_E + KP}{T}\right)} - \left(\frac{V_B T_E}{2KT_B} + \frac{V_C T_E}{2KT_C} + \frac{V_E}{2K}\right) \quad \ldots [3]$$

To develop Equation [4] consider the bulb to be at the minimum scale temperature T_1 and capillary and element to be at ambient temperature t. Substituting these values in Equation [13] gives

$$\frac{Kp_1^2}{t} + \left(\frac{V_B}{T_1} + \frac{V_C}{t} + \frac{V_E}{t}\right)p_1 - \frac{(V_B + V_C + V_E + KP)P}{T} = 0 \quad \ldots\ldots [15]$$

When bulb is taken to maximum scale temperature Equation [13] gives

$$\frac{K(p_1 + f)^2}{t} + \left(\frac{V_B}{T_2} + \frac{V_C}{t} + \frac{V_E}{t}\right)(p_1 + f) - \frac{(V_B + V_C + V_E + KP)P}{T} = 0 \quad \ldots\ldots [16]$$

Equating [15] and [16] and solving for p_1 gives

$$p_1 = \frac{T_2 f[(Kf + V_C + V_E)T_2 + V_B t]}{[(T_2 - T_1)V_B t - 2KfT_2T_1]} \quad \ldots\ldots [4]$$

For derivation of Equation [5], consider bulb to be at T_1, capillary and element at t, and charging temperature T to be ambient t. Substituting these values in Equation [13] gives

$$\frac{Kp_1^2}{t} + \left(\frac{V_B}{T_1} + \frac{V_C}{t} + \frac{V_E}{t}\right)p_1 - \frac{(V_B + V_C + V_E + KP)P}{t} = 0 \quad \ldots\ldots [17]$$

Rearranging, applying quadratic form, and reasoning as in solution for Equation [3] gives

$$P = \sqrt{\left(\frac{V_B + V_C + V_E}{2K}\right)^2 + \frac{tp_1}{K}\left(\frac{V_B}{T_1} + \frac{V_C}{t} + \frac{V_E}{t} + \frac{Kp_1}{t}\right)} - \frac{(V_B + V_C + V_E)}{2K} \quad \ldots\ldots [5]$$

Since the constant B has been eliminated in the foregoing expressions, any consistent set of units may be used as long as temperatures and pressures are absolute.

Example

A sample computation on a system whose physical characteristics approximate those in actual use follows, for the purpose of demonstrating the use of the expressions which have been developed.

Since small differences of large quantities are involved in the

use of the equations, it is necessary that a table of logarithms to seven places or a calculating machine be used to obtain significant results.

Consider a thermometer having a scale range of 0 to 500 F, the pressure-responsive element and linkage of which require a pressure change of 100 psi to move the pointer through full scale deflection. Maximum allowable pressure in element is 500 psig; bulb volume 5.0 cu in., capillary 0.1 cu in., element 0.2 cu in., and volume change of element 0.0002 cu in. per lb per sq in. Normal ambient temperature 70 F. This gives

$$f = 100 \qquad T_2 = 959.7$$
$$K = 0.0002 \qquad V_B = 5.0$$
$$t = 529.7 \qquad V_C = 0.1$$
$$T_1 = 459.7 \qquad V_E = 0.2$$

Substituting these values in Equation [4] gives

$$p_1 = \frac{459.7 \times 100[(0.0002 \times 100 + 0.1 + 0.2)959.7 + 5.0 \times 529.7]}{[(959.7 - 459.7)5.0 \times 529.7 - 2 \times 0.0002 \times 100 \times 959.7 \times 459.7]} = 103.99 \text{ psia}$$

which is the necessary pressure with bulb at 0 F, and capillary and element at 70 F to give a pressure change of 100 psi when bulb only is taken to 500 F. Note also that the pressure at 500 F bulb is within the maximum allowable limit for the element. Substituting the foregoing value of p_1 in Equation [5] gives

$$P = \sqrt{\left(\frac{5.0 + 0.1 + 0.2}{2 \times 0.0002}\right)^2 + \frac{529.7 \times 103.99}{0.0002}\left(\frac{5.0}{459.7} + \frac{0.1}{529.7} + \frac{0.2}{529.7} + \frac{0.0002 \times 103.99}{529.7}\right)} - \left(\frac{5.0 + 0.1 + 0.2}{2 \times 0.0002}\right)$$

$$P = 118.80 \text{ psia}$$

This is the necessary charging pressure with the complete system held at 70 F to give the required 100 psi pressure change when the bulb is taken through full-scale temperature change.

With the charging pressure P and temperature T determined, it becomes possible to calculate the pressure in the system under any temperature condition of bulb, capillary, and element by means of Equation [3]. The p-T_B curve is computed in the following, for 100 per cent, 75 per cent, 50 per cent, and 25 per cent of full-scale bulb temperature with T_C and T_E held constant at 70 F.

100 per cent scale bulb temperature, $T_B = 959.7$

$$p = \sqrt{\left(\frac{5.0 \times 529.7}{2 \times 0.0002 \times 959.7} + \frac{0.1 \times 529.7}{2 \times 0.0002 \times 529.7} + \frac{0.2}{2 \times 0.0002}\right)^2 + \frac{529.7 \times 118.80}{0.0002}\left(\frac{5.0 + 0.1 + 0.2 + 0.0002 \times 118.80}{529.7}\right)} - \left(\frac{5.0 \times 529.7}{2 \times 0.0002 \times 959.7} + \frac{0.1 \times 529.7}{2 \times 0.0002 \times 529.7} + \frac{0.2}{2 \times 0.0002}\right) = 203.98 \text{ psia}$$

The foregoing affords a check on the figures for p_1 and P, since $f = 203.98 - 103.99 = 99.99$ psi, which is within the accuracy of the computation, and within 0.01 per cent, of the original specified value of 100 psi.

75 per cent scale bulb temperature, $T_B = 834.7$

$$p = \sqrt{\left(\frac{5.0 \times 529.7}{2 \times 0.0002 \times 834.7} + \frac{0.1 \times 529.7}{2 \times 0.0002 \times 529.7} + \frac{0.2}{2 \times 0.0002}\right)^2 + \frac{529.7 \times 118.80}{0.0002}\left(\frac{5.0 + 0.1 + 0.2 + 0.0002 \times 118.80}{529.7}\right)} - \left(\frac{5.0 \times 529.7}{2 \times 0.0002 \times 834.7} + \frac{0.1 \times 529.7}{2 \times 0.0002 \times 529.7} + \frac{0.2}{2 \times 0.0002}\right) = 180.24 \text{ psia}$$

50 per cent scale bulb temperature, $T_B = 709.7$

$$p = \sqrt{\left(\frac{5.0 \times 529.7}{2 \times 0.0002 \times 709.7} + \frac{0.1 \times 529.7}{2 \times 0.0002 \times 529.7} + \frac{0.2}{2 \times 0.0002}\right)^2 + \frac{529.7 \times 118.80}{0.0002}\left(\frac{5.0 + 0.1 + 0.2 + 0.0002 \times 118.80}{529.7}\right)} - \left(\frac{5.0 \times 529.7}{2 \times 0.0002 \times 709.7} + \frac{0.1 \times 529.7}{2 \times 0.0002 \times 529.7} + \frac{0.2}{2 \times 0.0002}\right) = 155.66 \text{ psia}$$

25 per cent scale bulb temperature, $T_B = 584.7$

$$p = \sqrt{\left(\frac{5.0 \times 529.7}{2 \times 0.0002 \times 584.7} + \frac{0.1 \times 529.7}{2 \times 0.0002 \times 529.7} + \frac{0.2}{2 \times 0.0002}\right)^2 + \frac{529.7 \times 118.80}{0.0002}\left(\frac{5.0 + 0.1 + 0.2 + 0.0002 \times 118.80}{529.7}\right)} - \left(\frac{5.0 \times 529.7}{2 \times 0.0002 \times 584.7} + \frac{0.1 \times 529.7}{2 \times 0.0002 \times 529.7} + \frac{0.2}{2 \times 0.0002}\right) = 130.25 \text{ psia}$$

The foregoing values of pressure are given in Table 1, together with pressures corresponding to a linear curve through the minimum and maximum pressure, and the deviation of the actual from the linear value expressed in per cent of full-scale pressure change.

TABLE 1 VALUES OF PRESSURE AND OTHER DATA

T_B deg F	p psi	p (linear), psi	Deviation, per cent
0	103.99	103.99	0
125	130.25	128.99	+1.26
250	155.66	153.99	+1.67
375	180.24	178.99	+1.25
500	203.99	203.99	0

Customary practice is to set the instrument for zero error at mid-scale by means of a zero adjustment in the linkage, which would result in a —1.67 per cent error at maximum and minimum temperatures. This error can also be evenly divided at mid-scale and maximum and minimum points, which would result in a +0.84 per cent error at 250 F and a —0.84 per cent error at 0 and 500 F. The nonlinearity of the pressure-temperature curve can of course be reduced by increasing the bulb volume.

Equation [3] will now be used to determine the effect of ambient-temperature fluctuation. Consider the bulb to be at mid-scale 250 F with the element at 70 F, and assume the temperature of capillary to be increased to 120 F, $T_C = 579.7$

$$p = \sqrt{\left(\frac{5.0 \times 529.7}{2 \times 0.0002 \times 709.7} + \frac{0.1 \times 529.7}{2 \times 0.0002 \times 579.7} + \frac{0.2}{2 \times 0.0002}\right)^2 + \frac{529.7 \times 118.80}{0.0002}\left(\frac{5.0 + 0.1 + 0.2 + 0.0002 \times 118.80}{529.7}\right)} - \left(\frac{5.0 \times 529.7}{2 \times 0.0002 \times 709.7} + \frac{0.1 \times 529.7}{2 \times 0.0002 \times 579.7} + \frac{0.2}{2 \times 0.0002}\right) = 155.99 \text{ psia}$$

If temperature of element is increased to 120 F with capillary at 70 F, and bulb at 250 F, $T_E = 579.7$

$$p = \sqrt{\left(\frac{5.0 \times 579.7}{2 \times 0.0002 \times 709.7} + \frac{0.1 \times 579.7}{2 \times 0.0002 \times 529.7} + \frac{0.2}{2 \times 0.0002}\right)^2 + \frac{579.7 \times 118.80}{0.0002}\left(\frac{5.0 + 0.1 + 0.2 + 0.0002 \times 118.80}{529.7}\right)} - \left(\frac{5.0 \times 579.7}{2 \times 0.0002 \times 709.7} + \frac{0.1 \times 579.7}{2 \times 0.0002 \times 529.7} + \frac{0.2}{2 \times 0.0002}\right) = 156.42 \text{ psia}$$

TABLE 2 TEMPERATURES, PRESSURE, AND PER CENT ERROR

T_B, deg F	T_C, deg F	T_E, deg F	p, psi	Error, per cent
250	70	70	155.66	0
250	120	70	155.99	+0.33
250	70	120	156.42	+0.76

These values are given in Table 2, together with the error in per cent of full-scale pressure change when both capillary and element are at 70 F.

Discussion

W. I. Caldwell.[3] Another rather interesting solution of the author's equations leading to Equation [3] is possible. For convenience let

$$\eta = (V_c + V_E + KP)/V_B$$

$$\phi = \frac{T_B}{V_B}\left(\frac{V_c}{T_c} + \frac{V_E}{T_E}\right)$$

$$\alpha = \frac{PKT_B^2}{V_B T T_E}(1 + \eta)$$

[3] Director of Research, Taylor Instrument Companies, Rochester, N. Y.

Rearranging Equation [13] of the paper and introducing η and ϕ

$$\frac{PT_B}{T}(1 + \eta)\frac{1}{p^2} - (1 + \phi)\frac{1}{p} - \frac{K}{V_B}\frac{T_B}{T_E} = 0 \quad \ldots\ldots [18]$$

Solving for $1/p$ and inverting

$$p = \frac{PT_B}{T}\frac{1 + \eta}{\frac{1}{2}(1 + \phi) + \frac{1}{2}\sqrt{(1 + \phi)^2 + 4\alpha}} \quad \ldots\ldots [19]$$

where only the + sign has physical significance. Equation [19] is convenient to use when the value of K approaches zero. When $K = 0$

$$p = \frac{PT_B}{T}\frac{1 + 1/x}{1 + \phi}.$$

If in addition $T_c = T_E = t$

$$p = \frac{PT_B}{T}\frac{1 + 1/x}{1 + T_B/tx}$$

which is another form of the author's Equation [2].

Applying the approximation $\sqrt{1 + \epsilon} = 1 + \epsilon/2$ to the quadratic term in Equation [19], herewith, and rearranging

(Discussion continued with Equation [20] below)

$$p = \frac{PT_B}{T}\frac{(1 + \eta)}{1 + \phi + \alpha} \quad \ldots\ldots [20]$$

Using this approximation

$$\frac{\partial p}{\partial T_c} = \frac{P}{T}\frac{T_B^2}{T_c^2}\frac{V_c}{V_B}\frac{(1 + \eta)}{[1 + \phi + \alpha]^2}$$

Neglecting α, ϕ, and η

$$\frac{1}{f}\frac{\partial p}{\partial T_c} = \frac{P}{Tf}\frac{T_B^2}{T_c^2}\frac{V_c}{V_B} \quad \ldots\ldots [21]$$

Similarly

$$\frac{1}{f}\frac{\partial p}{\partial T_E} = \frac{P}{Tf}\frac{T_B^2}{T_E^2}\frac{V_E}{V_B}\left(1 + \frac{PKT_B}{V_B T}\right) \quad \ldots\ldots [22]$$

Equations [21] and [22] permit an easy approximation of the ambient-temperature errors of the capillary and element. Using the author's examples, one obtains

$$\frac{1}{f}\frac{\partial p}{\partial T_c}50 = 0.0034 \text{ or } 0.34 \text{ per cent}$$

$$\frac{1}{f}\frac{\partial p}{\partial T_E}50 = 0.78 \text{ per cent}$$

The author's values were 0.33 and 0.76 per cent.

To check the ambient errors of a proposed design prior to finding the filling pressure P, one can use the following approximation

$$\frac{f}{T_2 - T_1} = \frac{P}{T}$$

If this substitution is made in Equations [21] and [22] one finds for the author's example

$$\frac{1}{f}\frac{\partial p}{\partial T_a} 50 = 0.30 \text{ per cent}$$

and

$$\frac{1}{f}\frac{\partial p}{\partial T_g} 50 = 0.68 \text{ per cent}$$

While these approximations are not as good, they would provide a useful guide in the early stages of design.

Author's Closure

Mr. Caldwell's discussion represents a valuable addition to the paper in that his approximations are readily made by means of a slide rule for a tentative design before obtaining the tediously computed exact values by means of the author's expressions.

In order to avoid any possibility of confusing the reader, it is probably worth mentioning that the approximation used by Mr. Caldwell in obtaining Equation [20] has been applied twice in its general form $(1 + \epsilon)^m = 1 + m\epsilon$.

It is the author's hope that this preliminary work on the problem will stimulate interest in further analysis. Specifically, an expression for bulb volume, for a system with given physical characteristics, in terms of the maximum allowable error and ambient-temperature variation would be extremely useful.

Contributions of others are acknowledged by the author, with thanks to those who submitted written and verbal discussion, to the Theory Committee, IIRD of the ASME, in particular Mr. N. B. Nichols for valuable suggestions, and also to Jas. P. Marsh Corporation for co-operation in presentation of this paper.

The Pitot-Venturi Flow Element

By H. W. STOLL,[1] ROCHESTER, N. Y.

The Pitot-Venturi flow element is a velocity-measuring device having found wide use as an air-speed indicator, particularly during World War I. A considerable number of design changes have been made since, and this paper treats a specific form of the element and discusses the effect which the various components used in its assembly have on its calibration. Flow equations are developed and the method of determining the element's coefficient and exponent is described. The paper concludes with suggested methods of installation and an analysis of its position in the flow-measurement field.

Nomenclature

The following nomenclature is used in the paper:

- V = velocity in feet per second at flowing conditions
- K_{pv} = Pitot-Venturi flow coefficient (adapted form)
- H = differential pressure expressed in feet of flowing fluid
- h = differential pressure in inches of water
- n = differential pressure exponent established by test
- A = area, sq in.
- T = absolute temperature (deg F +460)
- t = temperature, deg F
- P = absolute pressure, psia
- G = specific gravity of gas at standard conditions (air = 1)
- g_l = specific gravity of liquid at base 60 F (water = 1)
- g_f = specific gravity of liquid at flow conditions (water = 1)
- D = inside pipe diameter, in.
- B = proportionality constant

Introduction

The Pitot-Venturi flow element as a velocity-measuring device has been well introduced in earlier literature complete with photographs, drawings, and performance data. This paper therefore will restrict its treatment of this element to a specific form being currently furnished and will emphasize particularly its design characteristics, factors influencing its coefficient, the development of its flow equations, installation considerations, and its place in the flow-measurement field.

As is known, one of the fundamental and simplest devices to measure fluid velocity in use today is the Pitot tube. However, a basic limitation of this element is the relatively small differential pressure which it develops and thus requires measuring instruments which have a high amplifying ability. There are numerous design and performance complications associated with instruments which must measure small variables, and hence any logical step which reduces the burden of the measurement can be viewed as a worth-while effort. The Pitot-Venturi flow element fits in with this approach for it develops differential pressures which vary from 5 to 10 times that developed by a Pitot tube over a velocity range of 25 fps to 90 fps.

[1] Taylor Instrument Companies.

Contributed by the Instruments and Regulators Division and Research Committee on Fluid Meters and presented at the Annual Meeting, New York, N. Y., November 26–December 1, 1950, of The American Society of Mechanical Engineers.

Note: Statements and opinions advanced in papers are to be understood as individual expressions of their authors and not those of the Society. Manuscript received at ASME Headquarters August 16, 1950. Paper No. 50—A-46.

Design Characteristics

Fig. 1 shows the element, and Fig. 2 is a cross-sectional drawing of it. Referring to Fig. 2, it is seen that it consists of two concentric Venturis arranged so that their openings lie in the same plane, the exit cone of the inner Venturi terminating in the throat section of the outer Venturi. The inner Venturi is held in place by a tube welded to its body and connecting to a chamber which terminates in a slit located in the throat. The mast support is welded to the outside surface of the outer Venturi and located so the tube from the inner Venturi passes through its center. The velocity impact hole is drilled into this mast-supporting piece at a point facing directly upstream. It is of relatively large diameter to minimize plugging.

The $^1/_4$-in. pipe which screws into the mast support serves as

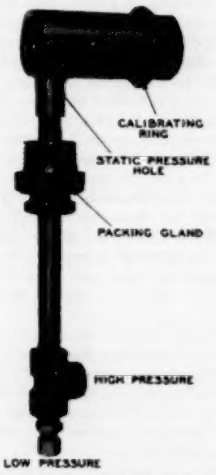

Fig. 1 Pitot-Venturi Flow Element

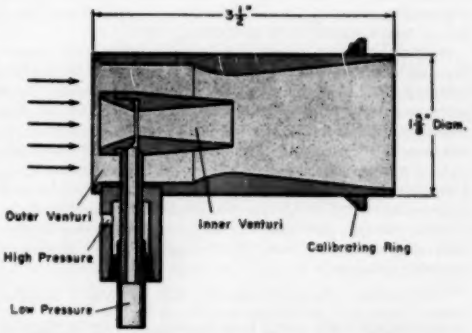

Fig. 2 Cross Section of Pitot-Venturi Flow Element

the mechanical support of the element and also conducts the static pressure to a tee where it ultimately connects to the upstream tap of a differential pressure instrument. The low-pressure line, which is the tube leading from the inner Venturi, passes through the center of this supporting pipe and terminates at the end of the mast so that it can be connected to the low-pressure tap of the differential pressure instrument. Concentric with the outer surface of the flow element and adjacent to it is a calibrating ring. Its function is to influence the relationship between velocity and differential pressure to the extent that a predetermined coefficient can be obtained.

In operation, fluid passing through the element enters the inner Venturi and also the area between the two Venturi tubes. Because of the relatively high forward velocity which occurs in the Venturi throat, additional fluid is made to pass through the inner Venturi due to fluid impact since its exit cone terminates in the throat of the outer Venturi.

Design Factors Influencing Pitot-Venturi's Coefficient

It is apparent that almost any change in internal dimensions or angles would exercise influences of varying degree on the Pitot-Venturi's coefficient. A primary requirement, however, is to select a design which will produce the greatest differential pressure and still keep within design proportions appropriate for this type of element. Experience has well proved the efficiency of current Venturi design, and hence the approach and exit-cone angles conform to present standard practice. On the other hand, recovery cone lengths (particularly the outside Venturi) have been shortened to permit the design of a more compact form.

The differential which is developed across a Venturi tube depends directly on the square of the flow through it and inversely on the fourth power of the throat diameter. With this being the case, it is clear that the throat dimensions both in the inner Venturi and the outer Venturi are highly critical. Also, since the "boosting" effect depends appreciably on the quantity of fluid passing between the inner and outer Venturis, the cross-sectional area ratio of these two components is of great importance.

Various compromises are necessary from a manufacturing standpoint, some of which reduce the over-all differential multiplying action of the element. For example, a greater annular area between the two Venturis at the approach would be desirable, but this would add unwarranted complication to the manufacture of the inner Venturi throat piece. The designed goal was a multiplying action of 10 compared to a Pitot tube alone with a velocity of 5000 fpm of air flowing at 14.70 psia and 70 F. From a report of the National Advisory Committee for Aeronautics,[2] it is seen that the Badin double Venturi, which has the greatest multiplying action of the six different models discussed, has a gain of approximately 11 at this velocity.

Multiplying action ranges from 5 to 8 at 5000 fpm in production models, and to bring the action up to a factor of 10, the calibrating ring is used. Observing its cross section, it is seen that it produces an outward swirl immediately downstream from it, and associated with this action is a momentary drop in pressure at the exit area of the element. The magnitude of this pressure decrease is a function of the ring's location on the element, and Fig. 3 illustrates the effect graphically. Because of this pronounced influence on the differential pressure produced, calibration can be obtained readily, and the importance of maintaining a high order of accuracy of various dimensions within the element is somewhat reduced.

[2] "The Altitude Effect on Air Speed Indicators," Part I, National Advisory Committee for Aeronautics, Report No. 110.
"The Altitude Effect on Air Speed Indicators," Part II, National Advisory Committee for Aeronautics, Report No. 156.

Any disturbance to the symmetry of the velocity wave front at the pressure-measuring slit located in the throat of the inner Venturi tends to decrease the multiplying action of the element. It is important therefore that the slit width be held to close tolerances. The effect of slit width on the performance of the Pitot-Venturi is shown in Fig. 4.

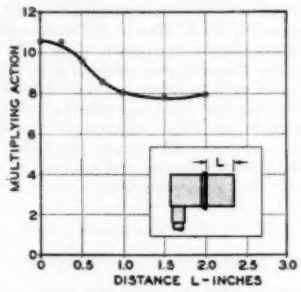

Fig. 3 Calibrating Ring Positions Versus Multiplying Action of Pitot-Venturi Flow Element

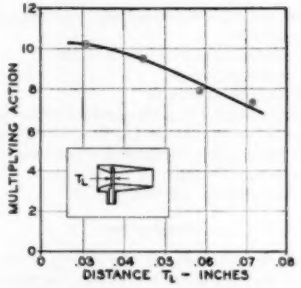

Fig. 4 Pressure-Slit Width Versus Multiplying Action of Pitot-Venturi Flow Element

For all practical purposes, it can be assumed that at any fixed velocity the quantity of flow material passing through the Pitot-Venturi remains unchanged when the inner throat diameter is varied slightly. As pointed out earlier, differential pressure and throat diameter bear a fourth-power relationship under fixed flow conditions, and hence the multiplying action of the Pitot-Venturi is similarly affected by any change in this dimension. Fig. 5 shows the magnitude of the loss in multiplying action as the bore is increased from its designed dimension.

Development of Pitot-Venturi Flow Equations

The constant-energy concept used in the determination of the relationship between velocity and differential applies also to the Pitot-Venturi flow element. However, as was found in earlier research, the multiplying action of the element is not constant, and the effect manifests itself as a variable coefficient. Fig. 6 illustrates how this action varies with velocity. Points have been included so that their distribution can be observed. The data have been obtained from a National Bureau of Standard's report dated February 10, 1950.

Plotting velocity against differential under constant density conditions on log-log paper, a straight line results which means that the equation can have the form

$$V = B(H)^n \quad [1]$$

This procedure of determining the flow equation is simple and straightforward. The exponent n is the slope of the line, and B can be found through direct substitution of test values. Other methods which utilize the constant-energy idea ultimately point to this solution, but there are a considerable number of assumptions which have to be made and hence still require actual flow tests. Equation [1] is applicable for any one given test

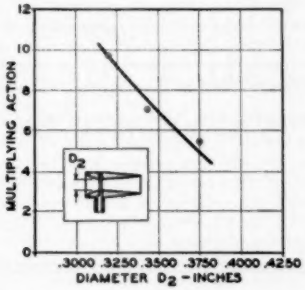

FIG. 5 THROAT DIAMETER VERSUS MULTIPLYING ACTION OF PITOT-VENTURI FLOW ELEMENT

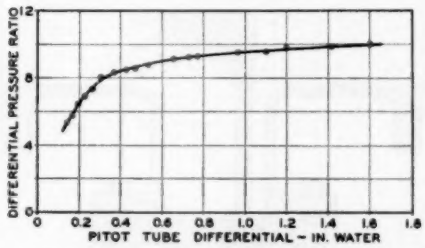

FIG. 6 RATIO OF PITOT-VENTURI DIFFERENTIAL TO PITOT-TUBE DIFFERENTIAL

condition. Converting it to a form which shows the influence of variables associated with installations, there is obtained

(*a*) For gas-velocity measurement

$$V_g = K_{pv}\left(\frac{123.7\,T\,h}{G\,P}\right)^n \text{ fps} \quad [2]$$

(*b*) For liquid-velocity measurement

$$V_L = K_{pv}\left(\frac{5.362\,h}{\theta_f}\right)^n \text{ fps} \quad [3]$$

The flow coefficient K_{pv} appearing in Equations [2] and [3] is characteristic of the Pitot-Venturi as an assembled unit. When n equals 0.500, K_{pv} is a pure number. On the other hand, when n equals some value other than 0.500, then K_{pv} is influenced by the nature of the material flowing through it. The magnitude of the effect depends on the difference between 0.500 and n.

With the Pitot-Venturi flow element located at the average velocity position, the differential reading can then be interpreted in terms of volumetric units. The flow rates given are expressed either in standard cubic feet per hour (SCFH) (14.70 psia and 60 F) or in gallons per minute at 60 F.

Gas flow in a duct having A sq in. area

$$Q_g\,(\text{SCFH}) = 884.3\,K_{pv}\,A\left(\frac{P}{T}\right)^{1-n}\left(\frac{123.7h}{G}\right)^n \quad [4]$$

If duct is circular with diameter D in.

$$Q_g\,(\text{SCFH}) = 694.6\,D^2\,K_{pv}\left(\frac{P}{T}\right)^{1-n}\left(\frac{123.7h}{G}\right)^n \quad [5]$$

Liquid flow through a circular duct of diameter D in. with rate expressed in gallons per minute

$$Q_L\,(\text{GPM at 60 F}) = \frac{2.448\,D^2}{g_t}\,K_{pv}(g_f)^{1-n}\,(5.362h)^n \quad [6]$$

The determination of K_{pv} and n can be accomplished by wind-tunnel tests. The slope of the curve on which there is plotted the log of velocity versus log of differential is n exactly. The procedure currently followed in determining K_{pv} is initially to establish an exact relationship between a Pitot tube of known coefficient and a certified Pitot-Venturi flow element.[3] Using this certified or test Pitot-Venturi element in a wind tunnel together with a Pitot tube located upstream from it, Pitot-tube readings can be taken for a group of predetermined differentials developed by the test Pitot-Venturi unit. The production Pitot-Venturi model can then be substituted for the test model at the same place in the tunnel and the Pitot-tube readings duplicated. Knowing n, as well as the air density, K_{pv} can then be found by substituting values in Equation [2]. Typical values of K_{pv} and n are 0.362 and 0.487, respectively. The importance of knowing n is evident from Fig. 7. Note that the error resulting from using

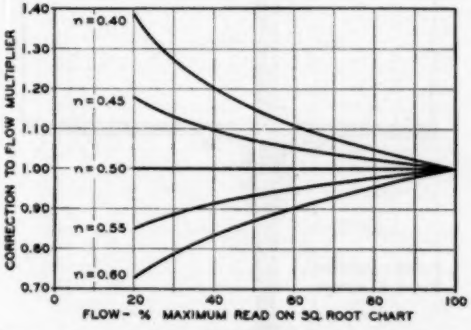

FIG. 7 CORRECTION FACTOR VERSUS DIFFERENTIAL EXPONENT FOR FLOWS READ ON SQUARE-ROOT CHART

a square-root chart increases rapidly with relatively small changes in n. Velocity versus differential-pressure curves for air and water are shown in Figs. 8 and 9, respectively. Points again have been included to show distribution. The air tests were conducted at the National Bureau of Standards' wind tunnel, and the water tests at the Bureau's hydraulic laboratory.

INSTALLATION CONSIDERATIONS

The Pitot-Venturi flow element may be mounted through the side wall of a pipe as shown in Fig. 10. Fig. 11 illustrates the method of installing the element through a 4-in. flange opening. In the event provision must be made to remove the flow element

[3] Certification of test standard was made by the National Bureau of Standards.

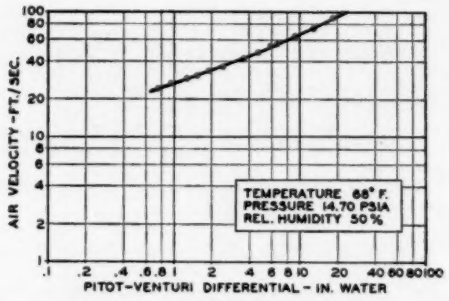

FIG. 8 AIR-VELOCITY VERSUS DIFFERENTIAL-PRESSURE CURVE FOR PITOT-VENTURI

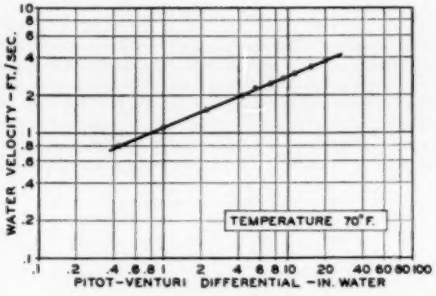

FIG. 9 WATER-VELOCITY VERSUS DIFFERENTIAL-PRESSURE-PRODUCED CURVE FOR PITOT-VENTURI

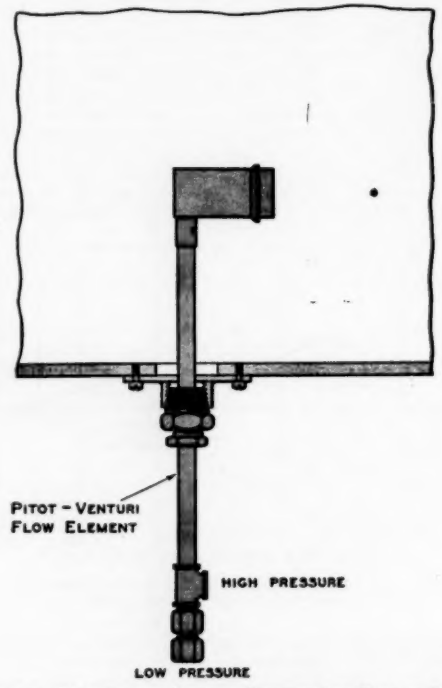

FIG. 10 PITOT-VENTURI MOUNTED THROUGH SIDE WALL OF PIPE

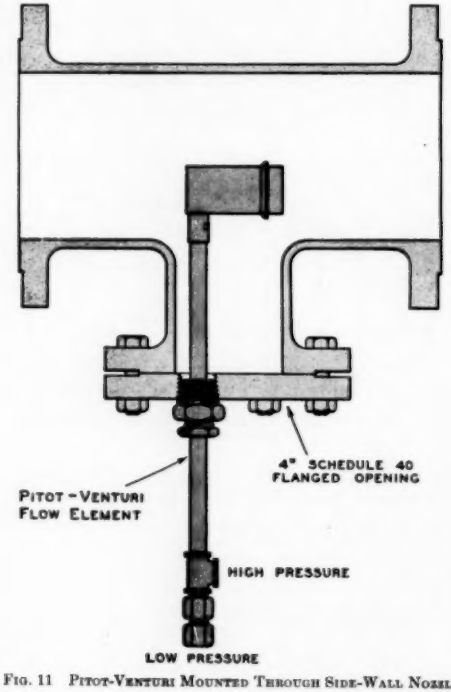

FIG. 11 PITOT-VENTURI MOUNTED THROUGH SIDE-WALL NOZZLE

without interrupting service in the main line, a 4-in. gate valve can be mounted on the 4-in. flange opening. The Pitot-Venturi support flange can then be matched to a short extension leading to the valve. The flow element can be removed by loosening the packing gland and withdrawing the element until it is located between the support flange and the gate valve. Upon closure of the valve, the support flange can be removed, and the element is then exposed for observation. The length of mast is chosen after the method of mounting has been established. It should be of sufficient length so that the element can touch the opposite surface of the pipe and have a 4-in. length external to the support flange.

This type of flow element should not be used in instances where gases are not completely free of condensables or when liquids contain solids. Because of the small clearances involved in the inner Venturi throat section, this element should not be used to measure steam velocities, nor should it be installed where continuous purge or blowback is required. In the latter instance, back pressure developed varies rapidly with purge flow rate and reflects in highly variable differential-pressure readings. In-

creasing the width of the slit in the inner Venturi throat would relieve this condition but, at the same time, seriously reduce the multiplying action of the element.

The influence of pipe sizes on the equation relating velocity and differential has not been established at this writing. However, analysis reveals that one limiting factor is the alteration of the wave front immediately downstream from the calibrating ring as would be caused by too small a duct. A second one is the effective reduction of cross-sectional area as a result of introducing the Pitot-Venturi in the flow line and thus produces a differential which is not predictably indicative of the true velocity of the fluid. At present, the recommended minimum pipe size is 6 in. No limitation is evident as to maximum pipe size apart from the physical requirements to be met when making surveys and providing for rigid suspension.

The effect on the multiplying action of the Pitot-Venturi flow element because its axis is not parallel to the axis of flow is shown in Fig. 12. As is seen, a deviation angle of 5 deg is readily permissible. Fluid impact and viscous drag cause the Pitot-Venturi to be deflected from its normal position. The effect of this is shown in graphic form in Fig. 13(*a*) and Fig. 13(*b*), for both brass and stainless-steel masts with various lengths exposed on the flow stream. Fig. 14 shows the deflection which would occur when the Pitot-Venturi is installed in a vertical pipe under no flow conditions. If the flow is downward, in a vertical pipe, values obtained from Figs. 13(*a*), 13(*b*), and 14 should be added, and if upward, they should be subtracted. Based on the assumption

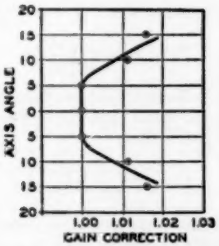

FIG. 12 ANGLE OF INCIDENCE VERSUS MULTIPLYING ACTION OF PITOT-VENTURI FLOW ELEMENT

that a 5-deg deviation between the Pitot-Venturi axis and the flow axis is permissible, the ratio of mast deflection to mast length for brass and steel should not exceed 0.031.

POSITION OF PITOT-VENTURI IN FLOW-MEASUREMENT FIELD

This element, being purely a velocity-measuring device, cannot be treated as a replacement for other proved flow elements. Instead, it takes its place among many other methods of flow measurement subject to review for adaptability and accuracy. When used in flow measurement, its location must be at the average velocity position, if Equations [4], [5], and [6] are to apply, and, since this position shifts with flow changes, the significance of the reading is similarly affected. At this writing, this type of element has proved itself useful in the measurement of gas flows over a temperature range of minus 100 F to plus 1700 F. Liquid-flow applications too have proved successful with ducts varying in size from 8 in. to 40 in.

CONCLUSION

The Pitot-Venturi flow element as a fluid-velocity measuring device is subject to all of the limitations of this type of primary element. At the same time, because of its ability to develop

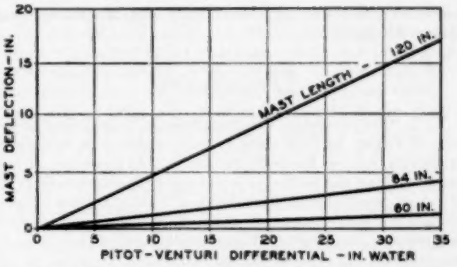

FIG. 13(a) BRASS PITOT-VENTURI MAST DEFLECTION PRODUCED BY FLUID FLOW

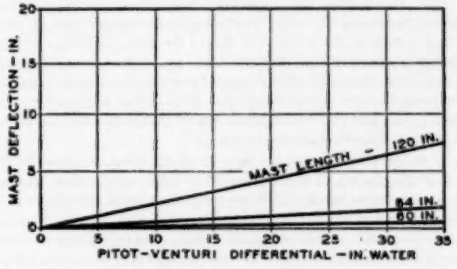

FIG. 13(b) STAINLESS-STEEL PITOT-VENTURI MAST DEFLECTION PRODUCED BY FLUID FLOW

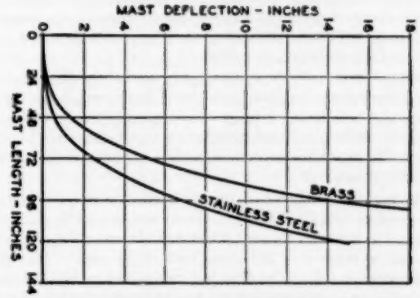

FIG. 14 PITOT-VENTURI MAST DEFLECTION, MAST IN HORIZONTAL POSITION

relatively high differentials when compared with a Pitot tube, it finds useful application when flow measurement must be made under no-pressure-loss conditions or when pipes are of a size where the customary primary element such as orifice, nozzle, or Venturi are not practical. Its use should be restricted to installations where at no time will the minimum velocity when expressed at 14.7 psia and 60 F be less than 25 fps since the points on the velocity-differential graph become quite scattered at lower velocity values. The maximum velocity at which data have been accumulated to date is 9000 fpm flowing at 15.0 psia and 75 F. These latter data were not assembled under precise control conditions, and, therefore, the points have not been included in Fig. 9.

ACKNOWLEDGMENT

The author wishes to express his appreciation for the very kind

assistance rendered by Mr. Russell Terry in making the drawings used in this paper.

Discussion

W. G. Brombacher.[4] The data obtained by the author on the ratio of Venturi to Pitot static pressure against flow should also be plotted against Reynolds number. This procedure is well known. Using this method of presentation permits data for fluids of various densities for a given design of Venturi tube to be summarized in a single graph, and definitely fixes the point at which the pressure ratio starts to fall in value as a function only of Reynolds number. It is hoped that this curve can be added to the paper.

C. B. Haughton, Jr.[5] The author has presented a very interesting discussion of a new variation of flow-measuring device, which is adaptable to very low fluid velocities. With his device special indicating instruments, such as micromanometers and draft gages, should be unnecessary for pressure measurement, as the magnification desired is inherent in the Pitot-Venturi element itself. In many applications this should eliminate much unnecessary expense for special instruments.

In the paper no mention was made of the considerations which led to the placing of the high-pressure holes on the downstream side of the mast support. Since magnification of the differential pressure is one of the prime advantages of this type of Venturi tube, it would appear that the greatest magnification possible would be desirable. A hole on the upstream side of the mast support would act as an impact hole whose increased pressure would be proportional to the fluid density times the square of the fluid velocity. Presumably the increased magnification would likewise be some function of this increased pressure. It would be interesting to know if the author made any tests on the element with the high-pressure hole so placed.

In Figs. 4, 5, and 12 of the paper, the trends shown by the curves seem to the writer to be based on scanty test data. If the curves had been drawn through the test points shown, the trends would be altered, and perhaps the test conclusions would be different. In Fig. 5, for example, one more test point might confirm the curve shown.

The installation shown in Fig. 11 is a useful one. Its usefulness possibly could be extended if some sort of a baffle plate were attached to the mast support, which would cover the flange opening and be flush with the inner wall of the pipe. This plate would serve to reduce the fluid turbulence around the high-pressure holes, and possibly allow the flow element to be placed much closer to the inner wall of the pipe without changing the basic calibration appreciably.

Several additional questions might be of interest: (1) What is the minimum practical size of the Pitot-Venturi flow element, and would the data presented in the paper be applicable to such a size? (2) Is the multiplying action shown in Figs. 3, 4, and 5, independent of the magnitude of the velocity?

The author has stated: "The differential which is developed across a Venturi tube depends directly upon the square of the flow through it, and inversely on the fourth power of the throat diameter." Since in a double Venturi there are two throats, it may be of interest to present the derivation of its flow equation in order to emphasize the author's statement:

The following nomenclature will be used:

A_1 = entrance area, outer Venturi
d_1 = entrance diameter, outer Venturi
d_2 = throat diameter, inner Venturi
d_3 = exit diameter, inner Venturi
d_4 = throat diameter, outer Venturi
g = acceleration of gravity
V_1 = stream velocity at entrance to outer Venturi
V_2 = throat velocity, inner Venturi
V_3 = exit velocity, inner Venturi
V_4 = throat velocity, outer Venturi
W = fluid flow rate
ΔP = pressure drop from free stream to inner Venturi throat
ρ = fluid density in free stream

The theoretical weight flow through the double Venturi is

$$W = \rho A_1 V_1 \quad [7]$$

By Bernoulli's theorem the change of pressure energy to velocity energy from the stream to the inner Venturi throat is

$$\frac{V_2^2}{2g} - \frac{V_1^2}{2g} = \frac{\Delta P}{\rho} \quad [8]$$

Also

$$V_2 = V_3 \times \left(\frac{d_3}{d_2}\right)^2 \quad [9]$$

by the continuity equation, and

$$V_3 = V_4 = V_1 \left(\frac{d_1}{d_4}\right)^2 \quad [10]$$

since the velocity at the exit of the inner Venturi is assumed equal to the velocity at the throat of the outer Venturi. Combining Equations [9] and [10], we have

$$V_2 = V_1 \left(\frac{d_1}{d_4}\right)^2 \left(\frac{d_3}{d_2}\right)^2 \quad [11]$$

Then if we substitute Equation [11] in Equation [8] and solve for the stream velocity V_1, we have

$$V_1 = \sqrt{\frac{2g\Delta P}{\rho\left[\left(\frac{d_1}{d_4}\right)^4 \left(\frac{d_3}{d_2}\right)^4 - 1\right]}} \quad [12]$$

Substituting Equation [12] in Equation [7] results in the theoretical weight flow through the double Venturi for any incompressible fluid

$$W = \frac{A_1\sqrt{2g\rho\Delta P}}{\sqrt{\left(\frac{d_1}{d_4}\right)^4 \left(\frac{d_3}{d_2}\right)^4 - 1}} \quad [13]$$

and if we solve for the Venturi differential we have

$$\Delta P = \frac{W^2}{2gA_1^2\rho}\left[\left(\frac{d_1}{d_4}\right)^4 \left(\frac{d_3}{d_2}\right)^4 - 1\right] \quad [14]$$

which agrees with the author's statement that the differential depends upon the square of the flow and inversely on the fourth power of the throat diameter. Note that both throat diameters (d_2) and (d_4) show this inverse relationship.

Author's Closure

It is quite true, as Dr. Brombacher intimated, that performance characteristics of primary elements used in flow measurement are

[4] Chief, Mechanical Instruments Section, National Bureau of Standards, Washington, D. C. Mem. ASME.

[5] Aircraft Gas Turbine Engineering Division, Aircraft Gas Turbine Laboratory, General Electric Company, West Lynn, Mass.

plotted as a function of Reynolds number. This procedure was not followed in the paper because of the special form of flow equations used. Specifically, the square-root relationship approach has been replaced by an exponential expression which automatically causes the Pitot-Venturi coefficient K_{pv} to be constant regardless of Reynolds number. A curve showing Reynolds number versus multiplying action would be important if the square-root law were used in the flow equations for then K_{pv} would not be constant. Previous to adopting this approach, the data were examined in the light of Reynolds number, and are shown in Fig. 15. Note that the abscissa is not a pure Reynolds number since there is no specific diameter which can be used in determining it. Inasmuch as only one form of element is furnished, it appears satisfactory to omit the diameter influence.

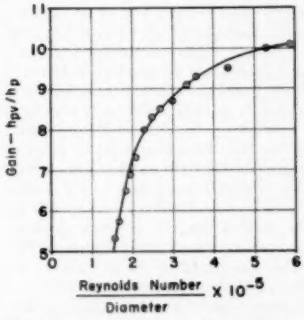

FIG. 15 GAIN VERSUS REYNOLDS NUMBER

In the discussion offered by Mr Haughton, a number of questions have been raised, and they will be answered in the same order in which they have been presented.

When the Pitot-Venturi element was first manufactured, the static pressure hole was located on the upstream face of the mast in order to take advantage of impact pressure. Complaints were soon received from the field to the effect that this impact hole plugged, rendering the unit inoperative. The holes were then relocated to the downstream position, namely, 135 deg measuring from the upstream face, and preliminary tests revealed that the unit would be satisfactory when furnished in this form. However, since the writing of this paper, it has been found that the flow equation developed for the unit was materially disturbed because of poor calibrating data, and interestingly enough, this condition was eliminated by restoring the static pressure hole to its upstream position. Apparently, the stream disturbance which the mast introduced had an effect on the static-pressure reading which differed considerably with each unit made. Our present practice is to furnish the element with the impact hole facing upstream, and if the installation is one which involves a high solid content, we do not recommend that the element be used. In the event that it must be used, the holes are located downstream to minimize operating difficulties.

It is recognized that the number of points shown in Figs. 4, 5, and 12 are inadequate. At the same time, tests have shown that their distribution varies terrificly from one unit to the next, and therefore it seemed unnecessary to show anything else but a trend in each instance.

Mr. Haughton suggested that a baffle plate be included when an installation is made as shown in Fig. 11. Thought was given to this arrangement, and we found that two difficulties presented themselves: (1) The installation of the baffle would prove somewhat difficult, and (2) the baffle would interfere when attempting to withdraw the element from the pipe line. For this reason we located the element on the leading edge of the nozzle opening so as to minimize the effect of turbulence which the nozzle opening might introduce.

The minimum practical size, from a manufacturing standpoint, which we have found is to make the unit with a $2^3/_4$ in. over-all length and a diameter of $1^1/_2$ in. However, we did not adopt this model, because the welding operation always causes some distortion and this influenced the performance characteristics of the element appreciably. The size furnished is somewhat larger and is less affected by these changes. It might be of interest to know that a die-cast model was made for us which had an outside diameter of about $^1/_2$ in. and a length of $1^1/_4$ in. Tests revealed that it was a poor performer and that any presence of dirt plugged the unit quite rapidly.

The multiplying action as affected by design changes is not independent of velocity. The influence is reduced as velocity is reduced, and the curves given in the paper were all determined at a velocity of 5000 ft per min.

A New Method of Determining Thermal Diffusivity of Solids at Various Temperatures

By D. ROSENTHAL[1] and A. AMBROSIO,[2] LOS ANGELES, CALIF.

The method under review affords a rapid means of determining thermal diffusivity and is especially suitable to measurements at high temperatures. The theory of moving heat sources is the basis for this method. When the theory is applied to the case of unidimensional heat flow in a long prismatic bar, being heated by a moving point heat source, an equation which permits the computation of thermal diffusivity at each temperature is obtained. The experimental technique involves the measurement of the temperature-time history at a single point of the bar, using two different heat-source velocities. The method was tried on a commercial "yellow" brass tube, but the equation derived for the computations proved to be unworkable owing to the poor accuracy attending the evaluation of the first and second-order derivatives of the temperature-time curves. To avoid this shortcoming another equation was derived by assuming that the thermal properties of the bar are constant in small intervals of temperature. This equation gives average values of diffusivity in the small intervals of temperature, rather than a specific value for each temperature. This approximation notwithstanding, the intervals of temperature could be made small enough to determine the values of thermal diffusivity of the brass specimen in the range 100 to 400 C with a repeatability of ±3 per cent. These computed values compare favorably with those found in the literature.

Introduction

THE advent of jet and rocket-propulsion power plants has made the use of engineering materials more and more dependent upon their physical properties at high temperatures. Yet, there are relatively few available data regarding these properties. This applies in particular to the thermal diffusivity,[3] a quantity which appears in all problems dealing with transient heat phenomena. One of the possible reasons for this shortcoming might be the lack of rapid and adequate methods of measurement, especially at high temperatures.

A survey of the available literature[4] has revealed that the current methods of determining thermal diffusivity have at least one of the following disadvantages or sources of error:

1 The thermal properties of the material are assumed to be constant over a wide range of temperatures.

2 The boundary condition required to obtain relatively simple equations for the thermal diffusivity is physically difficult to obtain and impose.

3 The mathematics must be simplified by approximations.

4 Sufficiently accurate data are difficult to obtain.

The new method, described in this paper, is believed to be free of most, if not all, of the afore-mentioned shortcomings. In addition, it has the advantage of affording a rapid determination of thermal diffusivity, and it appears to be well suited to high-temperature measurements.

Theory

The basic principles of the method under consideration are contained in the theory of moving heat sources developed by one of the authors.[5] Briefly, the method requires the establishment of the temperature-time history at a given point of the material as a result of the passage of a heat source.

In order to bring out the essential features of the theory, imagine a heat source moving at a constant velocity along the surface of a body and supplying a constant heat input to the body. Experiment shows[6] that if the extent of the body in both directions from the heat source is large as compared to the size of the source, and the source has been traveling for a long distance, a so-called "quasi-stationary" state characterized by a constant temperature distribution around the source occurs. That is, an observer stationed at the source fails to notice any change in the distribution of temperature around him. This is taken into account in the general equation of heat flow in solids by postulating that the temperature is independent of time if the system is referred to co-ordinates moving with the heat source.

This method of determining thermal diffusivity is concerned with the quasi-stationary state of heat flow in a long bar, whose thickness is small enough so that temperature changes in the cross section may be neglected. Furthermore, the heat losses from the surface to the surrounding medium are assumed to obey Newton's law of cooling at all points of the bar, except at the location of the heat source. Under these conditions, the differential equation of heat flow in terms of a co-ordinate system stationary with respect to the bar is

$$\frac{\partial}{\partial Z}\left(k\frac{\partial T'}{\partial Z}\right) = c\rho\frac{\partial T'}{\partial \theta} + \frac{Ph}{A}(T' - T_0') \quad \ldots\ldots [1]$$

where

Z = distance from a fixed point on the bar, cm

θ = time, sec

---

[1] Professor, Department of Engineering, University of California. Mem. ASME.

[2] Department of Engineering, University of California.

[3] "Metals Handbook," American Society of Metals, 1949.

[4] "A New Method of Determining Thermal Diffusivity of Solids at Various Temperatures," by A. Ambrosio, MS thesis, Department of Engineering, University of California, Los Angeles, Calif., June, 1949.

Contributed by the Heat Transfer Division and presented at the Semi-Annual Meeting, Toronto, Ont., Can., June 11–15, 1951, of The American Society of Mechanical Engineers.

Note: Statements and opinions advanced in papers are to be understood as individual expressions of their authors and not those of the Society. Manuscript received at ASME Headquarters, April 10, 1951. Paper No. 51—SA-39.

[5] "The Theory of Moving Sources of Heat and Its Application to Metal Treatment," by D. Rosenthal, Trans. ASME, vol. 68, 1946, pp. 849–866.

[6] "Temperature Measurements in Fusion Welding," by H. Bornefeld, *Technische Zentralblatt für Praktische Metal Bearbeitung*, vol. 43, 1933, pp. 14–18.

T' = temperature at point Z, deg C
T_0' = temperature of surrounding medium, deg C
k = thermal conductivity at temperature T', /(cal/sec cm² deg C/cm)
c = heat capacity at temperature T', (cal/g deg C)
ρ = density at temperature T', (g/cm³)
h = unit thermal conductance for surface heat losses associated with $(T' - T_0')$, (cal/sec cm² deg C)
P = perimeter, cm
A = cross-section area, cm²

To obtain the temperature as a function of the distance from the heat source, the transformaton $x = Z - v\theta$ is used. x(cm) = the distance measured from the heat source, and v (cm per sec) = the velocity of the heat source. With this transformation, Equation [1] becomes

$$\frac{\partial}{\partial x}\left(k\frac{\partial T'}{\partial x}\right) = -c\rho v\frac{\partial T'}{\partial x} + c\rho\frac{\partial T'}{\partial \theta} + \frac{Ph}{A}(T' - T_0') \quad [2]$$

As mentioned previously, when the bar is in the "quasi-stationary" state, the temperature distribution about the heat source is not a function of time. This condition is obtained in Equation [2] by setting $\frac{\partial T'}{\partial \theta} = 0$. Thus Equation [2] becomes

$$\frac{\partial}{\partial x}\left(k\frac{\partial T'}{\partial x}\right) = -c\rho v\frac{\partial T'}{\partial x} + \frac{Ph}{A}(T' - T_0') \quad [3]$$

If temperature measurements are made at a fixed point Z_0 on the bar, Equation [3] may be transformed to express the time-temperature relationship at this point on the bar. For this purpose let $x = Z_0 - v\theta$. Furthermore, by letting $(T = T' - T_0')$, Equation [3] becomes

$$\frac{1}{v^2}\frac{d}{d\theta}\left(k\frac{dT}{d\theta}\right) = c\rho\frac{dT}{d\theta} + \frac{Ph}{A}T \quad [4]$$

This equation may be rewritten to bring out explicitly the thermal diffusivity. Expand the left side of Equation [4], divide both sides by k, and define $H = (Ph)/(Ak)$. Since by definition, the thermal diffusivity is $\alpha = k/(c\rho)$, Equation [4] will now become

$$\frac{1}{v^2}\frac{d^2T}{d\theta^2} + \frac{1}{v^2}\frac{d(\ln k)}{dT}\left(\frac{dT}{d\theta}\right)^2 = \frac{1}{\alpha}\frac{dT}{d\theta} + HT \quad [5]$$

Equation [5] provides the theoretical basis for the experimental determination of the thermal diffusivity α.

The Exact Determination

In deriving Equation [5] only one assumption was made, namely, that the thermal characteristics of the material, as expressed by the quantities α, k, and H, are functions of the temperature and the temperature alone. Equation [5] relates these quantities to the temperature and its first and second derivatives which can be determined from the temperature-time history as measured at the point of observation. In order to compute the three unknowns α, k, and H, three different sets of values of $(dT)/(d\theta)$ and $(d^2T)/(d\theta^2)$ are required for the same temperature T. Two of these sets may be secured from one single experimental run, since, as may be seen in Fig. 1, the same temperature is obtained twice during a run. It is obtained once during the heating and once during the cooling portion of the temperature-time curve. In order to obtain the third set of values of $(dT)/(d\theta)$ and $(d^2T)/(d\theta^2)$ another run must be made with a different heat-source velocity. Since each run supplies two sets of values, an additional set is available for a check.

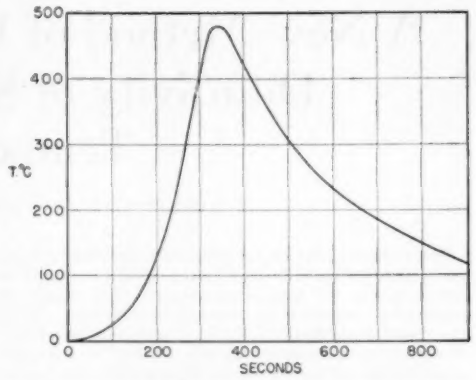

Fig. 1 Temperature-Time History of a Brass Tube in Quasi-Stationary-State Condition at a Heat-Source Velocity of 0.0610 Cm Per Sec

This procedure appears rather simple in theory. In practice, however, the first and second derivatives are exceedingly difficult to evaluate with any degree of accuracy. Several methods were attempted but none was sufficiently accurate to warrant the tedious work involved. It must be emphasized, however, that if an accurate means of evaluating derivatives from experimental data is developed, a method of determining diffusivity at each temperature is available.

The Approximate Determination

After the failure of the exact procedure, an approximate method was attempted. The assumption was made that the thermal properties of the material vary slowly enough with the temperature so that their change in a small interval of temperature may be neglected. Thus, in this small interval, the term

$$\frac{1}{v^2}\frac{d(\ln k)}{dT}\left(\frac{dT}{d\theta}\right)^2$$

in Equation [5] may be neglected, and Equation [5] becomes

$$\frac{1}{v^2}\frac{d^2T}{d\theta^2} = \frac{1}{\alpha}\frac{dT}{d\theta} + HT \quad [6]$$

It is known that an equation of the form

$$T = Be^{\beta\theta} \quad [7]$$

will satisfy the differential Equation [6] in each of the chosen intervals of temperature. It must be remembered, however, that both B and β may be of different values for each chosen interval. Substituting Equation [7] into Equation [6] results in the following relation

$$\frac{\beta^2}{v^2} - \frac{\beta}{\alpha} - H = 0 \quad [8]$$

On the other hand, Equation [7] may be rewritten to read

$$\ln T = \ln B + \beta\theta \quad [9]$$

Thus, if the experimental temperature-time curves are replotted on semilogarithmic scales, and the resultant curves are approxi-

mated by a series of short straight lines, a value of β may be computed for each short interval of temperature. The β thus determined will be a function of the temperature and the heat-source velocity used to obtain the data. Having two different values of β for the same interval of temperature, one can determine α and H from Equation [8]. This determination may be accomplished in two ways, (1) from a single curve, since the same interval of temperature is reached twice, on heating and cooling, or (2) from two curves, using either the heating or the cooling portion of the curves. This process may be formulated by means of the following equations

$$\beta = \frac{\ln T_1 - \ln T_2}{\theta_1 - \theta_2} \quad \ldots\ldots\ldots\ldots\ldots\ldots [10]$$

and

$$\alpha = \frac{\beta_1 - \beta_2}{\left(\frac{\beta_1}{v_1}\right)^2 - \left(\frac{\beta_2}{v_2}\right)^2} \quad \ldots\ldots\ldots\ldots\ldots\ldots [11]$$

An examination of Fig. 1 shows that the slope $(dT)/(d\theta)$ is positive on the heating side and negative on the cooling side of the temperature-time curve. The same is true for β, as may be seen in Fig. 2; hence, for greater precision, the determination of the diffusivity α should be made, using a β evaluated from the heating side of a curve in conjunction with a β evaluated from the cooling side of a curve.

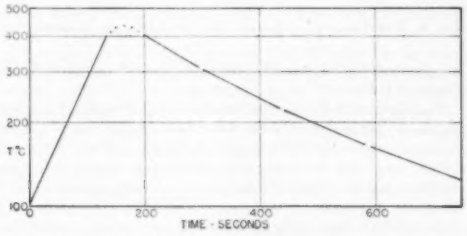

FIG. 2 TYPICAL LOG TEMPERATURE-TIME HISTORY OF BRASS TUBE AT A HEAT-SOURCE VELOCITY OF 0.0610 CM PER SEC

EXPERIMENTAL PROCEDURE

The material for which the diffusivity was determined is brass of the 65 per cent copper, 35 per cent zinc variety, the so-called "yellow" brass. The experimental equipment used to obtain the necessary data consisted of a test specimen with the requisite thermocouples attached, a heat source, and the instruments to measure the temperature-time relation.

The test specimen was made from a brass tube, 48 in. long, 3/4 in. diam, and with a wall thickness of 1/8 in. Number 20 chromel and alumel wires were used as thermocouples. They were pulled through the inside of the tube, and their junctions were silver-soldered to the tube wall. To permit the rotation of the specimen around the axis, the free ends of the thermocouple wires were attached to slip rings immersed in mercury pools, Fig. 3. Rotation of the specimen was desired in order to insure that the heat input to the specimen did not vary with respect to the circumference of the tube. To complete the electrical circuit, chromel and alumel wires were used to connect the mercury pools to the recorder.

A ring burner, designed to burn acetylene and air, was used as the heat source. To obtain a means of moving the heat source at a designated velocity, the tube was mounted in a lathe with one end held rigidly in the chuck and the other end supported by the steady rest. The ring burner was mounted in the tool post in such a manner that the tube was in the center of the ring and the plane of the ring was perpendicular to the longitudinal axis of the

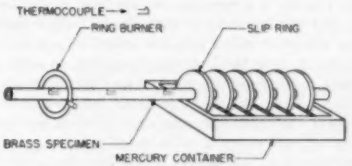

FIG. 3 ASSEMBLY OF EXPERIMENTAL EQUIPMENT

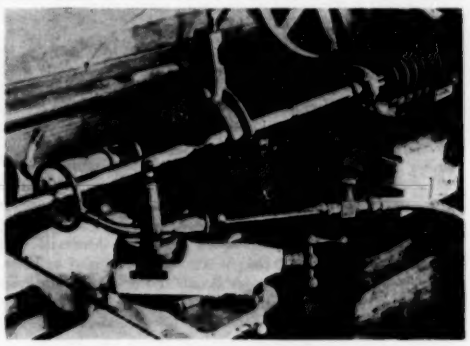

FIG. 4 VIEW OF RING BURNER, SLIP RINGS, AND MERCURY CONTAINER

tube, Fig. 4. By engaging the lead screw, the burner could be made to move along the length of the tube.

The voltages generated by the thermocouples on the tube were fed into a Brown sixteen-channel rapid recorder.

REMARKS ON EXPERIMENTAL PROCEDURE

The major difficulties encountered in the experimental development of this method of determining thermal diffusivity arose from the fact that it is physically impossible to attain a point heat source. Since the theory is valid only outside the region of the heat source, data obtained during the time the heat source is over the thermocouple are not usable. This primarily affects the data taken during the heating portion of the run. The distance from the thermocouple at which a noticeable change in temperature occurs is inversely proportional to the heat-source velocity.

Thus there is an upper limit to this velocity above which all of the heating data are obtained during the time the thermocouple is beneath the heat source. On the other hand, there is also a lower limit to the heat-source velocity which is determined by the length of the specimen and the lowest temperature which is desired on the cooling portion of the data.

Another consideration is the diffusivity of the specimen. The smaller the value of the diffusivity, the lower is the upper limit of the heat-source velocity. From the foregoing discussion it is seen that there is a definite range of useful velocities dependent upon

the width of the heat source and the thermal diffusivity of the specimen.

Another factor which must be considered is the maximum temperature to which the specimen may be exposed. This maximum temperature is, of course, a function of the melting point of the material. Experimentally, the maximum temperature which the specimen attains is a function of the heat input, heat-source velocity, and the diffusivity of the material. High maxima temperatures will be obtained with low velocities and low diffusivities. However, from the foregoing discussion, in order to obtain usable data, lower velocities must be used for materials with low diffusivities. Thus, unless one designs a heat source with a very wide range of controlled heat outputs, a different heat source may be needed for each material to be tested.

A final remark on this subject is that high-frequency response-recording equipment is essential in order to utilize the heating portion of the runs made with relatively high heat-source velocities.

Evaluation of Data

Data were obtained as curves of voltages developed by the thermocouple versus time. These voltages were converted into temperatures and the curves were replotted on semilogarithmic graph paper. The plotted points were then connected by segments of straight lines, and the slope of each segment was computed. This slope is, by Equation [10], the value of β. In this manner a set of β was determined for each heat-source velocity and interval of temperature. The β in each set were averaged for the heating and cooling curves separately. As a measure of the variation of β, the average of the standard deviation for a set of β was computed. The value for the set of β obtained from the cooling curves at $v = 0.0610$ cm per sec was determined to be less than 5 per cent. The average β and the corresponding heat-source velocity were substituted into Equation [11] to obtain the values for diffusivity.

Results

Data were taken at four heat-source velocities. At each velocity several runs were made at various points on the bar to check the establishment of the quasi-stationary state. The remaining runs were made using only one thermocouple. A typical temperature-time relationship is plotted in Fig. 1. From the data, values of diffusivity were computed at each interval of temperature by using the approximate procedure described. A plot of these values is shown in Fig. 5. By drawing the most probable straight line through the experimental points, the diffusivity of the brass specimen in the temperature range from 100 to 400 C is represented by the following equation

$$\alpha = 0.346(1 + 0.000715\,T) \pm 3 \text{ per cent} \quad [12]$$

A reference[7] was found which presented an equation for thermal conductivity of yellow brass as a function of temperature from 18 C to 200 C. This equation was converted into one for diffusivity by assuming the heat capacity and the density, which were also given, to be constant in the same range of temperatures. The converted equation was

$$\alpha = 0.365(1 + 0.001\,T) \quad [13]$$

Since the heat capacity of both copper and zinc increases with temperature,[8] it is presumed that the heat capacity of brass would do likewise and consequently the slope of Equation [13] should

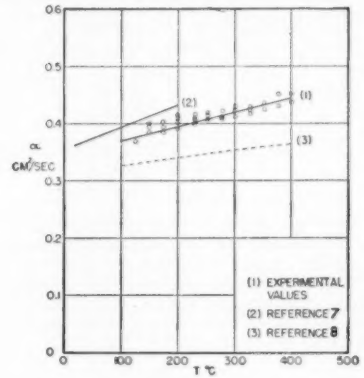

Fig. 5 Diffusivity of Brass as a Function of Temperature

be less than that obtained, that is, it should approach that of Equation [12].

Point values of the thermal conductivity of brass (70 per cent copper, 30 per cent zinc) from 0 to 400 C at intervals of 100 deg C were found in another reference.[8] Values of the thermal diffusivity were also computed using these point values of the conductivity and the values of heat capacity and density given in the handbook mentioned.[7] It is seen in Fig. 5 that the experimental values of the diffusivity lie between the sets of data obtained from the two references.

Conclusions

On the basis of the foregoing discussion it is concluded that the new method of determining thermal diffusivity of solids has definite advantages over the existing ones, especially with respect to the application to high temperatures. These advantages are as follows:

1 The properties of the material need be assumed constant only in small intervals of temperature.

2 The quasi-stationary state is easily obtained.

3 The mathematics involved in the calculation of the thermal diffusivity needs no simplification and is straightforward.

[7] "Copper and Brass Stock List and Handbook," Revere Copper and Brass Products, Pacific Metals Company, Ltd., Los Angeles, Calif., 1949.

[8] "Heat Transmission," by W. H. McAdams, McGraw-Hill Book Company, Inc., New York, N. Y., 1942.

A Standard Laboratory Corrosion Test for Metals in Phosphoric-Acid Service

By H. F. EBLING[1] and M. A. SCHEIL,[2] MILWAUKEE, WIS.

It is the purpose of this paper to show the need of a standard test for materials to be used in phosphoric-acid service. We propose and use a standard laboratory phosphoric-acid test to evaluate materials for phosphoric-acid service. This test is explored presenting some possible difficulties and their corrections. The relation between the laboratory test and our field experience is presented and illustrated. A table of laboratory corrosion test results is presented as a guide in selecting metals for phosphoric-acid service.

Introduction

PHOSPHORIC acid has many industrial and agricultural uses. It is produced by two methods: One is the wet process in which the phosphate rock is reacted with sulphuric acid, and phosphoric acid is produced by simple replacement. The second one is the thermal reduction process in which phosphate rock is reduced by carbon at about 1600 C. Under this condition elemental phosphorus is produced which in turn is volatilized, condensed, and collected under water. In peacetime, phosphorus is chiefly an intermediate product and is oxidized to phosphoric acid or phosphates before it has any wide industrial or agricultural application. By this method, phosphoric acid is produced in a pure, highly concentrated form, suitable for use in the food, chemical, and drug industries as well as for fertilizer purposes. Although about 75 per cent of the phosphorus products are used in the fertilizer industry, there are new and expanding markets for phosphoric acid and its compounds.

In the petroleum industry, phosphoric acid is used as a catalyst. About 15 years ago a process for the catalytic polymerization of propylenes and butylenes came into use. Refiners discovered that gases from cracking units could economically be polymerized to form a polymer gasoline of high blending octane value. During the last war large quantities of this poly-plant gasoline were hydrogenated to form aviation-gasoline stock.

Orthophosphoric acid is one of the most active catalysts employed in the polymerization process. Solid forms of the acid catalyst may consist of admixtures with kieselguhr, magnesia, alumina, sand, and so forth. The vessels containing the catalysts operate at temperatures ranging from 350 to 450 F and at pressures from 200 to 1000 psi.

At ordinary room temperature phosphoric acid is not considered as a very corrosive agent. However, at elevated temperatures and high concentrations phosphoric acid presents a serious corrosion problem. According to the "Chemical Engineers' Handbook,"[3] the only metals which are corrosion-resistant to phosphoric acid for all concentrations and temperatures are gold, platinum, platinum iridium, platinum rhodium, Durichlor, and Duriron. Silver was found satisfactory for all concentrations only up to 365 F. The Hastelloys B, C, and D, and Stellites were found to be resistant to boiling solutions while Worthite, Chlorimet, Durimet 20, lead, and Monel were resistant to high concentrations up to temperatures in the range of 200 to 250 F. The ordinary 18-8 stainless steels are limited to about 150 F for concentrations up to 80 per cent[4] or about a 45 per cent solution at its boiling temperature.

The results of a symposium are given by E. C. Fetter,[5] in which the manufacturers of corrosion-resistant materials discussed the suitability of their products for phosphoric-acid service. Referring to the metallic materials, we find the following limitations set forth:

1 Worthite, 85 per cent acid up to 250 F.
2 Illium G, 50 per cent acid up to boiling.
3 Hastelloy A, 50 per cent acid up to boiling.
Hastelloy B, 85 per cent acid up to boiling.
Hastelloy C, 50 per cent acid up to boiling.
Hastelloy D, 50 per cent acid up to boiling.
4 Stainless steel, solutions not over 200 F.
5 Copper and copper alloys, 90 per cent up to 185 F
6 Durimet T and 20, no figures given.
7 Nickel, 90 per cent, room temperature.
Inconel, 90 per cent, room temperature.
Monel, all concentrations to 220 F.

Another useful reference for the corrosion resistance of materials in phosphoric acid is to be found in "The Corrosion Handbook."[6]

Many of the observations listed were based upon the limited data of past tests, and full limitations of some of the materials have not been explored. It was noted that the test conditions can influence the test results greatly. Some of these conditions are as follows:

1 Acid purity, small amounts of acid of the halogen family greatly increase rates.
2 Degree of aeration.
3 Velocity of acid.

In 1948, the Tennessee Valley Authority issued a report[7] which lists materials tested in superphosphoric acid at elevated temperatures. The acid concentration used is given as 85 per cent P_2O_5 which is equivalent to about 118 per cent concentration in terms of orthophosphoric acid as shown in Fig. 1. The temperature generally used was 485 F. According to tests made under

---

[1] Metallurgist, Research Department, A. O. Smith Corporation.

[2] Director, Metallurgical Research, A. O. Smith Corporation.

[3] "Chemical Engineers' Handbook," by J. H. Perry, third edition, McGraw-Hill Book Company, Inc., New York, N. Y., 1950.

Contributed by the Petroleum Division and presented at the Fifth Annual Petroleum Mechanical Engineering Conference, New Orleans, La., Sept. 24-28, 1950, of The American Society of Mechanical Engineers.

Note: Statements and opinion advanced in papers are to be understood as individual expressions of their authors and not those of the Society. Manuscript received at ASME Headquarters, January 17, 1951.

[4] All references to acid concentration are in terms of orthophosphoric acid unless otherwise indicated.

[5] "Corrosion Forum," by various authors, *Chemical and Metallurgical Engineering*, vol. 53, July, August, and September, 1946.

[6] "The Corrosion Handbook," by H. H. Uhlig, The Electrochemical Society Inc., New York, John Wiley & Sons, Inc., New York, N. Y., 1948, p. 783.

[7] "Development of Processes and Equipment for Production of Phosphoric Acid," by M. M. Striplin, Jr., Tennessee Valley Authority, Engineering Report No. 2, Wilson Dam, Ala., 1948.

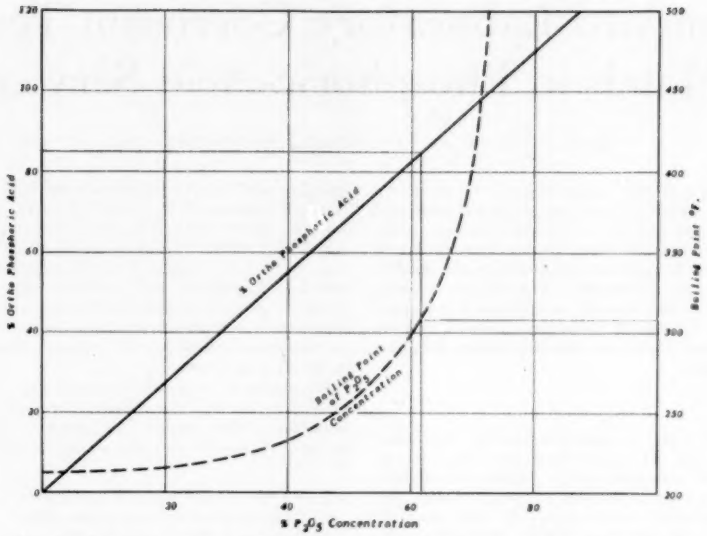

FIG. 1 P_2O_5 CONCENTRATION VERSUS PER CENT ORTHOPHOSPHORIC ACID AND BOILING POINT OF PHOSPHORIC-ACID SOLUTIONS

these conditions the following metallic materials were found to be satisfactory:

	Material	Corrosion rate
1	Tantalum	8 mils penetration per year
2	Hastelloy B	11 mils penetration per year
3	Sterling silver	12 mils penetration per year
4	Hastelloy A	23 mils penetration per year
5	Hastelloy C	35 mils penetration per year
6	Hastelloy D	35 mils penetration per year
7	Chlorimet 2	39 mils penetration per year
8	La Bour R-55	40 mils penetration per year

Satisfactory materials were those which had corrosion rates below 50 mils penetration per year. Here again we observed that the conditions of exposure influence the corrosion rates. Some tests were made in actual pilot-plant operation while others were made in the laboratory. Some specimens were exposed to static solutions while others were moved at various velocities or in agitated solutions.

From the data presented, we can see that there is a wide variation in the corrosion resistance of metallic materials and also variations in a particular material tested by different investigators. It is the purpose of this paper to set up a standard laboratory testing procedure for testing these metallic materials. It was noted in our past experience that there may be a very great variation in corrosion resistance in a particular type of alloy composition. For instance, in the proposed laboratory test, using phosphoric acid, we have tested a large number of type 316 heats to be used in phosphoric-acid service. Some heats had corrosion rates in the order of 2.50 inches penetration per year (IPY), while others were as low as 0.300 IPY. The wide range of results on this type of material was apparently due to residual elements which normally are thought of as unimportant. This will be presented later.

The establishment of a standard test procedure for phosphoric-acid service will furnish a standard of comparison for all materials. It would provide a gage with which one could measure whether a heat of a particular material was superior or inferior in corrosion resistance or if fabrication procedures altered its corrosion resistance. This test would have a similar role as the boiling nitric-acid test used in determining the corrosion resistance of austenitic stainless steels. It is well known that a laboratory test cannot select an alloy for a particular service condition, but it can provide a standard for testing the relative corrosion resistance of various heats of the alloy and the effects of fabrication procedures on them.

About 12 years ago the authors' company fabricated a number of alloy-lined vessels which were used for a gas-polymerization process using phosphoric acid as a catalyst. Type 317 material was used as the alloy for this service. At that time we used a phosphoric-acid test to select heats and to establish a fabrication procedure which would not impair the corrosion resistance of the material. A maximum of 1 in. per year penetration was set up as a standard for these vessels. During the last few years we have fabricated more of these vessels and received a number of inquiries concerning alloys for phosphoric-acid service. This led to the establishment of a standard testing procedure.

The phosphoric-acid test now used in our laboratory is as follows:

PHOSPHORIC-ACID TEST PROCEDURE

Preparation of Sample. The size of the specimen generally used for this test is approximately 2 in. long, 1 in. wide, and the full thickness of the supplied sheet. The identification of the sample is stamped at one end of the specimen. Any necessary heat-treatment of the sample should be carried out at this point. The specimen is then ground and polished to a 180 aloxite finish. Care is taken so that the specimen does not have cold-worked edges caused by shearing or overheated areas caused by prolonged or excessive grinding. New aloxite paper or cloth should be used for each alloy in order to prevent possible surface contamination. Micrometer measurements are taken of each di-

mension and the surface area is computed. The specimen then is weighed to the nearest milligram.

Apparatus and Supplies. The apparatus consists of the standard corrosion equipment in which a wide mouth 1 liter Pyrex erlenmeyer flask is used. The condenser for the apparatus is the cold-finger type. The specimens are introduced and taken out of the acid by means of a small glass basket as shown in Fig. 2.

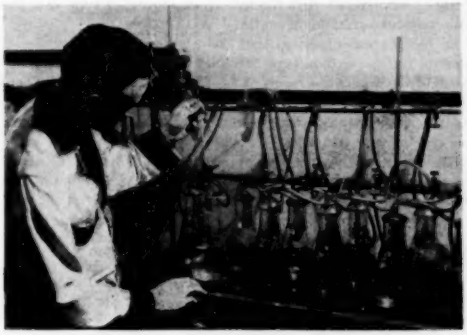

FIG. 2 REMOVING SPECIMEN FROM ACID SOLUTION

A standard electric hot plate is used to furnish sufficient heat so that the acid gently boils throughout the testing period. Baker's C. P. 85 per cent orthophosphoric acid is used. This acid has a specific gravity of 1.71 and boils at 160 C (320 F). No substitution should be made for this acid. The amount of acid used should be in proportion to the surface area of the specimen; a minimum of 60 ml of acid per sq in. of surface is used.

Test Procedure. The specimen is placed in a glass basket and is introduced into the cold acid, the condenser set into position, the assembly placed on the hot plate and brought to boil. The time is taken when the acid begins to boil. The time for one period or boil is 24 hr. At the end of the period the specimen is removed from the hot acid and washed in warm water. The specimen is dried by an air blast and again weighed to the nearest milligram. Only one specimen is run in each flask and fresh acid is used for each test period or boil. On most materials three 24-hr periods are generally sufficient to establish a uniform corrosion rate.

Calculation of Corrosion Rate. The penetration in inches per year is calculated for each period from the following formula:

$$\text{Corrosion rate in IPY} = \frac{W}{1.9x\ Dx\ Ax\ T}$$

where

IPY = inches penetration per year
W = loss in weight in milligrams expressed as a whole number
D = density of material
A = area, sq in.
T = time, hr

For an 18-8 alloy (density about 8) with the standard 24-hr period the formula becomes

$$\text{IPY} = \frac{\text{Milligrams lost}}{365 \times \text{area}}$$

Special Comments. It is absolutely necessary that the acid be kept boiling gently (approximately 160 C) during the test, as acid at a lower temperature will reduce appreciably the corrosion rate. It is recommended that a temperature reading be made at the end of the period to determine any change in the boiling point during the test.

The reflux condenser should be kept clean and fully inserted in the mouth of the erlenmeyer flask. Enough water should flow through the condensers to keep them cold to the hand to prevent leakage out of the top of the condenser. Loss of vapors by using poorly fitted condensers will cause a rapid increase in the acid concentration and its resulting boiling temperature.

Precautions should be taken against the possibility of flask breakage with the consequent spilling of hot acid, and flasks should be inspected for cracks before using. Rubber gloves are advisable when handling the hot acid.

Only phosphoric acid meeting Baker's analyzed quality and ACS standards shall be used. ACS standards are as follows:

Assay—not less than 85 per cent H_3PO_4
Chloride (Cl)—not more than 0.0005 per cent
Nitrate (NO_3)—to pass test (limit to about 0.0005 per cent)
Reducing substances (SO_2)—to pass test
Sulphate (SO_4)—not more than 0.003 per cent
Volatile acids (as acetic)—not more than 0.0015 per cent
Alkali and other phosphates—not more than 0.20 per cent as sulphates
Arsenic (As)—not more than 0.0002 per cent
Heavy metals—not more than 0.001 per cent as lead
Iron—not more than 0.005 per cent

REPRODUCIBILITY OF TESTS

We have made a large number of tests of ELC type 316 alloy in the phosphoric-acid procedure outlined. It was found that when good laboratory technique is employed with proper equipment, individual test-period results would not vary more than ±10 per cent of the average of the test periods. However, when we were required to make a large number of tests within a limited time, it was found that only about 75 per cent of the tests were within the 10 per cent variation limit. Almost all the tests were within a ±25 per cent variation. The reason for the wider variation under these test conditions was essentially the lack of control of the test temperature. Hot plates which were used and found satisfactory for other laboratory tests sometimes were found to be unsatisfactory for the phosphoric-acid test. Because of the high boiling temperature of the test solution some of the hot plates did not have sufficient capacity to keep the solutions boiling at all times. It was found that only slight drops in the line voltage would be sufficient to cause the solutions to stop boiling. This condition caused lower corrosion results.

The other difficulty was to prevent an increase in the temperature of the test solution. Since it was impossible to pair a particular flask with a condenser, there were occasions when an unusually large neck flask was used with a small condenser. The poor fit would allow some of the water vapor to escape from the test solution, thus concentrating the acid and raising the boiling point of the solution. This condition caused the higher corrosion results. This is the reason why a boiling-point determination was recommended at the end of each test period.

In spite of these difficulties, we found that the results of individual tests were within an acceptable range. When a large variation occurred in one of the periods in a test, a fourth period was run to verify the other two periods.

Not all materials show the tendency to establish a uniform corrosion rate over three periods like the type 316 and 317 alloys. A few test results on a heat of 27 per cent Cr alloy showed that there was a rapid increase in the corrosion rates from period to period, while the results on deoxidized copper showed a tendency to decrease from period to period.

Further tests on the reproducibility of this test were made with

the co-operation of one of the producers of low-carbon type 316 alloy. Since some of this alloy was purchased on the basis of the phosphoric-acid test, it was necessary that both the producer and consumer of the alloy could agree on the test results. Table 1 shows a series of results made by the two laboratories.

TABLE 1 COMPARISON OF PHOSPHORIC-ACID CORROSION-TEST RESULTS

ELC Type 316 Material
Tested in As Annealed Condition

Heat No.	Gage	Tested at	Rates in I.P.Y. Pd. 1	Pd. 2	Pd. 3	Ave.
1	.140"	Lab A	.485	.423	.451	.45
	.140"	Lab A	.507	.546	.456	.50
	.140"	A.O.S.	.402	.449	.509	.45
	.125"	A.O.S.	.567	.513	.459	.49
2	.140"	Lab A	.842	.638	.815	.56
	.140"	Lab A	.522	.567	.591	.59
	.140"	A.O.S.	.325	.461	.540	.44
	.125"	A.O.S.	.560	.555	.479	.53
3	.140"	Lab A	.508	.441	.462	.49
	.140"	Lab A	.434	.473	.468	.45
	.140"	A.O.S.	.427	.432	.477	.45
4	.140"	Lab A	.909	.660	.730	.77
	.140"	Lab A	.636	.538	.733	.63
	.140"	A.O.S.	.535	.534	.639	.58
	.109"	A.O.S.	.652	.589	.550	.60
5	.140"	Lab A	.662	.661	.988	.76
	.140"	Lab A	.540	.566	.625	.58
	.140"	A.O.S.	.532	.552	.510	.57

NOTE: Laboratory A refers to the steel vendor's results. A.O.S. refers to A. O. Smith Corporation Laboratory tests on similar materials.

Another point of interest to us concerning the reproducibility of the test was the determination of the variation in corrosion resistance within a particular heat of alloy. Figs. 3, 4, and 5 show the frequency distribution of a large number of tests on the particular heats. Figs. 6 and 7 show the frequency distribution of 13 heats of type 316 material made by one producer having similar analysis. With the amount of data presented we believe there is sufficient evidence that the phosphoric-acid test can provide reproducible results and can become a workable procedure in selecting acceptable materials for service in that medium.

Pure phosphoric acid attacks most of the austenitic stainless alloys by general corrosion. We have not observed any intergranular type of attack on ELC type 316 heats. Even standard type 316 and 317 alloys in a sensitized condition (precipitated carbide) never showed intergranular corrosion.

This is in opposition to the findings of Mears, Larrabee, and Fetner,[8] who stated that the attack of sensitized type 316 was generally intergranular in nature.[9]

In fact, it was observed that the corrosion characteristics of most of the low-carbon type 316 alloy heats did not change appreciably over a wide range of heat-treated conditions. There was a trend that stabilizing stress-annealing treatment at 1550–1650 F slightly improved the corrosion rates in some heats of low-carbon type 316 alloy. This heat-treatment showed lower corrosion rates when used on standard type 316 and 317 alloys than when the same alloy was fully annealed. Examples of this trend are as follows:

Heat no.	Average penetration annealed, IPY	Average penetration after 1550 F 15 hr AC, IPY
6	0.826	0.449
7	0.451	0.335
8	0.501	0.302
9	0.513	0.344

[8] "Comparative Corrosion Resistance of Stainless Steels in Various Acids," by R. B. Mears, C. P. Larrabee, and C. J. Fetner, Symposium on Evaluation Tests for Stainless Steel, Special Technical Publication No. 93, American Society for Testing Materials, p. 183.

[9] Apparently a difference of opinion exists on what is implied by the description of intergranular attack. We admit that the grain boundaries are more severely attacked and the surface is roughened. However, the attack does not proceed far enough to loosen grains and could not be described as "sugaring." In addition, no intergranular cracking was observed after bending the specimens.

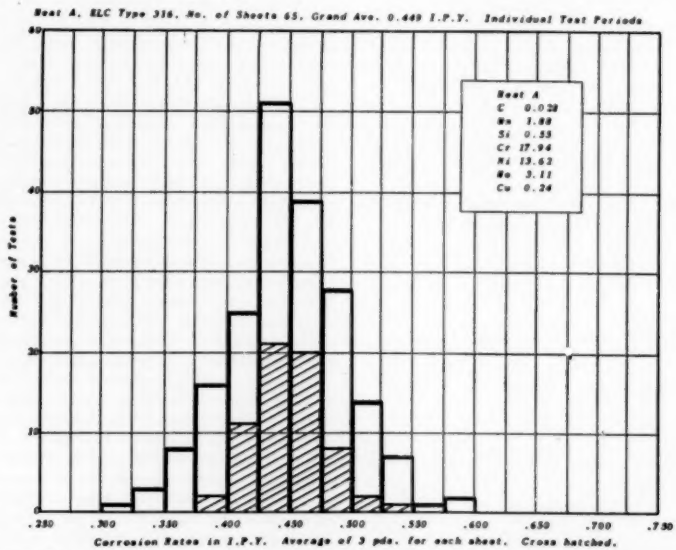

FIG. 3 FREQUENCY DISTRIBUTION OF CORROSION RESULTS IN BOILING 85 PER CENT PHOSPHORIC ACID

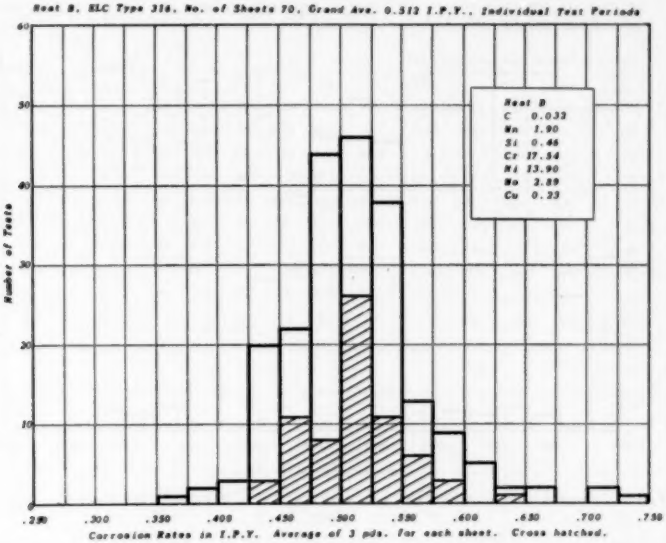

FIG. 4 FREQUENCY DISTRIBUTION OF CORROSION RESULTS IN BOILING 85 PER CENT PHOSPHORIC ACID

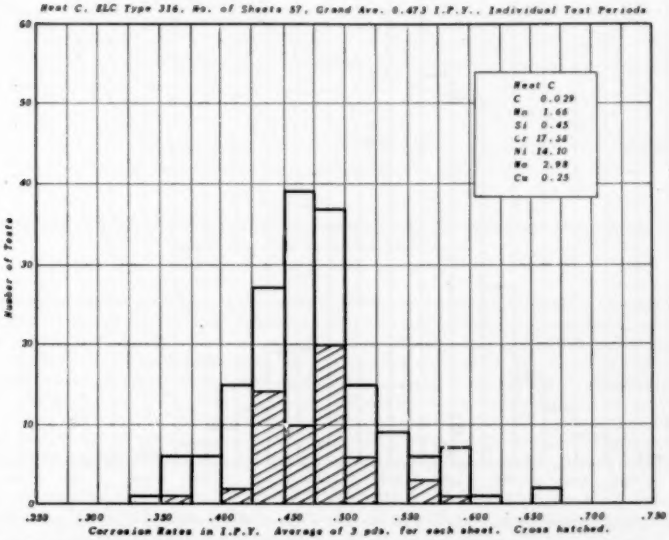

FIG. 5 FREQUENCY DISTRIBUTION OF CORROSION RESULTS IN BOILING 85 PER CENT PHOSPHORIC ACID

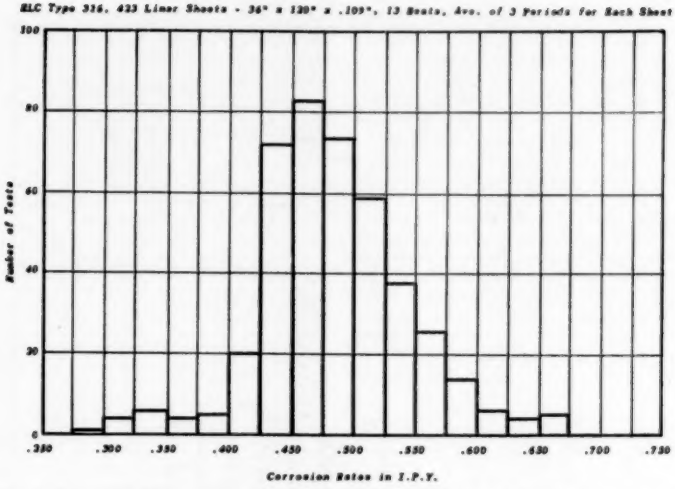

FIG. 6 FREQUENCY DISTRIBUTION OF CORROSION RESULTS IN BOILING 85 PER CENT PHOSPHORIC ACID

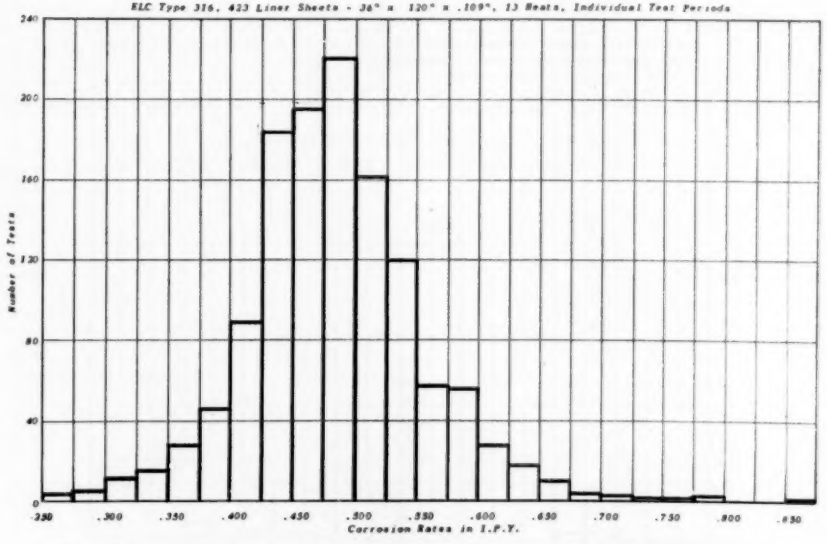

FIG. 7 FREQUENCY DISTRIBUTION OF CORROSION RESULTS IN BOILING 85 PER CENT PHOSPHORIC ACID

THE EFFECT OF COPPER

At the outset of the corrosion testing of low-carbon type 316 alloy in phosphoric acid, it was noted that one producer of alloy consistently met the required corrosion rate of 1 in. per year maximum, while a second producer could not meet the requirement. Typical corrosion rates on material supplied by the two producers are shown in Table 2.

The usual analysis of each heat is shown. It is to be noted that the standard analysis of elements of the heats did not give a clue as to their corrosion resistance in phosphoric acid. Some

TABLE 2 PHOSPHORIC-ACID TEST RESULTS ON ELC T316 MATERIAL FROM TWO PRODUCERS

Heat No.	Producer	Chemistry C	Mn	Si	Cr	Ni	Mo	Phosphoric Acid Test Results Annealed Condition—I.P.Y. Pd.1	Pd.2	Pd.3	Ave.	Copper Analysis
10	1	.02	1.30	.44	18.43	12.61	2.95	1.60	1.60	1.50	1.59	.04
11	1	.03	1.30	.39	18.47	13.78	3.11	1.55	1.51	1.43	1.54	.04
12	1	.03	1.38	.38	17.67	10.74	2.61	1.77	1.45	1.37	1.53	.04
13	1	.02	1.80	.39	18.09	11.85	3.00	2.15	2.43	—	—	.03
14	1	.03	0.83	.47	17.56	13.54	2.71	1.38	1.97	1.70	1.35	.03
15	2	.03	1.42	.32	17.61	12.94	2.89	.557	.442	.459	.486	.24
16	2	.03	1.54	.32	17.49	13.70	3.07	.489	.475	.472	.479	.26
17	2	.03	2.02	.72	17.66	13.52	2.71	.587	.562	.589	.580	.21
18	2	.03	1.86	.50	18.11	13.28	3.45	.930	.910	1.06	.970	.13
19	2	.03	1.79	.36	17.30	13.70	3.07	.675	.622	.582	.630	.16

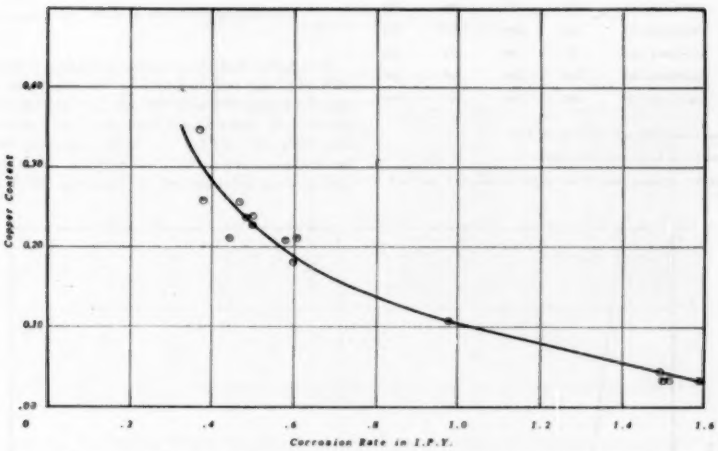

FIG. 8 EFFECT OF COPPER IN LOW-CARBON TYPE 316 ALLOY SHEETS ON CORROSION RESISTANCE AS DETERMINED BY PHOSPHORIC-ACID TEST

time later, spectrographic means were employed to determine the extent of residual elements in the alloy. The most suspicious residual element found was copper. A wet analysis of copper was made on each of the heats. This revealed that heats containing about 0.2 per cent or more of copper showed very good corrosion resistance in phosphoric acid. The copper analyses are shown in the last column of Table 2. Thus it is apparent that the residual-copper content is the important factor influencing the phosphoric acid corrosion resistance of type 316 material as shown in Fig. 8.

In order to confirm these results for weld metal, a series of tests were made on weld deposits made with 25 per cent Cr–20 per cent Ni–3 per cent Mo electrode with varying additions of copper. These results confirmed the importance of copper additions on the corrosion resistance of the weld deposits. Table 3 shows these results which are also shown in Fig. 9.

The mechanism which causes the copper to impart superior corrosion resistance to phosphoric acid is not known. Copper metal itself has a corrosion rate of about 2 in. per year, according to this test. It is probable that the copper fortifies the passive film on the surface of the metal. The same reaction occurs in the well-known Strauss test for austenitic stainless steels in which copper ions are added to a sulphuric-acid solution. The copper ions apparently inhibit the attack on material having a chromium content over a certain critical value (about 12 per cent) but not on the metal containing lesser amounts of chromium. Thus an annealed alloy will show no attack in this solution while sensitized alloy will be attacked intergranularly where there is a chromium depletion caused by carbide formation.

With this in mind, a series of tests were made using 85 per cent phosphoric acid with varying amounts of copper ions present. The presence of very small quantities of copper in the phosphoric acid remarkably reduced the corrosive attack of the acid on the type 316 alloys. These results are shown in Table 4 and also in Fig. 10. Similar effects were found in sulphuric-acid solutions by Kiefer and Renshaw.[10]

Numerous tests were made using the copper-inhibited phos-

[10] "The Behavior of the Chromium Nickel Stainless Steels in Sulfuric Acid," by G. C. Kiefer and W. G. Renshaw, *Corrosion*, vol. 6, August, 1950, p. 235.

TABLE 3 EFFECT OF COPPER IN 25 PER CENT Cr, 20 PER CENT Ni, 3 PER CENT Mo WELD DEPOSITS

Weld	Copper Addition	Heat Treatment	Phosphoric Acid Test Results in I.P.Y. Pd. 1	Pd. 2	Pd. 3	Ave.
1	None	As welded (1)	1.51	1.49	1.52	1.50
1	None	Sensitized (2)	1.96	2.12	2.04	2.04
1	None	Stabilized (3)	1.19	1.35	1.40	1.38
2	0.27% Cu	As welded (1)	.645	.502	.554	.567
2	0.27% Cu	Sensitized (2)	.384	.520	.472	.458
2	0.27% Cu	Stabilized (3)	.313	.504	.357	.408
3	0.44% Cu	As welded (1)	.409	.435	.481	.432
3	0.44% Cu	Sensitized (2)	.420	.365	.357	.381
3	0.44% Cu	Stabilized (3)	.257	.349	.304	.309
4	0.72% Cu	As welded (1)	.349	.285	.316	.350
4	0.72% Cu	Sensitized (2)	.318	.324	.314	.321
4	0.72% Cu	Stabilized (3)	.233	.233	.276	.247
5	1.06% Cu	As welded (1)	.264	.303	.294	.287
5	1.06% Cu	Sensitized (2)	.217	.228	.262	.236
5	1.06% Cu	Stabilized (3)	.180	.186	.193	.187
6	3.00% Cu	As welded (1)	.153	.125	.122	.141
6	3.00% Cu	Sensitized (2)	.140	.127	.136	.134
6	3.00% Cu	Stabilized (3)	.099	.108	.107	.105

(1) Deposit made seven beads wide and seven layers high

(2) Sensitized at 1250°F., 2 hours, furnace cooled

(3) Stabilized at 1525°F., 2 hours, heated and cooled between 1/2" and 1/4" stainless plates.

TABLE 4 EFFECT OF COPPER IONS IN PHOSPHORIC ACID

Test Solution	Corrosion Rates I.P.Y. Pd. 1	Pd. 2	Pd. 3	Ave.
1. 85% phosphoric acid, no copper ions	2.58	2.98	2.71	2.84
2. 85% phosphoric acid, .001% Cu^{++}	.125	.095	.153	.124
3. 85% phosphoric acid, .01% Cu^{++}	.262	.197	.218	.226
4. 85% phosphoric acid, .1% Cu^{++}	.039	.047	.049	.061

Material - Low Carbon Type 316 Annealed Condition

TABLE 5 EFFECT OF SENSITIZING HEAT-TREATMENT ON MATERIALS TESTED IN COPPER-INHIBITED PHOSPHORIC ACID

Material	Test Solution	Corrosion Rates In I.P.Y. Pd. 1	Pd. 2	Pd. 3	Ave.
ELC T316	85% H_3PO_4 + 0.1% Cu^{++}	.045	.068	.087	.067
ELC T316	85% H_3PO_4 + 0.001% Cu^{++}	.129	.097	.113	.113
Stand. T316	85% H_3PO_4 + 0.1% Cu^{++}	.485	.898	1.45	.978
Stand. T316	85% H_3PO_4 + 0.001% Cu^{++}	.079	.079	.043	.067

All Material Sensitized at 1250°F. for 2 Hours Air Cooled

It is noted that the corrosion resistance of the low-carbon type 316 alloy was not impaired by the sensitizing treatment. The standard type 316 alloy did not perform as well with the phosphoric acid containing 0.1 per cent Cu^{++} as with the acid with the 0.001 per cent Cu^{++}. It was noted on this particular test using the acid with the 0.1 per cent Cu^{++} that there was an excessive plating of copper on the specimen which appeared to peel

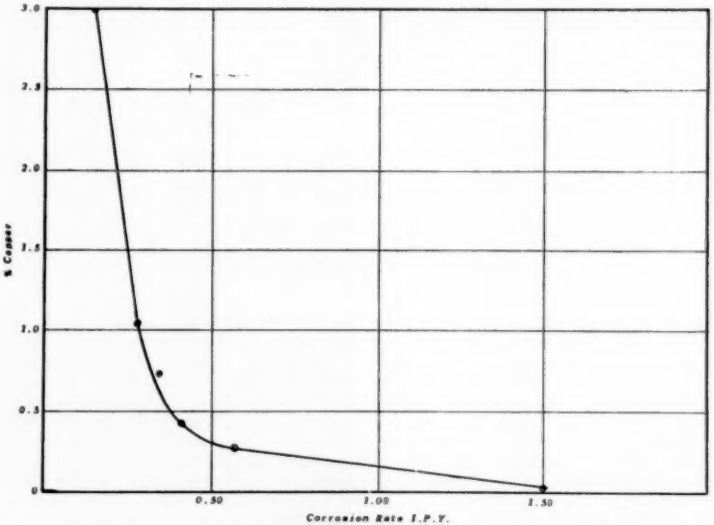

FIG. 9 EFFECT OF COPPER IN 25 CR, 20 NI, 3 MO WELD DEPOSITS ON CORROSION RESISTANCE AS DETERMINED BY PHOSPHORIC-ACID TEST

phoric-acid solutions on sensitized materials. These were made to determine if the copper ions were effective in inhibiting the attack on severely sensitized alloy. For these tests the low-carbon and standard type 316 alloys were used. The alloys were sensitized at 1250 F for 2 hr. The test results are shown in Table 5.

off at intervals. This action was not noticed on other specimens using this acid solution.

The success of the copper-inhibited phosphoric acid on type 316 alloys led to tests on other materials. One test using type 304 material showed that only the acid containing 0.1 per cent Cu^{++} was successful in producing an inhibiting action. This

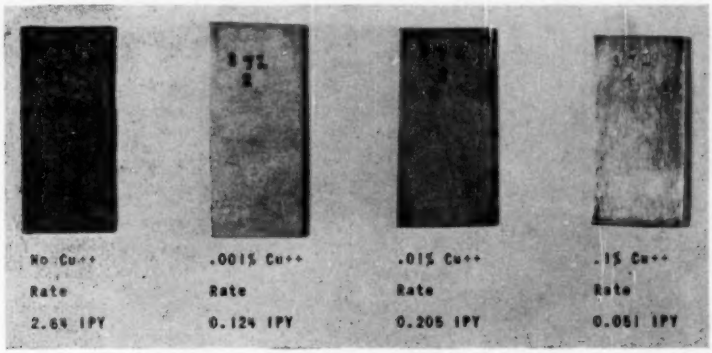

FIG. 10 PHOSPHORIC-ACID CORROSION TESTS IN BOILING 85 PER CENT PHOSPHORIC ACID WITH INDICATED AMOUNTS OF COPPER IONS
(ELC type 316 alloy with very low residual copper.)

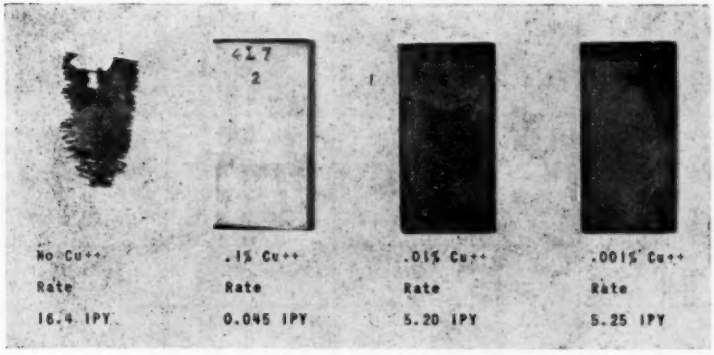

FIG. 11 PHOSPHORIC-ACID CORROSION TESTS IN BOILING 85 PER CENT PHOSPHORIC ACID WITH INDICATED AMOUNTS OF COPPER IONS
(ELC type 304 alloy with very low residual copper.)

TABLE 6 EFFECT OF COPPER-INHIBITED PHOSPHORIC CID ON TYPE 304 MATERIAL

Test Solution	Corrosion Rates In I.P.Y. Pd. 1	Pd. 2	Pd. 3	Ave.
1. 85% H_3PO_4 + 0.1% Cu^{++}	.058	.043	.038	.048
2. 85% H_3PO_4 + 0.01% Cu^{++}	5.25	--	--	--
3. 85% H_3PO_4 + 0.001% Cu^{++}	5.20	--	--	--
4. 85% H_3PO_4 + 0.0001% Cu^{++}	0.30	--	--	--

Material - ELC Type 304 - Annealed Condition

test showed the results listed in Table 6 and also in Fig. 11.

Other metallic ions were added to the phosphoric acid to determine whether they would have the same inhibiting action displayed by copper. Silver, cadmium, and tin ions were added to phosphoric-acid solutions and tested with type 316 alloy. Only silver displayed an inhibiting action similar to copper. Cadmium and tin did not show any inhibiting effect, Fig. 12.

Since copper was shown to be a powerful inhibiting agent in phosphoric acid, it was important to investigate the effect of copper in the test solution during a 24-hr period. To do this three alloy heats were chosen; (*a*) Carpenter No. 20 heat containing 3.36 per cent copper, (*b*) an ELC type 316 heat containing 0.25 per cent copper, and (*c*) an ELC type 316 heat containing 0.04 per cent copper. Specimens were prepared from each alloy and tested in the annealed condition. For this investigation the 85 per cent phosphoric acid was brought to the boiling point before placing the specimen in the solution. At the end of a predetermined time each specimen was taken out of the test solution, washed in warm water, dried, and weighed as quickly as possible and immediately replaced in the same boiling test solution.

The times of exposure to boiling acid were selected as one 5-min period, one 10-min period, one 15-min period, and one 30-min period. Then separate 1-hr periods were followed for a total of 5 or 6 hr. This was finally followed by one 17 or 18-hr period to finish up, giving a total of 24 hr.

On preliminary tests it was found that when the interval between weighings was too long, erratic corrosion rates resulted. It appeared that this was caused by a change in the surface condition of the specimens during the time they were exposed to air. The usual time consumed during the weighing intervals did not exceed 5 min.

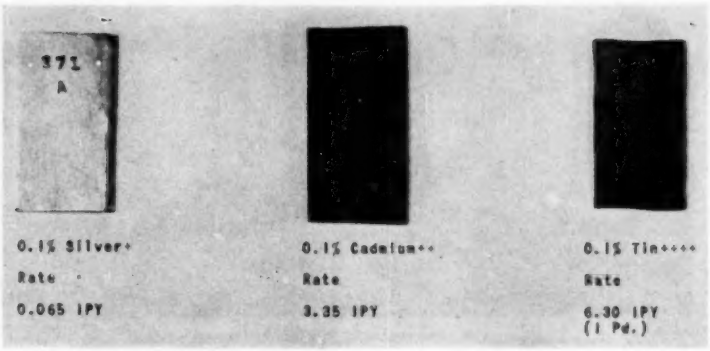

FIG. 12 PHOSPHORIC-ACID CORROSION TESTS IN BOILING 85 PER CENT PHOSPHORIC ACID WITH INDICATED AMOUNT OF METALLIC IONS
(ELC type 316 material with very low residual copper.)

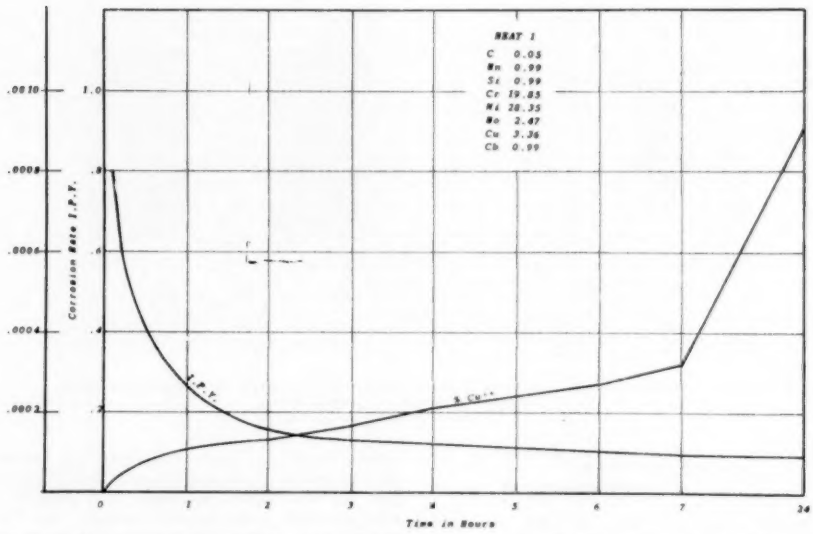

FIG. 13 CORROSION OF CARPENTER NO. 20 ALLOY—3.36 CU—IN BOILING 85 PER CENT PHOSPHORIC ACID DURING A 24-HR TEST

The copper content of these alloys is low enough to be considered in solid solution, and thus it is assumed that as a specimen dissolves, the ratio of the elements in solution is identical to the ratio of the elements in the alloy specimen.

With this procedure, the accumulated corrosion rate and copper content of the test solution were plotted for each alloy. Fig. 13 of the Carpenter No. 20 alloy shows the highest corrosion rate during the first 5 min of the test. As the copper content of the solution builds to 0.0001 per cent, the corrosion rate decreases. At about 0.00015 per cent copper in the test solution, the inhibiting action upon the phosphoric acid is apparent, and with copper in the solution between 0.00025 and 0.0009 per cent the corrosion rate is not appreciably changed. Fig. 14 of a low copper content type 316 stainless shows a remarkable decrease in corrosion rate as the copper content of the solution builds up to 0.0001 per cent. As the copper content increases up to 0.0004 per cent there is an additional decrease of the corrosion rate.

Fig. 15 of a type 316 stainless with only 0.04 per cent copper shows an increasing corrosion rate during the first hour of exposure or until the test solution builds up to 0.00005 per cent copper. As the copper content increases in the test solution up to about 0.0004 per cent, there is a continuous decrease of the corrosion rate.

It will be observed from these data that there appears to be a trend in the corrosion-rate results, depending on the copper content in the solution as well as the copper in the alloy. For an

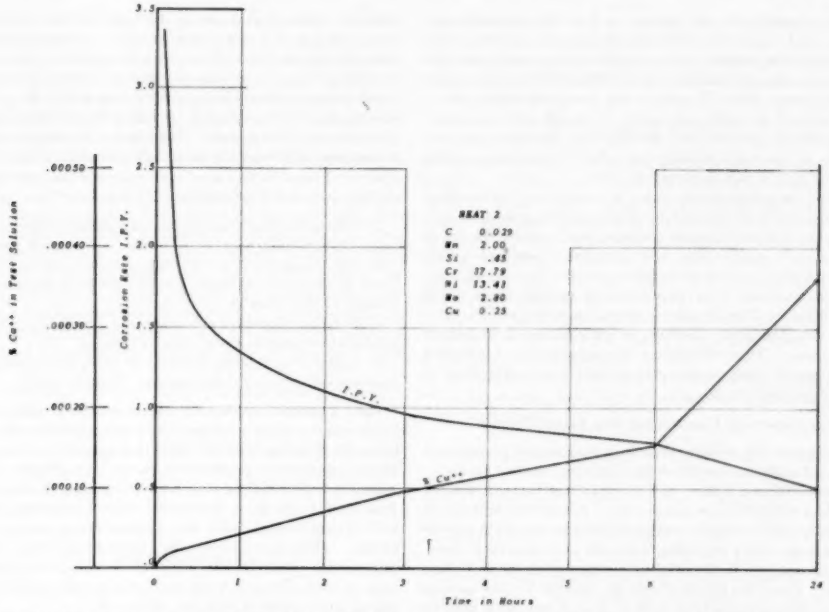

FIG. 14 CORROSION OF ELC T316 ALLOY—0.25 CU—IN BOILING 85 PER CENT PHOSPHORIC ACID DURING A 24-HR TEST

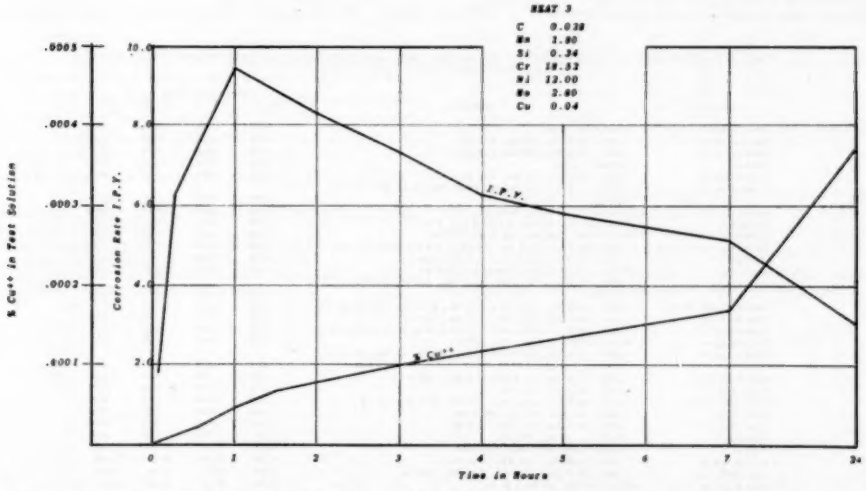

FIG. 15 CORROSION OF ELC T316 ALLOY—0.04 CU—IN BOILING 85 PER CENT PHOSPHORIC ACID DURING A 24-HR TEST

alloy with about 3 per cent copper, we find that approximately 0.0003 per cent copper is needed in the phosphoric acid to produce effective inhibiting action. For an alloy with about $^1/_4$ per cent copper, it is estimated that between 0.0005–0.001 per cent copper in the phosphoric acid will produce the lowest corrosion rates.

The effects of the inhibiting action of copper ions in aqueous acid solutions as well as other metallic ions should be explored more fully as these undoubtedly will affect the corrosion results in sulphuric acid as well as phosphoric acid.

From the foregoing observations, it is apparent that copper-bearing stainless alloys will exhibit high corrosion resistance only in service applications in which corrosion products are allowed to accumulate. In applications where corrosion products cannot be accumulated, it is quite reasonable to expect that the ultimate in corrosion resistance from copper-bearing stainless alloys would not be obtained. This fact also limits the accuracy of this corrosion test, but the same condition is inherent in all laboratory corrosion tests. This emphasizes the importance of selecting materials based upon actual service conditions rather than in laboratory corrosion tests.

Comparison of Laboratory and Field Testing

In the paper so far we have described a laboratory phosphoric-acid test and many factors which may influence the test results.

As was mentioned before, a laboratory test cannot select a material best suited for a certain process. It must be remembered that the only way a material can be selected for a certain process is by experience or by exploring materials in a controlled corrosion-testing program in the original equipment or in pilot-plant operations. Once the alloys which are suitable for the process are known, the variation from heat to heat of any alloy may be determined by the laboratory test.

It was noted that in the manufacture of phosphoric acid where very high concentrations of acid are handled, Hastelloy A, B, C, and D, tantalum, Chlorimet 2, La Bour R-55, and sterling silver were satisfactory materials. However, in a catalytic process using 65 per cent phosphoric acid under pressures of 1000 to 1350 psi and temperatures in the range of 500 to 600 F, only silver, copper, and some copper alloys were satisfactory. In a chemical process in which corrosion samples were exposed, it was found that copper and some of the copper alloys were not corrosion-resistant. However, type 316, 430, and a 27 per cent Cr alloy appeared to be very good. Hastelloy B alloy had only a fair resistance to corrosion. Thus, in these three processes where phosphoric acid was the principal corrodent, there was little agreement in selecting a good corrosion-resistant material. Some of the reasons for the disagreement are as follows:

1 Concentration, temperature, and pressure of the phosphoric-acid solutions influences the corrosion resistance of the material.

2 Small quantities of reducing mineral acids and the occurrence of formation of organic acids influences the corrosion resistance of the material.

3 Stagnant liquids or solids in contact with the surface of the material can cause localized attack or pitting.

4 Agitated or flowing solutions of phosphoric acid can cause a serious problem of erosion together with corrosion.

Field inspection reports on several company fabricated alloy-lined vessels, which were used in a gas-polymerization process, indicated that the type 317 alloy was subject to pitting attack. This type of attack probably was caused by a tarry or cokelike residue on the stainless alloy which is formed during operation. This residue acts like a sponge and tends to hold the phosphoric acid in close contact with the stainless lining, causing localized attack. These pits were repaired by welding during the inspection period. Later in the life of these vessels an intergranular type of failure became a serious factor which eventually caused vessels to be removed from this operation.

In the 7 years these vessels were in service, the only major change made was in the bottom heads. The original lining of $^7/_{64}$ in. thickness in the bottom head of each vessel was replaced at the end of the first year with a much thicker alloy lining. During the 7 years, the vessels were in operation 80 per cent of the total time. The 20 per cent time lost includes regeneration and re-

TABLE 7 CORROSION RESISTANCE OF SOME METALS TESTED IN BOILING 85 PER CENT PHOSPHORIC-ACID SOLUTION

Material	Analysis	Penetration Rate I.P.Y. Pd. 1	Pd. 2	Pd. 3	Ave.
Tantalum	Tantalum, pure	.000	.000	.000	.000
Hastelloy B	.10C, 64.5 Ni, 30 Mo, 5.0 Fe	.004	.006	.002	.004
Hastelloy B	.09C, 66.3 Ni, 28 Mo, 4.7 Fe	.003	.004	.004	.004
Silver	Silver, pure	.010	.006	.005	.007
Hastelloy B	.05C, 64.9 Ni, 28 Mo, 5.2 Fe	.047	.058	.047	.051
Carpenter 20	.05C, 1.08 Si, 20.30 Cr, 29.71 Ni, 2.38 Mo, 3.4 Cu, 1.0 Cb	.061	.050	.051	.054
Ampco 8	91.08 Cu, 2.0 Fe, 6.62 Al	.059	.058	.082	.066
Illium G	*N.A. 24 Cr, 56 Ni, 4 Mo, 8 Cu, 2 W	.086	.081	.074	.080
Durimen	*N.A. .09C, .35 Mn, 14.5 Si, 85 Fe	.099	.053	.090	.085
U731 (German alloy)	.07C, 23 Si, 14.05 Cr, 18.48 Ni, 4.06 Mo, 2.62 Cu	.094	.103	.070	.089
Durimet 7	.07C, 19.0 Cr, 23.0 Ni, 3.5 Mo, 1.0 Cu	.133	.110	.136	.126
Worthite	*N.A. 19 Cr, 24 Ni, 3 Mo, 2 Cu, 3 Si	.147	.109	.130	.129
Hastelloy C	.07C, 17.0 Cr, 52.5 Ni, 16.7 Mo, 4.9 W, 6.0 Fe, 1.6 Co	.114	.156	.130	.133
Armco 17-14 Cu Mo	.07C, 16.3 Cr, 14.8 Ni, 2.5 Mo, 2.1 Cu, .56 Cb, .3 Ti	.142	.130	.134	.135
Crucible 80	.07C, 20.9 Cr, 13.8 Ni, 1.2 Mo, 1.2 Cu	.171	.157	.140	.156
Hastelloy C	.06C, 17.2 Cr, 53.4 Ni, 17.2 Mo, 4.3 W, 5.0 Fe, .4 Co	.138	.129	.204	.180
Hastelloy D	*N.A. 85 Ni, 3 Cu, 2 Al, 10 Si	.279	.156	.091	.175
Hastelloy F	.08C, 21.9 Cr, 44 Ni, 6.3 Mo, .7 Ta, .4 Co, 23.5 Fe, .13 Cu, 1.4 Cb	.284	.225	.347	.287
KLC Type 316	.03C, 17.7 Cr, 14.2 Ni, 2.0 Mo, .32 Cu	.437	.432	.477	.448
Type 446	.18C, 26.2 Cr, .74 Ni	.175	.272	.949	.465
Crucible 90 Cb	.07C, 23.9 Cr, 12.6 Ni, 1.3 Mo, 1.2 Cu, .8 Cb	.290	.506	.610	.469
Type 430	.04C, .49 Mn, .37 Si, 16.6 Cr	.626	.670	.855	.735
Type 317	.07C, 18.6 Cr, 10.6 Ni, 3.3 Mo	.963	.882	.939	.928
Everdur	95.3 Cu, .8 Mn, 3.5 Si	1.18	.710	.980	.956
Copper	Copper ASTM B152-49T Type DHP	2.38	2.15	1.30	1.95
Carpenter 3	.21C, 19.6 Cr, .23 Ni, 1.34 Cu	1.35	1.47	1.43	1.42
KLC Type 310	.03C, 18.1 Cr, 11.4 Ni, 2.4 Mo, .02 Cu	1.62	1.57	1.79	1.66
Hastelloy A	*N.A. 59 Ni, 20 Mo, 20 Fe	1.25	3.16	3.06	2.49
Monel	.07C, 1.0 Mn, 66.9 Ni, 29.7 Cu, 2.1 Fe	4.45	4.60	--	--
Nickel A	98.9 Ni, 0.2 Fe	5.95	4.88	4.34	5.06
Type 329	.32C, 24.6 Cr, 2.4 Ni, 1.3 Mo	9.75	--	--	--
Nickel L	.03C Max, 99 Ni Min, .50 Fe Max	14.1	--	--	--
Inconel A	.05C, 14.6 Cr, 78.1 Ni, 6.6 Fe	14.6	--	--	--
Inconel B	.04C, 17.0 Cr, 75.0 Ni, 7.3 Fe	21.4	--	--	--
Type 405	.03C, .45 Mn, .32 Si, 12.3 Cr, .3 Al	78.0	--	--	--

*N.A., Nominal Analysis

placement of the catalyst, inspections, and necessary repairs.

From this experience, it is noted that the corrosion resistance of the material in this process was considerably better than that which was indicated by the phosphoric-acid test. It is believed that recent vessels fabricated of the extra low-carbon type 316 will display better corrosion resistance to phosphoric-acid attack, and also greatly lessen the possibility of intergranular attack which caused the ultimate failure of the alloy with the higher carbon contents.

Table 7 presents a list of metals which were tested in our laboratory in accordance with the proposed phosphoric-acid test. It was noted that considerable differences were found in the corrosion resistance of heats in a particular type of metal. This stresses the need of a standard test. From our experience we found that the corrosion rates obtained by the phosphoric-acid test are very much higher than those obtained on the same materials exposed to the conditions occurring in various processes. In this respect the phosphoric-acid test must be considered as an accelerated laboratory test.

It was noted that there was good agreement between the tests made with superphosphoric acid (85 per cent P_2O_5) at 485 F made at the TVA pilot plant and our boiling 85 per cent phosphoric-acid test. This agreement existed on the highly resistant materials. The lower resistant materials showed less agreement which is probably because of the difference found in the various heats of a particular alloy.

Discussion

M. G. FONTANA.[11] This paper emphasizes the fact that careful manipulation and good technique are mandatory in order to obtain reliable data from corrosion tests. The authors also point out the fact that a laboratory test in CP acid does not necessarily predict field performance under actual operating conditions. These two points are often overlooked.

The inhibiting effect of the copper ion in the acid and the improved resistance of copper-bearing 316 alloys in phosphoric acid are of interest. This is one of the reasons why alloys like Durimet 20 are superior to the 18–8-type steels for phosphoric acid. The copper ion in sulphuric acid shows strong inhibiting effects even under severe erosion-corrosion conditions as shown by Fontana and Luce,[12] and Fontana.[13] The superior corrosion resistance of chemical lead as compared to pure lead is due to approximately 0.06 per cent copper in the former.

Arsenic ions may also show similar inhibiting effects in phosphoric acid but the presence of this element would be undesirable in some of the uses for the finished acid.

A few remarks by the authors on the use of the "standard" nitric-acid test for materials for handling phosphoric acid would be of interest.

AUTHORS' CLOSURE

We thank Professor Fontana for information given in his discussion. We have not investigated arsenic ions as a possible inhibiting element in phosphoric acid. It appears that metals in Group 1B in the Periodic Table are effective inhibiting elements in phosphoric acid. One metal, cadmium, in Group 2 B was found to be ineffectual. There is no doubt that other elements or groups of elements may be found, but apparently little work has been done in this field.

The request for information on the use of the standard nitric-acid test for materials for handling phosphoric acid is summarized in the following tests.

Two heats of low-carbon type 316 from different manufacturers gave the results, Table 8, in the standard nitric-acid and phosphoric-acid tests.

TABLE 8 RATES IN IPY

Heat	Pd 1	Pd 2	Pd 3	Pd 4	Pd 5	Avg.
Nitric acid	.008	.008	.009	.010	.009	.009
Phosphoric acid	.427	.432	.477	—	—	.445
Heat y						
Nitric acid	.007	.006	.008	.009	.011	.008
Phosphoric acid	1.60	1.68	1.50	—	—	1.59

The two heats are similar in chemistry except for the residual copper content. As is seen, the nitric-acid test does not disclose any difference in corrosion resistance of these materials.

Tests made on Carpenter No. 20 alloy show that the nitric-acid test is more searching in so far as the effects of various heat-treatments are concerned. See Table 9.

TABLE 9 CARPENTER NO. 20 ALLOY—RATES IN IPY

		Pd 1	Pd 2	Pd 3	Pd 4	Pd 5	Avg.
Condition 1	Nitric acid	.009	.009	.011	.010	.010	.010
	Phosphoric acid	.088	.112	.070	—	—	.090
Condition 2	Nitric acid	.010	.016	.023	.034	.034	.023
	Phosphoric acid	.084	.092	.139	—	—	.105
Condition 3	Nitric acid	.043	.149	.329	—	—	—
	Phosphoric acid	.079	.094	.062	—	—	.078

Condition 1, as received.
Condition 2, nitric acid, 1100 F, 2 hr. Phosphoric acid, 1000 F, 3 hr.
Condition 3, 1625 F, 2 hr. Heated and cooled between 1/2 in. and 1/4 in. stainless plates.

Here again we see no relationship between the two tests. The nitric-acid test under conditions which show the higher rates, exhibits an attack which is intergranular in nature and the specimen "sugars." In the phosphoric-acid test the attack is general and apparently insensitive to the conditions causing the intergranular weakness as found by the nitric-acid test.

---

[11] Professor and Chairman, Department of Metallurgy, The Ohio State University, Columbus, Ohio.

[12] "Erosion-Corrosion of Metals and Alloys," by M. G. Fontana and W. A. Luce, *Corrosion*, vol. 5, 1949, pp. 189–193.

[13] "Erosion-Corrosion," by M. G. Fontana, *Industrial and Engineering Chemistry*, vol. 39, 1947, pp. 87A–88A.

Coal Sampling by Large-Increment Weights

By B. A. LANDRY[1] and W. W. ANDERSON[2]

A sampling experiment is described that was aimed at determining the variance in percentage ash of large-weight, single-increment samples of an Indiana coal. The observed variance is broken down into its component parts which are calculated from the data obtained. Results show that for increments of large weight, such as are taken by mechanical samplers, at large steam-generating stations, relatively few would be required, for the coal studied, to obtain a gross sample meeting present accuracy standards. The suggestion is made that studies on other coals should be made to confirm these findings which, if generally true, may lead to an upward revision of standards of accuracy in view of the practicability of taking larger numbers of increments mechanically.

Introduction

THE growing use of coal for steam and power generation, and the growing sale of these two forms of energy to large-scale distributors or consumers, coupled with the frequent changes that have taken place in the price of coal, have not reduced but have increased the necessity for acceptable accuracy in coal sampling. Contracts between steam-generating stations and customers now often contain a clause for adjusting sale price to the cost of the equivalent heat input to the boiler furnace. The calorific value of the fuel is an important factor in calculating heat input and, therefore, the accuracy with which the analysis of the sample represents the heating value of the coal burned is equally important.

The work of Morrow and Proctor[3] has demonstrated that the analysis of a sample of coal which is acceptably accurate for average ash content is also acceptably accurate for determining average calorific value. Hence all coal-sampling investigations, whether experimental or theoretical, have been limited generally to studies of the factors which affect the variability of ash content among coals and how best to cope with them in sampling. Sampling specifications that have resulted from such work, however, since they specify increments of small weight, can be said to belong still to the hand-shovel age of coal handling and to indicate a lack of recognition that the large daily tonnages of coal handled by modern steam plants, in effect, require mechanical sampling devices. Since these devices must take increments cutting completely across the stream of large cross section of rapidly moving coal being fed to pulverizers or stokers, the increments taken are necessarily of large weights, much larger than present specifications call for.

It has been quite generally accepted that sampling by larger increment weights would reduce the number of increments required to obtain a gross sample of acceptable accuracy. It also has been known that the reduction in the number of increments would not compensate for the increased weight of increment, so that the final gross sample obtained would be of larger weight. However, it was believed that mechanical methods of crushing the gross sample, before subdivision, would make it relatively easy to handle this part of the work of sampling.

The main problem was, therefore, that of ascertaining the exact extent to which the number of increments could be decreased, as the weight of increment was increased. The results of the experimental investigation described in this paper show that, after a certain weight of increment has been reached, there is no statistical gain in increasing weight further and, consequently, that a minimum number of increments must be taken, in any event, to compose the gross sample. On the other hand, it appears that this minimum number is relatively small, as compared with present specifications. This may make it feasible eventually to increase, above present nominal levels, the standards of so-called acceptable accuracy when sampling specifications for mechanical samplers are established.

This paper gives an account of an extensive sampling investigation made at the tipple of the Enos Coal Mining Company, in Pike County, Ind., in April, 1950, to determine the variance in percentage ash of samples of one increment, each weighing, approximately, 14, 40, 60, 80, and 100 lb. Thirty samples of each weight were taken, and each was reduced and analyzed separately. In addition, sixty increments of 50 lb each were taken for size-consist determination of the composite, and for float-and-sink separation, at seven specific gravities, of the seven size ranges obtained by screening. The set of data presented is believed to be more extensive than any yet made available on this subject for a single coal, and thus supplies long-needed missing data[4] on coal sampling. It is hoped that similar investigations can be carried on at the tipple of coal producers in various districts to obtain, on a wider basis, the sampling characteristics of United States coals.

Sampling Procedure

Mining and Tipple Operations. The coal used for this investigation is the product of strip mining in the Indiana No. 5 bed. The thickness of bed averages 4½ ft and that of the overburden, consisting of clay, shale, and limestone, averages 45 ft; a layer of black slate 1 to 3 in. thick lies immediately above the coal.

Coal is mined at five sites separated by a maximum distance of 8 miles and transported to the tipple by truck or by electric train. All coal is dumped into a common surge pit of large capacity in which considerable opportunity for mixing is afforded as the pieces roll and slide from various directions toward the bottom outlet. The discharged run-of-mine is then conveyed, at the rate of 900 tons per hr, to shaker screens giving nominal separation of the 2 × 0 in. size, which is conveyed to the rescreening plant on a rubber belt 36 in. wide traveling at the rate of 600 fpm.

Sampling Operations. All samples were collected from this belt. To avoid sampling bias, the belt was stopped for each of the thirty sampling operations, which were performed on the stationary belt as follows:

---

[1] Supervisor, Fuels Research, Battelle Memorial Institute, Columbus, Ohio. Mem. ASME.

[2] Technical Director, Commercial Testing and Engineering Company, Chicago, Ill.

[3] "Variables in Coal Sampling," by J. B. Morrow and C. P. Proctor, Trans. AIME, vol. 119, 1936, pp. 227–276.

Contributed by the Fuels Division of The American Society of Mechanical Engineers and presented at the Joint AIME-ASME Fuels Conference, Cleveland, Ohio, October 24–25, 1950.

Note: Statements and opinions advanced in papers are to be understood as individual expressions of their authors and not those of the Society. Manuscript received at ASME Headquarters, November 24, 1950.

[4] "The Missing Data on Coal Sampling," by B. A. Landry, Trans. ASME, vol. 67, 1945, pp. 78–79.

TABLE 1 WIDTH BETWEEN DIVIDERS AND CORRESPONDING APPROXIMATE WEIGHT OF SAMPLES OF ONE INCREMENT EACH

Section no.	Width between dividers, in.	Approximate weight of sample, lb	Distance between center line of sections, ft
1	5	14	
			5
2	18.5	50	
			4
3	14	40	
			4
4	21.5	60	
			5.5
5	28.5	80	
			5
6	18.5	50	
			4
7	36	100	

(*a*) Seven pairs of vertical dividers, each set a certain distance apart, were sliced through the coal ribbon, which was approximately 28 in. wide, down to the face of the belt.

(*b*) The material between each pair of dividers was raked and swept off the belt into receptacles.

(*c*) The dividers then were removed and the belt was started again.

Table 1 lists for each of the seven sections, in sampling order, the widths between dividers for each weight of sample and gives the distance on the belt between the center line of each section. All seven samples were collected within a belt distance of about 30 ft. A maximum of six such samplings could be made in one day, although five was the rule, and on the first and last days only two were made. Sampling dates were April 10, 11, 12, 13, 17 18, and 19, 1950.

Reduction of Samples for Ash Determination. Each of the 150 samples of one increment obtained for ash determination was weighed and then reduced to a laboratory pulp as follows:

(*a*) Each sample was crushed in its entirety, at the tipple, through a 10 × 15-in. hammer mill equipped with a $^3/_{16}$-in. round-hole perforated steel plate. By successive rifflings, a subsample of not less than $1^1/_4$ lb was obtained and shipped to the Chicago laboratory of Commercial Testing and Engineering Co.

(*b*) The entire amount of subsample received was crushed through a 7 × 6 in. hammer mill equipped with a $^1/_{16}$-in. round-hole perforated plate. A subsample of not less than 200 grams was obtained by successive rifflings.

(*c*) The entire amount of subsample was then pulverized through a Raymond hammer mill. The oversize on a 60-mesh screen was reduced to minus 60 mesh on a hard steel buckboard. A minimum of 50 grams was then riffled out for laboratory pulp. Dry-ash determinations were then made according to the ASTM method. Duplicate analyses were made from each pulp.

Results of Ash Determinations. Table 2 gives, for the thirty samples of five different weights taken, the determined weight of each sample (of one increment each), and the average of duplicate determinations of ash percentage. The average weights of samples and the grand average ash percentages are also shown in the table.

Screening of Composite Sample. As mentioned earlier, two 50-lb samples (of one increment each) were taken at each of the thirty stops of the belt. The compositive sample obtained weighed 3049.2 lb. The entire composite was screened over a $1^1/_2$-in. round-hole screen. The minus $1^1/_2$-in. material was riffled once, and one portion was screened successively over a $^3/_4$-in. and a $^5/_{16}$-in. round-hole screen. The minus $^5/_{16}$-in. material was riffled three times, and one remaining portion was screened successively on 10, 28, and 48-mesh (Tyler) screens. Table 3 summarizes the screening data obtained.

Gravity-Consist. All of the coal retained on the successive screens at the various stages of screening was later subjected to gravity separation, each cut being analyzed ultimately for its average ash content. Table 4 summarizes these data, and also gives the average ash percentage for each size interval; this average, of course, was obtained after weighting the percentage ash of each fraction by the relative weight of the fraction.

TABLE 3 SUMMARY OF SCREENING DATA

Size interval (round hole or Tyler), inch or mesh	First stage, lb	Second stage, lb	Third stage, grams	Weight per cent	Cumulative weight retained, per cent
Nom. 2 × $1^1/_2$ in.	257.3			8.5	8.5
$1^1/_2$ × $^3/_4$ in.		523.6		35.4	43.9
$^3/_4$ × $^5/_{16}$ in.		411.0		27.7	71.6
$^5/_{16}$ in. × 10 M			14,305	16.1	87.7
10 × 28 M			5,013	5.7	93.4
28 × 48 M			2,057	2.3	95.7
48 M × 0			3,811	4.3	
				100.0	

TABLE 2 WEIGHTS AND DRY-ASH CONTENTS OF SAMPLES OF ONE INCREMENT EACH

(Ash percentages are the average of duplicate determinations)

Approximate weight of sample, lb									
14		40		60		80		100	
Weight, lb	Ash, per cent	Weight, lb	Ash, per cent	Weight, lb	Ash, per cent	Weight, lb	Ash, per cent	Weight, lb	Ash, per cent
12.9	10.8	37.2	11.3	59.3	11.7	79.2	11.5	99.9	11.6
16.0	13.6	43.0	14.2	62.2	13.5	82.8	13.6	106.8	13.4
12.7	13.7	34.6	12.1	54.5	12.8	73.0	12.4	93.1	12.4
13.2	12.1	39.6	11.8	56.5	12.7	82.1	12.4	96.9	12.0
12.2	9.9	36.1	10.3	50.9	10.1	70.9	10.2	91.9	10.8
14.4	12.7	41.6	12.2	61.7	12.7	84.8	12.5	102.1	12.8
15.4	12.3	44.6	12.1	65.2	11.8	86.8	12.1	108.8	12.1
15.3	12.1	44.6	11.2	66.4	11.1	84.4	11.2	111.8	11.6
15.3	12.7	42.4	11.7	62.9	12.2	84.5	12.0	106.0	11.9
13.1	11.8	32.9	12.5	55.7	12.1	71.8	12.5	95.5	12.1
14.1	13.4	40.2	13.4	59.1	13.5	77.2	13.5	99.4	13.5
14.5	10.8	40.6	11.2	60.1	11.2	82.4	11.6	103.8	11.0
14.4	12.4	42.3	12.4	63.3	12.4	86.6	12.3	110.2	12.7
14.2	13.2	38.1	12.8	66.1	13.1	88.0	12.9	110.3	12.7
15.6	13.7	40.2	13.7	66.8	13.2	85.8	12.7	105.4	12.9
15.2	12.2	43.1	11.9	67.4	12.4	91.9	12.7	114.2	11.8
14.4	12.5	42.1	12.5	62.9	12.9	82.4	12.9	105.4	12.7
13.9	12.6	45.2	12.7	65.4	13.0	83.0	13.1	109.8	12.9
14.8	13.4	40.4	13.3	64.6	13.2	84.8	12.8	107.3	13.3
13.2	14.0	38.4	13.9	64.9	13.2	81.7	13.5	100.9	13.0
12.7	13.2	38.3	13.1	55.4	12.8	74.1	13.8	92.9	13.2
11.8	14.4	36.1	14.3	56.6	14.6	74.9	14.9	98.2	15.0
15.6	14.3	42.4	13.5	59.8	13.8	78.9	13.8	102.4	14.5
14.7	13.5	43.8	12.8	67.7	13.0	88.9	12.1	107.4	12.8
13.1	13.2	38.6	14.0	54.9	13.6	73.2	14.5	95.9	14.0
13.6	12.1	39.2	13.0	65.1	12.6	85.9	12.8	110.1	12.8
11.1	10.5	36.2	10.3	54.7	10.9	76.9	10.9	101.2	10.8
14.5	12.3	42.7	13.3	65.2	13.6	88.1	13.6	111.5	13.3
13.6	12.6	40.8	12.4	67.0	12.6	86.8	12.5	105.2	12.4
12.6	12.5	35.2	11.8	56.7	12.2	74.9	12.2	95.2	12.0
Avg. 13.9	12.6	40.0	12.5	61.3	12.6	81.6	12.6	103.3	12.6

TABLE 4 SUMMARY OF FLOAT-AND-SINK DATA

Specific gravity		Size interval, in. or Tyler mesh (M) — Weight, grams											
		Nom. 2 × 1½		1½ × ¾		¾ × ⅜		⅜ × 10 M		10 × 28 M		28 × 48 M		48 M × 0	
		114,585.6		235,951.9		187,232.6		14,280.2		4,998.1		2,043.6		1,814.1	
Sink	Float	Weight, per cent	Ash, per cent	Weight, per cent	Ash, per cent	Weight, per cent	Ash, per cent	Weight, per cent	Ash, per cent	Weight, per cent	Ash, per cent	Weight, per cent	Ash, per cent	Weight, per cent	Ash, per cent
	1.35	87.1	7.5	85.3	7.2	82.8	6.8	75.9	5.8	60.9	4.0	39.5	3.4	15.4	3.6
1.35	1.45	6.1	15.1	7.8	14.7	8.2	14.8	9.5	14.1	21.9	10.5	22.9	9.8	23.0	6.3
1.45	1.55	1.8	19.9	1.9	19.7	2.3	21.2	3.8	20.6	6.9	18.4	7.6	18.0	15.9	11.8
1.55	1.65	0.8	24.9	1.0	24.7	1.0	27.6	1.5	27.8	2.9	27.3	3.7	26.5	12.6	12.2
1.65	1.80	1.0	34.5	1.2	33.9	1.2	35.9	1.4	36.3	2.1	36.9	3.1	36.4	6.5	23.1
1.80	1.95	0.6	39.4	0.6	41.4	0.8	44.8	1.3	44.3	1.9	46.5	3.0	46.7	3.9	41.5
1.95	2.17	0.5	39.0	0.5	45.9	0.6	50.1	1.1	53.7	1.9	56.5	3.2	57.2	4.1	54.6
2.17		2.1	67.3	1.7	65.4	3.1	63.0	5.5	67.5	11.5	73.5	17.0	74.9	18.6	70.8
Total		100.0		100.0		100.0		100.0		100.0		100.0		100.0	
Average			10.2		9.9		10.7		12.3		17.6		23.9		24.0

Statistical Treatment of Data

Calculation of Variance of Samples. The variance in the percentage ash for each group of equal nominal weight of sample was calculated from the data listed in Table 1 by means of the standard formula

$$\sigma^2 = \frac{\Sigma(y_i)^2}{M} - \left(\frac{\Sigma y_i}{M}\right)^2 \quad \ldots\ldots\ldots\ldots [1]$$

where σ^2 is the observed variance, or (standard deviation)^2, for samples of a given weight, Σ is the summation sign, y_i refers to the percentage ash of each sample, and M is the number of samples of each weight taken, 30 in this instance. The summation limits are, therefore, from 1 to 30. Table 5 gives the variances

TABLE 5 DETERMINED VARIANCE OF PERCENTAGE ASH OF SAMPLES OF ONE INCREMENT EACH

Average weight of sample, lb	Variance, (standard deviation)^2
13.9	1.144
40.0	1.096
61.3	0.884
81.6	1.001
103.3	0.948

calculated by Equation [1] for each group of samples and also the average weights of these samples from Table 1. The tabulated results show that, although the observed variances are all of the same order of magnitude, yet there was a slight decrease in the variance with increase in weight of the one-increment samples. The fact that the result for the samples of average weight of 61.3 lb is out of line suggests that more than thirty samples, say, at the least, thirty-six samples, should have been taken to give a lower value of the standard error; in other words, with a number of single-increment samples larger than thirty, this point would probably have fallen in line.

The question of greater importance, in so far as the theory of coal sampling is concerned, is to investigate the nature of the statistical causes that led to the results of Table 5.

General Discussion on the Variance of Samples of One Increment. It is now generally agreed that the observed variance in percentage ash of samples of one increment is the sum of three variances, as follows:

(*a*) The variance which reflects how well any one sample of one increment represents the average ash of the "small" region of the lot of coal from which the increment was taken.[4, 5, 6, 7] This variance depends upon the variability in percentage ash of the individual pieces in the region, and decreases with increase in the number of contiguous pieces taken to form the increment; in other words, this variance decreases with increase in weight of the increment.

(*b*) The variance which reflects the essential variation in average ash of successive regions in the lot of coal being sampled.[6, 7] To all intents and purposes, this variance can be considered to be independent of the weight of increment, since the alternative of taking a sufficient number of increments, in an orderly manner, over the lot of coal sampled, to form a composite gross sample of acceptable accuracy, is always to be preferred to the taking of a substantial part of the entire lot for reduction prior to analysis.

(*c*) The variance which reflects the various departures from assured accuracy resulting from riffling of the gross sample, after each stage of crushing, plus any error in analysis.[5, 6, 7]

The problem is not unlike that of sampling a large community, to determine the average income of its members, if it is assumed that a number of groups having similar incomes not only exist but tend to reside in separate subcommunities. Obviously, in such sampling:

(*a*) The number of persons interviewed in any one subcommunity should increase as incomes range over wider limits between individuals.

(*b*) A minimum number of subcommunities must be sampled to insure that enough groups will be represented to meet the accuracy desired.

(*c*) Allowances should be made for the errors made by the interviewers.

Numerical estimates of the three component variances can be made, with certain assumptions, from the data obtained in this investigation. Obviously, results will apply only to the particular coal studied. The observed variance will be considered, therefore, as the sum of three independent variances

$$\sigma_o^2 = \sigma_W^2 + \sigma_R^2 + \sigma_{ra}^2 \quad \ldots\ldots\ldots\ldots [2]$$

when σ_W^2 is the variance within subregions, due to weight of increment, σ_R^2 is the lot variance due to the variation of average ash in all subregions, and σ_{ra}^2 is the variance introduced by the operations of sample reduction and analysis.

Calculation of Variance in Subregions, Due to Weight of Increment. The calculation of this component variance will be made from the formula[8]

$$\sigma_W^2 = \sigma_{\bar{w}}^2 \left(\frac{W}{w}\right)^{a-1} \quad \ldots\ldots\ldots\ldots [3]$$

where $\sigma_{\bar{w}}^2$ represents the variance in percentage ash for pieces of average weight $\bar{w}$, W is the weight of increment, w is the weight-weighted average weight of piece, and $(a - 1)$ is an index which measures the degree to which to coal of each subregion has been mixed, from its initial segregated state in the bed, toward a random arrangement of ash of pieces resulting from mining, trans-

[5] "Fundamentals of Coal Sampling," by B. A. Landry, U. S. Bureau of Mines, Bulletin No. 454.

[6] "Memorandum to Subcommittee XIII, Committee D-5, ASTM," by W. M. Bertholf, June, 1949.

[7] "Sampling of Coal and Washery Products," by J. Visman, Fuel Economy Conference of the World Power Conference, Section A2 Paper No. 4, The Hague, Holland, 1947, 12 pp.

[8] Reference 4, p. 72.

portation, and screening operations. As a first approximation in this calculation, it has been assumed that the mixing index of the coal, at the point of sampling, was equal to —1, corresponding to a perfectly random arrangement of ash percentage of pieces in each subregion. The variance in percentage ash on a piece-by-piece basis, σ_w^2, will be calculated from the float-and-sink data, and the weight-weighted average weight of piece, $\bar{w}$, will be calculated from the size-consist data. Substituting these calculated or assumed constants in Equation [3] will thus give σ_W^2 as a function of W.

Calculation of $\sigma_{\bar{w}}^2$. In the calculation of $\sigma_{\bar{w}}^2$, two steps were followed:

(*a*) The data from the float-and-sink tests were combined to give for all size intervals the total weight floating at each gravity, and the total weight of the final sink, from which the percentage by weight of the entire coal in each fraction was calculated. The determined ash percentages in one fraction, for each size interval, were then properly weighted and averaged, this process being repeated for all fractions. These calculations would have made it possible to plot average percentage ash in each fraction against cumulative weight of coal in the successive fractions. This plot of float-and-sink variability would not, however, exhibit the variability of ash percentages in terms of the individual pieces in the coal.

(*b*) Therefore, in order to pass from cumulative weight to cumulative number of pieces, the method of conversion previously suggested[9] was then followed of recalculating the length of each step of float, after the first, by multiplying by the inverse ratio of specific gravities; thus the new length of the second step was taken as (1.35/1.45 = 0.931) times the length of step on the weight basis, and so on. The length of the final step was adjusted on the basis of a ratio of 1.35/2.5 = 0.54, on the assumption that all material would float at a gravity of 2.5.

Fig. 1 is a plot of these data and thus shows as a step curve the variability in ash content of the pieces of Enos coal. The variance corresponding to the step curve shown was calculated by known methods,[10] giving $\sigma_w^2 = 72.27$.

Calculation of $\bar{w}$. The weight-weighted average weight of piece was calculated by the method previously described[11] of finding the Rosin-Rammler representation of the size consist, converting to weight consist, to give a curve of cumulative per cent passing against weight of piece, and performing a series integration to give the area between the curve and the vertical axis. The successive steps of this method will now be described.

Size-Consist Studies. Fig. 2 is a Bennett diagram on which curve A is a plot of the cumulative percentage retained from the screen analysis given in Table 3. It is seen that curve A bends upward asymptotically to a vertical line representing the size of the largest piece present in the nominal 2 × 0-in. coal screenings. The curvature shown in curve A is typical of all such

[9] Footnote 8, pp. 72–73.

[10] Reference 5, pp. 82–83.

[11] Ibid., pp. 115–126.

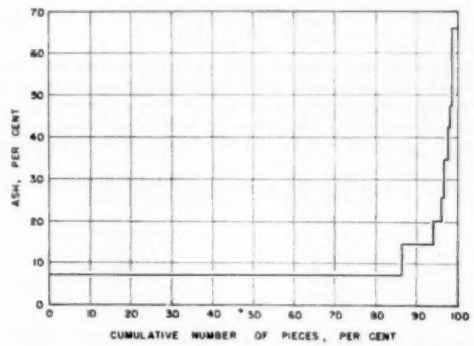

FIG. 1 FLOAT-AND-SINK ASH-VARIABILITY DATA FOR ENOS COAL

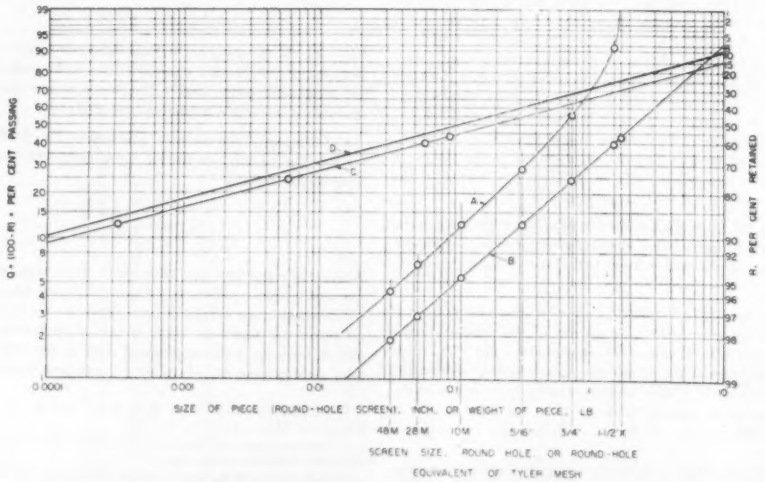

FIG. 2 BENNETT DIAGRAM REPRESENTATION OF (A) SCREEN ANALYSIS, (B) ROSIN-RAMMLER SIZE-CONSIST, (C) ROSIN-RAMMLER WEIGHT-CONSIST, ALL FOR ENOS COAL; (D) IS WEIGHT-CONSIST OF AVERAGE APPALACHIAN COAL (MALLEIS, 1933)

plottings of direct-screening data on the Bennett diagram. The diagram represents a method of linearizing the Rosin-Rammler equation

$$R = 100\, e^{-bx^n} \quad \ldots\ldots\ldots\ldots\ldots\ldots [4]$$

where R is the per cent retained at size x, b and n are parameters characteristic of the broken coal, and e is the base of natural logarithms. The Rosin-Rammler equation implies that pieces of all sizes, up to infinite size, are present in the broken coal. The diagram does not circumvent this difficulty; hence, since pieces larger than a certain practical size cannot be included in any screening data, these data when plotted will necessarily show the curvature of curve A.

Methods are available, however, for determining, from screening data, the percentage at which a Rosin-Rammler-represented coal must be considered to have been decapitated, that is, to have had all pieces above a certain size removed, by screening, in order that the undersize will exhibit the inner percentages obtained in a given screen analysis.

Application of one of these methods[12] to the data of curve A gave a value of 40 per cent for the percentage passing a $1^1/_2$-in. round-hole screen. Therefore it may be concluded that 60 per cent of the coal mined at Enos would be retained on the $1^1/_2$-in. screen. Moreover, since the cumulative weight passing the $1^1/_2$-in. screens was 100 — 8.5 = 91.5, the percentage passing the 2-in. (nominal) screen can be calculated to have been

$$\frac{(40)\,(100)}{91.5} = 43.7 \text{ per cent}$$

the corresponding percentage retained being 56.3.

The method mentioned also gives the values of the parameters b and n in Equation [4]. These were found to be, respectively, 0.36 and 0.86. The Rosin-Rammler size-consist expression for the Enos coal is therefore

$$R = 100\, e^{-0.36x^{0.86}} \quad \ldots\ldots\ldots\ldots\ldots\ldots [5]$$

Solving this equation for x, corresponding to $R = 56.3$, gave for x, the largest size present in the screenings, $x = 1.72$ in. (round hole). That this size is smaller than the 2-in. screen used is explained on the basis that, the coal being wet, pieces larger than this size presumably had enough fines sticking to them that they could not pass through a 2-in. round hole, particularly at the high speed at which the coal moved over the screens.

Curve B in Fig. 2 is a plot of Equation [5], the generalized Rosin-Rammler-represented coal, which probably represents quite accurately the size consist of the run-of-mine at Enos. Size consists, corresponding to any preassigned decapitation size can, of course, be calculated easily from curve B, thus avoiding the necessity of making complete screening tests.

Curve C corresponds to curve B, except that the abscissa has been transformed from size to weight of piece. The corresponding Rosin-Rammler equation is

$$R = 100\, e^{-Bw^N}$$

where

$$B = b/(w_1)^{n/3}$$

and

$$N = n/3 = 0.287$$

To find B, the weight of the 1-in. piece w_1, was taken to be 0.018 lb, in agreement with recent experiments.[13] Calculation gave $B = 1.14$. The equation of curve C is, therefore

$$R = 100\, e^{-1.14w^{0.287}} \quad \ldots\ldots\ldots\ldots\ldots\ldots [6]$$

Curve D is from a previously published Rosin-Rammler representation of the average consist of 38 Appalachian coals given by Malleis.[14] It is seen that curves C and D are very nearly parallel, indicating that the two types of coals have a very similar spread of sizes. The lateral displacement of the two lines stems mainly from the earlier assumed weight for a 1-in. piece, for curve D, for which reliable data did not exist at the time. The otherwise close agreement between curves C and D suggests that sampling specifications derived on the basis of Malleis' data can probably be used for all coals east of the Mississippi.

Fig. 3 is a plot on Cartesian co-ordinates of a portion of curve C, from Fig. 2, to show the weight consist of the Enos coal

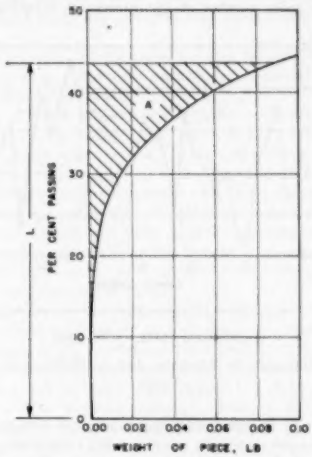

FIG. 3 WEIGHT-CONSIST CURVE FOR ENOS COAL
(Area A divided by L is $\bar{w} = 0.01225$.)

sampled. It can be shown[15] that the area A in Fig. 3 represents the sum of the squares of the weights of all pieces present in a sample of weight equal to the length of vertical side of the area. The weight-weighted average weight of piece, therefore, can be determined by dividing A by L, since

$$\bar{w} = \frac{\Sigma w_i^2}{W} = \frac{A}{L}$$

where area A is determined by planimeter.

Series Integration. An alternate method,[11] which does not require use of the planimeter was used, however, to determine $\bar{w}$. This consists essentially in obtaining the area A by integration of a series expansion of Equation [6]. Using the nomenclature given in the reference cited gives

$$\bar{w} = \frac{I - K}{Q} = \frac{5.8860 - 5.1506}{43.7} = 0.01225 \text{ lb}$$

Variance Equation for Subregions. Finally, therefore, the variance in subregions, due to weight of increment, can be ex-

[12] Footnote 10, pp. 121–123.

[13] "The Effect of Coal Size on the Sampling of Coal for Float-and-Sink Tests," by B. A. Landry and A. L. Bailey, presented at the Joint Fuels Conference, AIME-ASME, Cleveland, Ohio, October 24–25, 1950, fig. 1.

[14] Reference 5, fig. 36, p. 116.

[15] Ibid., pp. 113–115.

pressed after substituting for σ_w^2, $\bar{w}$, and $(a - 1)$ in Equation [3], as

$$\sigma_W^2 = 72.27 \left(\frac{W}{0.01225} \right)^{-1} \quad \ldots\ldots\ldots\ldots\ldots [7]$$

Significant numerical values of σ_W^2 and a plot of this equation are given later.

Estimate of Lot Variance. The variance which reflects the variation of average ash in all subregions of the coal can only be estimated, since samples were taken only during those periods when the belt was stopped, and since hundreds of tons of coal moved by the sampling point between samplings. To make the estimate, the percentages of ash of all five weights of samples taken at each belt stop were averaged.

Fig. 4 shows these grand averages of ash percentages plotted against the order number of the successive samplings or belt

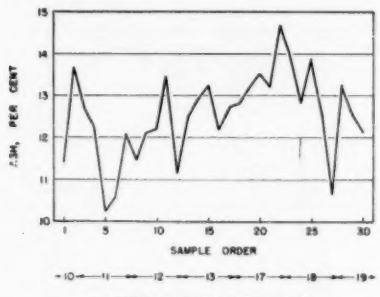

FIG. 4 VARIABILITY OF AVERAGE ASH OF SUBREGIONS FOR ENOS COAL

stops. If it is assumed that more frequent samplings would not have changed materially the variability exhibited by the curve drawn through the points obtained, then the process of calculating the variance by using Equation [1] can be justified. The indicated calculation gave $\sigma_s^2 = 0.935$, which will be used as the lot variance.

Variance of Sample Reduction and Analysis. No experimental work was done in this investigation that could supply direct information on the magnitude of the variance introduced as a result of the operations of sample reduction and analysis. Instead, by rewriting Equation [2] as

$$\sigma_{ra}^2 = \sigma_o^2 - (\sigma_W^2 + \sigma_S^2)$$

an estimate of this variance was obtained by calculating the difference between the observed variances of the samples and the sum of the variances associated with each subregion and with the lot. Use of this method implies that the arbitrary value of —1 taken for the mixing index in Equation [7] was appropriately chosen.

Table 6 gives the observed variances from Table 5 and each of the component variances. Term σ_W^2 was calculated by means of Equation [7] after substituting the corresponding weights of samples (of one increment) in the equation; σ_S^2 is the lot variance previously determined. The variances due to reduction and analysis, σ_{ra}^2, were obtained by difference.

Table 6 shows that the variance of reduction and analysis decreased steadily with increase in weight of the sample reduced. Whether this trend is real or whether it results from the several

TABLE 6 OBSERVED AND COMPONENT VARIANCES OF PERCENTAGE ASH OF SAMPLES OF ONE INCREMENT

Avg wt of sample, lb	Observed variance, σ_o^2	Component variances: Within regions, σ_W^2	Component variances: For all subregions, σ_S^2	Component variances: Reduction and analysis, σ_{ra}^2
13.9	1.144	0.064	0.935	0.145
40.0	1.096	0.022	0.935	0.139
61.3	0.884	0.014	0.935	.....
81.6	1.001	0.011	0.935	0.055
103.3	0.948	0.008	0.935	0.005

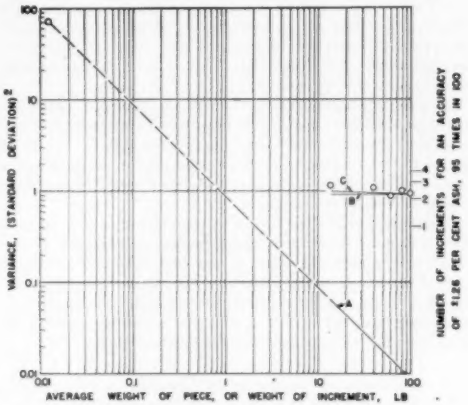

FIG. 5 RELATION OF NUMBER OF INCREMENTS REQUIRED TO THEIR WEIGHT, ENOS COAL

(Component variances: A, within subregions; B, from all subregions; C = A + B.)

assumptions made in calculating the other component variance is not known.

General Variance Relations. Fig. 5 is a log-log plot on which the various significant variables observed or calculated, that have been discussed, have been brought together.

The pivot point, in the upper left-hand corner, from which line A starts, represents the variance in percentage ash for the individual pieces of the coal sampled, σ_w^2. This variance has been plotted against the weight-weighted average weight of piece w. The slope of line A has been taken as —1 to represent perfect random mixing in the subregions. The decreasing variance shown by line A, as the weight of sample of one increment increases, represents the effect of the increase in number of pieces in decreasing the ash variability of the increments. Line A thus represents σ_W^2 as a function of W.

Horizontal line B represents the variance due to the variability of ash contents of the subregions, σ_S^2. This variance is taken to be constant over the range of increment weights taken. Curve C represents the sum of the variances represented by A and B. The observed variance points are indicated by circles. Any difference in variance between C and the observed points corresponds to the variances of reduction and analysis given in Table 6.

The right-hand scale in Fig. 5 shows the number of increments required to fulfill present ASTM standards of accuracy. This was calculated from the known formula[16]

$$\sigma^2 = (0.0026)\, \bar{y}^2 N$$

where $\bar{y}$ is the average ash of the coal and σ^2 is the variance of percentage ash in increments required to make N-increments necessary and sufficient. Fig. 5 shows that since the range of ob-

[16] Reference 4, p. 77.

served variance of increments of weights 14 to 100 lb was between 1.144 and 0.948, three increments of any such weight would constitute an adequate gross sample. It is understood that in taking these three increments, they should be obtained as uniformly as possible over the full time and tonnage periods involved, that is, about 6 days and 30,000 to 40,000 tons of coal, in this instance.

Conclusions and Future Work

The results of this investigation show that the strip-mined coal sampled was so well mixed, within each subregion, that a state of mixing very close to a random arrangement of pieces was achieved. By comparison, the variability resulting from variations in ash contents of the sublots sampled was far more important and was the main component of the observed variance in the samples taken. Taken together, however, all component variances added up to a small magnitude, which means that very few increments were found to be required, when sampling this coal, to meet present accuracy standards.

Inasmuch as some of the results obtained are unexpected, it is believed that data should be obtained at a number of other operations to show whether widely different trends will be uncovered and, if so, what may be their probable cause.

If it is found that the variance attached to increments of large weight is generally as low as this investigation has shown, it would appear that an increase in accuracy standards may be achieved with mechanical sampling devices by the simple process of taking a larger number of increments with them. Higher accuracy standards should be welcomed by all who are concerned with selling or buying steam or power.

Acknowledgments

The authors are greatly indebted to The Enos Coal Mining Company, and particularly to W. R. Caler, preparation manager, for the co-operation and aid extended in obtaining the coal samples.

The co-operation of Commercial Testing and Engineering Company in running the analyses and the float-and-sink separations is gratefully acknowledged.

Each author is also personally indebted to Battelle Memorial Institute and to Commercial Testing and Engineering Company, respectively, for their encouragement and support of the investigation.

Discussion

W. M. Bertholf.[17] Comment on the experimental work leading to the production of this paper is hardly necessary. It was of very high caliber and leaves little to be desired in the way of relevant information concerning the type of coal dealt with. While it is not the first experiment of its type, it appears to be the most fully documented of all coal-sampling experiments with which this commentator is acquainted.

The theory of coal sampling which was tested by this experiment requires no additional comment. It has been discussed informally in small groups for about 5 years and has been presented formally to several groups.[18] As was to be expected, this test fully confirms the theory that the observed variance is a "sum of component variances."

The statistical analysis of the data, as performed by the authors, yields results which are sufficiently different from those obtained by application of the most efficient[19] methods to warrant comment and comparison.

This experiment is of the type usually known in agricultural and biological research circles as "observations classified in one direction," i.e., the groups of increments are considered as being composed of "related" individuals although there is no implication of relationship between the groups as a whole. In such cases the method of "the analysis of variance" can be used to determine (most efficiently):

(*a*) The variance within groups.

(*b*) The variance between groups.

Essentially, these variances correspond directly to the variances (*a*) and (*b*) of the paper. It is not possible to determine variance (*c*) of the paper from the data of Table 2, directly nor indirectly—unless replicate pulps are prepared from each individual increment.

The best estimates of variances (*a*) and (*b*) are $5.026/w$ and 0.871, respectively. The corresponding estimates given in the paper are $0.886/w$ and 0.935.

The data of Tables 3 and 4 of the paper, when substituted in the formulas of Hassialis,[20] and Kassel-Guy,[21] indicate that variance (*a*) is between $4/w$ and $5/w$, probably nearer the latter figure. Ordinarily we would expect that the methods of Hassialis and Kassel-Guy would be consistent with any methods normally used for this purpose, i.e., there should be no serious discrepancy between these methods and the analysis of variance or any other legitimate method of estimating this "sampling constant."

Would the authors care to comment on the indicated discrepancy between the various methods?

When general agreement is reached on the appropriate methods of statistical analysis of data of this type, rapid progress should be made in the development of a body of data which will serve as the basis for improvement of sampling specifications, not only for coal but for other bulk materials. Until that time, comment on the sections, General Variance Relations and Conclusions and Future Work would be fruitless.

---

[17] Efficiency Engineer, By-Product Coke Plant, Colorado Fuel & Iron Corporation, Pueblo, Colo.

[18] A paper, "Notes on Coal Sampling," was presented at the annual meeting of the AIME in Chicago, Ill., 1946. Advance copies were sent to a representative group of well-informed sampling enthusiasts and comments were made by a number of these men, including the present authors. The theory then advanced was equivalent to the "now generally agreed" upon theory of compound variance; but it was a case of "no sale." The paper was withdrawn; but discussion has continued, as follows:

Correspondence with the chairman of Subcommittee XIII on Sampling, of ASTM Committee D-5, Coal and Coke, from 1945 to date.

A memorandum on "Use of a Sampling Chart," for sampling under "controlled" conditions was submitted to Subcommittee XIII in October, 1947.

A more complete memorandum, "The Design of Coal Sampling Procedures," covering the more complex theory of "field conditions" was submitted to this Subcommittee in June, 1949. (Presumably to be published in the ASTM Bulletin at an early date.)

At their invitation, a talk on "The Historical Development of Sampling Theory" was given in April, 1950, at a meeting of the Power Station Chemists of the Edison Electric Institute. This was followed by a series of conferences with a special committee on sampling, and certain points have been amplified by correspondence with the chairman, Mr. O. A. Blatter, and others.

A paper on the "Analysis of Variance in a Sampling Experiment" has recently been prepared. Included in this are the results of the Enos experiment, as well as five other experiments previously reported but analyzed by inefficient or inappropriate methods as originally reported.

[19] "Statistical Methods for Research Workers," by R. A. Fisher, eighth edition, sections 2 and 3, Oliver & Boyd, Edinburgh, Scotland, 1946.

[20] "Handbook of Mineral Dressing," by A. F. Taggert, John Wiley & Sons, Inc., New York, N. Y., section 19, particularly equation 16, and commentary thereon, 1945.

[21] "Determining Correct Weight of Sample in Coal Sampling," by L. S. Kassel and T. W. Guy, *Industrial and Engineering Chemistry*, Analytical Edition, vol. 7, 1935, pp. 112–115.

W. L. Webb.[22] The users of mechanical coal-sampling equipment should be much indebted to the authors and to the Enos Coal Mining Company and others who contributed to the study which made possible the presentation of these fundamental data on coal sampling by large-increment weights. Even though it is possible that the findings in this one instance with respect to the number of large increments needed to obtain a gross sample meeting ASTM standard of accuracy, may rarely apply, it is significant that in at least some instances the accuracy will be improved materially when ASTM minimum recommendations as to the number of increments are followed.

It is gratifying that the data given in the paper begin to clear up a discrepancy between two schools of thought, namely:

1 That the relationship between ash variance (i.e., the square of the standard division of ash), and the increment weight when plotted on a log-log chart such as is shown in Fig. 5 of the paper, is a straight line, the slope of which is the measure of the degree of mixing.

2 That the relationship is a curve, one end of which in the small-increment weight range is asymptotic to the previously mentioned straight line, and in the large-increment weight range becomes asymptotic to a line of constant variance.

The first theory was difficult to reconcile to practice as it meant that if a sufficiently large increment is taken, only one increment could represent amply the lot of coal under test. Such a situation was inconceivable to this discusser because of no knowledge of coal of unchanging quality. The second theory which the paper appears to confirm, in effect states that the number of increments required for a given sampling accuracy, as influenced by increasing increment weight, approaches a constant, and that beyond a specific increment weight, there is substantially negligible gain in sampling accuracy by further increasing the weight of the increment.

A consideration which is of particular concern to users of mechanical samplers is what sampling accuracies actually are being obtained with existing installations. This layman discusser gleans from the paper that, in a case involving a sampler, which employs a timer-operated primary cutter for taking increments from the falling coal stream and which crushes these increments and reduces them by means of a secondary continuously operated cutter, data to establish the sampling accuracy of the system could be obtained for a specific coal simply from determined ash values of pulps prepared from samples secured by causing the sampler to individually take, crush, and reduce perhaps 50 increments over a period covering the extreme range of coal characteristics.

In this instance, since the sampler takes substantially a fixed weight of increment at a constant conveyer rate, only this increment weight would be of concern. Having computed the variance of the ash values of the pulps and the average ash value, the number of increments required to secure the ASTM standard of accuracy could be computed from the known formula, reference (14) of the paper.

The foregoing procedure presumably would be acceptable only if there were no bias in taking the increments, in crushing and reducing them, and in preparing and analyzing the pulps. The determined variance would be the over-all variance, presumably the only one useful in measuring performance.

The authors' views on the foregoing procedure for testing one type of mechanical coal-sampling equipment will be most welcome.

This discusser wishes to take this opportunity to urge the users of mechanical coal samplers to become sufficiently interested in the performance of their samplers to be willing to spend the time and money necessary to make performance tests on their equipment. Apparently no recognized procedures have been developed to make such tests precisely. It is believed that the coal producers, electric utilities, and other large users of coal should urge upon ASTM Committee D-5 on Coal and Coke to develop suitable procedures, and ultimately to provide standards for mechanical sampling. The user of a mechanical sampler presumably is not only interested in the accuracy with which his sampler performs, but also what he can do to make it perform acceptably if the sampler accuracy is deficient.

The conducting of sampler performance tests will not only improve the coal buyer-seller relationship involved, but if presented in a paper, ultimately will provide the needed fund of knowledge to permit the intelligent design and operation of coal samplers.

[22] Mechanical Engineering Division, American Gas & Electric Service Corporation, New York, N. Y.

Authors' Closure

The authors are in full agreement with Mr. Bertholf that recognition of his views on the importance of the variance between lots has come too slowly. Erroneous conclusions in coal-sampling theory have often stemmed from incomplete data. We are happy to note that Mr. Bertholf approves of the data submitted with this paper.

The points raised by Mr. Bertholf regarding the method used of analyzing the data present a certain divergence of views that should be eventually resolved. It appears that Mr. Bertholf is in agreement with Equation [2] which states that the observed variances are the sum of *three* variances. Yet, in adapting R. A. Fisher's work to the calculation of component variances, Mr. Bertholf has developed a method which allows for the determination of only *two* variances, in such a way, as will be shown presently, that the sum of these two variances centers around the observed variances. This approach assumes in fact that the third variance is zero. The actual result is that the third variance is inextricably associated with the other two, and thus the estimates reached of both of these are open to question.

The estimates made by Mr. Bertholf can be summarized in Table 7 which is arranged in the same order as Table 6 of the paper.

TABLE 7

Bertholf's variance estimates					
Within regions	Between regions	Reduction, analysis	Total	Observed variance	Difference
0.361	0.871	0	1.232	1.144	+0.088
0.125	0.871	0	0.996	1.096	−0.100
0.082	0.871	0	0.953	0.884	+0.069
0.062	0.871	0	0.933	1.001	−0.068
0.048	0.871	0	0.919	0.948	−0.029

Because of the inherent elegance of Mr. Bertholf's method, we hope that it can be extended to the simultaneous determination of all three component variances of Equation [2]. This would avoid the necessity of making a number of the assumptions that we have had to make, would avoid the laborious screenings and float-and-sink determinations required by our method, and would not require the use that we have had to make of a difference method which is admittedly approximate.

We wish to thank Mr. Webb also for the points made in his discussion. There seems no question that the relations shown in Fig. 5 now are generally agreed upon. Whether coals will be found that depart significantly from these relations is a matter for the future to reveal.

Mr. Webb poses some very interesting questions regarding the best procedure to test the accuracy of an automatic sample involving the two steps of primary and secondary sampling, with a crushing stage between them. A committee of Subcommittee XIII of ASTM Committee D-5 has been appointed to study this question. It is hoped that planned tests will lead to important information on this type of sampling

The Integration of Organization and Management

By R. T. LIVINGSTON[1] and D. B. HERTZ,[2] NEW YORK, N. Y.

Management is a most important element contributing to our survival as a culture. Management, as an art, has provided no quantitative tools for study and use. Such tools must be provided by an adequate and testable theory of association and its operation, which deals with human behavior. The theory will be based upon the premise that human beings are the core of all associational activity. The mutual interactions and interdependencies of materials, machines, and men must be studied and measured, within the framework of the dynamic process of the social order, to provide the needed theory. The characteristics of groups, and the determinants of their activities are established, with brief details of organization structure. The practical aspects of an integrated theory of organization and management indicate that powerful tools can be made available in this field if sound premises are used for inquiry, experiment, and research.

Introduction

IT has often been said that the most important contribution to victory in World War II was America's capacity to produce. This capacity to produce was a product of an especial American genius, which is the talent of organizing and managing; the ability to envisage the means necessary to attain a goal, to break the task down, and to design a pattern of interrelations between the parts, and finally the ability to adjust the pattern and its performance as environment and occasion change.

Promises of social gains, of greater freedom from want and fear, and all those things which make up "the better life" remain but promises and dreams without production. In order to extend or even maintain the great social gains of the United States, we must expand a self-replenishing, productive economy which distributes its fruits equitably and provides the incentives which stimulate to action. Resources and manpower, energies, skills, drives, and ambitions, good will and kindliness are not special prerogatives of contemporary man. It is not only scientific accomplishment or technical ability which we can claim; rather, it is a way of thinking about men, using things, and working together in the pursuit of a common goal.

Today, however, in spite of great accomplishments, there is cause for us to pause. It has been demonstrated that there are great possibilities for continued advances in production and technology, but the demonstration of possibility does not prove that realization will follow. For example, the labor strife of recent years indicates the existence of unsolved problems in the application of management knowledge. The large number of industrial failures every year demonstrates that what appears to be known or understood by some, is not widely known or understood by all who must manage. Even where management knowledge is at its best, the increased speed of communications and transportation raises crucial and difficult problems, since the rapid changes in interaction and information available reduce the stability inherent in less dynamic processes. It is maintained here that our major problem of survival as a culture and a society will be determined by our ability to organize and manage those associations we have created (1).[3]

It is interesting that in spite of the fact that man has organized and managed since prehistoric times, there has yet to evolve a cogent philosophy, or a valid theory, of organization and management. Throughout history men have appeared, perhaps never in greater quantity than during the industrial development of this country, who have done outstanding jobs of either organization or management, or both. Yet they are not able to, or certainly have not, described in general terms the actions which have produced their success. Thus we may conclude that their practices must be called art. However, to call an activity an art does not preclude its study or analysis and does not mean that a science cannot be developed. For example, the fact that painting, sculpturing, and musical composition are arts and that great painters, sculptors, or composers are artists, does not mean there is not a parallel science, a logical body of rules, whereby people can learn to paint, to sculp, to compose. There is not yet a demonstrated relationship between practice and theory in the field of management. It is important, however, to make clear at this point that the possession of a knowledge of the technique of painting, of sculpturing, or composition will not guarantee that a practitioner will be a great, or even a good, artist. He may be dull, or uninspired but he should not make serious errors of technical application.

In a somewhat similar manner it should be possible to educate and train people to do at least an adequate job of management. This training can be of the greatest utility and will not in any way detract from the importance of those geniuses who have accomplished so much with little formal technology, unphrased philosophy, and chaotic and uncertain theory.

Preliminary Problems

In order to educate and train people, a group of techniques and disciplines are needed which is pertinent to the educational objective. These techniques must be related to one another and to a central core or theory or philosophy. There is at present no such philosophy. Not surprisingly, education and training for management vary. There is not even one single course, technique, or discipline that is universally recognized as essential for a person who desires to enter, and hopes to succeed in, the field of management. It is true that there are courses in "Management" in every school of business administration. As an indication of the difficulties of teaching this subject, it may be pointed out that the authors know of no book which presents a valid (testable) theory of management, and of no two books which

[1] Professor of Industrial Engineering, Executive Officer, Department of Industrial Engineering, Columbia University. Director of Research, Long Island Lighting Co. Mem. ASME.

[2] Assistant Professor of Industrial Engineering, Columbia University. Culpepper Herts Incorporated. Jun. ASME.

Contributed by the Management Division, Society for the Advancement of Management, and the American Institute of Industrial Engineers, and presented at the Spring Meeting, Atlanta, Ga., April 2–5, 1951, of The American Society of Mechanical Engineers.

Note: Statements and opinions advanced in papers are to be understood as individual expressions of their authors and not those of the Society. Manuscript received at ASME Headquarters on November 22, 1950. Paper No. 51—S-1.

[3] Numbers in parentheses refer to Bibliography at end of paper.

can be considered closely comparable except perhaps in paucity of fundamental theory.

It is the ambitious hope of this paper to outline the necessary premises upon which an integrated theory of organization and management may be constructed, and to present some tentative hypotheses which may form a part of such a theory.

Before an attempt is made to define the problem further it may be well to point out that the engineer has a necessary and rightful interest in it.

He must practice the "art" of management throughout his career, and his sympathetic attitude to both theory and practice makes him particularly qualified to undertake the solution of at least part of the problem. The engineering viewpoint and method of thinking and of approach have a great probability of accelerating reasonable and useful approximate solutions of problems in this field.

Jackson Martindell in a recent book (2) points out that there are nearly 100,000 "successfully" operating industrial units. It is reasonable to ask, therefore, why we at Columbia claim that it is necessary to review the field of management, and undertake research in organization.

Actually, there is the obvious answer: Scientific management tells us "there must be a better way," and, if scientific management has been at all successful in the past, we may suppose that its methods will continue to be valid. Therefore we may say that no matter how successful management is today it could be better. That, however, is not a really satisfactory reply since it does not answer the charge that what exists is already "good enough."

But is it good enough? Even if it were good enough that does not mean that it will be good enough. Communication and the economic tempo have greatly accelerated in the past 10 years. What was satisfactory in the past is not necessarily satisfactory today and certainly the new and different problems which will arise in the future will require more suitable general methods of solution. During the war, the Army, Navy, and Air Force brought in methods of mathematicians, social scientists, and physical scientists which were unique in the managerial field. These were used successfully in such techniques as "operations analysis." Today, private enterprise is faced with the fact that operation within the framework of increasingly complex controls will make its task even more difficult.

Therefore it is important, indeed necessary, for private enterprise to demonstrate its ability to understand its function and its operational genius. It can rest no longer upon its "rights" because if history has any meaning we must conclude that rights do not long outlive their social usefulness. Private enterprise is faced with a great challenge both externally and internally. If it meets the internal challenge there is little doubt of its ability to meet the external—but, in order to meet this challenge, research in its own area of operations is essential.

As an art, management has utilized the practice of taking action based upon personal interpretation of various types of facts and intuitive observations. What might have been called science has concerned itself with those areas in which the collection of data has been most highly developed—in the economic and technological spheres. Theories of costs and alternative choice have built strong foundations in these fields. But organization and management deal with costs and techniques only secondarily. Their primary concern is with people and their behavior. And here the art has had to rest upon the individual genius of the "good" managers and organizers. It is not that they would not have accepted or utilized valid theories if such existed, but rather that the means did not exist to collect the data concerning behavior. Organization depends upon people. In many respects, the choice of equipment, and theories of costs, are secondary to an understanding of the dynamics of their interrelationships with the personnel of an enterprise. In the opinion of the authors, the tools for the collection and measurement of facts concerning behavior are becoming available (1), and any valid theory of organization must present hypotheses which can be tested by the collection of such facts. No theory of management and organization can be considered completely valid which does not:

1 Deal directly with the behavior of the personnel of institutions and enterprises.

2 Present hypotheses concerning this behavior which are capable of test by observable facts.

The Basis of Management Theory

In the sense used here, organization is concerned with the design and construction of beterogeneous structures within which an association may be managed.

Thus we may say that organization consists of:

"A structuring of mutual dependencies which provides the means whereby man can most effectively pursue his activities within the framework of the social institutions."

And that management consists of "adjusting the available means as requisite to meet current internal and external change."

A valid theory of management will explain and integrate the following aspects of social groups:

1 Associative purpose, which will involve a consideraton of:

(*a*) Goals.
(*b*) The environment.
(*c*) Potential means of accomplishing purposes.
(*d*) Limiting factors and relationships.

2 Mechanisms of organized group behavior, which will include:

(*a*) A general description of the structural relationships.

(*b*) A description and analysis of communication, and the quantitative aspects of its effectiveness.

(*c*) Analysis of systems of value judgments or appraisal upon which an association acts.

3 An explanation of how the mechanism operates, that is to say, how management can function.

4 A description of these relationships in operational terms, so that the hypotheses of the theory may be tested.

Among the fields being observed to approach this theory are the following:

Historical and contemporary studies of industrial and other associations to determine how functions have evolved and how the patterns of organization and management have adjusted to meet changing circumstances.

Comparative studies in other areas, for example, biology and the physical sciences, of the problem of organization and the adjustment of the organism and groups of organisms to external forces.

The premises upon which an integrated theory of organization and management may be based include the following (3):

1 Management is primarily concerned with human beings grouped in associations, linking environmental elements together in a limited predictable pattern of dependence.

2 The patterns are determined in relation to the social order (4).

3 Management involves activity or actions on the part of "managers" according to some reproducible methodology and these actions produce actions in others in the association.

4 This activity and these actions take place in a time stream, that is, they involve predictions as to future events based upon

experience with past occurrences. The aim is to "tamper with" the uncontrolled probabilities of the future.

Human Resources

In the past, the engineer and others concerned with organization and management have done a superlative job as far as the physical aspects of industrial associations are concerned. It is hardly necessary to recognize here the accomplishments already made in methods analysis, work simplification, improvement and redesign of individual or group jobs and tasks, of processes, machines, and procedures. That this has been done at a price to the association and the contemporary social institutions is becoming increasingly apparent. It is now necessary to study and learn about the social costs of these procedures so that proper and effective use of the human resource can be made in the future. A profound change in thinking about "men at work" must take place. Wise management is now realizing that of all the resources available the human resource is the most important (and possibly the least effectively utilized). Human beings operate, activate, tend, repair, and otherwise perform tasks in connection with the specific and over-all operations of the association. The fundamental reason for association is co-operative and effective use of human resources (5), where effective means the best long-time use of all the assets that man can bring to the association, mental, and psychological, as well as physiological. Management must comprehend all of man—individually and as a group. Ideally, the maximum gain from association will be won only when all of man's needs are provided for. Only then will his true powers be realized, his creative abilities evoked, and only then will there be really effective integration of management and human associations.

The Association

An association of human beings may comprise anything from a momentary co-operation in a physical or emotional effort to the more familiar group seeking mutual protection or other benefits. Such associations include the industrial process, where machines and processes are utilized to produce something useful for exchange in the social environment. Basically the industrial process converts or otherwise adds value to raw materials, parts, or assemblies.

It is the physical characteristics of a mutual project which determine the obvious, although usually secondary, purpose of an association, and goals are generally established in relation to these physical characteristics. It is in terms of these goals that it may be said that the United States manager has done an outstanding job and has made extraordinary progress in the past 50 years.

If a useful theory for association management is to be evolved, it must be subject to test in the crucible of performance. In order to judge alternative solutions to a problem of association it will be necessary to measure accomplishment in various areas. Among the possible group accomplishments which may be measured are the following:

1 External effects of a method of management on:

(*a*) The state.

(*b*) The consumer.

(*c*) Other similar associations, i.e., competitive, and non-competitive.

(*d*) Other groups in the social framework.

2 Internal effects on:

(*a*) The association itself.

(*b*) The associators, that is, workers, management, and owners or investors.

The Social Order

The social institutions are all those associations in which man joins his fellows in order to implement, record, and limit his activities (6). The immediate institution such as the enterprise by which an industrial or business activity is carried on is of concern here. Others are the State and all the social associations which are external to the immediate institution and which limit, govern, control, and otherwise affect its internal arrangements and adjustments. Included also are other enterprises, associations, and institutions which form the remainder of the environment within which the activity is carried on—competitors, vendors, trade, labor or other associations, financial institutions, and the various institutions for communication and recording of information. The groups internal or related to the association, such as the family and specific informal groupings are of primary importance to any integration of management theory. It is with these latter groups that the social scientists, and especially the modern industrial sociologist and the cultural anthropologist, are concerned. There is no doubt that the organizer and the manager of the future must look increasingly to those fields for knowledge and help.

The Temporal Dimension

As Peter Drucker (7) so clearly pointed out, the enterprise is increasingly concerned with long-time persistency; trader philosophy is doomed in modern management. Decisions are now made which are concerned with more and more remote times in the future. The concern of top management is with long-time persistence rather than short-time gain, with loss avoidance as well as with profit. Therefore an enterprise may be considered as moving in a time stream, and every decision, while using the present as a point of reference, is based upon the past and is related to the future. Decisions are made, resulting in controlled action which is reviewed and appraised in preparation for another decision; an attempt to continue the status quo is such a decision. While time may be considered as a dimension, all action must be construed as cyclic, with decision constantly following decision (real or tacit), as the enterprise moves in the interactions which comprise its environment. This dimension may be considered as:

Cycle	Activity	
Before.....	Inquiry	Research
During.....	Evaluation	Design
After.....	Judgment	Control

and the cycle is continuously repeated.

Interaction and Change in Organization Theory

It is important to realize that all these components are related and are in a constant state of alteration. Not only do individuals grow and develop as individuals but also as groups. The working force—the human resource of 1951—is very different from that of 1925, if for no other reason than the fact that it has had on the average at least four more years of formal schooling—a matter which must have a profound effect but which has had very little formal or scientific consideration. The shifting age composition, the increased labor force in large numbers—all of these must be considered seriously.

There have been equally important changes in the other factors. The change of process is familiar to everyone, and some, Norbert Weiner (8) for example, see more and even greater changes ahead. Similarly, social institutions are modified and changed. During the past 100 years the use of the corporate form for industrial enterprise has evolved and, of necessity, there have been changes in the scope of governmental activity to com-

pensate for and control the great forces inherent in this form of institution.

All of these changes and developments are due not only to internal forces but also to adjustments and interaction to each other and to other factors. The problem is indeed one of dynamic process.

There are (at least) three major kinds of relationships which a theory linking management and organization must express:

1 The external relationships of the association; the environmental pattern.

2 The internal structural (functional) relationships; the "description" of the association.

3 The output-input (functioning) relationships; the effectiveness of operation.

The following statements set these forth in general terms.

The External Relationships of the Association

Considering the inter and intraactions, the receipt of stimuli and the responses, the change of the environment and the adjustment of an association thereto, it is possible to conceive of some physical model of an association.

An association may be conceived of as a group of organisms existing in a special set of interactions which we will define as the environment (9). This environment consists of specific relationships of one organism to another and to physical forces, some of which are known and whose influence is subject to prediction within probability limits. There are also other interactions present whose effect either individually or together under normal circumstances is minor, and under such normal circumstances can be neglected. However, from time to time these minor interactions, which it is suggested resemble a "chance system of causes," apparently for no reason, actually for no forseeable reason (under the existing state of knowledge), grow in intensity and either directly or by their effect upon other organisms and relationships in the environment impose an emergency upon the association. The ability of the association to withstand, to absorb and digest, or to resist and reject this emergency is a measure of the success of the association in one goal, self-preservation.

This association, exists, receives stimuli of various kinds from outside and reacts in a certain manner. At this point we will not consider the internal structure of the association. We are first interested in establishing a statement of the environment in which the association exists and the stimuli which it receives and reacts to, and what stimuli it in turn emits, and what effect these have upon environment.

For purposes of visualization we may consider the association as an object, in an n-dimensional sea of interactions. When these interactions are considered, three kinds or types can easily be recognized:

1 Physical
   (a) Regular
   (b) Intermittent
2 Temporal
3 Chance

The regular physical relationships are those which are apparent, can be measured and anticipated with reasonable forethought and intelligence. Their effect upon the association will vary. Some have direct effect and are recognized and reacted to rapidly; these are the ones for which the association is designed. Others are considered as a part of the environment within which the association is expected to operate. As long as their behavior remains as anticipated they will have little effect upon the association. However, the usual situation is that the behavior as predicted (and disregarding is a form of prediction) seldom is exactly the same as the actual behavior. In consequence, an association must adjust either continuously, or as more often happens in a discrete, noncontinuous fashion, from time to time as it is discovered that there is a significant difference between predicted and actual behavior.

These regular relationships are important, but they do not create the really difficult problems that the association has to meet. These difficult problems are caused by the intermittent ones. The real test of the "character" of an association is its ability to meet these intermittent emergencies, to absorb or reject, to recognize or ignore, and to continue to function. If intermittent interactions occur with sufficient frequency, they will (providing the association is successful) cease to be considered intermittent; they will become "predictable" and a part of the regular physical relationships which form the environment to which the association is adjusted.

The second class of interactions is related to the time stream in which the association exists, and may act upon the physical relationships as well as upon the entity which we consider the association. Thus a regular relationship may change its direction, it may wax or wane or indeed disappear. One class of such relationships has to do with the life of the physical property and the individuals which form parts of the structure of the association; another might have to do with the value of money. Still others represent the state of knowledge and information available about both internal and external matters.

Finally, there is the statistical "system of chance causes," comprising all those interactions that have not been taken into account in our plans. Generally, the more intelligent consideration has been given to the environment, the smaller will be this group of chance causes, and the smaller will be the variation (that is to say, a lesser standard deviation), and the greater will be the accuracy of prediction. One thing is important to consider and that is that this chance system of causes on the one hand, links together the intermittent and the regular relationships, and, on the other hand the physical and temporal. Thus it is a two-dimensional distribution, although the authors would hesitate to attempt to represent these dimensions graphically. Another interesting point is that any one of the chance systems of causes may move from this third category into either of the other two and, similarly, at any time one or more of the first two may subside and become classified with the chance system.

Description of the Association

Gillespie (10) sets forth that there are three fundamental characteristic units from which any industrial association is built. These he calls: "Inerts," "dynamics," "purposives," corresponding, respectively, to materials, machine or processes, and human beings. We believe it essential that groups be described in terms of physical factors, descriptive of their operational activity, and in terms of determinants of that activity. To integrate management and organization theory, it will be necessary to measure these factors and determinants so that predictions may be made with respect to management problems. Some of the more obvious and important variables which must be considered are as follows:

GROUPS AND THEIR CHARACTERISTICS

1 Physical factors:
   (a) Size—number
   (b) Personality and homogeneity
   (c) Relative geographic location
   (d) Communication facilities
   (e) Nonhuman content

2 Internal determinants:
- (a) Motivations and stimulations of
  - groups
  - individuals
- (b) Organizational factors
  - arrangement—structure
  - definition and specification
  - formal information exchange operations
- (c) Managerial factors
  - authority
    - how obtained
    - how exercised
  - policy
    - general
    - specific
- (d) The process
  - state of development
  - physical characteristics

3 External Determinants:
- (a) Relations to other associations of the industry
- (b) Relations to vendors
- (c) Relations to purchasers
- (d) Relations to other social institutions
- (e) Relations to economy as a whole
- (f) Historical influences
  - (may be internal as well)

One of the problems of measurement is an understanding of mutual relationships which exist among the three units which we have identified:

Materials versus machines
Materials versus human beings
Machines versus human beings

In each case there is a two-way relationship—a bond. These relationships are tentatively arranged in order of their potential ease of prediction. We must also recognize another order of relationship—self-relationships:

Materials versus materials
Machines versus machines
Human beings versus human beings

What are the relationships which exist between and among materials? Also between materials and machines and human beings? We may consider that materials have no "feeling," no impressions. However, it might be well to realize that even inerts have characteristics such as magnetic properties, hardness, flexibility, ductility, poisonousness, tendency to break, and so forth, which will force a pattern of behavior on the machines and human beings. However, these characteristics are usually closely predictable and largely do not change within a fixed environment. There is no personal element involved, and a material will not change its character due to the character of the machine or the human being. Even here a bit of caution is required as it is conceivable that the machine could, under certain circumstances, produce a change in the material.

We can conceive of a machine or a process as possessing certain invariant characteristics which can be described and predicted. In general, the machine and the human being assume an attitude or a position depending upon the characteristic of the material. In other words, the characteristics of the material may be considered a framework of reference, and, because these characteristics are largely fixed and unchangeable, the machine or the human being must adjust to meet their requirements. For example, a machine tool may "prefer" to have the adjustment to cut brass, for example (the preference merely means that there has been "adjustment" to prior experience) but if it has to cut cast iron it does not "object" to being readjusted to cut cast iron and certainly it cannot refuse to permit its adjustment to be changed if the possibility of adjustment has been foreseen. Otherwise the machine will "refuse to adjust" or, in other words, it will be "intransigent" and "stubborn."

Let us assume that phosphor bronze will poison flesh if handled hot and with sweaty hands; then the human being will wear gloves although he may not like to. In a word, the machine "doesn't care" if it adjusts but the human being has "pride" and so may "refuse to adjust," or only does so under "pressure."

Machines Versus Human Beings

Machines and processes are of various kinds. On the one hand, at the bottom of the scale is the hand tool—the artifact, the use of a physical "thing" to extend the abilities of the person. It seems clear that the relationship between this tool and the human being is simple. Originally, no doubt, the man made his tool and there was a personal element evolved. It was "his," he made it, it was therefore "good." It was his and there was little or no conflict. Even when he no longer made his tool, once he had obtained it, it was his; it was part of "his life," of his personality. It is not necessary nor important to distinguish this kind of tool from the human being that used it. There was no conflict. The human being had (owned) several, perhaps many, dynamics and, without his skill and his influence, they were of little importance. The number of people who could use what the individual had, was limited (he saw to it that they were, incidently), he had a position in society, a status due to his tools (dynamics) and his skills (the knowledge and ability to use the dynamics).

At the other end of the scale is the modern machine of which the computer is perhaps a good example. However, it may not be necessary to go that far to see the difficulties in the relationships. Any machine that requires more than one human operator raises a problem. Actually, the machine that taxes the abilities of a single human operator is probably the key. There are two directions of consideration. First, there is the situation, such as in weaving, where one operator tends more and more machines. He is still superior to the machine, until the point is reached where he cannot tend them all, and a feeling of irritation against the demands of the machine arises. On the other hand, there is the situation where two or more men are required to tend a single machine. Here another factor comes into play. The man is divisible, the machine is not. The individual man is less potent than the individual machine. In this case it is possible to develop a sense of "team play."

The Concept of the Individual

While material, of necessity, is often the focus of an association, it is so predictable, so stable that it presents no serious problem of conceptualization. Difficult as machines and processes may be, they too are closely predictable, and their interrelation with other machines and with materials presents no serious management problems. It is the human being that makes the problem difficult, and it is the human being about which we know the least.

The purposive, the individual, is the element which gives substance and meaning to an organization. It is true that it is possible to conceive of materials and machines as being "organized," but the concept is an incomplete one, in effect, lifeless.

Organization intuitively seems to convey the notion of adjustment or arrangement of different kinds of factors in the pursuit of a common goal. For operational purposes, the unit of organization may be defined as comprising a minimum of two factors, one of which must be a person.

Details of Organizational Structures

Organization seems to depend upon, and be structured by the transfer of information within and among such units. Management, on the other hand, is concerned with the substance of such

information, with obtaining, distributing, and utilizing it to make decisions.

The basic organizational group might consist of three units. There are fundamentally two types:

(*a*) Closed: 

Where (*a-b-c*) represents a unit. Communication is possible and the link is theoretically equally strong in all directions: *a-b*, *b-c*, *c-a*.

(*b*) Open: *a-b-c*

Where one unit is a center of communication. Thus, if *a* wishes to communicate with *c* it must pass through *b*.

It is possible that (*b*) could be considered a defective unit of the type (*a*). However, there is strong evidence that there are sufficient important differences and that the two types may be considered unrelated.

These are basic (and simple) communication patterns and have been explored at some length by Bavelas (11). Any other system of any kind can be built up from the so-called open grouping.

With more than three units in an organizational group the problem is difficult, although the grouping is only more complex in a magnitude sense. A group of four, for example, may be considered as two groups of three in which certain units have become foci; thus

* foci

The first practical test of an integrated theory of organization and management will be in its ability to predict the effects of the existence of these types of organizational groupings upon the operation of an association. Results of some quantitative work already undertaken have indicated the potential power of this type of theory (12). It must be admitted, however, that in certain cases, those groups providing the most individual satisfaction in work effort (closed) did not exhibit group problem solving ability as did others (open). It will be necessary to provide more experimental results before such conclusion may be stated finally.

Various relating forces will affect these groups in different ways. The social force of "coherence," for example, as distinguished from the isolating force of "individualism" will increase and then wane (13). Its behavior, however, will depend upon the particular association under consideration. Some of the forces which may be considered as contributing are (3):

1 Individual satisfactions.
2 Group satisfactions.
3 External interactions.
4 Cultural relationships.

Some of these have been measured, and the remainder must form a part of future management theory. There is a relationship between a person and a task which results in a "particular situation." That relation has an expected value which is determined by the invariate characteristics of the situation and the "normal" attitude of the individual. However, the attitude of the individual varies—with his state of health, his economic situation, and the like. Therefore the internal state of the combined organizational unit varies and the response to stimuli will vary. We must eliminate from our thinking the notion that not only is the situation invariate but also the person.

In other words, any association is created in order to achieve a certain objective or objectives; there is an answer to a stimulus, thereafter there is input of energy followed by output in the form of relationships and "production." It may not be possible ever to measure the real efficiency of an association but we can express the efficiency of an association in the usual engineering sense (where the measure approaches unit as a maximum) as

$$N_a = \frac{O - I}{O}$$

where

N_a = efficiency of association
O = "value" of output
I = "value" of input

Obviously, we must define value, but as long as both input and output are defined in the same units, we could escape the embarrasing necessity of describing it specifically. A defined efficiency such as this is one way of describing the effectiveness of an association but it is insufficient. The economists (14, 15) furnish us with an expression similar to the following

$$MMW = F_i(NR, HE, T)$$

or in words: "Man's material well-being" depends upon the "available natural resources" which are transformed by "human energies" applied "to tools" in finite time.

As set forth, this expression can describe anything from a single operation or by the use of summation signs, integrals, or very complicated differential equations (all of which might be done eventually) companies, industries, regions or economies. To bring it within the province with which engineers like to deal, let us look inside of the "bigger" picture and be microscopically "realistic." Now we may rephrase the expression somewhat and say:

"The effective accomplishment of an industrial association depends upon the physical resources which it has available but even more upon the intelligence with which it exploits its machines and processes."

We conceive of the association as consisting of a group of units of different characteristics, with certain individuals themselves members (in fact, centers, and foci) of certain definite groups, and also as individuals participating in the conformation which is the supra group, the associative entity. We will not at this point explore these intergroup interactions, merely pointing out that the external actions of each group form the intraactions of the supra group. It must not be forgotten that the total of all the external actions of the groups is "greater than" the intraaction of the ultra group and that this excess forms "a part of the output" of the association, which in turn becomes "the action of the association" upon the environment.

Practical Aspects of An Integrated Theory

Based upon our premises, and the definitions thus briefly set forth, it should be clear that the structure of organization may be described by the network of mutually dependent "situations" which are grouped to form associations. Management is the means whereby these situations are adjusted to meet changing stimuli. This concept is completely general, holding for all types of associations in the social order. However, our interest as engineers is primarily with the industrial productive association—the business or corporation.

To what practical purpose may be put a theoretical development such as this? In the first place, even as sketchily and incompletely developed as these concepts are here, it should be apparent that there is a great "engineering" advantage to viewing the complex structure of modern industry as a "system" of individual situations. Such a viewpoint provides the potentiality of a powerful working tool or methodology in the field of organization and management. This tool, which is our second practical advantage, is provided by statistical method—since any group of these situations becomes a "situation population," with cer-

tain homogeneous characteristics, that is, the interaction of individual with machine or process, and other individuals, provides a "measurable" distribution of performance probabilities (time, errors, etc.). The sums of these distributions, and their individual effect on over-all association performance, should furnish management with its quantitative tools of the future. Applications of this integrated concept have already been made with great success (12), and "systems research" is presently under way, at Columbia and elsewhere, to provide further bases for more complete and detailed utility.

Further, and by no means least, the integrated concept of organization and management provides a means for sound teaching of management "technique." This can provide society with managers who not only understand the relationships of man in his work situation, but are qualified to solve the pressing and complex problems of the industrial age. The students of this science may not be genuises, but they will be technically competent to determine realistic and sound solutions, using engineering methodology, and not merely repeat by rote the arts of individuals whose solutions were specific for other situations.

Finally, this theory of management deals with testable and operational hypotheses, and provides a basis for inquiry, experiment, and research. The situation population has been observed to exist stably in a number of associations—whether it exists in others is subject to test and proof. Within our framework, we feel that more than this need not be asked of any theory of management which is founded on the premise that the human being is the center of all associational activity.

BIBLIOGRAPHY

1 "Organization and Management at the Crossroads," by D. B. Hertz and R. T. Livingston, *Personnel*, vol. 27, 1950, pp. 36–42.
"Contemporary Organization Theory," by D. B. Hertz and R. T. Livingston, *Human Relations*, vol. 3, 1950.

2 "Scientific Appraisal of Management," by J. Martindell, Harper and Brothers, New York, N. Y., 1950.

3 "Structure and Process in Social Relations," *Psychiatry*, vol. 12, 1949, pp. 105–124.

4 "The Theory of Social Revolutions," by Brooks Adams, The Macmillan Company, New York, N. Y., 1913, pp. 207–208.

5 "On Being Human," by A. Montagu, H. Schuman, New York, N. Y., 1950.

6 "What Is Social Order," by L. K. Frank, *American Journal of Sociology*, vol. 49, March, 1944.

7 "The New Society," by P. Drucker, Harper and Brothers, New York, N. Y., 1950.

8 "Human Use of Human Beings," by N. Weiner, Houghton Mifflin Company, Boston, Mass., 1950.

9 "Teamwork and Productivity in a Shoe Factory," by C. Arensberg and A. B. Horsfall, *Human Organization*, vol. 1, Winter, 1949.

10 "The Principles of Rational Industrial Management," by J. J. Gillespie, Pitman Publishing Corporation, London, England, 1938.

11 "A Mathematical Model for Group Structures," by A. Bavelas, *Applied Anthropology*, vol. 1, 1948, pp. 16–30.

12 "Study of Communication in a Controlled Small Group Situation," by R. Goodnow and B. Norfleet (mimeographed).

13 "The Organizational Structure of a University Group as Reflected in the Pattern of Communications," by G. A. Robinson, Jr., and D. N. Edwards, master's essay, Columbia University, New York, N. Y., 1950.

14 "Economics, an Introductory Analysis," by P. A. Samuelson, McGraw-Hill Book Company, Inc., New York, N. Y., 1948.

15 "How We Live," by F. G. Clark and R. S. Rimanoczy, D. Van Nostrand Company, Inc., New York, N. Y., 1944.

Discussion

G. D. Wilkenson.[4] The writer is in thorough agreement with the authors on the need for engineers to consider the nonmechanical factors affecting their work. Because he does agree with them so completely, he feels that it is important to emphasize some aspects of the subject matter which the authors have not stressed. It is important to recognize that they are raising radical problems requiring more thought than the usual problems which engineers face. To solve them a type of thinking is required which is quite different from the habitual preoccupations of the engineer.

The engineer is primarily concerned with getting things done. He devotes himself to basic research if he is convinced that a machine is not functioning properly, but he seldom delves further into theory than is necessary to achieve the minimum of empirically successful operation. The problems the authors raise here are largely in the realm of theory. For the engineer, they have no apparent necessary empirical application. The social and economic structure may creak and groan, but the engineer is generally not convinced that maintenance measures must be superseded by inquiries into the basic design. Before general acceptance of the authors' views can be gained, therefore, a real reorientation of the engineer's thinking must be accomplished.

Moreover, no set of generally accepted rules has been developed that the engineer may apply. The "holistic" approach, of which this paper is an example, cannot give the ultimate solution. It is, indeed, a refreshing antidote to the frequently sterile attempts to examine man in abstraction, but it goes too far. Analysis is necessary for thought and action. It is true that man must be viewed as an integrated social being. It is also true that the limited human mind cannot comprehend the totality of qualities of any entity, and must abstract some of them before he can understand anything.

The falls at Niagara, for example, are both a setting for a honeymoon and a source of hydraulic power. They are many other things as well. Occasionally, legislators and treaty makers are faced with the problem of trying to evaluate the effect of a proposal to use one aspect of the falls upon the totality of aspects which makes the spot unique in northeastern United States. To admit this occasional need for a "holistic" approach to Niagara Falls does not require us to deny that analysis is sometimes required as well. An engineer would be a fool to insist upon discussing Niagara's hydraulic potential on his honeymoon. He would lose his job if he did not dismiss his thoughts of the honeymoon if he were commissioned to design a new turbine for the same spot.

In a parallel vein, we can agree that the engineer should take time to consider the patterns of human association, and to learn what other specialists have to contribute to the subject. He ought to aspire to make some contributions out of his own professional experience. But the engineer's experience, like the experience of the anthropologist, the sociologist, the psychologist, and the psychiatrist, is necessarily not with the totality of man, but with an abstraction of the particular characteristics which concern his specialty. The engineer need not castigate himself because he has treated human beings as sources of power, and as sensitive and versatile machines. It is his business to do so. Researches in the social sciences seem to indicate that he should modify his present ideas on the nature and use of this particular kind of machine. He would not be a good engineer if he did not give serious and thoughful consideration to these ideas. He could not remain a good engineer, however, harsh as it may sound to say it, if he ceased to view them only as factors affecting the human being as a machine.

Authors' Closure

The authors appreciate Mr. Wilkenson's views that a reorientation in engineering thinking is required if we are to achieve the ultimate limits in production efficiency. It should be clear that when production efficiency is mentioned, the total

[4] Paul B. Mulligan & Company, New York, N. Y. Mem. ASME.

concept is implied. It should be clear that long-range efficiency includes satisfactions and desires to produce on the part of those involved in the production process.

We do not deny that each element in the whole picture requires study and analysis on its own. The work of the department of industrial engineering of Columbia has included research in many of the individual determinants and characteristics of group operations listed in the paper. However, the element of bifurcation which has existed in the management, engineering, and social-science fields must be eliminated if constructive gains are to be made. Our paper has indicated the areas of integration which should prove fruitful.

For example, a "balanced" assembly line may be studied from a number of viewpoints. If the analysis of the individual elements of the particular process is invalid, then, of course, the production will be limited thereby. On the other hand, if the nature of the work is such that the individual operators do not have sufficient incentive to work efficiently, then the losses may be even higher. Cases may be cited of the use of self-structured teams instead of assembly lines in which the former produce considerably more than the latter.

It is to be hoped that the viewpoint of the human being as a machine alone will not continue to occupy the primary role in the minds of the engineers. Only by considering the total picture can *management* be integrated with engineering views of organization and production.

Analytical Studies in the Suppression of Wood Fires

By G. J. TAUXE[1] AND R. L. STOKER,[2] LOS ANGELES, CALIF.

This paper presents the results of two analytical studies associated with fire suppression of an idealized forest-type fuel; certain aspects of the studies, however, are applicable to wood fires in general. A qualitative discussion of the burning and the suppression of wood fires is presented in the introduction. The first study concerns the instantaneous interfacial temperatures that occur when a drop of water impinges upon the hot surface of a burning piece of wood and shows for typical cases that the drop will not vaporize instantaneously or bounce off, and that initially the relative wetting abilities of the suppressing agents may be of importance. The second study utilizes an electrical analog computer to investigate the simulated thermal behavior of wood as it burns and is extinguished by surface cooling, by penetration cooling, and by oxygen dilution. One important result indicates that the minimum theoretical ratio of the quantity of water for suppressing a typical fire to the volume of the burning wood is in the order of 1/150. Laboratory and field-test fires have given ratios in the order of 1/7, showing the large room for improvement in suppression techniques.

Nomenclature

The following nomenclature is used in the paper:

A = cross-sectional area, sq ft
a = subscript to T to indicate ambient temperature, or to E to indicate a voltage corresponding to T_a
b = subscript to T to indicate burning temperature, or to E to indicate a voltage corresponding to T_b
C = electrical or thermal capacitance, farads or Btu/deg F
c = subscript to T to indicate cooling temperature, or to E to indicate a voltage corresponding to T_c
c_p = specific heat, Btu/lb deg F
E = electrical potential, volts
e = subscript to indicate that a particular term is an electrical quantity
H = latent heat of vaporization, Btu/lb
h = combined unit thermal conductance for convection and radiation, Btu/sq ft deg F hr
i = electrical current, amperes
k = thermal conductivity, Btu/hr sq ft (deg F/ft)
L = length, ft
m = conversion constant, ratio of thermal to electrical capacitance, Btu/deg F farads
N = number of meshes or elements in a system
n = conversion constant, ratio of electrical to thermal time; also a subscript to indicate a varying number
p = penetration distance, ft
Q = quantity of electricity or heat flux, coulombs or Btu
q = heat flow rate, Btu/hr
R = electrical or thermal resistance, ohms or deg F/(Btu/hr)
r = radial distance, ft; also a subscript to T to indicate maximum reheating temperature or to E to indicate a voltage corresponding to T_r
s = subscript to time θ to indicate water spreading time between sectors for the cylinder with two-dimensional heat flow
T = temperature, deg F
t = subscript to indicate that a particular term is a thermal quantity
x = linear distance, ft
α = thermal diffusivity, sq ft/hr
δ = equivalent thickness of water layer, in.
γ = weight density, lb/cu ft
θ = time, sec or hr
ϕ = conversion constant, ratio of electrical potential to temperature, volts/deg F

Introduction

The spreading of fires in wood-type fuels and their suppression involve many factors which enter in complicated and interrelated ways. A general analytical treatment of the entire problem is impossible, but insight into the phenomena involved is possible by separate considerations given to certain of the important phases. The results of two such analytical studies are presented herein following a qualitative discussion of the burning and suppression of wood fires. The main emphasis in this work is toward typical forest-type fuels and situations; certain aspects, however, are applicable to wood fires in general.

Qualitatively, the combustion of wood may be divided into two categories which are (*a*) the burning of combustible gases and (*b*) the burning of carbon in the form of charcoal (1).[3] The two combustion processes probably occur simultaneously during most of the combustion history of any given piece of wood, and it is probably only near the end of burning that charcoal burning alone exists.

If attention is given to a particular specimen of wood in a burning system of similar specimens, one may deduce its subsequent history to be somewhat as follows. Prior to the actual arrival of the active flame, the surface of the specimen will be heated, usually first by radiation from the approaching flame, and later by convection, while its interior becomes heated by conduction. Under certain circumstances the fuel system and its ambient conditions may be such that the temperature of the specimen under consideration reaches its kindling or ignition point as a result of radiation alone. Under other circumstances, however, the specimen may not ignite and possess its own flame until after being "licked" by the oncoming flame. The relative importance of radiation, convection, and conduction in burning,

[1] Lecturer in Engineering, University of California, Los Angeles, Calif.

[2] Formerly Research Engineer, University of California, Los Angeles, Calif.; now Research Specialist, North American Aviation, Inc., Downey, Calif. Mem. ASME.

Contributed by the Wood Industries Division and the Society of American Foresters and presented at the Annual Meeting, New York, N. Y., November 26–December 1, 1950, of THE AMERICAN SOCIETY OF MECHANICAL ENGINEERS.

NOTE: Statements and opinions advanced in papers are to be understood as individual expressions of their authors and not those of the Society. Manuscript received at ASME Headquarters on February 2, 1951.

[3] Numbers in parentheses refer to the Bibliography at the end of the paper.

as well as in suppression, depends upon many factors which in turn may vary among different fires.

Before the specimen becomes ignited, several changes in it may have occurred because of heat absorption from its surroundings. Undoubtedly, the first change is its reduction in moisture content, beginning at the surface and then gradually drying toward the interior. The completeness of and the rapidity of the drying operation depend largely upon the specimen's size, structure, and initial moisture content. Conceivably occurring simultaneously with the latter part of this drying phase, there begins the destructive distillation of the numerous hydrocarbons, alcohols, acetic acid, and so forth, present in wood. These substances which are normally liquids are ultimately volatilized—even cracked in some cases—and are driven out through the pores of the wood along with the secondary thermal-reaction products, such as carbon monoxide, carbon dioxide, and hydrogen. Upon passing through the surface of the specimen into the immediate surrounding atmosphere, these gases may form a combustible mixture with the air, and their combustion will proceed directly if the surface temperature is high enough to ignite the mixture. Even if the surface temperature is below the ignition point of the combustible gases, they may be fired, nevertheless, by sparks or flames passing in the proximity of the specimen. In either case the specimen could be considered to be burning, although temporarily it might be playing the role of a gas burner with its own contained gas generator.

From observations of laboratory and field-test fires (**2**, **3**), it was not possible to detect a distinct transition from gaseous to charcoal burning. However, from the motion of the flame, and the lack of ash on observed specimens during the early stages of their combustion it was concluded that gaseous burning dominated. On the other hand, near the completion of combustion, after the specimens had been reduced to glowing embers with little or no apparent flame, it seemed reasonable that this phase was largely one of charcoal burning. During the intermediate phases of combustion, it was observed that occasional flaming gas jets issued from the burning specimens while the amount of ash accumulated. This indicated the presence of both types of burning. The presence of gaseous combustion can assist the burning of the charcoal by providing it with a hot ambient surrounding. Conversely, the burning charcoal provides a pilot light for the gases that issue out through the hot charcoal surface. Thus the two combustions are not only compatible but may actually assist each other.

The foregoing qualitative description of the elements of wood combustion provides a basis on which to analyze the mechanisms of suppression. The most direct means of suppressing a fire involve (*a*) cooling the fuel to a point below its kindling or ignition temperature and (*b*) changing or modifying the atmosphere surrounding the fuel, or altering the fuel itself, in such a manner that a combustible mixture no longer exists. There are, of course, such indirect methods as isolating the burning fuel so that it will burn itself out. Also, as each portion of a fire is extinguished, that portion will then no longer assist other regions to burn by aid of its transmitted heat, and this indirectly will have a beneficial effect in facilitating the suppression of the remainder.

The first two means of direct suppression mentioned are of principal interest here, and, although they will be discussed individually, it is difficult to separate the two effects in any actual experiment. For example, cooling undoubtedly is an important factor in the blowing out of a match, but at the same time there is a good possibility that the fast-moving stream of breath also dilutes the combustible mixture of air and the gases emitted from the match to such an extent that combustion is no longer possible. Hence it is not obvious whether the match flame is extinguished because the fuel is cooled below its ignition point or if the gas mixture is made too lean by an excess of air. Undoubtedly, both effects are responsible.

Extinguishment conceivably might be made with a very small amount of cooling, provided the cooling could all be applied suddenly to a very thin layer on the surface of the burning wood. Assisting the extinguishment, there is the possibility that the cooled surface charcoal may act as an absorbing medium for the gases generated in the interior, thus momentarily reducing or even stopping the flow of gases which otherwise would diffuse out to support gaseous combustion. Presumably, the surface could then be below the ignition temperature of either the charcoal or the generated gases. Consequently, the temperature would be redistributed throughout the wood, and a short time later the surface temperature might then again be well above the ignition temperatures of either the charcoal or the gases. However, if only the surface were cooled, there is no reason to expect that the generation of gases within the hot interior would cease. Thus, consequently, one can readily imagine the resumption of conditions that existed before the extinguishment. With sufficient heat removal in the last instance, the new distribution of temperature following the extinguishment would have been below the ignition point of the fuels. Hence, if enough heat to make up this deficit is not provided by the surroundings, the fire would remain extinguished unless appreciable gas generation continued and sparks or other external igniters were present.

Aside from immediate extinguishment, another desirable effect that can result from cooling is a reduction of the destructive distillation process. To accomplish this second benefit effectively, the cooling should be such that the temperature of the wood itself, and not merely that of the flame, is reduced. Thus it appears that the optimum cooling would require sufficient heat removal on the surface of the wood at least momentarily to stop the flame and enough interior cooling to suppress the destructive distillation and prevent rekindling after temperature readjustment.

It is practically impossible to apply an extinguishing agent on burning wood without in some way affecting the combustion mixture in the case of combustible gases or simply the oxygen availability in the case of charcoal burning. A low-velocity stream of air entering the combustion zone undoubtedly would enhance the burning since the fuel-to-oxygen ratio in wood fires is usually on the rich side. Only with a somewhat stronger blast would an overly lean mixture result. In the suppression of forest-type fires where explosives are used, this principle has questionable value because of the danger of spreading the fire by blasting burning materials into unburned areas. Rendering the fuel-air mixture too rich for combustion is much more feasible in fire suppression than making the mixture too lean. Typical tactics are smothering with dirt to keep out air or displacing the air by a gas which contains no available oxygen, such as carbon dioxide.

Undoubtedly, the most effective agent for the suppression of wood fires is water. Owing to its high specific heat as a liquid and its very high latent heat of vaporization, it is potentially an excellent coolant. Upon evaporization its high specific volume also makes it capable of displacing a correspondingly large volume of air, hence giving it good smothering qualities. In fact, upon evaporation at 212 F at atmospheric pressure, one unit volume of water becomes approximately 1700 volume units of steam. Furthermore, steam is a fairly good absorber of radiation and thus provides a shielding effect that might serve to reduce the radiant heat received from the adjoining flames by the fuel being sprayed.

From our present knowledge it is difficult to evaluate the relative importance of each of the foregoing functions of water in suppressing wood fires. All are useful and are present to some degree in water spray. In practice, however, not all of the spray

will reach the burning specimens and contribute directly to their cooling. Some of the spray will be carried away by wind and convection currents while some may be evaporated. Other drops may impinge on the hot surface but bounce or run off without providing any cooling. This latter loss of effectiveness may be remedied in part by increasing the affinity of water for wood as, for example, through the use of wetting agents.

A porous solid such as wood, under certain conditions, can be made to contain both adsorbed and absorbed water. Adsorbed water implies that a thin film of water exists over the surfaces of the porous walls (internal as well as external) whereas the absorbed water fills the interstices of the porous solid. To facilitate wetting wood in either manner, the water must have some affinity for the wood. This property can be enhanced by adding surface-active agents such as wetting agents to the water.

Some wetting agents may have strong "spread-wetting" characteristics. These agents must possess low surface tension, and consequently, probably aid adsorption. To have strong absorption characteristics, it would seem that strong capillarity and thus high surface tension would be needed. If this reasoning is correct, it would appear impossible to have both the best absorption and the best adsorption qualities simultaneously. Of course, from a practical standpoint the important thing may be to get sufficient water to the wood quickly and let the distribution between adsorption and absorption fall where it will.

One obvious difficulty to attaining well-distributed wetting in forest-fire control is that of approaching any burning specimen from more than one side. Consequently, only a portion of the surface area of any given specimen can be subjected directly to spray impingement. Even should the entire frontal area of the burning material experience spray impingement and become successfully wetted, there is no good reason to expect that this wetting alone would effect an extinguishment since roughly one half the original surface area involved in burning would remain unwetted. However, if the water would spread from the frontal surface around to the opposite side of each specimen, the situation would be greatly improved. Wetting agents should help accomplish this end.

The discussion to this point has centered around an individual specimen in a fire. It is felt that this approach should be the most logical one before attacking the over-all complicated situation where for forest fires one would have to consider such effects as the size, shape, compactness, density, moisture content, initial temperature, and surface emissivity or absorbtivity of the fuel, the air temperature and relative humidity, the barometric pressure, the wind velocity, the ground slope, the emissive power, temperature, and shape of the flame, the physical and thermal properties of the suppressing agent, its affinity for the fuel, and its technique of use. In spite of man's long experience with wood fires, he has a very incomplete understanding of the real basic mechanisms of the burning and the suppression of these fires. Much basic analysis and investigation remains to be done in understanding and devising more effective ways of combating this drain on our natural resources.

In analytical studies it is recognized that it is not feasible to make an exact mathematical analysis of the complete action of suppression agents as they impinge upon a burning piece of wood and affect the temperature distribution with time within the piece. Due to difficulties in accounting for the changes in properties of the wood with temperature, the charring of wood at a varying depth so that its composition gradually approaches that of charcoal, and the flow of volatile gases through the wood pores toward the atmosphere, a complete mathematical description is practically unobtainable. However, by assuming that the material is either wood or charcoal, depending upon the temperatures involved, it is possible by analyzing certain idealized systems to obtain results which are useful in indicating the order of magnitude of the desired quantities and their variations or in bracketing the results within certain limits.

The two analytical studies presented in this paper were conducted in order to gain an insight into the effect of the various heat-transfer mechanisms as they influence temperature distributions with time on the surface and within a piece of wood as it burns and the fire is suppressed. The first study of the instantaneous interfacial temperature at the time of water impingement has been made in order to estimate how high the temperature of burning wood may be before the water which strikes it commences to boil upon contact. The second study has been made to investigate the thermal behavior in wood during burning and suppression by surface cooling, by penetration cooling, and by oxygen dilution. The first study was rather concise and was mathematical in nature. The second study was quite comprehensive and was facilitated by the use of an electrical analog computer, herein referred to as the thermal analyzer.

Certain assumptions and properties of the involved materials were common to both studies and will be described. The following assumptions were used:

1 Each material was taken to be homogeneous.

2 The effect of diffusion of volatile gases or liquids in the material was neglected.

3 It was assumed that there were no heat sources or sinks within the material.

4 The properties of the materials were assumed to be constant and not vary with temperature.

Properties to represent water, wood, and charcoal, the materials encountered in the analyses, were chosen by referring to several handbooks and by suggestions from W. L. Fons on the basis of his work in the measurement of ignition temperatures (4). The properties of water employed were those for standard conditions. To represent wood, the average properties of ponderosa pine were used. Average values were likewise selected to represent charcoal. This information is presented in Table 1.

TABLE 1 PROPERTIES OF MATERIALS USED IN ANALYTICAL STUDIES

Quantity and symbol	Units	Water	Wood	Charcoal
Thermal conductivity, k	Btu/(hr) (sq ft) (deg F/ft)	0.36	0.1	0.05
Specific heat, c_p	Btu/lb	1.00	0.45	0.2
Weight density, γ	lb/cu ft	62.4	31	15
Thermal diffusivity, α ($\alpha = k/c_p \gamma$)	sq ft/hr	0.0058	0.0072	0.017

Instantaneous Interfacial Temperature on Water Impingement

The point might be raised that when burning wood is first attacked with water spray, the initial droplets impinging on the hot charred surface of the wood might immediately vaporize or bounce. This is because it seems impossible for a droplet to wet a surface that is well above the boiling point of the droplet. As an example of this phenomenon, one can envision the action of a drop of water placed on the hot surface of an iron skillet where the drop immediately starts to boil and skitters about rapidly. If this activity occurs when water first strikes burning wood, wetting agents would probably have little, if any, initial advantage as boiling action would overshadow wetting action, and the bulk of the cooling necessarily would have to occur without the assumed advantage of wetting.

To investigate these phenomena, use was made of a mathematical expression for the interfacial temperature of two semi-infinite solids following perfect contact with each other. This expression (derived in references 5, 9) is as follows.

$$T_0 = \frac{k_1 T_1/\sqrt{\alpha_1} + k_2 T_2/\sqrt{\alpha_2}}{k_1/\sqrt{\alpha_1} + k_2/\sqrt{\alpha_2}} \quad \ldots\ldots [1]$$

where T_0 is the interfacial temperature, T_1 and T_2 are the initial uniform temperatures of the two semi-infinite bodies indicated by the subscripts 1 and 2, and the remaining symbols are as defined in the nomenclature. This formula is valid at all times that these two semi-infinite solids of constant thermal properties are in perfect contact. Restricting attention to the instant of contact and a limited time thereafter, considerable freedom of choice is permitted for the conditions of the two bodies. Since finite times are required for all finite thermal changes to occur in the interior of the bodies following the contact, only the properties and conditions existing on the two surfaces just prior to their contact are needed to substitute in Equation [1] for computing the interfacial temperature at the instant of contact and a limited time thereafter. Thus, for the computation of T_0 the bodies may be finite and may even be liquid since a certain amount of time must elapse before convection within the liquid can affect the interfacial temperature. In particular, one of the bodies may be a piece of hot charcoal and the other a droplet of water, providing the initial interfacial temperature determined according to this equation does not exceed 212 F, the boiling point of water.

Equation [1] has been used to compute the family of straight lines shown in Fig. 1. Here the initial surface temperature of charcoal, wood, and iron have been plotted against the initial water temperature for the condition that the instantaneous interfacial temperature upon contact of the water on each of the solids would be 212 F. To make these computations it was necessary to determine only one additional point on each plot, since each relation is a straight line going through the 212 F point for both axes. Letting subscript 1 in Equation [1] apply to water, and subscript 2 apply to the solid materials, the solution was obtained by setting $T_1 = 0$ and by solving for T_2 to give a value of $T_0 = 212$ F. On substitution of $\alpha = k/c_p\gamma$ the following equation was obtained for these computations

$$T_2 = 212\left[1 + \sqrt{\frac{k_1 c_{p1}\gamma_1}{k_2 c_{p2}\gamma_2}}\right] \quad \ldots\ldots [2]$$

Values of the properties of the materials as given in Table 1 were substituted in Equation [2], and temperatures of 2810 and 1060 F were calculated for charcoal and wood, respectively. By using handbook values for its properties, a temperature of 233 F was similarly calculated for iron. Plotting these points yields the straight lines in Fig. 1.

In Fig. 1 the lines are dashed below an initial water temperature of 32 F to indicate that these values do not have any physical significance owing to the change in phase of water to ice. Similarly, the line for wood is dashed above an initial temperature of 800 F, since at temperatures above this wood would be converted to a material whose properties more nearly resemble those of charcoal.

In analyzing the results shown in Fig. 1 it is interesting to note that, for an initial water temperature of 75 F, water would not commence to boil at the instant of impingement on hot charcoal unless the initial temperature of the charcoal was approximately 1900 F. Even for water at 100 F, the charcoal would have to be at approximately 1600 F for instantaneous boiling to occur. On laboratory-scale fires (2) the highest temperatures measured on the surface of the burning wood were with one exception within 100 deg of 1570 F. If these results are representative (and they agree quite well with values reported by certain other investigators), it would indicate that the water drops will not instantaneously vaporize or bounce off upon impingement on

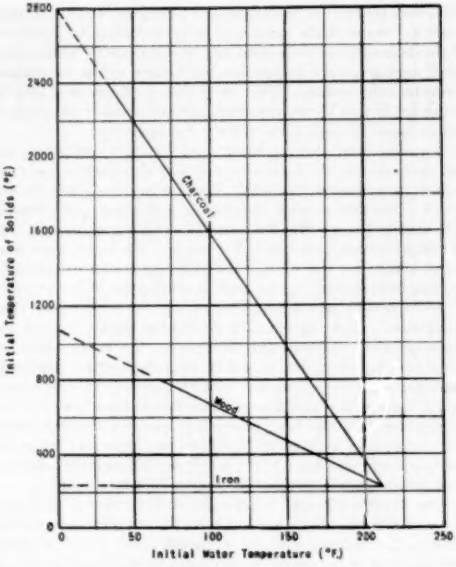

FIG. 1 TEMPERATURES OF WATER AND SOLIDS FOR AN INSTANTANEOUS INTERFACIAL TEMPERATURE OF 212 F

burning wood and that initially the wetting ability of a suppressing agent may be of importance.

In attempting to verify these calculations, a thermocouple was embedded just below the surface of a stick of charcoal, and heat was applied. The highest temperature obtainable in this experiment was 1300 F, and at this temperature water drops (initially at room temperature) wetted the surface instead of boiling instantaneously. Similar experiments were made using iron as the second material. For this the initial iron temperature which caused water drops to boil instantly was 225 F. This very closely checked the calculated temperature as may be seen by reference to Fig. 1 for an initial water temperature of 70 F.

ANALOGOUS STUDIES IN SUPPRESSION OF WOOD FIRES

Some of the complex phenomena involved in the burning and suppression of wood fires have been discussed qualitatively in the Introduction. Also it has been mentioned that in order to make a quantitative approach certain idealizations are necessary. Some of these idealizations were represented in the assumptions which were evolved in order that analytical solutions would be possible. Others entered in restricting the problem to typical cases representative of conditions actually encountered.

For these studies attention was focused on a single piece of wood and the analytical representation of the physical and thermal conditions encountered by it. The viewpoint was taken that this piece of wood was surrounded by like neighboring pieces, all of which simultaneously were undergoing the same sequence of treatment.

Certain values of temperature occurring during the sequence of burning, suppression, and reheating experienced by a piece of wood were selected for these studies. It was the aim to select temperatures as representative as possible of those occurring in the burning and the extinguishment of actual wood fires. Some of these were fixed by nature; however, most were selected as a

result of experimental measurements compared with values observed and reported by other investigators. The initial temperature of the material to be burned was taken to be 100 F. Similarly, the ambient-air temperature was selected as 100 F for the instances when no flame was present.

For the sequence of burning, the temperature at the surface of the piece of wood was taken to become 1500 F suddenly and to remain at that temperature until suppression started. The basis of this temperature selection is described briefly in the preceding section on interfacial temperatures. Assisted by radiation and convection from some source and by its own burning, the surface of the piece was assumed to be heated to this temperature while its interior was heated by conduction.

During burning, the transition of the wood to a substance whose properties resemble those of charcoal is somewhat gradual and depends upon the interior temperatures. On the basis of experimental measurements (3), a temperature of 800 F was selected for this transition of wood to charcoal. Consequently, wherever the interior of the piece was heated by conduction to between 800 and 1500 F, it was represented by a material having properties of charcoal; likewise, if heated below 800 F, the properties represented were those of wood.

Following the burning and attendant interior heating, suppression was represented by conditions made as typical as possible for surface cooling, penetration cooling, and oxygen dilution. For the first two of these methods where water cooling was involved, the temperature of the wetted surface or interior was assumed to be at the boiling point of water, 212 F, as long as the water for suppression existed on or in the stick. This temperature of the wetted portion was maintained until the water was completely vaporized with the amount of heat abstracted from the wooden piece by each pound of water vaporized being taken as equal to the latent heat of vaporization (970 Btu/lb). That the temperature of the wetted portion would be at or slightly less than 212 F was shown by the previously described studies of interfacial temperatures.

In these analytical studies the suppression of wood fires was idealized as consisting of two parts: (*a*) the flame and its associated heat generation was instantaneously stopped and (*b*) the surface temperature of the fuel was lowered and retained below its kindling temperature. The possibility of reignition due to combustible gases that might continue to be generated and be ignited by adjacent flame, sparks, and the like, and produce a flash back was not considered to exist in these analyses. Heat is necessarily removed from the fuel during part (*b*), but part (*a*) was assumed to be accomplished without the removal of heat.

Following the cooling period, after which the heat of vaporization of the applied water is utilized, the surface temperature of the piece of wood will begin to rise as heat is conducted toward the surface from the hot interior. Heat is also lost to the ambient by convection and by radiation at the surface, and this ultimately will cause the surface temperature to decrease. Thus at the surface a maximum temperature would be obtained at some time after the cooling period. If this maximum reheating temperature equaled or exceeded the assumed ignition temperature of the material, presumably reignition would occur with a resumption of burning about as it existed before the suppression. However, if the maximum reheating temperature were lower than the ignition temperature, presumably there would be complete extinguishment since conditions thereafter would improve with the surface temperature decreasing as time increased. Thus the definition of complete extinguishment as used in these studies involved the application of a suppressing agent to cool the wood at or close to its surface to 212 F for such a time that following this cooling period the surface temperature would not exceed the ignition temperature.

The ignition temperature for wood is not a fixed quantity and varies with many factors. For dry cellulose the ignition point may fall between 400 and 600 F and averages 540 F. The ignition points for typical combustible gases volatilized out of wood range from about 950 to 1400 F. Using oven temperatures of 1000 to 1200 F, W. L. Fons (4) obtained an ignition temperature for ponderosa pine of 650 F. In later work, using lower oven temperatures, Fons obtained values as high as 820 F. For these analytical studies a rekindling temperature of the wood was chosen to be 600 F. It might appear that this value is low in view of those just reported; however, the higher values were obtained for wood originally unburned and not for a wood material which had just been burned partially and suppressed. It seemed reasonable that reignition temperatures for this case would be lower than the original ignition temperature, and therefore a more conservative value was chosen.

For suppression by surface cooling, investigations were made which simulated the instantaneous application of water on the surface of the burning wood for particular periods of time. Different runs were made with different cooling times in order to obtain a rather complete range of the subsequent maximum reheating temperatures. During the cooling period, the simulated rate of heat removal was measured. By integrating this cooling rate over the cooling period, it was then possible to determine the total heat removal. From this and the latent heat of vaporization, the total amount of water and the thickness of the water layer applied to the surface could be calculated.

The so-called "penetration" type cooling was considered in an endeavor to evaluate the cooling effect that would result from the penetration of water into burning wood. Although the sort of cooling assumed involved a hypothetical penetration that would not occur in actual systems, it did lend itself readily to analysis and quite probably produced a comparable subsequent maximum reheating temperature to that which would result from more realistic penetration achieved with the same amount of cooling. Without attempting to elucidate the details of the mechanisms for accomplishing the end result, it was assumed that the penetration cooling runs represented the case where, after the initial burning, heat was removed suddenly so as to reduce the temperature to 212 F for a given depth into the material. The heat thus removed was taken to correspond to the latent heat of vaporization of a certain amount of water. This quantity of water might be assumed to be dispersed throughout the given depth instantaneously and to have no further effect beyond the cooling of the material to 212 F by its complete vaporization.

One aim of this investigation was to compare the effects of suppression by surface and by penetration cooling. To establish the equivalence of surface and penetration cooling, the various penetration distances p were taken in such a way that the heat removed by the instantaneous penetration cooling corresponded to the heat removed in a given time of surface cooling. This is illustrated in Fig. 2 where temperatures are plotted as ordinates against the distance within the slab from the surface as abscissas. Curve 1 illustrates, at the start of cooling, the distribution of temperature within the slab due to its burning. Curve 2 illustrates the temperature distribution at the end of a given time of surface cooling. The shaded area A_1 then represents the amount of heat that is removed during this surface-cooling period. For an equivalent penetration cooling run, the depth of penetration p was taken in such a way that the temperature was assumed to drop instantaneously to the cooling temperature T_0 = 212 F for this depth, resulting in the removal of an equal amount of heat. The heat so removed by this penetration cooling is represented in the sketch by the shaded area A_2 and as described $A_1 = A_2$. After making surface- and penetration-cooling runs with this same amount of cooling, their effectiveness was com-

pared by comparing their subsequent maximum reheating temperatures.

The oxygen-dilution runs represented the case where, after the initial burning, the flame of the burning wood was suddenly

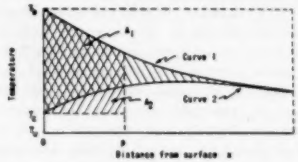

FIG. 2 TEMPERATURE DISTRIBUTION IN SURFACE AND PENETRATION COOLING

snuffed out (as though the extinguishment were being achieved with CO_2) and where with no applied cooling the surface temperature dropped gradually due to radiation and convection to the ambient. Complete extinguishment was represented for this method by finding the time required for the surface temperature to drop to 600 F.

Before going into details on the runs made on the various slabs or cylinders of wood with the three methods of suppression, information will be given on the general method of attack since that is believed to be of interest and as important as the immediate results.

Because of complications in the boundary conditions and in the involved phenomena, obviously it would be impractical, if not impossible, to solve these problems experimentally with the prototype of the thermal system or to make solutions mathematically even for the idealizations assumed. However, it is possible under certain circumstances to simulate systems involving heat conduction by means of fairly simple electrical systems. The relative ease of measuring electrical quantities, as compared to thermal quantities, often makes an electrical analogy an attractive method for studying such problems in heat conduction. Because of these reasons, the suppression studies were attacked using an electrical analog computer, called the thermal analyzer. The essential features of this analogy are developed for a one-dimensional heat-flow case. The development of the method for two and even three-dimensional heat flow is in principle an extension of this one-dimensional case and is not included.

The analogy is established by developing separately and then comparing the equations for temperature and for voltage in the thermal system and its electrical analog, respectively. Although the details establishing the thermal-electrical analogy are given in several articles and textbooks, they are offered here, using a somewhat different approach from that usually presented.

Considering the homogeneous rod or slab of uniform cross-sectional area, A, with the constant thermal properties depicted in Fig. 3 (a), the transient conduction of heat is defined by the Fourier-Poisson partial differential equation

$$\frac{\partial T}{\partial \theta_t} = \alpha \frac{\partial^2 T}{\partial x^2} \quad \ldots\ldots [3]$$

and by the boundary conditions at the two ends of the slab. Here the thermal diffusivity

$$\alpha = k/c_p \gamma \quad \ldots\ldots [4]$$

In these expressions the units of quantities are so chosen that distance x is measured in feet and time θ is measured in hours. The subscript t is used to indicate quantities in the thermal system.

Let the slab in Fig. 3 (a) be divided into N equal elements, each of length Δx as shown in Fig. 3 (b). The temperatures at the interfaces of each element will be designated as shown in this figure. The subscript n is used to indicate the interface between the nth and the n-plus-first element and may be given the successive values

$$1, 2, 3, \ldots n, \ldots (N-1)$$

In applying Equation [3] to Fig. 3 (b) at any instant of time, the

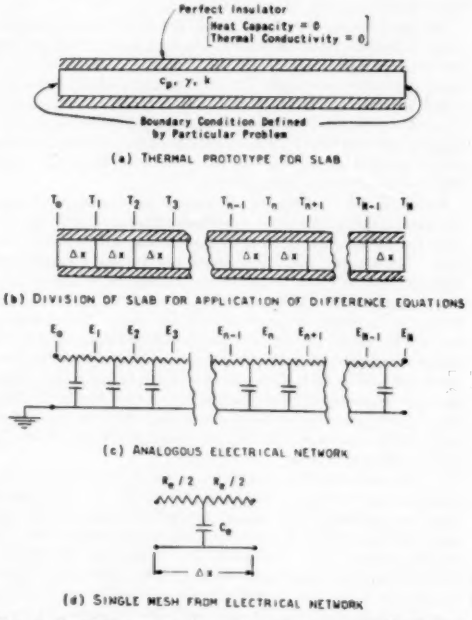

FIG. 3 ILLUSTRATION OF ANALOGOUS THERMAL AND ELECTRICAL CIRCUITS

second derivative term on the right-hand side of the equation can be approximated by an expression involving finite differences as

$$\frac{\partial^2 T_n}{\partial x^2} \cong \frac{(T_{n+1} - T_n)/\Delta x - (T_n - T_{n-1})/\Delta x}{\Delta x} = \frac{T_{n-1} - 2T_n + T_{n+1}}{(\Delta x)^2}$$

On substituting this in Equation [3] and by having n vary from 1 to $(N-1)$, the temperature conditions in the slab may be represented by a system of $(N-1)$ simultaneous approximate ordinary differential equations of the form

$$\frac{dT_n}{d\theta_t} \cong \frac{\alpha}{(\Delta x)^2}(T_{n-1} - 2T_n + T_{n+1}) \quad \ldots\ldots [5]$$

Expressions for the thermal resistance R_t and the thermal capacitance C_t of each element may be obtained by making use of the factor $\alpha/(\Delta x)^2$ in Equation [5]. By substituting values of

α from Equation [4] and by introducing the cross-sectional area of the slab A this factor may be written as

$$\frac{\alpha}{(\Delta x)^2} = \frac{kA}{\Delta x}\frac{1}{c_p\gamma A\Delta x} = \frac{1}{R_t}\frac{1}{C_t}$$

Thus, for each element

$$R_t = \frac{\Delta x}{kA} \quad [6]$$

$$C_t = c_p\gamma A\Delta x \quad [7]$$

On substituting these relationships in Equation [5] it becomes

$$\frac{dT_n}{d\theta_t} = \frac{1}{R_tC_t}(T_{n-1} - 2T_n + T_{n+1}) \quad [8]$$

To develop the analogy it will next be shown that the electrical network in Fig. 3 (*c*) satisfies a system of ordinary differential equations similar in form to those in Equation [8].

The electrical system in Fig. 3 (*c*) consists of a series of N-meshes, each of the type shown in Fig. 3 (*d*). The total electrical resistance in each mesh, which is the same as the resistance between condensers, is identical for each mesh and is equal to R_e ohms. (Quantities in the electrical system are distinguished by the use of the subscript e.) Likewise, all condensers are taken to have the same electrical capacitance C_e in farads. The voltages existing at the mesh junctions, which are midway between the condensers, are designated by the symbol E with subscripts like those for the temperature T to denote the various positions from points 0 to N. The electrical current flow in amperes in the corresponding resistors will be designated by the symbol i with the corresponding subscript. Thus, i_n represents the current flowing in the resistors joining at the point where E_n is obtained.

In order to indicate the voltage at the condenser halfway between the points where E_n and E_{n+1} are obtained, the designation $E_{n+1/2}$ will be used. Similarly $E_{n-1/2}$ represents the voltage at the condenser halfway between the points where E_{n-1} and E_n are obtained.

The voltage E_n at the mesh junction may be expressed as

$$E_n = \frac{1}{2}(E_{n-1/2} + E_{n+1/2}) \quad [9]$$

Taking the derivative of this expression with respect to time yields

$$\frac{dE_n}{d\theta_e} = \frac{1}{2}\left(\frac{dE_{n-1/2}}{d\theta_e} + \frac{dE_{n+1/2}}{d\theta_e}\right) \quad [10]$$

The general expression for the voltage developed across a condenser which is being charged with a current i is

$$E = \frac{1}{C_e}\int i\, d\theta_e$$

By applying this

$$E_{n-1/2} = \frac{1}{C_e}\int (i_{n-1} - i_n)\, d\theta_e$$

Taking the time derivative gives

$$\frac{dE_{n-1/2}}{d\theta_e} = \frac{1}{C_e}(i_{n-1} - i_n) \quad [11]$$

By a similar process there can be obtained

$$\frac{dE_{n+1/2}}{d\theta_e} = \frac{1}{C_e}(i_n - i_{n+1}) \quad [12]$$

Substituting Equations [11] and [12] into Equation [10] yields

$$\frac{dE_n}{d\theta_e} = \frac{1}{2C_e}(i_{n-1} - i_{n+1})$$

By applying Ohm's law to the resistances $R_e/2$ between the mid-point and the edges of the mesh, there can be obtained

$$i_{n-1} = \frac{E_{n-1} - E_{n-1/2}}{R_e/2}$$

$$i_{n+1} = \frac{E_{n+1/2} - E_{n+1}}{R_e/2}$$

On substituting these two relations in the expression directly preceding, there results

$$\frac{dE_n}{d\theta_e} = \frac{1}{R_eC_e}(E_{n-1} - E_{n-1/2} - E_{n+1/2} - E_{n+1})$$

Here the sum of the middle two terms in the bracket is equal to $-2E_n$ (from Equation [9]); therefore

$$\frac{dE_n}{d\theta_e} = \frac{1}{R_eC_e}(E_{n-1} - 2E_n + E_{n+1}) \quad [13]$$

If, in Equation [13], n is given the successive values from 1 to $(N-1)$, there will be obtained a system of $(N-1)$ ordinary differential equations which will represent the voltage conditions in the electrical network. These equations will be identical in form to the system of equations from Equation [8], except that these are exact equations whereas those for the thermal system are approximate equations. It should be noted that the degree of approximation depends upon the value of Δx; the smaller this is, the better the approximation becomes. Hence, except for this difference, the voltage in the electrical network in Fig. 3 (*c*) can be made analogous to the temperature in the thermal system of Fig. 3 (*a*) if the corresponding boundary conditions are imposed.

In Equation [13] standard electrical units are used for the electrical quantities. When this is done, time for the electrical system θ_e, is measured in units of seconds.

In order to interpret the quantities from the thermal system in terms of the analogous quantities from the electrical system, it is necessary to use certain conversion factors. These factors, designated as ϕ, m, and n, are defined as follows

$$\phi T = E \quad [14]$$

$$mC_e = C_t \quad [15]$$

$$n\theta_t = \theta_e \quad [16]$$

Here ϕ is a scale factor which may be selected arbitrarily in order to let a given number of volts potential difference represent a given value of temperature difference in degrees F. The factor m, which converts thermal to electrical capacitance, may also be arbitrarily selected within the limits of availability of the condensers. Time for the two systems is related by the factor n.

As indicated previously, units for the two systems are so chosen that time is measured in hours for the thermal system and in seconds for the electrical system. Thus, if n were to equal unity in Equation [16], 1 second of time on the thermal ana-

lyzer would represent the action during 1 hour in the thermal prototype. Obviously, this would be impractical particularly since manual switching was employed on the thermal analyzer. Therefore, it was necessary that the factor n be sufficiently large so that the timing would be accurate and so that significant amounts of time would not be lost in switching operations. On the other hand, if too much time were allowed for measurements, accuracy would be lost due to the action of the leakage resistance of the condensers in the thermal analyzer. It had been estimated that the time constant of this condenser leakage was in the order of 10^4 sec. Consequently, this indicated that a time factor should be selected so that runs could be made in less than 100 or 200 sec. As a compromise, it was decided that a factor of $n = 3600$ would be used for the tests. A further advantage of this factor was that 1 sec on the thermal-analyzer runs would correspond to 1 sec in the thermal system.

From a dimensional analysis of Equations [8] and [13], it can be seen that the RC product terms in these equations must be of the dimensions of time—actually the so called "time constant" for the respective parts. Therefore, it follows that

$$nR_tC_t = R_eC_e$$

By solving this expression for R_e and by substituting the capacitance ratio from Equation [15], the equation relating resistances in the two systems is obtained as

$$R_e = mnR_t \quad [17]$$

Another pair of analogous quantities is of interest. For the electrical system the quantity of electricity Q_e in coulombs is given by

$$Q_e = \int i\,d\theta_e = \int \frac{E}{R_e}\,d\theta_e = \int \frac{\phi T}{mnR_t}\,nd\theta_t = \frac{\phi}{m}\int \frac{T}{R_t}\,d\theta$$

with the equality being extended by using previously developed factors. By comparison of analogous quantities, it follows that the total heat flow Q_t in Btu is

$$Q_t = \int \frac{T}{R_t}\,d\theta_t$$

Therefore

$$Q_e = \frac{\phi}{m}\,Q_t \quad [18]$$

For a slab, the necessary expressions in order to solve for the circuit parameters of an electrical network which is to represent one-dimensional heat flow have now been indicated. First a cross-sectional area A is selected; this is usually either the area of the slab or a unit area in the slab. Next, the slab is divided along its length into a convenient number of elements of length Δx. Better results follow if the Δx-distances are made smaller in the regions where the greatest temperature changes are expected to occur; this is usually near the surface. From the values of A and Δx and the known thermal properties, k, c_p, and γ, values of R_t and C_t, the thermal resistance and the thermal capacitance, are computed from Equations [6] and [7] for each element. For this purpose each element with its area A and its corresponding Δx may be considered to define its elementary volume. In this volume the resistance is directly proportional to the length of path of the heat flow and inversely proportional to the cross-sectional area through which the heat flows. The capacitance is directly proportional to the volume and may be considered to be placed at the mean position of the mass represented in the element. These concepts are useful since they may also be employed for other configurations than those found in slabs.

From the values of R_t and C_t for each elementary volume, values of R_e and C_e may be computed using Equations [17] and [15]. First, the conversion factor m must be chosen so that the electrical capacities will fall within the range available as indicated. The foregoing procedure then yields a fixed value for R_e. If this value is not within a practical range, the quantities may be recomputed by selecting different values for m, A, or Δx.

Once computed, the electrical resistors and condensers may be arranged in the network as shown in Fig. 3 (*c*). However, it is usually more convenient to combine the adjacent pairs of resistors of value $R_e/2$ between condensers and to replace them by a single resistance.

The formulas used in making calculations for an electrical network to represent the one-dimensional heat flow in a cylinder (radial symmetry) are the same as for a slab, except for the formulas for the thermal resistance and the thermal capacitance. These new formulas may be derived from the considerations of heat flow in a cylinder where it varies as the logarithm of the radius or from the representations of quantities for elementary volumes selected for various radial increments and treated as described immediately in the foregoing for a slab. In either case the following expressions would be obtained

$$R_t = \frac{1}{2\pi Lk}\ln\frac{r_{n+1}}{r_n} \quad [19]$$

$$C_t = c_p\gamma L\pi(r_{n+1}^2 - r_n^2) \quad [20]$$

Here L represents a length parallel to the axis of the cylinder, ln indicates the natural logarithm, and r_{n+1} and r_n are successive radial boundaries of the annular-shaped elementary volume.

Calculating procedures for a cylinder are similar to those for a slab, except that an axial length L is selected instead of the area A and that Equations [19] and [20] are used instead of Equations [6] and [7]. For the cylinder a certain amount of cut-and-try operation is frequently required in order to get the desired balance of values for Δx, R_e, and C_e. The arrangement of the resistors and the condensers in the electrical network is also similar to that for Fig. 3 (*c*), with the position of each condenser representing the mean radial position of the mass for each elementary volume.

For two-dimensional heat flow in a cylinder the elementary volume is obtained by dividing the annulus-shaped elements into equal sectors. Thus the thermal capacitance representing the heat storage in the elementary volume is the same as that computed from Equation [20] divided by the number of radial sectors. The thermal resistance to heat flow in the radial direction is the same as that computed from Equation [19] multiplied by the number of radial sectors. By making use of Equation [6] the thermal resistance to heat flow in the tangential direction becomes

$$R_t = \frac{2\pi r_m}{kL\Delta r} \div (\text{no. of sectors}) \quad [21]$$

where r_m is the mean radial position of the mass for the elementary volume. By using the previously defined conversion factors, values of electrical resistance and capacity may be computed for the thermal quantities. The arrangement of these circuit elements in the network is shown in Fig. 9 and in the circuit diagram, Fig. 10.

A necessary part of the analytical studies was to represent the heat lost by a burned piece of wood through convection and

radiation to ambient temperatures. Evaluations for this may be made using Newton's law of cooling, recast as indicated.

$$q = hA(T_1 - T_2) = \frac{T_1 - T_2}{1/hA}$$

where

q = heat flow rate, Btu/hr
h = combined unit thermal conductance for convection and radiation, Btu/sq ft deg F hr
A = surface area, sq ft
T_1 = surface temperature of wood, deg F
$T_2 = T_a$ = ambient air temperature, deg F

Since temperature difference has been shown to be analogous to voltage difference, it will be seen upon comparison with Ohm's law $i = E/R$, that the quantity q is analogous to the electric current i and that the term $1/hA$ is analogous to the electrical resistance. The latter term must, therefore, be the thermal resistance due to the unit thermal conductance h and it may be written as

$$R_t = \frac{1}{hA}$$

Using Equation [17] to convert from thermal to electrical resistance and calling this electrical resistance R_h, there is obtained the expression

$$R_h = mn\frac{1}{hA} \qquad [22]$$

Numerical values were assigned to the unit thermal conductance h by a consideration of the heat lost by convection and radiation to the surrounding air. The unit thermal convective conductance h_c was evaluated for free convection around a cylinder by using information in reference (6). This was found to equal 2.5 Btu/sq ft deg F hr for $T_2 = 100$ F, $T_1 = 600$ F (taken as the average surface temperature of the wood during its reheating), and $r_0 = 0.025$ ft (the outside radius used for cases representing cylinders). The unit thermal radiative conductance h_r was evaluated from plots in reference (7), giving values of h_r for a Planckian (black-body) radiator for various values of temperatures. For ambient and surface temperatures of 100 and 600 F, respectively, h_r is given as 4.0 Btu/sq ft deg F hr. The total or combined unit thermal conductance h is the sum of h_r and h_c or 6.5 for the indicated temperatures. Actually, the average surface temperature following suppression is probably less than 600 F since it varies between 212 F and the maximum reheating temperature T_r. T_r might be anywhere between 212 F and 1000 F, but was in the neighborhood of 600 F for the runs of greatest interest. Since the time average would probably be less than 600 F, the value $h = 6.5$ may be high for most runs. On the other hand h_r is computed for free convection; actually, the composite effect of burning many sticks together would be to set up convection currents which would be greater than those that one stick alone could produce. The increased air velocity would cause a greater heat transfer, and h_r would be increased. After considering these effects, it was thought that a value of $h = 6$ probably would be most representative of actual conditions. However, to cover the possible deviations, various electrical resistors R_h were calculated and used in certain runs in the thermal analyzer to represent values of $h = 3.0$, 6.0, and 9.0 Btu/sq ft deg F hr. Physically, the resistor R_h is connected across the input terminals to the network as shown in Figs. 4 and 10.

Investigations were conducted on different networks representing slabs or cylinders with temperature variations in one or two dimensions. In each network electrical capacitors and resistors were chosen to represent the thermal capacity and resistance of the prototype material which was either wood or charcoal, depending upon the initial heating. For the one-dimensional case, the properties of the material in the slab or cylinder are represented by the resistors R_1 to R_N and the capacitors C_1 to C_N as shown in the schematic diagram, Fig. 4. To the left of the network is shown a direct-current power supply with a voltmeter V_1 to measure the voltage E_b which was set at 200 to represent the burning temperature, 1500 F. The ground or zero-voltage point, $E_a = 0$, was used to represent the initial and the ambient temperatures of 100 F. A small portion of the voltage appearing across the resistor R_h was amplified by a direct-current amplifier and applied to one channel of a two-channel Brush recorder, where it was recorded continuously against time. This voltage represented the temperature of the surface of the

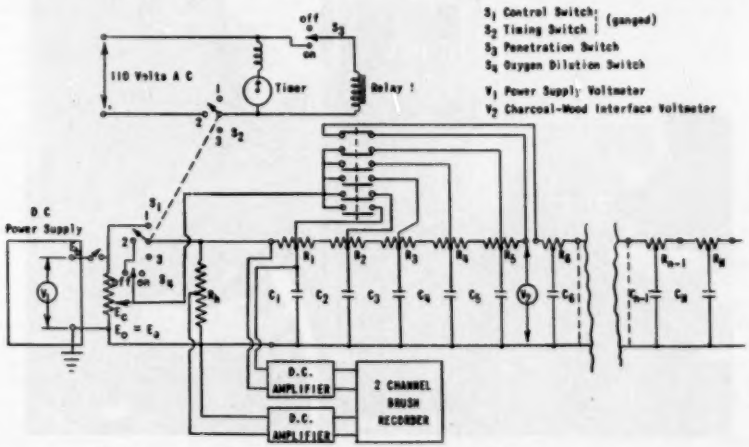

FIG. 4 SCHEMATIC DIAGRAM FOR THERMAL ANALYZER—ONE-DIMENSIONAL RUNS

slab or cylinder. By a similar arrangement the voltage drop across the first half of R_1 was recorded simultaneously on the second channel; from this voltage the current and then the heat-flow rate could be determined. The voltmeter V_2 were used to measure the voltage at the interface between the charcoal and the wood elements; here 100 volts were used to represent the demarcation temperature of 800 F. The timer and the switching and relay arrangement were used as part of the suppression sequence and will be described later.

Fig. 5 is a view of the thermal analyzer and its associated equipment. Aside from the switching panel in the top portion, the thermal analyzer is composed essentially of a series of electrical resistors and capacitances arranged with convenient receptacles in 45 units. Each unit consists of six fixed condensers and two variable resistors and may be used to form one mesh representing an elementary volume of a slab or a cylinder. The fixed condensers may be connected to have any nominal values in steps of 0.25 microfarad up to a maximum of 15.75 microfarads. Actual values as used were measured with a capacity bridge. The resistances could be varied up to 5 megohms. Connected externally to the thermal analyzer are the various meters, amplifiers, power supplies, timer, and two-channel automatic recorder.

The surface-cooling runs were simulated on the thermal analyzer by the use of an arrangement whereby the network input terminals could be switched at certain times to voltages representing the prescribed temperatures. With the network initially uncharged and with all switches in their normally "off" position, the ganged $S_1 - S_2$ control switch shown in Fig. 4 would be set in position 1. Then when the power-supply switch would be turned on, 200 volts simulating the burning temperature would be applied to the input terminals of the network until V_2 indicated 100 volts at the charcoal-wood interface position. At this time the control switch would be placed in position 2 to simulate the start of surface cooling. Section S_2 would start the timer; section S_1 would switch the network input terminals to $E_c = 16$ volts, obtained by a voltage-dividing arrangement from the 200-volt supply, to simulate the surface-cooling temperature of 212 F. This would be applied for times ranging usually from 0.10 to 16.00 sec. At the end of the surface-cooling period, as indicated by the timer, the control switch would be turned to position 3 where section 2 would stop the timer and where section 1 would cause the resistance R_A representing ambient, to be the only element connected across the input terminals to the network. Thus the voltage at the input terminals would rise and then fall, enabling the voltage representing the maximum reheating temperature T_r to be obtained from the recording tape. A typical tape record of a surface-cooling run is shown in Fig. 6.

The procedure used for the penetration-cooling runs was similar to that for the surface-cooling runs but with the following departures during the cooling period. It was necessary to short the condensers of the first few meshes to $E_c = 16$ volts in order to simulate the penetrating cooling which lowered the temperature to 212 F for the corresponding depths. The penetrating switch S_3 in Fig. 4 would be turned to the "on" position for these runs causing the relay R_1 to be actuated during the cooling period. This would cause six normally open contacts to close and short to the 16-volt point as many of the first six condensers of the network as were connected to the relay contacts. At the same time a pair of normally closed contacts would open the network just inside the point where the last condenser was shorted so that the remaining portion of the network would not be altered appreciably by these switching operations. Also, the cooling time for these runs was kept as short as possible, a matter of a few hundredths of a second, in order to minimize any change in the voltage distribution of the interior. Separate runs were made in which from one to as many as six of the condensers would be so shorted in order to simulate various penetration depths and to determine the effect on the subsequent maximum reheating temperature.

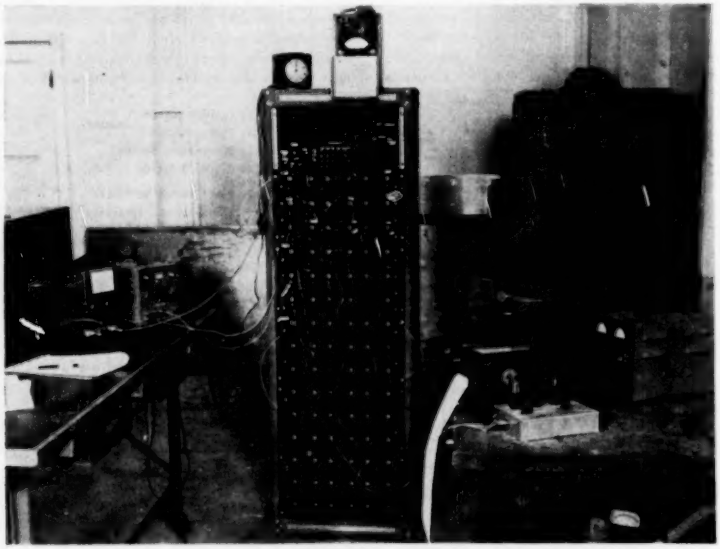

Fig. 5 Thermal Analyzer and Associated Equipment

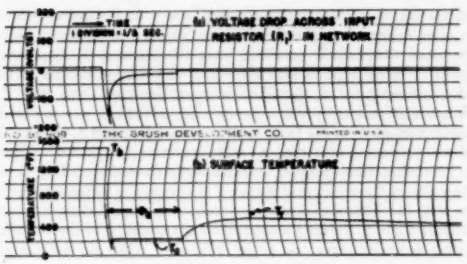

FIG. 6 TAPE RECORD OF TYPICAL THERMAL-ANALYZER SURFACE-COOLING RUN

The equivalence of the surface and the penetration-cooling runs was determined by comparing the quantity of electricity removed during the cooling periods. As was shown in Fig. 2 for the thermal prototype, this amounted to a comparison of the areas A_1 and A_2 which represented the amount of heat. For the surface-cooling runs the quantity of electricity Q_s was determined by recording versus time the voltage drop across the first half of R_1, Fig. 4; this was converted to current i and integrated from the recording tape with a planimeter to get Q_s (in effect using $Q_s = \int i \, d\theta_s$). For the penetration runs the quantity of electricity was determined by making use of the relation $Q_c = \int E \, dC_s$ and by taking into account the manner that both E and C_s varied with "depth" in the networks. The assumption was made that E varied linearly from $E_b = 200$ volts at the "surface" to $E = 100$ at the charcoal-wood interface. This assumption was valid to within 3 per cent since the charcoal-layer thickness was usually a small fraction of the total slab thickness or cylinder radius. The variation of C_s with depth was taken as it actually was computed and used in the networks. Thus Q_c could be obtained for every penetration-cooling run and compared by cross-plots with the corresponding surface-cooling runs in order to obtain an equivalent surface-cooling run having a particular cooling time. Since the same heat removal would be involved, the two equivalent runs would require the same amount of water for suppression as viewed in this study, and their effectiveness could be compared by observing their values of maximum reheating temperatures. The details in these comparisons required rather arduous calculations and are not included in this paper but are given in reference (3).

Calculations for the water-layer thickness δ for each run were made as follows. The quantity of electricity Q_s determined as indicated in the foregoing, was converted to a quantity of heat Q_t by using Equation [18]. This quantity of heat was taken to be that given up by the vaporization of water of density γ spread over an area A to a thickness δ. Thus $Q_t = H\gamma A\delta$ where H is the latent heat of vaporization of water. On equating the two expressions for Q_t there is obtained

$$\delta = \frac{mQ_s}{\phi H \delta A} \qquad [23]$$

Extinguishment by oxygen dilution was simulated in the runs by the aid of the oxygen-dilution switch S_4 which would be placed in the on position, Fig. 4. After the initial charging of the network, like that for the other types of runs, the control switch would be placed and left in position 2. Thus there would be no simulated cooling, and the network would discharge through R_A. From the tape recording, the time for the surface temperature being represented to drop to 600 F would be obtained.

The slab for which one-dimensional heat-flow investigations were made was simulated by 10 electrical meshes representing charcoal, followed by 13 meshes representing wood. In addition to the properties listed in Table 1, the following numerical quantities were used in computing the electrical parameters for this case

$$A = 0.1 \text{ sq ft}$$
$$\phi = \frac{1}{7} \text{ volts/deg F}$$
$$m = 300 \text{ Btu/deg F farads}$$
$$n = 3600 \text{ sec/hr}$$

Each of the 10 charcoal meshes represented a $\Delta x = 0.001$ ft, for which a typical mesh contained

$$R_s = 0.230 \text{ megohm}$$
$$C_s = 1.065 \text{ microfarads}$$

The wood meshes following had the first 5 meshes with $\Delta x = 0.001$ ft, and the next 8 meshes with $\Delta x = 0.002$ ft. This gave a slab of a nominal 0.030 ft thickness that could be viewed as being a 0.060-ft-thick slab which was suppressed simultaneously from both sides. For a value of $h = 6.0$ Btu/sq ft deg F hr, R_A was computed to equal 1.80 megohms.

To represent different degrees of establishment of the fire, various thicknesses of the charcoal layers were used in the runs. In addition to using 10 Δx (0.010 ft) of charcoal elements, runs were made with only 2 Δx (0.002 ft) and 5 Δx (0.005 ft) of charcoal elements on the surface of the wood. Also, in order to establish what was thought to represent the most severe condition of initial burning, a series of runs was made on a complete charcoal slab of 30 elements (0.20 ft), which was charged initially with a simulated uniform temperature of 1500 F throughout its thickness. For all practical purposes this was found to represent a semi-infinite slab since considerable reductions in the slab thickness did not affect conditions appreciably on the surface for the times employed.

The cylinder for the one-dimensional heat-flow investigations (radial symmetry) was simulated by 15 annular-shaped elements of wood at the center (0.020 ft in radius) with 10 elements of charcoal for a surface layer (0.080 ft thick), giving a total radius of 0.030 ft. In addition to the properties of the material, the following numerical quantities were used in computing the electrical parameters for this case:

$$L = 1.00 \text{ ft}$$
$$\phi = \frac{1}{7} \text{ volts/deg F}$$
$$m = 154 \text{ Btu/deg F farads}$$
$$n = 3600 \text{ sec/hr}$$

In Table 2 the circuit parameters for this case are tabulated.

Similar to that for the slab case, two degrees of burning were represented for the cylinder by making runs using 5 and 10 Δr of charcoal elements. Since the outside radius would change slightly with each of these charcoal-layer thicknesses, the values of R_A would also change. For example, with $h = 6.0$ Btu/sq ft deg F hr, R_A was found to equal 0.588 and 0.490 megohms for the respective 5 and 10 Δr of charcoal-layer thicknesses.

For the slabs and cylinders thus far described, the cooling was considered to be applied instantaneously over the entire external surface, and in these cases the heat flow was unidimensional. Consideration was also given to a progressive cooling extending over the external surface of a cylinder giving rise to a two-dimensional flow of heat, tangentially as well as radially. This treatment would approach conditions in practice where in fighting

TABLE 2 CIRCUIT PARAMETERS FOR CYLINDER WITH ONE-DIMENSIONAL HEAT FLOW

Mesh no.	Material represented	Distance from surface, ft	R_s, megohms	C_s, microfarads
1	Charcoal	0.0010	0.0585	3.542
2	Charcoal	0.0021	0.0655	3.724
3	Charcoal	0.0030	0.0635	3.325
4	Charcoal	0.0040	0.0632	3.08
5	Charcoal	0.0050	0.0691	3.27
6	Charcoal	0.0060	0.0708	3.17
7	Charcoal	0.0072	0.0874	3.15
8	Charcoal	0.0082	0.0775	2.80
9	Charcoal	0.0092	0.0808	2.63
10	Charcoal	0.0101	0.0775	2.33
11	Wood	0.0111	0.0454	10.63
12	Wood	0.0121	0.0481	10.29
13	Wood	0.0131	0.0488	9.66
14	Wood	0.0140	0.0480	9.16
15	Wood	0.0150	0.0572	8.87
16	Wood	0.0161	0.0662	8.86
17	Wood	0.0172	0.0727	8.39
18	Wood	0.0184	0.0864	8.31
19	Wood	0.0197	0.105	8.11
20	Wood	0.0213	0.147	8.45
21	Wood	0.0232	0.216	8.32
22	Wood	0.0258	0.429	8.18
23	Wood	0.0283	0.847	4.18
24	Wood	0.0290	0.447	0.507
25	Wood	0.0298	1.32	0.269

forest fires it is difficult to apply a suppressing agent on more than one side of the pieces of burning wood. Also, from observations of model laboratory fires (3) it was quite apparent that the frontal area of burning cylindrically shaped wood specimens on the side of the water spray was readily wetted but that the water spread rather slowly over the rear surface. This resulted in a much greater water requirement for complete extinguishment than when both the front and rear surfaces were sprayed simultaneously, even though spreading over the rear surface could be facilitated somewhat by the use of wetting agents. Some features of this action are shown in Fig. 7. The line of symmetry appearing on the sketch is to some extent an idealization not actually realized unless the axis of the cylinder is vertical, because gravity influences the water film above the line somewhat differently from that below the line. Notwithstanding this discrepancy, it was felt that the more salient characteristics of the actual cooling were retained when this symmetry was employed.

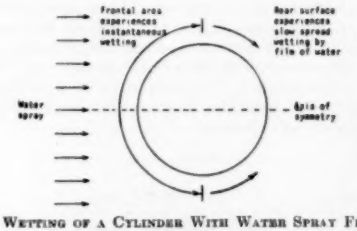

FIG. 7 WETTING OF A CYLINDER WITH WATER SPRAY FROM ONE SIDE

In order to use the thermal analyzer to study the surface temperature and the heat loss by this sort of cooling, the spreading of the surface cooling over the rear of the cylinder was necessarily done in discrete steps rather than continuously. The wood and the charcoal represented in this burning cylinder were divided into elements as indicated in Fig. 9. The six sectors were numbered from 1 through 6, and the four radial divisions were designated by letters *a*, *b*, *c*, and *d*. Essentially, the dimensions were the same as for the cylinder with one-dimensional heat flow with 5 Δr, and the same conversion factors were used in computing the electrical circuit parameters. The circuit parameters for one sector in this arrangement are given in Table 3. These are essentially the same for all sectors except for the small differences in values of C_s due to variations from their nominal values.

Fig. 8 illustrates the variations in surface temperature for each of the various sectors during a typical run. At the instant when cooling commenced, the cylinder was assumed to possess a temperature distribution resulting from the burning temperature, 1500 F, being applied uniformly over the outside surface until the temperature at the charcoal-wood interface was 800 F. When this was achieved, a temperature of 212 F was imposed instantaneously on the front surface sectors 1, 2, and 3, with 1500 F still prevailing over the rear surface sectors 4, 5, and 6. After a prescribed time interval, designated as θ_s, the spreading time per sector, the surface of sector 4 was reduced instantaneously to 212 F. This same stepwise cooling was applied in turn to sectors 5 and 6, yielding a condition corresponding to the wetting being extended over the entire cylinder. After an additional

TABLE 3 TYPICAL CIRCUIT PARAMETERS FOR ONE SECTOR OF CYLINDER WITH TWO-DIMENSIONAL HEAT FLOW

Annulus	Material represented	Distance from surface, ft	Radial resistor, megohms	Tangential resistor, megohms	C_s, microfarads
a	Charcoal	0–0.0010	0.870	142.	0.249
b	Charcoal	0.0010–0.0056	4.48	27.5	1.03
c	Wood	0.0056–0.0101	2.79	11.1	3.61
d	Wood	0.0101–0.0145	3.70	2.05	5.17

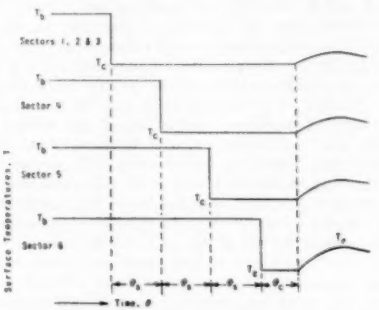

FIG. 8 SURFACE-TEMPERATURE VARIATIONS OF SECTORS FOR CYLINDER IN TWO-DIMENSIONAL RUNS

time interval representing the cooling time for the last sector θ_s the 212 F temperature was removed from the entire surface, and the surface temperatures of the various sectors were allowed to take whatever values they would as determined by the ambient conditions and by the existing internal distribution of temperature. It is obvious from the longer heating and shorter cooling of sector 6 that it would achieve the highest T_r and be the most critical region in regard to rekindling.

The schematic diagram for investigations on the cylinder with two-dimensional heat flow is given in Fig. 10. The network representing this case is shown in the lower part, and the details of switching are shown in the upper part. The voltages obtained from the direct-current power supply and the voltage divider were the same as those used for the other cases investigated. A ganged five-section, seven-position switch S_1 was used as the control switch. Section 1 was connected to the first three sectors of the network, while sections 2, 3, and 4 were connected to sectors 4, 5, and 6, respectively. Section 5 was used in the timer circuit in a manner similar to that for the one-dimensional cases in Fig. 4 and is not shown in this schematic diagram. With S_1 in position 1, the network was made ready for charging. On turning to position 2, the switch applied the voltage E_b to all sectors, causing the prescribed initial voltage distribution to be obtained in the network. When voltmeter V_2 at the charcoal-wood interface reached 100 volts, the switch was turned to position 3, producing a voltage E_s across the first three sectors. After a time θ, the

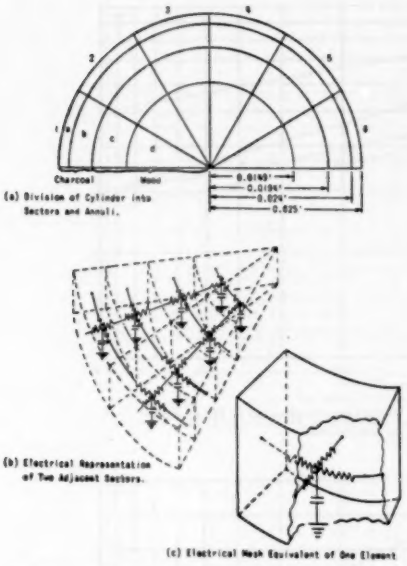

FIG. 9 SCHEMATIC REPRESENTATION OF CYLINDER FOR TWO-DIMENSIONAL HEAT FLOW

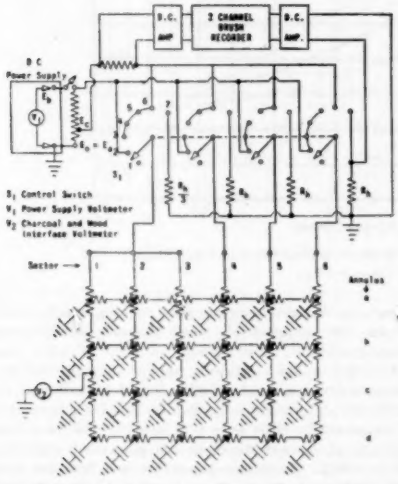

FIG. 10 SCHEMATIC DIAGRAM FOR THERMAL ANALYZER; TWO-DIMENSIONAL CYLINDRICAL RUNS

switch was turned to position 4, producing a voltage E_c across sector 4. In a similar fashion positions 5 and 6 connected the input terminals of sectors 5 and 6 to E_c. After the cooling time θ_c for sector 6 had elapsed, the input terminals of all sectors were switched to their respective R_h resistors, and the value of T_r for the last sector was measured using a direct-current amplifier and a Brush recorder to record the voltage across the last sector's R_h. Another direct-current amplifier and Brush recorder were employed to record the voltage across a small resistance in series with the leads from each sector to the divider where E_c was obtained. This enabled the quantity of electricity removed for the entire sequence of spread, wetting and cooling to be measured so that the corresponding heat removal and average water-film thickness might be calculated.

Only surface cooling runs with $h = 6.0$ Btu/sq ft deg F hr were employed in the investigations for the cylinder with two-dimensional heat flow. Spreading times θ_s of 0.25, 1.0, and 8.0 sec per sector were used with the cooling times θ_c for the last sector ranging from 0.25 to 8.0 sec. The value of R_h for each sector was 7.05 megohms. Since the first three sectors were treated identically, each of their R_h resistances was effectively in parallel and was replaced by a single resistor of value $R_h/3$.

Results from the previously described tests are presented in Figs. 11 to 15 and in Table 4. Though condensed considerably from a comprehensive research program, it is believed that the more representative and significant results are presented herein. In these figures T_r the maximum reheating temperature is plotted as ordinate. The cooling time θ_c is plotted as abscissa in Fig. 11, and on the rest, Figs. 12 to 15, the equivalent water-layer thickness δ is plotted as abscissa.

TABLE 4 SUMMARY OF OXYGEN-DILUTION RESULTS

Case investigated	No. of charcoal Δx or Δr	h (Btu/sq ft deg F hr)	Extinguishment time (sec)*
Slab	2	6.0	1.8
Slab	5	6.0	1.7
Slab	10	6.0	7.2
Slab	all	6.0	25.3
Cylinder	5	3.0	4.4
Cylinder	10	3.0	12.7
Cylinder	5	8.0	2.2
Cylinder	10	6.0	7.8
Cylinder	5	9.0	1.5

* Time for surface temperature to decrease from 1500 to 600 F.

The effect of the degree of establishment of the fire for slabs can be seen from the curves for surface cooling of Fig. 11 and Fig. 12. This effect is also shown for the cylinder with one-dimensional heat flow in Fig. 13 for both surface and penetration cooling. Comparisons of these curves show a definite increase in the equivalent water-layer thickness and the cooling time as the charcoal layer is made thicker, corresponding to the greater stored heat within the bodies in a more established fire.

A comparison of the effects of surface cooling and penetration cooling on extinguishment may be made from the curves plotted in Fig. 13 and Fig. 14 for the cylinder with one-dimensional heat flow. It would appear from these curves that there is no clear-cut advantage of penetration cooling over surface cooling. Therefore, one might conclude that as far as the effect of cooling is concerned in extinguishing a wood fire as viewed in these studies, the penetration ability of the suppressing agent is not of great importance. In the extinguishment of actual fires, however, there may be other factors or mechanisms present for which penetration of the suppressing agent may either directly or indirectly contribute to the over-all effectiveness. On the other hand, from observations made during laboratory and field-test fires, it appeared that spread wetting was a desirable action in order that the fire might be extinguished on the side of a stick away from the spray. It is even conceivable that penetration action may be detrimental in slowing down spread wetting by causing the front part of the stick to become saturated with an excess amount of water that must first penetrate before it can build up to a sufficient thickness on the surface to spread wet.

The effect of h, the combined unit thermal conductance for radiation and convection, on the results may be seen in Table 4

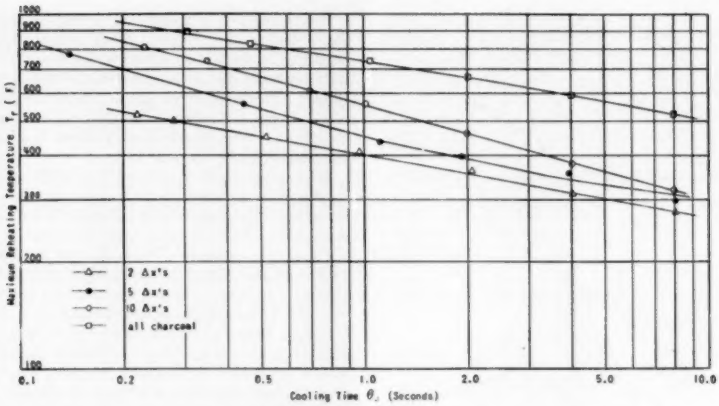

FIG. 11 THERMAL-ANALYZER RESULTS FOR SLABS WITH ONE-DIMENSIONAL HEAT FLOW
(h = 6.0 Btu/sq ft deg F hr; surface cooling.)

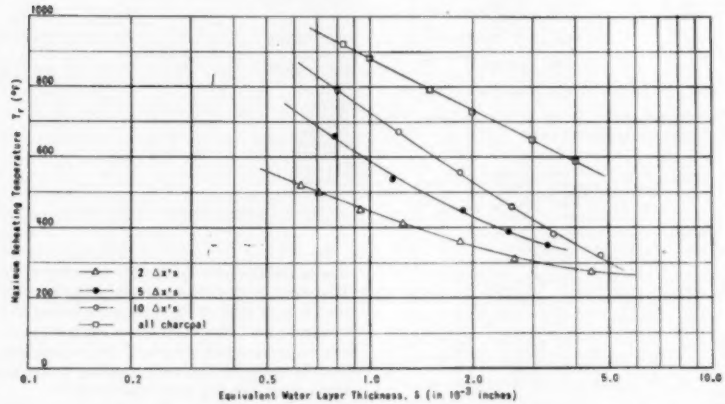

FIG. 12 THERMAL-ANALYZER RESULTS FOR SLABS WITH ONE-DIMENSIONAL HEAT FLOW
(h = 6.0 Btu/sq ft deg F hr; surface cooling.)

and in the curves in Fig. 14 for the cylinder with one-dimensional heat flow. For each type of extinguishment there was a noticeable spread in the results for h = 3.0, 6.0, and 9.0 Btu/sq ft deg F hr with greater amounts of the extinguishing agent needed for the smaller values of h.

The effect of the three spread-wetting rates used in the surface-cooling runs for the cylinder with two-dimensional heat flow may be seen in the curves in Fig. 15. Comparable curves are also plotted for one-dimensional heat flow in both the slab and the cylinder where instantaneous wetting on all sides was simulated. It was thought that the spread-wetting rate of 1 sec per sector most closely approximated the observed rates during suppression of laboratory model fires of similar sized specimens. Using this intermediate spreading rate, it can be seen that about two and one half times as much water was required for extinguishment as for the comparable instantaneous wetting case. Also it can be seen that the equivalent water-layer thickness is decreased if the spreading rate is increased.

What was thought to be the most striking result of all these tests was the comparatively small amounts of water required for extinguishment. For example, a layer of water approximately 0.001 in. thick suddenly applied over the surface of a 0.6-in-diam burning wood cylinder should be sufficient to suppress the fire and prevent rekindling in the subsequent rise of surface temperature. This gives a ratio of the volume of wood to the volume of water required for extinguishment approximately equal to 150/1. In certain laboratory and field-test fires (3), comparable ratios were in the order of 7/1,[4] thus showing the large room for improvement of techniques of extinguishing wood fires.

A comparison of curves for the one-dimensional-heat flow cases shows that results for a cylinder are fairly closely approximated by results for a slab with comparable number of elements of char-

[4] In recent tests (8), W. L. Fons has obtained ratios as high as 117/1, for laboratory model fires and 56/1 for field-test fires using burning stacks of logs.

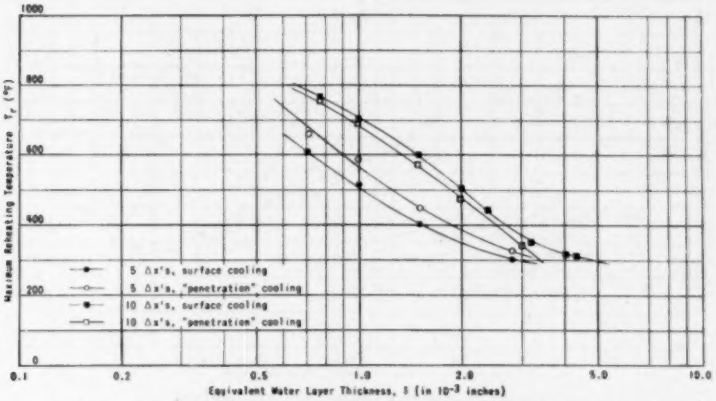

FIG. 13 THERMAL-ANALYZER RESULTS FOR CYLINDER WITH ONE-DIMENSIONAL HEAT FLOW (h = 6.0 Btu/sq ft deg F hr.)

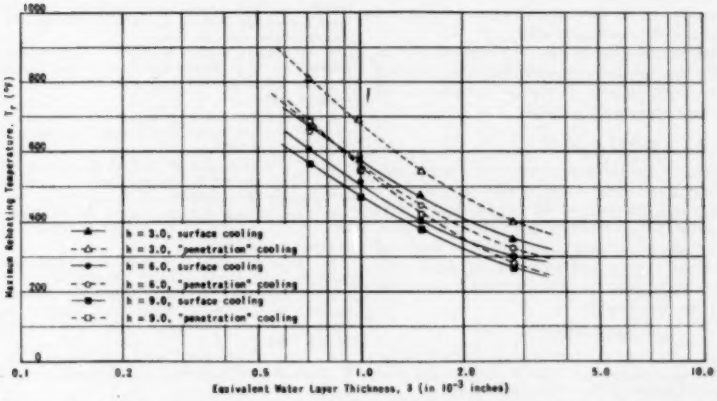

FIG. 14 THERMAL-ANALYZER RESULTS FOR CYLINDER WITH ONE-DIMENSIONAL HEAT FLOW; (5 Δx).

coal and values of h. This would tend to show that the geometry for these various cases does not influence the results as greatly as does the heat transfer in the portion of the material near the surface.

Times for extinguishment in the oxygen dilution runs are listed in Table 4. These decrease in about the manner expected with the higher values of h and with the smaller degree of fire establishment indicated by the lower number of charcoal elements. Except for the severe case of the uniformly heated complete charcoal slab, extinguishment times range from about 2 to 8 sec for the representative value of h = 6.0 Btu/sq ft deg F hr. These times are approximately 5 to 10 times greater than the water-cooling times from the comparable surface cooling runs where a T_r of 600 F was obtained.

CONCLUSIONS

1 When water at ordinary temperatures strikes burning wood, it will not boil instantaneously, and, consequently, initial wetting should be possible.

2 The thicker water layers required for the greater depths of charcoal show that more suppressing action is needed for extinguishing the more established fires.

3 There appears to be no significant difference in the values of the maximum reheating temperature obtained for the penetration-cooling runs and the equivalent surface-cooling runs.

4 For all types of extinguishment the value of the unit surface conductance h which affects the ambient cooling, has a significant influence on the maximum reheating temperature.

5 A layer of water approximately 0.001 in. thick suddenly applied over the surface of a 0.6-in-diam burning wood cylinder should be sufficient to extinguish the fire and prevent rekindling. This gives a ratio of the volume of wood to the volume of water equal approximately to 150/1.

6 If the frontal area of a 0.6-in-diam burning wood cylinder is wetted instantaneously and if four additional seconds are required for the wetting to cover the entire rear portion, owing to a finite rate of spread, the amount of water required for extinguishment will be about two and one-half times as great as would be required if the entire wetting were instantaneous.

7 The amount of water required to suppress a burning cylin-

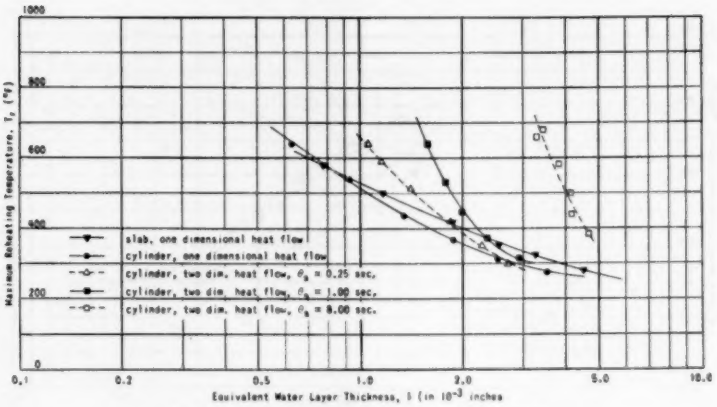

FIG. 15 COMPARATIVE THERMAL-ANALYZER RESULTS
(Surface cooling with 5 ΔT and h = 6.0 Btu/sq ft deg F hr.)

der of wood is decreased if the rate of spread wetting is increased.

8 For one-dimensional heat flow, results for a cylinder are fairly closely approximated by results for a slab.

9 Results for the oxygen-dilution runs, representing CO_2 extinguishing, indicate that the times required for extinguishment range between about 2 and 8 sec for conditions that are believed to be most representative of actual situations.

ACKNOWLEDGMENT

The research represented in this paper was performed as a part of a more extensive program under a co-operative agreement between the University of California and the United States Forest Service. For their helpful co-operation and valued assistance, the authors are particularly indebted to Messrs. W. L. Fons and I. C. Funk of the Forest Service, and Messrs. L. M. K. Boelter, R. Bromberg, and B. R. Mead of the Department of Engineering, University of California, Los Angeles.

BIBLIOGRAPHY

1 "The Chemistry of Wood," by L. F. Hawley and L. E. Wise, American Chemical Society Monograph Series No. 28, The Chemical Catalogue Company, Incorporated, New York, N. Y., p. 188.

2 "Technical Report Number 1—Engineering Fire Control Research," by G. J. Tauxe, C. K. Hadlock, and R. L. Stoker, Cooperative Agreement Number A5Fs-103-72, University of California, Los Angeles, Calif., June 30, 1948.

3 "Technical Report Number 2—Engineering Fire Control Research," by R. L. Stoker and G. J. Tauxe, Cooperative Agreement Number A5Fs-103-72, University of California, Los Angeles, Calif., January, 1949.

4 "The Heating and Ignition of Small Wood Cylinders," by W. L. Fons, California Forest and Range Experiment Station, Berkeley, Calif., April 16, 1948.

5 "The Conduction of Heat in Composite Infinite Bodies," by W. A. Mersman, W. P. Berggren, and L. M. K. Boelter, University of California Press, Berkeley, Calif., 1942, p. 9.

6 "Heat Transfer Notes," by L. M. K. Boelter, V. H. Cherry, H. A. Johnson, and R. C. Martinelli, University of California Press, Berkeley, Calif., 1946.

7 "Heat Transmission," by W. H. McAdams, McGraw-Hill Book Company, Inc., New York, N. Y., 1942, p. 63.

8 "Investigation of Use of Water and Chemicals for Forest Fire Suppression," by W. L. Fons, R. S. McBride, and E. E. Draves, California Forest and Range Experiment Station, Berkeley, Calif., May 9, 1950.

9 "Heat Conduction," by L. R. Ingersoll, O. J. Zobel, and A. C. Ingersoll, McGraw-Hill Book Company, Inc., New York, N. Y., p. 91.

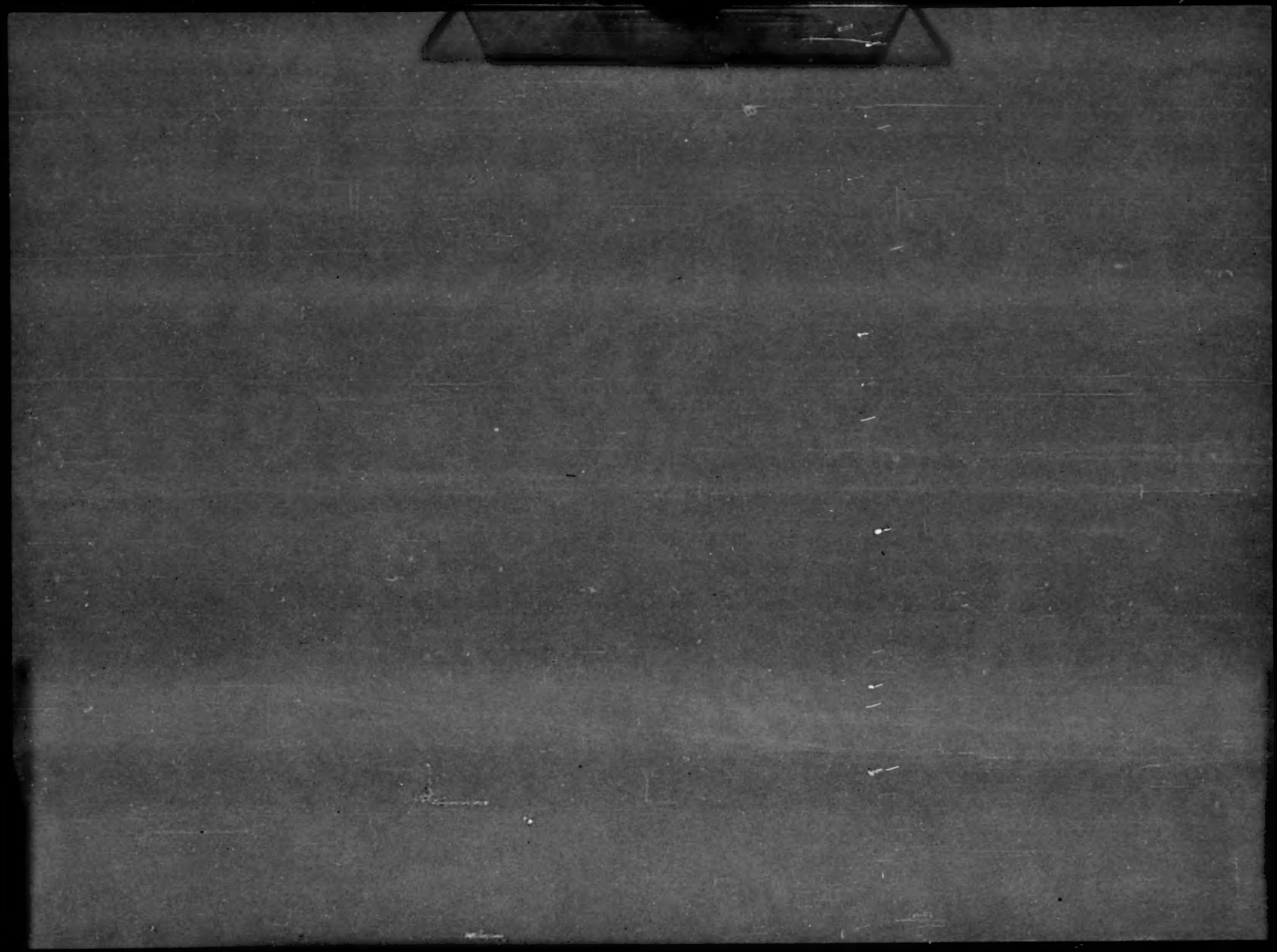

AN ASME PAPER

Its Preparation, Submission and Publication, and Presentation

To a large degree the papers prepared and presented under the ASME sponsorship are evidence by which its professional standing and leadership are judged. It follows, therefore, that to qualify for ASME sponsorship, a paper must not only present suitable subject matter, but it must be well written and conform to recognized standards of good English and literary style.

The pamphlet on "AN ASME PAPER" is designed to aid authors in meeting these requirements and to acquaint them with rules of the Society relating to the preparation and submission of manuscripts and accompanying illustrations. It also includes suggestions for the presentation of papers before Society meetings.

CONTENTS

Price 35¢. No discount allowed. *A remittance must accompany all orders for $2.00 or less. U.S. Postage Stamps are acceptable.*

THE AMERICAN SOCIETY OF MECHANICAL ENGINEERS

29 West 39th Street, New York 18, N. Y.